DECIPHERING PHAGOCYTE FUNCTIONS ACROSS DIFFERENT SPECIES

EDITED BY: Katrin Kierdorf, Marc S. Dionne, Yi Feng and Efstathios G. Stamatiades
PUBLISHED IN: Frontiers in Cell and Developmental Biology

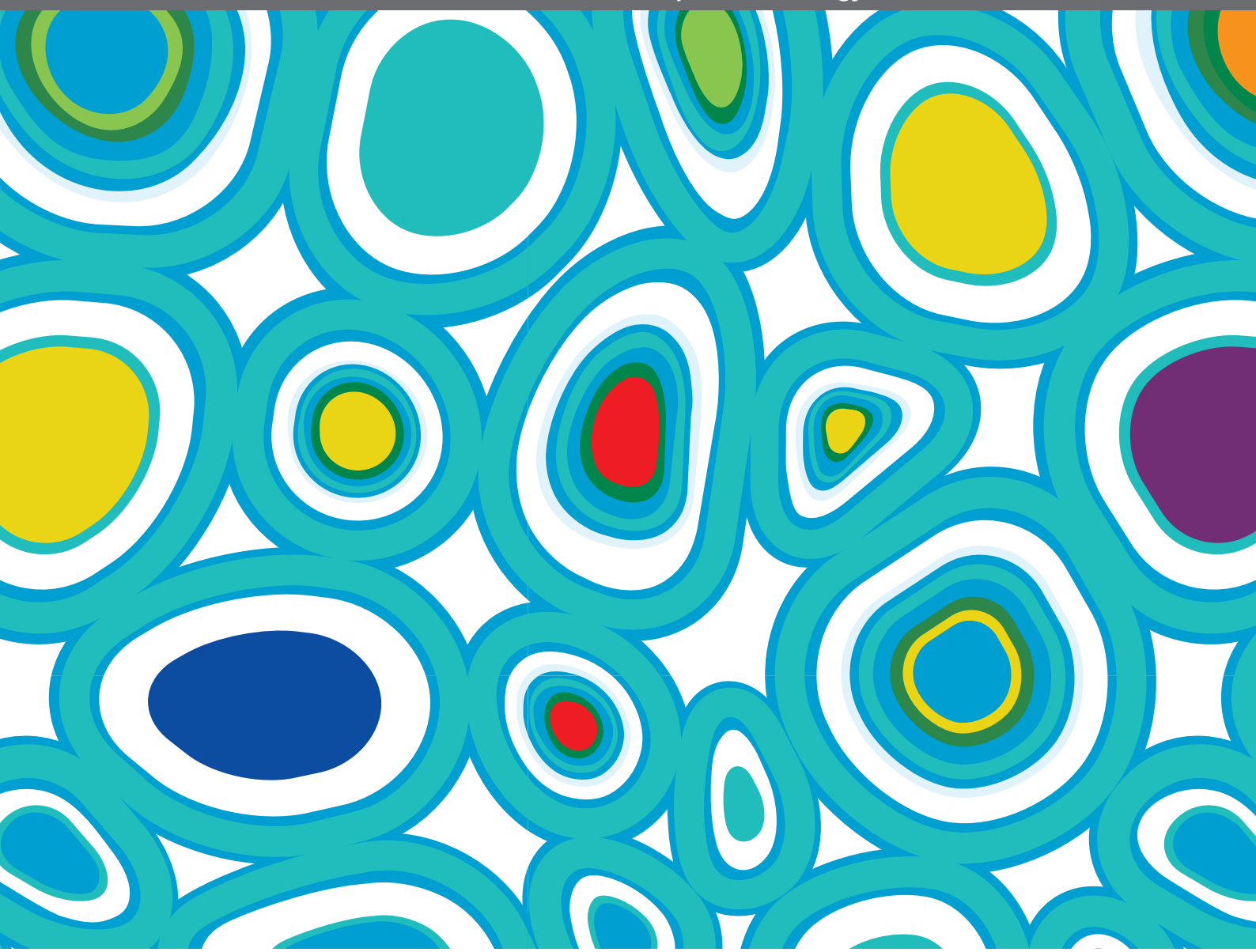

frontiers Research Topics

frontiers

ISSN 1664-8714
ISBN 978-2-88971-403-2
DOI 10.3389/978-2-88971-403-2

About Frontiers

Frontiers is more than just an open-access publisher of scholarly articles: it is a pioneering approach to the world of academia, radically improving the way scholarly research is managed. The grand vision of Frontiers is a world where all people have an equal opportunity to seek, share and generate knowledge. Frontiers provides immediate and permanent online open access to all its publications, but this alone is not enough to realize our grand goals.

Frontiers Journal Series

The Frontiers Journal Series is a multi-tier and interdisciplinary set of open-access, online journals, promising a paradigm shift from the current review, selection and dissemination processes in academic publishing. All Frontiers journals are driven by researchers for researchers; therefore, they constitute a service to the scholarly community. At the same time, the Frontiers Journal Series operates on a revolutionary invention, the tiered publishing system, initially addressing specific communities of scholars, and gradually climbing up to broader public understanding, thus serving the interests of the lay society, too.

Dedication to Quality

Each Frontiers article is a landmark of the highest quality, thanks to genuinely collaborative interactions between authors and review editors, who include some of the world's best academicians. Research must be certified by peers before entering a stream of knowledge that may eventually reach the public - and shape society; therefore, Frontiers only applies the most rigorous and unbiased reviews.
Frontiers revolutionizes research publishing by freely delivering the most outstanding research, evaluated with no bias from both the academic and social point of view. By applying the most advanced information technologies, Frontiers is catapulting scholarly publishing into a new generation.

What are Frontiers Research Topics?

Frontiers Research Topics are very popular trademarks of the Frontiers Journals Series: they are collections of at least ten articles, all centered on a particular subject. With their unique mix of varied contributions from Original Research to Review Articles, Frontiers Research Topics unify the most influential researchers, the latest key findings and historical advances in a hot research area! Find out more on how to host your own Frontiers Research Topic or contribute to one as an author by contacting the Frontiers Editorial Office: frontiersin.org/about/contact

DECIPHERING PHAGOCYTE FUNCTIONS ACROSS DIFFERENT SPECIES

Topic Editors:
Katrin Kierdorf, University of Freiburg, Germany
Marc S. Dionne, Imperial College London, United Kingdom
Yi Feng, University of Edinburgh, United Kingdom
Efstathios G. Stamatiades, Charité – Universitätsmedizin Berlin, Germany

Citation: Kierdorf, K., Dionne, M. S., Feng, Y., Stamatiades, E. G., eds. (2021). Deciphering Phagocyte Functions Across Different Species. Lausanne: Frontiers Media SA. doi: 10.3389/978-2-88971-403-2

Table of Contents

frontiers in Cell and Developmental Biology

EDITORIAL
published: 30 July 2021
doi: 10.3389/fcell.2021.712929

Editorial: Deciphering Phagocyte Functions Across Different Species

Yi Feng[1†], *Marc S. Dionne*[2†], *Efstathios G. Stamatiades*[3†] *and Katrin Kierdorf*[4,5,6*†]

[1] UoE Centre for Inflammation Research, Queen's Medical Research Institute, University of Edinburgh, Edinburgh, United Kingdom, [2] Medical Research Council Centre for Molecular Bacteriology and Infection and Department of Life Sciences, Imperial College London, London, United Kingdom, [3] Charité University Medical Centre, Institute of Microbiology, Infectious Diseases and Immunology, Berlin, Germany, [4] Faculty of Medicine, Institute of Neuropathology, University of Freiburg, Freiburg, Germany, [5] Center for Integrative Biological Signaling Studies Centre for Integrative Biological Signalling Studies, University of Freiburg, Freiburg, Germany, [6] Faculty of Medicine, Center for Basics in NeuroModulation (NeuroModulBasics), University of Freiburg, Freiburg, Germany

Keywords: phagocyte, macrophage, model organism, innate immunity, species

Editorial on the Research Topic

Deciphering Phagocyte Functions Across Different Species

Specialized innate immune cells are found across all metazoan organisms. Foundational experiments by Elie Metchnikoff revealed the existence of innate phagocytes which efficiently clear invading pathogens or cell debris in the sea star larva (Chang, 2009). The concept of phagocytic immune cells is conserved across insects to mammals and their counterparts are found in *Drosophila*, zebrafish, or mammals. These cells seem to serve two major functions: the clearance of invading pathogens and cell debris, as well as the release of immunomodulatory molecules and growth factors (Kierdorf and Dionne, 2016). Their functions cover a variety of tasks from combating infections or cancer to maintaining tissue homeostasis and repair.

This Research Topic contains a collection of original research articles and literature reviews pointing toward the importance of understanding phagocyte function in a cross-species approach, but also highlighting the necessity and elegance of experimental model organisms in biomedical research. More and more studies reveal that immune functions and ontogeny of many phagocyte subtypes are conserved across species (Gold and Brückner, 2014). By studying phagocyte function in different species we can obtain new insights into the innate immune function of human phagocytes such as granulocyte, monocytes, dendritic cells and macrophages (Geirsdottir et al., 2019; Zindel et al., 2021). Within this Research Topic Miah et al. outline the collective findings on prenatal human mononuclear phagocyte development in different organs and their role in embryonic and fetal organ development and to compare them to the more detailed data already obtained on phagocyte development in transgenic mouse models. They also highlight new data collected from single-cell multi-omic approaches and next-generation *ex-vivo* organ-on-chip models which could guide future studies into understanding human phagocyte development.

Depending on host tissue, phagocytes represent a heterogenous range of subtypes and functional diversity. In their study, Park et al. identify a new adherent intestinal phagocyte population in Atlantic salmon which has high phagocytic activity and expresses several macrophage specific genes. In a detailed review, Portilla et al. summarize the current knowledge on intestinal macrophages from different species. Starting with a description of the development and differentiation of phagocytes in different species during evolution, they further describe tissue specification of vertebrate macrophages and finally the highly adapted specialization of different intestinal macrophage subsets. Highlighting the complexity of the interplay of resident tissue macrophages with their niche, they also point toward the necessity to not only decipher heterogeneity across different phagocytes but also understand their interaction network within their specific tissue niche.

Edited and reviewed by:
You-Wen He,
Duke University, United States

****Correspondence:***
Katrin Kierdorf
katrin.kierdorf@uniklinik-freiburg.de

† These authors have contributed equally to this work

Specialty section:
This article was submitted to Cell Death and Survival, a section of the journal Frontiers in Cell and Developmental Biology

Received: *21 May 2021*
Accepted: *08 July 2021*
Published: *30 July 2021*

Citation:
Feng Y, Dionne MS, Stamatiades EG and Kierdorf K (2021) Editorial: Deciphering Phagocyte Functions Across Different Species. Front. Cell Dev. Biol. 9:712929. doi: 10.3389/fcell.2021.712929

Many immune defense pathways of phagocytes are conserved from invertebrates to vertebrates. Moghadam et al. describe recent data on the role and function of reactive oxygen species (ROS) produced by phagocytes from flies to humans. Here they also point to the importance of the collected data from model organisms which help to clarify the function of ROS and ROS deficiency during human disease. Bush et al. describe and compare the transcriptomic profile of sheep bone marrow derived macrophages (BMDMs) with BMDMs from other larger animals and rodents upon lipopolysaccharides (LPS) stimulation. This analysis highlights conserved transcriptional profiles between the species in genes clusters such as cell surface receptors and the endosome-lysosome pathway, but also differences in the induction of arginine metabolism and nitric oxide production.

A wide range of models for chronic disease, cancer and infection have been established in various model organisms and help us to understand phagocyte function *in vivo* (Dionne and Schneider, 2008; Feng and Martin, 2015). Kumar et al. present a new tool to study phagocytes in insect immunity by depleting phagocytes in *Drosophila melanogaster* and *Aedes aegypti* with clodronate liposomes. This depletion study demonstrates the central function of phagocytic immune cells in defense against invading pathogens. *Drosophila melanogaster* has emerged as a versatile tool to study immunometabolism and the interaction between immune signaling and adaptations in metabolism for example during infection but also how metabolic changes can trigger an immune response. Bajgar et al. summarize collective knowledge on the immunometabolism of hemocytes in *Drosophila* and discuss new hypotheses based on the available data. Using a mouse model for choroidal neovascularization (CNV) during age-related macular degeneration, Schlecht et al. demonstrate their findings on the role of macrophage-derived *secreted phosphoprotein-1* (*Spp1*) during CNV. Combining subsequent gene expression analysis of resident retinal microglia and *in vivo* inhibition of Spp1, they provide evidence that the Spp1 pathway could be a promising new target to modulate CNV in human patients.

Advances in *in vivo* imaging techniques now allow tracing of phagocytes in the living organism (Nimmerjahn et al., 2005; Stamatiades et al., 2016). The zebrafish is an excellent model system due to the high transparency of larvae and the availability of many transgenic reporter lines. Hu et al. use live imaging in zebrafish larvae to follow the migration behavior of neutrophils and macrophages in response to tail wounding. Interestingly, they find *toll like receptor 2* (*tlr2*) and *myeloid differentiation primary response 88* (*myd88*) are involved in modulating directional migration of distant neutrophils and macrophages to the wound. Detailed analysis of neutrophils and macrophage migration behavior revealed that the Tlr2-MyD88 pathway controls directional persistence and the migration speed of recruited cells. Future studies are now needed to further elucidate the mechanism as to how Tlr2-MyD88 signaling pathway cross talks to chemokine signaling to control neutrophil and macrophage responses to the wound signal. Recently new high-dimensional, high-throughput techniques, such as single cell RNA-sequencing (scRNA-seq) have allowed us to gain further insight on the heterogeneity of phagocytes in different species including embryonic and larval hemocytes in *Drosophila melanogaster* (Cattenoz et al., 2020; Cho et al., 2020; Tattikota et al., 2020). In this context, Cattenoz et al. compare the collective data from these three studies and identify eight hemocyte subgroups within all three datasets which are associated to distinct functions during embryonic and larval stages. Their comparison further highlights the distinct expression profile of larval hemocytes in peripheral tissues. The heterogenous functions of *Drosophila* macrophages in different organs during development, but also homeostasis, are summarized by Mase et al. In their contribution they give an overview of the recent knowledge on organ specific macrophage functions in *Drosophila*.

In the immunological field, there are few cross-species comparisons of phagocyte function. To our knowledge, the exchange of data between groups studying phagocyte function in different model organisms is most limited. How tissue-derived signals regulate phagocyte function is also barely understood. The articles and reviews collected for this Research Topic show that comparison and analysis of phagocyte function in different organisms might contribute to our knowledge about the innate immune system and help to understand immune responses during different diseases such as cancer, infection or metabolic disease.

AUTHOR CONTRIBUTIONS

All authors listed have made a substantial, direct and intellectual contribution to the work, and approved it for publication.

ACKNOWLEDGMENTS

The authors would like to dedicate this Research Topic to Katja Brueckner and her work on *Drosophila* plasmatocytes. She will be deeply missed by everyone in the field.

REFERENCES

Cattenoz, P. B., Sakr, R., Pavlidaki, A., Delaporte, C., Riba, A., Molina, N., et al. (2020). Temporal specificity and heterogeneity of *Drosophila* immune cells. *EMBO J.* 39:e104486. doi: 10.15252/embj.2020104486

Chang, Z.-L. (2009). Recent development of the mononuclear phagocyte system: in memory of Metchnikoff and Ehrlich on the 100th Anniversary of the 1908 Nobel Prize in Physiology or Medicine. *Biol. Cell* 101, 709–721. doi: 10.1042/BC20080227

Cho, B., Yoon, S.-H., Lee, D., Koranteng, F., Tattikota, S. G., Cha, N., et al. (2020). Single-cell transcriptome maps of myeloid blood cell lineages in *Drosophila*. *Nat. Commun.* 11:4483. doi: 10.1101/2020.01.15.908350

Dionne, M. S., and Schneider, D. S. (2008). Models of infectious diseases in the fruit fly *Drosophila melanogaster*. *Dis. Model Mech.* 1, 43–49. doi: 10.1242/dmm.000307

Feng, Y., and Martin, P. (2015). Imaging innate immune responses at tumour initiation: new insights from fish and flies. *Nat. Rev. Cancer* 15, 556–562. doi: 10.1038/nrc3979

Geirsdottir, L., David, E., Keren-Shaul, H., Weiner, A., Bohlen, S. C., Neuber, J., et al. (2019). Cross-species single-cell analysis reveals divergence of the primate microglia program. *Cell* 179, 1609–1622.e16. doi: 10.1016/j.cell.2019.11.010

Gold, K. S., and Brückner, K. (2014). *Drosophila* as a model for the two myeloid blood cell systems in vertebrates. *Exp. Hematol.* 42, 717–727. doi: 10.1016/j.exphem.2014.06.002

Kierdorf, K., and Dionne, M. S. (2016). The software and hardware of macrophages: a diversity of options. *Dev. Cell* 38, 122–125. doi: 10.1016/j.devcel.2016.07.008

Nimmerjahn, A., Kirchhoff, F., and Helmchen, F. (2005). Resting microglial cells are highly dynamic surveillants of brain parenchyma *in vivo*. *Science* 308, 1314–1318. doi: 10.1126/science.1110647

Stamatiades, E. G., Tremblay, M.-E., Bohm, M., Crozet, L., Bisht, K., Kao, D., et al. (2016). Immune monitoring of trans-endothelial transport by kidney-resident macrophages. *Cell* 166, 991–1003. doi: 10.1016/j.cell.2016.06.058

Tattikota, S. G., Cho, B., Liu, Y., Hu, Y., Barrera, V., Steinbaugh, M. J., et al. (2020). A single-cell survey of *Drosophila* blood. *Elife* 9:e54818. doi: 10.7554/eLife.54818.sa2

Zindel, J., Peiseler, M., Hossain, M., Deppermann, C., Lee, W. Y., Haenni, B., et al. (2021). Primordial GATA6 macrophages function as extravascular platelets in sterile injury. *Science* 371:eabe0595. doi: 10.1126/science.abe0595

Conflict of Interest: The authors declare that the research was conducted in the absence of any commercial or financial relationships that could be construed as a potential conflict of interest.

Publisher's Note: All claims expressed in this article are solely those of the authors and do not necessarily represent those of their affiliated organizations, or those of the publisher, the editors and the reviewers. Any product that may be evaluated in this article, or claim that may be made by its manufacturer, is not guaranteed or endorsed by the publisher.

frontiers in Cell and Developmental Biology

ORIGINAL RESEARCH
published: 21 July 2020
doi: 10.3389/fcell.2020.00661

Species-Specificity of Transcriptional Regulation and the Response to Lipopolysaccharide in Mammalian Macrophages

Stephen J. Bush[1†], Mary E. B. McCulloch[2†], Zofia M. Lisowski[2], Charity Muriuki[2], Emily L. Clark[2], Rachel Young[2], Clare Pridans[3,4], James G. D. Prendergast[2], Kim M. Summers[5‡] and David A. Hume[5‡]*

[1] Nuffield Department of Clinical Medicine, John Radcliffe Hospital, University of Oxford, Oxford, United Kingdom, [2] The Roslin Institute, The University of Edinburgh, Edinburgh, United Kingdom, [3] Centre for Inflammation Research, The University of Edinburgh, Edinburgh, United Kingdom, [4] Simons Initiative for the Developing Brain, Centre for Discovery Brain Sciences, The University of Edinburgh, Edinburgh, United Kingdom, [5] Mater Research Institute-University of Queensland, Translational Research Institute, Woolloongabba, QLD, Australia

OPEN ACCESS

Edited by:
Katrin Kierdorf, University of Freiburg, Germany

Reviewed by:
Andrew James Murphy, Baker Heart and Diabetes Institute, Australia
Alessandro Michelucci, Luxembourg Institute of Health, Luxembourg

***Correspondence:**
David A. Hume
david.hume@uq.edu.au

[†] These authors have contributed equally to this work
[‡] These authors share senior authorship

Specialty section:
This article was submitted to Cell Death and Survival, a section of the journal Frontiers in Cell and Developmental Biology

Received: *18 May 2020*
Accepted: *01 July 2020*
Published: *21 July 2020*

Citation:
Bush SJ, McCulloch MEB, Lisowski ZM, Muriuki C, Clark EL, Young R, Pridans C, Prendergast JGD, Summers KM and Hume DA (2020) Species-Specificity of Transcriptional Regulation and the Response to Lipopolysaccharide in Mammalian Macrophages. Front. Cell Dev. Biol. 8:661. doi: 10.3389/fcell.2020.00661

Mammalian macrophages differ in their basal gene expression profiles and response to the toll-like receptor 4 (TLR4) agonist, lipopolysaccharide (LPS). In human macrophages, LPS elicits a temporal cascade of transient gene expression including feed forward activators and feedback regulators that limit the response. Here we present a transcriptional network analysis of the response of sheep bone marrow-derived macrophages (BMDM) to LPS based upon RNA-seq at 0, 2, 4, 7, and 24 h post-stimulation. The analysis reveals a conserved transcription factor network with humans, and rapid induction of feedback regulators that constrain the response at every level. The gene expression profiles of sheep BMDM at 0 and 7 h post LPS addition were compared to similar data obtained from goat, cow, water buffalo, horse, pig, mouse and rat BMDM. This comparison was based upon identification of 8,200 genes annotated in all species and detected at >10TPM in at least one sample. Analysis of expression of transcription factors revealed a conserved transcriptional millieu associated with macrophage differentiation and LPS response. The largest co-expression clusters, including genes encoding cell surface receptors, endosome–lysosome components and secretory activity, were also expressed in all species and the combined dataset defines a macrophage functional transcriptome. All of the large animals differed from rodents in lacking inducible expression of genes involved in arginine metabolism and nitric oxide production. Instead, they expressed inducible transporters and enzymes of tryptophan and kynurenine metabolism. BMDM from all species expressed high levels of transcripts encoding transporters and enzymes involved in glutamine metabolism suggesting that glutamine is a major metabolic fuel. We identify and discuss transcripts that were uniquely expressed or regulated in rodents compared to large animals including *ACOD1*, CXC and CC chemokines, *CD163*, *CLEC4E*, *CPM*, *CSF1*, *CSF2*, *CTSK*, *MARCO*, *MMP9*, *SLC2A3*, *SLC7A7*, and *SUCNR1*. Conversely, the data confirm the conserved

regulation of multiple transcripts for which there is limited functional data from mouse models and knockouts. The data provide a resource for functional annotation and interpretation of loci involved in susceptibility to infectious and inflammatory disease in humans and large animal species.

Keywords: transcriptome, macrophage, LPS, feedback, network, conservation, species

INTRODUCTION

Macrophages and related members of the mononuclear phagocyte system (MPS) have many trophic roles in development and homeostasis and are the first line of defense against potential pathogens (Hume et al., 2019; Guilliams et al., 2020). The survival, proliferation and differentiation of macrophages depends upon signaling via the macrophage colony stimulating factor receptor (CSF1R), which mediates signals from colony stimulating factor 1 (CSF1; also known as macrophage colony stimulating factor) or interleukin 34 (IL34) (Stanley and Chitu, 2014; Hume et al., 2020). In response to pathogen challenge, resident macrophages are activated to produce cytokines and chemokines that drive recruitment of neutrophils and inflammatory monocytes. The activation of macrophages is mediated through pattern recognition receptors that bind to pathogen-associated molecules (Brubaker et al., 2015). The archetypal pattern recognition receptor is TLR4, which, with the coreceptor MD-2, recognizes endotoxin or lipopolysaccharide (LPS), a major constituent of the cell wall of Gram-negative organisms (Marongiu et al., 2019). TLR4 ligation initiates the up and down regulation of thousands of transcripts, including hundreds of transcription factors (Kaikkonen et al., 2013; Baillie et al., 2017). Many of the induced genes are required for defense against pathogens, but they are also responsible for symptoms such as fever and much of the pathology. Feedback control by numerous negative regulators is therefore required to ensure that the response to pathogens is limited and appropriate (Wells et al., 2005; Kondo et al., 2012).

Many studies of LPS signaling *in vitro* have used bone marrow-derived macrophages (BMDM), cells grown from bone marrow in the presence of CSF1, or monocyte-derived macrophages (MDM), matured from blood in the presence of CSF1. Previous network analysis of the time course of human MDM response to LPS revealed a sequential cascade of transient induction of feed forward and feedback regulators (Baillie et al., 2017). Not surprisingly, given the central role of macrophages in innate immunity, there are differences in the response to LPS of mouse and human macrophages grown in CSF1 (Schroder et al., 2012). The response to the endogenous anti-inflammatory agonists, glucocorticoids, is even more divergent, associated with gain and loss of functional glucocorticoid receptor binding sites in the genome (Jubb et al., 2016). Comparative analysis in the pig indicated that BMDM and monocyte-derived macrophages grown in CSF1 have very similar gene expression profiles. Both basal and LPS-induced gene expression profiles in pig were more similar to humans than were those in mice (Kapetanovic et al., 2012, 2013).

Nitric oxide (NO) production from arginine by NOS2 is a significant component of host defense in rodent species that is not conserved in large animals. Macrophages from humans and pigs do not produce NO in response to LPS and the enhancer elements involved in *NOS2* induction are not conserved in rodents (Kapetanovic et al., 2012; Schroder et al., 2012; Karagianni et al., 2017; Young et al., 2018). To further document the species specificity of regulated arginine metabolism we cultured BMDM from sheep, goat, cattle, water buffalo, pig, horse, and rat and incubated them with or without LPS. RNA-seq analysis of these populations revealed variation in arginine metabolism amongst the species including a divergence between bovids (cattle and water buffalo) and small ruminants (sheep and goats) (Young et al., 2018). In a separate study, the same primary RNA-seq data were used to document evolution and expression of the *ADGRE1* gene, encoding F4/80, a widely used marker for macrophage biology in mouse (Waddell et al., 2018). In these studies, the LPS response was analyzed at a single timepoint in each species (7 h) chosen to coincide with maximal induction of transcripts encoding inflammatory cytokines in human monocyte-derived macrophages (Baillie et al., 2017).

Macrophage immunometabolism is a burgeoning field based upon the view that metabolic requirements change with functional polarization (Hotamisligil, 2017; Castegna et al., 2020; Ryan and O'Neill, 2020). Published studies have focused on regulation of the tricarboxylic acid (TCA) cycle and accumulation of intermediates such as itaconate, succinate, and ketoglutarate as signaling molecules (Ryan and O'Neill, 2020). Like the NOS2 pathway, much of the evidence for roles of metabolic intermediates and enzymes in macrophage activation/polarization derives from *in vitro* studies of inbred mice, and at least some of the effects of LPS on mitochondrial function are mediated by endogenous NO (Van den Bossche et al., 2017). Itaconate, produced through the induction of the enzyme ACOD1, which diverts citrate from the TCA cycle, has been associated with anti-inflammatory roles (Mills et al., 2018). Similarly, a recent study of mice described the biosynthesis of anti-inflammatory fatty acids late in the LPS response as part of the feedback control network described above (Oishi et al., 2017). It is unclear how many of the findings can be translated to humans or other species.

The domestic sheep, like the pig, is an important livestock species, and also used extensively as a model in biomedical research. BMDM have previously been grown from sheep bone marrow in CSF1 and were shown to be responsive to LPS (Francey et al., 1992a,b). Like pig and human macrophages, sheep (and goat) macrophages make no detectable NO in response to LPS (Jungi et al., 1996; Young et al., 2018).

However, immunometabolism in sheep, a ruminant species, is potentially quite different from monogastric species such as humans and pigs. Mouse and rat macrophages have been shown to metabolize glutamine at a rapid rate (Curi et al., 2017). Glutamine metabolism in macrophages is regulated and inhibition of glutamine synthetase (GSS), which produces glutamine from glutamate, was shown to alter the polarization state of mouse macrophages (Jha et al., 2015; Palmieri et al., 2017). The circulating glutamine concentration in ruminants is three–fivefold lower than in monogastric species, due to a low glutamine synthetase capacity, and glutamine is not the predominant respiratory fuel for the intestine (Meijer et al., 1993). The sheep, as a ruminant, has high circulating levels of fermentative by-products, primarily volatile fatty acids (propionate, acetate, and butyrate), which are utilized within the liver for gluconeogenesis (Danfaer et al., 1995). Aside from acting as fuels, free fatty acids may be recognized by a large family of G protein coupled receptors (Kimura et al., 2020).

To extend our knowledge of the diversification of macrophage function amongst species, we have generated a time course of the transcriptomic response of sheep BMDM to LPS. Detailed analysis of this time course reveals those components that distinguish sheep from human macrophages. Comparative analysis with RNA-seq data from other species, including humans, is compromised by incomplete annotation, inconsistent naming and ambiguous orthology relationships (especially in multigene families). To enable such a comparison of sheep RNA-seq data with previously generated RNA-seq data for BMDM from goat, cow, water buffalo, horse, pig, and rat, and public domain data for two mouse species, we undertook an annotation effort to identify >8,000 macrophage-expressed genes that are clear orthologs between the species. We present a resource for functional annotation and interpretation of loci involved in susceptibility to infectious and inflammatory disease in humans and large animal species.

MATERIALS AND METHODS

Data Generation and Analysis

The protocol for the generation of bone marrow-derived macrophages (BMDM) in recombinant CSF1 was originally developed for pigs (Kapetanovic et al., 2012, 2013). Full details of the animals and the protocol for generation and activation of BMDM from sheep marrow are included with our high resolution sheep transcriptomic atlas where data for 3 male and 3 female cross-bred adult animals were originally described (Clark et al., 2017). The mRNA sequencing libraries generated for all time points were prepared using the Illumina TruSeq stranded mRNA library preparation kit (Illumina; Part: 15031047 Revision E) and sequenced to a depth of >25 million 125 bp paired-end reads per sample as described (Clark et al., 2017).

RNA-seq libraries for control and LPS-stimulated BMDM from additional species were downloaded from the European Nucleotide Archive (ENA). Details of all of the accessions are provided in **Supplementary Table S1.** This comparative dataset comprises eight additional species: buffalo, goat, cow, horse, mouse (both *Mus musculus* and its outbred relative, *Mus spretus*), pig and rat, as well as the sheep. For all species except mouse, the agonist used was *Salmonella minnesota* Re595 LPS, which is a pure TLR4 agonist (Young et al., 2018). In the case of the two mouse species, the agonist used was KLA (Kdo2-lipid A) the active core of LPS (Link et al., 2018) and samples were obtained after 6 h.

While publicly sourced RNA-seq libraries can differ both in preparation and sequencing methods, it is possible to process their data with a common normalization, producing comparable expression level estimates (Summers et al., 2019). Central to this process is reducing the distorting effects of differential sampling depth. To do so, each library was randomly down-sampled to a depth of 10 million reads, using seqtk v1.3[1] as previously described (Summers et al., 2019). Expression was then quantified as transcripts per million (TPM) using Kallisto v0.44.0 (Bray et al., 2016) with transcript-level expression estimates summed to the gene-level. To generate comprehensive Kallisto indices, we used (where available) the combined set of unique protein-coding transcripts from Ensembl and NCBI RefSeq as detailed in **Supplementary Table S2**.

For a meaningful cross-species comparison of expression levels, we also required a one-to-one relationship between gene names across species. This is complicated by the fact that some genes have multiple copies in one species but not others, as well as genomes differing in the completeness of the annotation. Should a gene name not be available in a given species, where possible we assigned a name on the basis of an ortholog in a near relative. For this purpose, orthology relationships were sourced from Ensembl BioMart (Kinsella et al., 2011) and required to be one-to-one, with ≥90% reciprocal identity and an 'orthology confidence' score of 1 (this score reflects a high whole genome alignment coverage and conservation of synteny, as described in Ensembl documentation[2], accessed 30th March 2020). If there are multiple possible orthologs, Ensembl classifies the relationship between each member of the set as one-to-many. However, if only one member of a one-to-many set of genes met the other two criteria (of reciprocal identity and orthology confidence score), we reconsidered this gene to be the most probable one-to-one ortholog. Genes renamed on the basis of orthology are indicated in **Supplementary Table S3**. These automatically assigned orthology relationships were only made within two sub-groups of the closest related species in the dataset: three ruminants (sheep, cow, and goat), and the three rodents (*M. musculus*, *M. spretus*, rat). No orthologs were sought for horse or pig (being relatively distant species) or buffalo (not yet available via Ensembl). The final dataset includes 9,478 genes for which there are candidate orthologs in at least 8 of 9 species (**Supplementary Table S3**). Of these, 8,249 genes were annotated in all 9 species and expressed >10TPM in at least one sample. These are shown as a list ranked on maximal expression in **Supplementary Table S4**. Transcription factors within this comparative dataset were identified based on the curated list of 1,639 known or likely human transcription factors published by Lambert et al. (2018).

[1] https://github.com/lh3/seqtk

[2] https://www.ensembl.org/info/genome/compara/Ortholog_qc_manual.html

Network and GO Term Enrichment Analysis

Network analysis was performed using Graphia, a computational tool which enables visualization and analysis of large correlation networks. This program is now available open-source as BioLayout.[3] The data provided in **Supplementary Tables** can also be reanalyzed with a new version of Graphia.[4] Networks created by Graphia were used in two ways. A sample-to-sample network was created to assess relationships between the nine species based on shared gene expression patterns between samples. The correlation co-efficient threshold of 0.8 was chosen to include all samples in the network. Gene-to-gene networks were created to determine co-expressed genes across all samples for the sheep BMDM time course and for the nine species responding to LPS. The correlation co-efficient for each of these gene co-expression networks (GCN) was chosen to optimise the number of nodes (transcripts) while minimizing the number of edges (correlations between nodes at or above the chosen correlation co-efficient) as shown in **Supplementary Figures S1, S2**. Enrichment of gene ontology (GO) terms for genes within the sheep clusters was assessed using DAVID,[5] with *Ovis aries* as the background. Only enrichments with Benjamini–Hochberg adjusted *p*-value of $\leq$0.05 were considered significant.

RESULTS

Response of Sheep Macrophages to LPS

Graphia is a computational tool which enables the analysis and visualization of large correlation networks. Amongst many applications it was used to identify cell and tissue-specific co-expression clusters in the sheep (Clark et al., 2017), pig (Summers et al., 2019) goat (Muriuki et al., 2019), water buffalo (Young et al., 2019), and chicken (Bush et al., 2018a) transcriptional atlas projects. Co-expression analysis of a detailed time course of the transcriptomic response of human MDM to LPS treatment based upon sequencing of CAGE (genome scale 5′ RACE) libraries revealed the transient induction of positive and negative regulators (Baillie et al., 2017). For the time course of sheep BMDM responding to LPS treatment, we chose 5 time points, 0, 2, 4, 7, and 24 h, to cover the major peaks identified in the human study. The full dataset for the six animals is provided in **Supplementary Table S5**. The 6 animals varied to some extent in the degree and temporal profile of their response to LPS. This variation increased the power to identify transcript clusters that were strictly co-regulated. For the purpose of this analysis, only transcripts detected above 10 TPM in at least one library were included. The expression data were clustered at an optimal Pearson correlation co-efficient of 0.75, which includes 9,304 transcripts in the network. The lists of genes in each cluster and the average expression profiles are provided in **Supplementary Table S6**. **Figure 1** shows the profiles for the eight largest clusters of interest annotated with specific index genes. With only 3 male and 3 female sheep in the dataset, it would not have been possible to detect subtle sex-specific gene expression but there was no obvious cluster that distinguished males and females.

Genes in the largest cluster, Cluster 1, containing more than half the total transcripts, were expressed constitutively and marginally down-regulated within 2 h by LPS. Cluster 6 and Cluster 7 each contain transcripts that were progressively down-regulated over the time course in all replicates, but the basal expression varied amongst the individual animals. These three clusters each contain multiple known macrophage-enriched transcripts (*CSF1R*, *C1QA*, *LGALS3*, and *IRF8*). Cluster 1 contains many components of the vacuolar ATPase, lysosomal enzymes and surface markers as well as the cell cycle transcriptional regulator *Foxm1* and many cell cycle-related transcripts (Giotti et al., 2019) and mitochondria-associated genes. Enriched GO terms and pathways include those related to lysosomes, endo- and exosomes, signaling, and cellular movement (**Supplementary Table S6**).

Cluster 2 contains transcripts that have a complex pattern of apparent transcriptional regulation; these were induced transiently at 2 h but then substantially and transiently down-regulated in all six replicates at 7 h.

Cluster 3 is the reciprocal to Cluster 2 and contains the largest set of inducible transcripts. The average expression of genes in this cluster peaks at 7 h and declines thereafter. It includes transcripts encoding transcriptional regulators, notably *AHR*, *ATF6*, *BATF3*, *EHF*, *IRF3*, *IRF7*, *IRF9*, and *STAT2* and numerous known interferon-inducible genes that are also induced by LPS in human macrophages, through autocrine IFNβ signaling and the MYD88-independent pathway (Baillie et al., 2017). The two type 1 interferon receptor genes (*IFNAR1/IFNAR2*) were highly expressed in unstimulated cells and the interferon-inducible feedback regulators, *SOCS1* and *SOCS3*, were induced by 2 h. However, the IFNβ genes in sheep are not currently annotated in Ensembl and the three IFNβ2-like transcripts did not meet the 10 TPM expression threshold at any time point. As such, the precise nature of the autocrine signal in sheep BMDM, if it exists, is unclear. Cluster 3 also contains transcripts encoding the classical pro-inflammatory cytokines *IL1B* and *IL6* and multiple chemokine genes (*CCL3*, *5*,*8*,*20; CXCL8*,*10*). The chemokine genes, notably *CXCL8* (encoding IL8), are amongst the most abundant transcripts in the LPS-induced state, collectively contributing > 100,000TPM. GO terms relating to antiviral response were enriched in this cluster.

Cluster 4 contains 395 transcripts that on average were induced transiently, peaking after 2–4 h and declining to basal levels by 24 h. These transcripts can be subdivided into several classes. They include classical early response genes encoding transcription factors (*EGR1*,*3*,*4; FOSB*, *FOSL1*, *FOSL2*, *IER3*, *IER5*, *JUNB*, *KDM6B*, *MYC*, and *NFKBIZ*) and negative regulators that were also induced in human MDM in response to LPS (*BCL3*, *BCOR*, *CISH*, *DUSP1*, *DUSP5*, *DUSP10*, *GADD45B*, *IL10*, *MEFV*, *NFKIA*, *NFKIB*, *SMAD7*, *SOC1*, *SOCS3*, *TNFAIP2*, *TNFAIP3*, *ZFP36*, and *ZC3H12A*) (Baillie et al., 2017) and were inferred to provide intrinsic limitation of the pro-inflammatory activation. The set of transient early response genes also included

[3]http://biolayout.org

[4]https://graphia.app

[5]https://david.ncifcrf.gov/home.jsp

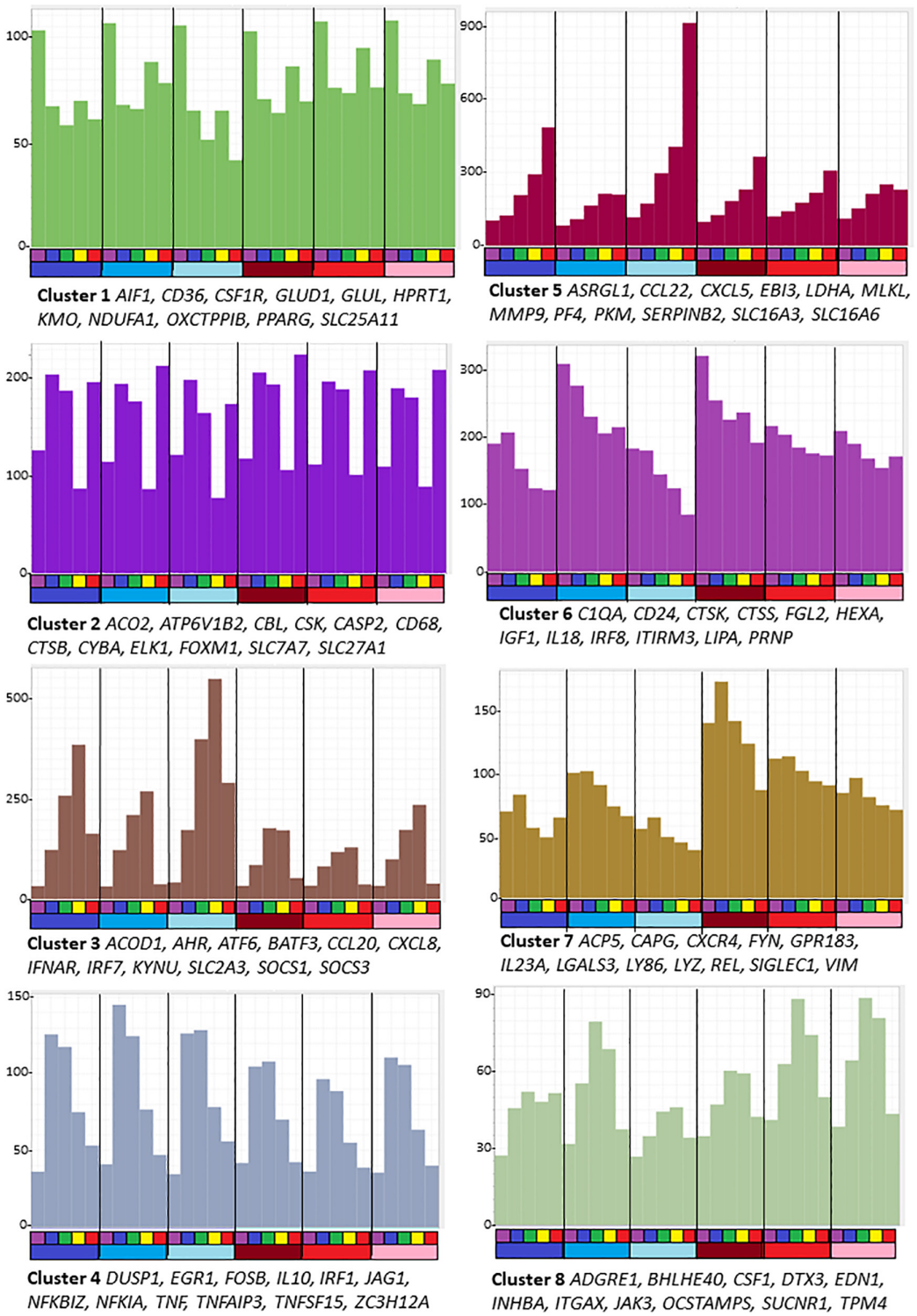

FIGURE 1 | Average gene expression profiles and genes of interest within the clusters of the largest eight clusters (>80 nodes) from the analysis of sheep BMDM treated with LPS. The primary data are in **Supplementary Table S5**, and full list of clusters and co-expressed transcripts is provided in **Supplementary Table S6**. Graphia network analysis performed at a Pearson correlation threshold $r \geq 0.75$ and MCL inflation 1.7. The *Y*-axis shows average expression (TPM) of genes in each cluster which indicates the shared pattern driving the correlated expression. For example, Cluster 5 contains transcripts that were each progressively up-regulated by LPS in all 6 animals. Genes named under each panel are representative of each cluster. The bars below the *X*-axis identify the samples. Each segment is the time course of an individual animal. The upper bar indicates the time point after adding LPS: purple = 0 h; blue – 2 h; green – 4 h; yellow – 7 h; red – 24 h. The lower bar indicates the sex of each individual: blue – males; red – females.

pro-inflammatory mediators such as *TNF* and *PTGS2*, and likely feed-forward regulators such as *IRF1*. A related cluster, Cluster 34, showed a similar average pattern but with more extreme induction from undetectable basal levels. It includes *CXCL1*, *JAG1*, *TNFSF15* and transcription factors *ETS2* and *KLF5*. More than 50 of the transcripts within Cluster 4 were unannotated on Ensembl. Around half of these could be confidently assigned gene names based upon clear orthology to human genes. Provisional annotations are shown in **Supplementary Table S6**. Amongst the most inducible and highest expressed were likely orthologs of transcription factors *CEBPD* and *KLF2*.

As in human macrophages responding to LPS, there was also a set of transcripts that continued to increase across the time course. Cluster 5 is the reciprocal cluster to Clusters 6 and 7. Transcripts in this cluster, as well as a subset of those in Cluster 3, are likely associated with resolution of inflammation. Amongst the most highly induced transcripts are those encoding matrix metalloproteinases, *MMP1*, *MMP3*, *MMP9*, *MMP12*, *MMP13*, *MMP14*, and *MMP25*. This cluster also contains ENSOARG00000006889, described as plasminogen activator inhibitor 2 and orthologous with *SERPINB2* of other mammals. *SERPINB2* is amongst the most highly induced transcripts in human monocytes (Baillie et al., 2017) and mouse macrophages (Costelloe et al., 1999) responding to LPS. There appears to be a gene duplication in ruminant genomes. Two *SERPINB2* family members have been found in cattle (ENSBTAG00000023198, described as serpin family B member 2, and ENSBTAG00000023026, described as serpin family B member 2-like). The sheep gene ENSOARG00000005159, described as plasminogen activator inhibitor 2-like, another sheep ortholog of *SERPINB2* in other mammals, also appears in Cluster 5 and was strongly induced by LPS.

As noted previously (Young et al., 2018) the sheep BMDM did not show induction of *NOS2* mRNA, nor of the inducible arginine transporter *SLC7A2* at any time point. Unlike human and pig macrophages, sheep BMDM expressed GTP cyclohydrolase (*GCH1*), required for the production of the NOS2 cofactor tetrahydrobiopterin, constitutively at low levels, but it was not LPS-inducible. In common with other ruminants (Young et al., 2018), sheep macrophages expressed the gene for the mitochondrial arginase enzyme, *ARG2*, which was substantially induced by LPS. *ARG2* is usually associated with the urea cycle in the liver and kidney (Caldwell et al., 2018). Annotation of the unannotated transcripts in Cluster 4 revealed that some are likely non-coding and have no orthologs in other species. Others reflect an issue also encountered in the recent pig atlas project (Summers et al., 2019) in which different Ensembl gene IDs are assigned to partial sequences/duplicates of known genes. For example, there are three *SLC7A1* transcripts in the sheep reference transcriptome, each showing the same pattern of rapid induction by LPS. *ENSOARG00000012028* maps immediately downstream of the annotated *SLC7A1* gene. Combining the TPM counts indicates that this transporter was, in fact, quite highly inducible by LPS. SLC7A1 transports arginine and ornithine. Ornithine decarboxylase (*ODC1*) was also highly expressed and further inducible in sheep macrophages. The high expression of ornithine amino transferase (*OAT*), which leads to the production of glutamate, suggests the main function of this pathway is to use arginine and ornithine as a fuel and support the unique arginine-urea biology of ruminants (Marini et al., 2004).

In humans and pigs, LPS promotes the uptake and metabolism of another amino acid, tryptophan, and its catabolism via the coordinated induction of three enzymes, indoleamine dioxygenase (IDO1), kynurenine monooxygenase (KMO) and kynureninase (KYNU) (Kapetanovic et al., 2012, 2013; Schroder et al., 2012). Curiously, *IDO1* mRNA was barely detected and was not LPS-inducible in sheep BMDM, whereas *KYNU* and *KMO* were highly expressed and *KYNU* was further induced by LPS. Kynurenine has assumed greater interest since the recognition of its role in immune modulation as an activator of the aryl hydrocarbon receptor (AHR) (Sinclair et al., 2018). *SLC7A5*, encoding a transporter which is required for the uptake of kynurenine, was highly inducible by LPS and peaked ahead of *KYNU*. Previous studies in other cell populations in sheep indicate that induction of *IDO1* depends upon stimulation with IFNγ (Entrican et al., 2009) which might synergise with LPS.

Metabolic Regulation in Sheep Macrophages

The emerging field of immunometabolism has focused on the regulation of intermediary metabolism in recruited monocytes and macrophages in various states of activation or polarization. Amongst emerging concepts is the view that M1 polarization (classical activation) is associated with aerobic glycolysis and mitochondrial dysfunction, whereas M2 polarization requires an active TCA cycle (Ryan and O'Neill, 2020). This M1/M2 dichotomy is not well-supported by transcriptome analysis in mice and humans or in other species which instead favors a broad spectrum of activation states (Hume, 2015; Murray, 2017). CSF1 as the sole stimulus is sometimes considered an M2 agonist (Murray et al., 2014). An alternative view is that CSF1 drives a differentiated state that resembles the resident macrophages of the wall of the gut (Baillie et al., 2017). LPS on the other hand is classed as an M1 agonist but is usually considered in combination with the classical Th1 lymphokine, IFNγ (Murray et al., 2014; Murray, 2017). In any case, there is no support for the regulation of mitochondrial function in macrophages in the sheep transcriptomic data. Cluster 1 contained the large majority of mitochondria-associated transcripts (and was enriched for GO terms and pathways relating to mitochondrial function and metabolism; **Supplementary Table S6**). The mitochondria-associated transcripts were highly expressed and there was no evidence of major up or down-regulation by LPS.

In many cases metabolic pathways are regulated at the level of solute transport (Curi et al., 2017). There were 150 annotated members of the large solute carrier (SLC) family detected in the sheep BMDM, of which 71 were within Cluster 1 and mainly expressed constitutively. Macrophages in mice depend to varying degrees upon glutamine, glucose and fatty acids as fuels and glutamine is an important immune regulator (Liu et al., 2017). 14 different solute carriers from 4 families have been shown to transport glutamine (Bhutia and Ganapathy, 2016). Of

the genes encoding these carriers, *SLC38A1*, contained within Cluster 3, was highly expressed and further inducible in the sheep BMDM. *SLC7A7* was constitutively expressed and *SLC1A5* and *SLC7A5* were both highly inducible within 2 h (Cluster 4). Consistent with the importance of glutamine as a fuel, transcripts encoding enzymes and mitochondrial carriers for glutamine metabolism (*GLS*, *GLUD1*, *GLUL*, and SLC25A11) were also highly expressed by sheep BMDM. One novel feature of the sheep BMDM was the very high expression of L-asparaginase (*ASRGL1* gene), which was further up-regulated later in the LPS response. Asparaginase may also possess glutaminase activity (Chan et al., 2014) and asparagine is likely taken up by SLC1A5 (also known as ASCT2). In humans, asparagine is a non-toxic carrier of residual ammonia to be eliminated from the body and regulates the uptake and metabolism of other amino acids, serine, arginine, and histidine, and thus protein and nucleotide synthesis (Krall et al., 2016). Interestingly, the *SDS* gene, encoding serine dehydratase, was also highly inducible by LPS. In non-ruminants, this enzyme is exclusive to the liver[6] and deaminates serine to pyruvate and threonine to 2-ketobutyrate to provide substrates for gluconeogenesis.

The use of glucose as a fuel is regulated primarily at the level of glucose transport. In mice, a myeloid-specific conditional deletion of *Slc2a1* confirmed that the encoded protein GLUT1 is the major glucose transporter in macrophages but the loss of glucose as a fuel had remarkably little impact on macrophage function (Freemerman et al., 2019). In the sheep BMDM, *SLC2A1* was up-regulated by LPS, but another transporter *SLC2A3* (GLUT3) was more highly expressed and was induced further within 2 h. *SLC2A6* is a lysosome-associated glucose transporter that was recently knocked out in the mouse genome (Caruana et al., 2019). It was induced >10-fold by 2 h in response to LPS. The glycolytic activator 6-phosphofructose-2-kinase/fructose-2,6-bisphosphatase encoded by *PFKFB3* is proposed to upregulate glycolysis and link glucose metabolism to cell proliferation and survival in mouse macrophages (Jiang et al., 2016). *PFKFB3* was highly expressed in the sheep BMDM and induced further by LPS. Pyruvate kinase, muscle (*PKM*, also known as *PKM2*) and both transcripts of lactate dehydrogenase (*LDHA/LDHB*), as well as *SLC16A3* (which encodes the monocarboxylate carrier MCT4) and *SLC16A6* were further elevated later in the response (Cluster 5). The TLR-inducible expression of *SLC16A3* is shared with mice, and in that species is proposed to mediate the export of lactate from glycolysis as part of a positive feedback mechanism (Tan et al., 2015).

In the TCA cycle, citrate is initially converted to *cis*-aconitate by mitochondrial aconitase 2 (*ACO2*). In LPS-stimulated mouse macrophages, the TCA cycle is diverted through the induction of a novel enzyme, *cis*-aconitate decarboxylase 1, encoded by *ACOD1* (also known as immune responsive gene 1; *IRG1*), which catalyzes the conversion of *cis*-aconitate to *cis*-itaconate (Ryan and O'Neill, 2020). *ACO2* was robustly expressed across the sheep BMDM time course, but not specifically regulated in response to LPS. *ACOD1* was induced by 4 hrs in response to LPS in all individual sheep but level of expression remained low. In mice, the induction of *ACOD1* leads indirectly to the accumulation of the downstream TCA cycle intermediates succinate, fumarate and malate. Succinate may be an important metabolite in innate immune signaling which enhances IL1B production (Tannahill et al., 2013). Interestingly, the G-protein-coupled receptor for succinate from the TCA cycle (encoded by *SUCNR1*, also known as *GPR91*) was highly upregulated in LPS stimulated sheep BMDM, whereas it is undetectable in mouse BMDM.

Given the unique metabolism of ruminants, we considered the possibility that ketone bodies would be a preferred fuel for sheep macrophages. In mice, *Slc27a1*, encoding the fatty acid transporter FATP1 [which also contributes to functional regulation in macrophages (Johnson et al., 2016)] is highly expressed in BMDM alongside carnitine acyl transferase genes (*Crat*, *Crot*) and repressed by LPS. In sheep BMDM, *SLC27A1* and *SLC27A2* were just detectable, but *CD36*, which encodes a transporter for long chain fatty acids, was constitutively highly expressed. *SLC16A3* may also mediate uptake of the ketone body, acetoacetate, in exchange for lactate (Dimmer et al., 2000). *OXCT*, encoding succinyl CoA:3-oxoacid CoA transferase, which catalyzes the first step in ketolysis, was also expressed constitutively.

Expression of Non-coding RNA in Sheep Macrophages

Genome-wide studies in multiple species have indicated that mammalian genomes are pervasively transcribed. Aside from protein-coding genes, several novel classes of non-coding RNAs (ncRNAs) contribute to transcriptional and translational regulation. Several thousand unique microRNAs have been identified in ruminant species (Bourdon et al., 2019). These have not been captured in our pipeline unless we captured their precursors. Another class of non-coding RNAs is derived from the transcriptional activation of enhancers; these were identified in LPS-stimulated mouse macrophages (Kaikkonen et al., 2013) and were also identified in genome-scale 5′RACE (CAGE) in human monocyte-derived macrophages responding to LPS (Baillie et al., 2017). These transcripts are rapidly degraded from the 3′ end by the exosome complex and are generally detected at <10 TPM with CAGE, and much lower with total RNA-seq. The final class of transcripts of interest is the long intergenic non-coding RNA (lincRNA). These have been attributed roles in transcriptional regulation and chromatin structure [reviewed in Ransohoff et al. (2018)]). By contrast to protein-coding mRNAs, they are commonly expressed at low levels but are more tissue or cell-type restricted. We recently combined RNA-seq data from multiple ruminant species to identify a consensus set of 5,350 lincRNA (Bush et al., 2018b). Of these predicted lincRNA, >4000 were detected in sheep BMDM, but the majority of these were expressed at <1 TPM (**Supplementary Table S7**). Only 230 were expressed >10 TPM in either the stimulated or unstimulated states; these are generally annotated as 'RNA gene' in Ensembl. Of the lincRNA, 54 were up-regulated > 2-fold and 13 down-regulated > 2-fold with LPS. We did not detect any obvious co-localisation of any inducible lincRNA with inducible protein-coding transcripts. Although mature microRNA were not detected because of the mRNA isolation protocol used, one of

[6]http://biogps.org

the most inducible non-coding RNA transcripts (MSTRG.36731) overlaps the large microRNA cluster on sheep chromosome 18 (18:64641285–64642220) suggesting that these microRNA have a role in innate immune regulation.

Comparative Analysis of Macrophage Gene Expression

Previous comparative analysis of inducible gene expression in BMDM from multiple species confirmed major differences in regulated expression of genes involved in arginine metabolism (Young et al., 2018). The large majority of analysis of transcriptional regulation and gene function in macrophages has been carried out in mouse and to a lesser extent in humans. To extend the cross-species comparison, we downloaded expression data for BMDM with and without TLR4 stimulation from 8 species in addition to sheep, and requantified expression as described in Section "Materials and Methods." The genome of each species has been annotated to a different extent and, as discussed for the sheep above, in many cases likely orthologies have not yet been adopted as gene names in Ensembl.

Supplementary Table S3 contains the full list of 10,770 genes expressed in at least one species for which we were able to identify orthologs in at least 3 species. The chosen time point to analyze the LPS response across mammalian species was 7 h in the large animals and rat and 6 h in the two mouse species. This captures the peak of response in the sheep where the majority of induced genes were increased in all 6 animals, consistent also with data from the human MDM time course (Baillie et al., 2017). This choice does omit analysis of immediate early genes (e.g., some genes within Clusters 4 and 34 in the sheep time course) where the induced expression had declined to baseline by 7 h.

There are averaged data for at least 3 animals in each species dataset and the culture conditions were almost identical for all species other than mouse. However, we know from previous studies in the pig (Kapetanovic et al., 2013), mouse (Raza et al., 2014; Buscher et al., 2017), and human (Fairfax et al., 2014) and the present study in sheep that there is considerable variation in the level of transcript expression and temporal profile between individuals and strains. As a first approximation to identify conserved regulation, **Supplementary Table S3** ranks the average fold induction of each gene for each species and then summarizes the sum of ranks, the range of ranks and describes the pattern of species-specificity. A low sum of ranks provides an indication of consistency of induction across species, and the top 10 genes induced by LPS on that basis are *IL1B*, *CXCL10*, *IL6*, *CCL5*, *ISG15*, *RSAD2*, *ACOD1*, *IL1A*, *IFIT1*, and *IL27* while the highest ranked transcription factor genes are *IRF1* and *IRF7*. Even within that set of most inducible transcripts the level of expression was highly variable amongst species. Notably, *IL1B* was very lowly expressed in pig, and *CXCL10*, *CCL5*, *RSAD2*, *ACOD1*, and *IRF7* were lowly expressed in sheep and goat. We were able to identify 8,240 genes for which there was a likely ortholog in all 9 species and in which expression was >10 TPM in at least one sample. These are provided separately in **Supplementary Table S4** ranked in order of maximum level of expression in any sample.

To determine whether the transcriptional basis of macrophage differentiation and activation was conserved, the profiles of genes encoding transcription factors (TF) were analyzed separately. A total of 421 TF genes were expressed in all 9 species at >10 TPM in at least one sample (**Supplementary Table S8**). The molecular basis of gene regulation during macrophage differentiation in mouse has been reviewed extensively (Fonseca et al., 2016; Hume et al., 2016; Monticelli and Natoli, 2017; Rojo et al., 2017). Although there were minor differences in the level of expression between the species, the core TF network was well-conserved. Master regulators such as *SPI1* (encoding the lineage-specific TF PU.1) and *MAFB* were constitutively expressed in BMDM in all species. The three members of the MITF family (*TFEB*, *TFEC*, and *MITF*), all of which are expressed in mouse macrophages (Rehli et al., 1999) and bind to regulatory elements in the promoters of many lysosome-associated transcripts (Hume et al., 2010) were also expressed in all species. One core TF absent from the conserved list was *CEBPB*. Annotation for this factor is missing in sheep. A BLAST search on Ensembl using the cow gene identified *ENSOARG00000013395* as the likely ortholog in sheep and as expected it was constitutively expressed in sheep BMDM and further induced by LPS as in all 8 other species (**Supplementary Table S3**). We conclude that the transcriptional network that controls macrophage differentiation and LPS responsiveness is largely conserved across mammals. In the light of discussion above about the role of interferon in sheep BMDM, one important exception is *IRF7*. In human monocytes, quantitative variation in LPS-inducible transcripts is associated with the level of *IRF7* (Hume and Freeman, 2014). As noted above, sheep and goat BMDM expressed very low levels of *IRF7* whereas it was highly inducible in all other species.

To identify sets of transcripts that vary in parallel between species we again used Graphia. **Figure 2A** shows the sample-to-sample matrix for the complete dataset. The graph reveals that control and LPS-stimulated datasets for three of the ruminant samples (sheep, cow, and water buffalo) cluster together as do the three rodent datasets. The goat dataset clustered separately from the other ruminants for reasons that become evident below, and pig and horse were also distinct. **Figure 2B** shows the GCN and **Supplementary Table S9** the contents of each of the clusters and their average expression profiles. Profiles of the largest clusters and index genes in each are shown in **Figure 3**. The two largest clusters contain genes that on average are constitutively expressed and marginally down-regulated by LPS. Cluster 1 was enriched around twofold in the rodent macrophages. It contains the macrophage-specific growth factor receptor, *CSF1R*. Cluster 2 and Cluster 7 have a similar profile to Cluster 1 but genes within them were on average more highly expressed in the pig BMDM relative to the ruminants and horse. Genes in Cluster 3 were highly expressed only in the goat BMDM and the cluster was strongly enriched for collagens and other mesenchyme-associated transcripts. These goat BMDM cultures were generated from 6 days old animals (**Supplementary Table S1**) when the marrow hematopoietic compartment may not have been fully established with residual mesenchymal cells contributing to the RNA pool. Cluster 5 is

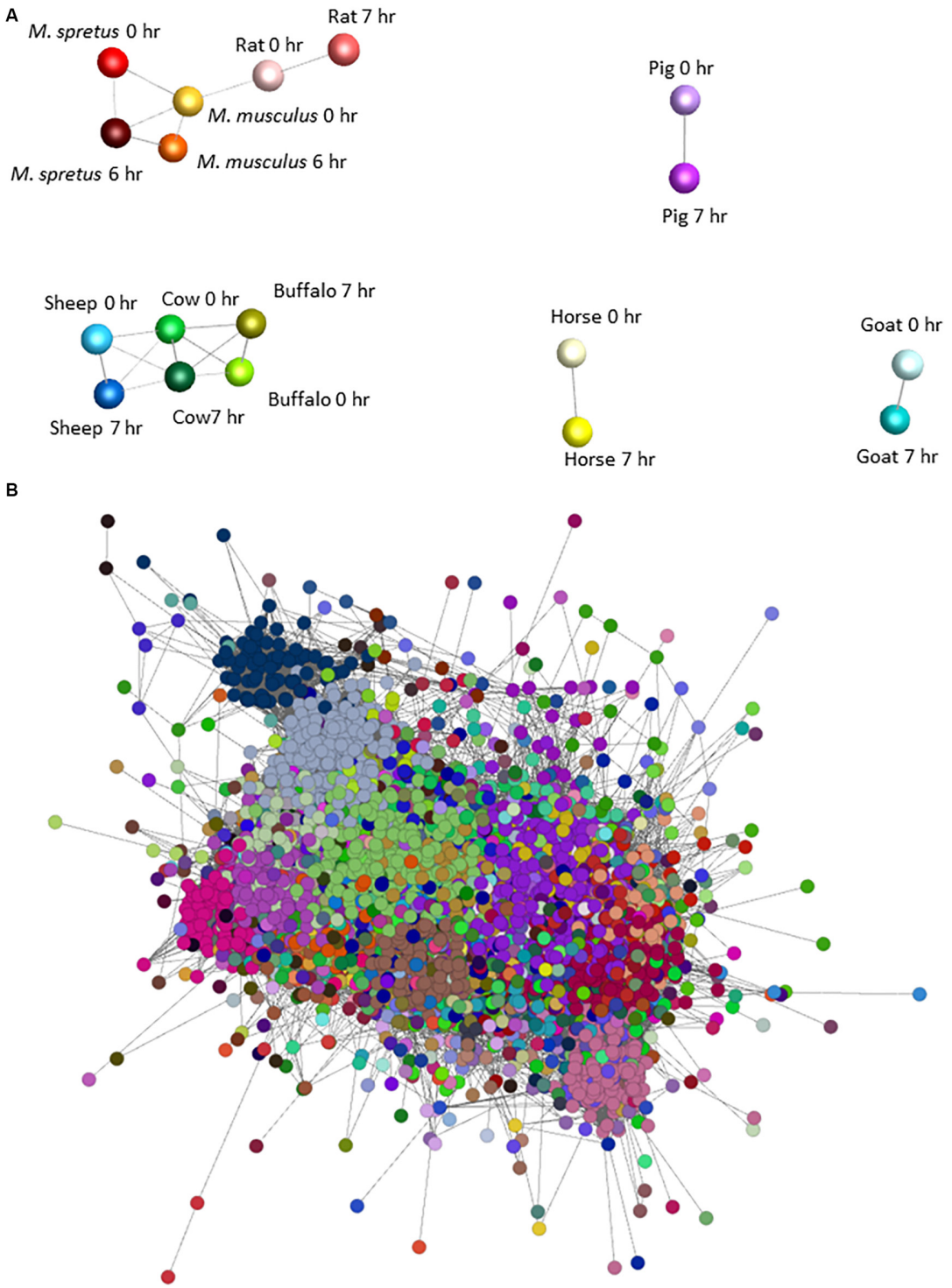

FIGURE 2 | Network analysis of BMDM from nine mammalian responding to stimulation with LPS. **(A)** Sample-to-sample 3D network of the BMDM treated with LPS. The Pearson correlation threshold was $r = 0.8$. Each node represents the BMDM from a species at 0 and 6 or 7 h post LPS exposure and the lines between them are connections above the threshold correlation coefficient. The layout demonstrates the separation of pig, goat and horse, and the close relationship among rodent samples and ruminant samples, and between the control and LPS-stimulated samples of each species. **(B)** Network graph for gene coexpression network for BMDM from each species with and without LPS stimulation. The Pearson correlation threshold was $r = 0.8$, MCL inflation value 1.7. Each node is a gene and the lines between them are connections above the threshold correlation coefficient. Nodes (genes) highlighted with the same color represent co-expression clusters determined by the MCL clustering algorithm with an inflation value of 1.7. Note that this is a 2D representation of a 3D network graph. The average expression profiles of genes within the largest clusters are shown in **Figure 3**.

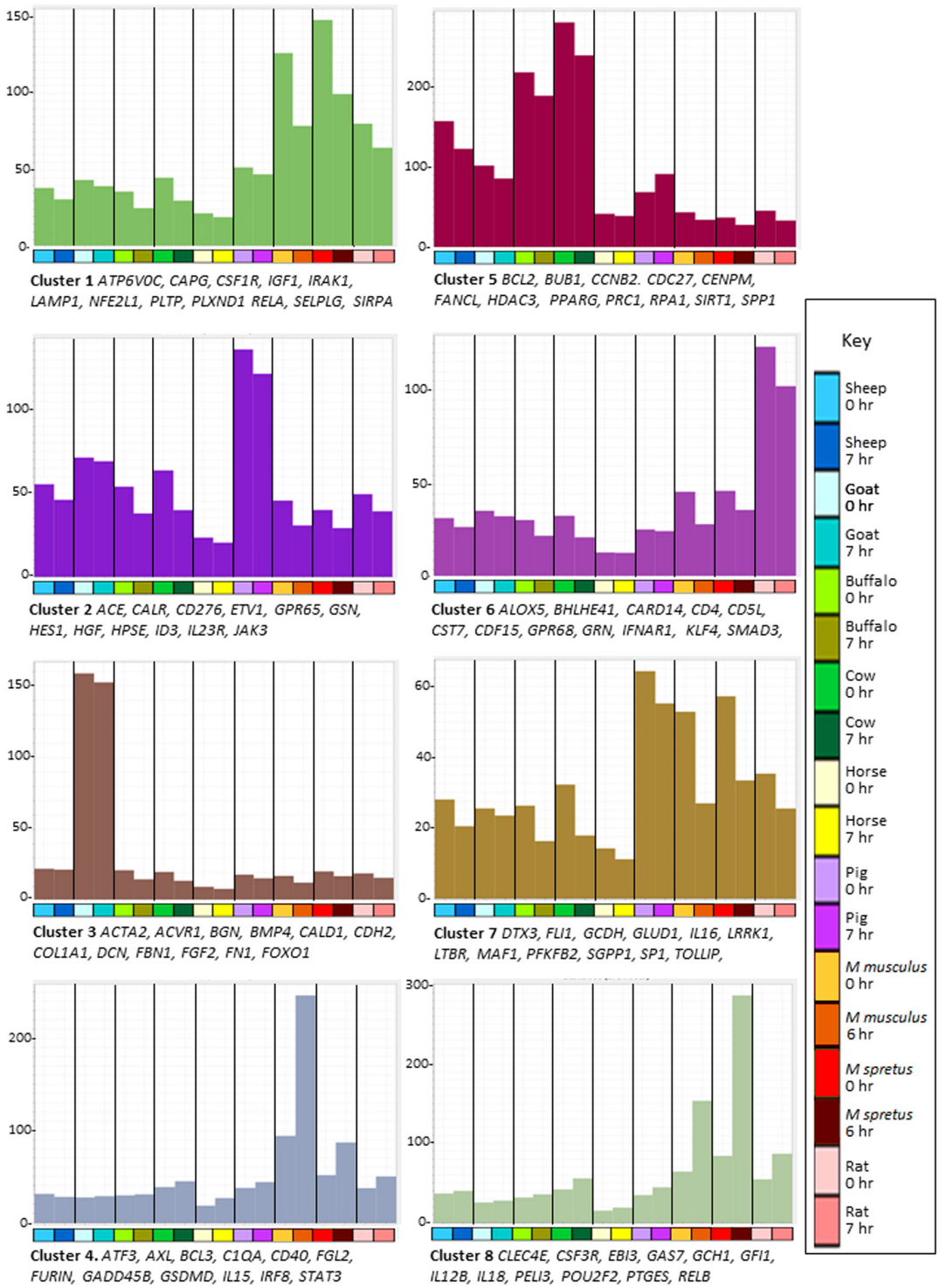

FIGURE 3 | Network analysis of BMDM from nine mammalian species responding to stimulation with LPS. Average gene expression profiles and genes of interest within the clusters of the largest eight clusters (>170 nodes) from the gene-to-gene analysis of BMDM with or without LPS shown in **Figure 2B**. Graphia network analysis performed at R ≥ 0.8, MCL inflation 1.7. *Y*-axis shows average expression of genes in each cluster (TPM) which indicates the shared pattern driving the correlated expression. For example, the basal expression of transcripts in Cluster 1 was enriched in the rodent BMDM and was down-regulated in all species by LPS. Genes named under each panel are representative of each cluster. The full set of genes in each cluster and all smaller clusters is provided in **Supplementary Table S9**. *X*-axis shows the samples. Bar indicates species: dark blue – sheep; light blue – goat; light green – buffalo; dark green – cow; yellow – horse; purple – pig; red – *Mus musculus*; dark red – *Mus spretus*; pink – rat. For each species the first column shows the average gene expression at 0 h and the second column shows the average gene expression after LPS treatment; 6 h for *M. musculus* and *M. spretus*; 7 h for all other species. Colors of the bars in the graphs are the same as those of the genes in that cluster in **Figure 2B**.

clearly enriched with genes previously annotated as cell cycle related (Giotti et al., 2019). The average expression was higher in the BMDM cultured from the four ruminant species and pigs and presumably reflects an ongoing proliferation at the time of harvest. Most transcripts in the cluster were repressed by LPS, consistent with the known growth inhibitory impacts of TLR signaling (Sester et al., 2005).

The average expression profiles of many of the smaller clusters vary between species, either in basal expression or pattern of regulation. Even within species, individual loci exhibit heritable differences in the level of expression (Fairfax et al., 2014). Species-enriched clusters such as Cluster 10 (buffalo), Cluster 11 (sheep), Cluster 12 (rat), Cluster 14 (cow), Cluster 16 (horse), and Cluster 36 (pig and horse) do not contain obvious transcriptional regulators that might act in *trans* so most species-specific variation is likely *cis*-acting. **Supplementary Table S9** shows the profiles and gene lists for these clusters.

Previous studies have indicated the substantive differences in regulated gene expression in macrophages between mice and large animals (humans and pigs) (Kapetanovic et al., 2012; Schroder et al., 2012). Clusters 4, 6, and 8 further highlight the difference between the rodent and large animal BMDM. Cluster 4 was enriched in the rodent BMDM, especially *M. musculus*, and further-induced by LPS. It includes TF genes *ATF3*, *CREB5*, *ETV6*, *FOXP1*, *IRF8*, and *STAT3*. Some transcripts within Cluster 4 (e.g., *C1QA* and *C1QB*) reflect the idiosyncrasies of the C57BL/6 mouse strain in which many transcripts are over-expressed or absent compared to other strains (Raza et al., 2014). Transcripts within Cluster 6 were highest in rat BMDM, again including multiple transcriptional regulators: *BHLHE41*, *CREB3*, *CUX1*, *ESRRA*, *ETV3*, *KLF4*, *NFATC1*, and *SMAD3*. Transcripts within Cluster 8 were also, on average, more highly expressed in rodents, and highly inducible by LPS. This cluster contains the rodent-specific macrophage marker *ADGRE1* (F4/80) and includes several lineage-enriched TF genes such as *AKNA*, *GFI1*, *KLF3*, *LMO4, NR1H3* and *SPI1*.

Several smaller clusters contain the transcripts that on average were induced by LPS in all species but with differences in relative activation. Clusters 37 and 39 contain most of the highest-ranked inducible transcripts in **Supplementary Table S3**, including *IL1A* and *IL1B*. Cluster 9 contains transcripts induced in all species but most highly in bovids (cow and water buffalo), including *BATF3*, *JUN*, *HIF1A*, *MITF*, *NFE2L3*, *NFIL3*, *PRDM1*, *STAT1* and transcripts encoding inflammatory effectors *CSF3* and *PTX3*. Transcripts in Clusters 19 (containing *IRF1*, *NR3C1*, and *REL*) and 38 (containing *IRF7*) were induced in all species but considerably less so in sheep and goats. This suggests that the comparatively low LPS-induced expression of a subset of interferon target genes discussed above is related to low expression of the key TFs IRF1 and IRF7. Similar variation in IRF gene family expression between individual humans (Hume and Freeman, 2014) and chickens (Freem et al., 2019) has also been associated with co-regulated expression of IRF target genes. The reciprocal Cluster 25 contains transcripts induced specifically in sheep and goat BMDM. It does not include obvious *trans*-acting factors, suggesting that these differences are locus-specific.

DISCUSSION

Feedback Regulation of the LPS Response in the Sheep

The analysis of the response of sheep BMDM to LPS confirms a pattern that was evident from a more extensive analysis of the response of human MDM to LPS (Baillie et al., 2017). The LPS response is a temporal cascade in which each peak of regulated gene expression includes both feed-forward activators and feedback inhibitors. The sheep BMDM response to LPS shares with the human macrophage response the rapid induction of numerous immediate early transcription factors. Amongst the most-inducible was the atypical NF-κB inhibitor protein gene, *NFKBIZ*, the product of which (IκBζ) interacts with Akirin2 to *trans*-activate inflammatory cytokine genes such as *IL6* and *IL12B* (Tartey et al., 2014). The canonical MyD88-independent TRIF/TRAM (TICAM1/2)-dependent pathway of IFN regulation determined from studies of mice involves the interactions of TRAF3 and the kinase TBK1 to phosphorylate IRF3, but this pathway is not conserved in humans (Schroder et al., 2012). In the sheep BMDM also, *IRF3*, *TBK1*, and *TRAF3* were expressed at very low levels and the most inducible member of the IRF family was *IRF1*. *TICAM1* was amongst the early LPS-responsive genes and in common with human, LPS induced *TRAF1*.The other feature shared with human macrophages was the rapid induction of genes encoding repressors of the TLR4 signal at multiple levels, including *BCL3*, *CISH*, *DUSP1/2/5/6*, *GADD45B*, *IL10*, *NFKB1/2*, *NFKBIA/B/D/E*, *PPP1R15A*, *SOCS1/3*, *TNFAIP3/6*, *TRIM25*, *ZFP36*, and *ZC3H12A*. Each of these inducible feedback regulators is shared with LPS-stimulated human MDM (Baillie et al., 2017). On the other hand, many of the negative regulators of TLR4 signaling identified in mice and discussed by Kondo et al. (2012) [e.g., *AHR*, *ATF3*, *ATG16L1*, *KLF3*, *MSK1/2*, *PDLIM2*, *PIN1*, *RPS6K* family (also known as MSP1/2)] were expressed constitutively in sheep BMDM as in human MDM (Baillie et al., 2017) and were not further-regulated by LPS. As discussed previously, the surprising feature of the feedback regulation of the LPS response is the apparent lack of redundancy, in that mutation or deletion of any of these regulators can lead to excessive TLR signals and inflammatory pathology in humans and model organisms (Wells et al., 2005).

Conserved Transcription Regulation in Macrophages

A comparative analysis of gene expression in the liver of 25 mammalian species concluded that the transcriptional profile and spectrum of lineage-specific TFs is largely conserved (Berthelot et al., 2018) despite the gain and loss of individual regulatory elements. We hypothesized that cells of the innate immune system could display greater diversity between species than hepatocytes as a consequence of the evolutionary pressure of pathogen selection which would differ between species.

Analysis of the response of mouse, human and pig macrophages to LPS (Schroder et al., 2012) and to glucocorticoids (GC) (Jubb et al., 2016) revealed the extensive gain and loss of *cis*-acting regulatory elements between the species that accounts for differences in inducible gene expression. This was especially obvious in the case of GC, where transcriptional activation derives from a single regulatory motif, unlike LPS-inducible gene expression which samples a smorgasbord of inducible TFs. The comparative analysis of the mammalian macrophage transcriptome presented here supports the evolutionary conservation of the overlying transcriptional network that drives macrophage biology. The set of constitutive and LPS-inducible TF transcripts was largely conserved across the 9 species we examined, and consistent with previous analysis of human MDM (Baillie et al., 2017).

As expected, amongst the most abundant transcripts shared by all macrophages are those encoding components of the endosome/lysosome pathway (e.g., *CD68*, *GPNMB*, *LAMP1*, and *NPC2*) and lysosomal hydrolases (*CTSB*, *CTSD*, *LGMN*, and *LIPA*). The largest divergence between the species separated the rodents from all the large animals and includes transcripts in Clusters 4, 6, and 8 (**Figure 3**). These differences need to be interpreted with some caution, because the clusters include multiple lineage-specific transcription factors such as *CEBPB*, *IRF8*, *NR1H3*, and *SPI1* that appear somewhat over-expressed in rodents, especially in the mouse samples. Unlike all of the other samples (which were generated by our group), the mouse BMDM were grown in L929 conditioned medium (as a source of CSF1) rather than recombinant CSF1, and in DMEM/high glucose with 20% fetal bovine serum (FBS) (Link et al., 2018) rather than RPMI 1640/10% FCS which is optimal for mouse BMDM proliferation (Hume and Gordon, 1983). One possibility we cannot eliminate is that the mouse BMDM are simply more fully differentiated as a result of the different culture conditions. Equally, there may be mouse-specific differences in CSF1 responsiveness, associated with the unique lack of autocrine *Csf1* expression by mouse BMDM (see above) which is also evident in independent datasets from our group.[6] The reciprocal immature phenotype is reflected in the cluster of cell cycle-associated transcripts which remain more highly expressed in the macrophages cultured from the large animals (Cluster 5, **Figure 3**).

Divergent Metabolic Regulation Amongst Mammalian Species

The shared high expression of genes involved in glutamine metabolism (*GLS*, *GLUL*, *GLUD1*, and *SLC25A11*) in BMDM from all species suggests that the use of this amino acid as a fuel by macrophages, demonstrated previously in mouse and human (Curi et al., 2017), is conserved amongst mammalian species. *SLC1A5*, which encodes a plasma membrane glutamine transporter, was also highly expressed in all the macrophage populations, especially ruminants (sheep and cow) where it was further induced by LPS. A variant isoform of SLC1A5 was shown recently to be involved in mitochondrial glutamine uptake in human tumor cells (Yoo et al., 2020).

Other metabolic pathways appeared more divergent. Our previous study documented the major differences in arginine metabolism and production of nitric oxide by these species and the underlying transcriptional basis for the difference (Young et al., 2018). Cluster 12 was most highly induced in the rodent BMDM and included *NOS2*, *ARG1* (encoding arginase 1), the gene for the inducible arginine transporter, SLC7A2, required for nitric oxide production in mouse macrophages (Kakuda et al., 1999) and arginosuccinate synthase (*ASS1*) which recycles citrulline to regenerate arginine (Qualls et al., 2012). As with *NOS2*, most of the genes in this cluster were also induced to a lesser extent in all the bovid BMDM in response to LPS and a temporal difference in the kinetics of induction cannot be eliminated. Interestingly, although *ACOD1* did not form part of Cluster 12, the level of induction by LPS was >10-fold lower in those species (goat, horse, pig, and sheep) in which *NOS2* induction was minimal. The induction of *ACOD1* may actually be a direct response to mitochondrial toxicity of NO (Jamal Uddin et al., 2016). The product of *ACOD1*, itaconate, induces *HMOX1* (Mills et al., 2018) which was also most inducible by LPS in the rat BMDM.

Notwithstanding the differential regulation of *IDO1* in sheep and goats, other genes involved in tryptophan metabolism (*KYNU*, *KMO*) were expressed and LPS-responsive only in BMDM from large animals, as shown previously in humans and pigs (Schroder et al., 2012). Accordingly, application of IDO1 inhibitors as therapeutic agents based upon rodent disease models (Prendergast et al., 2017) needs to be considered with caution. Kynurenine is an immune modulator, and studies in mouse T cells identified SLC7A5 as a transporter facilitating the uptake of this metabolite (Sinclair et al., 2018). In common with human macrophages where kynurenine has been attributed an anti-inflammatory role (Rotoli et al., 2018) an alternative kynurenine transporter, *SLC7A7* was constitutively expressed in BMDM from all the large animals. The macrophages from all species expressed high levels of the *SLC7A7* dimerization partner, *SLC3A2*, which forms the large/neutral amino acid transporter (y^+ LAT1) complex.

We speculated *a priori* that ruminant macrophages might be adapted to use fatty acids or ketone bodies as fuels because of the high levels of these metabolites produced by ruminant fermentation. This profile might potentially be shared with horses, which produce volatile fatty acids from hind gut fermentation. There was no evidence to support this hypothesis. Any such adaptation may be obscured by use of a common cell culture medium containing high glucose and relatively high oxygen. BMDM from the four ruminant species did share regulated high expression of other metabolism-associated transcripts noted from analysis of the sheep BMDM time course, including *ARG2*, *ASRGL1*, *LDHB*, *SDS*, and *SUCNR1*. The LPS-inducible expression of serine dehydratase (SDS) that was unique to the ruminants may also contribute pyruvate to support oxidative metabolism. Unlike rodents, BMDM from all of the large animals shared expression of *SLC2A3* (encoding GLUT3) although the level of expression and response to LPS differed. In humans, *SLC2A3* was expressed in blood monocytes and down-regulated during their maturation to

the CD16^{++} subset alongside increased oxidative metabolism (Schmidl et al., 2014). This pattern was recently confirmed in bovine monocytes (Eger et al., 2016). GLUT3 was first identified as a neuron-specific glucose transporter but subsequent studies revealed expression by human leukocytes and inducible translocation to the plasma membrane in response to stimulation [reviewed in Eger et al. (2016)]. GLUT3 has both the lowest K_m and the highest V_{max} of any of the glucose carriers, but it is unclear why this would be important for large animals compared to rodents. BMDM from all the species except horse also expressed the leukocyte-enriched hexokinase gene, *HK3*.

Species Specific Immune-Related Genes

The merged data in **Supplementary Tables S3, S4** and the cluster analysis of those (**Supplementary Table S9**) provide a resource to identify macrophage-expressed and LPS-inducible genes that are shared across all mammalian species. Other gene-specific differences amongst species may aid especially in the interpretation of studies using rodents as models to understand gene function. **Table 1** provides examples of transcripts for which there is some evidence of innate immune function in rodents, and which were up-regulated in all the mammalian macrophages. They include many additional examples of inducible feedback regulators highlighted in analysis of the sheep time course. In **Table 2**, we identify examples of transcripts that were expressed and/or regulated in macrophages and clearly highly divergent between rodents and large animals. Some families of genes are discussed in more detail below.

One gene and potential function that is clearly divergent between rodents and large animals is *APOBEC1* which is involved in RNA editing of cytosine to uracil (Harjanto et al., 2016). This transcript was expressed constitutively only in mouse BMDM. In human MDM, *APOBEC1* was not expressed but *APOBEC3A* was highly LPS-inducible (Baillie et al., 2017) and has been shown to mediate RNA editing in human monocytes and macrophages (Sharma et al., 2015). The APOBECs are a multigene family and cross-species orthologies are difficult to establish. The putative *APOBEC3A* gene in sheep (annotated as *APOBEC3Z1*) was highly induced in only 3 of the sheep BMDM analyzed. The highly LPS-inducible cytidine deaminase (*CDA*) gene might fulfill this function in ruminant macrophages.

The set of around 2,500 genes for which we detected expression but could not identify orthologs in all species includes genuine copy number variants (some of which are discussed below) and inconsistent gene names that require manual curation. There is a subset annotated only in the large animals or in rodents (e.g., the zinc finger proteins) where ortholog relationships are ambiguous. The Fc receptor family (FCGR), which are clearly important for macrophage effector functions (Bruhns and Jonsson, 2015) have copy number variants that are functionally important in humans,

TABLE 1 | Summary of novel genes induced by LPS in all mammalian BMDM.

Gene symbol	Gene name/description	Gene function	References
ALCAM	Activated leukocyte adhesion molecule	Regulator of cell trafficking, interacts with CD6	Zimmerman et al., 2006; Renard et al., 2020
ADAR	Adenosine deaminase, RNA-specific	A to I editing of mRNA.	Baal et al., 2019
CASP7	Caspase 7	Regulator of NF-κB-dependent transcription	Erener et al., 2012
CD274	Programmed cell death ligand 1	Regulation of T cell tolerance	Yamazaki et al., 2002
CFLAR	CASP8 and FADD-like apoptosis regulator (aka c-FLIP)	Regulator of inflammasome	Van Opdenbosch et al., 2017; Muendlein et al., 2020
DTX3L	Deltex E3 ubiquitin ligase	Forms complex with PARP9, regulates IFN response	Zhang et al., 2015
EPSTI1	Epithelial stromal interaction 1	Unknown function. Negative regulator of macrophage activation	Kim et al., 2018
IL27/EBI3	Interleukin 27	IL12-related. Heterodimeric cytokine, feedback regulator of IFN response	Bosmann and Ward, 2013; Aparicio-Siegmund and Garbers, 2015
PDE4B	Phosphodiesterase 4B	Feedback regulator of LPS response	Jin et al., 2005
PML	Promyelocytic leukemia	Regulator of apoptosis Required for LPS response	Lunardi et al., 2011
PNPT1	Polyribonucleotide nucleotidyltransferase 1	3′–5′ exonuclease associated with mitochondria	Sarkar and Fisher, 2006; Wang et al., 2010
RNF114	Ring-type zinc finger 114	Negative regulator of NF-κB. Interacts with TNFAIP3	Rodriguez et al., 2014
RNF19B	Ring-type zinc finger 19B (aka NKLAM)	E3 ubiquitin ligase, associated with phagosomes	Lawrence and Kornbluth, 2012; Lawrence et al., 2019
SDC4	Syndecan 4	Transmembrane heparan sulfate proteoglycan, regulator of LPS response *in vivo*	Ishiguro et al., 2001
TDRD7	Tudor domain containing 7	Inhibitor of AMPK and autophagy	Subramanian et al., 2018
TRIM21	Tripartite motif 21	E3 ubiquitin ligase, Inhibitor of IRF transcription factors	Labzin et al., 2019; Sjostrand et al., 2020
TRIM 23	Tripartite motif 23	E3 ubiquitin ligase, regulator of autophagy	Sparrer et al., 2017

Genes chosen were induced in all species and selected based upon limited related literature. References are primarily to studies in mice and provide evidence for a function in the response to LPS in vitro or in vivo.

TABLE 2 | Genes that show divergent regulation between large animals and rodents.

Gene symbol	Gene description	Gene function/regulation	Specificity	References
ADGRE1	Adhesion G protein- coupled receptor E1	F4/80 in mouse. Highly divergent expression, structure, sequence and function amongst species	Rodent	Waddell et al., 2018
CD163	Haptoglobin receptor	High in all large animals, absent from rodent BMDM. Regarded as M2 polarization marker.	Large animals	Vogel et al., 2014
CLEC4E	C type lectin 4E	Macrophage-induced C type lectin (Mincle). Role in fungal resistance induction by LPS is rodent-specific. Clec4 family expanded in rodents.	Rodent	Wells et al., 2008
C1QA, C1QB, C1QC	Complement 1Q	Very high expression in *Mus musculus* BMDM, known C57BL/6 strain-dependent	C57BL/6 *Mus musculus*	Raza et al., 2014
CPM	Carboxypeptidase M	Phosphoinositol-linked ectopeptidase. Marker of human MDM maturation from monocytes. Not expressed in rodent BMDM.	Not in rodents	Rehli et al., 2000
CTSK	Cathepsin K	Key gene in bone resorption, very high in all BMDM except *Mus musculus* (C57BL/6)	Not in *Mus musculus*	Drake et al., 2017
ENPP1	Ectonucleotide pyrophosphatase/ phosphodiesterase 1	Not expressed in rodent BMDM. Involved in regulation of calcification and signaling	Not in rodents	Roberts et al., 2019
MARCO	Macrophage receptor collagenous structure	Scavenger receptor. Mouse-specific, induced by LPS.	Mouse	Jing et al., 2013
MMP9	Matrix metalloproteinase 9	Inducible matrix degrading enzyme. Constitutive in all BMDM except mouse.	Not in mouse	Min et al., 2002
POU2F2	Oct-2 transcription factor	Expressed and induced by LPS only in rodent. Implicated in NOS2 regulation	Rodent	Lu et al., 2009
PTX3	Pentraxin 3	Humoral pattern recognition molecule. Many roles in inflammation. Not inducible in rodents.	Not inducible in rodents	Garlanda et al., 2018
SCIN	Scinderin (adseverin)	Gelsolin-related actin binding protein, implicated in osteoclast fusion in mice. High in all BMDM except rodents	Not in rodents	Wang et al., 2018
TNFAIP6	TNF alpha induced protein 6 (aka TSG6)	Secreted cytokine with IL4-like activity. Implicated in anti-inflammatory activity. Not induced by LPS in rodent BMDM	Not inducible in rodents	Mittal et al., 2016; Nepal et al., 2019
VSIG4	V set and immunoglobulin domain containing 4	Complement receptor (CRIg). Tissue resident macrophage marker. Low expressed in mouse BMDM	Low in mouse	Irvine et al., 2016

Genes shown are expressed or regulated only in rodents or large animals. References are to functional studies of the gene product or reviews where available.

with consequent confusion in orthology relationship with other species. There are many other genes currently annotated only as open-reading frames (Orf) in humans. The merged data confirms expression of these transcripts in macrophages of large animals. The large majority of these transcripts show no evidence of regulation in any species, likely reflecting the long-term focus of annotation efforts in all species on regulated genes. One exception is *C15orf48*, which was induced by LPS in all the large animal species and was also induced by LPS in human MDM (Baillie et al., 2017). Although the 83 amino acid Orf is conserved across species, this is also the host gene for miR-147, a microRNA induced by LPS in mouse macrophages and implicated in feedback regulation (Liu et al., 2009). *CXorf21*, expressed and further inducible by LPS in all the large animals, as in humans (Baillie et al., 2017), contains risk alleles for systemic lupus erythematosus and Sjögren's syndrome (Harris et al., 2019; Odhams et al., 2019). Although not in the pseudoautosomal region, the gene escapes X inactivation and is proposed to underly increased female autoimmune disease prevalence in humans. The protein product may regulate lysosome acidification (Harris et al., 2019). Another gene lacking functional annotation is *C9orf72*, the major locus implicated in human amyotrophic lateral sclerosis. This gene was highly expressed in human MDM (Baillie et al., 2017) and a mouse knockout led to macrophage dysfunction and neuroinflammation (O'Rourke et al., 2016). *C9orf72* was expressed in BMDM from all the species.

In view of the central role of CSF1 in macrophage homeostasis, the gene encoding this growth factor is of particular interest. Mouse BMDM express a very low level of *Csf1* mRNA and depend upon exogenous CSF1 for survival (Hume and Gordon, 1983). In humans, *CSF1* mRNA is undetectable in monocytes but rapidly induced *in vitro* as they differentiate to macrophages (Baillie et al., 2017). In mouse BMDM cultured by our group and analyzed using arrays,[6] *Csf1* mRNA was undetectable in untreated cells, but induced at 7 h by LPS. In the RNA-seq data from another group analyzed here, the result is similar. By contrast, in all other species *CSF1* mRNA was expressed constitutively in BMDM. In our experience, by contrast to mouse, BMDM and MDM produced from other species including rat do not depend upon exogenous CSF1 for survival. This difference may be important in the interpretation of rodent models of the impact of human *CSF1R* mutations (Hume et al., 2020). BMDM from the different species differ also in their expression of other myeloid growth factors and receptors. *CSF2* (granulocyte macrophage CSF) was undetected in mouse but highly LPS-inducible in the ruminant and rat BMDM. *CSF3* was also LPS-inducible, especially in cow and rat BMDM. All the BMDM expressed the CSF2 receptor gene (*CSF2RA*) but only mouse BMDM expressed high levels of *CSF3R*.

One of the hallmarks of inflammation is the rapid recruitment of neutrophils in response to inducible chemoattractants. Some chemokine genes were expressed constitutively by BMDM, whilst others are major LPS target genes. Neutrophil recruitment in humans is mediated mainly by the CXC family of chemokines acting on neutrophil receptors CXCR1 and CXCR2 (Petri and Sanz, 2018). The most abundant neutrophil chemoattractant *CXCL8* (IL8) has no ortholog in rodents. The annotated *CXCL* chemokine genes detected in BMDM were either expressed constitutively, induced or repressed by LPS in individual species. In rodents in particular, neutrophil chemotaxis may also be mediated by the CC chemokine family acting through CCR1 (Petri and Sanz, 2018). The BMDM from large animals and rats shared high constitutive expression of *CCR1*. Orthology relationships amongst the CC chemokines were also ambiguous and most were not assigned in all species. Individual CC chemokine transcripts (*CCL1-CCL9*, *CCL11*, *CCL12*, *CCL14*, and *CCL17*) were expressed constitutively, induced or repressed in an idiosyncratic manner. The chemokine gene *CCL20*, which was not expressed in rodents but induced by LPS in humans and pigs (Schroder et al., 2012) was also expressed in all the ruminant BMDM. The small ruminants (sheep and goats) showed the unique LPS induction of another chemokine gene (*CCL24*) but in keeping with the apparent low interferon response expressed low levels of *CXCL10* (also known as interferon inducible peptide 10kD, or IP10). Chemokine receptors have been favored targets for anti-inflammatory drugs since their first discovery, and the relative failure of efforts to target them has been attributed to the fact that both ligands and receptors are promiscuous in their binding activity. A recent review summarizes evidence for non-redundant functions of multiple ligands binding to a shared receptor and vice versa (Dyer, 2020). However, chemokine redundancy would also provide an explanation for rapid evolutionary functional divergence, and it may be that each animal species has its own unique solution to the recruitment of inflammatory cells.

Members of the S100 family of cytoplasmic calcium binding proteins have many proposed functions as intracellular regulators and secreted mediators in macrophages (Xia et al., 2017). *S100A4*, *S100A10*, and *S100A11* were expressed constitutively in BMDM from all species. Ruminant BMDM share with pig BMDM constitutive high expression of *S100A8* and *S100A9* (which form a functional heterotetramer known as calprotectin). *S100A1* was restricted to mouse BMDM whereas *S100A12*, a likely duplication of *S100A8* that is absent from rodent genomes, was also highly expressed and induced further by LPS in BMDM from all the large animals (**Supplementary Table S3**) as it was in human MDM (Baillie et al., 2017). *S100A6* was expressed by rodents, pigs and horses, but absent from ruminant BMDM. Conversely, the ruminant BMDM were unique in expressing *S100B*. It is not clear whether any of these closely related S100 family members has a unique species-specific function or there is simply functional redundancy.

Where orthology relationships were unambiguous there are genes identified in the GCN analysis that appear extremely divergent amongst species. The most highly expressed transcript in all 4 ruminants, *SPP1* (encoding osteopontin, also known as secreted phosphoprotein 1), was expressed constitutively at a level around 10-fold higher than in rodents. The sheep (Clark et al., 2017) and pig (Summers et al., 2019) atlases reveal that *SPP1* is massively enriched in macrophages relative to all tissues and other cells, where this is not the case in mouse.[6] *SPP1* is also amongst the most inducible transcripts in human MDM relative to blood monocytes (Baillie et al., 2017). There is a substantial literature on the many roles of osteopontin in innate immune regulation and mineral homeostasis, and genetic association with human disease susceptibility (Icer and Gezmen-Karadag, 2018). The numerous studies based upon the *Spp1* knockout mouse (Liaw et al., 1998) may not reveal the non-redundant functions of this gene in humans or large animals.

Manual curation reveals some examples where consistent expression is hidden by ambiguous annotation (e.g., *CD63*, annotated as the synonym *ITGA7* in the horse, is highly expressed in all species) and some examples (e.g., the absence of *CTSL* and *ATP6V0C* in both cattle and buffalo BMDM) where the lack of expression appears genuine. *CD163*, considered an M2 macrophage marker in mice (Murray et al., 2014) was expressed by BMDM from all the large animals but barely detected in mouse and rat. Horse BMDM showed uniquely high expression of *HSD11B1*, *IL5RA* and *TGFB3*. The inflammasome activator and cytoplasmic DNA sensor AIM2, known to be absent in pig and a pseudogene (low-expressed) in ruminants (Cridland et al., 2012) was LPS-inducible in horse BMDM. Genes within Cluster 14 that showed highest expression in the cow BMDM but were also highly expressed in other ruminants and pigs, include *ITGB3*, *MMP19*, *SLC31A2* (a copper transporter) and *VSIG4*. Genes within Cluster 10 that were most restricted to the buffalo include *CD34*, *CD247*, *CXCL2*, *IGF2*, *LDAH*, *LRR1*, *N2RF6*, *OSCAR*, and the zinc transporter *SLC39A2*. These transcripts could be associated with the adaptation of this species to tropical environments and high pathogen load.

CONCLUSION

We have presented a network analysis of the response of BMDM from individual sheep to LPS providing strong evidence of a conserved feedback regulatory framework in mammalian macrophages. We then extended the analysis to compare the response across mammalian species. On balance, although **Table 2** and the discussion highlight a number of clearly orthologous genes that show absolute expression differences among species, the number is small compared to the shared transcriptome and actually highlights the overall consistency of mammalian macrophage gene expression. We conclude that the vast majority of transcripts expressed constitutively or regulated by LPS in BMDM are detected in all species and most differences are quantitative rather than qualitative. In the analysis of multiple species we have used averaged data from outbred animals for every species other than *M. musculus* and rat. Based upon analysis of individuals in human, pig, and inbred mouse strains noted

above, and the analysis of six crossbred sheep presented here (**Figure 1**), it is likely that there is also substantial qualitative and quantitative variation within each species. Such variation may ensure that populations display a variety of responses to the diversity of pathogen challenges, an evolutionarily advantageous strategy. On the other hand, the combined dataset provides a resource for the prioritization of candidate genes within loci associated with heritable differences in disease susceptibility in humans and livestock animals.

DATA AVAILABILITY STATEMENT

The datasets presented in this study can be found in online repositories. The names of the repositories and accession numbers can be found in **Supplementary Table S1**.

ETHICS STATEMENT

All of the data analyzed herein were downloaded from publicly available datasets, generated independently in studies performed under appropriate Animal Ethics approvals, as detailed in the source publications.

AUTHOR CONTRIBUTIONS

SB, DH, and KS conceived the study, performed bioinformatic analysis, and wrote the manuscript. MM generated data for the sheep and performed bioinformatic analysis. EC and JP contributed to data generation and analysis and project supervision. ZL, CM, RY, and CP generated and contributed primary data for horse (ZL), goat and pig (CM), buffalo (RY), and rat (CP), respectively. All authors contributed to manuscript editing.

FUNDING

This work was supported in part by Biotechnology and Biological Sciences Research Council (BBSRC; https://bbsrc.ukri.org/) grants BB/L001209/1 ('Functional Annotation of the Sheep Genome') and BB/L004623/1 ('Transcriptome Analysis in Indian Buffalo and the Genetics of Innate Immunity') and Institute Strategic Program grants 'Farm Animal Genomics' (BBS/E/D/2021550), 'Blueprints for Healthy Animals' (BB/P013732/1), and 'Transcriptomes, Networks and Systems' (BBS/E/D/20211552). Edinburgh Genomics was partly supported through core grants from the BBSRC (BB/J004243/1), National Environment Research Council (NERC; https://nerc.ukri.org/) (R8/H10/56), and Medical Research Council (MRC; https://mrc.ukri.org/) (MR/K001744/1). MM received funding from the Royal (Dick) School of Veterinary Studies, University of Edinburgh. CM received Ph.D. scholarship support from the Newton Fund. ZL received a Ph.D. studentship from the Horserace Betting Levy Board. SB was supported by the Roslin Foundation. The Mater Research Institute-University of Queensland is grateful for funding from the Mater Foundation, Brisbane, Australia. The Translational Research Institute receives funding from the Australian Government.

SUPPLEMENTARY MATERIAL

The Supplementary Material for this article can be found online at: https://www.frontiersin.org/articles/10.3389/fcell.2020.00661/full#supplementary-material

FIGURE S1 | Graph size vs. correlation threshold for sheep BMDM treated with LPS. The correlation threshold chosen was 0.75, which included 9,304 nodes making 2,569,091 edges.

FIGURE S2 | Graph size vs. correlation threshold for nine species BMDM treated with LPS. The correlation threshold chosen was 0.8 (broken line), which included 8,129 nodes making 575,702 edges.

REFERENCES

Aparicio-Siegmund, S., and Garbers, C. (2015). The biology of interleukin-27 reveals unique pro- and anti-inflammatory functions in immunity. *Cytokine Growth. Factor. Rev.* 26, 579–586. doi: 10.1016/j.cytogfr.2015.07.008

Baal, N., Cunningham, S., Obermann, H. L., Thomas, J., Lippitsch, A., Dietert, K., et al. (2019). ADAR1 is required for dendritic cell subset homeostasis and alveolar macrophage function. *J. Immunol.* 202, 1099–1111. doi: 10.4049/jimmunol.1800269

Baillie, J. K., Arner, E., Daub, C., De Hoon, M., Itoh, M., Kawaji, H., et al. (2017). Analysis of the human monocyte-derived macrophage transcriptome and response to lipopolysaccharide provides new insights into genetic aetiology of inflammatory bowel disease. *PLoS Genet.* 13:e1006641. doi: 10.1371/journal.pgen.1006641

Berthelot, C., Villar, D., Horvath, J. E., Odom, D. T., and Flicek, P. (2018). Complexity and conservation of regulatory landscapes underlie evolutionary resilience of mammalian gene expression. *Nat. Ecol. Evol.* 2, 152–163. doi: 10.1038/s41559-017-0377-2

Bhutia, Y. D., and Ganapathy, V. (2016). Glutamine transporters in mammalian cells and their functions in physiology and cancer. *Biochim. Biophys. Acta* 1863, 2531–2539. doi: 10.1016/j.bbamcr.2015.12.017

Bosmann, M., and Ward, P. A. (2013). Modulation of inflammation by interleukin-27. *J. Leukoc. Biol.* 94, 1159–1165. doi: 10.1189/jlb.0213107

Bourdon, C., Bardou, P., Aujean, E., Le Guillou, S., Tosser-Klopp, G., and Le Provost, F. (2019). RumimiR: a detailed microRNA database focused on ruminant species. *Database* 2019:baz099. doi: 10.1093/database/baz099

Bray, N. L., Pimentel, H., Melsted, P., and Pachter, L. (2016). Near-optimal probabilistic RNA-seq quantification. *Nat. Biotechnol.* 34, 525–527. doi: 10.1038/nbt.3519

Brubaker, S. W., Bonham, K. S., Zanoni, I., and Kagan, J. C. (2015). Innate immune pattern recognition: a cell biological perspective. *Annu. Rev. Immunol.* 33, 257–290. doi: 10.1146/annurev-immunol-032414-112240

Bruhns, P., and Jonsson, F. (2015). Mouse and human FcR effector functions. *Immunol. Rev.* 268, 25–51. doi: 10.1111/imr.12350

Buscher, K., Ehinger, E., Gupta, P., Pramod, A. B., Wolf, D., Tweet, G., et al. (2017). Natural variation of macrophage activation as disease-relevant phenotype predictive of inflammation and cancer survival. *Nat. Commun.* 8:16041.

Bush, S. J., Freem, L., MacCallum, A. J., O'Dell, J., Wu, C., Afrasiabi, C., et al. (2018a). Combination of novel and public RNA-seq datasets to generate an mRNA expression atlas for the domestic chicken. *BMC Genomics* 19:594. doi: 10.1186/s12864-018-4972-7

Bush, S. J., Muriuki, C., McCulloch, M. E. B., Farquhar, I. L., Clark, E. L., and Hume, D. A. (2018b). Cross-species inference of long non-coding RNAs greatly expands the ruminant transcriptome. *Genet. Sel. Evol.* 50:20.

Caldwell, R. W., Rodriguez, P. C., Toque, H. A., Narayanan, S. P., and Caldwell, R. B. (2018). Arginase: a multifaceted enzyme important in health and disease. *Physiol. Rev.* 98, 641–665. doi: 10.1152/physrev.00037.2016

Caruana, B. T., Byrne, F. L., Knights, A. J., Quinlan, K. G. R., and Hoehn, K. L. (2019). Characterization of glucose transporter 6 in lipopolysaccharide-induced bone marrow-derived macrophage function. *J. Immunol.* 202, 1826–1832. doi: 10.4049/jimmunol.1801063

Castegna, A., Gissi, R., Menga, A., Montopoli, M., Favia, M., Viola, A., et al. (2020). Pharmacological targets of metabolism in disease: opportunities from macrophages. *Pharmacol. Ther* 2010:107521. doi: 10.1016/j.pharmthera.2020.107521

Chan, W. K., Lorenzi, P. L., Anishkin, A., Purwaha, P., Rogers, D. M., Sukharev, S., et al. (2014). The glutaminase activity of L-asparaginase is not required for anticancer activity against ASNS-negative cells. *Blood* 123, 3596–3606. doi: 10.1182/blood-2013-10-535112

Clark, E. L., Bush, S. J., McCulloch, M. E. B., Farquhar, I. L., Young, R., Lefevre, L., et al. (2017). A high resolution atlas of gene expression in the domestic sheep (*Ovis aries*). *PLoS Genet.* 13:e1006997. doi: 10.1371/journal.pgen.1006997

Costelloe, E. O., Stacey, K. J., Antalis, T. M., and Hume, D. A. (1999). Regulation of the plasminogen activator inhibitor-2 (PAI-2) gene in murine macrophages. Demonstration of a novel pattern of responsiveness to bacterial endotoxin. *J. Leukoc Biol.* 66, 172–182. doi: 10.1002/jlb.66.1.172

Cridland, J. A., Curley, E. Z., Wykes, M. N., Schroder, K., Sweet, M. J., Roberts, T. L., et al. (2012). The mammalian PYHIN gene family: phylogeny, evolution and expression. *BMC Evol. Biol.* 12:140. doi: 10.1186/1471-2148-12-140

Curi, R., de Siqueira Mendes, R., de Campos Crispin, L. A., Norata, G. D., Sampaio, S. C., and Newsholme, P. (2017). A past and present overview of macrophage metabolism and functional outcomes. *Clin. Sci.* 131, 1329–1342. doi: 10.1042/cs20170220

Danfaer, A., Tetens, V., and Agergaard, N. (1995). Review and an experimental study on the physiological and quantitative aspects of gluconeogenesis in lactating ruminants. *Comp. Biochem. Physiol. B. Biochem. Mol. Biol.* 111, 201–210. doi: 10.1016/0305-0491(94)00242-m

Dimmer, K. S., Friedrich, B., Lang, F., Deitmer, J. W., and Broer, S. (2000). The low-affinity monocarboxylate transporter MCT4 is adapted to the export of lactate in highly glycolytic cells. *Biochem. J.* 350(Pt 1), 219–227. doi: 10.1042/bj3500219

Drake, M. T., Clarke, B. L., Oursler, M. J., and Khosla, S. (2017). Cathepsin K inhibitors for osteoporosis: biology, potential clinical utility, and lessons learned. *Endocr. Rev.* 38, 325–350. doi: 10.1210/er.2015-1114

Dyer, D. P. (2020). Understanding the mechanisms that facilitate specificity, not redundancy, of chemokine mediated leukocyte recruitment. *Immunology* doi: 10.1111/imm.13200

Eger, M., Hussen, J., Koy, M., Danicke, S., Schuberth, H. J., and Breves, G. (2016). Glucose transporter expression differs between bovine monocyte and macrophage subsets and is influenced by milk production. *J. Dairy Sci.* 99, 2276–2287. doi: 10.3168/jds.2015-10435

Entrican, G., Wattegedera, S., Rocchi, M., and Wheelhouse, N. (2009). Pregnancy, indoleamine 2,3-dioxygenase (IDO) and chlamydial abortion: an unresolved paradox. *Vet. Microbiol.* 135, 98–102. doi: 10.1016/j.vetmic.2008.09.028

Erener, S., Petrilli, V., Kassner, I., Minotti, R., Castillo, R., Santoro, R., et al. (2012). Inflammasome-activated caspase 7 cleaves PARP1 to enhance the expression of a subset of NF-kappaB target genes. *Mol. Cell* 46, 200–211. doi: 10.1016/j.molcel.2012.02.016

Fairfax, B. P., Humburg, P., Makino, S., Naranbhai, V., Wong, D., Lau, E., et al. (2014). Innate immune activity conditions the effect of regulatory variants upon monocyte gene expression. *Science* 343:1246949. doi: 10.1126/science.1246949

Fonseca, G. J., Seidman, J. S., and Glass, C. K. (2016). Genome-wide approaches to defining macrophage identity and function. *Microbiol. Spectr.* 4:MCHD-0039-2016. doi: 10.1128/microbiolspec.MCHD-0039-2016

Francey, T., Jungi, T. W., Rey, O., and Peterhans, E. (1992a). Culture of ovine bone marrow-derived macrophages and evidence for serum factors distinct from M-CSF contributing to their propagation in vitro. *J. Leukoc. Biol.* 51, 525–534. doi: 10.1002/jlb.51.6.525

Francey, T., Schalch, L., Brcic, M., Peterhans, E., and Jungi, T. W. (1992b). Generation and functional characterization of ovine bone marrow-derived macrophages. *Vet. Immunol. Immunopathol.* 32, 281–301. doi: 10.1016/0165-2427(92)90051-q

Freem, L., Summers, K. M., Gheyas, A. A., Psifidi, A., Boulton, K., MacCallum, A., et al. (2019). Analysis of the progeny of sibling matings reveals regulatory variation impacting the transcriptome of immune cells in commercial chickens. *Front. Genet.* 10:1032. doi: 10.3389/fgene.2019.01032

Freemerman, A. J., Zhao, L., Pingili, A. K., Teng, B., Cozzo, A. J., Fuller, A. M., et al. (2019). Myeloid Slc2a1-deficient murine model revealed macrophage activation and metabolic phenotype are fueled by GLUT1. *J. Immunol.* 202, 1265–1286. doi: 10.4049/jimmunol.1800002

Garlanda, C., Bottazzi, B., Magrini, E., Inforzato, A., and Mantovani, A. (2018). PTX3, a humoral pattern recognition molecule, in innate immunity. Tissue Repair, and Cancer. *Physiol. Rev.* 98, 623–639. doi: 10.1152/physrev.00016.2017

Giotti, B., Chen, S. H., Barnett, M. W., Regan, T., Ly, T., Wiemann, S., et al. (2019). Assembly of a parts list of the human mitotic cell cycle machinery. *J. Mol. Cell Biol.* 11, 703–718. doi: 10.1093/jmcb/mjy063

Guilliams, M., Thierry, G. R., Bonnardel, J., and Bajenoff, M. (2020). Establishment and maintenance of the macrophage niche. *Immunity* 52, 434–451. doi: 10.1016/j.immuni.2020.02.015

Harjanto, D., Papamarkou, T., Oates, C. J., Rayon-Estrada, V., Papavasiliou, F. N., and Papavasiliou, A. (2016). RNA editing generates cellular subsets with diverse sequence within populations. *Nat. Commun.* 7:12145.

Harris, V. M., Harley, I. T. W., Kurien, B. T., Koelsch, K. A., and Scofield, R. H. (2019). Lysosomal pH is regulated in a sex dependent manner in immune cells expressing CXorf21. *Front. Immunol.* 10:578. doi: 10.3389/fimmu.2019.00578

Hotamisligil, G. S. (2017). Foundations of immunometabolism and implications for metabolic health and disease. *Immunity* 47, 406–420. doi: 10.1016/j.immuni.2017.08.009

Hume, D. A. (2015). The many alternative faces of macrophage activation. *Front. Immunol.* 6:370. doi: 10.3389/fimmu.2015.00370

Hume, D. A., Caruso, M., Ferrari-Cestari, M., Summers, K. M., Pridans, C., and Irvine, K. M. (2020). Phenotypic impacts of CSF1R deficiencies in humans and model organisms. *J. Leukoc. Biol.* 107, 205–219. doi: 10.1002/jlb.mr0519-143r

Hume, D. A., and Freeman, T. C. (2014). Transcriptomic analysis of mononuclear phagocyte differentiation and activation. *Immunol. Rev.* 262, 74–84. doi: 10.1111/imr.12211

Hume, D. A., and Gordon, S. (1983). Optimal conditions for proliferation of bone marrow-derived mouse macrophages in culture: the roles of CSF-1, serum. Ca2+, and adherence. *J. Cell. Physiol.* 117, 189–194. doi: 10.1002/jcp.1041170209

Hume, D. A., Irvine, K. M., and Pridans, C. (2019). The mononuclear phagocyte system: the relationship between monocytes and macrophages. *Trends Immunol.* 40, 98–112. doi: 10.1016/j.it.2018.11.007

Hume, D. A., Summers, K. M., Raza, S., Baillie, J. K., and Freeman, T. C. (2010). Functional clustering and lineage markers: insights into cellular differentiation and gene function from large-scale microarray studies of purified primary cell populations. *Genomics* 95, 328–338. doi: 10.1016/j.ygeno.2010.03.002

Hume, D. A., Summers, K. M., and Rehli, M. (2016). Transcriptional regulation and macrophage differentiation. *Microbiol. Spectr.* 4:MCHD-002402015. doi: 10.1128/microbiolspec.MCHD-0024-2015

Icer, M. A., and Gezmen-Karadag, M. (2018). The multiple functions and mechanisms of osteopontin. *Clin. Biochem.* 59, 17–24.

Irvine, K. M., Banh, X., Gadd, V. L., Wojcik, K. K., Ariffin, J. K., Jose, S., et al. (2016). CRIg-expressing peritoneal macrophages are associated with disease severity in patients with cirrhosis and ascites. *JCI Insight* 1:e86914.

Ishiguro, K., Kadomatsu, K., Kojima, T., Muramatsu, H., Iwase, M., Yoshikai, Y., et al. (2001). Syndecan-4 deficiency leads to high mortality of lipopolysaccharide-injected mice. *J. Biol. Chem.* 276, 47483–47488. doi: 10.1074/jbc.m106268200

Jamal Uddin, M., Joe, Y., Kim, S. K., Oh Jeong, S., Ryter, S. W., Pae, H. O., et al. (2016). IRG1 induced by heme oxygenase-1/carbon monoxide inhibits LPS-mediated sepsis and pro-inflammatory cytokine production. *Cell Mol. Immunol.* 13, 170–179. doi: 10.1038/cmi.2015.02

Jha, A. K., Huang, S. C., Sergushichev, A., Lampropoulou, V., Ivanova, Y., Loginicheva, E., et al. (2015). Network integration of parallel metabolic and transcriptional data reveals metabolic modules that regulate macrophage polarization. *Immunity* 42, 419–430. doi: 10.1016/j.immuni.2015.02.005

Jiang, H., Shi, H., Sun, M., Wang, Y., Meng, Q., Guo, P., et al. (2016). PFKFB3-driven macrophage glycolytic metabolism is a crucial component of innate antiviral defense. *J. Immunol.* 197, 2880–2890. doi: 10.4049/jimmunol.1600474

Jin, S. L., Lan, L., Zoudilova, M., and Conti, M. (2005). Specific role of phosphodiesterase 4B in lipopolysaccharide-induced signaling in mouse macrophages. *J. Immunol.* 175, 1523–1531. doi: 10.4049/jimmunol.175.3.1523

Jing, J., Yang, I. V., Hui, L., Patel, J. A., Evans, C. M., Prikeris, R., et al. (2013). Role of macrophage receptor with collagenous structure in innate immune tolerance. *J. Immunol.* 190, 6360–6367. doi: 10.4049/jimmunol.1202942

Johnson, A. R., Qin, Y., Cozzo, A. J., Freemerman, A. J., Huang, M. J., Zhao, L., et al. (2016). Metabolic reprogramming through fatty acid transport protein 1 (FATP1) regulates macrophage inflammatory potential and adipose inflammation. *Mol. Metab.* 5, 506–526. doi: 10.1016/j.molmet.2016.04.005

Jubb, A. W., Young, R. S., Hume, D. A., and Bickmore, W. A. (2016). Enhancer turnover is associated with a divergent transcriptional response to glucocorticoid in mouse and human macrophages. *J. Immunol.* 196, 813–822. doi: 10.4049/jimmunol.1502009

Jungi, T. W., Adler, H., Adler, B., Thony, M., Krampe, M., and Peterhans, E. (1996). Inducible nitric oxide synthase of macrophages. Present knowledge and evidence for species-specific regulation. *Vet. Immunol. Immunopathol.* 54, 323–330. doi: 10.1016/s0165-2427(96)05690-5

Kaikkonen, M. U., Spann, N. J., Heinz, S., Romanoski, C. E., Allison, K. A., Stender, J. D., et al. (2013). Remodeling of the enhancer landscape during macrophage activation is coupled to enhancer transcription. *Mol. Cell.* 51, 310–325. doi: 10.1016/j.molcel.2013.07.010

Kakuda, D. K., Sweet, M. J., Mac Leod, C. L., Hume, D. A., and Markovich, D. (1999). CAT2-mediated L-arginine transport and nitric oxide production in activated macrophages. *Biochem. J.* 340(Pt 2), 549–553. doi: 10.1042/bj3400549

Kapetanovic, R., Fairbairn, L., Beraldi, D., Sester, D. P., Archibald, A. L., Tuggle, C. K., et al. (2012). Pig bone marrow-derived macrophages resemble human macrophages in their response to bacterial lipopolysaccharide. *J. Immunol.* 188, 3382–3394. doi: 10.4049/jimmunol.1102649

Kapetanovic, R., Fairbairn, L., Downing, A., Beraldi, D., Sester, D. P., Freeman, T. C., et al. (2013). The impact of breed and tissue compartment on the response of pig macrophages to lipopolysaccharide. *BMC Genomics* 14:581. doi: 10.1186/1471-2164-14-581

Karagianni, A. E., Kapetanovic, R., Summers, K. M., McGorum, B. C., Hume, D. A., and Pirie, R. S. (2017). Comparative transcriptome analysis of equine alveolar macrophages. *Equine Vet. J.* 49, 375–382. doi: 10.1111/evj.12584

Kim, Y. H., Lee, J. R., and Hahn, M. J. (2018). Regulation of inflammatory gene expression in macrophages by epithelial-stromal interaction 1 (Epsti1). *Biochem. Biophys. Res. Commun.* 496, 778–783. doi: 10.1016/j.bbrc.2017.12.014

Kimura, I., Ichimura, A., Ohue-Kitano, R., and Igarashi, M. (2020). Free fatty acid receptors in health and disease. *Physiol. Rev.* 100, 171–210. doi: 10.1152/physrev.00041.2018

Kinsella, R. J., Kahari, A., Haider, S., Zamora, J., Proctor, G., Spudich, G., et al. (2011). Ensembl BioMarts: a hub for data retrieval across taxonomic space. *Database* 2011:bar030. doi: 10.1093/database/bar030

Kondo, T., Kawai, T., and Akira, S. (2012). Dissecting negative regulation of Toll-like receptor signaling. *Trends Immunol.* 33, 449–458. doi: 10.1016/j.it.2012.05.002

Krall, A. S., Xu, S., Graeber, T. G., Braas, D., and Christofk, H. R. (2016). Asparagine promotes cancer cell proliferation through use as an amino acid exchange factor. *Nat. Commun.* 7:11457.

Labzin, L. I., Bottermann, M., Rodriguez-Silvestre, P., Foss, S., Andersen, J. T., Vaysburd, M., et al. (2019). Antibody and DNA sensing pathways converge to activate the inflammasome during primary human macrophage infection. *EMBO J.* 38:e101365.

Lambert, S. A., Jolma, A., Campitelli, L. F., Das, P. K., Yin, Y., Albu, M., et al. (2018). The human transcription factors. *Cell* 172, 650–665.

Lawrence, D. W., and Kornbluth, J. (2012). E3 ubiquitin ligase NKLAM is a macrophage phagosome protein and plays a role in bacterial killing. *Cell Immunol.* 279, 46–52. doi: 10.1016/j.cellimm.2012.09.004

Lawrence, D. W., Shornick, L. P., and Kornbluth, J. (2019). Mice deficient in NKLAM have attenuated inflammatory cytokine production in a Sendai virus pneumonia model. *PLoS One* 14:e0222802. doi: 10.1371/journal.pone.0222802

Liaw, L., Birk, D. E., Ballas, C. B., Whitsitt, J. S., Davidson, J. M., and Hogan, B. L. (1998). Altered wound healing in mice lacking a functional osteopontin gene (spp1). *J. Clin. Invest.* 101, 1468–1478. doi: 10.1172/jci2131

Link, V. M., Duttke, S. H., Chun, H. B., Holtman, I. R., Westin, E., Hoeksema, M. A., et al. (2018). Analysis of genetically diverse macrophages reveals local and domain-wide mechanisms that control transcription factor binding and function. *Cell* 173, 1796–1809.e17. doi: 10.1016/j.cell.2018.04.018

Liu, G., Friggeri, A., Yang, Y., Park, Y. J., Tsuruta, Y., and Abraham, E. (2009). miR-147, a microRNA that is induced upon Toll-like receptor stimulation, regulates murine macrophage inflammatory responses. *Proc. Natl. Acad. Sci. U.S.A.* 106, 15819–15824. doi: 10.1073/pnas.0901216106

Liu, P. S., Wang, H., Li, X., Chao, T., Teav, T., Christen, S., et al. (2017). alpha-ketoglutarate orchestrates macrophage activation through metabolic and epigenetic reprogramming. *Nat. Immunol.* 18, 985–994. doi: 10.1038/ni.3796

Lu, S. C., Wu, H. W., Lin, Y. J., and Chang, S. F. (2009). The essential role of Oct-2 in LPS-induced expression of iNOS in RAW 264.7 macrophages and its regulation by trichostatin A. *Am. J. Physiol. Cell Physiol.* 296, C1133–C1139.

Lunardi, A., Gaboli, M., Giorgio, M., Rivi, R., Bygrave, A., Antoniou, M., et al. (2011). A role for PML in innate immunity. *Genes Cancer* 2, 10–19.

Marini, J. C., Klein, J. D., Sands, J. M., and Van Amburgh, M. E. (2004). Effect of nitrogen intake on nitrogen recycling and urea transporter abundance in lambs. *J. Anim. Sci.* 82, 1157–1164. doi: 10.2527/2004.8241157x

Marongiu, L., Gornati, L., Artuso, I., Zanoni, I., and Granucci, F. (2019). Below the surface: the inner lives of TLR4 and TLR9. *J. Leukoc. Biol.* 106, 147–160.

Meijer, G. A., van der Meulen, J., and van Vuuren, A. M. (1993). Glutamine is a potentially limiting amino acid for milk production in dairy cows: a hypothesis. *Metabolism* 42, 358–364. doi: 10.1016/0026-0495(93)90087-5

Mills, E. L., Ryan, D. G., Prag, H. A., Dikovskaya, D., Menon, D., Zaslona, Z., et al. (2018). Itaconate is an anti-inflammatory metabolite that activates Nrf2 via alkylation of KEAP1. *Nature* 556, 113–117.

Min, D., Moore, A. G., Bain, M. A., Breit, S. N., and Lyons, J. G. (2002). Activation of macrophage promatrix metalloproteinase-9 by lipopolysaccharide-associated proteinases. *J. Immunol.* 168, 2449–2455. doi: 10.4049/jimmunol.168.5.2449

Mittal, M., Tiruppathi, C., Nepal, S., Zhao, Y. Y., Grzych, D., Soni, D., et al. (2016). TNFalpha-stimulated gene-6 (TSG6) activates macrophage phenotype transition to prevent inflammatory lung injury. *Proc. Natl. Acad. Sci. U.S.A.* 113, E8151–E8158.

Monticelli, S., and Natoli, G. (2017). Transcriptional determination and functional specificity of myeloid cells: making sense of diversity. *Nat. Rev. Immunol.* 17, 595–607. doi: 10.1038/nri.2017.51

Muendlein, H. I., Jetton, D., Connolly, W. M., Eidell, K. P., Magri, Z., Smirnova, I., et al. (2020). cFLIPL protects macrophages from LPS-induced pyroptosis via inhibition of complex II formation. *Science* 367, 1379–1384. doi: 10.1126/science.aay3878

Muriuki, C., Bush, S. J., Salavati, M., McCulloch, M. E. B., Lisowski, Z. M., Agaba, M., et al. (2019). A mini-atlas of gene expression for the domestic Goat (Capra hircus). *Front. Genet* 10:1080. doi: 10.3389/fgene.2019.01080

Murray, P. J. (2017). Macrophage polarization. *Annu. Rev. Physiol.* 79, 541–566.

Murray, P. J., Allen, J. E., Biswas, S. K., Fisher, E. A., Gilroy, D. W., Goerdt, S., et al. (2014). Macrophage activation and polarization: nomenclature and experimental guidelines. *Immunity* 41, 14–20. doi: 10.1016/j.immuni.2014.06.008

Nepal, S., Tiruppathi, C., Tsukasaki, Y., Farahany, J., Mittal, M., Rehman, J., et al. (2019). STAT6 induces expression of Gas6 in macrophages to clear apoptotic neutrophils and resolve inflammation. *Proc. Natl. Acad. Sci. U.S.A.* 116, 16513–16518. doi: 10.1073/pnas.1821601116

Odhams, C. A., Roberts, A. L., Vester, S. K., Duarte, C. S. T., Beales, C. T., Clarke, A. J., et al. (2019). Interferon inducible X-linked gene CXorf21 may contribute to sexual dimorphism in systemic lupus erythematosus. *Nat. Commun.* 10:2164. doi: 10.1038/s41467-019-10106-2

Oishi, Y., Spann, N. J., Link, V. M., Muse, E. D., Strid, T., Edillor, C., et al. (2017). SREBP1 contributes to resolution of pro-inflammatory TLR4 signaling by reprogramming fatty acid metabolism. *Cell Metab.* 25, 412–427. doi: 10.1016/j.cmet.2016.11.009

O'Rourke, J. G., Bogdanik, L., Yanez, A., Lall, D., Wolf, A. J., Muhammad, A. K., et al. (2016). C9orf72 is required for proper macrophage and microglial function in mice. *Science* 351, 1324–1329. doi: 10.1126/science.aaf1064

Palmieri, E. M., Menga, A., Martin-Perez, R., Quinto, A., Riera-Domingo, C., De Tullio, G., et al. (2017). Pharmacologic or genetic targeting of glutamine synthetase skews macrophages toward an M1-like phenotype and inhibits tumor metastasis. *Cell Rep.* 20, 1654–1666. doi: 10.1016/j.celrep.2017.07.054

Petri, B., and Sanz, M. J. (2018). Neutrophil chemotaxis. *Cell Tissue Res.* 371, 425–436.

Prendergast, G. C., Malachowski, W. P., DuHadaway, J. B., and Muller, A. J. (2017). Discovery of IDO1 inhibitors: from bench to bedside. *Cancer Res.* 77, 6795–6811. doi: 10.1158/0008-5472.can-17-2285

Qualls, J. E., Subramanian, C., Rafi, W., Smith, A. M., Balouzian, L., DeFreitas, A. A., et al. (2012). Sustained generation of nitric oxide and control of mycobacterial infection requires argininosuccinate synthase 1. *Cell Host Microbe* 12, 313–323. doi: 10.1016/j.chom.2012.07.012

Ransohoff, J. D., Wei, Y., and Khavari, P. A. (2018). The functions and unique features of long intergenic non-coding RNA. *Nat. Rev. Mol. Cell Biol.* 19, 143–157. doi: 10.1038/nrm.2017.104

Raza, S., Barnett, M. W., Barnett-Itzhaki, Z., Amit, I., Hume, D. A., and Freeman, T. C. (2014). Analysis of the transcriptional networks underpinning the activation of murine macrophages by inflammatory mediators. *J. Leukoc. Biol.* 96, 167–183. doi: 10.1189/jlb.6hi0313-169r

Rehli, M., Krause, S. W., and Andreesen, R. (2000). The membrane-bound ectopeptidase CPM as a marker of macrophage maturation in vitro and in vivo. *Adv. Exp. Med. Biol.* 477, 205–216. doi: 10.1007/0-306-46826-3_23

Rehli, M., Lichanska, A., Cassady, A. I., Ostrowski, M. C., and Hume, D. A. (1999). TFEC is a macrophage-restricted member of the microphthalmia-TFE subfamily of basic helix-loop-helix leucine zipper transcription factors. *J. Immunol.* 162, 1559–1565.

Renard, H. F., Tyckaert, F., Lo Giudice, C., Hirsch, T., Valades-Cruz, C. A., Lemaigre, C., et al. (2020). Endophilin-A3 and Galectin-8 control the clathrin-independent endocytosis of CD166. *Nat. Commun.* 11:1457.

Roberts, F., Zhu, D., Farquharson, C., and Macrae, V. E. (2019). ENPP1 in the regulation of mineralization and beyond. *Trends Biochem. Sci.* 44, 616–628. doi: 10.1016/j.tibs.2019.01.010

Rodriguez, M. S., Egana, I., Lopitz-Otsoa, F., Aillet, F., Lopez-Mato, M. P., Dorronsoro, A., et al. (2014). The RING ubiquitin E3 RNF114 interacts with A20 and modulates NF-kappaB activity and T-cell activation. *Cell Death Dis.* 5:e1399. doi: 10.1038/cddis.2014.366

Rojo, R., Pridans, C., Langlais, D., and Hume, D. A. (2017). Transcriptional mechanisms that control expression of the macrophage colony-stimulating factor receptor locus. *Clin. Sci.* 131, 2161–2182. doi: 10.1042/cs20170238

Rotoli, B. M., Barilli, A., Visigalli, R., Ingoglia, F., Milioli, M., Di Lascia, M., et al. (2018). Downregulation of SLC7A7 Triggers an inflammatory phenotype in human macrophages and airway epithelial cells. *Front. Immunol.* 9:508. doi: 10.3389/fimmu.2018.00508

Ryan, D. G., and O'Neill, L. A. J. (2020). Krebs cycle reborn in macrophage immunometabolism. *Annu. Rev. Immunol.* 38, 289–313. doi: 10.1146/annurev-immunol-081619-104850

Sarkar, D., and Fisher, P. B. (2006). Molecular mechanisms of aging-associated inflammation. *Cancer Lett.* 236, 13–23. doi: 10.1016/j.canlet.2005.04.009

Schmidl, C., Renner, K., Peter, K., Eder, R., Lassmann, T., Balwierz, P. J., et al. (2014). Transcription and enhancer profiling in human monocyte subsets. *Blood* 123, e90–e99. doi: 10.1182/blood-2013-02-484188

Schroder, K., Irvine, K. M., Taylor, M. S., Bokil, N. J., Le Cao, K. A., Masterman, K. A., et al. (2012). Conservation and divergence in Toll-like receptor 4-regulated gene expression in primary human versus mouse macrophages. *Proc. Natl. Acad. Sci. U.S.A.* 109, E944–E953.

Sester, D. P., Trieu, A., Brion, K., Schroder, K., Ravasi, T., Robinson, J. A., et al. (2005). LPS regulates a set of genes in primary murine macrophages by antagonising CSF-1 action. *Immunobiology* 210, 97–107. doi: 10.1016/j.imbio.2005.05.004

Sharma, S., Patnaik, S. K., Taggart, R. T., Kannisto, E. D., Enriquez, S. M., Gollnick, P., et al. (2015). APOBEC3A cytidine deaminase induces RNA editing in monocytes and macrophages. *Nat. Commun.* 6:6881.

Sinclair, L. V., Neyens, D., Ramsay, G., Taylor, P. M., and Cantrell, D. A. (2018). Single cell analysis of kynurenine and System L amino acid transport in T cells. *Nat. Commun.* 9:1981.

Sjostrand, M., Carow, B., Nyberg, W. A., Covacu, R., Rottenberg, M. E., and Espinosa, A. (2020). TRIM21 controls Toll-like receptor 2 responses in bone-marrow-derived macrophages. *Immunology* 159, 335–343. doi: 10.1111/imm.13157

Sparrer, K. M. J., Gableske, S., Zurenski, M. A., Parker, Z. M., Full, F., Baumgart, G. J., et al. (2017). TRIM23 mediates virus-induced autophagy via activation of TBK1. *Nat. Microbiol.* 2, 1543–1557. doi: 10.1038/s41564-017-0017-2

Stanley, E. R., and Chitu, V. (2014). CSF-1 receptor signaling in myeloid cells. *Cold Spring Harb. Perspect. Biol.* 6:a021857. doi: 10.1101/cshperspect.a021857

Subramanian, G., Kuzmanovic, T., Zhang, Y., Peter, C. B., Veleeparambil, M., Chakravarti, R., et al. (2018). A new mechanism of interferon's antiviral action: Induction of autophagy, essential for paramyxovirus replication, is inhibited by the interferon stimulated gene, TDRD7. *PLoS Pathog.* 14:e1006877. doi: 10.1371/journal.ppat.1006877

Summers, K. M., Bush, S. J., Wu, C., Su, A. I., Muriuki, C., Clark, E. L., et al. (2019). Functional annotation of the transcriptome of the Pig, Sus scrofa, based upon network analysis of an RNAseq transcriptional atlas. *Front. Genet.* 10:1355. doi: 10.3389/fgene.2019.01355

Tan, Z., Xie, N., Banerjee, S., Cui, H., Fu, M., Thannickal, V. J., et al. (2015). The monocarboxylate transporter 4 is required for glycolytic reprogramming and inflammatory response in macrophages. *J. Biol. Chem.* 290, 46–55. doi: 10.1074/jbc.m114.603589

Tannahill, G. M., Curtis, A. M., Adamik, J., Palsson-McDermott, E. M., McGettrick, A. F., Goel, G., et al. (2013). Succinate is an inflammatory signal that induces IL-1beta through HIF-1alpha. *Nature* 496, 238–242.

Tartey, S., Matsushita, K., Vandenbon, A., Ori, D., Imamura, T., Mino, T., et al. (2014). Akirin2 is critical for inducing inflammatory genes by bridging IkappaB-zeta and the SWI/SNF complex. *EMBO J.* 33, 2332–2348. doi: 10.15252/embj.201488447

Van den Bossche, J., O'Neill, L. A., and Menon, D. (2017). Macrophage Immunometabolism: where are we (Going)? *Trends Immunol.* 38, 395–406. doi: 10.1016/j.it.2017.03.001

Van Opdenbosch, N., Van Gorp, H., Verdonckt, M., Saavedra, P. H. V., de Vasconcelos, N. M., Goncalves, A., et al. (2017). Caspase-1 engagement and TLR-induced c-FLIP expression suppress ASC/Caspase-8-dependent apoptosis by inflammasome sensors NLRP1b and NLRC4. *Cell Rep.* 21, 3427–3444. doi: 10.1016/j.celrep.2017.11.088

Vogel, D. Y., Glim, J. E., Stavenuiter, A. W., Breur, M., Heijnen, P., Amor, S., et al. (2014). Human macrophage polarization in vitro: maturation and activation methods compared. *Immunobiology* 219, 695–703. doi: 10.1016/j.imbio.2014.05.002

Waddell, L. A., Lefevre, L., Bush, S. J., Raper, A., Young, R., Lisowski, Z. M., et al. (2018). ADGRE1 (EMR1, F4/80) is a rapidly-evolving gene expressed in mammalian monocyte-macrophages. *Front. Immunol.* 9:2246. doi: 10.3389/fimmu.2018.02246

Wang, G., Chen, H. W., Oktay, Y., Zhang, J., Allen, E. L., Smith, G. M., et al. (2010). PNPASE regulates RNA import into mitochondria. *Cell* 142, 456–467. doi: 10.1016/j.cell.2010.06.035

Wang, Y., Galli, M., Shade Silver, A., Lee, W., Song, Y., Mei, Y., et al. (2018). IL1beta and TNFalpha promote RANKL-dependent adseverin expression and osteoclastogenesis. *J. Cell Sci.* 131:jcs213967. doi: 10.1242/jcs.213967

Wells, C. A., Ravasi, T., and Hume, D. A. (2005). Inflammation suppressor genes: please switch out all the lights. *J. Leukoc. Biol.* 78, 9–13. doi: 10.1189/jlb.1204710

Wells, C. A., Salvage-Jones, J. A., Li, X., Hitchens, K., Butcher, S., Murray, R. Z., et al. (2008). The macrophage-inducible C-type lectin, mincle, is an essential component of the innate immune response to *Candida albicans*. *J. Immunol.* 180, 7404–7413. doi: 10.4049/jimmunol.180.11.7404

Xia, C., Braunstein, Z., Toomey, A. C., Zhong, J., and Rao, X. (2017). S100 proteins as an important regulator of macrophage inflammation. *Front. Immunol.* 8:1908. doi: 10.3389/fimmu.2017.01908

Yamazaki, T., Akiba, H., Iwai, H., Matsuda, H., Aoki, M., Tanno, Y., et al. (2002). Expression of programmed death 1 ligands by murine T cells and APC. *J. Immunol.* 169, 5538–5545. doi: 10.4049/jimmunol.169.10.5538

Yoo, H. C., Park, S. J., Nam, M., Kang, J., Kim, K., Yeo, J. H., et al. (2020). A Variant of SLC1A5 Is a mitochondrial glutamine transporter for metabolic reprogramming in cancer cells. *Cell Metab.* 31:e12.

Young, R., Bush, S. J., Lefevre, L., McCulloch, M. E. B., Lisowski, Z. M., Muriuki, C., et al. (2018). Species-specific transcriptional regulation of genes involved in nitric oxide production and arginine metabolism in macrophages. *Immunohorizons* 2, 27–37. doi: 10.4049/immunohorizons.1700073

Young, R., Lefevre, L., Bush, S. J., Joshi, A., Singh, S. H., Jadhav, S. K., et al. (2019). A gene expression atlas of the domestic water buffalo (*Bubalus bubalis*). *Front. Genet.* 10:668. doi: 10.3389/fgene.2019.00668

Zhang, Y., Mao, D., Roswit, W. T., Jin, X., Patel, A. C., Patel, D. A., et al. (2015). PARP9-DTX3L ubiquitin ligase targets host histone H2BJ and viral 3C protease to enhance interferon signaling and control viral infection. *Nat. Immunol.* 16, 1215–1227. doi: 10.1038/ni.3279

Zimmerman, A. W., Joosten, B., Torensma, R., Parnes, J. R., van Leeuwen, F. N., and Figdor, C. G. (2006). Long-term engagement of CD6 and ALCAM is essential for T-cell proliferation induced by dendritic cells. *Blood* 107, 3212–3220. doi: 10.1182/blood-2005-09-3881

Conflict of Interest: The authors declare that the research was conducted in the absence of any commercial or financial relationships that could be construed as a potential conflict of interest.

frontiers in Cell and Developmental Biology

ORIGINAL RESEARCH
published: 15 October 2020
doi: 10.3389/fcell.2020.580848

Adherent Intestinal Cells From Atlantic Salmon Show Phagocytic Ability and Express Macrophage-Specific Genes

*Youngjin Park[1], Qirui Zhang[2], Geert F. Wiegertjes[3], Jorge M.O. Fernandes[1] and Viswanath Kiron[1]**

[1] Faculty of Biosciences and Aquaculture, Nord University, Bodø, Norway, [2] Division of Clinical Genetics, Lund University, Lund, Sweden, [3] Aquaculture and Fisheries Group, Wageningen University & Research, Wageningen, Netherlands

OPEN ACCESS

Edited by:
Yi Feng,
The University of Edinburgh, United Kingdom

Reviewed by:
Dimitar Borisov Iliev, Institute of Molecular Biology (BAS), Bulgaria
Sherri L. Christian, Memorial University of Newfoundland, Canada

***Correspondence:**
Viswanath Kiron
kiron.viswanath@nord.no

Specialty section:
This article was submitted to Cell Death and Survival, a section of the journal Frontiers in Cell and Developmental Biology

Received: *07 July 2020*
Accepted: *22 September 2020*
Published: *15 October 2020*

Citation:
Park Y, Zhang Q, Wiegertjes GF, Fernandes JMO and Kiron V (2020) Adherent Intestinal Cells From Atlantic Salmon Show Phagocytic Ability and Express Macrophage-Specific Genes. Front. Cell Dev. Biol. 8:580848. doi: 10.3389/fcell.2020.580848

Our knowledge of the intestinal immune system of fish is rather limited compared to mammals. Very little is known about the immune cells including the phagocytic cells in fish intestine. Hence, employing imaging flow cytometry and RNA sequencing, we studied adherent cells isolated from healthy Atlantic salmon. Phagocytic activity and selected gene expression of adherent cells from the distal intestine (adherent intestinal cells, or AIC) were compared with those from head kidney (adherent kidney cells, or AKC). Phagocytic activity of the two cell types was assessed based on the uptake of *Escherichia coli* BioParticles^{TM}. AIC showed phagocytic ability but the phagocytes were of different morphology compared to AKC. Transcriptomic analysis revealed that AIC expressed genes associated with macrophages, T cells, and endothelial cells. Heatmap analysis of selected genes indicated that the adherent cells from the two organs had apparently higher expression of macrophage-related genes. We believe that the adherent intestinal cells have phagocytic characteristics and high expression of genes commonly associated with macrophages. We envisage the possibilities for future studies on enriched populations of adherent intestinal cells.

Keywords: adherent, intestinal cells, ImageStream®^{X}, Atlantic salmon, phagocytosis, RNA-Seq, macrophages

INTRODUCTION

Teleost fishes have both organized and diffuse lymphoid tissues. However, these tissues differ from those of mammals morphologically and functionally. Fish lack bone marrow and lymph nodes found in mammals. Therefore, they rely on thymus, (head) kidney and spleen as their key lymphoid organs. The head kidney (or anterior kidney), is the main source of cytokine-producing lymphoid cells (Geven and Klaren, 2017), macrophages, and plasma cells, which find their way to specific sites, including those in the intestine, to replenish tissue-resident cell populations (Kratofil et al., 2017). Furthermore, the head kidney recruits specific cell types during disease conditions like inflammation (Parra et al., 2015). The head kidney is also a well-known primary B cell organ in fishes (Li et al., 2006; Parra et al., 2015).

This makes the head kidney the main hematopoietic organ in teleost fish. In addition, fish possess mucosa-associated lymphoid tissues (MALTs), but these tissues are more diffuse compared to those in mammals (Parra et al., 2015). Among these MALTs, gut-associated lymphoid tissues (GALTs) contain two main populations of immune cells: (1) intraepithelial lymphocytes, which include mainly T cells located between the epithelial cells; and (2) lamina propria leukocytes, which are comprised of lymphocytes, macrophages, granulocytes and plasma cells (Rombout et al., 2011). In-depth knowledge of these immune cells present in GALT is necessary to understand the crosstalk between antigens and the epithelium as well as the immunological functions of both the key lymphoid organs and GALT. However, the lack of appropriate cell markers and complexity of isolation protocols are still hampering the progress of research on leukocyte cell populations in the fish intestine.

The most common practice is to collect adherent cells from specific organs in order to characterize them through further analysis. Cell adhesion refers to the ability of cells to adhere to other cells or extracellular matrix (Khalili and Ahmad, 2015). This process not only stimulates communication between cells but also helps to retain the tissue structure and functions (Khalili and Ahmad, 2015). The cells isolated from tissues or organs are mostly adherent types, and the known mammalian adherent cells are macrophages (Selvarajan et al., 2011), T cells (Bierer and Burakoff, 1988; Shimizu et al., 1991), endothelial cells (Braniste et al., 2016), epithelial cells (Kihara et al., 2018) and dendritic cells (DC, only upon antigen exposure) (Yi and Lu, 2012). Mammalian cell culture methods are frequently adopted to culture and study monocyte-derived macrophage-like cells from fish immunological tissues such as spleen (Iliev et al., 2013) and head kidney (Joerink et al., 2006; Iliev et al., 2019). However, our knowledge of the cell types including phagocytic cells that are involved in the fish intestinal immune response is rather limited compared to mammals.

As for the intestinal cells of fish, McMillan and Secombes (1997) were the first researchers to describe protocols to isolate them from rainbow trout, *Oncorhynchus mykiss*. After a decade, several research groups put in effort to effectively isolate and characterize intestinal immune cells from different fish species such as rainbow trout (Bernard et al., 2006), gilthead seabream, *Sparus aurata* (Salinas et al., 2007) and Atlantic salmon, *Salmo salar* (Attaya et al., 2018). Although there is ample information about the adherent cells from the head kidney in teleost fishes, knowledge about the intestinal cells has to be gathered by employing next generation techniques.

Therefore, this study investigated the adherent cells isolated from the distal intestine by employing the cells from the head kidney of Atlantic salmon as reference. We adopted two high-throughput techniques, imaging flow cytometry (IFC) and RNA sequencing. First, using IFC we explored the adherent cells from the aforementioned organs to decipher the characteristics of the populations and their phagocytic activity. Subsequently, a transcriptomic study was carried out to profile the expression of (1) cell type (macrophage, dendritic cell, endothelial cell, T and B cells)-related genes and (2) other immune genes (cytokines, chemokines, mucins and toll-like receptors) to delineate if the adherent cells expressed genes associated with phagocytes.

MATERIALS AND METHODS

Experimental Fish and Sampling Procedure

Atlantic salmon post smolts of about 70 g were purchased from a commercial producer (Sundsfjord Smolt, Nygårdsjøen, Norway) and maintained at the Research Station of Nord University, Bodø, Norway. Fish were fed a commercial feed (Ewos Micro, Ewos AS, Bergen, Norway) to satiation, and reared in a flow-through sea water system (temperature: 7–8°C, dissolved oxygen saturation: 87–92%, 24-h light cycle). Fish (of the weight range 510–590 g) was used in this study. The fish were starved for 24 h and were killed with an over dose of MS-222 (Tricaine methane sulfonate; Argent Chemical Laboratories, Redmond, United States; 80 mg/L). Head kidney (HK) and distal intestine (DI) samples were then collected.

Cell Isolation and Culture

Immune cells from the head kidney (HK) and distal intestine (DI) were isolated and grown at 12°C in Leibovitz's L-15 Medium (L-15; Sigma-Aldrich, Oslo, Norway) as described previously by Park et al. (2020) and Salinas et al. (2007), respectively. The osmolality of cell culture media was adjusted to 380 mOsm by adding a solution consisting of 5% (v/v) 0.41 M NaCl, 0.33 M $NaHCO_3$ and 0.66 (w/v) D-glucose (Sigma).

Briefly, HK from salmon ($n = 6$) were sampled and transferred to 15 mL centrifuge tubes to make a total volume of 4 mL in ice-cold L-15 + [L-15 medium with 50 U/mL penicillin (Sigma), 50 μg/mL streptomycin (Sigma), 2% fetal bovine serum (FBS; Sigma) and 10 U/mL heparin (Sigma)]. The tissues were passed through a sterile 100-μM cell strainer (Falcon, New York, United States) with ice-cold L-15 + . Thereafter, the cell suspensions were layered on 40%/60% Percoll (Sigma) to separate HK leukocytes and centrifuged at 500 × *g* for 30 min, at 4°C. Cells at the interface were collected and washed twice with ice-cold L-15-FBS free (L-15 medium with 50 U/mL penicillin, 50 μg/mL streptomycin) by centrifugation (500 × *g*, 5 min, 4°C).

For intestinal cell isolation, DI samples from salmon ($n = 6$) were transferred to a cell culture dish (Nunc EasyDish, Thermo Fisher Scientific, Oslo, Norway) with 2 mL ice-cold PBS. The tissues were cut open longitudinally and washed with ice-cold PBS to remove gut contents. After washing they were cut into small pieces (1–2 cm fragments) and transferred to 15 mL centrifuge tubes to make a total volume of 4 mL in DTT solution (0.145 mg/mL dithiothreitol + 0.37 mg/mL EDTA in Ca^{2+} and Mg^{2+} free HBSS, Sigma) at room temperature for 20 min to break disulfide bonds in the mucus. Next, the tissue fragments were washed with L-15 + supplemented with DNAse (0.05 mg/ml; Sigma) to prevent cell clumping and wash out excess DTT. Thereafter, the washed fragments were transferred to 15 mL centrifuge tubes to make a total volume of 6 mL in the digestive solution (0.37 mg/mL collagenase IV, Thermo Fisher Scientific). The centrifuge tubes

were incubated in a shaking incubator (200 rpm) at RT for 60 min. The tissue fragments and supernatants were then passed through a sterile 100-μM cell strainer with ice-cold L-15 + , and the cell suspensions were layered on 25%/75% Percoll. The tubes containing the cells and Percoll were centrifuged at 500 × *g* for 30 min, at 4°C to separate DI leukocytes. Cells at the interface were collected and washed twice with ice-cold L-15-FBS free by centrifugation (500 × *g*, 5 min, 4°C).

Both HK and DI leukocytes (mentioned under flow cytometry studies) were allowed to adhere on a cell culture dish with 2 mL L-15 + for 2 days at 12°C. After collecting the supernatant containing non-adherent cells, the dish with the adherent cells was placed on ice for 10 min, and the cells were detached by washing three times with 1.5 mL ice-cold PBS supplemented with 5 mM EDTA. The cells obtained were centrifuged (500 × *g*, 5 min, 4°C) and re-suspended in 1 mL L-15 + . Then, the cells were counted using a portable cell counter (Scepter 2.0 cell counter, EMD Millipore, Darmstadt, Germany). To confirm the quality of the harvested cells, we observed the cells using a live cell imager (ZOE Fluorescent Cell imager, Bio-Rad, Oslo, Norway). With our improved protocols, we were able to harvest many cells with high viability. We checked the quality of the isolated cells by observing them through microscope and with the help of live/dead cell assays using propidium iodide.

Flow Cytometry Studies

To understand the cell populations and their functions we isolated and cultured cells from HK and DI. These cells were studied employing the ImageStream$^{®X}$ Mk II Imaging Flow Cytometer (Luminex Corporation, Austin, TX, United States) equipped with two argon-ion lasers (488 and 642 nm) and a side scatter laser (785 nm). The acquired cell data were analyzed using IDEAS 6.1.822.0 software (Luminex). All flow cytometry assays were performed as described previously (Park et al., 2020).

Cell Population

To study the cell populations − (i) whole leukocytes, (ii) supernatants and (iii) adherent cells − from three cell suspensions from HK or DI, aliquots containing > 5 × 10^5 cells were washed with 500 μL PBS by centrifugation (500 × *g*, 5 min, 4°C) and resuspended in 50 μL PBS. Prior to loading the tubes containing the cells in the flow cytometer, 1 μL of propidium iodide (PI, 1 mg/mL, Sigma) was added to differentiate between the dead and live cells as well as to estimate the cell types based on the morphology of their nucleus. From each sample, more than 10,000 cell images were acquired using two lasers with optimized voltage levels, 488 nm (1 mW) and 785 nm (0.47 mW). Thereafter, using IDEAS software, dead cells were excluded based on PI positivity; both are shown in a brightfield (BF) area (cell size) vs. side scatter (SSC) intensity (cell granularity) plot.

Phagocytosis Assay

To compare the phagocytic activity of whole leukocytes and adherent cells (i and iii mentioned under flow cytometry studies), aliquots containing 0.5 × 10^5 cells in 100 μL L-15 + were incubated with fluorescent bio-particles (pHrodo^{TM} Red *Escherichia coli* Bioparticles, Thermo Fisher Scientific), at a cell and particle ratio of 1:5 for 2 h at 12°C. After incubation, the cells were washed once with 500 μL PBS by centrifugation (500 × *g*, 5 min, 4°C) and resuspended in 50 μL PBS. Thereafter, the tubes containing cells were loaded in the flow cytometer and more than 10,000 cell images were acquired using two lasers with optimized voltage levels, 488 nm (50 mW) and 785 nm (0.47 mW). Data analyses were performed following our previous protocol (Park et al., 2020). Phagocytic ability was measured as the percent of phagocytic cells in total cells while phagocytic capacity was calculated as the mean number of particles in each phagocyte as described previously (Park et al., 2020).

Transcriptomic Analysis

The main aim of the RNA-Seq analysis was to obtain a snapshot of the expression profiles of selected genes. To compare the expression of genes linked to the adherent cells from HK and DI, 12 libraries were prepared (n = 6). The list of selected genes used in this study is comprised of (1) 34 cell type (macrophage, dendritic cell, endothelial cell, T and B cells)-related genes and (2) 42 other immune-related (cytokines, chemokines, mucins and toll-like receptors) genes, as shown in **Tables 1** and **2**, respectively.

RNA Isolation, Library Preparation and Illumina Sequencing

Total RNA was extracted from the adherent cells that were isolated from HK and DI (<500,000 cells) using the PicoPure RNA isolation kit (Thermo Fisher Scientific) according to the manufacturer's protocol. The quality and quantity of total RNA were assessed using Agilent RNA high sensitivity screen tape kits and Bioanalyzer 2200 TapeStation system (Agilent Technologies, Santa Clara, CA, United States). RNA sequencing libraries were prepared using the NEBNext Ultra II Directional RNA library preparation kit with poly (A) mRNA magnetic isolation module (NEB #E7490; New England BioLabs® , Herts, United Kingdom), according to the manufacturer's protocol. For the first and second strand cDNA synthesis, 50 ng of total RNA having high RNA integrity number (RIN > 8) was enriched with Oligo(dT)-conjugated magnetic beads and fragmented to ∼200 nt. Thereafter, the resulting cDNA were end-repaired for adaptor ligation. The ligated cDNAs were amplified with barcoded primers on a thermal cycler for 14 cycles. The PCR products were purified using AMPure XP beads (Beckman Coulter Inc., Brea, CA, United States) to avoid contamination from residual adapter dimers and unwanted (smaller) fragments. After library preparation, the quality and quantity of individual libraries were assessed using Agilent DNA high sensitivity screen tape kits and Bioanalyzer 2200 TapeStation system. These barcoded individual libraries were pooled at equimolar ratios and sequenced as single−end reads (75 bp) on an Illumina NextSeq 500 sequencer (Illumina, San Diego, CA, United States) with

TABLE 1 | List of abbreviations and details of genes expressed in macrophages, dendritic cells, endothelial cells, T and B cells.

Abbreviations	Gene name	Ensembl/GenBank ID
cd68	CD68	ENSSSAG00000002993
cd200r1	CD200 receptor 1A-like	ENSSSAG00000039924
mmd	monocyte to macrophage differentiation protein	ENSSSAG00000001828
csf1r	macrophage receptor MARCO-like	ENSSSAG00000063051
marco	macrophage colony stimulating factor receptor-like protein	ENSSSAG00000061479
mpeg1	macrophage expressed 1	ENSSSAG00000076214
capg	macrophage-capping protein-like	ENSSSAG00000003660
h2-eb1	H-2 class II histocompatibility antigen, I-E beta chain	XM_014133067
cd74	HLA class II histocompatibility antigen gamma chain-like	ENSSSAG00000004635
cd80	CD80-like	ENSSSAG00000056420
cd83	CD83 antigen	ENSSSAG00000057240
cd209	CD209 antigen-like	XM_014194638
cd3gda	CD3gammadelta-A	ENSSSAG00000009995
cd3z	CD3zeta-1	ENSSSAG00000055061
cd42al	truncated CD4-2A-like protein	ENSSSAG00000076595
cd8a	CD8 alpha	ENSSSAG00000065860
cd8b	CD8 beta	ENSSSAG00000045680
cd28	T-cell-specific surface glycoprotein CD28-like	ENSSSAG00000060163
cd2l	T-cell surface antigen CD2-like	XM_014129565
cd96	T-cell surface protein tactile-like	XM_014129863
trbc1	T-cell receptor beta-1 chain C region-like	NC_027300
trgc2	T-cell receptor gamma chain C region C10.5-like	NC_027319
cd6l	T-cell differentiation antigen CD6-like	ENSSSAG00000057293
tcd80l	T-lymphocyte activation antigen CD80-like	ENSSSAG00000056420
tagap	T-cell activation GTPase activating protein	ENSSSAG00000061533
igm	IgM	XM_014203125
cd48l	CD48 antigen-like	ENSSSAG00000064252
cd79a	B-cell antigen receptor complex-associated protein alpha chain-like	ENSSSAG00000003014
blnk	B-cell linker	ENSSSAG00000065613
bcap29	B cell receptor associated protein 29	ENSSSAG00000074312
bcl9l	B-cell CLL/lymphoma 9 protein-like	ENSSSAG00000063108
ecscr	endothelial cell-specific chemotaxis regulator-like	XM_014129374
cd151al	CD151 antigen-like	ENSSSAG00000065694
pecam	platelet endothelial cell adhesion molecule-like	ENSSSAG00000001458

NextSeq 500/550 high output v2 reagents kit (Illumina) at the sequencing facility of Nord University, Bodø, Norway.

Bioinformatics Analyses

All bioinformatics analyses of RNA-Seq data were performed as described previously by Zhang et al. (2018). The obtained raw sequencing data was deposited in the Gene Expression Omnibus (GEO, NCBI); the accession number is GSE154142. Briefly, raw sequence data were converted to FASTQ format with bcl2fastq2 (v2.17, Illumina). The adapter sequences were removed using cutadapt (version 1.12) with the following the parameters: -q 20 –quality-base = 33 -m 20 –trim-n. The quality of the trimmed fastq files (clean reads) was then assessed using FastQC (Andrews, 2010), and the reads with quality > Q30 were mapped to the Atlantic salmon genome ICSASG_v2 from RefSeq[1]. The mapped reads were quantified and then annotated using gff3 annotation file. The generated data was normalized using DESeq2 (Love et al., 2014), and the normalized data was used for statistical comparisons, i.e., to determine the differences in the expression of selected immune-related genes in AIC and AKC. The package, DESeq2 employs shrinkage estimation for dispersions and fold changes. The R packages ggplot2 version 3.1.1 (Wickham, 2016) were employed to prepare and format the graphs. A heatmap was prepared using the functions from the package ComplexHeatmap (Gu, 2015).

Statistical Analyses

Statistical analysis was performed using RStudio version 1.1.463. Normality of the flow cytometry and gene expression data was tested by Shapiro-Wilk Test, and the assumption of equal variance was checked by Bartlett's Test. Comparisons between groups were performed using unpaired Student's *t*-test. The differences were considered significant at $p < 0.05$.

[1]https://www.ncbi.nlm.nih.gov/assembly/GCF_000233375.1/

TABLE 2 | List of abbreviations and details of genes coding for selected cytokines, chemokines, mucins, and toll-like receptors.

Abbreviations	Gene name	Ensembl/GenBank ID
tgfbr1	Transforming growth factor beta receptor type-1-like	ENSSSAG00000079756
tgfbr2	Transforming growth factor beta receptor type-2	ENSSSAG00000071570
tab2	Transforming growth factor beta-activated kinase 1 and MAP3K7-binding protein 2-like	ENSSSAG00000074549
traf2	Tumor necrosis factor receptor associated factor 2	ENSSSAG00000046864
tnfa2	Tumor necrosis factor alpha-2 precursor	ENSSSAG00000053783
tnfaip2	Tumor necrosis factor alpha-induced protein 2-like	XM_014143804
tnfrsf6b	Tumor necrosis factor receptor superfamily member 6b	ENSSSAG00000044783
tnfrsf10a	Tumor necrosis factor receptor superfamily member 10A-like	ENSSSAG00000049387
tnfsf11	Tumor necrosis factor superfamily member 11	ENSSSAG00000053734
tnfrsf13b	Tumor necrosis factor receptor superfamily member 13B-like	ENSSSAG00000079103
il1b-like	Interleukin-1 beta-like	ENSSSAG00000060993
irak3-like	Interleukin-1 receptor-associated kinase 3-like	ENSSSAG00000051931
il1rl1	Interleukin-1 receptor-like protein	ENSSSAG00000069876
il1rap	Interleukin 1 receptor accessory protein	ENSSSAG00000043510
il6r	Interleukin-6 receptor subunit alpha	ENSSSAG00000052467
il6rb	Interleukin-6 receptor subunit beta-like	ENSSSAG00000061284
il8	Interleukin 8	ENSSSAG00000006498
il12rb2	Interleukin-12 receptor beta-2 chain	ENSSSAG00000042273
il17rcl	Interleukin-17 receptor C-like	ENSSSAG00000007189
il17rel	Interleukin-17 receptor E-like	XM_014134812
il31ra	Interleukin-31 receptor A	ENSSSAG00000062925
cxcr1l	C-X-C chemokine receptor type 1-like	ENSSSAG00000042001
ccl2l	C-C motif chemokine 2-like	XM_014191804
cxcr3l	C-X-C chemokine receptor type 3-like	ENSSSAG00000051147
ccr3	C-C chemokine receptor type 3	ENSSSAG00000042484
cxcr4l	C-X-C chemokine receptor type 4-like	ENSSSAG00000050781
cxcr5l	C-X-C chemokine receptor type 5-like	ENSSSAG00000040121
ccr5l	C-C chemokine receptor type 5-like	ENSSSAG00000072678
ccr6l	C-C chemokine receptor type 6	ENSSSAG00000076547
ccr9l	C-C chemokine receptor type 9-like	ENSSSAG00000070198
ccl19l	C-C motif chemokine 19-like	ENSSSAG00000002773
ccl20l	C-C motif chemokine 20-like	ENSSSAG00000051350
ccl25	C-C motif chemokine 25	ENSSSAG00000071212
muc1	mucin 1, cell surface associated	XM_014160723
muc5acl	Mucin-5AC-like	ENSSSAG00000080927
muc13l	Mucin-13-like	ENSSSAG00000069082
muc17l	Mucin-17-like	ENSSSAG00000047784
cd164l2	CD164 sialomucin-like 2 protein	XM_014143111
tlr2	Toll-like receptor 2	ENSSSAG00000003781
tlr6	Toll-like receptor 6	ENSSSAG00000079217
tlr8	Toll-like receptor 8	ENSSSAG00000074528
tlr13	Toll-like receptor 13	ENSSSAG00000077966

RESULTS

Diverse Cells Among Salmon Distal Intestine Cell Population

We explored the cell populations from salmon DI by employing IFC. After dead cell exclusion, approximately 90% of viable cells (negative for PI) were obtained; shown in a BF area (cell size) vs. SSC intensity (cell granularity) plot (**Figure 1A**). Because we have already revealed the identity of the HK cell population in our previous study (Park et al., 2020) here we show only the DI cell population in **Figure 1**. The gating strategy that was developed previously by Park et al. (2020) was employed for DI cell populations (**Figure 1A**: LYM, lymphocyte; MON, monocyte/macrophage; R1, macrophage-like cells). Nucleus morphologies were revealed through PI staining (**Figures 1B,C**). Only PI negative live cells (**Figure 1B**) were considered for the gating shown in **Figure 1A**; cells in the gates LYM, MON, and R1 had spherical and fairly rigid nuclei while those in the gate R2 had relatively smaller and different shaped nuclei. We found that there are diverse cells in the isolated salmon DI cell population.

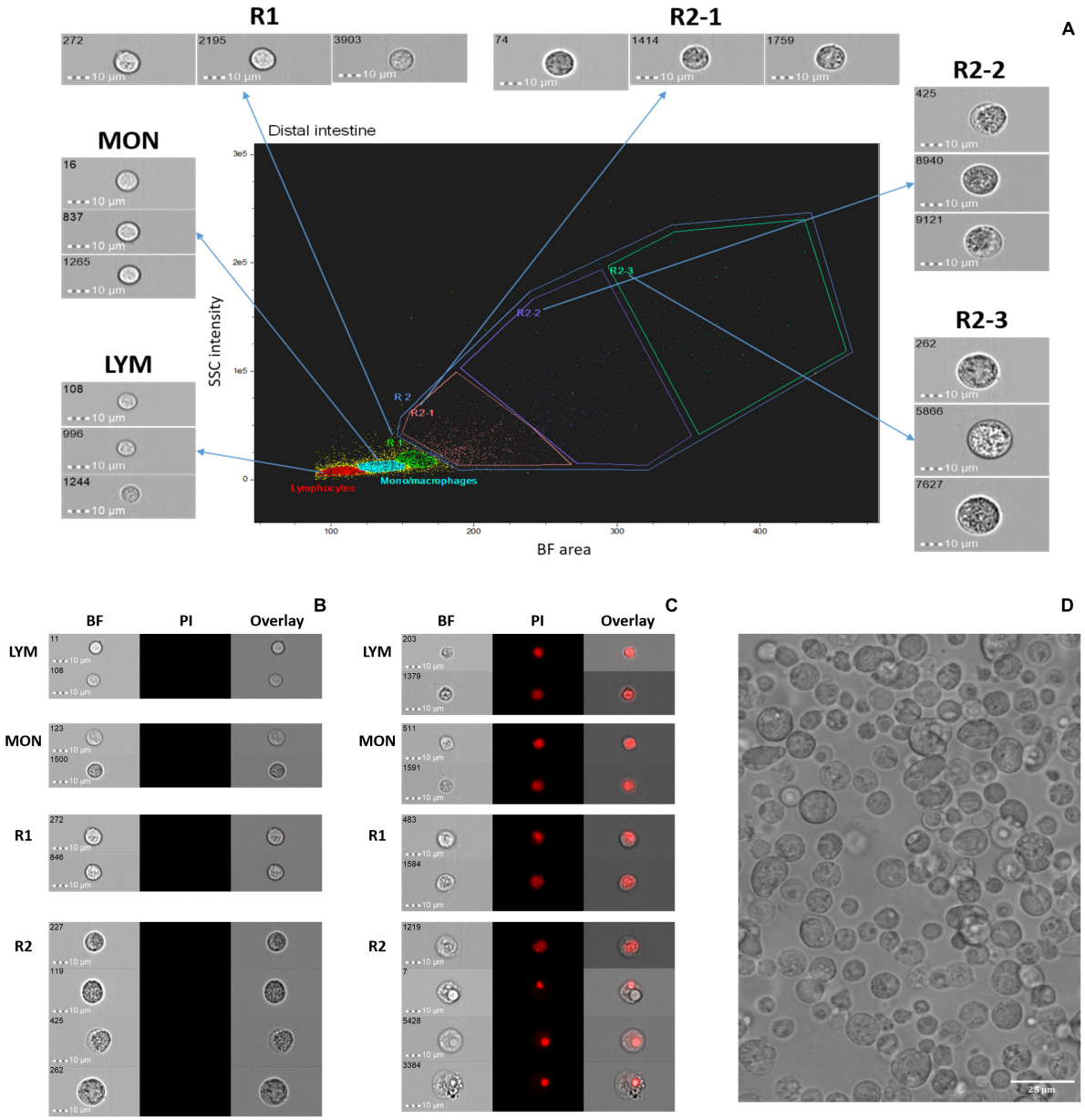

FIGURE 1 | Cell populations from Atlantic salmon distal intestine. **(A)** Live cells are shown in a brightfield (BF) area (cell size) vs. side scatter (SSC) intensity plot (cell granularity). Representative images (40 × objective, scale bar = 10 μm) from each gate are shown separately. Intestinal cells were identified based on nucleus morphologies. Using propidium iodide, live or no-stained cells **(B)** and dead or nucleus-stained cells **(C)** are shown. **(D)** A representative image captured by fluorescent imager (20 × objective, scale bar = 25 μm) shows salmon intestinal cell population. LYM, lymphocytes; MON, monocytes/macrophages; R, region: R1, macrophage-like cells; R2, unknown cells; R2-1, R2-2, presumptive granulocytes; R2-3, presumptive vacuolated cells.

A representative image of the DI cell images from among 6 images captured (to confirm the quality of the harvested DI cells) by the fluorescent imager is shown in **Figure 1D**.

Adherent Cells From Salmon Distal Intestine Exhibit Phagocytic Ability

The cell populations – whole leukocytes (HKL and DIL, respectively), supernatants (HS and DS, respectively) and adherent cells (AKC and AIC, respectively) – from three cell suspensions from HK or DI are shown in **Figures 2A–C** and **Figures 2E–G**, respectively. The reference AKC had macrophage population, located in higher BF area and higher SSC intensity compared to those of head kidney supernatant-derived cells (HS, red gates; **Figures 2B–D**). In the DI cells, the cell populations were more scattered, as evident in the dotplot (considering the BF area values). However, AIC apparently had a lower percentage of the cells in the gated area compared to those of distal intestine supernatant-derived cells (DS, red gates; **Figures 2F–H**).

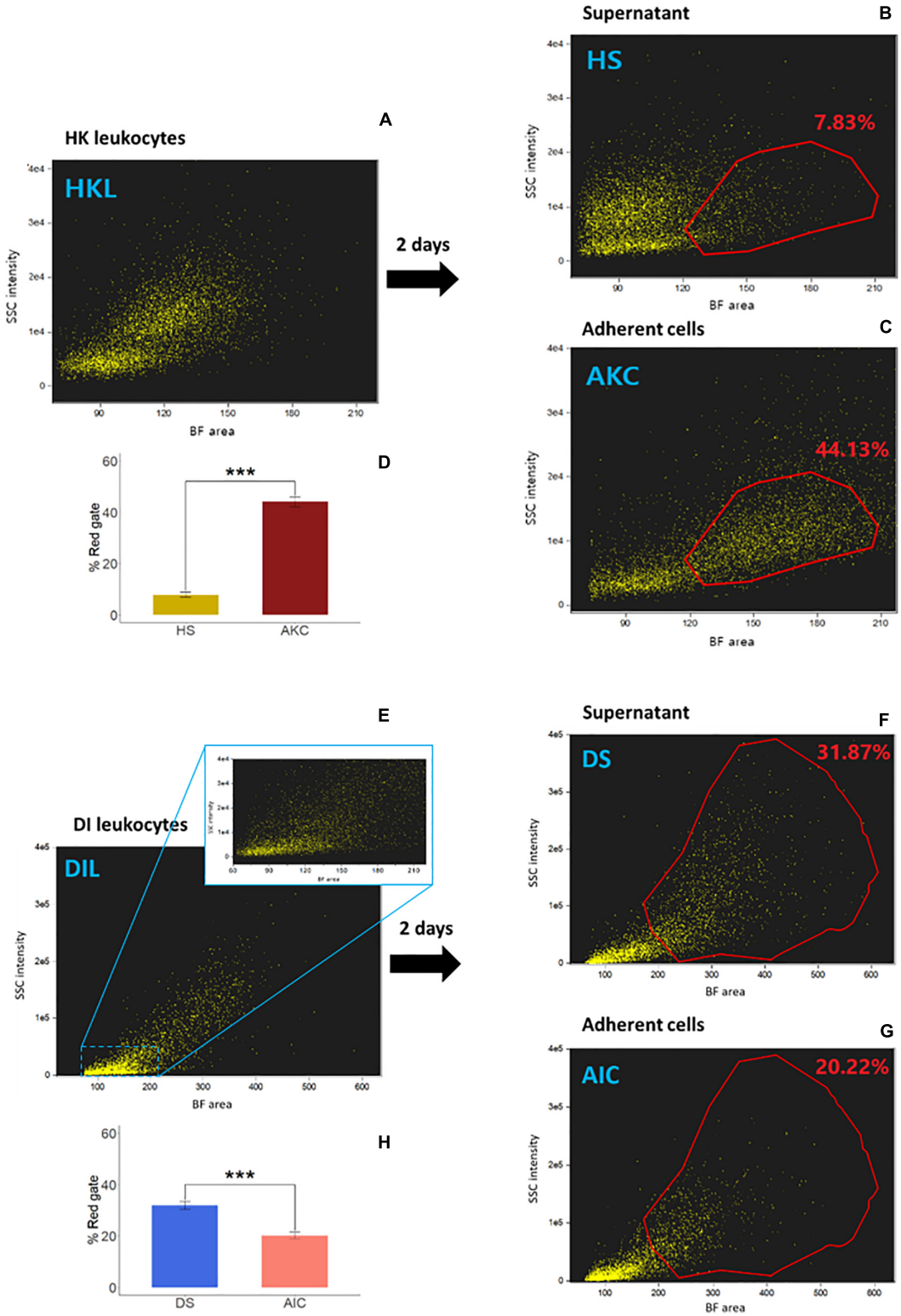

FIGURE 2 | Examination of adherent cell population from Atlantic salmon head kidney and distal intestine by imaging flow cytometry. We compared cell populations from three cell suspensions; (**A** and **E**) whole leukocytes (HKL and DIL, respectively), (**B** and **F**) supernatants (HS and DS, respectively) and (**C** and **G**) adherent cells (AKC and AIC, respectively) in a brightfield (BF) area (cell size) vs. side scatter (SSC) intensity plot (cell granularity) using IFC. The bar plots (**D** and **H**) indicate percent of the cells in the red gates in supernatants (**B** and **F**) vs. those in adherent cells (**C** and **G**, respectively). Statistically significant differences ($p < 0.001$) are indicated using asterisks. Bar plots show the mean ± SD ($n = 6$).

To compare the phagocytic activity of whole leukocytes and adherent cells from HK (**Figures 3A–C**) and DI (**Figures 4A–C**), we quantified the uptake of *E. coli* BioParticles™ by the cells (Park et al., 2020). The phagocytic abilities of AKC and AIC were significantly higher than those of HKL and DIL (**Figures 3A**, **4A**), respectively. The phagocytes from AIC had different morphologies compared to AKC (**Figures 3C**, **4C**). Among AICs, along with single and round shaped phagocytes, we found oval shaped (5.69% of total phagocytes, **Figure 4D**) and doublets consisting of a phagocytic cell and an interacting cell (1.15% of total phagocytes, **Figure 4E**).

Adherent Cells From Distal Intestine of Salmon Express Macrophage and Immune-Related Genes

To understand the identity of cell types in AIC, the expression of selected genes in AIC was compared with those of AKC. We obtained over 312 million cleaned reads from 12 (6 from AIC and 6 from AKC) samples after adapter trimming and quality filtering. Of them, over 285 million reads were mapped to Atlantic salmon genome. Average mapping percentage among samples was 91.36% (**Supplementary Table 1**). The dispersion of the genes decreased with increase in mean of normalized counts (**Supplementary Figure 1**).

Employing the normalized read counts from DESeq2 analyses, we describe the expression of 34 cell-specific (macrophage, dendritic cell, endothelial cell, T and B cells) genes and 42 immune-related (cytokines, chemokines, mucins and toll-like receptors) genes in AIC compared to AKC. Lack of appropriate cell markers and unavailability of easy intestinal cell isolation techniques hamper the characterization of adherent cells. Therefore, we adopted the targeted analysis strategy to delineate the cell types by linking them to known genes.

The expression of 34 genes associated with macrophages, dendritic cells (DC), endothelial cells, T and B cells in AIC were compared to those in AKC (**Figures 5**, **6**). Among the 9 macrophage-related genes, the expression of 8 genes (*h2-eb1*, *cd74*, *cd68*, *marco*, *capg*, *mpeg1*, *cd200r1*, and *csf1r*) was significantly lower in AIC compared to AKC (**Figure 5A**). As for the DC specific genes (**Figure 5B**), AIC had significantly lower expression of *cd209* and *cd83* than those of AKC. As for the endothelial cell-related genes, the expression of *ecscr* and *cd151l* was significantly higher in AIC than in AKC though this was not the case for the *pecam* gene (**Figure 5C**).

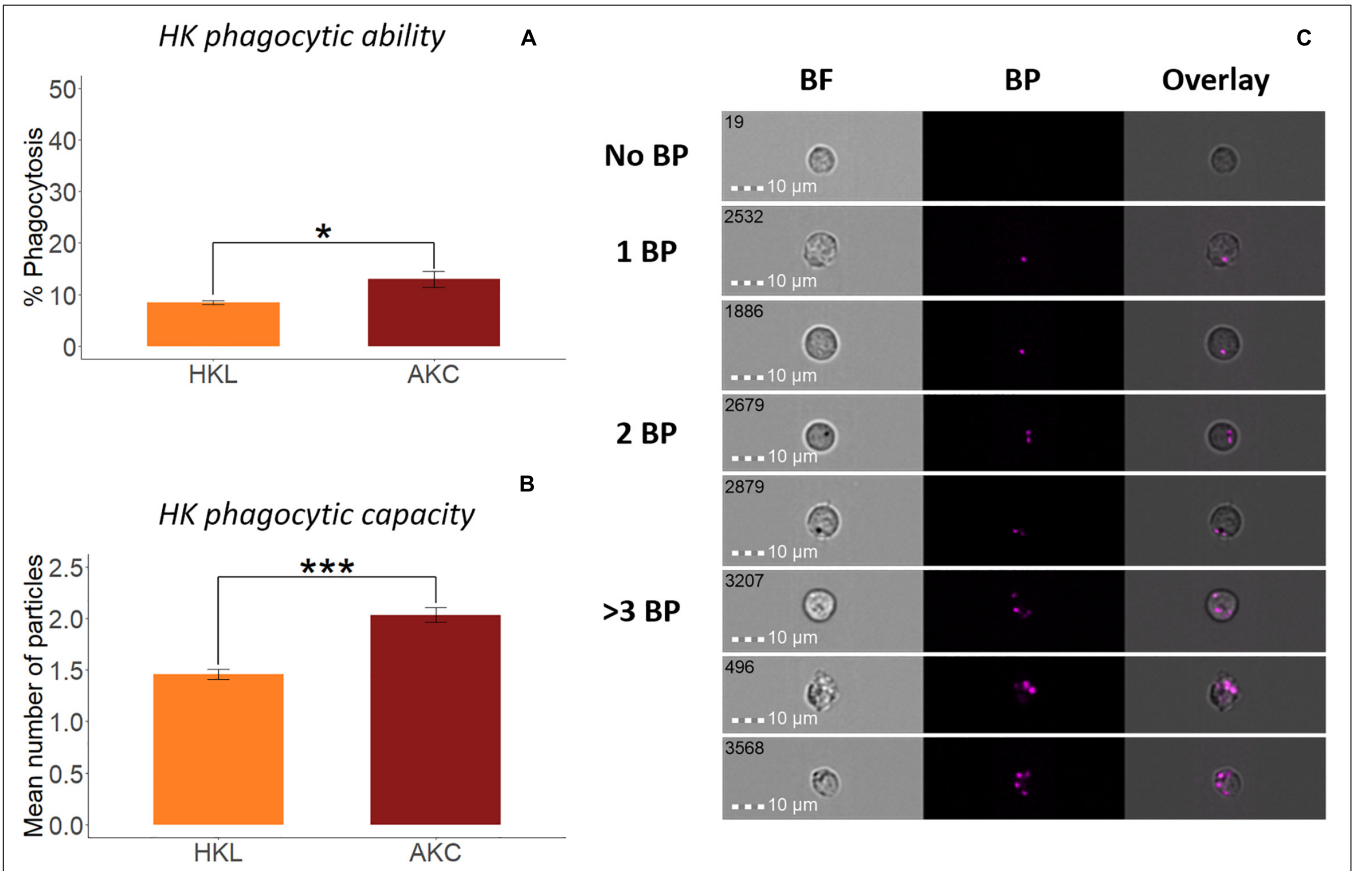

FIGURE 3 | Phagocytic activity of whole leukocytes and adherent cells from Atlantic salmon head kidney. Percent of phagocytic cells or phagocytic ability **(A)** and mean number of bio-particles (BP) ingested per phagocytic cell or phagocytic capacity **(B)** are shown. **(C)** Representative cell images show cells with no BP, and 1BP, 2BP, and >3BP. Statistically significant differences ($p < 0.05$) are indicated using asterisks. Bar plots show the mean ± SD ($n = 6$). All cell images were captured with 40 × objective. Scale bar = 10 µm. BF, brightfield; 1 BP, 2 BP, and > 3 BP, 1–3 internalized bio-particles.

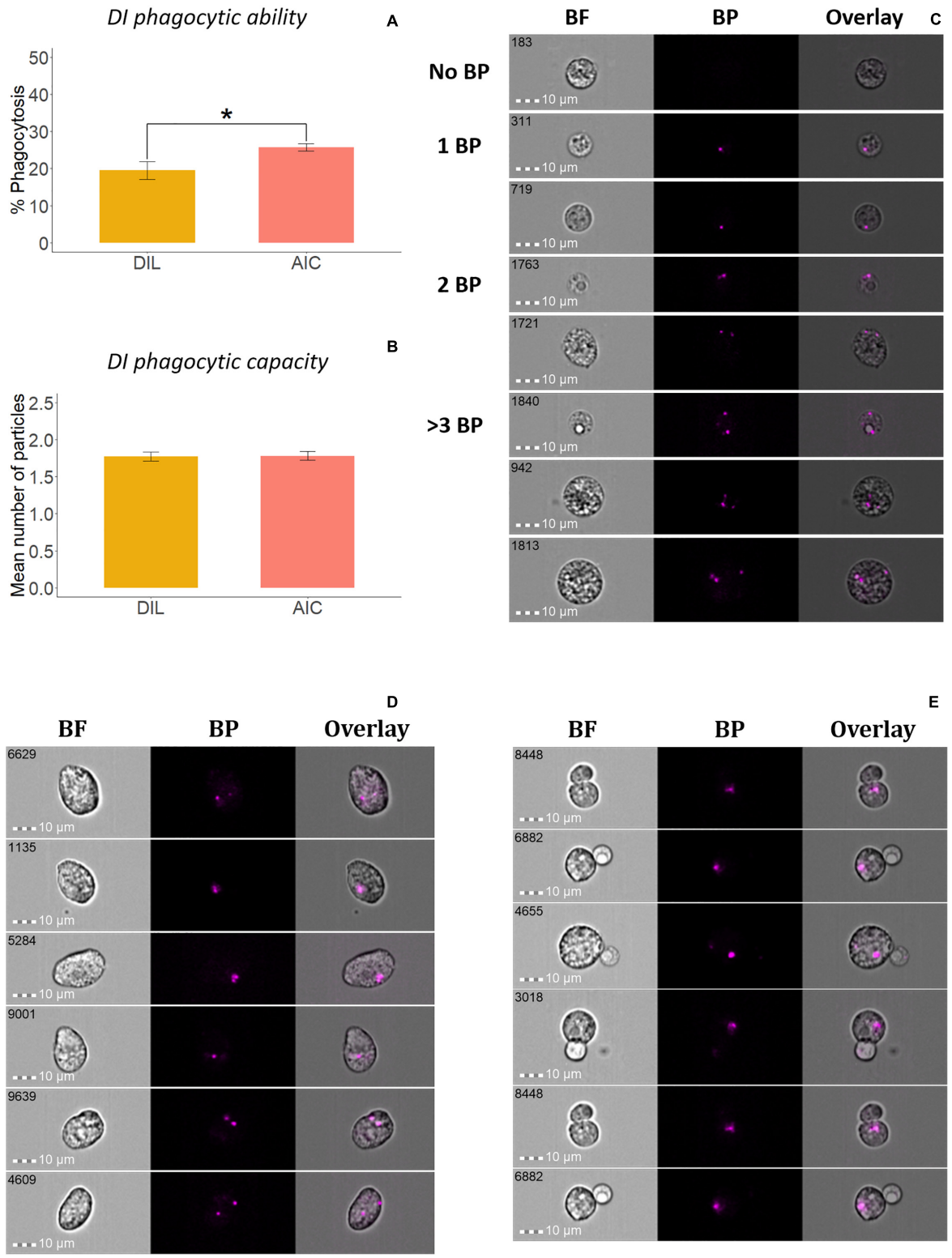

FIGURE 4 | Phagocytic activity of whole leukocytes and adherent cells from Atlantic salmon distal intestine. Percent of phagocytic cells or phagocytic ability **(A)** and mean number of bio-particles (BP) ingested per phagocytic cell or phagocytic capacity **(B)** are shown. **(C)** Representative cell images show cells with no BP, and 1BP, 2BP, and >3BP. Statistically significant differences ($p < 0.05$) are indicated using asterisks. In addition, oval shaped phagocytes **(D)** and doublets containing a phagocyte that interacts with a lymphocyte-like cell **(E)** were found among the adherent intestinal cells. Bar plots show the mean ± SD ($n = 6$). All cell images were captured with 40 × objective. Scale bar = 10 µm. BF, brightfield; 1 BP, 2 BP, and >3 BP, 1–3 internalized bio-particles.

Regarding the T and B cell-specific gene profile (**Figure 6**), AIC had significantly higher expression of most T cell-related genes (*cd96*, *tagap*, *cd3gda*, *cd8b*, *cd8a*, *cd6l*, *cd42al*, *cd28*, *trbc1*, *cd2l,* and *trgc2*), but significantly lower expression of B cell-related genes (*igm*, *blnk*, and *cd79a*).

The expression of 21 immune-related cytokine genes were also considered for the AIC vs. AKC comparisons (**Figure 7**). AIC had significantly lower expression of interleukin 1 and 6 receptors (*il1rap* and *il6r*) while the expression of tumor necrosis factor (TNF)-related genes (*tnfrsf10a*, *tnfsf11, traf2,* and *tnfrsf6b*) was significantly higher. Among the transforming growth factor (TGF)-related genes, the expression of TGFβ receptors (*tgfbr1* and *tgfbr2*) were significantly higher, while the expression of TGFβ activated kinase binding protein (*tab2*) was significantly lower in AIC.

Twelve immune-related genes of chemokines were also studied in AIC and AKC (**Figure 8A**). The expression levels of *ccr9l*, *ccl20l*, *ccr6l,* and *ccr5l* were significantly higher, while the expression of, *cxcr3l*, *ccr3*, *ccl25*, *cxcr4l*, *cxcr1l,* and *cxcr5l* was significantly lower in AIC.

The expression of 9 immune-related genes for mucin and toll-like receptor (TLR) were also compared to understand the differences in AIC and AKC (**Figures 8B,C**). Mucin-related genes (*muc13l*, *muc1*, *cd164l2*, and *muc5acl*) were mainly expressed in AIC but several TLR genes (*tlr13*, *tlr8*, *tlr2* and *tlr6*) were not predominantly expressed in AIC.

Hierarchical clustering-based heatmap along with the boxplot annotation shown in **Figure 9** reveals the gene profiles associated with AIC and AKC. Although the expression of the genes associated with AKC macrophages was significantly higher than those of AIC, both showed predominantly higher expression of the macrophage-specific genes than those of other cell types such as T and B cells.

DISCUSSION

The intestine has a key role in sustaining the health of fishes. Various cells in the intestine act in harmony to maintain the local (Okumura and Takeda, 2016) as well as systemic homeostasis (Biteau et al., 2011; Ramakrishnan et al., 2019). Of these cells,

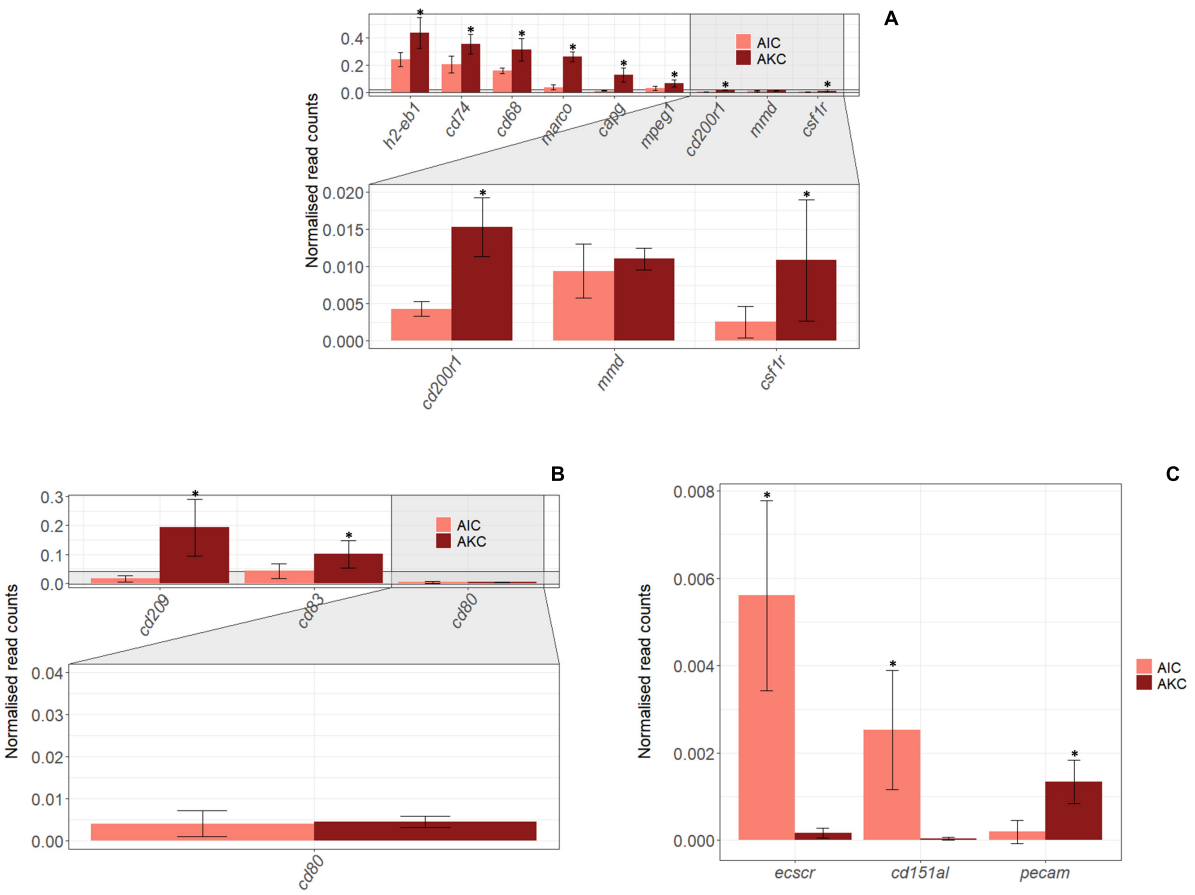

FIGURE 5 | The expression of genes linked to macrophages, dendritic cells and endothelial cells in the adherent cells from Atlantic salmon distal intestine and head kidney. Employing the normalized read counts from DESeq2 analyses, the expression of genes related to macrophages **(A)**, dendritic cells **(B)** and endothelial cells **(C)** were determined, and the expression levels between the adherent cells from salmon distal intestine (AIC) and head kidney (AKC) were compared. Statistically significant differences ($p < 0.05$) are indicated using asterisks. Bar plots show the mean ± SD. Sample size = 6.

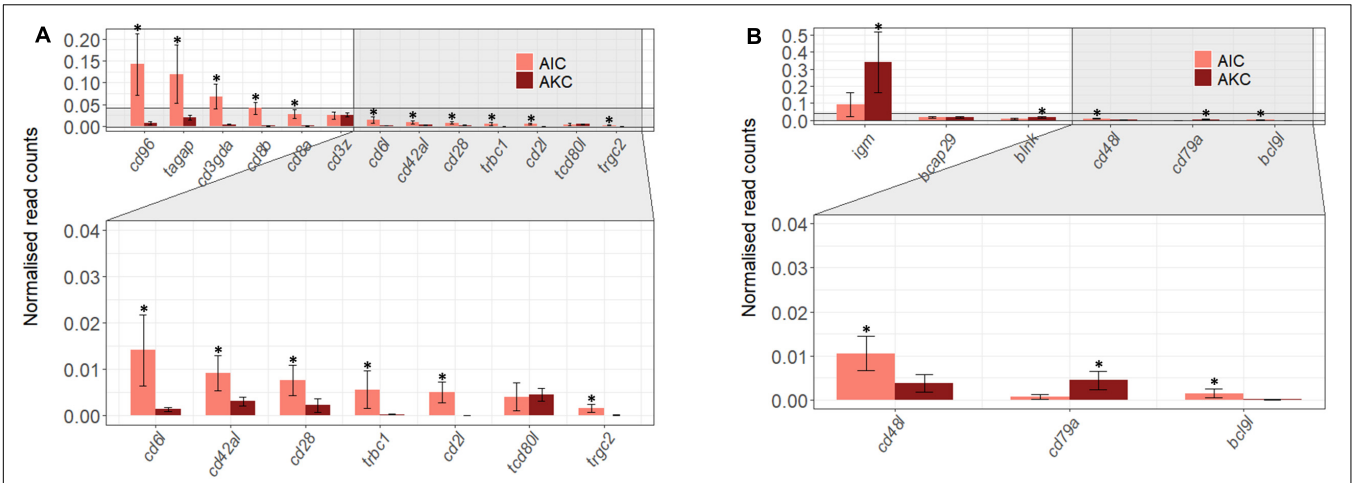

FIGURE 6 | The expression of genes related to T and B cells in the adherent cells from Atlantic salmon distal intestine and head kidney. Employing the normalized read counts from DESeq2 analyses, the expression of T **(A)** and B cells **(B)** associated genes in the adherent cells from salmon distal intestine (AIC) and head kidney (AKC) were compared. Statistically significant differences ($p < 0.05$) are indicated using asterisks. Bar plots show the mean ± SD ($n = 6$).

the GALT cells are imperative in responding to antigens, both benign and pathogenic. The immune cells that are developed in the main lymphoid site enter the circulation, and along with the GALT cells they surveil the host immune status. In the present study, we obtained leukocytes from DI and HK of Atlantic salmon and then separated the adherent cells from the two cell populations.

Employing IFC, we examined the phagocytic activity of the adherent intestine cells and compared it with those of adherent head kidney cells. We also examined the expression of immunologically relevant genes through RNA-Seq of the cells from the two key immune organs of Atlantic salmon.

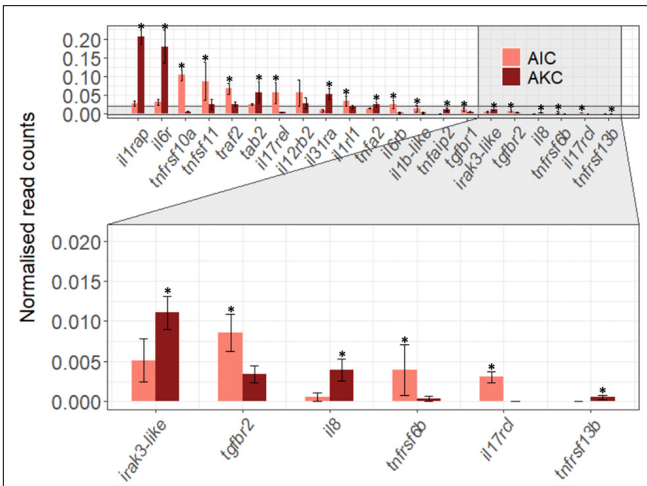

FIGURE 7 | The expression of cytokine-related genes in the adherent cells from Atlantic salmon distal intestine and head kidney. Employing the normalized read counts from DESeq2 analyses, the expression of cytokine-related genes in the adherent cells from salmon distal intestine (AIC) and head kidney (AKC) were compared. Statistically significant differences ($p < 0.05$) are indicated using asterisks. Bar plots show the mean ± SD ($n = 6$).

AIC had distinct cell population; the cells were less diverse than the whole leukocyte population. Other researchers were also able to isolate cells from the intestine of Atlantic salmon (Attaya et al., 2018) and gilthead seabream (Salinas et al., 2007), but they did not specifically examine adherent cells. The major phagocytes in vertebrates are neutrophils, monocytes, macrophages, mast cells, and immature dendritic cells (Robinson and Babcock, 1998). In the present study, we confirmed the phagocytic ability of AIC, which had different shapes compared with those of AKC. Unlike monocyte-derived macrophages which have mainly stretched shapes, the AIC appeared larger and rounded as shown in a mice study (Vereyken et al., 2011). Rombout et al. (1998) reported that the carp intestinal cells are diverse compared to the cells from other immunological tissues such as spleen and head kidney. In addition to many round-shaped cells, the oval shaped phagocytes, similar to the ones we observed, are reported as endothelial cells in mammals, and they were shown to have the ability to internalize pathogenic bacteria (Rengarajan et al., 2016). Furthermore, Lindell et al. (2012) showed that oval-shaped skin epithelial cells in trout can perform phagocytosis of *Vibrio anguillarum*. However, their identity has to be validated by employing specific cell markers. As for the doublets in the adherent cells, the phagocytes in them resembled macrophage-like cells (R1, **Figure 1A**) while the interacting small cells had a morphology similar to that of lymphocytes. A study that investigated mouse intestinal cells using imaging flow cytometry (Zhao et al., 2014) indicated that similar doublets consisted of $CD103^+$ intestinal dendritic cells and $CD4^+$ T cells. From our results, we infer that the oval-shaped cells similar to endothelial cells or epithelial cells with phagocytic ability may have special roles in mucosal immune system. In addition, the presence of the doublets indicates the interaction between

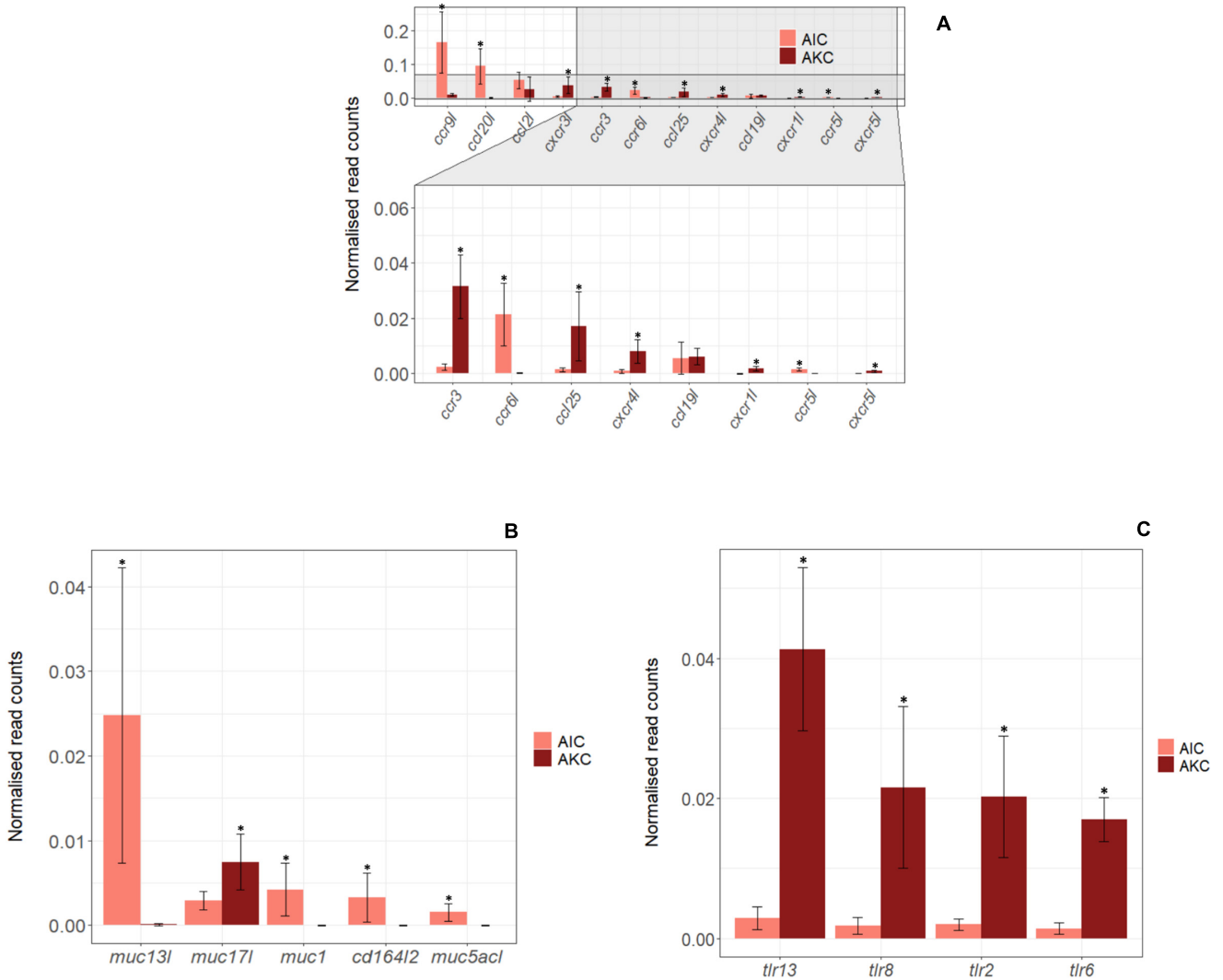

FIGURE 8 | The expression of genes related to chemokines, mucins and toll-like receptors in the adherent cells from Atlantic salmon distal intestine and head kidney. Employing the normalized read counts from DESeq2 analyses, the expression of genes related to chemokines **(A)**, mucins **(B)** and toll-like receptors **(C)** in the adherent cells from salmon distal intestine (AIC) and head kidney (AKC) were compared. Statistically significant differences ($p < 0.05$) are indicated using asterisks. Bar plots show the mean ± SD ($n = 6$).

phagocytes and lymphocyte-like cells that cooperate with them in immune defense.

In the present study, considering the phagocytic ability and high expression levels of macrophage genes in AIC we presume that majority of cell types in AIC are macrophages. Salmon macrophages can be effectively harvested after culturing adherent cells from HK (Paulsen et al., 2001). The presence of macrophages in adherent cells from fish intestine and their phagocytic properties have not been reported yet. In the present study, high levels of TNF-related genes (*tnfrsf10a*, *tnfsf11*, *traf2* and *tnfsf6b*) and TGFβ receptors (*tgfbr1* and *tgfbr2*) in AIC can be linked to activation and proliferation of macrophages (Luckett-Chastain et al., 2016; Yu et al., 2017) and T cells (McKarns and Schwartz, 2005; Mehta et al., 2018) while high levels of *il1* and *il6* in AKC can be linked to the classical activation of macrophages (Luckett-Chastain et al., 2016). We have also found that the expression of eight macrophage-related genes (*h2-eb1*, *cd74*, *cd68*, *marco*, *capg*, *mpeg1*, *cd200r1*, and *csf1r*) was highest in AIC among selected cell type linked genes (**Figure 9**) although the expression in AKC was significantly higher than those of AIC (**Figure 5**). Our results are in agreement with another HK transcriptomic study; carp HK macrophage-like cells had higher expression of *cd68* and *mcsfr* compared to those of HK leukocytes (Hu et al., 2018). Furthermore, a study conducted by Jenberie et al. (2018) revealed the higher expressions of *csf1r* and *marco* in HK macrophage-like cells. Another salmon study indicated the higher expression of MHCIIβ in the adherent cells from the head kidney (Iliev et al., 2019), and we found that the expression of *h2-eb1* gene was higher in AKC. This gene in association with MHC class II plays a role in the

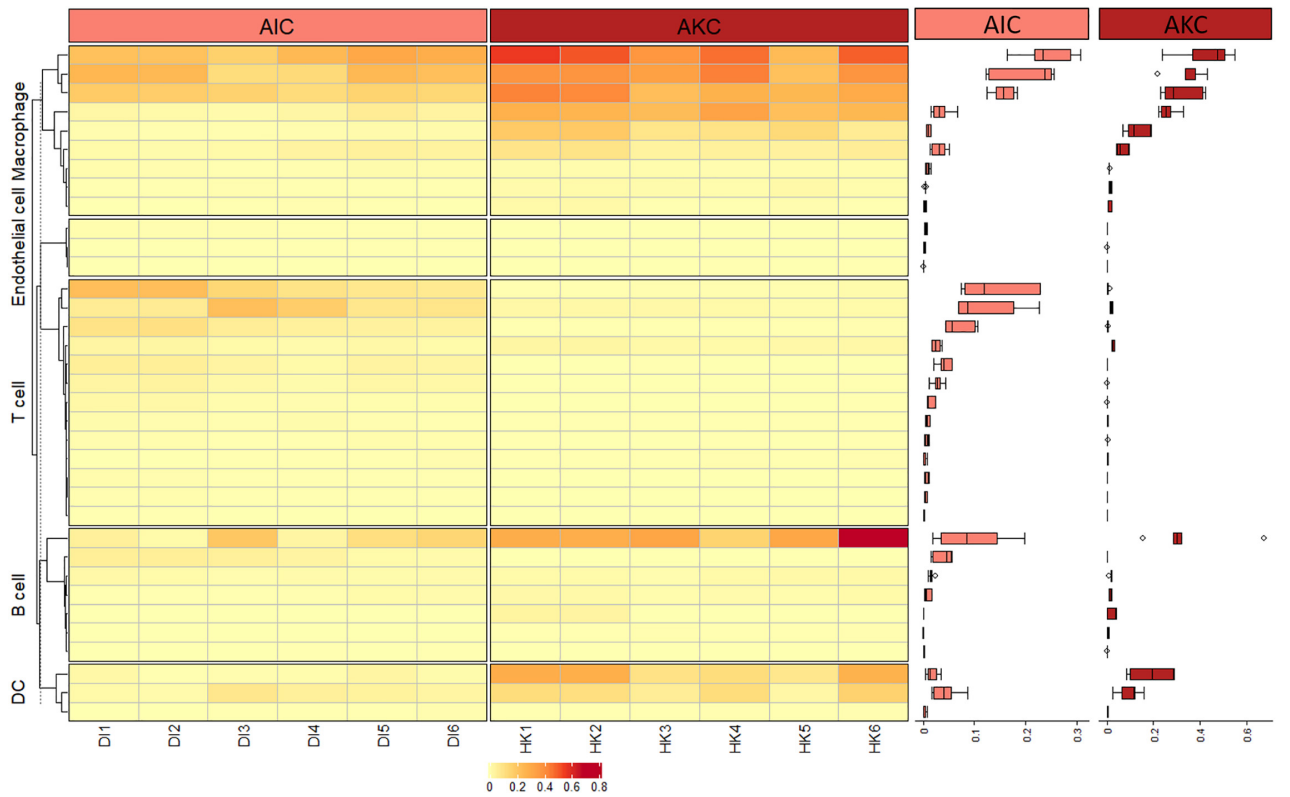

FIGURE 9 | Heatmap of the expression of selected genes in the adherent cells from Atlantic salmon distal intestine and head kidney. Box plots indicate the expression of genes related to macrophages, dendritic cells, endothelial cells, T and B cells. The color gradient from light yellow to dark red in the heatmap indicates increasing transcript levels.

processing and presentation of antigens (Adamus et al., 2012), and teleost mucosa has major T cells receptors (TCR) such as TCRαβ and TCRγδ, and their respective co-receptors, namely CD4 and CD8, which facilitate antigen recognition (Toda et al., 2011). The presence of T cells in fish intestine was reported years ago by Rombout et al. (1998). Another study (Romano et al., 2007) also indicated the abundance of T cells and TCRβ$^+$ lymphocytes in the posterior intestine and mid-intestine of seabass, respectively. In addition, CD3ε$^+$ cells are abundant in salmonid immune organs including intestine (Koppang et al., 2010). Our results about the higher expression of T cell-related genes and *h2-eb1* in AIC and the doublets could be pointing to the cooperation between the adherent cell populations. AIC had higher expression of chemokines, probably those related to T cells. Furthermore, three chemokines (*ccr9l*, *ccl20l,* and *ccr6l*) were dominantly expressed in AIC. It has been reported that mammalian CD4$^+$ T cells express *ccr9* (Cosorich et al., 2019) while *ccl20* and *ccr6* are expressed on CD8$^+$ T cell (Kondo et al., 2007; Kish, 2015). The chemokines that are highly expressed in AKC are related to macrophage activation: teleost macrophage-like cells express *cxcr3l* (Lu et al., 2017), *ccl25* (Aquilino et al., 2016) and *cxcr4l* (Chia et al., 2018) while mammalian macrophages express *ccr3* (Park et al., 1999). In present study, higher expression levels of *ccr9l*, *ccl20l,* and *ccr6l* may be indicating the presence of T cells in AIC. Furthermore, considering our hypothesis that the adherent cells could be mainly phagocytes, the expression of T cell-related genes in the intestine could be suggestive of their critical role in mucosal immune system. A study on zebrafish (Wan et al., 2017) showed that γδ T cells which are generally abundant in the intestinal epithelium have potent phagocytic ability. In addition, the phagocytic activity of AIC and the finding of a previous study on the ability of oval-shaped mammalian endothelial cells to internalize pathogens (Rengarajan et al., 2016) likely indicate the phagocytic property of endothelial cells in AIC. We found that AIC had significantly higher expression of endothelial genes (*ecscr* and *cd151l*) while AKC had higher expression of *pecam* gene. Both *ecscr* and *cd151* are known as general signatures of mammalian endothelial cells (Verma et al., 2010; Yang et al., 2017) though they have not yet been reported in fish. On the other hand, *pecam* (or *cd31*) is a gene associated with endothelial cell adhesion molecule and it was highly expressed within blood vascular compartment (Privratsky and Newman, 2014). Furthermore, the presence of the mucin-like receptor, *cd164* could be an indication of the ability of certain cells in AIC to adhere to endothelial cells (Havens et al., 2006).

In summary, employing IFC and transcriptomics, we were able to characterize the adherent cell populations from DI, based on the genes reported as specific to certain cell types.

AIC had different-shaped phagocytes and expressed genes associated with macrophages, T cells, and endothelial-like cells. Overall (selected) gene profiles show that AIC predominantly express macrophage-related genes. Further investigation on the transcriptomic responses of the intestinal cells to different antigens will help to expand our understanding of their crosstalk at the mucosal surfaces in teleosts.

DATA AVAILABILITY STATEMENT

The obtained raw sequencing data was deposited in the Gene Expression Omnibus (GEO, NCBI); the accession number is GSE154142.

ETHICS STATEMENT

The animal study was reviewed and approved by National Animal Research Authority in Norway (Mattilsynet; FOTS ID 10050).

AUTHOR CONTRIBUTIONS

YP, JF, and VK conceived and designed the study. YP performed the experiments on the cells and wrote the first draft of the manuscript. YP and QZ conducted RNA sequencing and data analysis. GW provided suggestions to improve the manuscript. YP, QZ, GW, JF, and VK read, revised and approved the manuscript for submission. All authors contributed to the article and approved the submitted version.

FUNDING

The INFISH project (272004) funded by the Regionale Forskningsfond Nord-Norge partly supported this study. YP is a recipient of the Korean Government Scholarship—National Institute for International Education, South Korea.

ACKNOWLEDGMENTS

The authors, especially YP, is grateful to Bisa Saraswathy for her valuable support in data analyses, discussions and comments on the manuscript. The authors would like to thank the staff at the Research Station, Nord University for their help in the laboratory.

SUPPLEMENTARY MATERIAL

The Supplementary Material for this article can be found online at: https://www.frontiersin.org/articles/10.3389/fcell.2020.580848/full#supplementary-material

Supplementary Figure 1 | Dispersion estimation plot. The plot indicates the shrinkage of the gene-wise dispersions.

Supplementary Table 1 | Details of raw reads, cleaned reads and mapped reads from different samples.

REFERENCES

Adamus, G., Brown, L., Andrew, S., Meza-Romero, R., Burrows, G. G., and Vandenbark, A. A. (2012). Neuroprotective effects of recombinant T-cell receptor ligand in autoimmune optic neuritis in HLA-DR2 mice. *Invest. Ophthalmol. Vis. Sci.* 53, 406–412. doi: 10.1167/iovs.11-8419

Andrews, S. (2010). *FastQC: A Quality Control Tool for High Throughput Sequence Data. Babraham Bioinformatics*. Cambridge: Babraham Institute.

Aquilino, C., Granja, A. G., Castro, R., Wang, T., Abos, B., Parra, D., et al. (2016). Rainbow trout CK9, a CCL25-like ancient chemokine that attracts and regulates B cells and macrophages, the main antigen presenting cells in fish. *Oncotarget* 7, 17547–17564. doi: 10.18632/oncotarget.8163

Attaya, A., Wang, T., Zou, J., Herath, T., Adams, A., Secombes, C. J., et al. (2018). Gene expression analysis of isolated salmonid GALT leucocytes in response to PAMPs and recombinant cytokines. *Fish Shellf. Immunol.* 80, 426–436. doi: 10.1016/j.fsi.2018.06.022

Bernard, D., Six, A., Rigottier-Gois, L., Messiaen, S., Chilmonczyk, S., Quillet, E., et al. (2006). Phenotypic and functional similarity of gut intraepithelial and systemic T cells in a teleost fish. *J. Immunol.* 176, 3942–3949. doi: 10.4049/jimmunol.176.7.3942

Bierer, B. E., and Burakoff, S. J. (1988). T cell adhesion molecules. *FASEB J.* 2, 2584–2590.

Biteau, B., Hochmuth, C. E., and Jasper, H. (2011). Maintaining tissue homeostasis: dynamic control of somatic stem cell activity. *Cell Stem Cell* 9, 402–411. doi: 10.1016/j.stem.2011.10.004

Braniste, T., Tiginyanu, I., Horvath, T., Raevschi, S., Cebotari, S., Lux, M., et al. (2016). Viability and proliferation of endothelial cells upon exposure to GaN nanoparticles. *Beilstein J. Nanotechnol.* 7, 1330–1337. doi: 10.3762/bjnano.7.124

Chia, K., Mazzolini, J., Mione, M., and Sieger, D. (2018). Tumor initiating cells induce Cxcr4-mediated infiltration of pro-tumoral macrophages into the brain. *eLife* 7:e31918.

Cosorich, I., Mcguire, H. M., Warren, J., Danta, M., and King, C. (2019). CCR9 expressing T helper and T follicular helper cells exhibit site-specific identities during inflammatory disease. *Front. Immunol.* 9:2899. doi: 10.3389/fimmu.2018.02899

Geven, E. J., and Klaren, P. H. (2017). The teleost head kidney: integrating thyroid and immune signalling. *Dev. Compar. Immunol.* 66, 73–83. doi: 10.1016/j.dci.2016.06.025

Gu, Z. (2015). *Complexheatmap: Making Complex Heatmaps. R Package Version 1.*

Havens, A. M., Jung, Y., Sun, Y. X., Wang, J., Shah, R. B., Bühring, H. J., et al. (2006). The role of sialomucin CD164 (MGC-24v or endolyn) in prostate cancer metastasis. *BMC Cancer* 6:195. doi: 10.1186/1471-2407-6-195

Hu, Y., Wei, X., Liao, Z., Gao, Y., Liu, X., Su, J., et al. (2018). Transcriptome analysis provides insights into the markers of resting and LPS-activated macrophages in grass carp (*Ctenopharyngodon idella*). *Intern. J. Mol. Sci.* 19:3562. doi: 10.3390/ijms19113562

Iliev, D. B., Lagos, L., Thim, H. L., Jørgensen, S. M., Krasnov, A., and Jørgensen, J. B. (2019). CpGs induce differentiation of Atlantic salmon mononuclear phagocytes into cells with dendritic morphology and a proinflammatory transcriptional profile but an exhausted allostimulatory activity. *Front. Immunol.* 10:378. doi: 10.3389/fimmu.2019.00378

Iliev, D. B., Thim, H., Lagos, L., Olsen, R., and Jørgensen, J. (2013). Homing of antigen-presenting cells in head kidney and spleen-salmon head kidney hosts diverse APC types. *Front. Immunol.* 4:137. doi: 10.3389/fimmu.2018.00137

Jenberie, S., Thim, H. L., Sunyer, J. O., Skjødt, K., Jensen, I., and Jørgensen, J. B. (2018). Profiling Atlantic salmon B cell populations: CpG-mediated TLR-ligation enhances IgM secretion and modulates immune gene expression. *Sci. Rep.* 8, 1–12. doi: 10.1038/s41598-018-21895-9

Joerink, M., Ribeiro, C. M., Stet, R. J., Hermsen, T., Savelkoul, H. F., and Wiegertjes, G. F. (2006). Head kidney-derived macrophages of common carp (*Cyprinus carpio* L.) show plasticity and functional polarization upon differential stimulation. *J. Immunol.* 177, 61–69. doi: 10.4049/jimmunol.177.1.61

Khalili, A. A., and Ahmad, M. R. (2015). A review of cell adhesion studies for biomedical and biological applications. *Intern. J. Mol. Sci.* 16, 18149–18184. doi: 10.3390/ijms160818149

Kihara, H., Kim, D. M., Nagai, M., Nojiri, T., Nagai, S., Chen, C.-Y., et al. (2018). Epithelial cell adhesion efficacy of a novel peptide identified by panning on a smooth titanium surface. *Intern. J. Oral Sci.* 10, 1–8. doi: 10.1038/s41368-018-0022-1

Kish, D. (2015). Roles of the CCL20-CCR6 axis and CXCR3 in CD8 T cell-mediated contact hypersensitivity (CCR5P. 211). *J. Immunol.* 194:186.13.

Kondo, T., Takata, H., and Takiguchi, M. (2007). Functional expression of chemokine receptor CCR6 on human effector memory CD8+ T cells. *Eur. J. Immunol.* 37, 54–65. doi: 10.1002/eji.200636251

Koppang, E. O., Fischer, U., Moore, L., Tranulis, M. A., Dijkstra, J. M., Köllner, B., et al. (2010). Salmonid T cells assemble in the thymus, spleen and in novel interbranchial lymphoid tissue. *J. Anat.* 217, 728–739. doi: 10.1111/j.1469-7580.2010.01305.x

Kratofil, R. M., Kubes, P., and Deniset, J. F. (2017). Monocyte conversion during inflammation and injury. *Arterioscler. Thromb. Vasc. Biol.* 37, 35–42. doi: 10.1161/atvbaha.116.308198

Li, J., Barreda, D. R., Zhang, Y.-A., Boshra, H., Gelman, A. E., Lapatra, S., et al. (2006). B lymphocytes from early vertebrates have potent phagocytic and microbicidal abilities. *Nat. Immunol.* 7, 1116–1124. doi: 10.1038/ni1389

Lindell, K., Fahlgren, A., Hjerde, E., Willassen, N.-P., Fällman, M., and Milton, D. L. (2012). Lipopolysaccharide O-antigen prevents phagocytosis of *Vibrio anguillarum* by rainbow trout (*Oncorhynchus mykiss*) skin epithelial cells. *PLoS One* 7:e37678. doi: 10.1371/journal.pone.0037678

Love, M. I., Huber, W., and Anders, S. (2014). Moderated estimation of fold change and dispersion for RNA-seq data with DESeq2. *Genome Biol.* 15:550. doi: 10.1186/s13059-014-0550-8

Lu, X.-J., Chen, Q., Rong, Y.-J., Chen, F., and Chen, J. (2017). CXCR3. 1 and CXCR3. 2 differentially contribute to macrophage polarization in teleost fish. *J. Immunol.* 198, 4692–4706. doi: 10.4049/jimmunol.1700101

Luckett-Chastain, L., Calhoun, K., Schartz, T., and Gallucci, R. M. (2016). IL-6 influences the balance between M1 and M2 macrophages in a mouse model of irritant contact dermatitis. *J. Immunol.* 196:196.17.

McKarns, S. C., and Schwartz, R. H. (2005). Distinct effects of TGF-β1 on CD4+ and CD8+ T cell survival, division, and IL-2 production: a role for T cell intrinsic Smad3. *J. Immunol.* 174, 2071–2083. doi: 10.4049/jimmunol.174.4.2071

McMillan, D. N., and Secombes, C. J. (1997). Isolation of rainbow trout (*Oncorhynchus mykiss*) intestinal intraepithelial lymphocytes (IEL) and measurement of their cytotoxic activity. *Fish Shellf. Immunol.* 7, 527–541. doi: 10.1006/fsim.1997.0099

Mehta, A. K., Gracias, D. T., and Croft, M. (2018). TNF activity and T cells. *Cytokine* 101, 14–18. doi: 10.1016/j.cyto.2016.08.003

Okumura, R., and Takeda, K. (2016). Maintenance of gut homeostasis by the mucosal immune system. *Proc. Jpn. Acad. Ser. B* 92, 423–435. doi: 10.2183/pjab.92.423

Park, I.-W., Koziel, H., Hatch, W., Li, X., Du, B., and Groopman, J. E. (1999). CD4 receptor-dependent entry of human immunodeficiency virus type-1 env-pseudotypes into CCR5-, CCR3-, and CXCR4-expressing human alveolar macrophages is preferentially mediated by the CCR5 coreceptor. *Am. J. Respir. Cell Mol. Biol.* 20, 864–871. doi: 10.1165/ajrcmb.20.5.3547

Park, Y., Abihssira-García, I. S., Thalmann, S., Wiegertjes, G. F., Barreda, D. R., Olsvik, P. A., et al. (2020). Imaging flow cytometry protocols for examining phagocytosis of microplastics and bioparticles by immune cells of aquatic animals. *Front. Immunol.* 11:203. doi: 10.3389/fimmu.2018.00203

Parra, D., Reyes-Lopez, F. E., and Tort, L. (2015). Mucosal immunity and B cells in teleosts: Effect of vaccination and stress. *Front. Immunol.* 6:354. doi: 10.3389/fimmu.2018.00354

Paulsen, S. M., Engstad, R. E., and Robertsen, B. (2001). Enhanced lysozyme production in Atlantic salmon (*Salmo salar* L.) macrophages treated with yeast β-glucan and bacterial lipopolysaccharide. *Fish Shellf. Immunol.* 11, 23–37. doi: 10.1006/fsim.2000.0291

Privratsky, J. R., and Newman, P. J. (2014). PECAM-1: regulator of endothelial junctional integrity. *Cell Tissue Res.* 355, 607–619. doi: 10.1007/s00441-013-1779-3

Ramakrishnan, S. K., Zhang, H., Ma, X., Jung, I., Schwartz, A. J., Triner, D., et al. (2019). Intestinal non-canonical NFκB signaling shapes the local and systemic immune response. *Nat. Commun.* 10, 1–16. doi: 10.1038/s41467-019-08581-8

Rengarajan, M., Hayer, A., and Theriot, J. A. (2016). Endothelial cells use a formin-dependent phagocytosis-like process to internalize the bacterium *Listeria monocytogenes*. *PLoS Pathog.* 12:e1005603. doi: 10.1371/journal.pone.1005603

Robinson, J. P., and Babcock, G. F. (1998). *Phagocyte Function: A Guide for Research and Clinical Evaluation*. New York, NY: Wiley-Liss.

Romano, N., Rossi, F., Abelli, L., Caccia, E., Piergentili, R., Mastrolia, L., et al. (2007). Majority of TcRβ+ T-lymphocytes located in thymus and midgut of the bony fish, *Dicentrarchus labrax* (L.). *Cell Tissue Res.* 329, 479–489. doi: 10.1007/s00441-007-0429-z

Rombout, J., Joosten, P., Engelsma, M., Vos, A., Taverne, N., and Taverne-Thiele, J. (1998). Indications for a distinct putative T cell population in mucosal tissue of carp (*Cyprinus carpio* L.). *Dev. Compar. Immunol.* 22, 63–77. doi: 10.1016/s0145-305x(97)00048-7

Rombout, J. H., Abelli, L., Picchietti, S., Scapigliati, G., and Kiron, V. (2011). Teleost intestinal immunology. *Fish Shellf. Immunol.* 31, 616–626. doi: 10.1016/j.fsi.2010.09.001

Salinas, I., Meseguer, J., and Esteban, M. (2007). Assessment of different protocols for the isolation and purification of gut associated lymphoid cells from the gilthead seabream (*Sparus aurata* L.). *Biol. Proc.* 9:43. doi: 10.1251/bpo132

Selvarajan, K., Moldovan, L., Chandrakala, A. N., Litvinov, D., and Parthasarathy, S. (2011). Peritoneal macrophages are distinct from monocytes and adherent macrophages. *Atherosclerosis* 219, 475–483. doi: 10.1016/j.atherosclerosis.2011.09.014

Shimizu, Y., Newman, W., Gopal, T. V., Horgan, K. J., Graber, N., Beall, L. D., et al. (1991). Four molecular pathways of T cell adhesion to endothelial cells: Roles of LFA-1, VCAM-1, and ELAM-1 and changes in pathway hierarchy under different activation conditions. *J. Cell Biol.* 113, 1203–1212. doi: 10.1083/jcb.113.5.1203

Toda, H., Saito, Y., Koike, T., Takizawa, F., Araki, K., Yabu, T., et al. (2011). Conservation of characteristics and functions of CD4 positive lymphocytes in a teleost fish. *Dev. Compar. Immunol.* 35, 650–660. doi: 10.1016/j.dci.2011.01.013

Vereyken, E. J., Heijnen, P. D., Baron, W., De Vries, E. H., Dijkstra, C. D., and Teunissen, C. E. (2011). Classically and alternatively activated bone marrow derived macrophages differ in cytoskeletal functions and migration towards specific CNS cell types. *J. Neuroinflamm.* 8:58. doi: 10.1186/1742-2094-8-58

Verma, A., Bhattacharya, R., Remadevi, I., Li, K., Pramanik, K., Samant, G. V., et al. (2010). Endothelial cell-specific chemotaxis receptor (ecscr) promotes angioblast migration during vasculogenesis and enhances VEGF receptor sensitivity. *Blood J. Am. Soc. Hematol.* 115, 4614–4622. doi: 10.1182/blood-2009-10-248856

Wan, F., Hu, C.-B., Ma, J.-X., Gao, K., Xiang, L.-X., and Shao, J.-Z. (2017). Characterization of γδ T cells from zebrafish provides insights into their important role in adaptive humoral immunity. *Front. Immunol.* 7:675. doi: 10.3389/fimmu.2018.00675

Wickham, H. (2016). *ggplot2: Elegant Graphics for Data Analysis*. Berlin: Springer.

Yang, X., Li, S., Zhong, J., Zhang, W., Hua, X., Li, B., et al. (2017). CD151 mediates netrin-1-induced angiogenesis through the Src-FAK-Paxillin pathway. *J. Cell. Mol. Med.* 21, 72–80. doi: 10.1111/jcmm.12939

Yi, H.-J., and Lu, G.-X. (2012). Adherent and non-adherent dendritic cells are equivalently qualified in GM-CSF, IL-4 and TNF-α culture system. *Cell. Immunol.* 277, 44–48. doi: 10.1016/j.cellimm.2012.05.014

Yu, X., Buttgereit, A., Lelios, I., Utz, S. G., Cansever, D., Becher, B., et al. (2017). The cytokine TGF-β promotes the development and homeostasis of alveolar macrophages. *Immunity* 47, 903–912. doi: 10.1016/j.immuni.2017.10.007

Zhang, Q., Kopp, M., Babiak, I., and Fernandes, J. M. (2018). Low incubation temperature during early development negatively affects survival and related innate immune processes in zebrafish larvae exposed to lipopolysaccharide. *Sci. Rep.* 8, 1–14. doi: 10.1038/s41598-018-22288-8

Zhao, W., Minderman, H., and Russell, M. W. (2014). Identification and characterization of intestinal antigen-presenting cells involved in uptake and processing of a nontoxic recombinant chimeric mucosal immunogen based on cholera toxin using imaging flow cytometry. *Clin. Vaccine Immunol.* 21, 74–84. doi: 10.1128/CVI.00452-13

Conflict of Interest: The authors declare that the research was conducted in the absence of any commercial or financial relationships that could be construed as a potential conflict of interest.

frontiers in Cell and Developmental Biology

ORIGINAL RESEARCH
published: 28 January 2021
doi: 10.3389/fcell.2020.618598

Secreted Phosphoprotein 1 Expression in Retinal Mononuclear Phagocytes Links Murine to Human Choroidal Neovascularization

Anja Schlecht[1], Peipei Zhang[1], Julian Wolf[1], Adrian Thien[1], Dennis-Dominik Rosmus[2], Stefaniya Boneva[1], Günther Schlunck[1], Clemens Lange[1] and Peter Wieghofer[2]**

[1] Eye Center, Medical Center, Medical Faculty, University of Freiburg, Freiburg, Germany, [2] Institute of Anatomy, Leipzig University, Leipzig, Germany

OPEN ACCESS

Edited by:
Efstathios G. Stamatiades,
Charité—Universitätsmedizin Berlin, Germany

Reviewed by:
Thomas Langmann,
Universität zu Köln, Germany
Jian Liu,
University of Bristol, United Kingdom

***Correspondence:**
Peter Wieghofer
peter.wieghofer@medizin.uni-leipzig.de
Clemens Lange
clemens.lange@uniklinik-freiburg.de

Specialty section:
This article was submitted to Cell Death and Survival, a section of the journal Frontiers in Cell and Developmental Biology

Received: 17 October 2020
Accepted: 01 December 2020
Published: 28 January 2021

Citation:
Schlecht A, Zhang P, Wolf J, Thien A, Rosmus D-D, Boneva S, Schlunck G, Lange C and Wieghofer P (2021) Secreted Phosphoprotein 1 Expression in Retinal Mononuclear Phagocytes Links Murine to Human Choroidal Neovascularization. Front. Cell Dev. Biol. 8:618598. doi: 10.3389/fcell.2020.618598

Age-related macular degeneration (AMD) represents the most common cause of blindness in the elderly in the Western world. An impairment of the outer blood-retina barrier and a localized inflammatory microenvironment cause sprouting of choroidal neovascular membranes (CNV) in neovascular AMD that are in intimate contact with surrounding myeloid cells, such as retinal microglia, and ultimately lead to visual impairment. The discovery of novel target molecules to interfere with angiogenesis and inflammation is vital for future treatment approaches in AMD patients. To explore the transcriptional profile and the function of retinal microglia at sites of CNV, we performed a comprehensive RNA-seq analysis of retinal microglia in the mouse model of laser-induced choroidal neovascularization (mCNV). Here, we identified the angiogenic factor Osteopontin (*Opn*), also known as "secreted phosphoprotein 1" (*Spp1*), as one of the most highly expressed genes in retinal microglia in the course of CNV formation. We confirmed the presence of SPP1 at the lesion site in recruited retinal microglia in *Cx3cr1*^{CreER}:*Rosa26-tdTomato* reporter mice by confocal microscopy and in whole retinal tissue lysates by ELISA highlighting a massive local production of SPP1. Inhibition of SPP1 by intravitreal injection of an anti-SPP1 antibody significantly increased the lesion size compared to IgG-treated control eyes. In line with our results in rodents, we found an increased *SPP1* mRNA expression in surgically extracted human choroidal neovascular (hCNV) membranes by the quantitative RNA-seq approach of massive analysis of cDNA ends (MACE). Numerous IBA1^{+}SPP1^{+} myeloid cells were detected in human CNV membranes. Taken together, these results highlight the importance of SPP1 in the formation of CNV and potentially offer new opportunities for therapeutic intervention by modulating the SPP1 pathway.

Keywords: AMD, CNV, Osteopontin, OPN, SPP1, microglia, *Cx3cr1*^{CreERT2}

HIGHLIGHTS

- *Spp1* emerges as one of the top differentially regulated angiogenic genes in murine microglia in the model of laser-induced CNV.
- SPP1 protein expression is highly increased in CNV tissue and present in retinal microglia.
- Scavenging of SPP1 by an anti-SPP1 antibody leads to increased lesion size in CNV.
- SPP1 expression is highly induced in surgically extracted human choroidal neovascularization membranes on both RNA and protein levels.

INTRODUCTION

Microglia represent the resident tissue-macrophages of the retina and the brain and originate from the extra-embryonic yolk sac early during development (Ginhoux et al., 2010; Kierdorf et al., 2013; Goldmann et al., 2016; O'Koren et al., 2019; Wieghofer et al., in press). In the context of neurodegeneration, neuroinflammation, or other insults, the composition as well as the gene and protein expression signatures of myeloid cells can dramatically change (Ajami et al., 2018; O'Koren et al., 2019; Wieghofer et al., in press). These changes include microglia activation leading to relevant functional alterations. The mode of action can thereby be beneficial but also detrimental depending on the disease model affecting microglia in the brain or retina (Reyes et al., 2017; Masuda et al., 2020).

Choroidal neovascularisation (CNV) is a common cause of irreversible vision loss in patients with age-related macular degeneration (AMD), which is the leading cause of blindness in the elderly (Fine et al., 2000). In a previous study, we showed that myeloid cells represent a heterogeneous cell population that accumulates at sites of CNV and modulates its formation in a laser-induced CNV mouse model, which is a widely used model for nAMD (Lambert et al., 2013; Wieghofer et al., in press). The close interplay between myeloid cells and blood vessel formation has been extensively studied in the past; however, the origin of accumulating myeloid cells in this model has long remained unclear (Oh et al., 1999; Fantin et al., 2010; Dejda et al., 2016; Usui-Ouchi et al., 2020). Recently we have shown that retinal microglia are the dominant innate immune cell population at sites of CNV and are characterized by a specific disease-associated gene expression signature similar to other disease models, including *Spp1* encoding the secreted phosphoprotein 1 (SPP1), *Lgals3* (lectin, galactose binding, soluble 3), and *Apoe* (Apolipoprotein E) (Keren-Shaul et al., 2017; O'Koren et al., 2019; Wieghofer et al., in press). In particular, the role of secreted SPP1 in vascular diseases and its potential to serve as an easily accessible biomarker present in blood serum and other body fluids has gained attention recently (Lok and Lyle, 2019). SPP1 is a multifaceted protein involved in homeostatic functions and pathophysiological processes like bone morphogenesis, vascular remodeling, recruitment of leukocytes, cell adhesion, and extracellular matrix remodeling (Lok and Lyle, 2019). The broad spectrum of features is reflected by the cell types expressing SPP1 including leukocytes, epithelial and endothelial cells, and neurons in humans (Kunii et al., 2009).

As a matricellular cytokine SPP1 binds to integrin receptors, like α_V integrins, and certain splice variants of the hyaluronic acid receptor CD44, which are expressed by endothelial cells (Lok and Lyle, 2019). The angiogenic capacity combined with its potential to shape myeloid cell recruitment highlights SPP1 as a promising target in vascular diseases (Yu et al., 2017; Lok and Lyle, 2019).

The goal of our study was to explore gene expression signatures of native and CNV-associated retinal microglia by comprehensive bulk RNA-seq. Furthermore, we investigated the role of SPP1 in CNV formation by local intraocular application of an antibody directed against SPP1. Finally, we correlated our findings in mice to human CNV samples from nAMD patients. Our results underline the importance of SPP1 in the formation of CNV in mice and humans, thus paving the way for new therapeutic interventions by modulating the SPP1 pathway.

RESULTS

Identification of the Angiogenic *Spp1* Gene in Experimental Choroidal Neovascularization

To gain more insight into the transcriptional profile and angiogenic capacity of microglia during development of experimental choroidal neovascularization, we conducted bulk RNA-seq of flow cytometry-isolated $CD45^{lo}CD11b^{+}CX_3CR1^{+}Ly6C^{-}Ly6G^{-}$ retinal microglia at CNV d3 (**Figure 1A**). The principal component analysis clearly showed distinct gene expression patterns between the lasered group 3 days after experimental laser treatment and unlasered control mice (**Figure 1B**). Next, we determined the differentially expressed genes (DEG) between CNV-associated MG and control microglia and found that 654 DEG were significantly increased in microglia in association with CNV formation. Among the top five DEG increased in CNV-associated MG were *Fn1* (log2FC = 9.8, padj. = 2.9×10^{-15}), *Spp1* (log2FC = 6.6, padj = 3.8×10^{-25}), *Ifi27I2a* (log2FC = 2.9, padj = 7.7×10^{-8}), *Cd74* (log2FC = 2.7, padj = 7.9×10^{-7}), and *Cd72* (log2FC= 2.4, padj = 2.2×10^{-24}) (**Figures 1C,D**). Also *Apoe* (log2FC = 1.7, padj = 3.3×10^{-12}) was significantly upregulated and is an important regulator for the transition into disease-associated microglia (Song and Colonna, 2018). In addition, genes typically expressed by antigen-presenting cells, such as *H2-Ab1* (log2FC = 2.1, padj = 9.3×10^{-6}) and *Cd74,* or involved in interferon signaling, like *Ifitm3* (log2FC = 1.59, padj = 0.005) and *Ifi27I2a,* were present among the upregulated genes in CNV (**Figures 1C,D**). To identify functionally associated genes, we performed a gene ontology (GO) analysis and found genes relevant for the biological processes "myeloid leukocyte migration," "extracellular matrix binding," and "tissue remodeling" (**Figure 1E**). These genes include *Ccl2* (log2FC = 2.5, padj = 4.2×10^{-7}) encoding a chemokine attracting peripheral blood monocytes and *Lgals3* (log2FC = 3.1, padj = 8.2×10^{-10}) that has been described in disease-associated

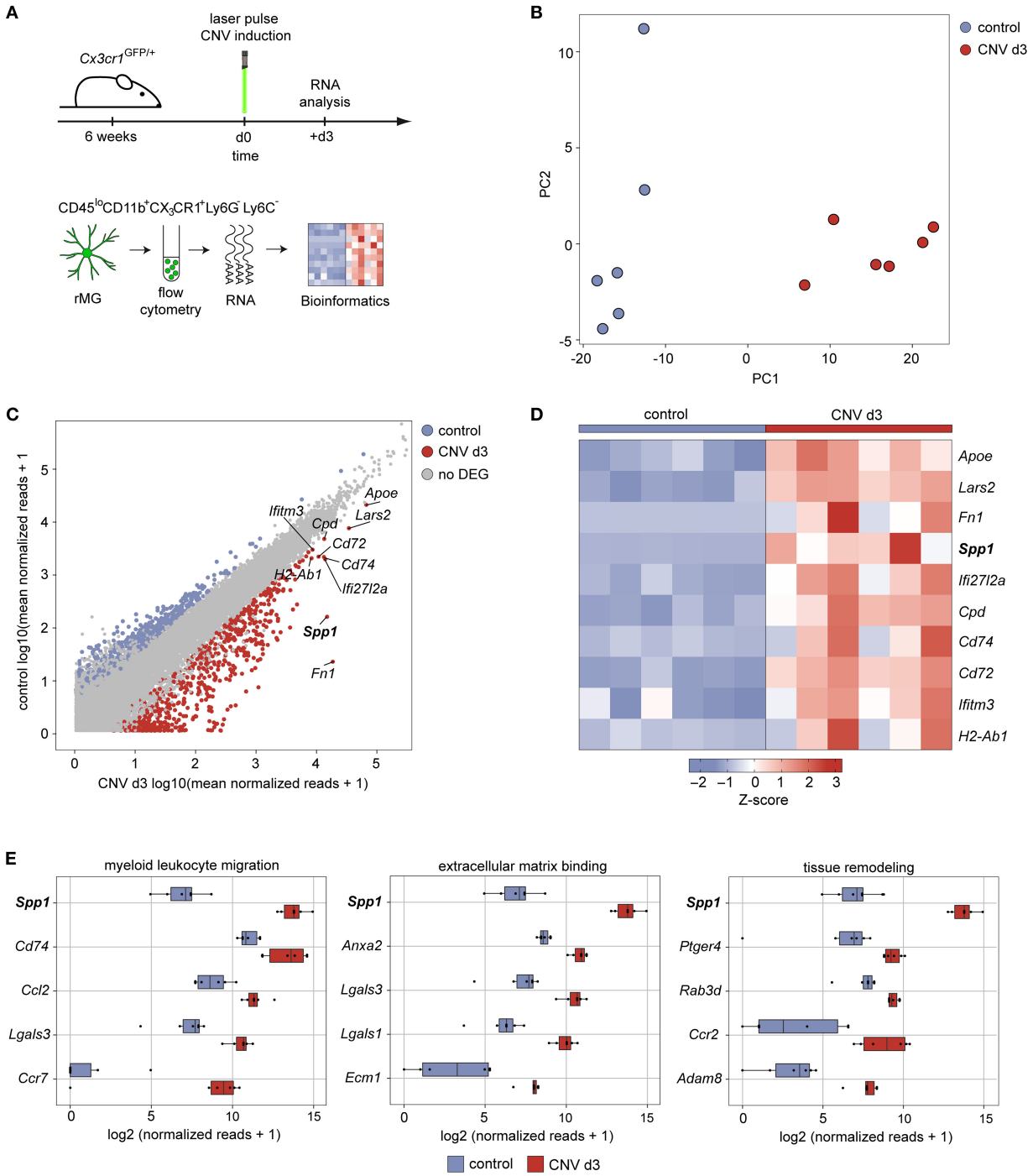

FIGURE 1 | Expression of secreted phosphoprotein 1 increases upon experimental induction of choroidal neovascularization in mice. **(A)** Experimental scheme depicting the workflow for isolation of viable and single CD45^{lo}CD11b^{+}CX$_3$CR1^{+}Ly6C^{-}Ly6G^{-} cells from the retina under healthy conditions and experimental choroidal neovascularization at d3 after induction for unbiased RNA-seq. Six focal argon laser burns were applied to each retina to induce microglia activation and subsequent choroidal neovascularization formation in mice (mCNV). **(B)** Principal component analysis of transcripts analyzed by RNA-seq. **(C)** Scatter plot using the log2 transformation of normalized counts visualizing differentially expressed genes between healthy conditions (y-axis) and experimental choroidal neovascularization on d3 after laser treatment (x-axis). The top 10 highest expressed genes are labeled. Definition of differentially expressed genes: abs(log2FC) > 1.5 & padjusted < 0.05. **(D)** Heatmap of the top 10 differentially expressed genes between healthy conditions and experimental choroidal neovascularization on d3 after laser treatment according to the mean expression in the laser group. The z-score represents the gene expression in relation to its mean expression by standard deviation units (red: upregulation, blue: downregulation). **(E)** Box plots illustrating the top five factors of the most disease-relevant GO terms ordered according to the mean expression in the laser group.

microglia and is responsible for interaction with the extracellular matrix (O'Koren et al., 2019; Boeck et al., 2020) (**Figure 1D**). Nevertheless, besides its known role in angiogenesis, *Spp1* was also the most highly expressed gene within all three biological processes GO terms, which prompted us to investigate its role in further detail (**Figure 1E**).

Validation and Interference With SPP1 on the Protein Level in CNV Mice

To validate the expression of SPP1 protein we used conditional *Cx3cr1*^{CreER}*:Rosa26-tdTomato* reporter mice to specifically label microglia in the CNV model (Goldmann et al., 2013; Wieghofer et al., 2015, in press). Eight weeks after Tamoxifen treatment to induce Tomato expression in retinal microglia, mice were laser-treated to induce CNV (d0) and sacrificed 3 days later for immunofluorescent staining and confocal imaging (**Figures 2A,B**). Here, we found numerous Tomato^{+} microglia cells expressing SPP1 and exhibiting an amoeboid appearance, which indicates an activated phenotype in contrast to their ramified state under homeostatic conditions (**Figure 2B**). Tomato^{-}SPP1^{+} cells were present indicating that other cell types than microglia are also involved in CNV formation. In accordance with our RNA-seq data, a strong increase of SPP1 protein in whole CNV tissue was detectable by ELISA (CNV: 62.30 $\pm$ 6.90, control: 6.00 $\pm$ 2.03, $p < 0.0001$) (**Figure 2C**). These findings prompted us to inhibit SPP1 in the course of CNV development by an intravitreal administration of an anti-SPP1 antibody 1 day after CNV laser-induction. The contralateral eyes were treated with an IgG control (**Figure 2D**). The increase in lesion size was clearly visible over time by funduscopic imaging and showed severely enhanced vascular leakage under anti-SPP1 treatment visualized by angiography (**Figure 2E**). The quantification of the lesion size based on Collagen IV immunoreactivity revealed a more than 2-fold increase of the lesioned area (2.25 $\pm$ 1.05, $p = 0.0004$) in eyes treated with anti-SPP1 compared to IgG controls. Consequently, the intraocular application of anti-SPP1 antibodies suggested a protective, anti-angiogenic function of SPP1 during CNV formation (**Figure 2E**).

SPP1 Expression in Mice Can Be Linked to Human Neovascular AMD

To generalize our findings, we next explored the expression of SPP1 in human CNV by conducting a *post-hoc* analysis of already available RNA-seq data from surgically extracted human membranes of choroidal neovascularization (hCNV) (**Figure 3A**) (Schlecht et al., 2020). Interestingly, also in human CNV, *SPP1* was one of the most prominent upregulated angiogenic genes when compared to healthy controls (CNV: 18.41 $\pm$ 11.38 reads, controls: 0.70 $\pm$ 0.64 reads, *padj* = 0.019) (**Figure 3B**). Next, we investigated the expression of SPP1 protein in human body donor tissue as compared to human CNV membranes by immunofluorescence (**Figure 3C**). In retinal IBA1^{+} microglia, SPP1 was barely detectable in healthy control tissue, which is in line with previous studies (Masuda et al., 2019) (**Figure 3C**). Only in the choroid, a faint staining for SPP1 was observed in IBA1^{+} macrophages, whereas in CNV tissue a strong expression of SPP1 was detected in IBA1^{+} cells. Non-myeloid IBA1^{-}SPP1^{+} cells were also present at the site of the lesion, similar to our findings in mice (**Figures 2B**, **3C**). Overall, we found comparable expression of *SPP1* RNA and SPP1 protein in both murine and human tissue samples, suggesting a functional relevance of the molecule in CNV formation.

DISCUSSION

Retinal microglia cells are key players in the modulation of disease course and severity across disease models including retinal degeneration, diabetic retinopathy, retinal light damage, and CNV (O'Koren et al., 2019; Van Hove et al., 2020; Wieghofer et al., in press). The concept of disease-associated microglia (DAM), initially introduced for brain disease models involving microglia activation, was recently successfully applied to retinal microglia (Keren-Shaul et al., 2017; O'Koren et al., 2019; Wieghofer et al., in press).

Single-cell RNA-seq (scRNA-seq) of fresh tissue samples is advantageous to characterize subtypes of all kinds of cell types. However, fresh human CNV tissue is not available as surgical CNV extraction became obsolete due to novel treatment strategies and archived samples are not amenable to scRNA-seq preparation (Masuda et al., 2019, 2020; Schlecht et al., 2020). To compare gene expression signatures across species, we applied bulk RNA-seq approaches on experimentally induced murine and archived human choroidal neovascularization tissue samples.

Gene expression profiling of retinal microglia by RNA-seq revealed a CNV-associated phenotype clearly distinguishable from the profile of retinal microglia in untreated control mice. Significant changes were observed for transcripts functionally relevant in fibrosis (*Fn1*), antigen-presentation (*Cd74*, *H2-Ab1*), myeloid cell migration (*Cd74*, *Ccl2*, *Lgals3*), phagocytosis (*Lgals3*), and inflammation (*Ifi27l2a*, *Ifitm3*, *Lgals3*). With regard to antigen presentation, we recently demonstrated that *Cd74* is not expressed in retinal microglia under homeostatic conditions but induced together with *H2-Aa*, encoding MHCII, upon CNV induction, which is in line with the present study (Wieghofer et al., in press). Of note, the induced expression of MHCII (*H2-Aa*) was also confirmed on the protein level in mice and in human CNV membranes (Wieghofer et al., in press). The observed increase of *Apoe* expression further supports the induction of the DAM gene expression signature mediated by binding to the triggering receptor of myeloid cells 2 (TREM2), like it was shown in the brain (Song and Colonna, 2018). Furthermore, *Apoe* was highly expressed in DAM in a model of retinal light damage and, most importantly, in mononuclear phagocytes in the subretinal space in AMD patients (Levy et al., 2015a,b; O'Koren et al., 2019). In another study, SPP1 was found to be key for the promotion of macrophage survival in the subretinal space in the CNV model (Beguier et al., 2020).

The highly significant induction of *Spp1* in retinal microglia points to this gene as a key mediator of CNV pathology, which could be functionally associated with three major hallmarks of the CNV model: angiogenesis, macrophage recruitment,

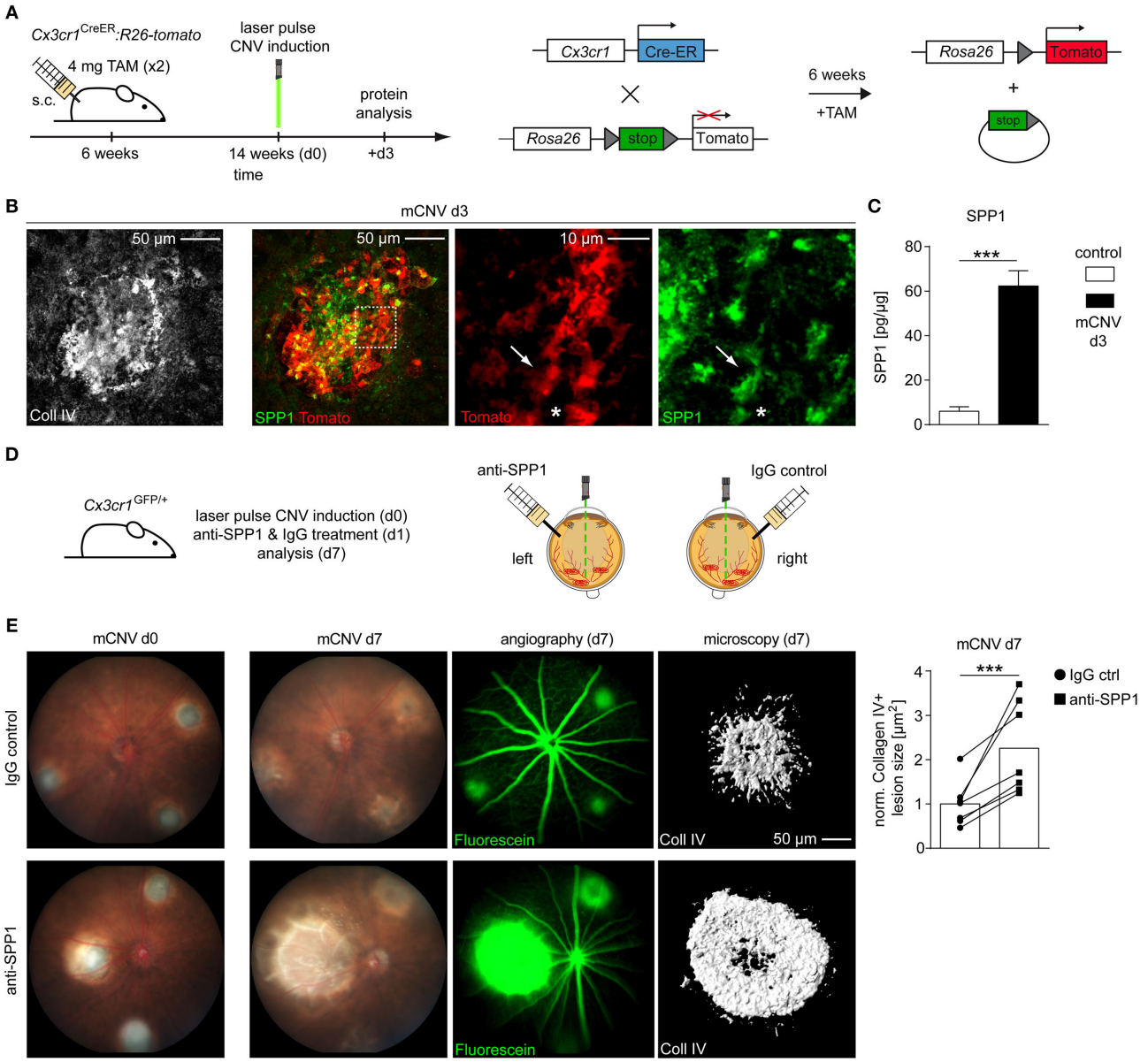

FIGURE 2 | Interference with SPP1 on protein level changes the outcome of experimental choroidal neovascularization. **(A)** Experimental scheme. Six weeks old *Cx3cr1*^{CreER}*:Rosa26-tdTomato* mice were exposed to TAM to induce microglia-specific Tomato labeling. Eight weeks later three focal argon laser burns were applied to each retina to induce microglia activation and subsequent choroidal neovascularization (mCNV). Mice were sacrificed at CNV d3 for immunofluorescence stainings. **(B)** Representative immunofluorescence images for collagen IV (white), Tomato (red), and SPP1 (green) in *Cx3cr1*^{CreER}*:Rosa26-tdTomato* mice on d3 after CNV induction. Arrows point to a Tomato^{+}SPP1^{+} rMG while asterisks indicate a Tomato^{+}SPP1^{-} rMG. Representative pictures of seven mice out of two independent experiments are displayed. **(C)** SPP1 levels in lesioned RPE tissue (mCNV) of wildtype mice compared to untreated controls d3 after CNV induction as measured by ELISA (control: $n = 7$, CNV: $n = 8$ from two independent experiments). Bars represent means ± s.e.m. ***$p < 0.0001$, Unpaired *t*-test. **(D)** Experimental scheme. Choroidal neovascularization was laser induced at day 0 (d0) in *Cx3cr1*$^{GFP/+}$ mice. At d1, 50 ng anti-SPP1 (dissolved in 1 µL PBS injection volume) was injected intravitreally into one eye and the same amount of IgG control antibody (again dissolved in PBS) into the contralateral eye. Mice were sacrificed at d7 after evaluation of fundus and fluorescence angiography. **(E)** Exemplary funduscopic image of lesions directly after laser burn-induced mCNV at day 0 (left) and d7 (right) under treatment with IgG control (top row) or anti-SPP1 antibody (bottom row). Fluorescence angiography indicates leakage of intraperitoneally applied Fluorescein. Representative Imaris reconstruction of collagen IV immunoreactivity and corresponding quantification of CNV size in mice that underwent laser treatment and subsequent injection of either anti-SPP1 into the left eye (squares) or IgG isotype controls into the right eye (circles). Each symbol represents the mean lesion size within one eye of one mouse, based on Collagen IV area of individual lesions imaged by confocal microscopy and normalized to the IgG control. Corresponding values from left and right eye are displayed as pairs. Bar graphs represent the overall mean value of seven mice in total. All values were normalized to the IgG control mean value. Bars represent mean ± s.e.m. ***$p < 0.001$, ratio paired *t*-test.

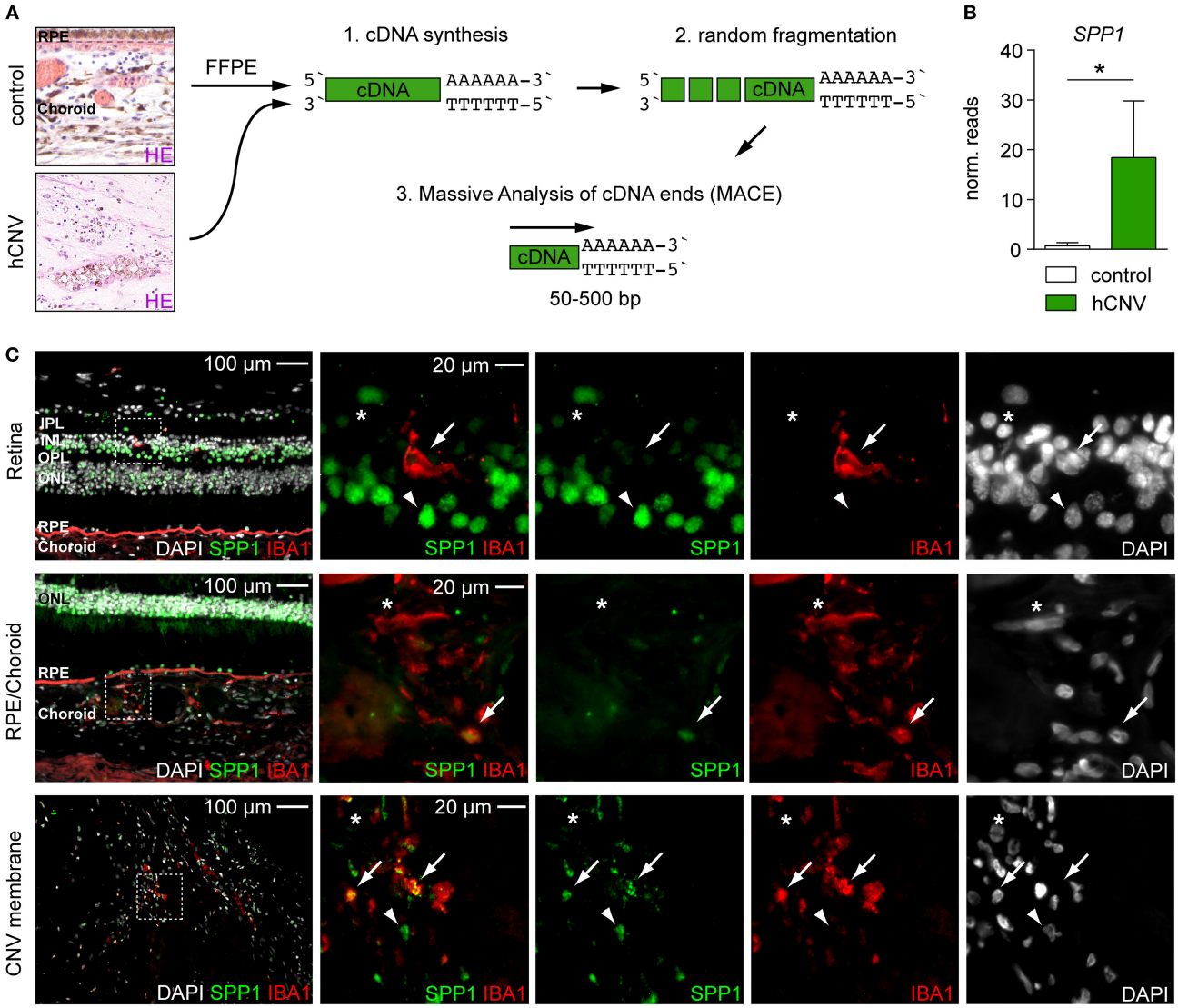

FIGURE 3 | Quantitative RNA-seq analysis and immunofluorescence reveal the presence of SPP1 in human CNV tissue. **(A)** Experimental scheme. RNA was extracted from formalin-fixed and paraffin-embedded human healthy choroid and CNV membranes for massive analysis of cDNA ends (MACE) RNA-seq analysis. Retinal pigment epithelium is abbreviated with RPE. **(B)** *SPP1* expression was quantified by RNA-seq (MACE) in four control samples and four CNV membranes ($p = 0.019$). Bars represent mean ± s.e.m. **(C)** Immunofluorescence for DAPI (white), SPP1 (green), and IBA1 (red) in the retina and RPE/choroid of one body donor and in a CNV membrane of a patient diagnosed with neovascular age-related macular degeneration. $IBA1^{+}SPP1^{+}$ macrophages (arrow) could be found in both healthy RPE/choroid and CNV membranes in line with the RNA-seq (MACE) results, next to $IBA1^{+}SPP1^{-}$ macrophages (asterisk). Arrowheads point to $IBA1^{-}SPP1^{+}$ cells. Dashed white squares indicate the region of interest shown as magnifications on the right side. The layering is indicated for the inner and outer plexiform layer (IPL, OPL), inner and outer nuclear layer (INL, ONL), retinal pigment epithelium (RPE), and choroid.

and tissue remodeling of the extracellular matrix (Tobe et al., 1998; Lambert et al., 2013). Also in a murine model of light-induced neurodegeneration, *Spp1* was highly induced in a specific microglial cluster that also expressed *Lgals1* and *Lgals3* as distinctive marker for subretinal DAM (O'Koren et al., 2019).

In line with previous CNV studies, the lesion size was affected by varying degrees in $Spp1^{-/-}$ mice or after systemic application of an antibody directed against SPP1 (Fujita et al., 2011; Ong et al., 2011; Beguier et al., 2020). In these experiments, which are based on systemic inhibition of SPP1, CNV size is decreased (Fujita et al., 2011; Ong et al., 2011), whereas in the current study, local inhibition of SPP1 by antibodies leads to larger lesions. This can be explained by several factors. The systemic inhibition of SPP1 not only leads to smaller lesions but also to severe changes in the hematopoiesis of myeloid cells in the bone marrow, which, as previously shown, is reflected by a reduced number of the monocyte-macrophage dendritic cell progenitors (MDP) (Magdaleno et al., 2018). A systemic treatment could thereby alter the overall composition of myeloid cells in the blood, finally leading to lower numbers of recruited macrophages and smaller lesions (Fujita et al., 2011). In the clinical routine an antibody against vascular endothelial growth factor (VEGF) is applied

intravitreally in patients suffering from neovascular AMD to achieve high local concentration and reduce the possibility of side effects. Therefore, we administered anti-SPP1 in a more specific approach by applying it locally into the eye to minimize its influence on peripheral immune compartments. In a recent study, the same antibody was successfully applied *in vivo* proving its suitability and bioactivity after intravitreal injection (Beguier et al., 2020) besides its use *in vitro* (Hosaka et al., 2017; Hulsmans et al., 2018). Despite the same mode of application in the CNV model, anti-SPP1 was only given in combination with other factors, and the significantly differing treatment regimen with respect to dosage, time points, and frequency of applications together with a later time point of analysis after CNV does not allow a direct comparison (Beguier et al., 2020). In contrast to previous studies including CNV experiments in constitutive $Spp1^{-/-}$ mice, we found a more than 2-fold increase in lesion size at CNV d7 with anti-SPP1 treatment (Ong et al., 2011). Our findings support a protective function of SPP1 during CNV development that could be mediated at the level of myeloid cells but also through other sources of SPP1 (Lok and Lyle, 2019). Several studies point toward a microglia-related effect. First, this is supported by the fact that microglia were shown to be the predominant myeloid cell type at the lesion site (Wieghofer et al., in press) and their expression of SPP1 upon CNV induction, as confirmed on RNA and protein levels. Furthermore, treatment with SPP1 *in vitro* revealed functionally relevant changes in microglia response to external stimuli (Tambuyzer et al., 2012; Patouraux et al., 2014; Rabenstein et al., 2016). In LPS-stimulated microglia, the production of pro-inflammatory cytokines, like IL-6 and TNFα, was significantly reduced under SPP1 treatment, thereby promoting an anti-inflammatory phenotype (Rabenstein et al., 2016). In addition, the presence of SPP1 significantly improved the survival of microglia under stress conditions and increased the phagocytic activity of microglia *in vitro* (Tambuyzer et al., 2012; Rabenstein et al., 2016). A dose-dependent decrease in superoxide production was found, as well, which is in line with an increase of iNOS expression upon SPP1 decrease in a macrophage cell line (Tambuyzer et al., 2012; Patouraux et al., 2014). In the same study, the authors could reverse the SPP1-mediated increased proliferation rate of microglia by applying an anti-OPN antibody *in vitro* (Tambuyzer et al., 2012), which resembles our antibody-mediated interference with SPP1 in the experimental CNV model. Of note, secreted SPP1 stimulates macrophages to produce CCL2, which was also detected in CNV-associated retinal microglia and acts as a potent chemokine for the recruitment of peripheral myeloid cells (Rowe et al., 2014). These cells could further modulate angiogenesis but represent only a fraction of the overall myeloid cell composition dominated by microglia (Wieghofer et al., in press). However, if the aforementioned *in vitro* observations in microglial biology would apply to the *in vivo* situation, the blockage of SPP1 would have an escalating effect on the basic functions of microglia, like pro-inflammatory cytokine and production of reactive oxygen species, leading to a worsening of tissue damage at the lesion site. The availability of conditional CreERT2 deleter strains targeting microglia like the $Cx3cr1^{\mathrm{CreER}}$ mouse model opens not only the possibility to label microglia specifically but also create conditional knockout mice (Droho et al., 2020; Wieghofer et al., in press). This strategy was successfully applied in the past and will decipher microglial functions in a much more specific setting in the future (Lückoff et al., 2016; Wolf et al., 2020).

Beside the observed role of microglia, we cannot completely rule out a functionally relevant effect of the anti-SPP1 treatment on other non-myeloid cells. For example, SPP1 is also expressed by endothelial and smooth muscle cells and loss of stroma-derived SPP1 led to enhanced tumor progression in mice (O'Brien et al., 1994; Szulzewsky et al., 2017). Interestingly, the interaction of a CD44v6 splice variant, acting as a receptor for SPP1, with VEGF receptor 2 (VEGFR2) on endothelial cells suggests an interference with SPP1 signaling across cell types (Tremmel et al., 2009). Furthermore, our study shows a considerable expression of SPP1 in human retinal neurons, which is consistent with findings in rat retina (Chidlow et al., 2008). Thus, an indirect effect of anti-SPP1 treatment via modulation of the SPP1 pathway in neurons cannot be excluded. RNA-seq analysis of whole human CNV membranes revealed *SPP1* as one of the most highly regulated genes within the disease-relevant GO terms "extracellular structure organization" and "response to wounding," similar to our findings in mice (Schlecht et al., 2020). Our immunofluorescent analysis revealed that SPP1 was predominantly expressed in $IBA1^{+}$ mononuclear phagocytes in human CNV, which strongly resembled the situation present in the murine experimental CNV model, suggesting a highly conserved phenomenon across species. Given the increasing expression of SPP1 in human microglia with age (Sankowski et al., 2019), the SPP1 signaling pathway in MG may modulate CNV development in patients with neovascular AMD and therefore represent a therapeutic target in the future.

Taken together, this study shows that Spp1 is significantly expressed at RNA and protein level in murine and human CNV. The intravitreal application of anti-SPP1 antibodies led to increased CNV lesion size suggesting an anti-angiogenic effect of SPP1. Our results provide new insights into the biology of retinal microglia during health and CNV formation and open new avenues for the treatment of ophthalmological diseases like neovascular AMD.

MATERIALS AND METHODS

Mice

In this study, C57BL/6J mice were used as wildtype (WT) mice. All transgenic lines [$Cx3cr1^{GFP/+}$, $Cx3cr1^{CreERT2}$, and *Rosa26-fl-stop-fl-tdTomato* (*Rosa26-tdTomato*)] were bred on a C57BL/6J background under specific pathogen-free conditions and devoid of *Crb1* (*RD8*) mutations. $Cx3cr1^{CreERT2}$ were crossed to *Rosa26-tdTomato*. All animal experiments were approved by local administration and were performed in accordance with the respective national, federal, and institutional regulations.

Tamoxifen Treatment

For induction of the nuclear CreER-T2 recombinase activity in adult animals, 6–8-week-old $Cx3cr1^{CreER}$ mice were treated with 4 mg Tamoxifen (TAM, T5648-1G, Sigma-Aldrich, Taufkirchen,

Germany) dissolved in 200 µl corn oil (Sigma-Aldrich, C8267-500 ml) and injected subcutaneously at two time points 48 h apart.

Laser-Induced Choroidal Neovascularization Model

Mice were anesthetized with a mixture of ketamine (100 mg/kg) and xylazine (6 mg/kg), and pupils were dilated with a combination of 0.5% tropicamide and neosynephrine-POS 5%. Corneal gel was applied to maintain hydration of the cornea and reduce media opacifications. Mice were placed in front of an argon laser (VISULAS 532s, ZEISS) after the pupils were completely dilated. A cover slip with a drop of gel was placed on the eye as a contact lens to convert the curved cornea into a planar surface. Three laser burns at equal distance from the optic disc were induced by an Argon laser with a wavelength of 532 nm, a power of 150 mW, a fixed diameter of 100 µm, and duration of 100 ms. Only burns that produced a bubble as a sign for retinal pigment epithelial rupture were included in the study. For immunohistochemical analyses, three laser burns were applied per eye. For molecular analyses (RNA sequencing and ELISA) six laser burns were applied per eye to maximize the enrichment with diseased tissue. Prior to tissue processing, the peripheral part of the retina (RNA sequencing) or choroid (ELISA) was removed with small scissors to use only the central part of the respective tissue (containing the laser lesions) for analyses. Control eyes without laser treatment were dissected in the same way. After laser treatment, mice were then placed on a pre-warmed warming plate at 35°C until they had recovered from anesthesia.

Antibody Treatment During Laser-Induced Choroidal Neovascularization

Choroidal neovascularization was laser-induced at day 0 (d0) in *Cx3cr1*$^{GFP/+}$ mice, as described above, with the following variations (Tobe et al., 1998). At d1 mice received an intravitreal injection of 50 ng anti-SPP1 (R&D Systems, AF808) solved in 1 µL PBS in one eye, whereas the same amount of IgG control antibody was injected in the same PBS volume in the contralateral eye (Nanofil Syringe 10 µl equipped with Nanofil 34 G needle, World Precision Tools, Sarasota, USA). Mice were sacrificed at d7 after performing fundus imaging and fluorescence angiography (Fluorescein (ALCON 10%, H12588-0113) was diluted 1: 20 with 0.9% NaCl and 40 µL per 20 g mouse were injected). After enucleation, eye cups were dissected to perform a collagen IV staining for the evaluation of the lesion size in the flat-mounts. Animals with subretinal bleedings or confluent lesions were excluded from further analysis. Lesion area was normalized to the size in IgG control. Normality was given using the Kolmogorov-Smirnov-Test and a ratio paired *t*-test was applied.

Fluorescence Microscopy

After transcardial perfusion with phosphate-buffered saline (PBS), eyes were fixed in 4% PFA for 1 h at RT and processed, as previously described, for flatmounts (Pitulescu et al., 2010). Primary antibodies goat anti-mouse Collagen IV (Merck Millipore, MAB769, Burlington, USA) and rabbit anti-mouse SPP1 (LifeSpan Biosciences, LSBio, LS-B10122, Inc., Seattle, USA) were added overnight in a 1:500 (Collagen IV) or 1:1,000 (SPP1) dilution at 4°C (flatmount). Secondary antibody was applied in a dilution of 1:500 (Alexa Flour® 488 and Alexa Fluor® 647, Thermo Fisher Scientific, Waltham, USA) overnight at 4°C (flatmount). Images were taken using a conventional fluorescence microscope (Olympus BX-61 with a color camera [Olympus DP71]) (Olympus, Tokyo, Japan) and the confocal pictures were taken with a DMi-8 (Leica) with a 20x NA 0.75 CS2 (Leica 506517).

Protein Analysis

Proteins were isolated from choroidal tissue using RIPA buffer (R0278, Sigma) containing protease (Complete Tablets Mini, 0463159001, Roche) and phosphatase inhibitors (Phosstop, 04906845001, Roche). The amount of recovered protein was evaluated by colorimetric assay (BCA kit; Pierce, Rockford, IL). Content of SPP1 (Osteopontin) in 1.25 µg of purified protein was analyzed by using an Osteopontin Mouse ELISA Kit (Thermo Fisher Scientific) according to the manufacturer's instructions.

RNA Sequencing and Analysis

Cx3cr1$^{GFP/+}$ mice were analyzed at the age of 8 weeks. For isolation of microglia, cells were stained with antibodies against CD45 (30-F11, 103133, BioLegend, San Diego, CA, USA), CD11b (M1/70, 17-0112-83, eBioscience, Thermo Fisher Scientific), Ly6C (AL-21, 45-5932-82, eBioscience, Thermo Fisher), and Ly6G (1A8, 551460, BD Pharmingen, BD Biosciences). FVD780 (eBioscience) was used to exclude dead cells. Total bulk RNA was extracted directly into RNAprotect buffer (QIAGEN, Hilden, Germany) from viable FACS-sorted $CD45^{lo}CD11b^{+}CX3CR1^{+}Ly6C^{-}Ly6G^{-}$ retinal microglia according to the "Purification of total RNA from animal and human cells" protocol of the RNeasy Plus Micro Kit (QIAGEN). In brief, cells were stored and shipped in RNAprotect buffer at 2–8°C. After pelleting, the RNAprotect buffer was replaced by RLT Plus buffer (QIAGEN) and the samples were homogenized by vortexing for 30 s. Genomic DNA contamination was removed using gDNA Eliminator spin columns. Next, ethanol was added and the samples were applied to RNeasy MinElute spin columns followed by several wash steps. Finally, total RNA was eluted in 12 µl of nuclease free water. Purity and integrity of the RNA was assessed on the Agilent 2100 Bioanalyzer with the RNA 6000 Pico LabChip reagent set (Agilent, Palo Alto, CA, USA).

The SMARTer Ultra Low Input RNA Kit for Sequencing v4 (Clontech Laboratories, Inc., Mountain View, CA, USA) was used to generate first strand cDNA from 150 to 600 pg total-RNA. Double-stranded cDNA was amplified by LD PCR (12–14 cycles) and purified via magnetic bead clean-up. Library preparation was carried out, as described in the Illumina Nextera XT Sample Preparation Guide (Illumina, Inc., San Diego, CA, USA). Then, 150 pg of input cDNA were tagmented (tagged and fragmented) by the Nextera XT transposome. The products were purified and amplified via a limited-cycle PCR program to generate multiplexed sequencing libraries. For the PCR step 1:5

dilutions of index 1 (i7) and index 2 (i5) primers were used. The libraries were quantified using the KAPA SYBR FAST ABI Prism Library Quantification Kit (Kapa Biosystems, Inc., Woburn, MA, USA). Equimolar amounts of each library were pooled, and the pools were used for cluster generation on the cBot with the Illumina TruSeq SR Cluster Kit v3. The sequencing run was performed on an HiSeq 1000 instrument using the indexed, 50 cycles single-read (SR) protocol and the TruSeq SBS v3 Reagents according to the Illumina HiSeq 1000 System User Guide. Image analysis and base calling resulted in.bcl files, which were converted into.fastq files with the bcl2fastq v2.18 software. RNA extraction, library preparation and RNA-seq were performed at the Genomics Core Facility "KFB—Center of Excellence for Fluorescent Bioanalytics" (University of Regensburg, Regensburg, Germany).

Sequencing data were uploaded to and analyzed on the Galaxy web platform (usegalaxy.eu) (Afgan et al., 2018), as previously described (Boneva et al., 2020). Quality control was performed with FastQC Galaxy Version 0.72 (http://www.bioinformatics.babraham.ac.uk/projects/fastqc/ last access on 07/30/2020). Reads were mapped to the mouse reference genome [Gencode (Frankish et al., 2019), version M25] with RNA STAR (Dobin et al., 2013) Galaxy Version 2.7.2b (default parameters) using the Gencode main annotation file [Gencod (Frankish et al., 2019), version M25]. Two BAM files for each sample (one for each flow cell) were combined in one BAM file per sample using Merge BAM files Galaxy Version 1.2.0. Reads mapped to the mouse reference genome were counted by featureCounts Galaxy Version 1.6.4 (Liao et al., 2014) (default parameters) using the aforementioned annotation file. The output of featureCounts was imported into R Studio (Version 1.2.1335, R Version 3.5.3). Gene symbols were determined based on ENSEMBL (Yates et al., 2020) release 100 (Mouse genes, download at 08/01/2020). Genes with 0 reads in all samples were removed from the analysis. After principal component analysis (Love et al., 2014), differential gene expression was analyzed using the R package DESeq2 Version 1.22.2 (default parameters) (Love et al., 2014). Transcripts with log2fold change (log2FC) > 1.5 or < -1.5 and Benjamini-Hochberg adjusted $p < 0.05$ were considered as differentially expressed genes (DEG). Gene enrichment analysis was performed using the R package clusterProfiler 3.10.1 (Yu et al., 2012). Heatmaps were created using the R package ComplexHeatmap 1.20.0 (Gu et al., 2016). Other data visualization was performed using the ggplot2 package (Wickham, 2009). The sequencing data are available in the Gene Expression Omnibus Database under the accession number GSE160011.

RNA Sequencing Using Massive Analysis of cDNA Ends (MACE)

Total RNA was isolated from formalin-fixed and paraffin-embedded (FFPE) sections of all specimens using the Quick-RNA FFPE Kit (Zymo Research, USA). Following a DNAse I digestion using the Baseline-ZERO kit (Epicenter, USA), the RNA concentration was measured with the Qubit RNA HS Assay Kit on a Qubit Fluorometer (Life Technologies, USA). The RNA quality was determined with the RNA Pico Sensitivity Assay on a LabChip GXII Touch (PerkinElmer, USA). The fragment size of all RNA samples ranged between 120 and 150 bp. The preparation of massive analysis of cDNA ends (MACE) libraries was carried out using 1 μg of total RNA, as previously described (Zajac et al., 2015). The barcoded libraries (four CNV membranes and four control samples) were sequenced simultaneously on the NextSeq 500 (Illumina, USA) with 1 × 75 bp. Data analysis was conducted as described above with the following modifications: Reads were mapped to the human reference genome (hg38, Galaxy built-in reference genome) with RNA STAR Galaxy Version 2.6.0b-2 6 (default parameters) using the Gencode annotation file (Gencode 31, release June 2019, downloaded on 08/05/2019, https://www.gencodegenes.org/human/releases.html). The sequencing data are available in the Gene Expression Omnibus Database under the accession number GSE146887.

Human Tissue

Whole human eyes (ciliary body melanoma) or eye tissue (CNV membrane) were acquired after an informed consent form was signed by the patients prior to surgery at the Eye Center, University Medical Center Freiburg. At the Institute of Anatomy, eyes were enucleated in consent with the body donors, secured by contract, and no data other than age, sex, and cause of death were disclosed. MACE RNA Sequencing was performed on four FFPE-treated CNV membranes extracted from patients with neovascular AMD during vitreoretinal surgery between 1992 and 1999. Four age-matched FFPE RPE-choroidal specimens were obtained from the macular region of enucleated eyes suffering from ciliary body melanoma serving as controls. The macular RPE and choroid was unaffected in these eyes as confirmed by routine histology. FFPE tissue was sliced with 7 μm thickness and placed on glass slides. For immunofluorescence, deparaffinization (15 min xylol followed by descending ethanol concentrations with 5 min per concentration [100, 96, and 70%]) was conducted, followed by adding aqua dest at room temperature and citrate buffer (pH = 6) for 2 × 5 min at 95°C. After washing 3 × 10 min with PBS TritonX 0.3% (PBS-T), blocking solution (PBS-T, 5% goat serum) was applied for 30 min at RT. Primary antibodies (IBA1, 234 013, Synaptic Systems; mouse-anti human SPP1/Osteopontin, LS-C169155, clone 7C5H12, LifeSpan BioSciences, Inc., Seattle, USA) were diluted in PBS 0.5% bovine serum albumine (BSA) for incubation overnight at 4°C. After washing with PBS-T, slides were incubated with secondary antibodies goat anti-mouse Alexa Fluor® 647 and goat anti-rabbit Alexa Fluor® 568 for 1 h at RT. After washing with aqua dest, autofluorescence was quenched with Sudan Black B (0.3% in 70% ethanol overnight stirring at 50°C, filtrated twice and incubated for 5 min at 37°C on the slides) and nuclei were counterstained with 4′,6-Diamidin-2-phenylindol (DAPI) 1:10,000 for 10 min, washed three times with aqua dest, and embedded in Fluorescence Mounting Medium (Agilent Dako).

Statistical Analysis

Statistical analysis was performed using GraphPad Prism (GraphPad Software, Version 6.0, La Jolla, USA). Data were tested for normality applying the Kolmogorov–Smirnov test. If normality was given, an unpaired *t*-test was applied, if not indicated otherwise. If the data did not meet the criteria of normality, the Mann–Whitney test was applied. Differences were considered significant when $P < 0.05$.

DATA AVAILABILITY STATEMENT

The original contributions presented in the study are publicly available. This data can be found at: https://www.ncbi.nlm.nih.gov/geo/query/acc.cgi?acc=GSE160011.

ETHICS STATEMENT

The studies involving human participants were reviewed and approved by Ethics committee of the University of Freiburg. The patients/participants provided their written informed consent to participate in this study. The animal study was reviewed and approved by Regierungspräsidium Freiburg i. Br.

AUTHOR CONTRIBUTIONS

AS, PZ, AT, D-DR, and PW conducted experiments and analyzed data. SB provided CNV tissue and human RNA-seq data. JW analyzed bulk RNA-seq data. PW wrote the manuscript with support from AS, SB, GS, and CL. CL and PW supervised the project. All authors contributed to the article and approved the submitted version.

FUNDING

AS and CL were supported by the SFB/TRR167.

ACKNOWLEDGMENTS

The authors thank Marc Leinweber, Gabriele Prinz, Constance Hobusch, Jana Brendler, Heidrun Kuhrt, and Sylvia Zeitler for excellent technical assistance, M. Follo and team at Lighthouse fluorescence technologies Core Facility, University Medical Center Freiburg for cell sorting, CEMT at University of Freiburg for excellent animal care, KFB, Center of Excellence for Fluorescent Bioanalytics, Regensburg for RNA-seq analysis, GenXPro, Frankfurt a. M. for MACE and analysis, Claudia Auw-Hädrich for providing tissue. We are grateful to the body donors at the Institute of Anatomy. We acknowledge support from the Leipzig University for Open Access Publishing.

REFERENCES

Afgan, E., Baker, D., Batut, B., van den Beek, M., Bouvier, D., Cech, M., et al. (2018). The galaxy platform for accessible, reproducible and collaborative biomedical analyses: 2018 update. *Nucleic Acids Res.* 46, W537–W544. doi: 10.1093/nar/gky379

Ajami, B., Samusik, N., Wieghofer, P., Ho, P. P., Crotti, A., Bjornson, Z., et al. (2018). Single-cell mass cytometry reveals distinct populations of brain myeloid cells in mouse neuroinflammation and neurodegeneration models. *Nat. Neurosci.* 21, 541–551. doi: 10.1038/s41593-018-0100-x

Beguier, F., Housset, M., Roubeix, C., Augustin, S., Zagar, Y., Nous, C., et al. (2020). The 10q26 risk haplotype of age-related macular degeneration aggravates subretinal inflammation by impairing monocyte elimination. *Immunity* 53, 429–441.e8. doi: 10.1016/j.immuni.2020.07.021

Boeck, M., Thien, A., Wolf, J., Hagemeyer, N., Laich, Y., Yusuf, D., et al. (2020). Temporospatial distribution and transcriptional profile of retinal microglia in the oxygen-induced retinopathy mouse model. *Glia* 68, 1859–1873. doi: 10.1002/glia.23810

Boneva, S., Schlecht, A., Böhringer, D., Mittelviefhaus, H., Reinhard, T., Agostini, H., et al. (2020). 3′ MACE RNA-sequencing allows for transcriptome profiling in human tissue samples after long-term storage. *Lab. Invest.* 100, 1345–1355. doi: 10.1038/s41374-020-0446-z

Chidlow, G., Wood, J. P. M., Manavis, J., Osborne, N. N., and Casson, R. J. (2008). Expression of osteopontin in the rat retina: effects of excitotoxic and ischemic injuries. *Invest. Ophthalmol. Vis. Sci.* 49, 762–771. doi: 10.1167/iovs.07-0726

Dejda, A., Mawambo, G., Daudelin, J.-F., Miloudi, K., Akla, N., Patel, C., et al. (2016). Neuropilin-1-expressing microglia are associated with nascent retinal vasculature yet dispensable for developmental angiogenesis. *Invest. Ophthalmol. Vis. Sci.* 57, 1530–1536. doi: 10.1167/iovs.15-18598

Dobin, A., Davis, C. A., Schlesinger, F., Drenkow, J., Zaleski, C., Jha, S., et al. (2013). STAR: ultrafast universal RNA-seq aligner. *Bioinformatics* 29, 15–21. doi: 10.1093/bioinformatics/bts635

Droho, S., Thomson, B. R., Makinde, H. M., Cuda, C. M., Perlman, H., and Lavine, J. A. (2020). Ocular macrophage origin and heterogeneity during steady state and experimental choroidal neovascularization. *J. Neuroinflamm.* 17:341. doi: 10.1186/s12974-020-02010-0

Fantin, A., Vieira, J. M., Gestri, G., Denti, L., Schwarz, Q., Prykhozhij, S., et al. (2010). Tissue macrophages act as cellular chaperones for vascular anastomosis downstream of VEGF-mediated endothelial tip cell induction. *Blood* 116, 829–840. doi: 10.1182/blood-2009-12-257832

Fine, S. L., Berger, J. W., Maguire, M. G., and Ho, A. C. (2000). Age-related macular degeneration. *N. Engl. J. Med.* 342, 483–492. doi: 10.1056/NEJM200002173420707

Frankish, A., Diekhans, M., Ferreira, A.-M., Johnson, R., Jungreis, I., Loveland, J., et al. (2019). GENCODE reference annotation for the human and mouse genomes. *Nucleic Acids Res.* 47, D766–D773. doi: 10.1093/nar/gky955

Fujita, N., Fujita, S., Ogata, N., Matsuoka, M., Okada, Y., Kon, S., et al. (2011). Endogenous osteopontin involvement in laser-induced choroidal neovascularization in mice. *Invest. Ophthalmol. Vis. Sci.* 52, 9310–9315. doi: 10.1167/iovs.10-7050

Ginhoux, F., Greter, M., Leboeuf, M., Nandi, S., See, P., Gokhan, S., et al. (2010). Fate mapping analysis reveals that adult microglia derive from primitive macrophages. *Science* 330, 841–845. doi: 10.1126/science.1194637

Goldmann, T., Wieghofer, P., Jordão, M. J. C., Prutek, F., Hagemeyer, N., Frenzel, K., et al. (2016). Origin, fate and dynamics of macrophages at central nervous system interfaces. *Nat. Immunol.* 17, 797–805. doi: 10.1038/ni.3423

Goldmann, T., Wieghofer, P., Muller, P. F., Wolf, Y., Varol, D., Yona, S., et al. (2013). A new type of microglia gene targeting shows TAK1 to be pivotal in CNS autoimmune inflammation. *Nat. Neurosci.* 16, 1618–1626. doi: 10.1038/nn.3531

Gu, Z., Eils, R., and Schlesner, M. (2016). Complex heatmaps reveal patterns and correlations in multidimensional genomic data. *Bioinformatics* 32, 2847–2849. doi: 10.1093/bioinformatics/btw313

Hosaka, K., Rojas, K., Fazal, H. Z., Schneider, M. B., Shores, J., Federico, V., et al. (2017). Monocyte chemotactic protein-1-interleukin-6-osteopontin pathway of intra-aneurysmal tissue healing. *Stroke* 48, 1052–1060. doi: 10.1161/STROKEAHA.116.015590

Hulsmans, M., Sager, H. B., Roh, J. D., Valero-Muñoz, M., Houstis, N. E., Iwamoto, Y., et al. (2018). Cardiac macrophages promote diastolic dysfunction. *J. Exp. Med.* 215, 423–440. doi: 10.1084/jem.20171274

Keren-Shaul, H., Spinrad, A., Weiner, A., Matcovitch-Natan, O., Dvir-Szternfeld, R., Ulland, T. K., et al. (2017). A unique microglia type associated with restricting development of Alzheimer's disease. *Cell* 169, 1276–1290.e17. doi: 10.1016/j.cell.2017.05.018

Kierdorf, K., Erny, D., Goldmann, T., Sander, V., Schulz, C., Perdiguero, E. G., et al. (2013). Microglia emerge from erythromyeloid precursors via Pu.1- and Irf8-dependent pathways. *Nat. Neurosci.* 16, 273–280. doi: 10.1038/nn.3318

Kunii, Y., Niwa, S., Hagiwara, Y., Maeda, M., Seitoh, T., and Suzuki, T. (2009). The immunohistochemical expression profile of osteopontin in normal human tissues using two site-specific antibodies reveals a wide distribution of positive cells and extensive expression in the central and peripheral nervous systems. *Med. Mol. Morphol.* 42, 155–161. doi: 10.1007/s00795-009-0459-6

Lambert, V., Lecomte, J., Hansen, S., Blacher, S., Gonzalez, M.-L. A., Struman, I., et al. (2013). Laser-induced choroidal neovascularization model to study age-related macular degeneration in mice. *Nat. Protoc.* 8, 2197–2211. doi: 10.1038/nprot.2013.135

Levy, O., Calippe, B., Lavalette, S., Hu, S. J., Raoul, W., Dominguez, E., et al. (2015a). Apolipoprotein E promotes subretinal mononuclear phagocyte survival and chronic inflammation in age-related macular degeneration. *EMBO Mol. Med.* 7, 211–226. doi: 10.15252/emmm.201404524

Levy, O., Lavalette, S., Hu, S. J., Housset, M., Raoul, W., Eandi, C., et al. (2015b). APOE isoforms control pathogenic subretinal inflammation in age-related macular degeneration. *J. Neurosci.* 35, 13568–13576. doi: 10.1523/JNEUROSCI.2468-15.2015

Liao, Y., Smyth, G. K., and Shi, W. (2014). featureCounts: an efficient general purpose program for assigning sequence reads to genomic features. *Bioinformatics* 30, 923–930. doi: 10.1093/bioinformatics/btt656

Lok, Z. S. Y., and Lyle, A. N. (2019). Osteopontin in vascular disease. *Arterioscler. Thromb. Vasc. Biol.* 39, 613–622. doi: 10.1161/ATVBAHA.118.311577

Love, M. I., Huber, W., and Anders, S. (2014). Moderated estimation of fold change and dispersion for RNA-seq data with DESeq2. *Genome Biol.* 15:550. doi: 10.1186/s13059-014-0550-8

Lückoff, A., Caramoy, A., Scholz, R., Prinz, M., Kalinke, U., and Langmann, T. (2016). Interferon-beta signaling in retinal mononuclear phagocytes attenuates pathological neovascularization. *EMBO Mol. Med.* 8, 670–678. doi: 10.15252/emmm.201505994

Magdaleno, F., Ge, X., Fey, H., Lu, Y., Gaskell, H., Blajszczak, C. C., et al. (2018). Osteopontin deletion drives hematopoietic stem cell mobilization to the liver and increases hepatic iron contributing to alcoholic liver disease. *Hepatol. Commun.* 2, 84–98. doi: 10.1002/hep4.1116

Masuda, T., Sankowski, R., Staszewski, O., Böttcher, C., Amann, L., Sagar, et al. (2019). Spatial and temporal heterogeneity of mouse and human microglia at single-cell resolution. *Nature* 566, 388–392. doi: 10.1038/s41586-019-0924-x

Masuda, T., Sankowski, R., Staszewski, O., and Prinz, M. (2020). Microglia heterogeneity in the single-cell era. *Cell Rep.* 30, 1271–1281. doi: 10.1016/j.celrep.2020.01.010

O'Brien, E. R., Garvin, M. R., Stewart, D. K., Hinohara, T., Simpson, J. B., Schwartz, S. M., et al. (1994). Osteopontin is synthesized by macrophage, smooth muscle, and endothelial cells in primary and restenotic human coronary atherosclerotic plaques. *Arterioscler. Thromb.* 14, 1648–1656. doi: 10.1161/01.ATV.14.10.1648

Oh, H., Takagi, H., Takagi, C., Suzuma, K., Otani, A., Ishida, K., et al. (1999). The potential angiogenic role of macrophages in the formation of choroidal neovascular membranes. *Invest. Ophthalmol. Vis. Sci.* 40, 1891–1898.

O'Koren, E. G., Yu, C., Klingeborn, M., Wong, A. Y. W., Prigge, C. L., Mathew, R., et al. (2019). Microglial function is distinct in different anatomical locations during retinal homeostasis and degeneration. *Immunity* 50, 723–737.e7. doi: 10.1016/j.immuni.2019.02.007

Ong, S. S., Malek, G., Espinosa-Heidmann, D. G., Wu, K., Saloupis, P., Spiga, M. G., et al. (2011). Osteopontin drives fibrosis in a mouse model of neovascular age related macular degeneration. *Invest. Ophthalmol. Vis. Sci.* 52, 942–942.

Patouraux, S., Rousseau, D., Rubio, A., Bonnafous, S., Lavallard, V. J., Lauron, J., et al. (2014). Osteopontin deficiency aggravates hepatic injury induced by ischemia-reperfusion in mice. *Cell Death Dis.* 5:e1208. doi: 10.1038/cddis.2014.174

Pitulescu, M. E., Schmidt, I., Benedito, R., and Adams, R. H. (2010). Inducible gene targeting in the neonatal vasculature and analysis of retinal angiogenesis in mice. *Nat. Protoc.* 5, 1518–1534. doi: 10.1038/nprot.2010.113

Rabenstein, M., Vay, S. U., Flitsch, L. J., Fink, G. R., Schroeter, M., and Rueger, M. A. (2016). Osteopontin directly modulates cytokine expression of primary microglia and increases their survival. *J. Neuroimmunol.* 299, 130–138. doi: 10.1016/j.jneuroim.2016.09.009

Reyes, N. J., O'Koren, E. G., and Saban, D. R. (2017). New insights into mononuclear phagocyte biology from the visual system. *Nat. Rev. Immunol.* 17, 322–332. doi: 10.1038/nri.2017.13

Rowe, G. C., Raghuram, S., Jang, C., Nagy, J. A., Patten, I. S., Goyal, A., et al. (2014). PGC-1α induces SPP1 to activate macrophages and orchestrate functional angiogenesis in skeletal muscle. *Circ. Res.* 115, 504–517. doi: 10.1161/CIRCRESAHA.115.303829

Sankowski, R., Böttcher, C., Masuda, T., Geirsdottir, L., Sagar, null, Sindram, E., et al. (2019). Mapping microglia states in the human brain through the integration of high-dimensional techniques. *Nat. Neurosci.* 22, 2098–2110. doi: 10.1038/s41593-019-0532-y

Schlecht, A., Boneva, S., Gruber, M., Zhang, P., Horres, R., Bucher, F., et al. (2020). Transcriptomic characterization of human choroidal neovascular membranes identifies calprotectin as a novel biomarker for patients with age-related macular degeneration. *Am. J. Pathol.* 190, 1632–1642. doi: 10.1016/j.ajpath.2020.04.004

Song, W. M., and Colonna, M. (2018). The identity and function of microglia in neurodegeneration. *Nat. Immunol.* 19, 1048–1058. doi: 10.1038/s41590-018-0212-1

Szulzewsky, F., Schwendinger, N., Güneykaya, D., Cimino, P. J., Hambardzumyan, D., Synowitz, M., et al. (2017). Loss of host-derived osteopontin creates a glioblastoma-promoting microenvironment. *Neuro Oncol.* 20, 355–366. doi: 10.1093/neuonc/nox165

Tambuyzer, B. R., Casteleyn, C., Vergauwen, H., Van Cruchten, S., and Van Ginneken, C. (2012). Osteopontin alters the functional profile of porcine microglia *in vitro*. *Cell Biol. Int.* 36, 1233–1238. doi: 10.1042/CBI20120172

Tobe, T., Ortega, S., Luna, J. D., Ozaki, H., Okamoto, N., Derevjanik, N. L., et al. (1998). Targeted disruption of the FGF2 gene does not prevent choroidal neovascularization in a murine model. *Am. J. Pathol.* 153, 1641–1646. doi: 10.1016/S0002-9440(10)65753-7

Tremmel, M., Matzke, A., Albrecht, I., Laib, A. M., Olaku, V., Ballmer-Hofer, K., et al. (2009). A CD44v6 peptide reveals a role of CD44 in VEGFR-2 signaling and angiogenesis. *Blood* 114, 5236–5244. doi: 10.1182/blood-2009-04-219204

Usui-Ouchi, A., Usui, Y., Kurihara, T., Aguilar, E., Dorrell, M. I., Ideguchi, Y., et al. (2020). Retinal microglia are critical for subretinal neovascular formation. *JCI Insight* 5:e137317. doi: 10.1172/jci.insight.137317

Van Hove, I., De Groef, L., Boeckx, B., Modave, E., Hu, T.-T., Beets, K., et al. (2020). Single-cell transcriptome analysis of the Akimba mouse retina reveals cell-type-specific insights into the pathobiology of diabetic retinopathy. *Diabetologia* 63, 2235–2248. doi: 10.1007/s00125-020-05218-0

Wickham, H. (2009). *ggplot2: Elegant Graphics for Data Analysis*. New York, NY: Springer-Verlag. doi: 10.1007/978-0-387-98141-3

Wieghofer, P., Knobeloch, K.-P., and Prinz, M. (2015). Genetic targeting of microglia. *Glia* 63, 1–22. doi: 10.1002/glia.22727

Wieghofer, P., Hagemeyer, N., Sankowski, R., Schlecht, A., Staszewski, O., Amann, L., et al. (in press). Mapping the origin and fate of myeloid cells in distinct compartments of the eye by single-cell profiling. *EMBO J.* doi: 10.15252/embj.2020105123

Wolf, A., Herb, M., Schramm, M., and Langmann, T. (2020). The TSPO-NOX1 axis controls phagocyte-triggered pathological angiogenesis in the eye. *Nat. Commun.* 11:2709. doi: 10.1038/s41467-020-16400-8

Yates, A. D., Achuthan, P., Akanni, W., Allen, J., Allen, J., Alvarez-Jarreta, J., et al. (2020). Ensembl 2020. *Nucleic Acids Res.* 48, D682–D688. doi: 10.1093/nar/gkz966

Yu, G., Wang, L.-G., Han, Y., and He, Q.-Y. (2012). clusterProfiler: an R package for comparing biological themes among gene clusters. *OMICS* 16, 284–287. doi: 10.1089/omi.2011.0118

Yu, H., Liu, X., and Zhong, Y. (2017). The effect of osteopontin on microglia. *Biomed. Res. Int.* 2017:1879437. doi: 10.1155/2017/1879437

Zajac, B. K., Amendt, J., Horres, R., Verhoff, M. A., and Zehner, R. (2015). *De novo* transcriptome analysis and highly sensitive digital gene expression profiling of *Calliphora vicina* (*Diptera*: *Calliphoridae*) pupae using MACE (massive analysis of cDNA ends). *Forensic. Sci. Int. Genet.* 15, 137–146. doi: 10.1016/j.fsigen.2014.11.013

Conflict of Interest: The authors declare that the research was conducted in the absence of any commercial or financial relationships that could be construed as a potential conflict of interest.

frontiers in Cell and Developmental Biology

BRIEF RESEARCH REPORT
published: 02 February 2021
doi: 10.3389/fcell.2021.627976

Use of Clodronate Liposomes to Deplete Phagocytic Immune Cells in *Drosophila melanogaster* and *Aedes aegypti*

Jyothsna Ramesh Kumar[1,2†], Jessica P. Smith[2†], Hyeogsun Kwon[2] and Ryan C. Smith[2]*

[1] *Interdepartmental Graduate Program in Immunobiology, Iowa State University, Ames, IA, United States,* [2] *Department of Entomology, Iowa State University, Ames, IA, United States*

The innate immune system is the primary defense response to limit invading pathogens for all invertebrate species. In insects, immune cells are central to both cellular and humoral immune responses, however few genetic resources exist beyond *Drosophila* to study immune cell function. Therefore, the development of innovative tools that can be widely applied to a variety of insect systems is of importance to advance the study of insect immunity. Here, we have adapted the use of clodronate liposomes (CLD) to deplete phagocytic immune cells in the vinegar fly, *Drosophila melanogaster,* and the yellow fever mosquito, *Aedes aegypti*. Through microscopy and molecular techniques, we validate the depletion of phagocytic cell populations in both insect species and demonstrate the integral role of phagocytes in combating bacterial pathogens. Together, these data demonstrate the wide utility of CLD in insect systems to advance the study of phagocyte function in insect innate immunity.

Keywords: phagocytosis, hemocytes, immune cells, phagocyte depletion, clodronate liposomes, *Aedes (Ae.) aegypti*, *Drosophila melanogaster*

OPEN ACCESS

Edited by:
Marc S. Dionne,
Imperial College London,
United Kingdom

Reviewed by:
Alysia Vrailas-Mortimer,
Illinois State University, United States
Shruti Yadav,
Molecular Medicine Research Institute, United States

***Correspondence:**
Ryan C. Smith
smithr@iastate.edu

† These authors have contributed equally to this work

Specialty section:
This article was submitted to Cell Death and Survival, a section of the journal Frontiers in Cell and Developmental Biology

Received: *10 November 2020*
Accepted: *11 January 2021*
Published: *02 February 2021*

Citation:
Ramesh Kumar J, Smith JP, Kwon H and Smith RC (2021) Use of Clodronate Liposomes to Deplete Phagocytic Immune Cells in Drosophila melanogaster and Aedes aegypti. Front. Cell Dev. Biol. 9:627976. doi: 10.3389/fcell.2021.627976

INTRODUCTION

Insects rely on conserved cellular and humoral responses as the primary defense to invading pathogens. Immune cells, known as hemocytes, can directly participate in cellular responses such as phagocytosis and encapsulation (Lemaitre and Hoffmann, 2007; Hillyer and Strand, 2014), as well as mediate humoral signaling responses (Foley and O'Farrell, 2003; Wu et al., 2012) that limit pathogen survival. Studies in *Drosophila* have been aided by a wealth of genetic tools that include mutant and transgenic lines (Braun et al., 1997, 1998; Kurucz et al., 2003; Zettervall et al., 2004), as well as genetic techniques to ablate populations of plasmatocytes (Charroux and Royet, 2009; Defaye et al., 2009) that have significantly advanced our understanding of insect immune cells. However, the lack of genetic resources in non-model insect systems has severely limited studies of immune cell function. In mosquitoes, there has been a dependence on RNAi for reverse-genetic studies of hemocytes (Pinto et al., 2009; Ramirez et al., 2014; Smith et al., 2015, 2016), yet due to the absence of hemocyte markers and the systemic nature of gene-silencing, there have been significant limitations to address gene function in specific tissues or immune cell-types.

Evidence from vertebrate systems has demonstrated that chemical approaches can be utilized to target immune cells (Shek and Lukovich, 1982; Kagan and Hartmann, 1984;

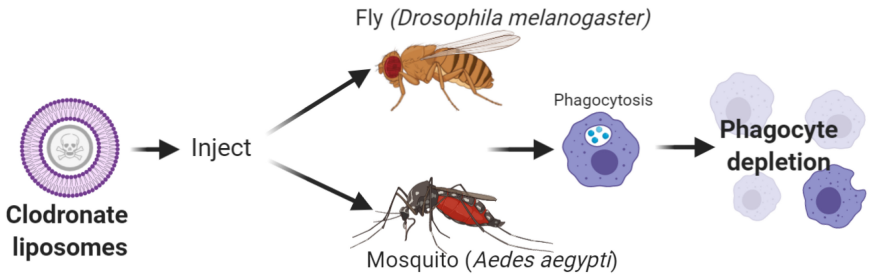

GRAPHICAL ABSTRACT | Overview of phagocyte depletion experiments using clodronate liposomes to in *Drosophila melanogaster* or *Aedes aegypti*. Created with BioRender.com.

van Rooijen and Sanders, 1994), overcoming specific requirements for genetic tools to study immune cell function. Among these chemical approaches, clodronate liposomes (CLD) have shown the most promise and have been widely used in vertebrate systems to examine macrophage function (van Rooijen and Sanders, 1994; Lehenkari et al., 2002; van Rooijen and Hendrikx, 2010). Relying on the phagocytic properties of a subset of immune cells, CLD can be specifically delivered to macrophage populations, where after being phagocytosed they are degraded by the lysosome to promote apoptosis (van Rooijen and Sanders, 1994; van Rooijen and Hendrikx, 2010). Non-target cells lacking phagocytic abilities and lysosomal components are not affected by CLD treatment (van Rooijen and Sanders, 1994; van Rooijen and Hendrikx, 2010). This methodology has been widely applied in mammalian systems to understand autoimmune disease and macrophage contributions to infection biology (Jordan et al., 2003; Cockburn et al., 2010; Cha et al., 2015).

A recent study in mosquitoes described the use of CLD to deplete phagocytic immune cell populations in *Anopheles gambiae* (Kwon and Smith, 2019), demonstrating for the first time that CLD can be utilized in an invertebrate. Based on the highly conserved phagocytic properties of immune cells, the use of CLD has significant potential as a tool to study invertebrate immune function, overcoming many of the technical hurdles for non-model insect species. To further examine its applicability to insect species, in this study we examine the use of CLD to similarly investigate phagocytic immune cell function in *Drosophila melanogaster* and *Aedes aegypti*. Through these studies, we demonstrate that CLD can effectively deplete phagocytic cell populations of both species, illustrating the broad application of the use of CLD to study innate immune cell function across insects.

METHODS

Fly Stocks

Drosophila melanogaster fly stocks were maintained at 25°C on standard molasses-based fly medium (Archon Scientific). Previously described SRP-mCherry (w[1118]; P{w[+ mC] = srpHemo-3XmCherry}; stock #78358) and HeGal4-UAS-GFP (w[*]; P{w[+ mC] = He-GAL4.Z}85, P{w[+ mC] = UAS-GFP.nls}8; stock #8700) transgenic lines (Zettervall et al., 2004; Gyoergy et al., 2018) which express fluorescent proteins under universal larval hemocyte markers were obtained from the Bloomington Stock Center.

Mosquito Rearing

Aedes aegypti (Liverpool strain) mosquitoes were reared at 27°C and 80% relative humidity with a 14:10 h light/dark period. Larvae were reared on a 50:50 diet of ground fish flakes (Tetramin, Tetra) and milk bone dog biscuits. Adults were maintained on a 10% sucrose solution. All experimental techniques were performed on cohorts of 4–6 days old adult female mosquitoes.

Phagocytic Cell Depletion Using Clodronate Liposomes

Adult flies (2–3 days old) and mosquitoes (3–5 days old) were intra-thoracically injected with 69 nl of control liposomes (LP) or CLD (Standard macrophage depletion kit, Encapsula NanoSciences LLC) using a Nanoject III injector (Drummond Scientific) as previously described (Kwon and Smith, 2019). To determine the ideal concentrations for each species to maximize CLD efficacy on phagocyte depletion while minimizing effects on survival, dilutions of commercially available stock solutions of LP (24.3 mM L-alpha-phosphatidylcholine, 10.9 mM cholesterol) and CLD (24.3 mM L-alpha-phosphatidylcholine, 10.9 mM cholesterol, 18.4 mM Clodronate [(Dichloro-phosphono-methyl)phosphonate) were prepared in 1X PBS (1 (stock), 1:2, 1:3, 1:4 (only *Aedes*), 1:5] and compared to 1× PBS serving as an injection control. Based on the resulting experiments, a 1:5 dilution was chosen for all subsequent experiments in *Drosophila*, while a 1:4 dilution of LP and CLD was used for experiments with *Ae. aegypti*.

Hemolymph Perfusion and Counting of Hemocytes

To evaluate the efficacy of phagocyte depletion experiments, hemolymph perfusions were performed as previously (Smith et al., 2015; Kwon et al., 2017; Kwon and Smith, 2019) using anticoagulant buffer (vol/vol 60% Schneider's insect medium, 10% fetal bovine serum and 30% citrate buffer, 98 mM NaOH, 186 mM NaCl, 1.7 mM EDTA, 41 mM citric acid, pH

4.5). Perfused hemolymph was placed onto a hemocytometer (Neubauer, C-Chip DHC-N01, INCYTO) where approximately 50 cells were counted per individual fly or approximately 200 cells per individual mosquito for both LP and CLD treated sub-groups. Hemocyte sub-populations were differentiated by morphology (size and shape) or fluorescence (red or green) in the *Drosophila* transgenic lines.

Drosophila samples were examined 48h post-injection, while *Aedes* were evaluated at both 24 and 48h post-injection. Additionally, to examine the effects of blood feeding, blood-fed mosquitoes were examined 24 h post blood-meal (48 h post-injection) after challenge with defibrinated sheep blood (Hemostat Laboratories) using an artificial membrane feeding system.

Bacterial Challenge Following Clodronate Treatment

Cultures of *Serratia marcesens* and *Staphylococcus aureus* were grown overnight in LB at 37°C. For *Drosophila* experiments, bacterial cultures were centrifuged at 8,000 rpm for 5 min, washed twice with 1× PBS, and resuspended in 1× PBS at a concentration of OD_{600} = 0.1. Approximately 24 h after pre-treatment with LP or CLD, adult SRP-mCherry *Drosophila* (n = 20 per replicate) were injected with 23 nl (∼1 × 10^8 CFU/ml) of either bacterial suspensions (*S. marcescens* or *S. aureus*) using a Nanoject III injector as previously described (Troha and Buchon, 2019). Following challenge, flies were maintained at room temperature and survival was monitored every 24 h for 8 days.

For mosquito experiments, *S. marcescens* or *S. aureus* cultures were centrifuged at 8,000 rpm for 5 min, washed twice with 1× PBS and resuspended to a final concentration of OD_{600} = 0.4. OD. A 100× dilution of the bacterial cultures (∼4 × 10^6 CFU/ml) were injected (69 nl) into naïve adult mosquitoes (n = 30 per replicate) 48 h post-treatment with LP or CLD as previously (Kwon and Smith, 2019). The injection of 1× PBS was included as an additional control. The survival of mosquitoes following bacterial challenge was monitored every 24 h for 8 days to determine the effects of phagocyte depletion on mosquito survival.

Gene Expression Analysis Following Clodronate Treatment

Total RNA was isolated from pooled whole fly or mosquito samples using TRIzol (Thermo Fisher Scientific), of which 2 μg of total RNA was used a template for cDNA synthesis using the RevertAid First Strand cDNA Synthesis kit (Thermo Fisher Scientific). To examine gene expression following phagocyte depletion, qRT-PCR was performed using PowerUp SYBR Green Master Mix (Thermo Fischer Scientific) on control- or clodronate-treated treated fly and mosquito samples.

To validate phagocyte depletion in *Drosophila*, primers directed at either GFP or mCherry were examined in their respective transgenic lines using RpL32 as an internal control (**Supplementary Table 1**) using the following cycling conditions: 95°C for 10 min, 40 cycles with 95°C for 15 s and 65°C for 60 s. Similarly, phagocyte depletion was evaluated in *Aedes* using primers directed at the granulocyte-enriched genes, nimrod, and eater, with rpS17 as an internal control (**Supplementary Table 1**). qRT-PCR was performed for 40 cycles using the following cycling conditions: 98°C for 10s, 60°C for 10s and 72°C for 30 s. For both fly and mosquito samples, relative expression was evaluated using a comparative C_T ($2^{-\Delta\Delta Ct}$) method (Livak and Schmittgen, 2001).

RESULTS

To determine the applicability of using CLD to deplete phagocytic cell populations in other insect species (Kwon and Smith, 2019), we first examined the use of CLD in *Drosophila melanogaster*. Following the injection of either LP (empty) or CLD at different dilutions (1:2 or 1:5 in 1× PBS, **Figure 1A**), adult *Drosophila* (SRP-mCherry) were monitored over an 8-day period to examine the potential effects of liposome treatment on fly survival (**Figure 1B**). When compared to PBS-injected controls, LP treatment had no effect on survival [Mantel-Cox; PBS: LP (1:2), P = 0.0811; PBS: LP (1:5), P = 0.0551] (**Figure 1B**). In addition, no differences in *Drosophila* survival were seen between LP and CLD treatments [Mantel-Cox; LP (1:2):CLD (1:2), P = 0.5506; LP (1:5):CLD (1:5), P = 0.6947] (**Figure 1B**). Using the 1:5 dilutions of LP and CLD, we then evaluated the efficacy of phagocyte depletion by perfusing flies two days post-injection (**Figure 1A**). Taking advantage of transgenic stocks that express fluorescent proteins in phagocytic plasmatocyte populations (Zettervall et al., 2004; Gyoergy et al., 2018), we demonstrate that CLD treatment significantly reduces the percentage of $mCherry^+$ (**Figure 1C**) and $EGFP^+$ (**Supplementary Figure 1**) plasmatocytes in *Drosophila* adults. We further validated these depletion experiments in the SRP-mCherry line using qRT-PCR, demonstrating a significant reduction in *mCherry* expression 24 h after CLD treatment (**Figure 1D**). Similar qRT-PCR experiments with the *Hemese*Gal4-UAS-GFP line did not display differences in *GFP* expression when evaluated 24 h post-treatment or at 48 h post-treatment to allow at additional incubation time (**Supplementary Figure 1**). Given the reduction of $EGFP^+$ immune cells following clodronate treatment (**Supplementary Figure 1**), the lack of change to *GFP* expression levels may be due to *GFP* expression in other tissues beyond plasmatocyte populations as previously noted (Zettervall et al., 2004). Together, these data suggest that CLD are able to effectively deplete *Drosophila* phagocyte populations.

Similar experiments were also performed in the yellow fever mosquito, *Aedes aegypti*, to evaluate the use of CLD for phagocyte depletion (**Figure 2A**). Concentrations of either LP or CLD at 1:2, 1:4, or 1:5 dilutions were examined, with none of the concentration having measurable impacts on adult mosquito survival (**Figure 2B**). Both the 1:4 and 1:5 dilutions were able to significantly reduce the percentage of granulocytes at 24- or 48-h post-treatment (**Supplementary Figure 2**), although phagocyte depletion was more effective at 48 h and with the 1:4 dilution (**Supplementary Figure 2**). Moreover, CLD treatment was able to effectively reduce phagocyte populations in mosquitoes under both naïve (**Figure 2C**) and blood-fed conditions (**Figure 2D**).

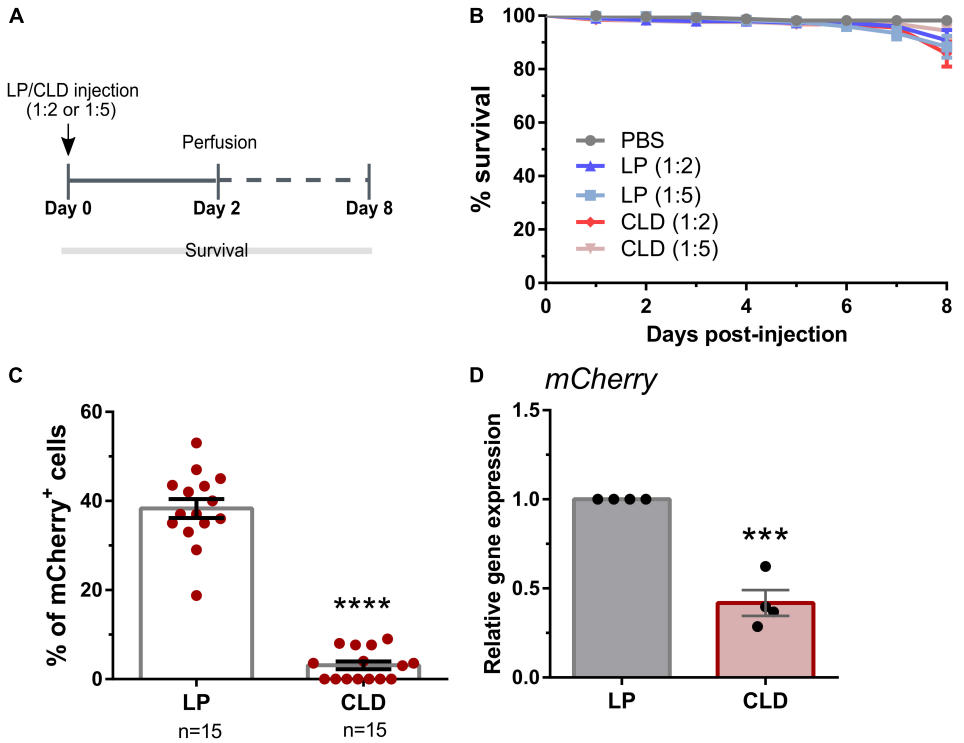

FIGURE 1 | Use of clodronate liposomes to deplete *Drosophila* plasmatocytes. **(A)** Overview of clodronate liposome experiments in *Drosophila* (SRP-mCherry). Control (LP)- or clodronate liposomes (CLD) were diluted at 1:2 or 1:5 in 1X PBS and intrathoracically injected into adult female flies. Survival was then monitored over an eight-day period **(B)**. Error bars represent the mean ± SEM of three independent replicates. In each replicate, 20 female adult flies were used for each experimental condition. LP treatment had no effect on survival [Mantel-Cox; PBS: LP (1:2), $P = 0.0811$; PBS: LP (1:5), $P = 0.0551$], nor were there differences between LP and CLD treatments [Mantel-Cox; LP (1:2):CLD (1:2), $P = 0.5506$; LP (1:5):CLD (1:5), $P = 0.6947$]. Following perfusion two-days post-injection, the percentage of mCherry^{+} hemocytes were evaluated in LP- and CLD-treated flies (1:5 dilution) **(C)**. Data represent the pooled mean ± SEM of three independent experiments and were analyzed by a Mann–Whitney test to determine significance. To further validate phagocyte depletion, *mCherry* expression was examined in whole flies by qRT-PCR **(D)**. Relative *mCherry* transcripts were significantly reduced following CLD-treatment. Data represent the pooled mean ± SEM of four independent experiments and were analyzed using an unpaired t test to determine significance. n = number of individual flies examined. Asterisks denote significance (***$P < 0.001$, ****$P < 0.0001$).

These morphological observations were further validated using qRT-PCR on *eater* and *nimrod*, two transcripts associated with hemocyte phagocytic function (Kocks et al., 2005; Kurucz et al., 2007; Kwon and Smith, 2019). For both *eater* and *nimrod*, clodronate treatment significantly reduced the relative transcript abundance in naïve and blood-fed mosquitoes (**Figure 2E**). Together, these data suggest that CLD can effectively be used to study *Ae. aegypti* phagocyte function.

To determine the effects of phagocyte depletion on immune function and host survival, we challenged adult flies and mosquitoes with bacteria after treatment with LP or CLD (**Figure 3**). *Drosophila* displayed significantly reduced survival following phagocyte depletion when challenged with *S. marcescens* and *S. aureus* (**Figure 3A**) similar to previous reports in which plasmatocytes were depleted through genetic experiments (Charroux and Royet, 2009; Defaye et al., 2009). However, these effects were considered more moderate when compared to the strong phenotypes resulting from similar experiments in *Ae. aegypti,* where the survival of CLD-treated mosquitoes was severely reduced upon challenge of either *S. marcescens* or *S. aureus* (**Figure 3B**). Similar to previous work in the mosquito *Anopheles gambiae* (Kwon and Smith, 2019), *S. marcescens* challenge caused significant pathogenicity in control- and clodronate-treated *Ae. aegypti*, although phagocyte depletion led to significant mortality within 3 days post-challenge (**Figure 3B**). *S. aureus* challenge also led to severe mortality in the phagocyte-depleted background with little effect in control mosquitoes (**Figure 3B**). In agreement with previous studies implicating phagocytic immune cells in mediating insect responses to bacterial challenge (Kocks et al., 2005; Kurucz et al., 2007; Hashimoto et al., 2009; Kwon and Smith, 2019), these results provide further support that CLD can serve as a valuable tool to study cellular immune function and phagocyte contributions to innate immune responses to pathogens across a variety of insect systems.

DISCUSSION

Insects have developed a robust innate immune system for defense against a variety of microorganisms that are the result of developments in diverse ecological systems and environments,

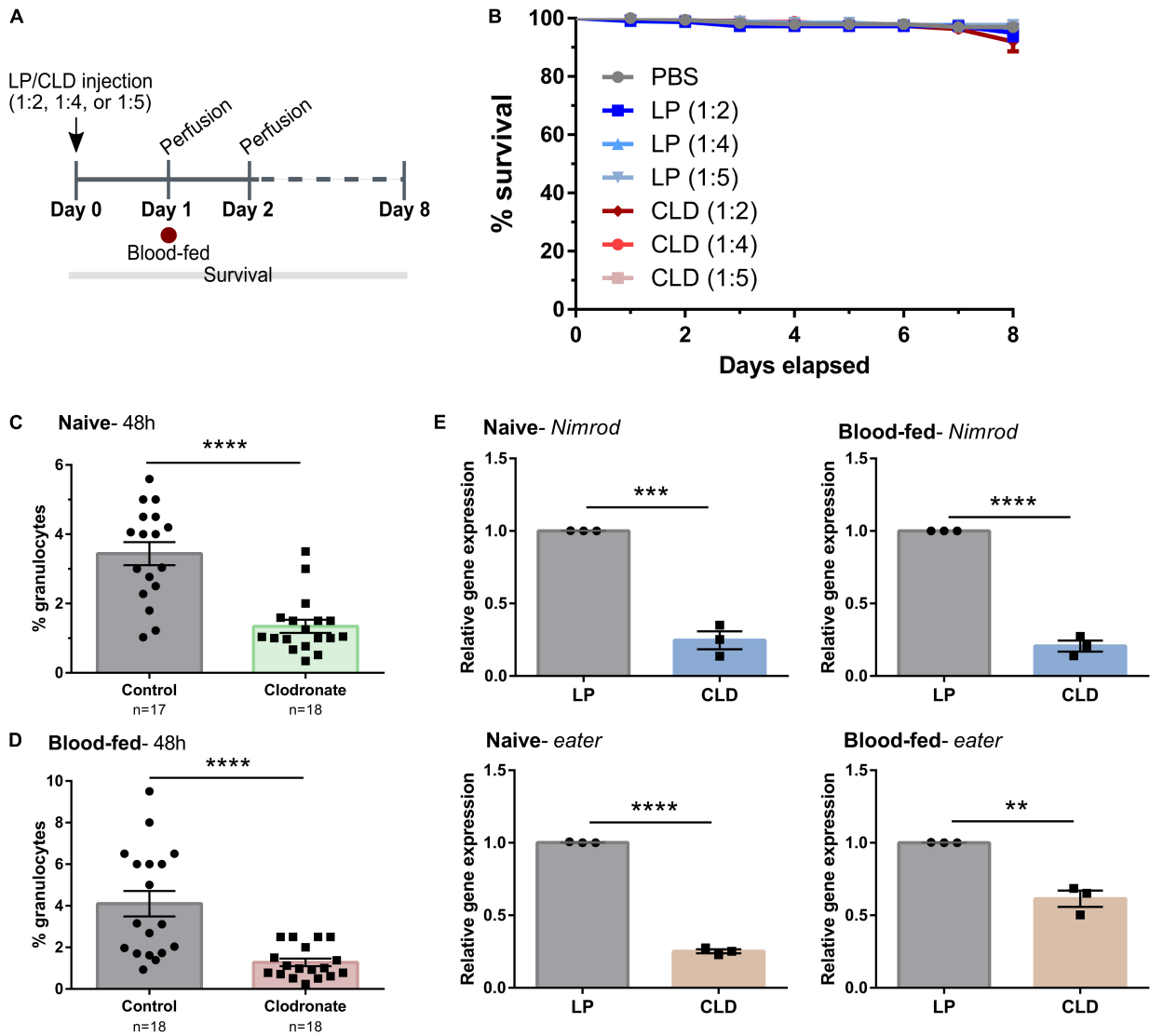

FIGURE 2 | Application of clodronate liposomes to deplete *Ae. aegypti* phagocytic immune cells. **(A)** Overview of clodronate liposome experiments in mosquitoes. Control (LP)- or clodronate liposomes (CLD) were diluted at 1:2, 1:4, or 1:5 in 1X PBS and intrathoracically injected into adult female mosquitoes. Survival was then monitored over an eight-day period **(B)**. Error bars represent the mean ± SEM of two independent replicates. In each replicate, 30 adult female adult mosquitoes were used for each experimental condition. LP treatment had no effect on survival [Mantel-Cox; PBS: LP (1:2), $P = 0.4464$; PBS: LP (1:4), $P = 0.7120$; PBS: LP (1:5), $P = 0.7978$] and there were no differences in survival between LP and CLD treatments [Mantel-Cox; LP (1:2):CLD (1:2), $P = 0.9425$; LP (1:4):CLD (1:4), $P = 0.7992$; LP (1:5):CLD (1:5), $P = 0.8361$]. To evaluate phagocyte depletion, the percentage of granulocytes were examined by light microscopy two-days (48 h) post-injection (1:4 dilution) under either naïve **(C)** or blood-fed conditions **(D)**. Data represent the pooled mean ± SEM of three independent experiments that were analyzed by a Mann–Whitney test to determine significance. To further validate phagocyte depletion, molecular marker of phagocytic cells, *nimrod* and *eater*, were examined in whole mosquitoes by qRT-PCR **(E)**. Relative *nimrod* and *eater* transcripts were significantly reduced following CLD-treatment under both naïve and blood-fed conditions. Data represent the pooled mean ± SEM of three independent experiments that were analyzed using an unpaired t test to determine significance. *n* = number of individual mosquitoes examined. Asterisks denote significance (**$P < 0.01$, ***$P < 0.001$, ****$P < 0.0001$).

as well as the hematophagous behaviors that expose many insect species to bacterial, viral, fungal, and parasitic pathogens. With evidence of immune memory (Pham et al., 2007; Rodrigues et al., 2010; Cooper and Eleftherianos, 2017) and the conservation of immune signaling pathways with mammalian systems (Buchon et al., 2014; Hillyer, 2016), the study of insect immunity offers several advantages for comparative immunology. Moreover, insects have integral roles in the transmission of disease that influence agriculture or that are of veterinary or medical importance. While *Drosophila* has served as an excellent model for insect systems, it is not representative of the diversity in insect systems where studies of non-model insects have been limited by the lack of genetic tools.

Herein, we expand on previous reports in *An. gambiae* (Kwon and Smith, 2019) to describe the use of CLD in *D. melanogaster* and *Ae. aegypti* to deplete phagocytic immune cells. Widely

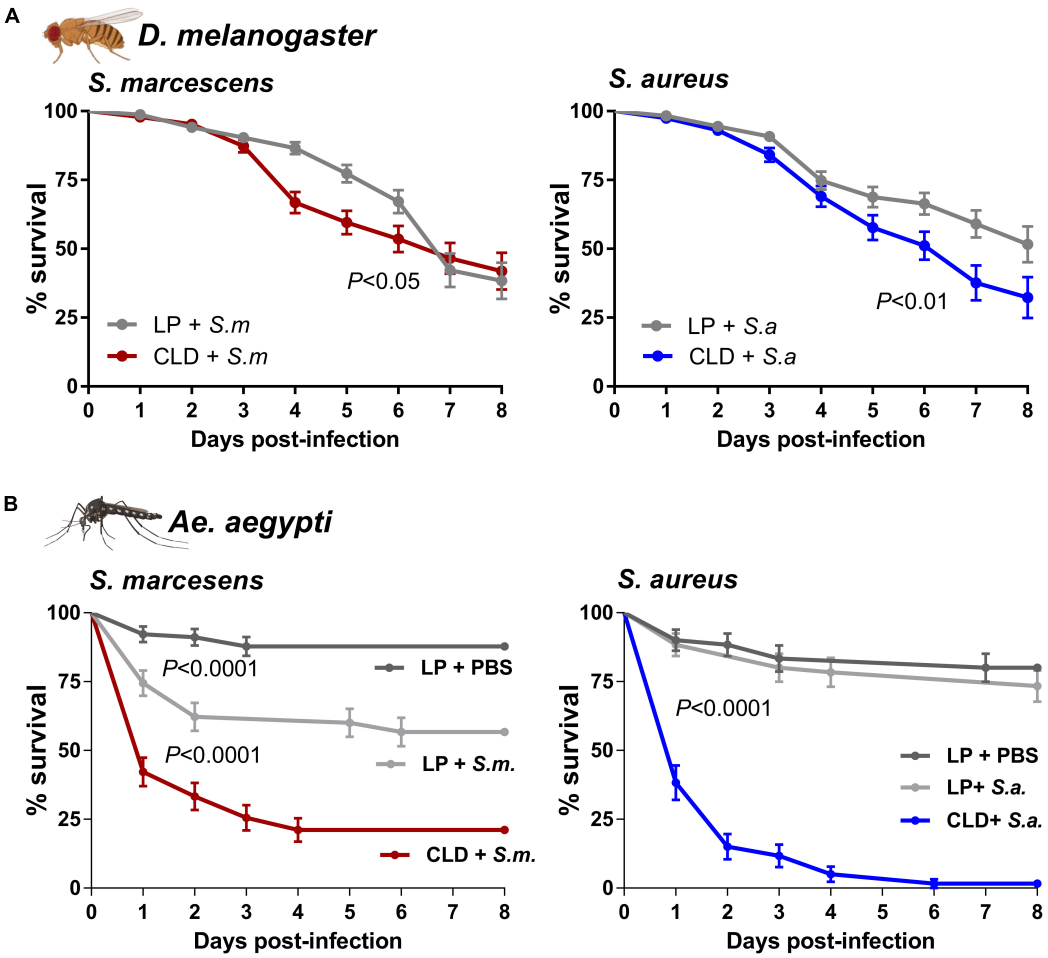

FIGURE 3 | The depletion of phagocytic immune cells influences survival after bacterial challenge. Bacterial challenge assays were performed in flies **(A)** or mosquitoes **(B)** following treatment with control (LP)- or clodronate liposomes (CLD). Survivorship was monitored in every day over an 8-day period to evaluate the effects of *S. marcescens* or *S. aureus* challenge. For mosquito challenge experiments **(B)**, an additional control was added in which LP-treated mosquitoes were challenged with the injection of sterile PBS. Error bars represent the mean ± SEM of three independent replicates for *Drosophila* (20 per replicate) and *Ae. aegypti* (30 per replicate). Data were analyzed using a log-rank (Mantel-Cox) test using GraphPad Prism 6.0. Fly and mosquito images were created with BioRender.com.

used in mammalian systems to deplete macrophage populations function (van Rooijen and Sanders, 1994; Lehenkari et al., 2002; van Rooijen and Hendrikx, 2010), our results provide further evidence that CLD can also be utilized in a variety of insect systems and is supported by conserved, functional similarities between insect and mammalian phagocytes (Browne et al., 2013).

In our proof of principle experiments, we demonstrate through microscopy and qRT-PCR techniques that CLD can significantly reduce phagocytic plasmatocyte or granulocyte populations respectively in adult *D. melanogaster* and *Ae. aegypti*. While mutations (Braun et al., 1997, 1998) or other methods of genetic ablation (Charroux and Royet, 2009; Defaye et al., 2009) to study phagocyte function already exist in *Drosophila*, similar tools have not yet been developed in mosquitoes. Alternative methods to inhibit phagocyte function have been utilized in both *Drosophila* (Elrod-Erickson et al., 2000; Lamiable et al., 2016) and mosquitoes (Castillo et al., 2017) that rely on saturating the phagocytic machinery via the injection of polystyrene beads, yet may not fully impair phagocyte function. Therefore, we believe that the use of CLD provides a convenient method to study phagocyte function in non-model insects, as well as an alternative methodology for model systems such as *Drosophila*. Moreover, the ability to deplete phagocytic cell populations also enables the study of phagocyte contributions to insect-pathogen interactions. This is supported by recent experiments demonstrating phagocyte contributions to anti-*Plasmodium* immunity in *An. gambiae* (Kwon and Smith, 2019) and may be similarly utilized in the future to examine phagocyte function in the context of arbovirus infection in *Ae. aegypti*.

Additional experiments demonstrate the importance of phagocyte function for insect survival following bacterial challenge, wherein both flies and mosquitoes display reduced survival to gram (−) and gram (+) bacteria following phagocyte depletion similar to previous experiments (Charroux and Royet, 2009; Defaye et al., 2009; Kwon and Smith, 2019). Of interest, these survival phenotypes were much stronger

in *Ae. aegypti* where few mosquitoes survived challenge with either *S. marcescens* or *S. aureus*, and may potentially represent differences in the cellular and humoral defenses to bacterial pathogens between mosquitoes and flies that warrant further study.

In summary, we believe that our experiments with CLD support their utility to deplete phagocytes in flies and mosquitoes, providing new or alternative methods to study the cellular and humoral contributions of phagocytes to the defense of invading pathogens. With the conserved utility of CLD in mammals and insects, as well as its ease of use, we believe that CLD can be a significant new resource for the study of invertebrate immunity.

DATA AVAILABILITY STATEMENT

The original contributions presented in the study are included in the article/**Supplementary Material**, further inquiries can be directed to the corresponding author.

AUTHOR CONTRIBUTIONS

JR, JS, and HK performed the experiments and analyzed the results. RS conceived the experiments, analyzed data, and wrote the initial draft of the manuscript. All authors contributed to the editing and writing of the final manuscript.

FUNDING

This work was supported in part by R21AI149118 from the National Institutes of Health, National Institute of Allergy and Infectious Diseases (to RS).

ACKNOWLEDGMENTS

Stocks obtained from the Bloomington Drosophila Stock Center (NIH P40OD018537) were used in this study.

SUPPLEMENTARY MATERIAL

The Supplementary Material for this article can be found online at: https://www.frontiersin.org/articles/10.3389/fcell.2021.627976/full#supplementary-material

REFERENCES

Braun, A., Hoffmann, J. A., and Meister, M. (1998). Analysis of the *Drosophila* host defense in domino mutant larvae, which are devoid of hemocytes. *Proc. Natl. Acad. Sci.* 95, 14337–14342. doi: 10.1073/pnas.95.24.14337

Braun, A., Lemaitre, B., Lanot, R., Zachary, D., and Meister, M. (1997). *Drosophila* immunity: Analysis of larval hemocytes by P-element-mediated enhancer trap. *Genetics* 147, 623–634. doi: 10.1093/genetics/147.2.623

Browne, N., Heelan, M., and Kavanagh, K. (2013). An analysis of the structural and functional similarities of insect hemocytes and mammalian phagocytes. *Virulence* 4, 597–603. doi: 10.4161/viru.25906

Buchon, N., Silverman, N., and Cherry, S. (2014). Immunity in *Drosophila melanogaster*-from microbial recognition to whole-organism physiology. *Nat. Rev. Immunol.* 14, 796–810. doi: 10.1038/nri3763

Castillo, J. C., Beatriz, A., Ferreira, B., Trisnadi, N., and Barillas-Mury, C. (2017). Activation of mosquito complement antiplasmodial response requires cellular immunity. *Sci. Immunol.* 2:eaal1505. doi: 10.1126/sciimmunol.aal1505

Cha, S.-J., Park, K., Srinivasan, P., Schindler, C. W., van Rooijen, N., Stins, M., et al. (2015). CD68 acts as a major gateway for malaria sporozoite liver infection. *J. Exp. Med.* 212, 1391–1403. doi: 10.1084/jem.20110575

Charroux, B., and Royet, J. (2009). Elimination of plasmatocytes by targeted apoptosis reveals their role in multiple aspects of the *Drosophila* immune response. *Proc. Natl. Acad. Sci. U. S. A.* 106, 9797–9802. doi: 10.1073/pnas.0903971106

Cockburn, I. A., Chen, Y. C., Overstreet, M. G., Lees, J. R., van Rooijen, N., Farber, D. L., et al. (2010). Prolonged antigen presentation is required for optimal CD8+ T cell responses against malaria liver stage parasites. *PLoS Pathog.* 6, 1–13. doi: 10.1371/journal.ppat.1000877

Cooper, D., and Eleftherianos, I. (2017). Memory and specificity in the insect immune system: Current perspectives and future challenges. *Front. Immunol.* 8:539. doi: 10.3389/fimmu.2017.00539

Defaye, A., Evans, I., Crozatier, M., Wood, W., Lemaitre, B., and Leulier, F. (2009). Genetic ablation of *Drosophila* phagocytes reveals their contribution to both development and resistance to bacterial infection. *J. Innate Immun.* 1, 322–334. doi: 10.1159/000210264

Elrod-Erickson, M., Mishra, S., and Schneider, D. (2000). Interactions between the cellular and humoral immune responses in *Drosophila*. *Curr. Biol.* 10, 781–784. doi: 10.1016/s0960-9822(00)00569-8

Foley, E., and O'Farrell, P. H. (2003). Nitric oxide contributes to induction of innate immune responses to gram-negative bacteria in Drosophila. *Genes Dev.* 17, 115–125. doi: 10.1101/gad.1018503

Gyoergy, A., Roblek, M., Ratheesh, A., Valoskova, K., Belyaeva, V., Wachner, S., et al. (2018). Tools allowing independent visualization and genetic manipulation of *Drosophila melanogaster* macrophages and surrounding tissues. *G3 Genes Genomes Genet.* 8, 845–857. doi: 10.1534/g3.117.300452

Hashimoto, Y., Tabuchi, Y., Sakurai, K., Kutsuna, M., Kurokawa, K., Awasaki, T., et al. (2009). Identification of lipoteichoic acid as a ligand for draper in the phagocytosis of *Staphylococcus aureus* by *Drosophila* hemocytes. *J. Immunol.* 183, 7451–7460.

Hillyer, J. F. (2016). Insect immunology and hematopoiesis. *Dev. Comp. Immunol.* 58, 102–118. doi: 10.1016/j.dci.2015.12.006

Hillyer, J. F., and Strand, M. R. (2014). Mosquito hemocyte-mediated immune responses. *Curr. Opin. Insect Sci.* 3, 14–21. doi: 10.1016/j.cois.2014.07.002

Jordan, M. B., Van Rooijen, N., Izui, S., Kappler, J., and Marrack, P. (2003). Liposomal clodronate as a novel agent for treating autoimmune hemolytic anemia in a mouse model. *Blood* 101, 594–601. doi: 10.1182/blood-2001-11-0061

Kagan, E., and Hartmann, D. P. (1984). [32] Elimination of macrophages with silica and asbestos. *Methods Enzymol.* 108, 325–335. doi: 10.1016/s0076-6879(84)08099-x

Kocks, C., Cho, J. H., Nehme, N., Ulvila, J., Pearson, A. M., Meister, M., et al. (2005). Eater, a transmembrane protein mediating phagocytosis of bacterial pathogens in *Drosophila*. *Cell* 123, 335–346. doi: 10.1016/j.cell.2005.08.034

Kurucz, É, Márkus, R., Zsámboki, J., Folkl-Medzihradszky, K., Darula, Z., Vilmos, P., et al. (2007). Nimrod, a putative phagocytosis receptor with EGF Repeats in *Drosophila* plasmatocytes. *Curr. Biol.* 17, 649–654. doi: 10.1016/j.cub.2007.02.041

Kurucz, E., Zettervall, C.-J., Sinka, R., Vilmos, P., Pivarcsi, A., Ekengren, S., et al. (2003). Hemese, a hemocyte-specific transmembrane protein, affects the cellular immune response in *Drosophila*. *Proc. Natl. Acad. Sci. U. S. A.* 100, 2622–2627. doi: 10.1073/pnas.0436940100

Kwon, H., Arends, B. R., and Smith, R. C. (2017). Late-phase immune responses limiting oocyst survival are independent of TEP1 function yet display strain specific differences in *Anopheles gambiae*. *Parasit. Vectors* 10:369.

Kwon, H., and Smith, R. C. (2019). Chemical depletion of phagocytic immune cells in *Anopheles gambiae* reveals dual roles of mosquito hemocytes in anti-*Plasmodium* immunity. *Proc. Natl. Acad. Sci.* 116, 14119–14128. doi: 10.1073/pnas.1900147116

Lamiable, O., Arnold, J., da Silva, de Faria, I. J., Proveti Olmo, R., Bergami, F., et al. (2016). Analysis of the contribution of hemocytes and autophagy to *Drosophila* antiviral immunity. *J. Virol.* 90, JVI.238–JVI.216.

Lehenkari, P. P., Kellinsalmi, M., Näpänkangas, J. P., Ylitalo, K. V., Mönkkönen, J., Rogers, M. J., et al. (2002). Further insight into mechanism of action of clodronate: inhibition of mitochondrial ADP/ATP translocase by a nonhydrolyzable, adenine-containing metabolite. *Mol. Pharmacol.* 61, 1255–1262. doi: 10.1124/mol.61.5.1255

Lemaitre, B., and Hoffmann, J. (2007). The host defense of *Drosophila melanogaster*. *Annu. Rev. Immunol.* 25, 697–743.

Livak, K. J., and Schmittgen, T. D. (2001). Analysis of relative gene expression data using real-time quantitative PCR and. *Methods* 25, 402–408. doi: 10.1006/meth.2001.1262

Pham, L. N., Dionne, M. S., Shirasu-Hiza, M., and Schneider, D. S. (2007). A specific primed immune response in *Drosophila* is dependent on phagocytes. *PLoS Pathog.* 3:e26. doi: 10.1371/journal.ppat.0030026

Pinto, S. B., Lombardo, F., Koutsos, A. C., Waterhouse, R. M., McKay, K., An, C., et al. (2009). Discovery of *Plasmodium* modulators by genome-wide analysis of circulating hemocytes in *Anopheles gambiae*. *Proc. Natl. Acad. Sci. U. S. A.* 106, 21270–21275.

Ramirez, J. L., Garver, L. S., Brayner, F. A., Alves, L. C., Rodrigues, J., Molina-Cruz, A., et al. (2014). The role of hemocytes in *Anopheles gambiae* antiplasmodial immunity. *J. Innate Immun.* 6, 119–128. doi: 10.1159/000353765

Rodrigues, J., Brayner, F. A., Alves, L. C., Dixit, R., and Barillas-Mury, C. (2010). Hemocyte differentiation mediates innate immune memory in *Anopheles gambiae* mosquitoes. *Science* 329, 1353–1355. doi: 10.1126/science.1190689

Shek, P. N., and Lukovich, S. (1982). The role of macrophages in promoting the antibody response mediated by liposome-associated protein antigens. *Immunol. Lett.* 5, 305–309. doi: 10.1016/0165-2478(82)90118-3

Smith, R. C., Barillas-Mury, C., and Jacobs-Lorena, M. (2015). Hemocyte differentiation mediates the mosquito late-phase immune response against *Plasmodium* in *Anopheles gambiae*. *Proc. Natl. Acad. Sci.* 112, E3412–E3420.

Smith, R. C., King, J. G., Tao, D., Tomescu, O., Brando, C., Thallinger, G. G., et al. (2016). Molecular profiling of phagocytic immune cells in *Anopheles gambiae* reveals integral roles for hemocytes in mosquito innate immunity. *Mol. Cell. Proteomics* 15, 3373–3387. doi: 10.1074/mcp.m116.060723

Troha, K., and Buchon, N. (2019). Methods for the study of innate immunity in *Drosophila melanogaster*. *Wiley Interdiscip. Rev. Dev. Biol.* 8, 1–25.

van Rooijen, N., and Hendrikx, E. (2010). Liposomes for specific depletion of macrophages from organs and tissues. *Methods Mole. Biol.* 605, 189–203. doi: 10.1007/978-1-60327-360-2_13

van Rooijen, N., and Sanders, A. (1994). Liposome mediated depletion of macrophages: mechanism of action, preparation of liposomes and applications. *J. Immunol. Methods* 174, 83–93. doi: 10.1016/0022-1759(94)90012-4

Wu, S. C., Liao, C. W., Pan, R. L., and Juang, J. L. (2012). Infection-induced intestinal oxidative stress triggers organ-to-organ immunological communication in *Drosophila*. *Cell Host Microbe* 11, 410–417. doi: 10.1016/j.chom.2012.03.004

Zettervall, C.-J., Anderl, I., Williams, M. J., Palmer, R., Kurucz, E., Ando, I., et al. (2004). A directed screen for genes involved in *Drosophila* blood cell activation. *Proc. Natl. Acad. Sci. U. S. A.* 101, 14192–14197. doi: 10.1073/pnas.0403789101

Conflict of Interest: The authors declare that the research was conducted in the absence of any commercial or financial relationships that could be construed as a potential conflict of interest.

frontiers in Cell and Developmental Biology

ORIGINAL RESEARCH
published: 15 February 2021
doi: 10.3389/fcell.2021.624571

A Novel Function of TLR2 and MyD88 in the Regulation of Leukocyte Cell Migration Behavior During Wounding in Zebrafish Larvae

*Wanbin Hu[1], Leonie van Steijn[2], Chen Li[3], Fons J. Verbeek[1,3], Lu Cao[3], Roeland M. H. Merks[1,2] and Herman P. Spaink[1]**

[1] Institute of Biology, Leiden University, Leiden, Netherlands, [2] Mathematical Institute, Leiden University, Leiden, Netherlands, [3] Leiden Institute of Advanced Computer Science, Leiden University, Leiden, Netherlands

OPEN ACCESS

Edited by:
Yi Feng, University of Edinburgh, United Kingdom

Reviewed by:
Felix Ellett, Massachusetts General Hospital and Harvard Medical School, United States
Qing Deng, Purdue University, United States
Milka Sarris, University of Cambridge, United Kingdom

***Correspondence:**
Herman P. Spaink
h.p.spaink@biology.leidenuniv.nl

Specialty section:
This article was submitted to Cell Death and Survival, a section of the journal Frontiers in Cell and Developmental Biology

Received: *31 October 2020*
Accepted: *22 January 2021*
Published: *15 February 2021*

Citation:
Hu W, van Steijn L, Li C, Verbeek FJ, Cao L, Merks RMH and Spaink HP (2021) A Novel Function of TLR2 and MyD88 in the Regulation of Leukocyte Cell Migration Behavior During Wounding in Zebrafish Larvae. Front. Cell Dev. Biol. 9:624571. doi: 10.3389/fcell.2021.624571

Toll-like receptor (TLR) signaling via myeloid differentiation factor 88 protein (MyD88) has been indicated to be involved in the response to wounding. It remains unknown whether the putative role of MyD88 in wounding responses is due to a control of leukocyte cell migration. The aim of this study was to explore *in vivo* whether TLR2 and MyD88 are involved in modulating neutrophil and macrophage cell migration behavior upon zebrafish larval tail wounding. Live cell imaging of tail-wounded larvae was performed in *tlr2* and *myd88* mutants and their corresponding wild type siblings. In order to visualize cell migration following tissue damage, we constructed double transgenic lines with fluorescent markers for macrophages and neutrophils in all mutant and sibling zebrafish lines. Three days post fertilization (dpf), tail-wounded larvae were studied using confocal laser scanning microscopy (CLSM) to quantify the number of recruited cells at the wounding area. We found that in both *tlr2*$^{-/-}$ and *myd88*$^{-/-}$ groups the recruited neutrophil and macrophage numbers are decreased compared to their wild type sibling controls. Through analyses of neutrophil and macrophage migration patterns, we demonstrated that both *tlr2* and *myd88* control the migration direction of distant neutrophils upon wounding. Furthermore, in both the *tlr2* and the *myd88* mutants, macrophages migrated more slowly toward the wound edge. Taken together, our findings show that *tlr2* and *myd88* are involved in responses to tail wounding by regulating the behavior and speed of leukocyte migration *in vivo*.

Keywords: TLR2, MyD88, leukocyte migration, neutrophils, macrophages, zebrafish, tail wounding

INTRODUCTION

Acute inflammation is characterized by the directed migration of leukocytes, which can be triggered by tissue damage (Lieschke et al., 2001; Soehnlein and Lindbom, 2010). The function of directed leukocyte migration is to eliminate cell debris and invading pathogens, with the aim of maintaining homeostasis upon tissue damage (Serhan et al., 2007). Neutrophils and macrophages are the two

crucial immune cells that engage in this process (Soehnlein and Lindbom, 2010; Li et al., 2012). Neutrophils are the first cells to rapidly respond to the site of injury, and produce cytokines and chemokines to mediate the recruitment of other cells (Nathan, 2006; Li et al., 2012). However, persisting neutrophil recruitment can release toxic granule contents to further damage tissue, and thereby is a hallmark of chronic inflammatory disease (Weiss, 1989; Serhan et al., 2007; Brazil et al., 2013). In comparison, distant macrophages move slower and accumulate later at the wounded area and are considered to play a role in eliminating the debris of apoptotic cells and assist in regeneration of wounded tissue (Martin and Leibovich, 2005; Soehnlein and Lindbom, 2010; Li et al., 2012; Mescher, 2017). Leukocyte migration must be tightly regulated to avoid negative effects on tissue repair or further damage. Despite myriad studies on leukocyte migration in response to wounding, the underlying mechanisms are not yet completely understood (Hopkin et al., 2019).

Neutrophils and macrophages depend on membrane-localized pattern recognition receptors (PRRs) to sense invading microbes and associated tissue damage (Hato and Dagher, 2015). PRRs play a crucial role to recognize pathogen associated molecular patterns (PAMPs) of invading microbes in open wounds and damage associated molecular patterns (DAMPs) released by lysing cells (Janeway and Medzhitov, 2002; Niethammer, 2016). Toll-like receptors (TLRs) are prominent recognition factors for PAMPs and DAMPs to regulate inflammatory responses (Yu et al., 2010; Vijay, 2018). Extensive studies have demonstrated that cellular distribution is different for each TLR. TLRs recognize different classes of PAMPs and trigger the production of cytokines and chemokines during infection. Two typical examples are TLR2, which senses bacterial lipoproteins (Quesniaux et al., 2004), and TLR4, which recognizes bacterial lipopolysaccharide (LPS) (Poltorak et al., 1998). Accumulating evidence shows that high-mobility group box 1 protein (HMGB1), which is the best well known endogenous danger signal, activates inflammation by forming complexes with other DAMPs (such as single-stranded DNA, nucleosomes and LPS) to be recognized by IL-1R as well as TLR2, TLR4, and TLR9 to induce inflammatory responses (Bianchi, 2009; Yanai et al., 2009; Soehnlein and Lindbom, 2010). After interacting with these PAMPs and DAMPs, TLRs initiate downstream signaling cascades that ultimately result in producing cytokines and chemokines. Importantly, the activation of downstream signaling pathways by HMGB1 has been shown to be dependent on the TLR down-stream signaling mediated by myeloid differentiation factor 88 protein (MyD88) (Soehnlein and Lindbom, 2010; Teixeira et al., 2020).

TLR2 is one of the best known PRRs and acts as a heterodimer with TLR1 or TLR6 to recognize gram positive bacteria including mycobacteria, presumably based on the specific binding to their cell wall components, such as glycolipids and glycoproteins (Quesniaux et al., 2004; Oliveira-Nascimento et al., 2012). TLR2 is expressed and activated after tissue injury even in the absence of infections, like in acute ischemic injury as well as in acute liver and kidney injury (Schauber et al., 2007; Castoldi et al., 2012; Xu et al., 2013; Moles et al., 2014). In the study of Mojumdar et al. (2016), it was shown that macrophage infiltration was reduced into normal muscle following acute injury in TLR2 deficiency mice (Mojumdar et al., 2016). In addition, Kim et al. demonstrated that TLR2 contributes to macrophage infiltration in the dorsal root ganglia after peripheral nerve injury in mice (Kim et al., 2011). Such injury-induced TLR2 expression and activation has therefore been hypothesized to be important for human health (Seki et al., 2011; Miura et al., 2013; Moles et al., 2014). Following ischemic injury in mice, TLR2 activation promotes cell permeability, lymphocyte invasion and endothelial cell migration and mediates the release of TNF-α and IL-6 (Xu et al., 2013). TLR2-deficient mice have a defective ability to recruit neutrophils to an injured liver and fail to induce the neutrophil chemokine CXCL-2 (Moles et al., 2014). Additionally, TLR2 contributes to chronic liver disease in a mouse model by mediating MAPK and NF-κB signaling pathways (Ji et al., 2014). However, there is little knowledge of the function of TLR signaling in cell migration of myeloid cells to epithelial wounding sites (Deng et al., 2012).

MyD88 is an essential adaptor protein for all TLRs, except TLR3 (Takeda and Akira, 2004; Chen et al., 2020). MyD88 is responsible for activating downstream signaling through binding to the TIR domain of TLRs (Takeda and Akira, 2004; Chen et al., 2020). A few studies have shown changes in MyD88 expression after tissue injury. Similar to *Tlr2*, the gene expression of *Myd88* is upregulated following ischemic injury in mice (Wagner et al., 2020). Moreover, the expression of *Myd88* and *Tlr2* is significantly increased in diabetic wounded mice (Dasu et al., 2010). In addition, some evidence indicate that Myd88 is involved in the modulation of wound healing (Macedo et al., 2007; Houseright et al., 2020), but the underlying mechanism is still unclear. Although TLR signaling is important for chemokine production, little is known about the role of MyD88 in leukocyte migratory responses to tissue injuries in the absence of pathogenic infections.

In this paper we use zebrafish larvae as a model for studying leukocyte cell migration after tail wounding. The zebrafish model has become an important vertebrate model for studying human diseases. The small size and transparency of their larvae are useful characteristics for the screening and imaging of transgenic reporter lines (Meijer and Spaink, 2011). Zebrafish larvae are a popular model for studying functions involved in wound repair (Renshaw et al., 2006; Niethammer et al., 2009; Xie et al., 2019; Bernut et al., 2020; Katikaneni et al., 2020; Sommer et al., 2020b). The availability of mutants in TLR signaling genes *tlr2* and *myd88* make it possible to study their roles in leukocyte migratory behavior upon tail wounding in zebrafish (Henry et al., 2013; van der Vaart et al., 2013; Hu et al., 2019; Xie et al., 2019; Sommer et al., 2020b). Tlr2 and Myd88 show a highly conserved structure in mammals and zebrafish (Meijer et al., 2004). In a previous study, we demonstrated the conserved role of *tlr2* in zebrafish as a PRR to recognize the mammalian TLR2 ligand Pam3CSK4, and identified a set of genes that are specifically expressed by activation of the downstream pathway of zebrafish *tlr2* (Yang et al., 2015). Moreover, He et al. (2020) confirmed that *tlr2* gene expression can be upregulated upon wounding in zebrafish larvae

which is consistent with previous studies in mice. In addition, the study of Sommer et al. (2020a) suggests that *myd88* is required for induction of chemokine gene expression, such as *ccl2* and *cxcl11aa,* following tail wounding.

In the present study, live fluorescent imaging was used to investigate the effect of the *tlr2* mutation and the *myd88* mutation on leukocyte migration upon tail wounding. We found reduced numbers of recruited neutrophils and macrophages at the wounding area in both *tlr2* mutants and *myd88* mutants, compared to their sibling controls. Leukocyte migration in the *tlr2* and *myd88* mutants upon wounding was analyzed using quantitative analyses of cell migration tracks. Our results demonstrate that the *tlr2* and the *myd88* mutations affect distant neutrophil migration upon wounding by negatively affecting their directional persistence, but not their migration speed. Not only the directional persistence of distant macrophages was significantly decreased in the *tlr2* and the *myd88* mutants, but also their migration speed. This study shows for the first time that TLR signaling is directly involved in controlling behavior of cell migration of neutrophils and macrophages during wounding, stimulating further studies also in other model systems.

MATERIALS AND METHODS

Zebrafish Maintenance and Strain Construction

All animal experiments described in this study were performed at the University of Leiden according to standard protocols (zfin.org) and adhered to the international guidelines specified by the EU Animal Protection Directive 2010/63/EU. The culture of adult fish was approved by the local animal welfare committee (DEC) of the university (License number: protocol 14,198). No adult zebrafish were sacrificed for this study. All experiments were done on 3 days post fertilization (dpf) fish, therefore prior to the free-feeding stage and did not fall under animal experimentation law according to the EU Animal Protection Directive 2010/63/EU. Eggs and larvae were grown at 28.5°C in egg water (60 g/ml Instant Ocean sea salts). For living imaging and tail wounding experiments, 3 dpf larvae were anesthetized with egg water containing 0.02% buffered 3-aminobenzoic acid ethyl ester (Tricaine, Sigma-Aldrich, Netherlands).

The *tlr2*^{sa19423} mutant and *myd88*^{hu3568} mutant lines were identified by the sequencing of an ENU-mutagenized zebrafish library (van der Vaart et al., 2013; Hu et al., 2019). To investigate the effect of the *tlr2* and the *myd88* mutations on leukocyte development, double fluorescent lines *tlr2*$^{+/+}$ *Tg (mpeg1:mCherry-F);TgBAC (mpx: EGFP)*, *tlr2*$^{-/-}$ *Tg (mpeg1:mCherry-F);TgBAC (mpx: EGFP), myd88*$^{+/+}$ *Tg (mpeg1:mCherry-F);TgBAC (mpx: EGFP)*, *myd88*$^{-/-}$ *Tg (mpeg1:mCherry-F);TgBAC (mpx: EGFP)* were used. Both homozygous mutants were outcrossed with the double transgenic line *Tg (mpeg1:mCherry-F);TgBAC (mpx: EGFP)* (Renshaw et al., 2006; Bernut et al., 2014). Subsequently, their heterozygous offspring with both positive GFP and mCherry fluorescence were imaged and then used for in-cross. F1 heterozygous in-cross offspring with both positive GFP and mCherry fluorescence were imaged blindly and genotyped post-imaging to produce the homozygous mutants and wild type siblings. In the present study, the double transgenic lines were used for the quantification of cell numbers, cell recruitment assays upon wounding, and leukocyte living imaging experiments.

Tail Wounding

In the present study, a caudal fin wounding model was applied as previously described (Renshaw et al., 2006; Chatzopoulou et al., 2016; Xie et al., 2019). 3 dpf *tlr2* zebrafish larvae were anesthetized with egg water containing 0.02% tricaine (Sigma Aldrich). Subsequently, the caudal fins of larvae were wounded by using a 1 mm sterile sapphire blade scalpel (World Precision Instruments) on a 2% agarose covered petri-dish. To avoid damaging the notochord and other tissues of zebrafish larvae, all of the wounding experiments were performed under a MZ16FA Fluorescence Stereo Microscope (Leica Microsystems, Wetzlar Germany) equipped with a DFC420C color camera (Leica Microsystems). After the wounding, the egg water with 0.02% tricaine was changed with untreated egg water. Wounded larvae were put back into an incubator at 28.5°C. Subsequently, the wounded larvae were collected or fixed for follow up experiments.

Imaging and Quantification

For the quantification of the recruited cell number upon wounding, the double transgenic *tlr2* and *myd88* larvae were wounded with the method described before. 1, 2, 4, and 6 h post wounding (hpw), larvae were collected and fixed with 4% paraformaldehyde (PFA) in PBS overnight at 4°C and washed with PBS the next day. The wounded tail area of fixed samples from each group were imaged by using a Leica MZ16FA fluorescence stereo microscope equipped with a DFC420C color camera. Cells localized within an area of 200 μm from the wounding edge toward the body trunk were counted as recruited cells. Analysis was performed by combining three independent experiments.

For detailed cell migration behavior analyses, larvae (3 dpf) were mounted into 1% low melting point agarose (Sigma Aldrich) with 0.02% tricaine and imaged under a Leica TCS SP8 confocal microscope (Leica Microsystems) with a 10× objective (N.A. 0.40). Data were saved as maximum projection images for further cell counting. The number of neutrophils and macrophages in the tail region were manually quantified.

Live Imaging

All time-lapse imaging was performed on 3 dpf larvae. Larvae for each condition (unchallenged/wounded) were mounted in the method described before and visualized in the CLSM with 1 min time interval for 2 h image capture using a 20× objective (N.A. 0.75). For the manual cell tracking analysis, all time-lapse images were saved as maximum projection images.

We first defined the role of *tlr2* and *myd88* in leukocyte migration under the unchallenged condition. The caudal hematopoietic tissue (CHT) of double transgenic lines was imaged using the CLSM with unchallenged condition. To investigate the effect of the *tlr2* and *myd88* mutations on leukocyte migration upon wounding, the double transgenic

line *Tg (mpeg1:mCherry-F);TgBAC (mpx: EGFP)* larvae in the *tlr2*, *myd88* mutant or their wild type background were wounded and performed for real time imaging from 1 to 3 hpw.

Cell Tracking and Its Quantification

The cell tracking of macrophages and neutrophils was either performed manually by using a manual tracking plug-in from Fiji (Meijering et al., 2012; Torraca et al., 2015) or automatically by using automatic 3D cell tracking algorithms (Tinevez et al., 2017; Ulman et al., 2017). In this paper, we applied a Viterbi Algorithm, proposed by Magnusson et al. for quantifying leukocyte migration speed (Magnusson et al., 2015). The Viterbi Algorithm follows a global linking strategy which can find the optimal path based on a probabilistically motivated scoring function. The algorithm incorporates six different cell behaviors which include cell migration, migration into or out of image based on probability framework, and cell count, mitosis, apoptosis based on logistic regression. In our application, we did not take into account mitosis and apoptosis. An operation called "swaps" is applied in the Viterbi Algorithm. It can modify links in preexisting tracks if there is a better linking way during a creation of new tracks.

The distance to the wound, mean speed, net displacement, meandering index (M.I.), mean square displacement (MSD), cell diffusivity (D), velocity in anteroposterior direction (V_{AP}), and V_{AP} over time were calculated in different groups by manual tracking data. The calculation and explanation of the parameters are shown in **Figure 4**. The distance to the wound is defined as the shortest Euclidean distance to the wound edge (**Figure 4A**). For the velocity in the anteroposterior direction, tracks were rotated such that the spines of the larvae were aligned (**Figure 4B**). Then, for each cell the average velocity in the anteroposterior axis was calculated. For V_{AP} over time, the V_{AP} of all cells within a group was averaged over three consecutive time frames. Net displacement, total displacement, meandering index and mean speed are shown in **Figure 4C** and **Table 1** (Eqs 1–4). The net displacement is the distance of the cell between the first and final time frame (**Figure 4C**), i.e., the Euclidian distance traveled being: $d_{net} = d\left(p_i, p_N\right)$ (**Table 1**, Eq. 1). The total displacement is the length of the total cell track, i.e., the sum of the net displacements between two successive frames $[d_{tot} = \sum_{i=1}^{N-1} d\left(p_i, p_{i+1}\right)]$ (**Figure 4C** and **Table 1**, Eq. 2). Cells can reorient between two frames, such that this measure may underestimate the actual distance traveled. However, we used the same frame rate of 1 min in all experiments, such that the results are comparable with one another. Meandering index is most simply defined as the net distance traveled divided by the total distance traveled ($\text{M.I} = \frac{d_{net}}{d_{tot}}$) (Stokes et al., 1991; **Figure 4C** and **Table 1**, Eq. 3). Mean speed is the total displacement divided by traveled time ($\bar{v} = \frac{1}{N-1} \sum_{i=1}^{N-1} v_i$) (**Table 1**, Eq. 4). The MSD at time t was calculated for each group by averaging the squared displacement from starting time t_1 = 1 hpw to time t over all cells (K) within that group $[MSD\ (t) = \frac{1}{K} \sum_{i=1}^{K} \left(d\ \left(p_{i,1}\ ,\ p_{i,\ 1+t}\right)\right)^2]$ (**Figure 4D** and **Table 1**, Eq. 5). For persistent random walkers, an analytical expression for the MSD exists: $Fitted\ MSD\ (t) = 2v^2\ \tau t - 2(v\tau)^2\ (1 - e^{\frac{-t}{\tau}})$ (**Table 1**, Eq. 6), with v the intrinsic cell velocity and τ the persistent time, which can be fit to the MSD calculated from cell tracks (Selmeczi et al., 2005). The cell diffusivity constant D and MSD(t) at large t are related through $D = 1/2n\ \frac{dMSD(t)}{dt}$, with n = 2 the dimension, which for persistent random walkers results in $D = 1/2\ v^2\ \tau$ (**Table 1**, Eq. 7). We assume that distant neutrophils and macrophages can behave like persistent random walkers during the time span of imaging (Taylor et al., 2013). We fit Eq. 6 to the MSD curve (**Table 1**, Eq. 5) using a non-linear least squares method. The obtained parameters v and τ are then used to compute the approximated cell diffusivity D. For distant neutrophils, the fit was performed on the first 80 min of tracking, for distant macrophages, the entire 2 h tracking period was used.

TABLE 1 | Formulas of calculated track measures and derived measures.

Measure	Definition	No.
Net displacement (μm)	$d_{net} = d(p_i, p_N)$	Eq. 1
Total displacement (μm)	$d_{tot} = \sum_{i=1}^{N-1} d(p_i, p_{i+1})$	Eq. 2
Meandering index	$\text{M.I.} = d_{net}/d_{tot}$	Eq. 3
Mean speed (μm/min)	$\bar{v} = \frac{1}{N-1} \sum_{i=1}^{N-1} v_i$	Eq. 4
Mean squared displacement (μm^2)	$MSD\ (t) = \frac{1}{K} \sum_{i=1}^{K} (d\ (p_{i,1}\ ,\ p_{i,\ 1+t}))^2$	Eq. 5
Fitted mean squared displacement (μm^2)	$MSD\,(t) = 2v^2\ \tau t - 2\,(v\tau)^2\ \left(1 - e^{\frac{-t}{\tau}}\right)$	Eq. 6
Cell diffusivity constant D (μm^2/min)	$D = 1/2\ v^2\ \tau$	Eq. 7

The movement behavior of cells can change after they arrive at the wound edge (**Supplementary Figure S1**). To analyze the behavior of leukocyte tracks more accurately, we defined categories of distant and local resident cell movements based on their starting location in the first frame of the time lapse. Cells with a starting point of movements localized further than 200 μm from the wound edge toward to the trunk were categorized as distantly localized cells (in brief called distant cells). Cells with a starting point of movements localized within a distance of up to 200 μm from the wound edge toward to the trunk were categorized as wound-residing cells (in brief called local resident cells, **Supplementary Figure S1A**). Although there is no difference between distant neutrophils and local resident neutrophils in mean speed (**Supplementary Figure S1C**), net displacement and meandering index are significantly decreased in the local resident neutrophil groups compared to the distant neutrophil groups (**Supplementary Figures S1D,E**). Furthermore, mean speed, net displacement and meandering index are all significantly decreased in the local resident macrophage groups (**Supplementary Figures S1F–H**). Thus, the cell movement behavior is quantified by

separating distant and local resident cell movements in this study.

Statistical Analysis

Graphpad Prism software (Version 8.1.1; GraphPad Software, San Diego, CA, United States) was used for statistical analysis. Computations of distance to the wound, MSD and V_{AP} were performed using a Python script including the SciPy stats library for statistical testing. Shaded regions of MSD and V_{AP} over time indicate standard error of mean, the other experiment data are shown as mean ± *SD*. Statistical significance of differences was determined by using an unpaired, two-tailed *t*-test for comparing the difference between wild type and *tlr2* and *myd88* mutant (ns, no significant difference; $^{*}P < 0.05$; $^{**}P < 0.01$; $^{***}P < 0.001$; $^{****}P < 0.0001$).

RESULTS

Tlr2 and myd88 Mutations Do Not Affect Development and Basal Motility of Leukocytes

To determine the leukocyte development in *tlr2* and *myd88* mutants, the double-transgenic line *tlr2*$^{+/+}$ *Tg (mpeg1:mCherry-F);TgBAC (mpx: EGFP)*, *tlr2*$^{-/-}$ *Tg (mpeg1:mCherry-F);TgBAC (mpx: EGFP)*, *myd88*$^{+/+}$ *Tg (mpeg1:mCherry-F);TgBAC (mpx: EGFP)* and *myd88*$^{-/-}$ *Tg (mpeg1:mCherry-F);TgBAC (mpx: EGFP)* were constructed. The lines were imaged at 3 dpf to count the number of macrophages and neutrophils in their tail region, and then compared with their wild type siblings (**Figure 1A**). Embryos of the *tlr2* and *myd88* mutants showed similar numbers of macrophages and neutrophils as their wild type siblings (**Figures 1B–E**). This result is consistent with our previous studies of the same *myd88* mutant at 3 dpf and the *tlr2* mutant at 2 dpf (van der Vaart et al., 2013; Hu et al., 2019). With the aim of investigating the importance of the *tlr2* and the *myd88* mutations for leukocyte behavior under unchallenged condition, the CHT region was analyzed in the double transgenic lines of *tlr2* and *myd88* using CLSM by taking time-lapse images (**Figure 1A**). No significant effect was observed on leukocyte basal motility in the CHT tissue in the *tlr2* and *myd88* mutants compared with their wild type sibling control (**Figures 1F–M**). Representative images are shown in **Supplementary Figures S2, S3**.

Tlr2 and myd88 Regulate Neutrophil Recruitment to a Tail Wound

To study the effect of the *tlr2* and *myd88* mutations on the recruitment of neutrophils toward a site of injury, a tail wound method was used in 3 dpf zebrafish larvae as a model for inflammation. To quantify the number of recruited neutrophils to the wound, we counted the number of neutrophils that were located in a range closer than 200 μm from the wound edge of the tail at 1, 2, 4, and 6 hpw (**Figure 2A**). Our results show that the *tlr2* mutation had a significant negative effect on the recruitment of neutrophils after 2, 4, and 6 hpw (**Figures 2B,C**). However, there is no significant difference in recruited neutrophil numbers between wild type and *tlr2*$^{-/-}$ at 1 hpw (**Figures 2B,C**). Notably, a significant difference of recruited neutrophil numbers was already observed at 1 hpw in *myd88* zebrafish larvae and remained significant until 6 hpw (**Figures 2D,E**).

Tlr2 and myd88 Regulate Macrophage Recruitment to a Tail Wound

To assess the role of the *tlr2* and *myd88* mutations in regulating the recruitment of macrophages to a site of the tail wound, we counted the recruited macrophage numbers by the same method as for measuring the neutrophil recruitment to the wound (**Figure 3A**). Both *tlr2*$^{-/-}$ and *myd88*$^{-/-}$ mutant zebrafish larvae displayed diminished macrophage responses upon wounding (**Figure 3**). Significantly decreased numbers of recruited macrophages toward the injury were measured in the *tlr2*$^{-/-}$ group at 2, 4, and 6 hpw (**Figures 3B,C**). Similarly, there is no significant difference in recruited macrophage numbers between wild type and *tlr2*$^{-/-}$ at 1 hpw (**Figure 3C**). A significant difference of recruited macrophage numbers was already observed from 1 hpw in *myd88* zebrafish larvae, the same as was observed with neutrophil recruitment (**Figures 3D,E**).

Live Imaging Reveals That the *tlr2* and *myd88* Mutations Affect Distant Neutrophil Directional Persistence, but Not Migration Speed Upon Tail Wounding

To investigate how neutrophils migrate in the absence of *tlr2* or *myd88* after tail wounding, a time-lapse microscopy experiment was performed by using CLSM between 1 to 3 hpw (**Figures 5**, **6**). The definition of distant and local resident neutrophils is shown in panel A of **Figures 5**, **6** and **Supplementary Figures S4, S5**. Neutrophils located closer than 200 μm to the wound were defined as local resident neutrophils and further than 200 μm were defined as distant neutrophils. Measurement of the distance to the wound over time of all distant neutrophils in the *tlr2*$^{-/-}$ group indicated a trend of impaired infiltration toward the wound (**Figures 5B,C**, up panel). In total, the group of distant neutrophils in the *tlr2*$^{+/+}$ group that arrived at the wound edge and stayed within a distance of 20 μm to the wound comprises 84% of a total of 25 tracked neutrophils (**Figure 5C**, up panel). The local resident neutrophils in this group all remained at the wound (**Supplementary Figure S4B,C**, up panel). In contrast, the group of the distant neutrophils in the *tlr2*$^{-/-}$ group that arrived at the wound within 2 h time-lapse cell tracking comprises only approximately 36% (**Figures 5B,C**, bottom panel). Moreover, approximately 33% of local resident neutrophils in the *tlr2*$^{-/-}$ group already migrated away from the wound edge within 3 hpw (**Supplementary Figures S4B,C**, bottom panel).

In general, distant neutrophils in the *myd88*$^{+/+}$ group showed more chemotaxis to the wound compared to *myd88*$^{-/-}$ neutrophils (**Figures 6B,C**). Approximately 96.7% distant neutrophils arrived at the wound (within a distance of 20 μm to the wound) in the *myd88*$^{+/+}$ group in total (**Figure 6C** up panel). However, only 86.4% distant neutrophils arrived to

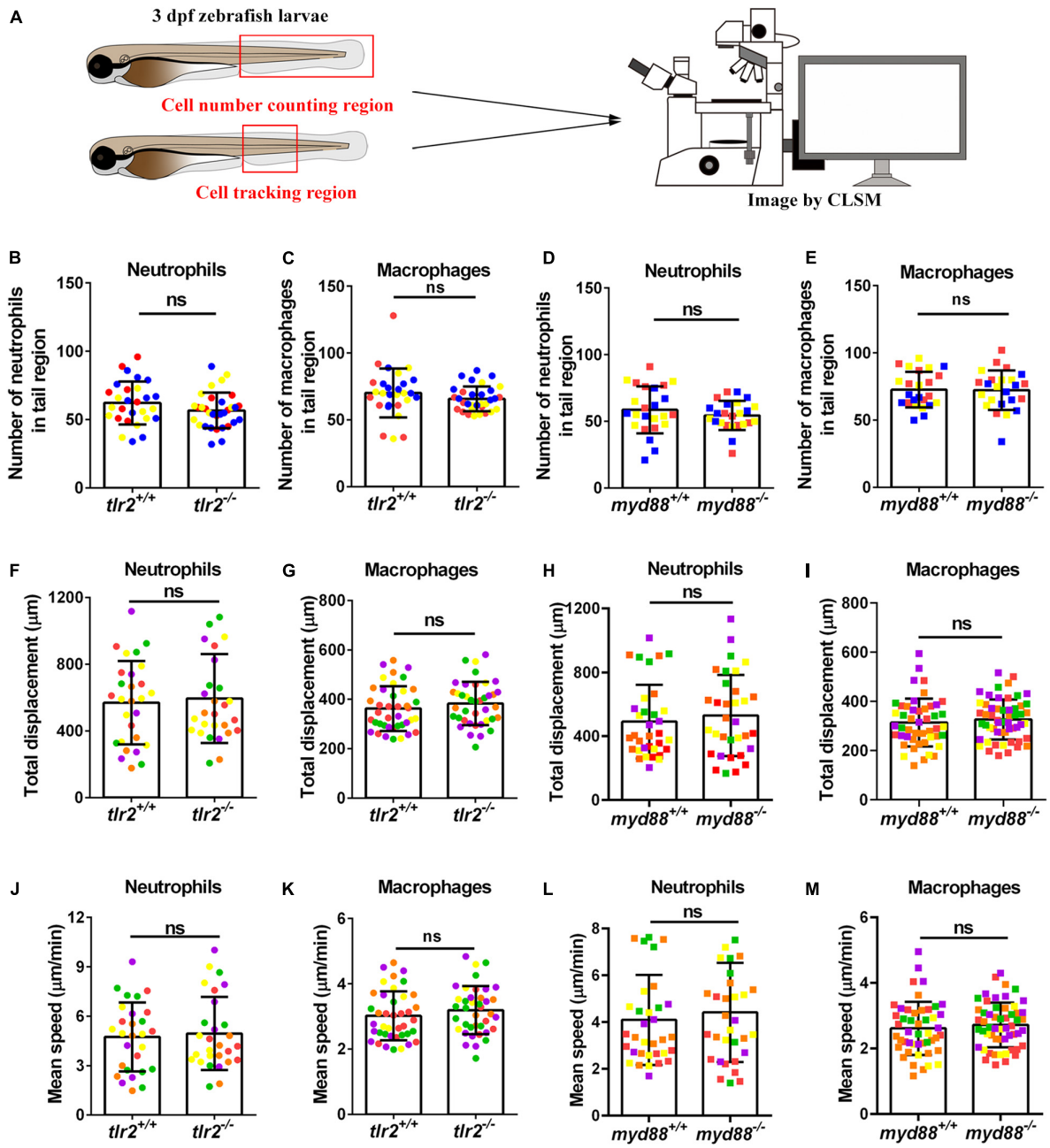

FIGURE 1 | Quantification of macrophage and neutrophil numbers and their basal migratory capability in the 3 dpf *tlr2 and myd88* mutants and wild sibling controls larvae. **(A)** Experimental scheme. At 3 dpf, numbers and basal migratory capability of GFP-labeled neutrophils and mCherry-labeled macrophages in tail region were quantified using Leica TCS SP8 confocal laser scanning microscopy (CLSM). Red boxes show the area in which cells were counted or tracked. **(B–E)** The quantification of neutrophil and macrophage numbers in tail region by using *tlr2* and *myd88* zebrafish larvae. Data (mean ± *SD*) are combined from three pools of zebrafish larvae. No significant differences (ns) in the number of neutrophils **(B,D)** and macrophages **(C,E)** was detected with an unpaired, two-tailed *t*-test. Each point represents one larva and different colors represent different pools. Sample size (*n*): 28, 32 **(B,C)**; 24, 24 **(D,E)**. **(F,G,J,K)** Quantification of basal migratory capability in 3 dpf *tlr2* zebrafish. The total displacement and mean speed of individual neutrophils **(F,J)** and macrophages **(G,K)** were quantified by using a manual tracking plugin. Data (mean ± *SD*) are combined from 5 larvae of $tlr2^{+/+}$ *Tg (mpeg1:mCherry-F);TgBAC (mpx: EGFP)* and $tlr2^{-/-}$ *Tg (mpeg1:mCherry-F);TgBAC (mpx: EGFP)* larvae, respectively. Each color indicates a different larva. No significant differences (ns) in the total displacement and mean speed of neutrophils **(F,J)** and macrophages **(G,K)** were detected with an unpaired, two-tailed *t*-test. Sample size (*n*): 28, 28 **(F,J)**; 40, 39 **(G,K)**. Cell tracking movies are shown in **Supplementary Movies S1–S4**) **(H,I,L,M)** Quantification of basal migratory capability in 3 dpf *myd88* zebrafish. The total displacement and mean speed of individual neutrophils **(H,L)** and macrophages **(I,M)** were quantified by using a manual tracking plugin. Data (mean ± *SD*) are combined from 5 larvae of $myd88^{+/+}$ *Tg (mpeg1:mCherry-F);TgBAC (mpx: EGFP)* and $myd88^{-/-}$ *Tg (mpeg1:mCherry-F);TgBAC (mpx: EGFP)* larvae, respectively. Each color indicates a different larva. No significant differences (ns) in the total displacement and mean speed of neutrophils **(H,L)** and macrophages **(I,M)** were detected with an unpaired, two-tailed *t*-test. Sample size (*n*): 34, 33 **(H,L)**; 47, 55 **(I,M)**. Cell tracking movies are shown in **Supplementary Movies S5–S8**).

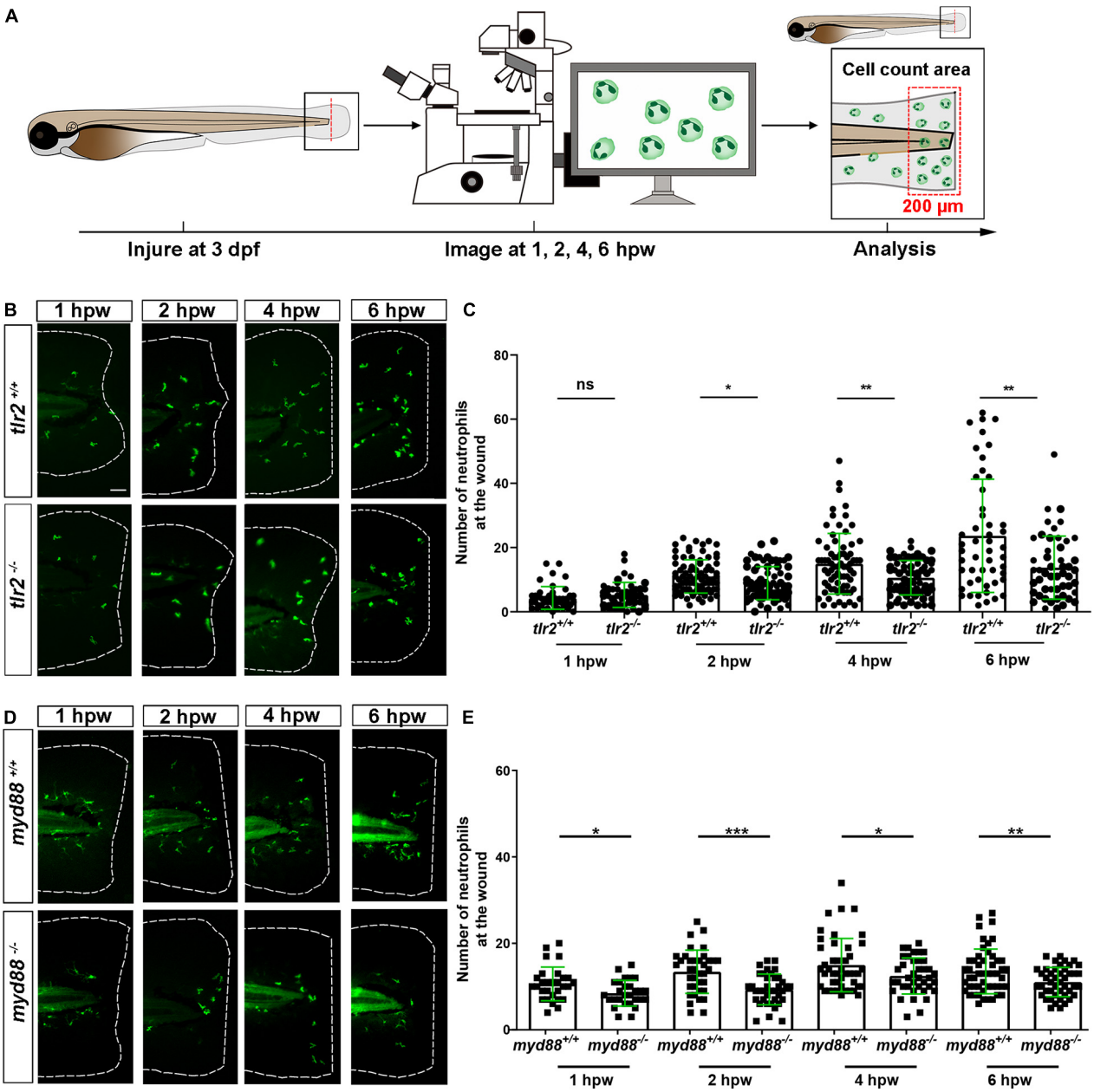

FIGURE 2 | The number of neutrophils recruited to the wounded area in the *tlr2* and *myd88* mutants and wild type sibling controls larvae. **(A)** Experimental scheme. *Tlr2* and *myd88* homozygous mutants and sibling control larvae were wounded at 3 dpf. Their tails were wounded to the tip of the notochord. The red dashed line shows the site of wounding. Recruited neutrophils at the wound were imaged at 1, 2, 4, and 6 hpw by using CLSM. For recruited cell counting analysis, cells localized within an area of 200 μm from the wounding edge toward the body trunk were counted as recruited cells. The red dashed box shows the area where neutrophils were counted as recruited neutrophils. **(B,D)** Representative images of 3 days dpf larvae at 1, 2, 4, and 6 h post-wounding (hpw). Scale bar: 50 μm. **(C)** Quantification of recruited neutrophil numbers to the wounded area at 1, 2, 4, and 6 hpw in 3 dpf $tlr2^{+/+}$ and $tlr2^{-/-}$ larvae. Each point represents a different larva. Sample size (*n*): 45, 46, 82, 72, 74, 68, 50, 50. **(E)** Quantification of recruited neutrophil numbers to the wounded area at 1, 2, 4, and 6 hpw in 3 dpf $myd88^{+/+}$ and $myd88^{-/-}$ larvae. Each point represents a different larva. Sample size (*n*): 29, 28, 37, 38, 45, 39, 51, 45. In all cases, statistical analyses were done from three independent experiments. An unpaired, two-tailed *t*-test was used to assess significance (ns, no significant difference, $^{*}P < 0.05$, $^{**}P < 0.01$, $^{***}P < 0.001$) and data are shown as mean ± *SD*.

the wound (within a distance of 20 μm to the wound) in the $myd88^{-/-}$ group (**Figure 6C**, bottom panel). The local resident neutrophils in this group all remained at the wound except for a few outliers (**Supplementary Figure S5C**). In summary, the general trend of distant neutrophils migration in the *myd88* mutant and sibling zebrafish groups was consistent with the result in the *tlr2* mutant and sibling zebrafish groups, respectively (**Figure 6C**).

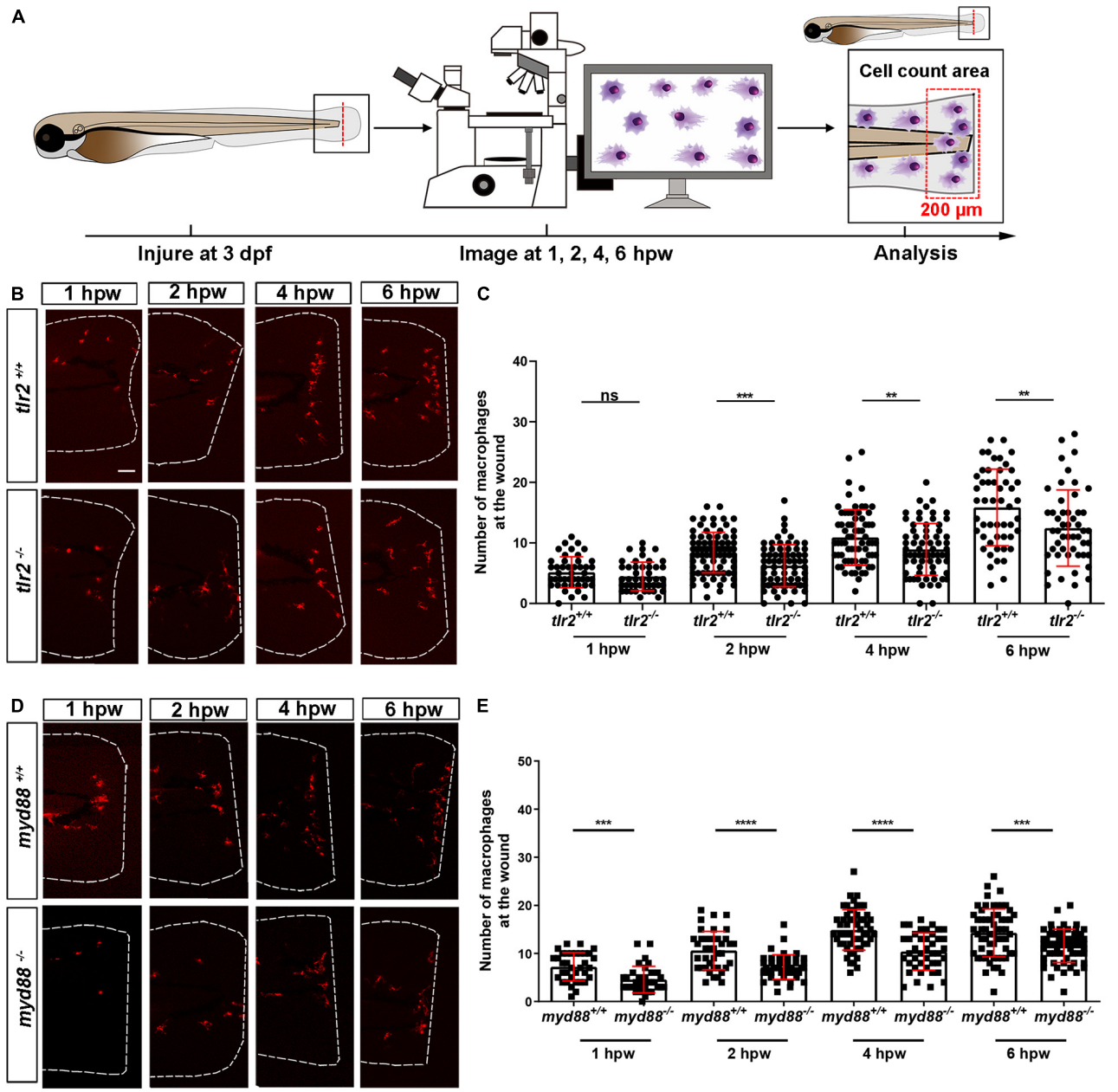

FIGURE 3 | The number of macrophages recruited to the wounded area in the *tlr2* and *myd88* mutants and wild type sibling controls larvae. **(A)** Experimental scheme. *Tlr2* and *myd88* homozygous mutants and sibling control larvae were wounded at 3 dpf. Their tails were wounded to the tip of the notochord. The red dashed line shows the site of wounding. Recruited macrophages at the wound were imaged at 1, 2, 4, and 6 hpw by using CLSM. For recruited cell counting analysis, cells localized within an area of 200 μm from the wounding edge toward the body trunk were counted as recruited cells. The red dashed box shows the area where macrophages were counted as recruited macrophages. **(B,D)** Representative images of 3 dpf larvae at 1, 2, 4, and 6 hpw. Scale bar: 50 μm. **(C)** The quantification of recruited macrophage numbers to the wounded area at 1, 2, 4, and 6 hpw in 3 dpf $tlr2^{+/+}$ and $tlr2^{-/-}$ larvae. Each point represents a different larva. Sample size (*n*): 45, 45, 82, 71, 69, 68, 51, 50. **(E)** The quantification of recruited macrophage numbers to the wounded area at 1, 2, 4, and 6 hpw in 3 dpf $myd88^{+/+}$ and $myd88^{-/-}$ larvae. Each point represents a different larva. Sample size (*n*): 35, 34, 40, 43, 56, 42, 60, 58. In all cases, statistical analyses were done with data of three independent experiments. An unpaired, two-tailed *t*-test was used to assess significance (ns, no significant difference, $^{**}P < 0.01$, $^{***}P < 0.001$, $^{****}P < 0.0001$) and data are shown as mean ± *SD*.

To quantify differences in neutrophil migration behavior between *tlr2* and *myd88* mutants and their wild type siblings, we first analyzed whether the deficiency of *tlr2* and *myd88* can affect neutrophil mean migration speed upon wounding. The results showed that the *tlr2* and the *myd88* mutations do not affect the mean speed of both distant and local resident neutrophils upon the wounding (**Figures 5D**, **6D**, and **Supplementary Figures S4D, S5D**). In addition to manual cell tracking analysis we

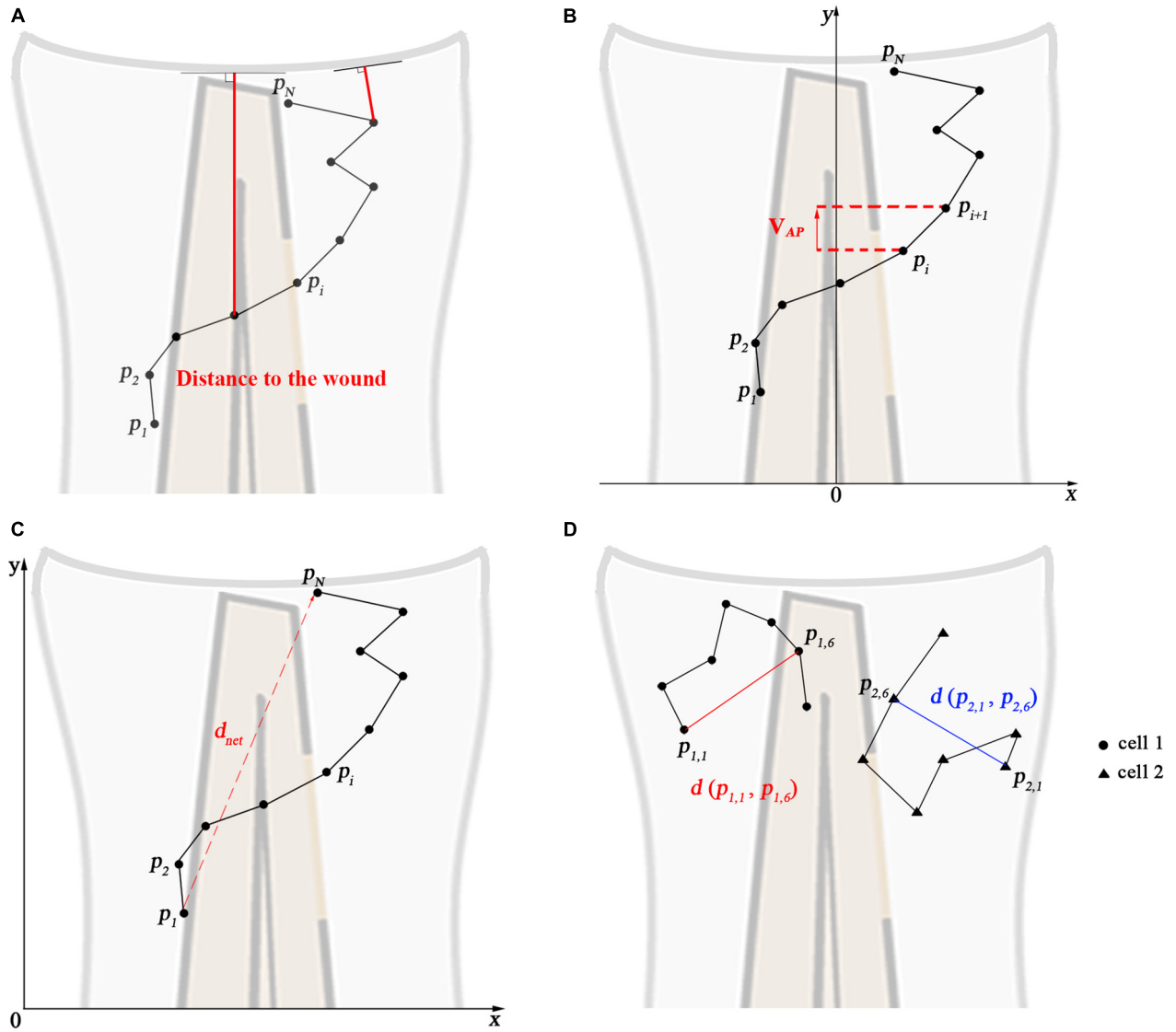

FIGURE 4 | Calculated track measures. **(A)** Depiction of distance to the wound. It measured for each frame as the shortest distance from the cell's current position to the entire line of the wound, i.e., the orthogonal projection to the wound. **(B)** Depiction of V_{AP}: velocity in anteroposterior axis direction. The visible part of the spine is taken as the *y*-axis. **(C)** Depiction of the net displacement, total displacement, meandering index, and mean speed: the net displacement is the distance of the cell between the first and final time frame. Total displacement is the sum of the net displacement between two successive frames. Meandering index corresponds to the net displacement divided by the total displacement. Mean speed is the total displacement divided by traveled time. Formulas show in **Table 1** (Eqs 1–4). **(D)** Depiction of the construction of the mean squared displacement: the displacement between the first time frame and time frame *t* from all cells is squared and averaged (see **Table 1**, Eq. 5).

also performed automatic 3D cell tracking by using a Viterbi Algorithm (Magnusson et al., 2015). The results, shown in **Supplementary Figure S8**, confirm that there is no difference in mean speed between mutant and sibling neutrophils. However, automatic tracking of living cells showed to be very challenging due to the complex leukocyte cell behaviors. Since in the automated method there are cell disappearing and appearing leading to gaps in the time series images it is currently still outperformed by manual tracking.

We also tested the effect of the *tlr2* and the *myd88* mutations on the movement direction of neutrophils upon wounding by the quantification of net displacement, whose definition is shown in **Figure 4** and **Table 1**. We observed that the net displacement of distant neutrophils had a decreased trend in the $tlr2^{-/-}$ group compared to the $tlr2^{+/+}$ group (**Figure 5E**). Moreover, cell diffusivity determined by the fitting Eq. 6 to the MSD curve (**Table 1**) did not differ much between the $tlr2^{-/-}$ group (277 μm^2/min) and the $tlr2^{+/+}$ group (268 μm^2/min) (**Figure 5G**). A significant decrease in net displacements was consistently observed in the *myd88* mutant group (**Figure 6E**). Also, $myd88^{-/-}$ neutrophils have lower diffusivity (274 μm^2/min) than $myd88^{+/+}$ neutrophils (412 μm^2/min) as measured from

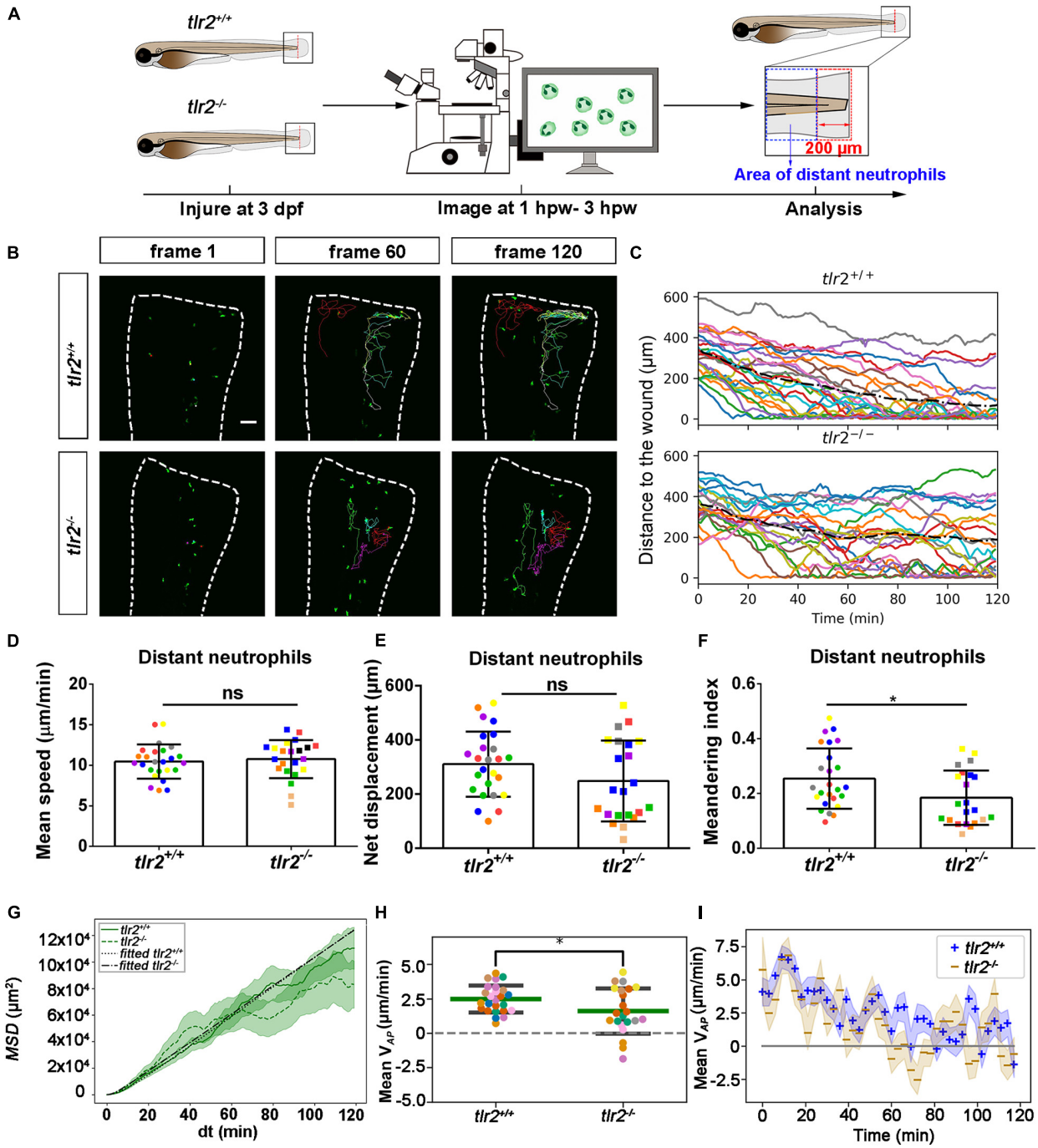

FIGURE 5 | Quantification of distant neutrophils behavior in wounded *tlr2* mutant and sibling control larvae. **(A)** Experimental scheme. *Tlr2*$^{+/+}$ and *tlr2*$^{-/-}$ larvae were wounded at 3 dpf. The red dashed line shows the site of wounding. Neutrophils of wounded zebrafish larvae were tracked for 2 h and images were taken every 1 min by using CLSM. For cell tracking analysis, cells localized outside an area of 200 µm from the wounding edge toward the body trunk were counted as distant cells. Blue dashed box shows the area where distant neutrophils were tracked. **(B)** Representative images of distant neutrophil tracks in the wounded tail fin of 3 dpf *tlr2*$^{+/+}$ or *tlr2*$^{-/-}$ larvae at frame 1, frame 60 and frame 120. Time interval between two successive frames is 1 min. Each color track represents an individual neutrophil. Cell tracking movies are shown in **Supplementary Movies S9, S10**). Scale bar: 50 µm. **(C)** Distance to the wound. Black dash line represents average distance to the wound. Each color line represents one cell. **(D–I)** Quantification of distant neutrophil tracks. In **(D–F,H)**, each color indicates a different larva. There was no significant difference between the groups in terms of mean speed **(D)**, net displacement **(E)**, and MSD (green) and fitted MSD (black) **(G)**. However, meandering index **(F)** and mean V_{AP} **(H)** of neutrophils at the wound in *tlr2*$^{+/+}$ is greater than in *tlr2*$^{-/-}$ larvae. The fitted MSD (**G**, black) was fitted for $dt < 80$ min. The shaded regions in MSD **(G)** and mean V_{AP} over time **(I)** indicate standard error of the mean. Statistical analyses were done with 7 and 8 fish, respectively, for each group. An unpaired, two-tailed *t*-test was used to assess significance (ns, non-significance, $^*P < 0.05$) and data are shown as mean ± *SD*. Sample size (*n*): 25, 22 **(D–F,H)**.

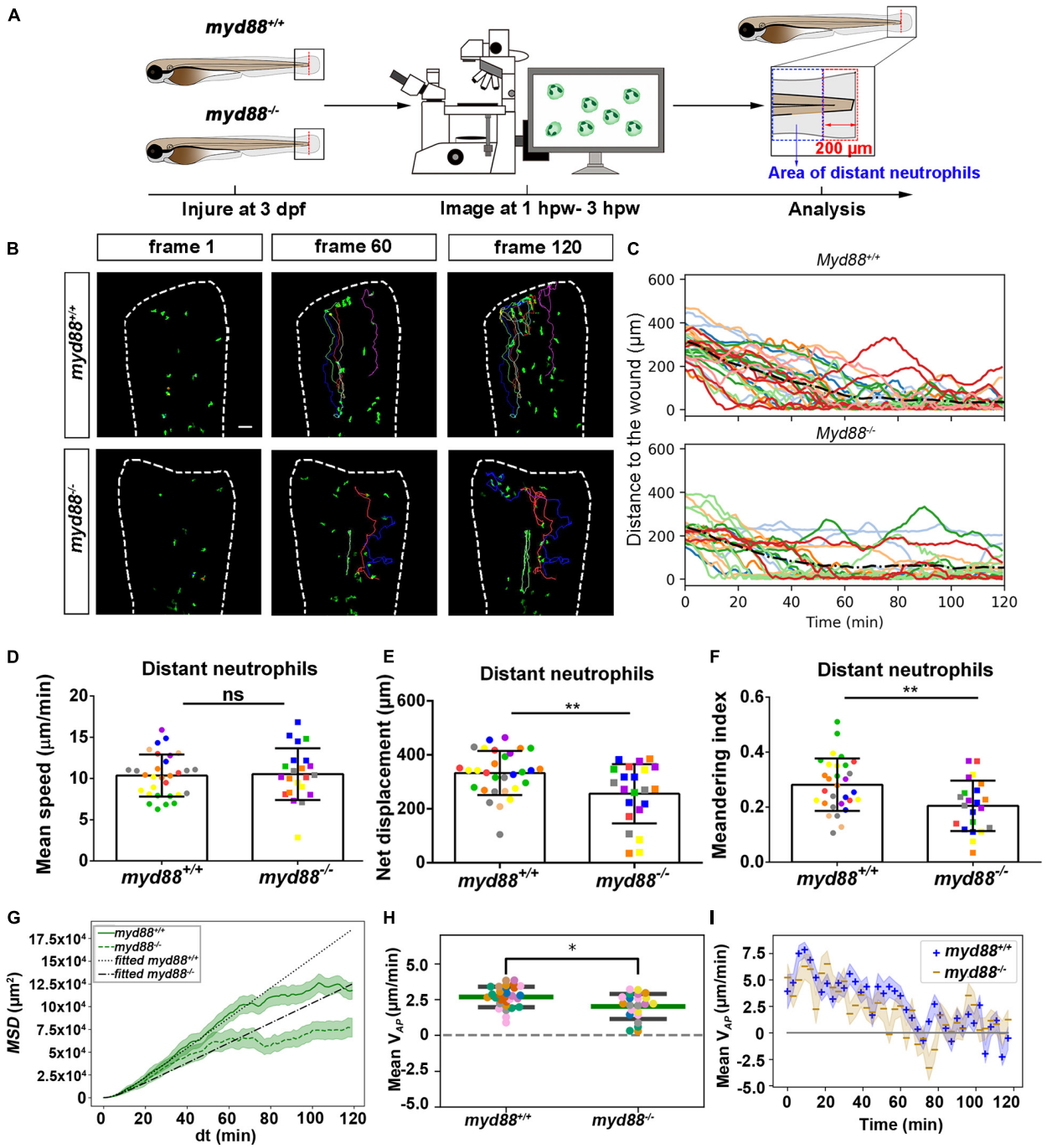

FIGURE 6 | Quantification of distant neutrophils behavior in wounded *myd88* mutant and sibling control larvae. **(A)** Experimental scheme. *Myd88*$^{+/+}$ and *myd88*$^{-/-}$ larvae were wounded at 3 dpf. The red dashed line shows the site of wounding. Neutrophils of wounded *myd88* zebrafish larvae were tracked for 2 h and images were taken every 1 min by using CLSM. For cell tracking analysis, cells localized outside an area of 200 μm from the wounding edge toward the body trunk were counted as distant cells. Blue dashed box shows the area where distant neutrophils were tracked. **(B)** Representative images of distant neutrophil tracks in the wounded tail fin of 3 dpf *myd88*$^{+/+}$ or *myd88*$^{-/-}$ larvae at frame 1, frame 60, and frame 120. Time interval between two successive frames is 1 min. Each color track represents an individual neutrophil. Cell tracking movies are shown in **Supplementary Movies S11, S12**). Scale bar: 50 μm. **(C)** Distance to the wound. Black dash line represents average distance to the wound. Each color line represents one cell. **(D–I)** Quantification of distant neutrophil tracks. In **(D–F,H)**, each color indicates a different larva. There was no significant difference between the groups in terms of mean speed **(D)**. However, the net displacement **(E)**, meandering index **(F)**, MSD (green) and fitted MSD (black) **(G),** and mean V_{AP} **(H)** of neutrophils at the wound in *myd88*$^{+/+}$ is greater than in *myd88*$^{-/-}$ larvae. The shaded regions MSD **(G)** and in mean V_{AP} over time **(I)** indicate standard error of the mean. The fitted MSD (**G**, black) was fitted for $dt < 80$ min. Statistical analyses were done with 8 and 7 fish, respectively, for each group. An unpaired, two-tailed *t*-test was used to assess significance (ns, non-significance, $^{*}P < 0.05$, $^{**}P < 0.01$) and data are shown as mean ± *SD*. Sample size (*n*): 30, 22 **(D–F,H)**.

the slopes of the MSD plots (**Figure 6G**). As the cell speed of *myd88*$^{-/-}$ neutrophils does not differ from that of *myd88*$^{+/+}$ neutrophils (**Figure 6D**), the reduced diffusivity may be due to more frequent or sharper changes of direction of the *myd88*$^{-/-}$ neutrophils. As neutrophils reach the wound edge, their diffusivity is limited in space. This is also visible in the flattening of the MSD at later time frames. Hence, fitting Eq. 6 to the MSD curve was limited to $dt < 80$.

To further study the effect of the *tlr2* and *myd88* mutations on the neutrophil migration direction, we determined the meandering index and mean V_{AP} (**Figures 5F,H**, **6F,H**). The meandering index and mean V_{AP} are all significantly decreased in the distant neutrophils of both *tlr2*$^{-/-}$ and *myd88*$^{-/-}$ mutants compared to their wild type sibling controls (**Figures 5F,H**, **6F,H**). However, no significant difference of meandering index was found in local resident neutrophils of the *tlr2*$^{-/-}$ and *myd88*$^{-/-}$ mutants compared to the wild type siblings (**Supplementary Figures S4F, S5F**). The mean V_{AP} over time qualitatively shows again the impaired chemotaxis of *tlr2*$^{-/-}$and *myd88*$^{-/-}$neutrophils compared to the *tlr2*$^{+/+}$ and *myd88*$^{+/+}$ neutrophils, respectively (**Figures 5I**, **6I**). As more and more neutrophils approach the wound (**Figures 5C**, **6C**), the mean V_{AP} drops. For almost every time point, mean V_{AP} of *tlr2*$^{+/+}$ exceeds mean V_{AP} of *tlr2*$^{-/-}$ (**Figure 5I**). Similar results were observed for *myd88*$^{+/+}$ and *myd88*$^{-/-}$ distant neutrophils (**Figure 6I**).

Live Imaging Reveals That the *tlr2* and *myd88* Mutations Affect Distant Macrophage Migration Speed and Directional Persistence Upon Tail Wounding

To study the effect of the *tlr2* and *myd88* mutations on macrophage migration upon wounding, we compared macrophage behavior with their wild type siblings. The definition of distant macrophage and local resident macrophage is shown in panel A of **Figures 7**, **8** and **Supplementary Figures S6, S7**. Macrophages located closer than 200 μm to the wound were defined as local resident macrophages and further than 200 μm were defined as distant macrophages. In contrast to neutrophils, the majority of macrophages do not reach the wound within the measured time period. By measuring their distance to the wound over time, we can see a trend that distant macrophages show less chemotaxis in the *tlr2*$^{-/-}$ and *myd88*$^{-/-}$ mutant groups compared to their wild type sibling groups (**Figures 7B,C**, **8B,C**). Within 50 μm to the wound, the local resident macrophages all remained at the wound in both the *tlr2* and *myd88* mutants and their wild type sibling controls (**Supplementary Figures S6B,C, S7B,C**). Within a distance of 200 μm, but outside 50 μm to the wound, local resident macrophages tend to migrate to the wound direction (**Supplementary Figures S6B,C, S7B,C**).

To quantify differences in macrophage migration behavior between *tlr2* and *myd88* mutants and their wild type siblings, we first analyzed whether the deficiency of *tlr2* and *myd88* can affect macrophage mean migration speed upon wounding. Following tail wounding, both distant and local resident macrophages migrate more slowly in the *tlr2*$^{-/-}$ and *myd88*$^{-/-}$ mutant groups than in the wild type sibling controls (**Figures 7D**, **8D** and **Supplementary Figures S6D, S7D**). In addition to manual cell tracking analysis we also performed automatic cell tracking by using a Viterbi Algorithm (Magnusson et al., 2015; **Supplementary Figure S8**). The results from this automated 3D cell tracking confirm the significant difference in mean speed between mutant and sibling macrophages (**Supplementary Figure S8**).

Subsequently, we studied the directional persistence of macrophage migration upon wounding. To this end, we quantified the net displacement, meandering index and mean V_{AP} in the *tlr2* and *myd88* mutants and siblings. The net displacement of the distant macrophages (**Table 1**, Eq. 1) was reduced in the *tlr2*$^{-/-}$ and *myd88*$^{-/-}$ mutants compared to the controls (**Figures 7E**, **8E**). The meandering index (**Table 1**, Eq. 3) and mean V_{AP} of distant macrophages were also significantly decreased in the *tlr2*$^{-/-}$ and *myd88*$^{-/-}$ groups (**Figures 7F,H**, **8F,H**). However, no significant differences in net displacement were found in local resident *tlr2* and *myd88* macrophage groups (**Supplementary Figures S6E, S7E**). The trend of mean V_{AP} over time is similar to the one observed for distant neutrophils, in that *tlr2*$^{+/+}$ and *myd88*$^{+/+}$ macrophages have a higher mean V_{AP} than *tlr2*$^{-/-}$ and *myd88*$^{-/-}$ macrophages during the entire tracking period. The mean V_{AP} of macrophages is positive for a longer period of time compared to the neutrophils, as the majority of macrophages have not reached the wound site during the 2 h time span.

The differences in speed and directionality also became apparent from the differences in MSD between the *tlr2*$^{+/+}$ and *myd88*$^{+/+}$ distant macrophages vs. the *tlr2*$^{-/-}$ and *myd88*$^{-/-}$ distant macrophages (**Figures 7G**, **8G**). The MSD (**Table 1**, Eq. 5) is lower for the *tlr2*$^{-/-}$ and *myd88*$^{-/-}$ macrophages, which can reflect a speed reduction and/or a lowered directional persistence. A decreased directional persistence can also be seen through the shape of the MSD curve. For *tlr2*$^{+/+}$ and *myd88*$^{+/+}$ distant macrophages, the MSD curve, especially at short time intervals dt, has a parabolic shape, indicating straight cell trajectories. For *tlr2*$^{-/-}$ and *myd88*$^{-/-}$, however, the MSD curve has a more linear shape, indicating random cell motility. Finally, the cell diffusivity D is also decreased in the *tlr2*$^{-/-}$ (38 μm^2/min) and *myd88*$^{-/-}$ (221 μm^2/min) macrophage groups compared to the *tlr2*$^{+/+}$ (132 μm^2/min) and *myd88*$^{+/+}$ (284 μm^2/min) macrophage groups. In summary, the data show that both *tlr2* and *myd88* mutations affect distant macrophage migration speed and directional persistence upon tail wounding.

DISCUSSION

In this study we visualized cell migration in *tlr2* and *myd88* mutants using live-imaging in a zebrafish tail wounding model. Thereby we demonstrated that these genes play a crucial role to control the migration of both neutrophils and macrophages upon tissue wounding. Like in mammals, neutrophils and macrophages play a dominant role in the wounding response during the first several hours after zebrafish tail fin wounding

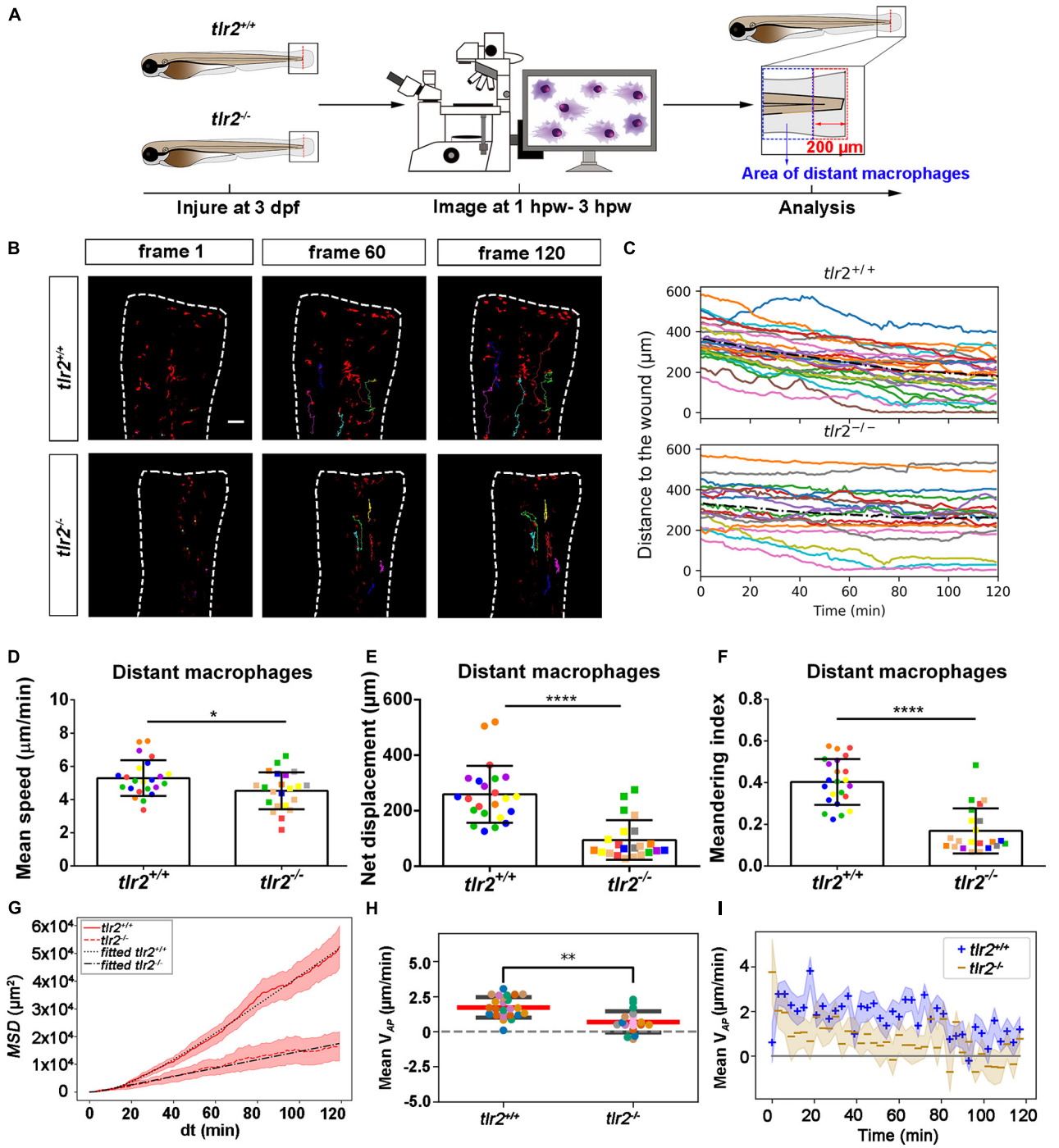

FIGURE 7 | Quantification of distant macrophage behavior in wounded *tlr2* mutant and sibling control larvae. **(A)** Experimental scheme. *Tlr2*$^{+/+}$ and *tlr2*$^{-/-}$ larvae were wounded at 3 dpf. The red dashed line shows the site of wounding. Macrophages of wounded *tlr2* zebrafish larvae were tracked for 2 h and images were taken every 1 min by using CLSM. For cell tracking analysis, cells localized outside an area of 200 μm from the wounding edge toward the body trunk were counted as distant cells. Blue dashed box shows the area where distant macrophages were tracked. **(B)** Representative images of distant macrophage tracks in the wounded tail fin of 3 dpf *tlr2*$^{+/+}$ or *tlr2*$^{-/-}$ larvae at frame 1, frame 60, and frame 120. Time interval between two successive frames is 1 min. Each color track represents an individual macrophage. Cell tracking movies are shown in **Supplementary Movies S13, S14**). Scale bar: 50 μm. **(C)** Distance to the wound. Black dash line represents average distance to the wound. Each color line represents one cell. **(D–I)** Quantification of distant macrophage tracks. In **(D–F,H)**, each color indicates a different larva. There was a significant difference between the groups in terms of mean speed **(D)**, net displacement **(E)**, meandering index **(F)**, MSD (red) and fitted MSD (black) **(G)**, and mean V_{AP} **(H)** of macrophages. The shaded regions in MSD **(G)** and mean V_{AP} over time **(I)** indicate standard error of the mean. Statistical analyses were done with 6 and 8 fish, respectively, for each group. An unpaired, two-tailed *t*-test was used to assess significance (ns, non-significance, $^{*}P < 0.05$, $^{**}P < 0.01$, $^{****}P < 0.0001$) and data are shown as mean ± *SD*. Sample size (*n*): 23, 22 **(D–F,H)**.

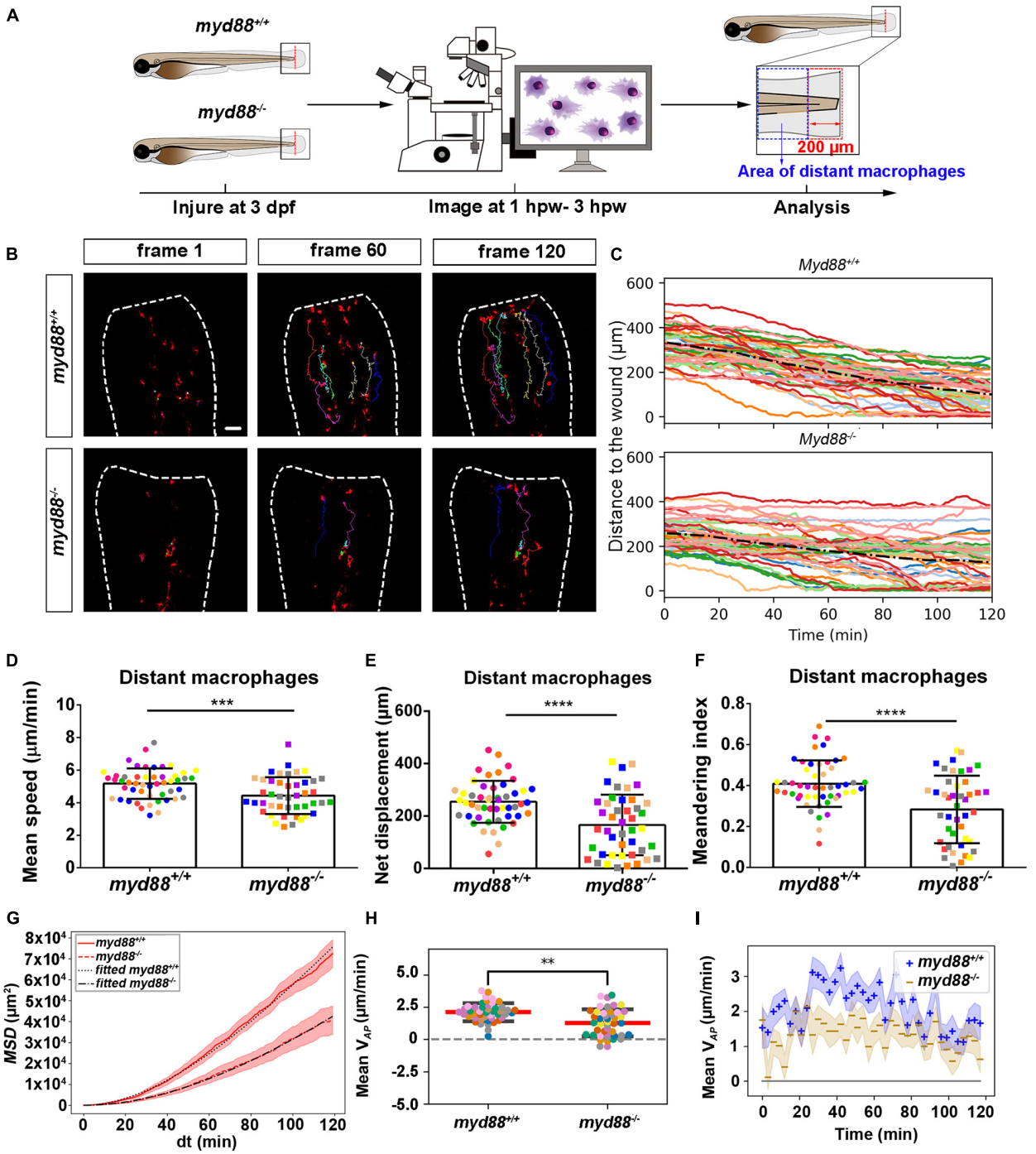

FIGURE 8 | Quantification of distant macrophages behavior in wounded *myd88* mutant and sibling control larvae. **(A)** Experimental scheme. *Myd88*$^{+/+}$ and *myd88*$^{-/-}$ larvae were wounded at 3 dpf. The red dashed line shows the site of wounding. Macrophages of wounded zebrafish larvae were tracked for 2 h and images were taken every 1 min by using CLSM. For cell tracking analysis, cells localized outside an area of 200 µm from the wounding edge toward the body trunk were counted as distant cells. Blue dashed box shows the area where distant macrophages were tracked. **(B)** Representative images of distant macrophage tracks in the wounded tail fin of 3 dpf *myd88*$^{+/+}$ or *myd88*$^{-/-}$ larvae at frame 1, frame 60 and frame 120. Time interval between two successive frames is 1 min. Each color track represents an individual macrophage. Cell tracking movies are shown in **Supplementary Movies S15, S16**). Scale bar: 50 µm. **(C)** Distance to the wound. Black dash line represents average distance to the wound. Each color line represents one cell. **(D–I)** Quantification of distant macrophage tracks. In **(D,F,H)**, each color indicates a different larva. There was a significant difference between the groups in terms of mean speed **(D)**, net displacement **(E)**, meandering index **(F)**, MSD (red) and fitted MSD (black) **(G)** and mean V_{AP} **(H)** of macrophages. Statistical analyses were done with 9 and 8 fish, respectively, for each group. The shaded regions in MSD **(G)** and mean V_{AP} over time **(I)** indicate standard error of the mean. An unpaired, two-tailed *t*-test was used to assess significance (ns, non-significance, $^{**}P < 0.01$, $^{***}P < 0.001$, $^{****}P < 0.0001$) and data are shown as mean ± *SD*. Sample size (*n*): 50, 44 **(D–F,H)**.

(Gray et al., 2011; Li et al., 2012; Xie et al., 2019). In mice, it has been shown previously that TLR signaling plays a role in controlling infiltration of neutrophils and macrophages into injured tissue (Schauber et al., 2007; Castoldi et al., 2012; Xu et al., 2013; Moles et al., 2014). The function of TLR signaling in migration to epithelial wounds has only been studied so far in zebrafish larvae (Deng et al., 2012). This study found that knock-down of *myd88* by morpholinos impairs the infiltration of neutrophils into the wound area, but the mechanisms underlying such reduced wound infiltration remained unknown. By using double transgenic lines, here we show that *tlr2* and *myd88* are both essential for directed migration of distant neutrophils and macrophages to the wounded tissue. The meandering index (**Figure 4** and **Table 1**, Eq. 3) of distant neutrophils and macrophages was significantly decreased in *tlr2* and *myd88* mutant larvae compared with wild type sibling control groups (**Figures 5F**, **6F**, **7F**, **8F**). Moreover, the migration speed of distant and local resident macrophages was decreased upon wounding in the *tlr2* and *myd88* mutants (**Figures 7D**, **8D** and **Supplementary Figures 6D, 7D**), but not in unchallenged larvae. In summary, our data suggest that TLR signaling regulates neutrophil and macrophage migration upon wounding by controlling their directional persistence and the migration speed of macrophages (**Figure 9**).

The difference in directional persistence of the distant neutrophils and macrophages in the mutant shows already within 3 h post wounding, suggesting that TLR signaling is involved in direct sensing of signals from the wound at the post-transcriptional level. However, since TLRs have not been implied in sensing meandering gradients, we assume that this function involves other receptors. Tlr2 has been shown to be essential for the regulation of cytokines and chemokines expression in both mice and zebrafish (Moles et al., 2014; Hu et al., 2019). For instance, we have shown that a *tlr2* mutant shows a significant lower expression of *cxcl11aa* and also of a related chemokine, *cxcl11ac*, during mycobacterial infection. The CXCR3-CXCL11 chemokine-signaling axis has been demonstrated to play an essential role not only in the infection process and but also in the inflammation process by regulating leukocyte trafficking (Torraca et al., 2015; Sommer et al., 2020b). It is possible that an insufficient level of basal transcripts for chemokines at the time of wounding is responsible for the observed defects in leukocyte migration behavior. It is also possible that DAMPs released by dead cells around the wound do not lead to secretion of chemokines in the absence of TLR signaling. DAMPs are well known for activating PRRs and then activating downstream chemokines and cytokines secretion (Niethammer, 2016). Molecules that can function as DAMPs and associated recognition factors during tissue injury such as hyaluronic acid and HMGB1, have been shown to be directly recognized by TLRs in tissues (Jiang et al., 2005; Bianchi, 2009; Komai et al., 2017). Chemokines can be produced by leukocytes which are exposed to reactive oxygen species (ROS) produced by injury (Yamamoto et al., 2008; Soehnlein and Lindbom, 2010). Moreover, previous studies have demonstrated that ROS are required for leukocyte recruitment upon wounding in the zebrafish larval model, showing its function in long range chemotaxis to arachidonic acid (Niethammer et al., 2009; Katikaneni et al., 2020). It has been demonstrated that the generation of ROS is related to TLR signaling in inflammation and tissue injury (Mittal et al., 2014). For example, Shishido et al. (2006) found that TLR2 mediates the generation of ROS after vascular injury. Thus, it is interesting to further study whether the generation of ROS may be altered in *tlr2* and *myd88* mutant

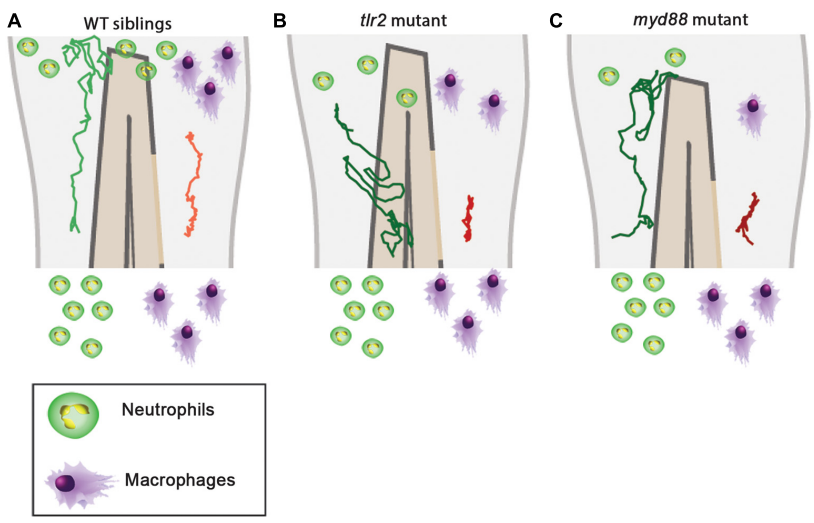

FIGURE 9 | Graphic summary of the data of cell migration behavior in the *tlr2* and *myd88* mutants and wild type siblings. **(A)** Cell migration behavior in the wild type siblings. **(B)** Cell migration behavior in the *tlr2* mutant. **(C)** Cell migration behavior in the *myd88* mutant. In all cases, the green and red tracks are representative for the medians of the measured total displacements and net displacements in the anteroposterior axis of distant neutrophils and macrophages, respectively. The number of drawn leukocytes at the wound are only representing estimates of the relative numbers in the different genotypes. For the wild type sibling the *tlr2*$^{+/+}$ sibling was used as an example **(A)**.

zebrafish larvae. In addition, it is possible that the function of other TLRs can be affected in a TLR2 mutant upon tissue wounding. For example, the mRNA expression of TLR4 was decreased in TLR2-deficient mice, which indicated that TLR2 can cooperate with TLR4 to play a role upon tissue wounding (Suga et al., 2014; Chen and DiPietro, 2017). Taken together, these studies suggest that TLR signaling is implicated in the sensitivity to signaling molecules secreted by the wound, explaining why less infiltration of neutrophils and macrophages is observed in tail wounds of the *tlr2* and *myd88* mutants. Future research should be aimed at experiments investigating the cell autonomous nature of the function of TLR signaling in leukocyte cell migration behavior in response to wounding.

To study the mechanistic basis of the differences in cell migratory behavior, mathematical and computational models can also provide insights. Chemokine and ROS gradients can easily be modeled by partial differential equations (PDEs). These can also be incorporated into cell chemotaxis models, such as random walk models, phase field models, or the Cellular Potts model, with varying degrees of cell resolution, to study the chemotaxis of leukocytes. Such models could provide quantitative insights into how chemokine and ROS gradients affect the migration behavior of the leukocytes, and how the cells change these gradients by binding or secretion of chemokines or absorption and metabolizing ROS (Donà et al., 2013) which is known to affect the robustness of chemotaxis (Tweedy et al., 2016). Using Bayesian inference on tracking data, one can infer a number of chemotaxis parameters, such as the flow rate, diffusion coefficient and production time of the chemoattractant (Manolopoulou et al., 2012). Furthermore, simulated tracks can be compared to experimentally derived tracks. Altogether, such quantitative approaches in close interaction with new experiments could help demonstrate that the chemokine or ROS gradients are affected by the *tlr2* and *myd88* mutations. For such experiments we will need larger data sets than were currently obtained. This was partially due to the limitations of manual cell tracking. Therefore, in follow-up experiments with larger datasets, the tracking needs to be automated. Consequently, we plan to develop further optimized automatic tracking methods based on the used Viterbi algorithm to quantify larger data sets.

Better theoretical cell migration analysis methods will also be useful for studying subsequent phases of the inflammatory response after wounding (Soehnlein and Lindbom, 2010). This can assist us in future studies focused on examining the involvement of the TLR signaling in neutrophil reverse migration and in the repair of wounded tissue. Previously we have reported that *myd88* mutant larvae that were raised under germ-free conditions show increased macrophage and decreased neutrophil numbers in the gut (Koch et al., 2019). This indicates that the function of TLR signaling in leukocyte migration is dependent on the gut microbiota. It will be highly interesting to test whether the response of leukocytes to tail wounding is also dependent on the microbiome.

DATA AVAILABILITY STATEMENT

The original contributions presented in the study are included in the article/**Supplementary Material**, further inquiries can be directed to the corresponding author/s.

ETHICS STATEMENT

The animal study and the breeding of adult fish was approved by the local animal welfare committee (DEC) of the University of Leiden.

AUTHOR CONTRIBUTIONS

WH performed all biological experiments and manual cell tracking analyses and wrote the first version of the manuscript. LS performed analyses of cell migration behavior and assisted with statistical analyses. CL and LC developed a script and performed automated cell tracking analyses. RM, FV, and HS supervised the study. HS initiated the study and has the final responsibility of the manuscript. All authors delivered input for the final version of the manuscript and agreed with its contents.

FUNDING

WH was supported by grants from the China Scholarship Council (CSC). RM was supported by NWO Vici 865.17.004. The funding bodies had no role in the design of the study and collection, analysis, and interpretation of data, and in writing the manuscript.

ACKNOWLEDGMENTS

We acknowledge Ulrike Nehrdich and Guus van der Velden for the assistance in adult zebrafish care.

SUPPLEMENTARY MATERIAL

The Supplementary Material for this article can be found online at: https://www.frontiersin.org/articles/10.3389/fcell.2021.624571/full#supplementary-material

REFERENCES

Bernut, A., Herrmann, J. L., Kissa, K., Dubremetz, J. F., Gaillard, J. L., Lutfalla, G., et al. (2014). Mycobacterium abscessus cording prevents phagocytosis and promotes abscess formation. *Proc. Natl. Acad. Sci. U S A.* 111, E943–E952. doi: 10.1073/pnas.1321390111

Bernut, A., Loynes, C. A., Floto, R. A., and Renshaw, S. A. (2020). Deletion of cftr leads to an excessive neutrophilic response and defective tissue repair in a

zebrafish model of sterile inflammation. *Front. Immunol.* 11:1733. doi: 10.3389/fimmu.2020.01733

Bianchi, M. E. (2009). HMGB1 loves company. *J. Leukoc Biol.* 86, 573–576. doi: 10.1189/jlb.1008585

Brazil, J. C., Louis, N. A., and Parkos, C. A. (2013). The role of polymorphonuclear leukocyte trafficking in the perpetuation of inflammation during inflammatory bowel disease. *Inflamm. Bowel. Dis.* 19, 1556–1565. doi: 10.1097/MIB.0b013e318281f54e

Castoldi, A., Braga, T. T., Correa-Costa, M., Aguiar, C. F., Bassi, E. J., Correa-Silva, R., et al. (2012). TLR2, TLR4 and the MYD88 signaling pathway are crucial for neutrophil migration in acute kidney injury induced by sepsis. *PLoS One* 7:e37584. doi: 10.1371/journal.pone.0037584

Chatzopoulou, A., Heijmans, J. P., Burgerhout, E., Oskam, N., Spaink, H. P., Meijer, A. H., et al. (2016). Glucocorticoid-Induced attenuation of the inflammatory response in zebrafish. *Endocrinology* 157, 2772–2784. doi: 10.1210/en.2015-2050

Chen, L., and DiPietro, L. A. (2017). Toll-Like receptor function in acute wounds. *Adv. Wound Care* 6, 344–355. doi: 10.1089/wound.2017.0734

Chen, L., Zheng, L., Chen, P., and Liang, G. (2020). Myeloid differentiation primary response protein 88 (MyD88): the central hub of TLR/IL-1R signaling. *J. Med. Chem.* 63, 13316–13329. doi: 10.1021/acs.jmedchem.0c00884

Dasu, M. R., Thangappan, R. K., Bourgette, A., Dipietro, L. A., Isseroff, R., and Jialal, I. (2010). TLR2 expression and signaling-dependent inflammation impair wound healing in diabetic mice. *Lab. Invest.* 90, 1628–1636. doi: 10.1038/labinvest.2010.158

Deng, Q., Harvie, E. A., and Huttenlocher, A. (2012). Distinct signalling mechanisms mediate neutrophil attraction to bacterial infection and tissue injury. *Cell Microbiol.* 14, 517–528. doi: 10.1111/j.1462-5822.2011.01738.x

Donà, E., Barry, J. D., Valentin, G., Quirin, C., Khmelinskii, A., Kunze, A., et al. (2013). Directional tissue migration through a self-generated chemokine gradient. *Nature* 503, 285–289. doi: 10.1038/nature12635

Gray, C., Loynes, C. A., Whyte, M. K., Crossman, D. C., Renshaw, S. A., and Chico, T. J. (2011). Simultaneous intravital imaging of macrophage and neutrophil behaviour during inflammation using a novel transgenic zebrafish. *Thromb Haemost.* 105, 811–819. doi: 10.1160/TH10-08-0525

Hato, T., and Dagher, P. C. (2015). How the innate immune system senses trouble and causes trouble. *Clin. J. Am. Soc. Nephrol.* 10, 1459–1469. doi: 10.2215/CJN.04680514

He, M., Halima, M., Xie, Y. F., Schaaf, M. J. M., Meijer, A. H., and Wang, M. (2020). Ginsenoside Rg1 acts as a selective glucocorticoid receptor agonist with anti-inflammatory action without affecting tissue regeneration in zebrafish larvae. *Cells* 9:1107. doi: 10.3390/cells9051107

Henry, K. M., Loynes, C. A., Whyte, M. K., and Renshaw, S. A. (2013). Zebrafish as a model for the study of neutrophil biology. *J. Leukoc Biol.* 94, 633–642. doi: 10.1189/jlb.1112594

Hopkin, S. J., Lewis, J. W., Krautter, F., Chimen, M., and Mcgettrick, H. M. (2019). Triggering the resolution of immune mediated inflammatory diseases: can targeting leukocyte migration be the answer? *Front. Pharmacol.* 10:184. doi: 10.3389/fphar.2019.00184

Houseright, R. A., Rosowski, E. E., Lam, P. Y., Tauzin, S. J. M., Mulvaney, O., Dewey, C. N., et al. (2020). Cell type specific gene expression profiling reveals a role for complement component C3 in neutrophil responses to tissue damage. *Sci. Rep.* 10:15716. doi: 10.1038/s41598-020-72750-9

Hu, W., Yang, S., Shimada, Y., Munch, M., Marin-Juez, R., Meijer, A. H., et al. (2019). Infection and RNA-seq analysis of a zebrafish tlr2 mutant shows a broad function of this toll-like receptor in transcriptional and metabolic control and defense to *Mycobacterium marinum* infection. *BMC Genom.* 20:878. doi: 10.1186/s12864-019-6265-1

Janeway, C. A. Jr., and Medzhitov, R. (2002). Innate immune recognition. *Annu. Rev. Immunol.* 20, 197–216. doi: 10.1146/annurev.immunol.20.083001.084359

Ji, L., Xue, R., Tang, W., Wu, W., Hu, T., Liu, X., et al. (2014). Toll like receptor 2 knock-out attenuates carbon tetrachloride (CCl4)-induced liver fibrosis by downregulating MAPK and NF-kappaB signaling pathways. *FEBS Lett.* 588, 2095–2100. doi: 10.1016/j.febslet.2014.04.042

Jiang, D., Liang, J., Fan, J., Yu, S., Chen, S., Luo, Y., et al. (2005). Regulation of lung injury and repair by Toll-like receptors and hyaluronan. *Nat. Med.* 11, 1173–1179. doi: 10.1038/nm1315

Katikaneni, A., Jelcic, M., Gerlach, G. F., Ma, Y., Overholtzer, M., and Niethammer, P. (2020). Lipid peroxidation regulates long-range wound detection through 5-lipoxygenase in zebrafish. *Nat. Cell Biol.* 22, 1049–1055. doi: 10.1038/s41556-020-0564-2

Kim, D., You, B., Lim, H., and Lee, S. J. (2011). Toll-like receptor 2 contributes to chemokine gene expression and macrophage infiltration in the dorsal root ganglia after peripheral nerve injury. *Mol. Pain* 7:74. doi: 10.1186/1744-8069-7-74

Koch, B. E. V., Yang, S., Lamers, G., Stougaard, J., and Spaink, H. P. (2019). Author correction: intestinal microbiome adjusts the innate immune setpoint during colonization through negative regulation of MyD88. *Nat. Commun.* 10:526. doi: 10.1038/s41467-019-08456-y

Komai, K., Shichita, T., Ito, M., Kanamori, M., Chikuma, S., and Yoshimura, A. (2017). Role of scavenger receptors as damage-associated molecular pattern receptors in Toll-like receptor activation. *Int. Immunol.* 29, 59–70. doi: 10.1093/intimm/dxx010

Li, L., Yan, B., Shi, Y. Q., Zhang, W. Q., and Wen, Z. L. (2012). Live imaging reveals differing roles of macrophages and neutrophils during zebrafish tail fin regeneration. *J. Biol. Chem.* 287, 25353–25360. doi: 10.1074/jbc.M112.349126

Lieschke, G. J., Oates, A. C., Crowhurst, M. O., Ward, A. C., and Layton, J. E. (2001). Morphologic and functional characterization of granulocytes and macrophages in embryonic and adult zebrafish. *Blood* 98, 3087–3096. doi: 10.1182/blood.V98.10.3087.h8003087_3087_3096

Macedo, L., Pinhal-Enfield, G., Alshits, V., Elson, G., Cronstein, B. N., and Leibovich, S. J. (2007). Wound healing is impaired in MyD88-deficient mice: a role for MyD88 in the regulation of wound healing by adenosine A2A receptors. *Am. J. Pathol.* 171, 1774–1788. doi: 10.2353/ajpath.2007.061048

Magnusson, K. E. G., Jalden, J., Gilbert, P. M., and Blau, H. M. (2015). Global linking of cell tracks using the viterbi algorithm. *Ieee Trans. Med. Imag.* 34, 911–929. doi: 10.1109/TMI.2014.2370951

Manolopoulou, I., Matheu, M. P., Cahalan, M. D., West, M., and Kepler, T. B. (2012). Bayesian spatio-dynamic modeling in cell motility studies: learning nonlinear taxic fields guiding the immune response. *J. Am. Stat. Assoc.* 107, 855–865.

Martin, P., and Leibovich, S. J. (2005). Inflammatory cells during wound repair: the good, the bad and the ugly. *Trends Cell Biol.* 15, 599–607. doi: 10.1016/j.tcb.2005.09.002

Meijer, A. H., Gabby Krens, S. F., CityMedina Rodriguez, I. A., He, S., Bitter, W., Ewa Snaar-Jagalska, B., et al. (2004). Expression analysis of the Toll-like receptor and TIR domain adaptor families of zebrafish. *Mol. Immunol.* 40, 773–783. doi: 10.1016/j.molimm.2003.10.003

Meijer, A. H., and Spaink, H. P. (2011). Host-pathogen interactions made transparent with the zebrafish model. *Curr. Drug Targets* 12, 1000–1017. doi: 10.2174/138945011795677809

Meijering, E., Dzyubachyk, O., and Smal, I. (2012). Methods for cell and particle tracking. *Methods Enzymol.* 504, 183–200. doi: 10.1016/B978-0-12-391857-4.00009-4

Mescher, A. L. (2017). Macrophages and fibroblasts during inflammation and tissue repair in models of organ regeneration. *Regeneration (Oxf)* 4, 39–53. doi: 10.1002/reg2.77

Mittal, M., Siddiqui, M. R., Tran, K., Reddy, S. P., and Malik, A. B. (2014). Reactive oxygen species in inflammation and tissue injury. *Antioxid Redox. Signal.* 20, 1126–1167. doi: 10.1089/ars.2012.5149

Miura, K., Yang, L., Van Rooijen, N., Brenner, D. A., Ohnishi, H., and Seki, E. (2013). Toll-like receptor 2 and palmitic acid cooperatively contribute to the development of nonalcoholic steatohepatitis through inflammasome activation in mice. *Hepatology* 57, 577–589. doi: 10.1002/hep.26081

Mojumdar, K., Giordano, C., Lemaire, C., Liang, F., Divangahi, M., Qureshi, S. T., et al. (2016). Divergent impact of Toll-like receptor 2 deficiency on repair mechanisms in healthy muscle versus *Duchenne muscular* dystrophy. *J. Pathol.* 239, 10–22. doi: 10.1002/path.4689

Moles, A., Murphy, L., Wilson, C. L., Chakraborty, J. B., Fox, C., Park, E. J., et al. (2014). A TLR2/S100A9/CXCL-2 signaling network is necessary for neutrophil recruitment in acute and chronic liver injury in the mouse. *J. Hepatol.* 60, 782–791. doi: 10.1016/j.jhep.2013.12.005

Nathan, C. (2006). Neutrophils and immunity: challenges and opportunities. *Nat. Rev. Immunol.* 6, 173–182. doi: 10.1038/nri1785

Niethammer, P. (2016). The early wound signals. *Curr. Opin. Genet. Dev.* 40, 17–22. doi: 10.1016/j.gde.2016.05.001

Niethammer, P., Grabher, C., Look, A. T., and Mitchison, T. J. (2009). A tissue-scale gradient of hydrogen peroxide mediates rapid wound detection in zebrafish. *Nature* 459, 996–999. doi: 10.1038/nature08119

Oliveira-Nascimento, L., Massari, P., and Wetzler, L. M. (2012). The role of TLR2 in infection and immunity. *Front. Immunol.* 3:79. doi: 10.3389/fimmu.2012.00079

Poltorak, A., He, X., Smirnova, I., Liu, M. Y., Van Huffel, C., Du, X., et al. (1998). Defective LPS signaling in C3H/HeJ and C57BL/10ScCr mice: mutations in Tlr4 gene. *Science* 282, 2085–2088. doi: 10.1126/science.282.5396.2085

Quesniaux, V. J., Nicolle, D. M., Torres, D., Kremer, L., Guerardel, Y., Nigou, J., et al. (2004). Toll-like receptor 2 (TLR2)-dependent-positive and TLR2-independent-negative regulation of proinflammatory cytokines by mycobacterial lipomannans. *J. Immunol.* 172, 4425–4434. doi: 10.4049/jimmunol.172.7.4425

Renshaw, S. A., Loynes, C. A., Trushell, D. M., Elworthy, S., Ingham, P. W., and Whyte, M. K. (2006). A transgenic zebrafish model of neutrophilic inflammation. *Blood* 108, 3976–3978. doi: 10.1182/blood-2006-05-024075

Schauber, J., Dorschner, R. A., Coda, A. B., Buchau, A. S., Liu, P. T., Kiken, D., et al. (2007). Injury enhances TLR2 function and antimicrobial peptide expression through a vitamin D-dependent mechanism. *J. Clin. Invest.* 117, 803–811. doi: 10.1172/JCI30142

Seki, E., Park, E., and Fujimoto, J. (2011). Toll-like receptor signaling in liver regeneration, fibrosis and carcinogenesis. *Hepatol. Res.* 41, 597–610. doi: 10.1111/j.1872-034X.2011.00822.x

Selmeczi, D., Mosler, S., Hagedorn, P. H., Larsen, N. B., and Flyvbjerg, H. (2005). Cell motility as persistent random motion: theories from experiments. *Biophys. J.* 89, 912–931. doi: 10.1529/biophysj.105.061150

Serhan, C. N., Brain, S. D., Buckley, C. D., Gilroy, D. W., Haslett, C., O'neill, L. A., et al. (2007). Resolution of inflammation: state of the art, definitions and terms. *FASEB J.* 21, 325–332. doi: 10.1096/fj.06-7227rev

Shishido, T., Nozaki, N., Takahashi, H., Arimoto, T., Niizeki, T., Koyama, Y., et al. (2006). Central role of endogenous Toll-like receptor-2 activation in regulating inflammation, reactive oxygen species production, and subsequent neointimal formation after vascular injury. *Biochem. Biophys. Res. Commun.* 345, 1446–1453. doi: 10.1016/j.bbrc.2006.05.056

Soehnlein, O., and Lindbom, L. (2010). Phagocyte partnership during the onset and resolution of inflammation. *Nat. Rev. Immunol.* 10, 427–439. doi: 10.1038/nri2779

Sommer, F., Ortiz Zacari, As, N. V., Heitman, L. H., and Meijer, A. H. (2020a). Inhibition of macrophage migration in zebrafish larvae demonstrates in vivo efficacy of human CCR2 inhibitors. *Dev. Comp. Immunol.* 116:103932. doi: 10.1016/j.dci.2020.103932

Sommer, F., Torraca, V., Kamel, S. M., Lombardi, A., and Meijer, A. H. (2020b). Frontline science: antagonism between regular and atypical Cxcr3 receptors regulates macrophage migration during infection and injury in zebrafish. *J. Leukoc Biol.* 107, 185–203. doi: 10.1002/JLB.2HI0119-006R

Stokes, C. L., Lauffenburger, D. A., and Williams, S. K. (1991). Migration of individual microvessel endothelial cells: stochastic model and parameter measurement. *J. Cell Sci.* 99(Pt 2), 419–430.

Suga, H., Sugaya, M., Fujita, H., Asano, Y., Tada, Y., Kadono, T., et al. (2014). TLR4, rather than TLR2, regulates wound healing through TGF-beta and CCL5 expression. *J. Dermatol. Sci.* 73, 117–124. doi: 10.1016/j.jdermsci.2013.10.009

Takeda, K., and Akira, S. (2004). Microbial recognition by Toll-like receptors. *J. Dermatol. Sci.* 34, 73–82. doi: 10.1016/j.jdermsci.2003.10.002

Taylor, H. B., Liepe, J., Barthen, C., Bugeon, L., Huvet, M., Kirk, P. D. W., et al. (2013). P38 and JNK have opposing effects on persistence of in vivo leukocyte migration in zebrafish. *Immunol. Cell Biol.* 91, 60–69. doi: 10.1038/icb.2012.57

Teixeira, H. S., Zhao, J., Kazmierski, E., Kinane, D. F., and Benakanakere, M. R. (2020). TLR3-Dependent activation of TLR2 endogenous ligands via the MyD88 signaling pathway augments the innate immune response. *Cells* 9:1910. doi: 10.3390/cells9081910

Tinevez, J. Y., Perry, N., Schindelin, J., Hoopes, G. M., Reynolds, G. D., Laplantine, E., et al. (2017). TrackMate: an open and extensible platform for single-particle tracking. *Methods* 115, 80–90. doi: 10.1016/j.ymeth.2016.09.016

Torraca, V., Cui, C., Boland, R., Bebelman, J. P., Van Der Sar, A. M., Smit, M. J., et al. (2015). The CXCR3-CXCL11 signaling axis mediates macrophage recruitment and dissemination of mycobacterial infection. *Dis. Model. Mech.* 8, 253–269. doi: 10.1242/dmm.017756

Tweedy, L., Knecht, D. A., Mackay, G. M., and Insall, R. H. (2016). Self-Generated chemoattractant gradients: attractant depletion extends the range and robustness of chemotaxis. *PLoS Biol.* 14:e1002404. doi: 10.1371/journal.pbio.1002404

Ulman, V., Maska, M., Magnusson, K. E. G., Ronneberger, O., Haubold, C., Harder, N., et al. (2017). An objective comparison of cell-tracking algorithms. *Nat. Methods* 14, 1141–1152. doi: 10.1038/nmeth.4473

van der Vaart, M., Van Soest, J. J., Spaink, H. P., and Meijer, A. H. (2013). Functional analysis of a zebrafish myd88 mutant identifies key transcriptional components of the innate immune system. *Dis. Model. Mech.* 6, 841–854. doi: 10.1242/dmm.010843

Vijay, K. (2018). Toll-like receptors in immunity and inflammatory diseases: past, present, and future. *Int. Immunopharmacol.* 59, 391–412. doi: 10.1016/j.intimp.2018.03.002

Wagner, N., Reinehr, S., Palmhof, M., Schuschel, D., Tsai, T., Sommer, E., et al. (2020). Microglia activation in retinal ischemia triggers cytokine and toll-like receptor response. *J. Mol. Neurosci.* Online ahead of print. doi: 10.1007/s12031-020-01674-w

Weiss, S. J. (1989). Tissue destruction by neutrophils. *N. Engl. J. Med.* 320, 365–376. doi: 10.1056/NEJM198902093200606

Xie, Y., Tolmeijer, S., Oskam, J. M., Tonkens, T., Meijer, A. H., and Schaaf, M. J. M. (2019). Glucocorticoids inhibit macrophage differentiation towards a pro-inflammatory phenotype upon wounding without affecting their migration. *Dis. Model. Mech.* 12:dmm037887. doi: 10.1242/dmm.037887

Xu, Y., Zhou, Y., Lin, H., Hu, H., Wang, Y., and Xu, G. (2013). Toll-like receptor 2 in promoting angiogenesis after acute ischemic injury. *Int. J. Mol. Med.* 31, 555–560. doi: 10.3892/ijmm.2013.1240

Yamamoto, S., Shimizu, S., Kiyonaka, S., Takahashi, N., Wajima, T., Hara, Y., et al. (2008). TRPM2-mediated Ca2+influx induces chemokine production in monocytes that aggravates inflammatory neutrophil infiltration. *Nat. Med.* 14, 738–747. doi: 10.1038/nm1758

Yanai, H., Ban, T., Wang, Z., Choi, M. K., Kawamura, T., Negishi, H., et al. (2009). HMGB proteins function as universal sentinels for nucleic-acid-mediated innate immune responses. *Nature* 462, 99–103. doi: 10.1038/nature08512

Yang, S., Marin-Juez, R., Meijer, A. H., and Spaink, H. P. (2015). Common and specific downstream signaling targets controlled by Tlr2 and Tlr5 innate immune signaling in zebrafish. *BMC Genom.* 16:547. doi: 10.1186/s12864-015-1740-9

Yu, L., Wang, L., and Chen, S. (2010). Endogenous toll-like receptor ligands and their biological significance. *J. Cell Mol. Med.* 14, 2592–2603. doi: 10.1111/j.1582-4934.2010.01127.x

Conflict of Interest: The authors declare that the research was conducted in the absence of any commercial or financial relationships that could be construed as a potential conflict of interest.

frontiers in Cell and Developmental Biology

REVIEW
published: 15 February 2021
doi: 10.3389/fcell.2021.629238

Polarization of Macrophages in Insects: Opening Gates for Immuno-Metabolic Research

Adam Bajgar, Gabriela Krejčová and Tomáš Doležal*

Department of Molecular Biology and Genetics, University of South Bohemia, Ceske Budejovice, Czechia

Insulin resistance and cachexia represent severe metabolic syndromes accompanying a variety of human pathological states, from life-threatening cancer and sepsis to chronic inflammatory states, such as obesity and autoimmune disorders. Although the origin of these metabolic syndromes has not been fully comprehended yet, a growing body of evidence indicates their possible interconnection with the acute and chronic activation of an innate immune response. Current progress in insect immuno-metabolic research reveals that the induction of insulin resistance might represent an adaptive mechanism during the acute phase of bacterial infection. In *Drosophila*, insulin resistance is induced by signaling factors released by bactericidal macrophages as a reflection of their metabolic polarization toward aerobic glycolysis. Such metabolic adaptation enables them to combat the invading pathogens efficiently but also makes them highly nutritionally demanding. Therefore, systemic metabolism has to be adjusted upon macrophage activation to provide them with nutrients and thus support the immune function. That anticipates the involvement of macrophage-derived systemic factors mediating the inter-organ signaling between macrophages and central energy-storing organs. Although it is crucial to coordinate the macrophage cellular metabolism with systemic metabolic changes during the acute phase of bacterial infection, the action of macrophage-derived factors may become maladaptive if chronic or in case of infection by an intracellular pathogen. We hypothesize that insulin resistance evoked by macrophage-derived signaling factors represents an adaptive mechanism for the mobilization of sources and their preferential delivery toward the activated immune system. We consider here the validity of the presented model for mammals and human medicine. The adoption of aerobic glycolysis by bactericidal macrophages as well as the induction of insulin resistance by macrophage-derived factors are conserved between insects and mammals. Chronic insulin resistance is at the base of many human metabolically conditioned diseases such as non-alcoholic steatohepatitis, atherosclerosis, diabetes, and cachexia. Therefore, revealing the original biological relevance of cytokine-induced insulin resistance may help to develop a suitable strategy for treating these frequent diseases.

Keywords: *Drosophila*, macrophages, insulin resistance, cachexia, cytokines, immuno-metabolism, aerobic glycolysis

OPEN ACCESS

Edited by:
Katrin Kierdorf,
University of Freiburg, Germany

Reviewed by:
Dan Hultmark,
Umeå University, Sweden
Helen Weavers,
University of Bristol, United Kingdom

****Correspondence:***
Adam Bajgar
bajgaradam@seznam.cz

Specialty section:
This article was submitted to Cell Death and Survival, a section of the journal Frontiers in Cell and Developmental Biology

Received: *13 November 2020*
Accepted: *11 January 2021*
Published: *15 February 2021*

Citation:
Bajgar A, Krejčová G and Doležal T (2021) Polarization of Macrophages in Insects: Opening Gates for Immuno-Metabolic Research. Front. Cell Dev. Biol. 9:629238. doi: 10.3389/fcell.2021.629238

INTRODUCTION

Both cachexia and insulin resistance are in the spotlight of immuno-metabolic research and represent the most important comorbidities that often accompany acute and chronic inflammatory states and complicate their treatment (Fonseca et al., 2020). Cachexia, literally meaning "bad condition," is a metabolic syndrome of excessive weight loss and muscle wasting caused by alterations in appetite and the overall metabolic setup (Yang et al., 2020). The progressive development of insulin resistance to pre-cachexia and cachexia, which is defined as a loss of more than 5% of the cell body mass over 12 months or less, is known to be a hallmark for a wide range of seemingly unrelated diseases, such as obesity, cancer, chronic obstructive pulmonary disease, acute kidney disease, and sepsis (Mak and Cheung, 2006; Koehler et al., 2007; Srikanthan et al., 2010; Honors and Kinzig, 2012). Nevertheless, the mechanism of induction of these frequently occurring metabolic syndromes remains to be elucidated.

The origin of insulin resistance and cachexia relies on the activity of immune cell-derived signaling factors and is thus a result of excessive activation of the immune system (Olefsky and Glass, 2010). However, the biological relevance of such signaling has not been fully comprehended yet. It is mainly due to the prevailing perception of the cytokine-induced insulin resistance as a mere side effect of pathological syndromes and insufficient effort to reveal its adaptive meaning. The complexity of the mammalian immune system, as well as pleiotropic effects of most immune cell-derived factors, further complicate the resolution of this intricate relationship (Stenholm et al., 2008; Del Fabbro et al., 2011).

Recent progress in insect immuno-metabolic research revealed that cytokine-induced insulin resistance is not a mechanism occurring exclusively in vertebrates. Indeed, we may observe several physiological conditions in which immune cells release cytokines to affect the systemic metabolism via induction of insulin resistance in *Drosophila,* such as metabolic misbalance and development, as well as immune response (Rajan and Perrimon, 2011; Woodcock et al., 2015; Lee et al., 2018; Dolezal et al., 2019). These states document the preservation of this mechanism among such evolutionarily distant groups as insects and mammals. To be maintained in the evolution, we might presume that cytokine-induced insulin resistance represents an ancient adaptive process of systemic metabolic rearrangement.

Here, we would like to present several recent observations depicting that *Drosophila* activated immune cells affect systemic metabolism via the induction of insulin resistance to ensure sufficient supplementation with nutrients for their function (**Figure 1** and **Box 1**). Although this mechanism is necessary for the acute phase of the immune response (Yang et al., 2015; Bajgar and Dolezal, 2018; Dolezal et al., 2019), it may lead to nutrient wastage if chronic, and prolonged reallocation of sources may become the basis for the development of many serious pathological conditions.

Innate immune cells performing the phagocytic function represent the front line of protection against invading pathogens (Franken et al., 2016). Individuals, therefore, tend to maximize the number of these protectors participating in phagocytosis and clearance of pathogen (Kacsoh and Schlenke, 2012; Mihajlovic et al., 2019). Nevertheless, the maintenance of an excessive number of metabolically demanding phagocytes would be highly energy-intensive with subsequent adverse impact on concurrent energy-consuming processes, such as growth and reproduction (Wolowczuk et al., 2008). Therefore, animals have developed a strategy to overcome these evolutional constraints by maintaining a sufficient number of immune cells in a quiescent state as well as by proliferation of their progenitors upon immune challenge. Quiescent phagocytes exhibiting only a basal metabolic rate are thus waiting for the activation stimuli ready to be metabolically awakened and to participate in the acute immune response (Mosser and Edwards, 2008). In plentiful times, individuals can fully exploit the surplus energy to maintain homeostasis, growth, and reproduction as processes based mainly on anabolic metabolism (Wang et al., 2019). That is in sharp contrast to the situation of life-threatening infection. In response to the recognition of pathogen-associated molecular patterns, activated immune cells such as monocytes, macrophages, dendritic cells, and neutrophils, must react rapidly to limit the pathogen burden and adopt a bactericidal polarization phenotype (Galván-peña and O'Neill, 2014; Loftus and Finlay, 2016). However, the immediate activation of a large number of these cells toward the bactericidal phenotype (also known as pro-inflammatory) represents an immense energy load for the organism (Demas, 2004; Edholm et al., 2017). The nutritional investments connected with the acute phase response are further increased by the proliferation of immune cell progenitors and their differentiation toward effector cells upon activation of the immune response.

Professional phagocytes must rewire their cellular metabolism greatly to become efficient in bacterial killing (Pavlou et al., 2017). It is well established particularly for mammalian bactericidal macrophages that they undergo metabolic polarization toward aerobic glycolysis as a predominant source of energy and a precursors essential for bactericidal function (Benoit et al., 2008). Similarly to macrophages, the increased glycolytic rate and other metabolic adjustments were later confirmed also for neutrophils, dendritic cells, effector lymphocytes, and natural killer cells (Loftus and Finlay, 2016). Interestingly, adoption of aerobic glycolysis by immune cells may originate not only in response to bacterial invaders but can also be induced by excessive lipid uptake (**Box 2**).

Although the term "aerobic glycolysis" *sensu stricto* refers to lactic acid fermentation of glucose, here we perceive it as a complex phagocyte metabolic program including, in addition, increased pentose phosphate pathway, lipid synthesis, and the mevalonate pathway, as well as a rewired flow of the Krebs cycle (Mills and O'Neill, 2016; Nonnenmacher and Hiller, 2018). Such metabolic adaptation affects also nutritional demands of these cells and makes them functionally dependent on external supplementation. Since the availability of nutrients may become limiting for the adoption of bactericidal polarization (Nagy and Haschemi, 2015; Ganeshan et al., 2019), they have to secure sufficient availability of sources in circulation and gain an advantage over the surrounding tissues in their use.

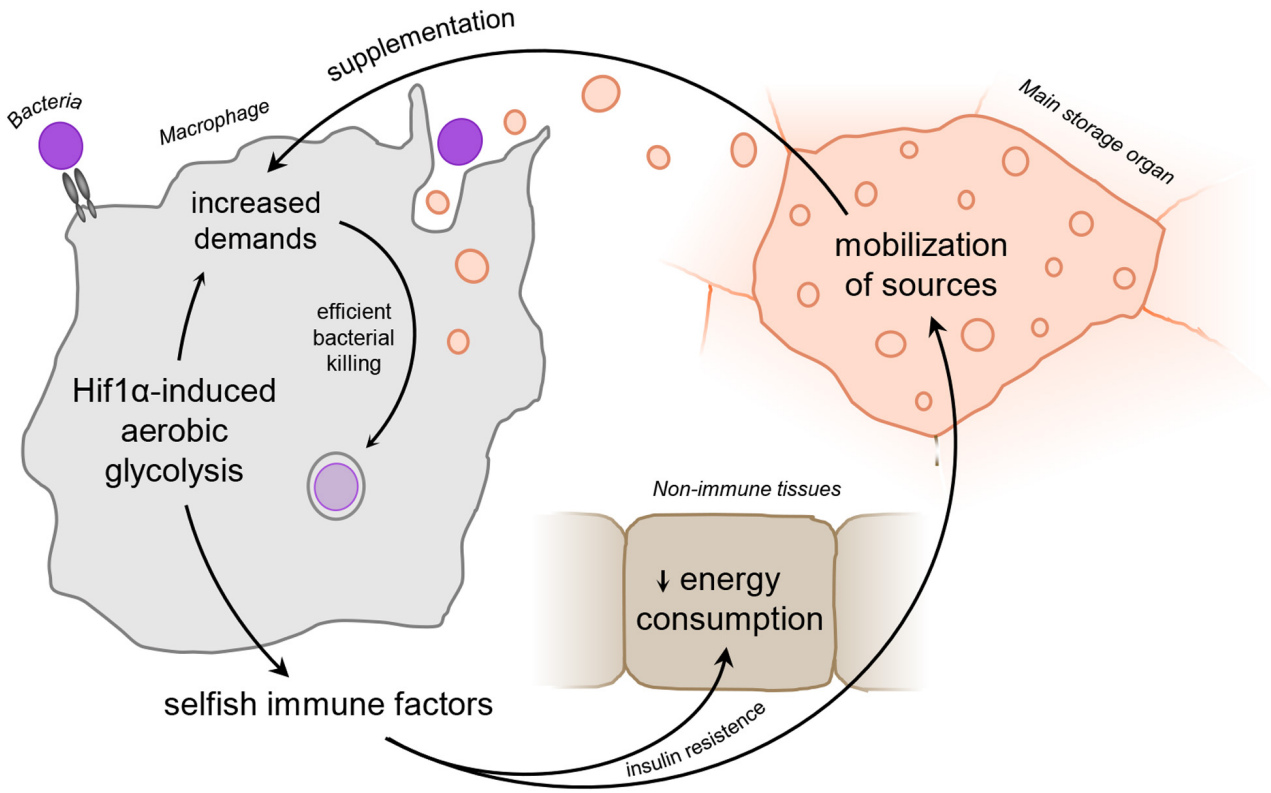

FIGURE 1 | Schematic representation of the "selfish immune system theory." Infection-activated macrophages adopt Hif1α-induced aerobic glycolysis and subsequently release signaling factors to ensure sufficient amount of nutrients to supplement the immune function. Hif1α, hypoxia-inducible factor 1 α.

Therefore, activated professional phagocytes release signaling factors regulating both local and systemic energy in order to usurp enough sources for an acute immune response (Khovidhunkit et al., 2004; Soeters and Soeters, 2012; Straub, 2014; Dolezal, 2015; **Figure 1** and **Box 1**).

Besides the mobilization of sources from central energy-storing organs, such as adipose tissue and the liver, it is fundamental to limit the consumption of nutrients by other processes unrelated to the immune response (Almajwal et al., 2019). The privileged status of immune cells in reaching the nutrients is justified since making the immune response the most efficient is often a question of life and death. Although such behavior of the immune cells is for the sake of the individual, the usurpation of sources may be interpreted as selfish if viewed from the perspective of inter-organ competition for sources. Immune cell-derived signaling factors responsible for such systemic metabolic switch may be hence called selfish immune factors (SIFs) (Bajgar et al., 2015; Dolezal et al., 2019).

BOX 1 | Hypothesis.
We hypothesize that activated phagocytes produce signaling factors to reflect their current nutritional demands upon adoption of aerobic glycolysis. These factors induce mobilization of nutrients and silence their consumption by non-immune tissues via insulin resistance, leaving thus enough of sources for the activated immune system. Release of these signaling factors is thus beneficial for the acute immune response; however, it may lead to energy wasting and development of severe pathologies if produced chronically (**Figure 1**).

Insulin signaling is the central signaling pathway regulating the balance between anabolic and catabolic processes in the body (Schwartsburd, 2017). We may, therefore, presume that antagonism of insulin signaling is the most straightforward strategy to reroute energy flows from maintenance, growth, and reproduction to its fast utilization by the activated immune system. Cytokine-induced deterioration of insulin signaling leads to an increased titer of circulating energy-rich compounds such as glucose, lipoproteins, and amino acids (Felig et al., 1969; Salazar et al., 2018; Cho et al., 2019). The impact of infection-induced insulin insensitivity on the systemic metabolism highly resembles hyperglycemia and hyperlipidemia as hallmark states of chronic insulin resistance and cachexia (Khovidhunkit et al., 2004; de Luca and Olefsky, 2008; Shi et al., 2019). However, the regulation of energy homeostasis in mammals is substantially influenced also by other metabolism-related hormones such as cortisol and catecholamines, particularly noradrenalin and norepinephrine that should not be omitted for their effects on nutrient mobilization in situation of metabolic stress (Marik and Bellomo, 2013).

In the presented perspective, insulin resistance and subsequent pre-cachectic state induced by immune cell-derived factors may be perceived as an adaptive metabolic adjustment

BOX 2 | Excessive lipids induce adoption of macrophage pro-inflammatory phenotype.

It is of particular interest that the adoption of pro-inflammatory MI polarization can be induced even without the presence of a pathogen. That is in concordance with the previously mentioned fact that HIFIα stabilization, central for induction of bactericidal macrophage polarization, may be achieved either by TLR4 activation or by metabolic feedback from mitochondrial metabolism (Iommarini et al., 2017). It underpins many metabolically induced inflammatory diseases with a significant impact on human well-being, such as obesity, non-alcoholic fatty liver disease, atherosclerosis, and diabetes (Kraakman et al., 2014; Castoldi et al., 2016; Kazankov et al., 2019).

Exposure of macrophages to excessive amounts of lipids can lead to the adoption of pro-inflammatory polarization of macrophages. The effect of lipids on macrophages is dual. The increased concentration of lipids in the extracellular space is recognized by TLR4 and, analogically to infection, leads to the stabilization of HIFIα via the NFκB signaling pathway (Hubler and Kennedy, 2016; Korbecki and Bajdak-Rusinek, 2019). In addition, lipids are efficiently internalized by macrophages via receptor-mediated endocytosis (Park, 2014). Because there is no feedback on lipid uptake by macrophages, it leads to a massive accumulation of oxidized lipids and cholesterol in the cytosol of these cells, followed by disruption of mitochondrial function (Gibson et al., 2018). Lipid peroxidation catalyzed by free iron ions, together with ROS accumulation, leads to disruption of mitochondrial function by activating the transcription factor *nuclear factor erythroid 2-related factor 2* (NRF2) (Dodson et al., 2019). NRF2 triggers the expression of a number of genes responsible for the sequestration of free iron and enzymes that neutralize the oxidative potential of ROS (Tonelli et al., 2018). Therefore, the accumulation of both internal and external lipids results in HIFIα stabilization and the adoption of AG. It seems that macrophages are predetermined for this detoxification function by exploiting a whole set of genes involved in lipid metabolism and thus help to cope with ectopic lipid deposition (Bobryshev et al., 2016).

Under conditions in which macrophages are exposed to excessive lipids for a time-restricted period, such as aerobic exercise, intermittent fasting, and caloric restriction, induction of mild mitochondrial stress may be beneficial for the organism. This phenomenon, called mitohormesls, alleviates systemic insulin signaling, which has a positive impact on lifespan (Ristow and Schmeisser, 2014). Nevertheless, prolonged exposure of macrophages to lipids leads to the adoption of pro-inflammatory phenotypes and chronic insulin resistance (Shin et al., 2017). During obesity, macrophages are thought to cause cytokine-induced insulin resistance in adipose tissue, the liver, and, subsequently, the whole organism (Marette, 2002; Tilg and Hotamisligil, 2006; Makki et al., 2013).

Activation of macrophages by excessive lipids may explain several metabolic syndromes such as adipose tissue inflammation, non-alcoholic liver steatosis, atherosclerosis, diabetes, and cachexia. This hypothesis is in concordance with clinical observations and experiments carried out on mice, in which the amelioration of macrophage polarization by anti-inflammatory agents and drugs affecting lipid metabolism leads to significant improvement of these syndromes in obese individuals (Bellucci et al., 2017; Koelwyn et al., 2018).

essential for the effective fight of invading pathogens. However, mobilization of nutrients and their altered distribution in the body may become detrimental if chronic and may progress to the development of several human pathological states.

In the following paragraphs, we would like to present several lines of evidence supporting this perspective. Although gained mostly by the research of immuno-metabolism in insects, these observations are in concordance with many data from mice models and humans. Since the metabolic switch of innate immune cells is best comprehended for macrophages, we will focus in this review mainly on these cells. The hypothetical model discussed in this review is based on knowledge of biology of both mammalian macrophages as well as *Drosophila* professional phagocytes, called plasmatocytes. Their basic characteristics and the features resembling mammalian macrophages and neutrophils are further described in **Box 3**. To specify that the presented information concerns *Drosophila* phagocytes, these cells will be always denoted here as plasmatocytes.

We believe that we present here a compelling set of information to change the general conception of insulin resistance and pre-cachexia as clearly pathological states. This may help to better comprehend medical treatment in many human diseases.

MACROPHAGE ADOPTION OF A BACTERICIDAL PHENOTYPE IS NUTRITIONALLY DEMANDING

Macrophages, as highly versatile cells, fulfill various tasks in the organism. Besides representing the front line of protection against invading pathogens, macrophages also clear apoptotic cellular debris, maintain tissue homeostasis, and participate in the formation of many morphological structures during development (Wynn et al., 2013; Gordon and Martinez-Pomares, 2017; Theret et al., 2019).

Not surprisingly, the various macrophage tasks require specific settings of cellular metabolism to obtain the optimal amount of metabolites and precursors required for the desired function. That may be depicted, for instance, in the metabolism of amino acid arginine. While macrophages participating in wound healing metabolize arginine to generate growth-promoting ornithine essential for wound reconstruction, bactericidal macrophages use the same amino acid as a precursor for the production of nitric oxide later applied as an efficient bactericidal agent (Mills et al., 2015). This revelation led to later identification of the full spectrum of macrophage polarization states characterized by their metabolic program, with the extremes represented by healing and bactericidal polarizations (Mosser and Edwards, 2008). Interestingly, the metabolic settings are determinative of macrophage function, and a mere metabolic setting has the potential to change the polarization phenotype (Galván-peña and O'Neill, 2014).

Upon pathogen infiltration, macrophages have to recognize, entrap, engulf, and destroy the invaders in the phagolysosome (Diskin and Pålsson-McDermott, 2018). There is no doubt that these processes are connected with excessive energy expenditure and a need for a synthesis of a high amount of precursors for the production of bactericidal agents, signaling molecules, as well as remodeling of cytoskeleton and cellular membrane. It has been estimated that the cellular membrane of activated macrophage turns over completely every 30 min due to accelerated endocytosis and micropinocytosis (Werb and Cohn, 1972). Besides membrane remodeling, phagocytosis also requires a high amount of energy. The ATP required for phagocytosis of a single polystyrene particle has been estimated to cost about 10^9 ATP molecules (Karnovsky, 1962). The subsequent generation of a sufficient amount of ROS and myeloperoxidase for bacterial

BOX 3 | *Drosophila* as a model for immuno-metabolic research.

Over the last century, *Drosophila* has become a very universal and suitable model organism for the study of many human diseases. The simplicity of *Drosophila,* the existence of readily available transgenic strains, as well as the possibility of tissue-specific and time-limited knockdown of a particular gene make *Drosophila* one of the most suitable model organisms for the study of complex systemic metabolic syndromes (Duffy, 2002). In addition, approaches that previously could not be applied due to the lack of input material from such a small organism are now possible due to the greater sensitivity of analytical techniques in recent years (Cheng et al., 2018).

The *Drosophila* immune system consists of several layers of protection of an individual, which consist of two main branches of the humoral and cellular immune response. In addition to immune cells, the fat body also participates in immune responses, as the central metabolic organ supports the immune response by releasing resources and producing antimicrobial peptides (Melcarne et al., 2019). Although *Drosophila* may develop a characteristic immune response against underlying types of pathogens, such as gram-positive and gram-negative bacteria, viruses, and fungi, the adaptive immune response in *Drosophila* has not been reliably demonstrated (Ferrandon et al., 2007). The *Drosophila* and mammalian immune systems display a surprising level of homology in the major immune signaling pathways. The antibacterial response consists of the activation of the Toll and Imd signaling pathways, supported by the usual JNK and HIFIα stress response (De Gregorio et al., 2002).

Some observations suggest that the innate immune response to invading pathogens shows certain features of trainability, but the mechanism of this process remains unclear. *Drosophila* immune cells, called hemocytes, include prohemocytes, plasmatocytes, crystall cells, and lamellocytes. While crystal cells and plasmatocytes are mainly involved in the encapsulation and melanization of foreign objects in the hemolymph, plasmatocytes represent a population of professional phagocytes (Melcarne et al., 2019; **Figure 2**).

Plasmatocytes are the most abundant population of cells in both larvae and adult flies (**Figure 2A**). These functionally versatile cells are involved in many biological processes (**Figure 2F**), from embryonic morphogenesis, metamorphosis, and wound healing to protection against invading pathogens (Banerjee et al., 2019). Because phagocytosis and bacterial killing are highly conserved at the level of cell biology, *Drosophila* plasmatocytes show an exceptional level of similarity to cells of the mammalian innate immune system, especially macrophages and neutrophils. Indeed, plasmatocytes use the same metabolic and signaling pathways for pathogen uptake and destruction in phagolysosomes (**Figure 2C**) as their mammalian counterparts, including the involvement of a plethora of homologous genes (Browne et al., 2013).

Although plasmatocytes are predominantly considered in the literature as a homogeneous population of phagocytic cells, a single cell transcriptomic analysis of the immune-stimulated larval hemocytes revealed a surprising level of their variability. However, the research of the plasmatocyte subpopulation is still at the beginning and far from distinguishing tissue-resident or specifically primed plasmatocyte subsets (Cattenoz et al., 2020; Tattikota et al., 2020).

Recently, the concept of immuno-metabolism has been developed in mammals, which indicates that several populations of mammalian immune cells must adopt a specific cellular metabolism in order to perform the desired function (Galván-peña and O'Neill, 2014). Although there are still some doubts about an analogous mechanism for *Drosophila* plasmatocytes, several publications and transcriptomic data document this ability (Krejčová et al., 2019; Cattenoz et al., 2020; Ramond et al., 2020; Tattikota et al., 2020). These observations are necessary not only for a comprehensive understanding of the antibacterial immune response but may become a base for research of many other human diseases that are connected with the pathological metabolic polarization of mammalian immune cells.

Despite the undeniable benefits of the *Drosophila* model for the study of human diseases, there are certain limits because many *Drosophila* organs and tissues show a lower level of complexity than in mammals.

Drosophila is currently used extensively to study insulin resistance. *Drosophila* and mammalian insulin signaling share major components at the level of cell biology (Álvarez-Rendón et al., 2018). However, certain significant differences also need to be taken into account. *Drosophila* carries eight insulin-like peptides (DILP1-8) that show structural homology to either mammalian insulin or relaxin. Analogous to mammals, *Drosophila* insulin signaling also reflects the current metabolic status of the individual. DILPs 2, 3, and 5 are thus released by specialized neurosecretory cells in the *Drosophila* CNS to regulate reproduction, growth and lifespan. While most DILPs activate a single *Drosophila* insulin receptor, DILP8 binds to its own LGR3 receptor. The situation in humans is even more complicated because, in addition to insulin, we can recognize two insulin-like growth factors, relaxin, as well as several insulin-like peptides. Insulin signaling activity is affected by many convergent signaling pathways and factors, such as hormones of a lipophilic nature, as well as insulin-binding proteins and IGFs (Nässel et al., 2015; Nässel and Broeck, 2016). Thus, an analogy can also be observed in the manner of insulin resistance induction.

Therefore, we believe that ongoing research on the role of the *Drosophila* immune system in the regulation of systemic metabolism will lead to new discoveries that can be generalized to human medical research.

killing in the phagolysosome is another metabolically demanding process. The production of ROS, as well as compensation of its cytotoxicity, depends on sufficient availability of NADPH in cells. Therefore, macrophages must substantially increase the flow rate of the metabolic pathways producing this reducing agent (Panday et al., 2015).

To cover the sudden requirements arising from bactericidal function, macrophage has to adjust the overall metabolic setup, i.e., glycolysis, pentose phosphate pathway, mevalonate pathway, as well as the mitochondrial cycle of tricarboxylic acids and oxidative phosphorylation (Galván-peña and O'Neill, 2014). Such a complex rearrangement is orchestrated by central metabolic regulator Hypoxia-inducible factor 1 alpha—*Hif1α* (Corcoran and O'Neill, 2016; Wang et al., 2017). This stress-related transcription factor, originally discovered in research of hypoxia, is constitutively produced and degraded by all cells in the body (Marxsen et al., 2004). That is particularly important for immediate initiation of Hif1α activity since mere inhibition of its degradation suffices to stimulate expression of its target genes (Watts and Walmsley, 2019). Stabilized HIF1α triggers the expression of more than a hundred genes under the control of the hypoxia response element (Dengler et al., 2014). The unique metabolic program established by the activity of HIF1α is generally called aerobic glycolysis. Between HIF1α-target genes, we can find mostly enzymes directly participating in metabolic pathways upregulated in aerobic glycolysis or regulating their flow rate, as will be mentioned below (**Figure 3**).

Many different signaling cascades converge on prolyl hydroxylase dehydrogenase (PHD), the enzyme responsible for HIF1α degradation. PHD requires several metabolic products as essential cofactors for its enzymatic activity. From the most prominent, we should mention oxygen, Fe^{2+} ions, and α-ketoglutarate as a product of canonically running Krebs cycle (Iommarini et al., 2017). Although originally described in hypoxia, HIF1α stabilization may be achieved even under normoxic conditions as may be observed in macrophages stimulated by pathogen-associated molecular patterns or pro-inflammatory cytokines (Iommarini et al., 2017). These ligands

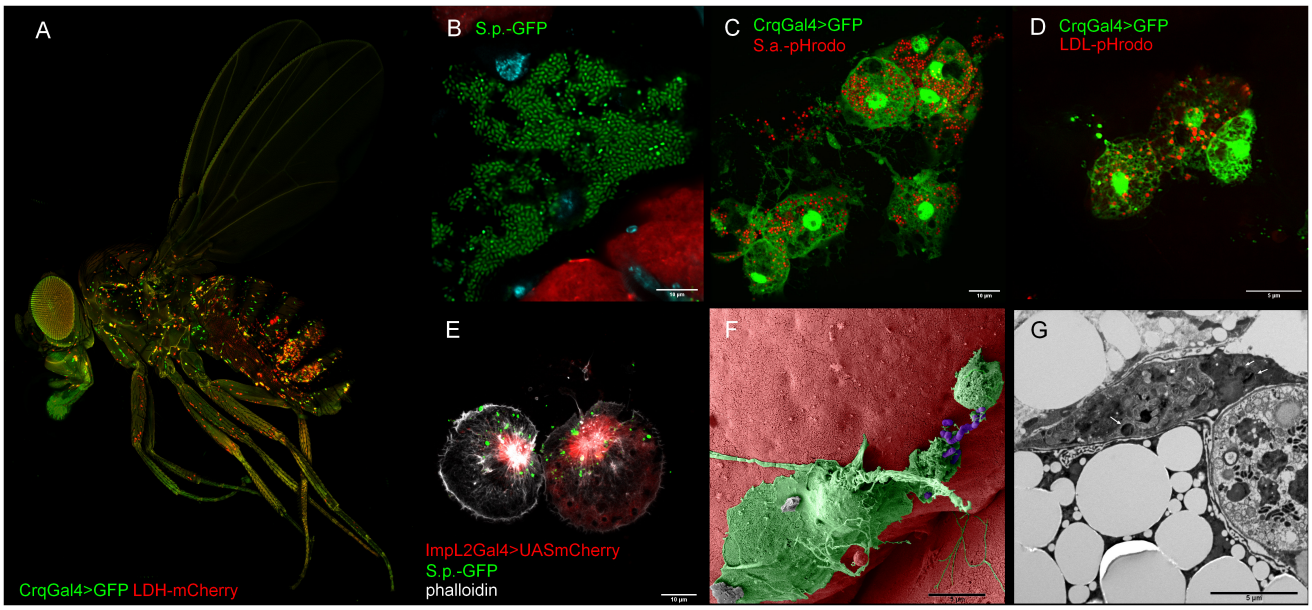

FIGURE 2 | Representative confocal and electron microscopy images of *Drosophila* macropahges. **(A)** Adult *Drosophila* bearing a genetic construct that enables visualization of macrophages (in green HmlGal4 > UAS2xeGFP) and tissue expressing lactate dehydrogenase (LDH-mCherry). **(B)** Confocal image depicting growth of streptococcus in dissected *Drosophila* abdomen (green—*S. pneumoniae*, red pericardial cells, cyan—DAPI). **(C)** Confocal image depicting phagocytic events by injection of *Drosophila* adult with pHrodo^{TM} Red *S. aureus* Bioparticles^{TM} Conjugate. Macrophages are visualized by endogenously expressed GFP (Crq > GFP) (green—macrophages, red—phagolysosomes). **(D)** Confocal image depicting endocytosis of low-density lipoproteins by injection of adult fly with pHrodo^{TM} Red-LDL. Macrophages are visualized by endogenously expressed GFP (Crq > GFP) (green—macrophages, red—LDL-containing late endosomes). **(E)** ImpL2-expressing macrophages interacting with fluorescently labeled *S. pneumoniae* (green—*S. pneumoniae*, red—ImpL2 Gal4 > UAS mCherry, white—phalloidin). **(F)** Pseudo-colored scanning electron micrograph of a macrophage interacting with *S. pneumoniae* (green—macrophage, purple—*S. pneumoniae*). **(G)** Transmission electron micrograph of *S. pneumoniae* bacteria (white arrows) in a macrophage. Crq, croquemort; ImpL2, imaginal morphogenesis protein late 2; LDL, low-density lipoproteins; S.p., *Streptococcus pneumoniae*.

activate toll-like receptor 4 (TLR4), which further enhances a Nuclear Factor kappa B (NF-κB)-signaling pathway. As an outcome of NFkB activity, the cytosolic $Fe2^{+}$ ions are sequestered by the major iron-storage protein ferritin. Lack of Fe^{2+} as a crucial cofactor of PHD thus causes HIF1α stabilization and substantial remodeling of overall cellular metabolism (Siegert et al., 2015). It should be noted that TLR4 may also be activated by endogenous ligands such as extracellular matrix components, oxidized lipids, and lipoproteins (Erridge, 2010).

Besides extracellular stimuli, HIF1α stabilization may be achieved by the cytosolic accumulation of several metabolic intermediates originating from the mitochondrial Krebs cycle. It has been documented that lactate, succinate, itaconate, pyruvate, and 2-hydroxyglutarate impair PHD ability to degrade HIF1α (Koivunen et al., 2007; Bailey and Nathan, 2018). This interconnection seems to be adaptive for overcoming hypoxic states since an accumulation of these metabolites in the cytosol is a hallmark of mitochondrial dysfunction (Garedew and Moncada, 2008; Prabakaran, 2015). Even though this mechanism enables cells to reflect their current metabolic state, it makes HIF1α stabilization dependent on elevated flow through metabolic pathways enhanced in aerobic glycolysis. Therefore, cells employing aerobic glycolysis are highly sensitive to the availability of sources. Early experiments using LPS as a classic way to activate macrophages showed that macrophages functionally depend on sufficient concentrations of glucose, glutamine, and lipids in the culture medium (Newsholme et al., 1986). Further *in vitro* investigation of nutrient uptake and trafficking fully elucidated the complexity of HIF1a-mediated metabolic changes and the utilization of these nutrients by bactericidal macrophages (Stunault et al., 2018).

An immense uptake of glucose is one of the hallmarks of bactericidal macrophages. That may be explained by its utilization as a primary energy resource as well as a substrate for the generation of NADPH and nucleotides in the pentose phosphate pathway (Yamashita et al., 2014). Consistently, *glucose-6-phosphate dehydrogenase*, which catalyzes the first step in pentose phosphate pathway, is known to be triggered by HIF1α (Gao et al., 2004). Interestingly, the glucose energy potential is not fully exploited since pyruvate as the end-product of glycolysis is not entering the mitochondria for its full oxidation. Due to HIF1α transcriptional activity, it is instead preferentially converted to lactate by *lactate dehydrogenase* and excluded from the cell through *monocarboxylate transporter 4* (Firth et al., 1995; Kim et al., 2006). Via increased glycolytic flux, cells avoid the time-consuming transport of pyruvate into the mitochondrial lumen that otherwise represents the rate-limiting step of ATP generation (Thomas and Halestrap, 1981). Thanks to that, the glycolytic flux may be increased even a hundred times, thus fully compensating for the lower efficiency of ATP generation.

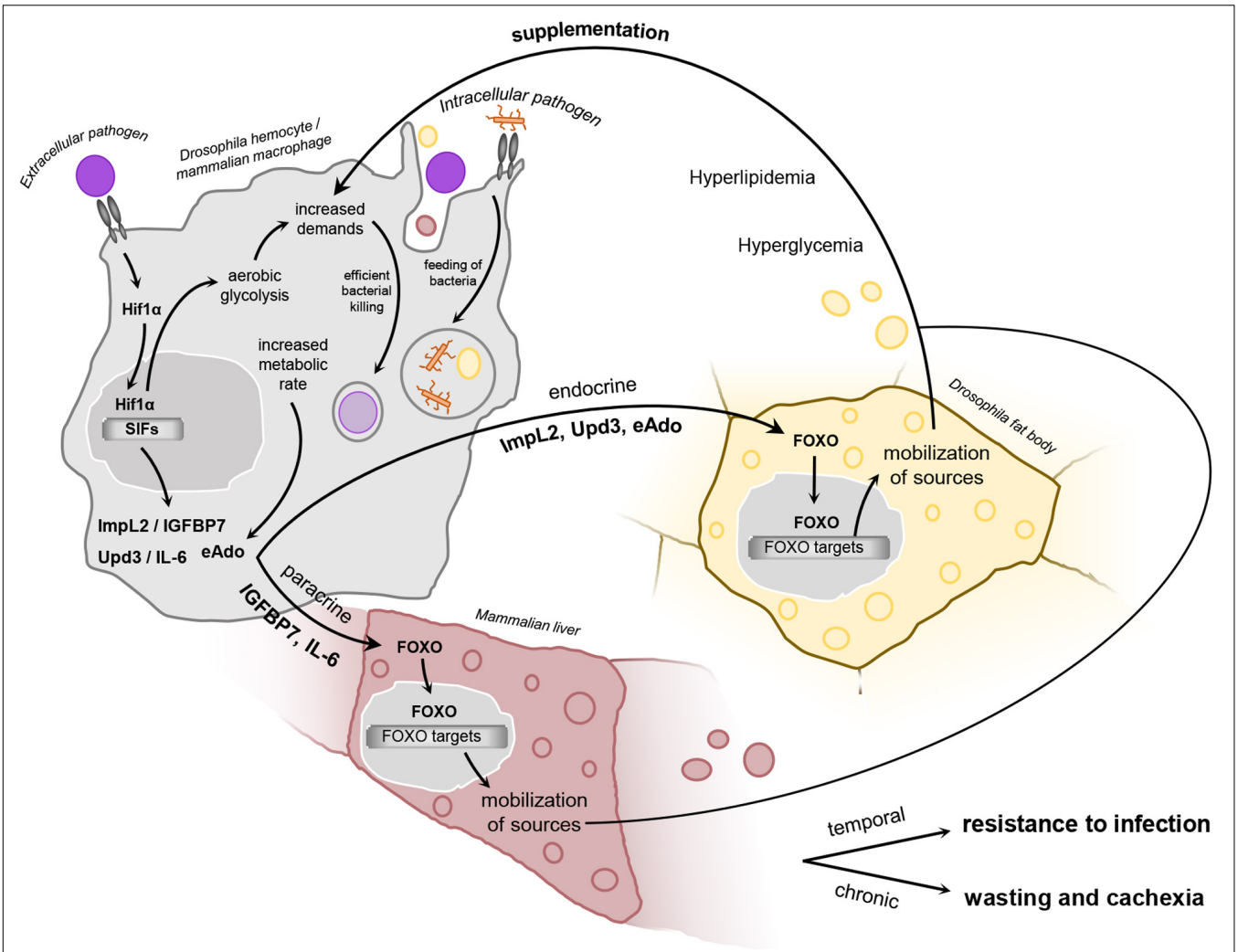

FIGURE 3 | Schematic representation of the proposed hypothetical model. In infection-activated macrophages, HIF1α stabilization leads to adoption of aerobic glycolysis, which is a highly energy demanding metabolic program. Aerobic glycolysis is interconnected with the production of selfish immune factors. These molecules affect remotely the metabolism of the main storage organs via induction of insulin resistance, leading to FOXO nuclear translocation and induction of mobilization of sources. This results in elevated titer of circulating carbohydrates and lipids, which are thus utilized by bactericidal macrophages to supplement their increased energy demands. Such inter-organ communication is essential for resistance to infection by extracellular pathogen, but may be maladaptive upon its chronic activation or in case of infection by intracellular bacteria. Hif1α, hypoxia-inducible factor 1 α; FOXO, forkhead box O; Upd3, unpaired 3; ImpL2, Imaginal morphogenesis protein late 2; IGFBP7, insulin-growth factor binding protein 7; IL-6, interleukin 6; eAdo, extracellular adenosine; SIFs, selfish immune factors.

The acceleration of glycolysis is also under the control of HIF1α, which regulates the expression of rate-limiting glycolytic enzymes *hexokinase II* and *phosphofructokinase-1* (Riddle et al., 2000; Obach et al., 2004). Pyruvate conversion into lactate, together with pentose phosphate pathway, serves as a mechanism generating sufficient amounts of NADPH to be utilized for ROS production as well as self-protection against its detrimental effects (Riganti et al., 2012).

Despite the generation of sufficient amounts of ATP by glycolysis, mitochondrial metabolism is still crucial for activated macrophages (Sancho et al., 2017). Indeed, many Krebs cycle intermediates have been shown to be essential for macrophage bactericidal function. Since HIF1α-elevated expression of *pyruvate dehydrogenase kinase* diverts the pyruvate from entering the mitochondria, there must be an alternative way for Krebs cycle supplementation. The flow of the Krebs cycle is sustained by using glutamate as an initial precursor for the synthesis of Krebs cycle intermediates. To supplement the Krebs cycle by glutamate, HIF1α increases the expression of glutamine transporters SLC1A5 and SLC38A2 (Chen et al., 2001). Since the Krebs cycle is replenished from a different direction than usual, it produces several intermediates in opposite directions and was therefore referred to as the "broken Krebs cycle" (O'Neill, 2015). Consequently, the concentration of several Krebs cycle intermediates varies substantially in the cytosol. While overproduced itaconate and fumarate are used directly to fight the pathogen extracellularly, citrate is used as a substrate for the synthesis of fatty acids and glutathione (Rouzer et al., 1982).

However, the broken Krebs cycle does not generate enough precursors to fuel the oxidative phosphorylation. The canonical function of oxidative phosphorylation is thus disabled, and cells cannot employ cellular respiration (Ramond et al., 2019). Although bactericidal macrophages generate ATP independently from oxygen, their activity is often associated with a high oxygen consumption rate (OCR) when metabolically analyzed under controlled *in vitro* conditions (Van den Bossche et al., 2015). This can be explained by the massive utilization of oxygen for the generation of reactive oxygen and nitric species (ROS/RNS) later used for bacterial killing in phagolysosomes and oxidative burst (Forman and Torres, 2002). Indeed, an expressional increase in *Nitric oxide synthase* is triggered by the transcriptional activity of HIF1α (Matrone et al., 2004). ROS are produced by the NADPH-oxidase complex as well as the reversed mitochondrial electron transport chain. Production of ROS/RNS thus depends on the utilization of ATP, NADPH, and their effective regeneration (Xu et al., 2016; Scialò et al., 2017).

A considerable amount of ROS must be generated for bacterial killing in phagolysosomes. However, with increasing concentration of ROS, also the risk of lipid peroxidation and subsequent cell death rises. Bactericidal macrophages invest many sources to cascades producing a sufficient amount of neutralizing reductive compounds. Citrate and glutamate are exploited for the generation of glutathione, which protects thus macrophages from self-harming by otherwise bactericidal ROS (Kwon et al., 2019).

Finally, yet importantly, the difference can also be seen in the utilization of lipids if comparing quiescent and bactericidal macrophages. While resting macrophages use a relatively small amount of lipids mainly as a source of energy from fatty acid oxidation, upon infection, HIF1α-induced activity of sterol regulatory element-binding proteins and peroxisome proliferator-activated receptors lead to the accumulation of fatty acids and cholesterol (Shen and Li, 2017; Mylonis et al., 2019). That may be attributed to increased uptake of lipids in the form of lipoproteins as well as a rise in lipid synthesis. Uptake of lipoproteins [via scavenger receptor CD36, very-low-density lipoprotein receptor (VLDL-R) and low-density lipoprotein receptor-related protein 1 (LRP1)] as well as their synthesis increases in a HIF1α-dependent manner (Krishnan et al., 2009; Castellano et al., 2011; Mylonis et al., 2012; Shen et al., 2012; Maier et al., 2017), which further supports the perception of HIF1α as a master-regulator of aerobic glycolysis in bactericidal macrophages. However, the involvement of this regulation upon infection has not been fully comprehended yet. Contrary, the utilization of fatty acids for energy generation via fatty acid oxidation is significantly decreased upon HIF1α stabilization (Remmerie and Scott, 2018). Even though the use of lipids by macrophages upon infection has not been fully elucidated yet, we can presume their deployment for remodeling of the cellular membrane, formation of cholesterol rafts, synthesis of catecholamines, trained immunity, as well as inflammasome activation (Bekkering et al., 2018; Remmerie and Scott, 2018).

As we depicted above, the adjustment of macrophage central metabolic pathways is fundamental for the engulfment of bacteria and its killing. However, this relationship has been omitted for a long time in insects. Nevertheless, phagocytosis and clearance of invading pathogens is an evolutionarily highly conserved process even on the molecular level and, therefore, plasmatocytes as *Drosophila* professional phagocytes (**Figure 2** and **Box 3**) should have the same requirements for energy and precursors (Stuart and Ezekowitz, 2008; Browne et al., 2013). The position of plasmatocytes in fly's body (**Figure 2A**), their morphology (**Figures 2C–G**), as well as their ability to phagocytose bacteria (**Figures 2C,E–G** and **Box 3**) and uptake LDLs (**Figure 2D**) are depicted in **Figure 2**.

Thus, we can hypothesize that basically, all professional phagocytes performing bactericidal function should undergo the switch toward aerobic glycolysis upon their activation. This notion is supported by observations made by Anderson and his colleagues, who investigated the metabolic demands of cockroach hemocytes during phagocytosis *in vitro*. They revealed that insect hemocytes are functionally dependent on uptake of glucose, glutamine, and lipids from cultivation media (Anderson et al., 1973; Ratcliffe and Rowley, 1975). That may be supported by transcriptomic data characterizing *Drosophila* immune cells with various stimuli. In larvae, both differentiating and proliferating immune cells display hallmarks of increased glycolytic rate and conversion of pyruvate to lactate resembling aerobic glycolysis (Irving et al., 2005; Johansson et al., 2005; Bajgar et al., 2015; Ramond et al., 2020). The versatility of *Drosophila* immune cells and their metabolic response to the activating stimuli may be further documented by the single-cell transcriptomic analysis published recently (Tattikota et al., 2020), which shows the above-mentioned patterns in raw data. According to these data, larval hemocytes display increased expression levels of lipid-scavenging receptors and genes for import and metabolism of lipids in the Krebs cycle. Moreover, a subpopulation of immune cells bearing lamellocyte markers displays metabolic shift toward aerobic glycolysis upon wasp infestation.

It has been proven experimentally that even adult fly plasmatocytes perform the switch to aerobic glycolysis upon streptococcal infection *in vivo* (Krejčová et al., 2019). In analogy to their mammalian counterparts, *Drosophila* plasmatocytes require the activity of HIF1α for induction of aerobic glycolysis and, in response to infection, display substantially increased glucose and lipid uptake (Krejčová et al., 2019, 2020). In concordance with that, the rate of glycolysis, as well as the production of lactate, is increased in these cells. However, the complex metabolic characterization concerning particularly mitochondrial metabolism still remains to be fully explored. In this experimental setup, plasmatocyte function is central for limiting the bacterial burden during the first 24 h post-infection. Decreased efficiency of phagocytosis and bacterial killing leads to the death of the individuals. Interestingly, the cellular metabolic switch is accompanied by an adjustment of the systemic metabolism of flies when both adoption of aerobic glycolysis by plasmatocytes and induction of hyperglycemia and hyperlipidemia are essential for resistance during the acute phase of the infection. Since adoption of aerobic glycolysis by plasmatocytes is epistatic to adjustment of systemic metabolism, we may anticipate the existence of signaling factors

mediating this interorgan crosstalk (Bajgar and Dolezal, 2018; Krejčová et al., 2019, 2020; **Figure 1** and **Box 1**).

In conclusion, the adoption of aerobic glycolysis as a metabolic program fundamental for effective bactericidal function results in increased demands for external sources. Since these sources may be depleted rapidly in the local microenvironment (Kedia-Mehta and Finlay, 2019), we suggest that one of the possible ways how to ensure resource supplementation is the release of immune cell-derived signaling factors to affect systemic metabolism (**Figure 1** and **Box 1**). The character of these signaling factors will be considered in the following paragraphs.

ADOPTION OF AEROBIC GLYCOLYSIS IS CONNECTED WITH THE RELEASE OF SYSTEMIC SIGNALING FACTORS

As described in the previous paragraphs, macrophage activation is connected with enhanced nutritional demands due to the adoption of aerobic glycolysis and a high activity of these cells. Macrophages are expected to release signaling factors to usurp enough sources from other non-immune organs and tissues. Thus, the immune response becomes a privileged physiological process above other processes in the body. However, redistribution of sources may be limiting for concurrent physiological processes based mainly on anabolic metabolism (Ganeshan et al., 2019; Kedia-Mehta and Finlay, 2019). From the perspective of inter-organ signaling, the immune system behaves selfishly in competition for energy sources and releases SIFs that mediate this signaling (**Figure 1** and **Box 1**). Based on the knowledge of insect SIFs, we may propound several hypothetical features to be met by these factors. This approach may help to identify possible novel SIFs in mammals.

Firstly, we expect the SIFs to be released by activated immune cells as a reflection of their nutritional status and adoption of HIF1α-driven aerobic glycolysis. There are two ways to translate the information about the increased demands linked to the adoption of aerobic glycolysis into the production of SIFs. SIF production may be a part of the transcriptional program associated with the metabolic switch directed by either HIF1α or other transcriptional factors involved in immune cell polarization—for example, JNK and NfKB. Thus, the remodeling of cellular metabolism of these cells and concurrent production of SIFs may be intimately interlinked. Alternatively, certain metabolites, generated as a product of some highly active metabolic pathways in aerobic glycolysis, may serve as potential SIFs as well (**Figure 3**).

Whether or not SIFs are linked to a transcriptional program or to the metabolic status of the cells, they should be released during the early phase of the acute immune response. Although it has been shown that macrophages are endowed with certain nutritional stores, they barely suffice for the initial few hours of their activation (Ma et al., 2020). This fact has been documented by many clinical data as well as experimental studies describing the progress of infection (Imran and Smith, 2007; Scott et al., 2019). Last, but not least, we should consider the potential of SIFs to spread through the body and affect systemic nutrient expenditure.

Assuming that the nutritional requirements of activated immune cells are the primary motivation for SIF release, we can look for a parallel in neoplastic tumors and hypoxic tissues, because they all use HIF1α-driven aerobic glycolysis (Escoll and Buchrieser, 2018; Miska et al., 2019; **Box 4**). Based on that presumption, we may preselect several cancer-derived cachectic factors that also occur in hypoxia. In the following paragraphs, we will address three immune signaling factors that meet the above criteria and represent the potential SIFs in *Drosophila* [extracellular adenosine (eAdo), insulin/IGF antagonist Imaginal morphogenesis protein late 2 (ImpL2), and cytokine Unpaired3 (Upd3)] (**Figure 3**).

Adenosine is a purine metabolite naturally occurring at low concentrations in all living cells. Nevertheless, its concentration

BOX 4 | Cancer and bactericidal macrophages display a similar cellular metabolic setup.

It is almost 100 years since the discovery that cancer cells preferentially employ glucose fermentation as an oxygen-independent source of ATP even when sufficiently supplied with oxygen (Warburg et al., 1927; Warburg, 1956). This metabolism was thought to be unique for cancer cells and was called the Warburg effect, named after its discoverer. Since the adoption of the Warburg effect yields eighteen times less ATP generated from one molecule of glucose compared to oxidative phosphorylation, the benefits arising from the use of such a metabolic program appeared unlikely. The adoption of the Warburg effect was thus attributed to disturbed mitochondrial function. However, this explanation cannot elucidate the similar observations made in yeasts that often use anaerobic metabolism despite the constant level of oxygen in the culture. This phenomenon is known as the Crabtree effect, which suggests an adaptive significance for such metabolic settings (de Deken, 1966; Diaz-Ruiz et al., 2011). Later research has shown that this mechanism is also utilized by other highly active or dividing cells, such as embryonic stem cells and activated bactericidal macrophages, and the term aerobic glycolysis has been introduced for this metabolic adaptation (Jones and Bianchi, 2015). This motivated scientists to find an explanation for why cells in certain situations prefer to switch to this metabolic regime and what the benefits are.

Using modern metabolomics techniques, it has been found that the lower yield of ATP is compensated by the increased glycolytic rate and that this metabolic setting represents an advantage in the production of essential precursors promoting cell growth, division, and active participation in many biological processes (Burns and Manda, 2017). As a result, these cells are dependent on an increased supply of nutrients. It is now clear that neoplastic cancer cells alter all major cellular metabolic pathways and that there is a high similarity in metabolism between cancer and bactericidal macrophages (Escoll and Buchrieser, 2018). It is generally accepted that neoplastic cancer cells represent a significant energy burden for patients compared to benign tumors of the same size. The malignancy of these tumors depends on the induction of systemic metabolic changes such as insulin resistance and cachexia (Nagao et al., 2019).

Interestingly, the pro-cachectic effect of tumors is interconnected with the adoption of HIFIα -dependent aerobic glycolysis (Koltai, 2020). It has been outlined that cancer may be perceived as a metabolic syndrome comprising cancer-induced insulin resistance and cachexia as mechanisms to usurp enough nutrition from the host's anabolic processes to support tumor growth and metastatic spreading (Porporato, 2016). In concordance with that, cachexia is thought to cause about 20% of deaths in cancer patients and accompany up to 80% of advanced cancer states (Fonseca et al., 2020). Besides metabolic profile, cancer cells also share with bactericidal macrophages the production of several pro-inflammatory cytokines with impact on systemic metabolism (Liou, 2017). Therefore, research on these factors and their involvement in the induction of insulin resistance and cachexia upon infection should be considered.

may rise substantially as a reflection of increased activation of cellular metabolism (Eltzschig, 2013). Adenosine is formed in the cells as an outcome of the enormous consumption of ATP, the increased number of methylation events, as well as generation of reductive potential (Ham and Evans, 2012; Tehlivets et al., 2013; Sarkar et al., 2020). Accumulation of intracellular adenosine serves as a negative feedback signal on cellular metabolism via AMPK activation leading to quiescence (Aymerich et al., 2006). That is contradictory to the desired tasks of an activated immune system, and immune cells thus must expel excessive adenosine extracellularly (Sag et al., 2008). Since the quantification of intracellular adenosine is technically challenging under natural physiological conditions, its production by immune cells has to be presumed from indirect evidence. Nonetheless, the processes leading to the generation of intracellular adenosine are accelerated in activated macrophages employing aerobic glycolysis (Leonard et al., 1978; Vijayan et al., 2019; Silva et al., 2020). Aside from the intracellular source of adenosine, we should not omit its generation in an extracellular space, where it may be produced by ectonucleotidases bound to the surface of the immune cells (Zanin et al., 2012). Characteristic producers of adenosine in mammals are hypoxic endothelial and smooth muscle cells, activated immune cells, as well as cancerous tissues (Grenz et al., 2011; Silva-Vilches et al., 2018; Boison and Yegutkin, 2019). Recently, it has been shown that intracellular adenosine may be released by cultured human macrophages infected by *Leishmania* (Hsu et al., 2012). It is in concordance with an observation made in *Drosophila,* in which activated immune cells release adenosine via equilibrative nucleoside transporters upon an infestation of larvae by parasitoid wasps (Bajgar et al., 2015). Extracellular production of adenosine has also been described for murine macrophages upon their classic activation by LPS (Zanin et al., 2012). Although local rise in adenosine concentration has rather anti-inflammatory effects in mammals (Haskó and Cronstein, 2013), its systemic spreading may support immune response by mobilizing required energy substrates (Tadaishi et al., 2018). As an outcome of paracrine and systemic adenosine effects, we may observe overall metabolic suppression in the organism inducing thus, e.g., fatigue or hibernation (Davis et al., 2003; Olson et al., 2013). That is analogous to the observation made in infected *Drosophila* where adenosine directs mobilization of carbohydrates from adipose tissue and concurrently limits glucose consumption by other than immune tissues (Bajgar et al., 2015; Bajgar and Dolezal, 2018). Although the release of adenosine has not yet been experimentally linked to the adoption of aerobic glycolysis in activated immune cells, it is well established that many genes involved in adenosine signaling are HIF1α targets (Bowser et al., 2017). Thus, we hypothesize that adenosine production may be directly linked to the adoption of aerobic glycolysis. This is in concordance with the observation of eAdo release from cancer cells, hypoxic tissues, as well as activated immune system (Schrader et al., 1977; Alam et al., 2015; Bajgar and Dolezal, 2018; Arab and Hadjati, 2019).

The second SIF—ImpL2—has been identified as a *Drosophila* cancer-derived cachectic factor (Kwon et al., 2015). This putative functional homolog of mammalian *insulin-like growth factor-binding protein 7* (IGFBP7) is known to be released from experimentally induced cancer cells in adult flies. ImpL2 affects the metabolism of adipose tissue via insulin resistance and induces the mobilization of nutrients subsequently exploited by the tumor for its own growth (Kwon et al., 2015; Figueroa-Clarevega and Bilder, 2015). ImpL2 is documented to be released from tumors, which growth was induced either by loss of cell polarity or overexpression of transcription coactivator *Yorkie* (Bunker et al., 2015; Kwon et al., 2015). Importantly, these tumors are known to rely metabolically on aerobic glycolysis (Wang et al., 2016).

A remarkable release of ImpL2 was also observed from tissues undergoing experimentally-induced hypoxia and mitohormesis, where its expression reflected the mitochondrial dysfunction (Allee, 2011; Owusu-Ansah et al., 2013). The link between HIF1α and ImpL2 production has been revealed by comparing ImpL2 transcript abundance in response to hypoxia for wild-type and HIF1α homozygous mutant adult flies. Moreover, experimentally increased HIF1α expression is sufficient for enhanced ImpL2 protein levels (Allee, 2011). The role of HIF1α in the regulation of ImpL2 production has been suggested for infection-activated plasmatocytes (Krejčová et al., 2020). It has been revealed that the rise in ImpL2 expression in plasmatocytes (**Figure 2E**) is dependent on HIF1α activity in these cells upon infection. Thus, HIF1α directs not only the metabolic switch to aerobic glycolysis but also ImpL2 expression. That is further supported by the occurrence of four hypoxia response elements in the regulatory sequence of the ImpL2 genomic region. We thus may claim that bactericidal plasmatocytes produce ImpL2 as a reflection of HIF1α-driven aerobic glycolysis (Krejčová et al., 2020). Interestingly, plasmatocytes produce ImpL2 not only in response to the recognition of invading pathogens but also in response to their exposure to excessive lipids, as it has been documented for high-fat-diet fed flies (Morgantini et al., 2019). Since ImpL2 is known to bind *Drosophila* insulin-like peptides, its effects on systemic metabolism can be accounted to the abrogation of insulin signaling (Honegger et al., 2008).

The last SIF discussed here is a *Drosophila* cytokine Upd3. Based on its structural and functional similarities, it is considered to be a functional homolog of mammalian cytokine IL6 (Oldefest et al., 2013). In analogy to its mammalian counterpart, Upd3 also acts as a ligand for the JAK-STAT signaling pathway. Upd3 production is crucial in the regulation of many physiological processes, ranging from embryogenesis and larval growth and development to stress response, such as in tissue damage, loss of cell polarity, metabolic stress, and bacterial infection (Jiang et al., 2009; Wang et al., 2014; Woodcock et al., 2015). Under such situations, Upd3 production is triggered by the activation of JNK by loss of cell polarity, recognition of bacterial pathogens, or increased accumulation of ROS (Jiang et al., 2009). Immune cells are one of the prominent producers of Upd3 in adult flies. In response to tissue damage, bacterial infection, or exposure to oxidized lipids, Upd3 expression rises in these cells substantially (Agaisse et al., 2003; Woodcock et al., 2015; Chakrabarti et al., 2016; Shin et al., 2020). Systemic Upd3 subsequently triggers JAK-STAT signaling in non-immune tissues and activates a stress response primarily in the gut and the fat body. While in the

gut, Upd3 induces regenerative proliferation and maintenance of integrity, in the fat body, it induces a Foxo-driven transcriptomic program, leading to a mobilization of lipid stores (Chakrabarti et al., 2016; Shin et al., 2020).

Interestingly, Upd3 production is induced under a similar condition to ImpL2. Indeed, both are produced from cancer and hypoxic cells as well as from plasmatocytes responding to bacterial infection, excessive lipids, or tissue damage (Agaisse et al., 2003; Bunker et al., 2015; Shin et al., 2020). The interconnection of Upd3 production with HIF1α transcriptional activity has been observed for hypoxia-responsive neurons in the central nervous system of *Drosophila* larvae. Upd3 released by these cells has a remote impact on insulin signaling in adipose tissue and, thus, supports the proliferation of immune cell progenitors in lymph glands (Cho et al., 2018).

From the above-mentioned, we may suggest that Upd3 production reflects a situation of cellular metabolic stress. However, the direct link between plasmatocyte aerobic glycolysis and Upd3 production has not been satisfactorily studied to date. A systemic effect of Upd3 may be attributed to the activation of a JAK-STAT cascade, which often leads to an alleviation of the insulin signaling pathway in target tissues (Yang et al., 2015; Kierdorf et al., 2020; Shin et al., 2020).

We propose that all three SIFs discussed here are produced by bactericidal immune cells due to their increased metabolic activity and the adoption of HIF1α-driven aerobic glycolysis. It is particularly interesting that the informing of metabolic demands is mediated by multiple factors involving the body's central metabolic organs. However, it seems that their cooperative action ensures the supplementation of the immune system with sources (**Figure 3**).

IMMUNE CELL-DERIVED FACTORS INDUCE MOBILIZATION AND TARGETED DELIVERY OF NUTRIENTS

The task of SIFs is to ensure sufficient supplementation of their producers with energy resources and nutrients necessary for their function.

The mechanism of resource redistribution consists of two parallel processes, the mobilization of resources from reserves and their subsequent delivery to the activated immune system. The energy suddenly required for protection against pathogen attack is usurped from anabolic processes such as the building of reserves, maintenance, growth, and reproduction. Therefore, SIFs are expected to mobilize the nutrients from central energy-storing organs and concurrently minimize their consumption by other immune response-unrelated tissues.

Since most physiological processes based on anabolism depend on the insulin signaling pathway (Schwartsburd, 2017), we can assume that the transition between insulin sensitivity and resistance may represent such a mechanism. We hypothesize here that ImpL2, Upd3, and adenosine represent examples of possible SIFs. Therefore, their impact on systemic metabolism with emphasis on the induction of insulin resistance will be considered in the following paragraphs.

Recently, it has been deciphered that ImpL2 is released from infection-activated plasmatocytes during acute immune response in *Drosophila* (Krejčová et al., 2020; **Figure 3**). However, a recently published RNA-Seq analysis of *Drosophila* larval plasmatocytes revealed neither an increase in ImpL2 transcripts upon septic injury nor enriched expression of ImpL2 in plasmatocytes (Ramond et al., 2020). That is in concordance with other observations showing that larval ImpL2 is expressed in the fat body rather than in circulating immune cells. That suggests a different role of ImpL2 in larva and adult immune system since, in adult flies, the subpopulation of plasmatocytes clearly displays a strong ImpL2 expression level, particularly of ImpL2 RA isoform (Krejčová et al., 2020). Interestingly, another single-cell analysis displays a clear subpopulation of larval plasmatocytes denoted according to a high level of ImpL2 expression as ImpL2-positive (Cattenoz et al., 2020).

Krejčová shows that ImpL2 subsequently affects the mobilization of carbohydrates and lipoproteins from the fat body, which results in their increased titer in circulation and their subsequent utilization by activated plasmatocytes (**Figure 3**). Several independent approaches document its impact on nutrient mobilization. It was shown that ImpL2 induces morphological changes in the fat body of infected individuals. The adipocytes display a significantly reduced amount of lipid stores, which are dispersed in the cytoplasm in an increased number of smaller lipid droplets. It is believed that the reduced diameter of the lipid droplets is advantageous for cells undergoing increased lipolysis since it makes the triglycerides more accessible to lipases located on their surface (Kühnlein, 2012). That is in concordance with the induction of Forkhead Box O (Foxo)-driven transcriptomic program, which triggers the expression of enzymes responsible for lipolysis and assembly and release of lipoproteins (**Figure 3**). Lipid mobilization in the form of lipoproteins is further supported by the change of relative representation of individual lipid classes in the fat body on behalf of phospholipids. Interestingly, a mere overexpression of ImpL2 in plasmatocytes is able to mimic the effects of infection in the fat body (Krejčová et al., 2020).

Foxo is known to regulate adipocyte metabolism upon metabolic stress conditions such as starvation, hypoxia, and elicitation of immune response. It has been reported that when starving or eliciting an immune response, Foxo is triggered by immune signaling cascades such as NF-κB, Toll, and IMD in the fat body (Molaei et al., 2019; Texada et al., 2019). Nevertheless, adipocyte insulin signaling has the power to counteract this nutrient-deliberating mechanism completely (Lee and Dong, 2017). Therefore, it is central for the organism to alleviate insulin signaling in these cells to induce mobilization of stores. ImpL2 is a perfect candidate for this role since it is known for its high affinity to *Drosophila insulin-like peptides* as well as experimentally administered human insulin (Honegger et al., 2008). Although the production of ImpL2 by plasmatocytes appears to be sufficient to induce changes in lipid metabolism of adipose tissue upon infection, another plasmatocyte-derived factor, Upd3, surprisingly targets the same signaling pathway in this organ (Krejčová et al., 2020; Shin et al., 2020).

There is a striking similarity between the effects accounted for ImpL2 and Upd3. Contrary to ImpL2, Upd3 affects the FOXO nuclear translocation via activation of the JAK/STAT signaling pathway in the fat body and induces insulin resistance in adipocytes downstream of insulin receptor (Shin et al., 2020). That may be accomplished via affecting the phosphorylation status of effector kinase AKT. Interestingly, also Upd3 itself can induce mobilization of lipid stores into the circulation (Woodcock et al., 2015). Redundancy of ImpL2 and Upd3 effects suggests that it is adaptive to inhibit insulin signaling in adipose tissue by multiple SIFs to secure mobilization of sources upon infection. Also eAdo affects adipose tissue metabolism in response to infection in *Drosophila*. While the effects of ImpL2 and Upd3 are manifested mainly by the mobilization of lipid stores, eAdo affects the level of expression of glycogen metabolizing enzymes through its receptor. eAdo induces hyperglycemia upon infection via depletion of adipose tissue glycogen stores (Bajgar and Dolezal, 2018). However, its effect on lipid metabolism has not been sufficiently investigated yet.

We may conclude that immune cell-derived SIFs induce adipocyte insulin resistance leading to mobilization of sources from adipose tissue and their utilization by activated immune cells (**Figure 3**).

Besides mobilization of sources, SIFs also often silence the nutrient consumption of tissues that are not involved in the immune response. Interestingly, all the SIFs discussed here are known to silence anabolic processes in these tissues in certain situations. Production of one factor by macrophages thus regulates concurrently both mobilization of sources and suppression of physiological processes competing with the immune response for resources.

The effect of ImpL2 on anabolic processes has been observed during the fly's development and upon experimental induction of cancer. An increased titer of circulating ImpL2 alleviated insulin signaling and thus decreased metabolic muscle rate and caused fragmentation of muscle mitochondria (Figueroa-Clarevega and Bilder, 2015; Kwon et al., 2015; Lee et al., 2018). In addition, these individuals displayed disrupted ovary maturation and mobilization of sources leading to wasting-induced cachexia (Figueroa-Clarevega and Bilder, 2015; Kwon et al., 2015). We can hypothesize that plasmatocyte-derived ImpL2 may have similar effects upon infection, although not with as significant phenotypes as in cancer because upregulation of the ImpL2 gene in these experimental systems resulted in concentrations far beyond those occurring naturally.

Also, the effects of Upd3 on muscle metabolism have been investigated. Plasmatocyte-derived Upd3 has been shown to limit remote lipid accumulation in muscles to maintain lipid homeostasis in the tissue via alleviation of insulin signaling in these cells through activation of the JAK-STAT singling pathway, which is documented by decreased pAKT occurrence (Kierdorf et al., 2020). We suggest that such a mechanism may also be involved in the regulation of muscle lipid uptake upon infection, during which Upd3 expression in plasmatocytes is markedly elevated (Péan et al., 2017). A similar mechanism may be observed in larvae infested by wasp parasitoids, in which Upd3-induced JAK-STAT signaling in muscles is essential for an effective immune response (Yang et al., 2015). This may indicate that muscle insulin resistance is essential to effectively combat wasp parasitic infestation. However, in their follow-up study, Yang and Hultmark (2017) showed that insulin signaling in muscles, in contrast to fat body and plasmatocytes, is essential for the effective encapsulation of invaders. Muscle-specific knockdown of insulin receptor resulted in reduced resistance to infection and encapsulation rate. However, these effects can be explained by developmental defects caused by changes in feeding behavior and subsequent malnutrition, as this experimental treatment was induced throughout the life of individuals. Nonetheless, this publication nicely depicts the impact of experimentally induced muscle insulin resistance on systemic carbohydrate metabolism.

The impact of eAdo on decreased energy consumption by non-immune tissues has also been described in *Drosophila* larva upon wasp infestation. eAdo released by activated immune cells silences consumption of C^{14}-labeled glucose by virtually all non-immune tissues, leading to decreased growth of imaginal wing discs and delayed metamorphosis. Consequently, this mechanism allows the glucose uptake by immune cells to be increased up to threefold. These effects were mediated by eAdo activation of the adenosine receptors in target tissues (Bajgar et al., 2015).

Based on the aforementioned data, we may say that the effects of macrophage-derived SIFs are dual. They induce nutrient mobilization from central storage organs and concurrently limit their consumption by non-immune tissues and physiological processes. While these effects are essential for the acute-phase response to infection, they may cause nutrient waste and cachexia if activated chronically (**Figure 3**).

IMMUNE CELL-MEDIATED METABOLIC CHANGES ARE NOT ALWAYS BENEFICIAL UPON INFECTION

Immune cell-derived SIFs increase the titer of circulating carbohydrates and lipids, which are then available to be exploited by the immune system. Subsequently, these nutrients are utilized by activate phagocytes to feed the suddenly increased energy and nutritional demands. Thus, we may presume that this signaling is important for resistance to infection.

Indeed, experimental knockdown of ImpL2 and Upd3 in infection-activated plasmatocytes or systemic abrogation of adenosine signaling pathway leads to the reduced ability of plasmatocytes to fight the pathogens. That manifests in decreased resistance to bacterial infection accompanied by elevated pathogen load in these individuals (Agaisse et al., 2003; Bajgar and Dolezal, 2018; Krejčová et al., 2020). Further studies suggested that such a decrease in resistance to infection is due to reduced availability of nutrients for immune cells. Notably, a mere twofold increase in glucose concentration in fly diet is sufficient to rescue phenotypes caused by a lack of eAdo signaling (Bajgar et al., 2015).

Although SIF signaling is essential for an adequate immune response to acute bacterial infection, it may become maladaptive under certain conditions. Since SIFs mobilize sources primarily

for the needs of phagocytes, they may be exploited by the bacteria growing intracellularly. It is well documented that many intracellular pathogens affect the metabolic profile of macrophages to be literarily nourished by the host cell (Teng et al., 2017). Indeed, it has been described for each of the SIFs discussed here that their effects have become maladaptive upon infection with intracellular pathogens such as *Listeria monocytogenes* or *Mycobacterium tuberculosis* (Péan et al., 2017; Bajgar and Dolezal, 2018; Krejčová et al., 2020).

Not only the type of bacterial threat but also the duration of SIF action seems to be central. Prolonged SIF production leads to uncontrolled wasting of nutrients, cachexia, and irreversible damage of tissues silenced by insulin resistance. Indeed, for instance, the production of eAdo by plasmatocytes has to be time-restricted by eAdo degrading enzyme Adenosine deaminase-related growth factor A (Adgf-A). Interestingly, this enzyme is produced by plasmatocytes as well, with an 8 h delay after adenosine. Lack of adgf-A function leads to wasting of glycogen stores and slow-down of development (Bajgar and Dolezal, 2018).

Also, the ImpL2 production by plasmatocytes must be time-restricted. Chronically increased ImpL2 production by plasmatocytes leads to developmental malformations, reduced body size of the individual, and excessive melanization of immune cells (Krejčová et al., 2020). Moreover, the overproduction of ImpL2 causes insulin resistance and cachexia in the *Drosophila* cancer model (Figueroa-Clarevega and Bilder, 2015; Kwon et al., 2015).

Although eAdo, ImpL2, and Upd3 meet the criteria of a selfish immune factor released by the *Drosophila* plasmatocytes, analogous signaling in mammals remains controversial. However, all of these factors have their signaling counterparts in mammals. While the Upd3 functional homolog has been identified as IL6, studied mostly for its signaling and metabolic effects in immune response, the ImpL2 mammalian putative functional homolog IGFBP7, known for its ability to attenuate insulin signaling, has not yet been explored in the context of infection. Therefore, we speculate about the evolutionary conservation of the role of these SIFs in the following paragraphs.

THE FUNCTION OF IMMUNE CELL-DERIVED SIFS MAY BE CONSERVED BETWEEN INSECTS AND MAMMALS

Experimental studies performed on insects demonstrate that plasmatocytes release signaling factors to affect systemic metabolism and thus ensure a sufficient supply of resources. Here, we would like to consider the possibility that such a mechanism is also valid for mammals (**Figure 3**). The connection between aerobic glycolysis in activated phagocytic immune cells and the adjustment of systemic metabolism has been considered for mammals in recent review based mainly on clinical data of chronically ill patients (van Niekerk et al., 2017). Moreover, it may represent the essence of many human diseases, as will be discussed later.

A plethora of cytokines and chemokines are released from activated immune cells upon the adoption of a bactericidal polarization state. These are generally known as "pro-inflammatory cytokines" due to their potential to guide other myeloid cells toward inflammatory polarization. Here, we suggest their role in the regulation of systemic metabolism via the induction of insulin resistance upon bacterial infection.

From several experimental and clinical studies, it is clear that macrophage production of pro-inflammatory cytokines is associated with HIF1α transcriptional activity and subsequent metabolic rearrangement toward aerobic glycolysis (Palazon et al., 2014; Corcoran and O'Neill, 2016). However, it is difficult to distinguish whether their production reflects either cellular metabolic switch or adopted pro-inflammatory state since both are intimately interconnected (Diskin and Pålsson-McDermott, 2018). To solve this problem, we must focus on the production of cytokines by cells utilizing HIF1α-mediated aerobic glycolysis in non-inflammatory context, such as neoplastic tumors and hypoxic tissues (He et al., 2014; Edwardson et al., 2017).

There is a compelling list of publications describing the release of pro-inflammatory cytokines from cancer and hypoxic tissues (Dinarello, 2006; Peyssonnaux et al., 2007; Popa et al., 2007; Heikkilä et al., 2008; Xing and Lu, 2016; Lewis and Elks, 2019; Kammerer et al., 2020). Recently, a transcriptomic meta-analysis of human cancers varying in degree of their pro-cachectic potential has been performed to identify new cachectic factors (Freire et al., 2020). Many of the identified factors were cytokines and chemokines well-known for their participation in the acute immune response. That is in concordance with other studies documenting the pro-cachectic features of Il1β, TNFα, and Il6 (Zhang et al., 2007; Narsale and Carson, 2014; Patel and Patel, 2017).

Consistent with this hypothesis, hypoxic tissues also release a number of cytokines with pro-cachectic properties. Surprisingly, the elicitation of hypoxic response employs several immune-related signaling pathways such as JNK, NF-κB, and Hif1α (Jin et al., 2000; D'Ignazio and Rocha, 2016). Their activation leads to the adjustment of cellular metabolism to overcome periods of mitochondrial dysfunction. Although pro-inflammatory cytokines were originally investigated in the context of LSP-induced sepsis (Pizarro and Cominelli, 2007; Rossol et al., 2011), they also reflect the metabolic status and nutritional requirements of their producers and thus serve as potential regulators of systemic metabolism.

According to the proposed theory, the central mechanism that changes the systemic metabolism from anabolism to catabolism is the induction of insulin resistance. In adipose tissue, the lack of insulin signaling serves as a signal for potentiation of lipolysis and subsequent fatty acid mobilization (Langin, 2013). Therefore, infection-induced lipodystrophy results in a substantial release of lipid stores during the acute phase of the immune response. Deliberated fatty acids are further metabolized in the liver and enwrapped into lipoproteins as a lipid form suitable for transport to distant tissues on the periphery (Perry et al., 2014). The liver is

known to respond differently to a lack of insulin signaling from most tissues in the body, which is called the "liver insulin resistance paradox " (Santoleri and Titchenell, 2019). Indeed, contrary to other tissues silenced by a lack of insulin signal, hepatic insulin resistance accelerates lipid synthesis, gluconeogenesis, and absorption of circulating amino acids (Biddinger et al., 2008). All of these metabolic changes lead to increased mobilization of lipoproteins and glucose into circulation, resulting in the development of hyperglycemia and hyperlipidemia (Lewis et al., 2002). It is known that stress-related hyperglycemia, as a result of insulin resistance in critically ill and septic patients, is beneficial under certain conditions. In the acute phase of stress response, hyperglycemia appears to support metabolically stressed tissues and immune cell function, whereas in context of its chronic activation, it may result in development of glucotoxicity, exaggerated glycosylation, and chronic inflammation. The function of mammalian immune cells is affected by insulin signaling with different context-dependent effects (Van den Berghe, 2002; Marik and Bellomo, 2013; van Niekerk et al., 2017).

An opposite effect of insulin resistance can be observed in muscles, where a lack of insulin signal leads to a significant reduction of its metabolic rate and induction of autophagy (Lim et al., 2014; Ryter et al., 2014). Autophagy covers basal nutritional demands of silenced cells and concurrently generates amino acids utilized for gluconeogenesis in hepatocytes (Cui et al., 2019). In line with the energy-saving program, insulin resistance in the brain also significantly reduces its energy consumption, leading to a lower intellectual capacity, bad moods, and depressions (Kullmann et al., 2020). Nevertheless, metabolic adaptation to metabolic stress is a tremendously complex process in mammals, which is affected by many hormonal and signaling cues. Particularly effect of several stress-related hormones, such as cortisol, noradrenaline, or norepinephrine on the mobilization of nutrients from adipose tissue and the liver is well established. In this context, the role of immune cell-derived factors on these signaling pathways should also be considered.

Besides the systemic impact on insulin resistance, we should also take into account the paracrine effects of cytokines in the liver. The liver is the central metabolic organ that coordinates the systemic metabolic changes upon infection (Bernal, 2016). In addition, the liver hosts a specialized population of tissue-resident macrophages known as Kupffer cells (KC). KCs serve as sentinel cells reflecting changes in the titers of metabolites and endotoxins in the blood. Although KCs tolerate some levels of endotoxins being permanently present in the circulation without eliciting an immune response, their increase above a certain limit leads to KC activation (Zeng et al., 2016). KCs recognize endotoxins via TLR4, which in turn leads to the activation of NF-κB and its classical M1 polarization (Gandhi, 2020). This process is accompanied by the stabilization of HIF1α and the adoption of aerobic glycolysis (Roth and Copple, 2015). Subsequently, KCs release the pro-inflammatory cytokines Il1β, TNFα, and IL6 into the extracellular space. Consequently, these signaling factors induce hepatocyte insulin resistance via their paracrine signaling (Bartolomé et al., 2008). The lack of insulin signaling in hepatocytes leads to a nuclear translocation of the transcription factor FOXO and the subsequent induction of its specific transcriptomic program. FOXO increases the expression of genes involved in lipogenesis and glycogenolysis, as well as the production and release of lipoproteins (Puigserver et al., 2003). This mechanism is strikingly reminiscent of the process observed in insect adipose tissue. Although the role of KC-derived IL1β, Il6, and TNFα in inducing hepatocyte insulin resistance has been reliably demonstrated, their mere administration cannot fully mimic the effects of KCs (Bartolomé et al., 2008). This suggests the involvement of additional KC-derived signaling factors. IGFBP7, a mammalian putative functional homolog of *Drosophila* ImpL2, may be a potential candidate (**Figure 3**).

It has been shown that IGFBP7 expression increases fourfold in the culture of human THP-1 macrophages in response to their exposure to *Streptococcus pneumoniae* (Krejčová et al., 2020). In addition, IGFBP7 expression increases sixfold in response to the exposure of KCs to excessive lipids in obese mice. Subsequently, IGFBP7 induces hepatocyte insulin resistance, hyperlipidemia, and hyperglycemia prior to the production of KC-derived pro-inflammatory cytokines (Morgantini et al., 2019). Although the experimental data connecting the adoption of aerobic glycolysis by KCs to the production of IGFBP7 are missing, we suggest that this mechanism may be relevant for the mobilization of nutrients for immune cells, upon infection. The role of IGFBP7 and IL6 in the induction of insulin resistance and cachexia is further supported by their increased plasma titer in patients suffering from diseases often accompanied by cachexia, such as morbid obesity, cancer, chronic obstructive pulmonary disease, acute kidney diseases, and liver fibrosis (Liu et al., 2015; Gunnerson et al., 2016; Ruan et al., 2017; Martínez-Castillo et al., 2020). Although nowadays IGFBP7 is associated with diseases accompanied by chronic inflammatory and pathological conditions, we suggest that its beneficial role in nutrient mobilization during an acute immune response should also be considered (**Figure 3**).

SUMMARY

This review brings the new perspective that systemic insulin resistance represents an essential mechanism for overcoming the acute phase of bacterial infection. Insulin resistance is induced by immune cell-derived cytokines, which are produced as a reflection of their elevated metabolic demands resulting from the adoption of aerobic glycolysis. These cytokines induce both the mobilization of sources from the storage organs and their suppressed consumption by non-immune tissues. Titers of nutrients thus elevate in circulation to be utilized by the activated immune system. While such metabolic adaptation is fundamental for resistance to extracellular pathogens, it may become maladaptive upon infection by intracellular bacteria exploiting phagocyte cellular stores for its own benefits. Although cytokine-induced insulin resistance is beneficial during acute phase response, its chronic activation may progress into the wasting of nutrients and cachexia (**Figure 3**), which are severe metabolic disorders accompanying several serious diseases. Understanding

the adaptive significance of cytokine-induced insulin resistance may therefore provide new insights into these maladies.

Induction of insulin resistance in hepatocytes is central for the progress of obesity and obesity-associated diseases, such as non-alcoholic steatohepatitis, atherosclerosis, and diabetes. According to the presented hypothesis, liver and systemic insulin resistance are induced by chronically adopted aerobic glycolysis in activated liver macrophages. Reversal of macrophage metabolic switch may thus represent a powerful therapeutic strategy.

AUTHOR CONTRIBUTIONS

AB, GK, and TD discussed the topic, conceptualized, wrote, and revised the manuscript. GK created the figures. AB and GK captured the microscopy images. All authors contributed to the article and approved the submitted version.

FUNDING

The authors confirm funding from the Grant Agency of the Czech Republic AB (Project 20-14030S; www.gacr.cz) and TD (Project 20-09103S; www.gacr.cz).

ACKNOWLEDGMENTS

We would like to thank Lucie Hrádková, Pavla Nedbalová, Marcela Jungwirthová, and other members of our laboratory for stimulating discussions and eternal support for our work. We thank Hanka Sehadová and Lucie Pauchová for introducing us to the fascinating world of electron microscopy. We appreciate Rebecca Collier for her enthusiasm and positive mood, which helped us overcome difficult moments in the preparation of the manuscript.

REFERENCES

Agaisse, H., Petersen, U.-M., Boutros, M., Mathey-Prevot, B., and Perrimon, N. (2003). Signaling role of hemocytes in *Drosophila* JAK/STAT-dependent response to septic injury. *Dev. Cell* 5, 441–450. doi: 10.1016/S1534-5807(03)00244-2

Alam, M., Costales, M., Cavanaugh, C., and Williams, K. (2015). Extracellular adenosine generation in the regulation of pro-inflammatory responses and pathogen colonization. *Biomolecules* 5, 775–792. doi: 10.3390/biom5020775

Allee, J. P. (2011). *ImpL2 Represses Insulin Signaling in Response to Hypoxia*, Thesis, University of Oregon, Eugene, OR.

Almajwal, A., Alam, I., Zeb, F., and Fatima, S. (2019). Energy metabolism and allocation in selfish immune system and brain: a beneficial role of insulin resistance in aging. *Food Nutr. Sci.* 10, 64–80. doi: 10.4236/fns.2019.101006

Álvarez-Rendón, J. P., Salceda, R., and Riesgo-Escovar, J. R. (2018). *Drosophila melanogaster* as a model for diabetes type 2 progression. *Biomed Res. Int.* 2018, 1–16. doi: 10.1155/2018/1417528

Anderson, R. S., Holmes, B., and Good, R. A. (1973). Comparative biochemistry of phagocytizing insect hemocytes. *Comp. Biochem. Physiol. Part B Comp. Biochem.* 46, 595–602. doi: 10.1016/0305-0491(73)90099-0

Arab, S., and Hadjati, J. (2019). Adenosine blockage in tumor microenvironment and improvement of cancer immunotherapy. *Immune Netw.* 19:e23. doi: 10.4110/in.2019.19.e23

Aymerich, I., Foufelle, F., Ferré, P., Casado, F. J., and Pastor-Anglada, M. (2006). Extracellular adenosine activates AMP-dependent protein kinase (AMPK). *J. Cell Sci.* 119, 1612–1621. doi: 10.1242/jcs.02865

Bailey, P., and Nathan, J. (2018). Metabolic regulation of hypoxia-inducible transcription factors: the role of small molecule metabolites and iron. *Biomedicines* 6:60. doi: 10.3390/biomedicines6020060

Bajgar, A., and Dolezal, T. (2018). Extracellular adenosine modulates host-pathogen interactions through regulation of systemic metabolism during immune response in *Drosophila*. *PLoS Pathog.* 14:e1007022. doi: 10.1371/journal.ppat.1007022

Bajgar, A., Kucerova, K., Jonatova, L., Tomcala, A., Schneedorferova, I., Okrouhlik, J., et al. (2015). Extracellular adenosine mediates a systemic metabolic switch during immune response. *PLoS Biol.* 13:e1002135. doi: 10.1371/journal.pbio.1002135

Banerjee, U., Girard, J. R., Goins, L. M., and Spratford, C. M. (2019). *Drosophila* as a genetic model for hematopoiesis. *Genetics* 211, 367–417. doi: 10.1534/genetics.118.300223

Bartolomé, N., Arteta, B., Martínez, M. J., Chico, Y., and Ochoa, B. (2008). Kupffer cell products and interleukin 1? directly promote VLDL secretion and apoB mRNA up-regulation in rodent hepatocytes. *Innate Immun.* 14, 255–266. doi: 10.1177/1753425908094718

Bekkering, S., Arts, R. J. W., Novakovic, B., Kourtzelis, I., van der Heijden, C. D. C. C., Li, Y., et al. (2018). Metabolic induction of trained immunity through the mevalonate pathway. *Cell* 172, 135–146.e9. doi: 10.1016/j.cell.2017.11.025

Bellucci, P. N., González Bagnes, M. F., Di Girolamo, G., and González, C. D. (2017). Potential effects of nonsteroidal anti-inflammatory drugs in the prevention and treatment of type 2 diabetes mellitus. *J. Pharm. Pract.* 30, 549–556. doi: 10.1177/0897190016649551

Benoit, M., Desnues, B., and Mege, J.-L. (2008). Macrophage polarization in bacterial infections. *J. Immunol.* 181, 3733–3739. doi: 10.4049/jimmunol.181.6.3733

Bernal, W. (2016). The liver in systemic disease: sepsis and critical illness. *Clin. Liver Dis.* 7, 88–91. doi: 10.1002/cld.543

Biddinger, S. B., Hernandez-Ono, A., Rask-Madsen, C., Haas, J. T., Alemán, J. O., Suzuki, R., et al. (2008). Hepatic insulin resistance is sufficient to produce dyslipidemia and susceptibility to Atherosclerosis. *Cell Metab.* 7, 125–134. doi: 10.1016/j.cmet.2007.11.013

Bobryshev, Y. V., Ivanova, E. A., Chistiakov, D. A., Nikiforov, N. G., and Orekhov, A. N. (2016). Macrophages and their role in atherosclerosis: pathophysiology and transcriptome analysis. *Biomed Res. Int.* 2016, 1–13. doi: 10.1155/2016/9582430

Boison, D., and Yegutkin, G. G. (2019). Adenosine metabolism: emerging concepts for cancer therapy. *Cancer Cell* 36, 582–596. doi: 10.1016/j.ccell.2019.10.007

Bowser, J. L., Lee, J. W., Yuan, X., and Eltzschig, H. K. (2017). The hypoxia-adenosine link during inflammation. *J. Appl. Physiol.* 123, 1303–1320. doi: 10.1152/japplphysiol.00101.2017

Browne, N., Heelan, M., and Kavanagh, K. (2013). An analysis of the structural and functional similarities of insect hemocytes and mammalian phagocytes. *Virulence* 4, 597–603. doi: 10.4161/viru.25906

Bunker, B. D., Nellimoottil, T. T., Boileau, R. M., Classen, A. K., and Bilder, D. (2015). The transcriptional response to tumorigenic polarity loss in *Drosophila*. *eLife* 4:e03189. doi: 10.7554/eLife.03189

Burns, J., and Manda, G. (2017). Metabolic pathways of the warburg effect in health and disease: perspectives of choice, chain or chance. *Int. J. Mol. Sci.* 18:2755. doi: 10.3390/ijms18122755

Castellano, J., Aledo, R., Sendra, J., Costales, P., Juan-Babot, O., Badimon, L., et al. (2011). Hypoxia stimulates low-density lipoprotein receptor-related protein-1 expression through hypoxia-inducible factor-1α in human vascular smooth muscle cells. *Arterioscler. Thromb. Vasc. Biol.* 31, 1411–1420. doi: 10.1161/ATVBAHA.111.225490

Castoldi, A., Naffah de Souza, C., Câmara, N. O. S., and Moraes-Vieira, P. M. (2016). The macrophage switch in obesity development. *Front. Immunol.* 6:637. doi: 10.3389/fimmu.2015.00637

Cattenoz, P. B., Sakr, R., Pavlidaki, A., Delaporte, C., Riba, A., Molina, N., et al. (2020). Temporal specificity and heterogeneity of *Drosophila* immune cells. *EMBO J.* 39:e104486. doi: 10.15252/embj.2020104486

Chakrabarti, S., Dudzic, J. P., Li, X., Collas, E. J., Boquete, J.-P., and Lemaitre, B. (2016). Remote control of intestinal stem cell activity by haemocytes in *Drosophila*. *PLoS Genet.* 12:e1006089. doi: 10.1371/journal.pgen.1006089

Chen, C., Pore, N., Behrooz, A., Ismail-Beigi, F., and Maity, A. (2001). Regulation of glut1 mRNA by Hypoxia-inducible Factor-1. *J. Biol. Chem.* 276, 9519–9525. doi: 10.1074/jbc.M010144200

Cheng, L., Baonza, A., and Grifoni, D. (2018). *Drosophila* models of human disease. *Biomed. Res. Int.* 2018:7214974. doi: 10.1155/2018/7214974

Cho, B., Spratford, C. M., Yoon, S., Cha, N., Banerjee, U., and Shim, J. (2018). Systemic control of immune cell development by integrated carbon dioxide and hypoxia chemosensation in *Drosophila*. *Nat. Commun.* 9:2679. doi: 10.1038/s41467-018-04990-3

Cho, Y.-R., Ann, S. H., Won, K.-B., Park, G.-M., Kim, Y.-G., Yang, D. H., et al. (2019). Association between insulin resistance, hyperglycemia, and coronary artery disease according to the presence of diabetes. *Sci. Rep.* 9:6129. doi: 10.1038/s41598-019-42700-1

Corcoran, S. E., and O'Neill, L. A. J. (2016). HIF1α and metabolic reprogramming in inflammation. *J. Clin. Invest.* 126, 3699–3707. doi: 10.1172/JCI84431

Cui, P., Shao, W., Huang, C., Wu, C.-J., Jiang, B., and Lin, D. (2019). Metabolic derangements of skeletal muscle from a murine model of glioma cachexia. *Skelet. Muscle* 9:3. doi: 10.1186/s13395-018-0188-4

Davis, J. M., Zhao, Z., Stock, H. S., Mehl, K. A., Buggy, J., and Hand, G. A. (2003). Central nervous system effects of caffeine and adenosine on fatigue. *Am. J. Physiol. Integr. Comp. Physiol.* 284, R399–R404. doi: 10.1152/ajpregu.00386.2002

de Deken, R. H. (1966). The crabtree effect: a regulatory system in yeast. *J. Gen. Microbiol.* 44, 149–156. doi: 10.1099/00221287-44-2-149

De Gregorio, E. (2002). The Toll and Imd pathways are the major regulators of the immune response in *Drosophila*. *EMBO J.* 21, 2568–2579. doi: 10.1093/emboj/21.11.2568

de Luca, C., and Olefsky, J. M. (2008). Inflammation and insulin resistance. *FEBS Lett.* 582, 97–105. doi: 10.1016/j.febslet.2007.11.057

Del Fabbro, E., Hui, D., Dalal, S., Dev, R., Nooruddin, Z. I., and Bruera, E. (2011). Clinical outcomes and contributors to weight loss in a cancer Cachexia clinic. *J. Palliat. Med.* 14, 1004–1008. doi: 10.1089/jpm.2011.0098

Demas, G. E. (2004). The energetics of immunity: a neuroendocrine link between energy balance and immune function. *Horm. Behav.* 45, 173–180. doi: 10.1016/j.yhbeh.2003.11.002

Dengler, V. L., Galbraith, M. D., and Espinosa, J. M. (2014). Transcriptional regulation by hypoxia inducible factors. *Crit. Rev. Biochem. Mol. Biol.* 49, 1–15. doi: 10.3109/10409238.2013.838205

Diaz-Ruiz, R., Rigoulet, M., and Devin, A. (2011). The Warburg and Crabtree effects: on the origin of cancer cell energy metabolism and of yeast glucose repression. *Biochim. Biophys. Acta – Bioenerg.* 1807, 568–576. doi: 10.1016/j.bbabio.2010.08.010

D'Ignazio, L., and Rocha, S. (2016). Hypoxia induced NF-κB. *Cells* 5:10. doi: 10.3390/cells5010010

Dinarello, C. A. (2006). The paradox of pro-inflammatory cytokines in cancer. *Cancer Metast. Rev.* 25, 307–313. doi: 10.1007/s10555-006-9000-8

Diskin, C., and Pålsson-McDermott, E. M. (2018). Metabolic modulation in macrophage effector function. *Front. Immunol.* 9:270. doi: 10.3389/fimmu.2018.00270

Dodson, M., Castro-Portuguez, R., and Zhang, D. D. (2019). NRF2 plays a critical role in mitigating lipid peroxidation and ferroptosis. *Redox Biol.* 23, 101107. doi: 10.1016/j.redox.2019.101107

Dolezal, T. (2015). Adenosine: a selfish-immunity signal? *Oncotarget* 6, 32307–32308. doi: 10.18632/oncotarget.4685

Dolezal, T., Krejcova, G., Bajgar, A., Nedbalova, P., and Strasser, P. (2019). Molecular regulations of metabolism during immune response in insects. *Insect Biochem. Mol. Biol.* 109, 31–42. doi: 10.1016/j.ibmb.2019.04.005

Duffy, J. B. (2002). GAL4 system in *drosophila*: a fly geneticist's swiss army knife. *Genesis* 34, 1–15. doi: 10.1002/gene.10150

Edholm, E.-S., Rhoo, K. H., and Robert, J. (2017). "Evolutionary aspects of macrophages polarization," in *Macrophages. Results and Problems in Cell Differentiation*, Vol. 62, ed. M. Kloc (Cham: Springer), 3–22. doi: 10.1007/978-3-319-54090-0_1

Edwardson, D. W., Boudreau, J., Mapletoft, J., Lanner, C., Kovala, A. T., and Parissenti, A. M. (2017). Inflammatory cytokine production in tumor cells upon chemotherapy drug exposure or upon selection for drug resistance. *PLoS One* 12:e0183662. doi: 10.1371/journal.pone.0183662

Eltzschig, H. K. (2013). Extracellular adenosine signaling in molecular medicine. *J. Mol. Med.* 91, 141–146. doi: 10.1007/s00109-013-0999-z

Erridge, C. (2010). Endogenous ligands of TLR2 and TLR4: agonists or assistants? *J. Leukoc. Biol.* 87, 989–999. doi: 10.1189/jlb.1209775

Escoll, P., and Buchrieser, C. (2018). Metabolic reprogramming of host cells upon bacterial infection: why shift to a Warburg-like metabolism? *FEBS J.* 285, 2146–2160. doi: 10.1111/febs.14446

Felig, P., Marliss, E., and Cahill, G. F. (1969). Plasma amino acid levels and insulin secretion in obesity. *N. Engl. J. Med.* 281, 811–816. doi: 10.1056/NEJM196910092811503

Ferrandon, D., Imler, J. -L., Hetru, C., and Hoffmann, J. A. (2007). The *Drosophila* systemic immune response: sensing and signalling during bacterial and fungal infections. *Nat. Rev. Immunol.* 7, 862–874. doi: 10.1038/nri2194

Figueroa-Clarevega, A., and Bilder, D. (2015). Malignant *Drosophila* tumors interrupt insulin signaling to induce Cachexia-like wasting. *Dev. Cell* 33, 47–55. doi: 10.1016/j.devcel.2015.03.001

Firth, J. D., Ebert, B. L., and Ratcliffe, P. J. (1995). Hypoxic regulation of lactate Dehydrogenase A. *J. Biol. Chem.* 270, 21021–21027. doi: 10.1074/jbc.270.36.21021

Fonseca, G. W. P., da Farkas, J., Dora, E., von Haehling, S., and Lainscak, M. (2020). Cancer cachexia and related metabolic dysfunction. *Int. J. Mol. Sci.* 21:2321. doi: 10.3390/ijms21072321

Forman, H. J., and Torres, M. (2002). Reactive oxygen species and cell signaling. *Am. J. Respir. Crit. Care Med.* 166, S4–S8. doi: 10.1164/rccm.2206007

Franken, L., Schiwon, M., and Kurts, C. (2016). Macrophages: sentinels and regulators of the immune system. *Cell. Microbiol.* 18, 475–487. doi: 10.1111/cmi.12580

Freire, P. P., Fernandez, G. J., Moraes, D., Cury, S. S., Dal Pai-Silva, M., Reis, P. P., et al. (2020). The expression landscape of cachexia-inducing factors in human cancers. *J. Cachexia. Sarcopen. Muscle* 11, 947–961. doi: 10.1002/jcsm.12565

Galván-peña, S., and O'Neill, L. A. J. (2014). Metabolic reprograming in macrophage polarization. *Front. Immunol.* 5:420. doi: 10.3389/fimmu.2014.00420

Gandhi, C. R. (2020). Pro- and anti-fibrogenic functions of gram-negative bacterial Lipopolysaccharide in the liver. *Front. Med.* 7:130. doi: 10.3389/fmed.2020.00130

Ganeshan, K., Nikkanen, J., Man, K., Leong, Y. A., Sogawa, Y., Maschek, J. A., et al. (2019). Energetic trade-offs and hypometabolic states promote disease tolerance. *Cell* 177, 399–413.e12. doi: 10.1016/j.cell.2019.01.050

Gao, L., Mejıìas, R., Echevarrıìa, M., and López-Barneo, J. (2004). Induction of the glucose-6-phosphate dehydrogenase gene expression by chronic hypoxia in PC12 cells. *FEBS Lett.* 569, 256–260. doi: 10.1016/j.febslet.2004.06.004

Garedew, A., and Moncada, S. (2008). Mitochondrial dysfunction and HIF1 stabilization in inflammation. *J. Cell Sci.* 121, 3468–3475. doi: 10.1242/jcs.034660

Gibson, M. S., Domingues, N., and Vieira, O. V. (2018). Lipid and non-lipid factors affecting macrophage dysfunction and inflammation in atherosclerosis. *Front. Physiol.* 9:654. doi: 10.3389/fphys.2018.00654

Gordon, S., and Martinez-Pomares, L. (2017). Physiological roles of macrophages. *Pflügers Arch. Eur. J. Physiol.* 469, 365–374. doi: 10.1007/s00424-017-1945-7

Grenz, A., Homann, D., and Eltzschig, H. K. (2011). Extracellular adenosine: a safety signal that dampens hypoxia-induced inflammation during ischemia. *Antioxid. Redox Signal.* 15, 2221–2234. doi: 10.1089/ars.2010.3665

Gunnerson, K. J., Shaw, A. D., Chawla, L. S., Bihorac, A., Al-Khafaji, A., Kashani, K., et al. (2016). TIMP2●IGFBP7 biomarker panel accurately predicts acute kidney injury in high-risk surgical patients. *J. Trauma Acute Care Surg.* 80, 243–249. doi: 10.1097/TA.0000000000000912

Ham, J., and Evans, B. A. J. (2012). An emerging role for adenosine and its receptors in bone homeostasis. *Front. Endocrinol.* 3:113. doi: 10.3389/fendo.2012.00113

Haskó, G., and Cronstein, B. (2013). Regulation of inflammation by adenosine. *Front. Immunol.* 4:85. doi: 10.3389/fimmu.2013.00085

He, Q., Yang, Q., Zhou, Q., Zhu, H., Niu, W., Feng, J., et al. (2014). Effects of varying degrees of intermittent hypoxia on proinflammatory cytokines and adipokines in rats and 3T3-L1 adipocytes. *PLoS One* 9:e86326. doi: 10.1371/journal.pone.0086326

Heikkilä, K., Ebrahim, S., and Lawlor, D. A. (2008). Systematic review of the association between circulating interleukin-6 (IL-6) and cancer. *Eur. J. Cancer* 44, 937–945. doi: 10.1016/j.ejca.2008.02.047

Honegger, B., Galic, M., Köhler, K., Wittwer, F., Brogiolo, W., Hafen, E., et al. (2008). Imp-L2, a putative homolog of vertebrate IGF-binding protein 7, counteracts insulin signaling in *Drosophila* and is essential for starvation resistance. *J. Biol.* 7:10. doi: 10.1186/jbiol72

Honors, M. A., and Kinzig, K. P. (2012). The role of insulin resistance in the development of muscle wasting during cancer cachexia. *J. Cachexia. Sarcopen. Muscle* 3, 5–11. doi: 10.1007/s13539-011-0051-5

Hsu, C.-L., Lin, W., Seshasayee, D., Chen, Y.-H., Ding, X., Lin, Z., et al. (2012). Equilibrative nucleoside transporter 3 deficiency perturbs lysosome function and macrophage homeostasis. *Science* 335, 89–92. doi: 10.1126/science.1213682

Hubler, M. J., and Kennedy, A. J. (2016). Role of lipids in the metabolism and activation of immune cells. *J. Nutr. Biochem.* 34, 1–7. doi: 10.1016/j.jnutbio.2015.11.002

Imran, M., and Smith, H. L. (2007). The dynamics of bacterial infection, innate immune response, and antibiotic treatment. *Discret. Contin. Dyn. Syst. B* 8, 127–143. doi: 10.3934/dcdsb.2007.8.127

Iommarini, L., Porcelli, A. M., Gasparre, G., and Kurelac, I. (2017). Non-canonical mechanisms regulating hypoxia-inducible factor 1 alpha in cancer. *Front. Oncol.* 7:286. doi: 10.3389/fonc.2017.00286

Irving, P., Ubeda, J.-M., Doucet, D., Troxler, L., Lagueux, M., Zachary, D., et al. (2005). New insights into *Drosophila* larval haemocyte functions through genome-wide analysis. *Cell. Microbiol.* 7, 335–350. doi: 10.1111/j.1462-5822.2004.00462.x

Jiang, H., Patel, P. H., Kohlmaier, A., Grenley, M. O., McEwen, D. G., and Edgar, B. A. (2009). Cytokine/Jak/Stat signaling mediates regeneration and homeostasis in the *Drosophila* Midgut. *Cell* 137, 1343–1355. doi: 10.1016/j.cell.2009.05.014

Jin, N., Hatton, N., Swartz, D. R., Xia, X., Harrington, M. A., Larsen, S. H., et al. (2000). Hypoxia Activates jun-n-terminal kinase, extracellular signal-regulated protein kinase, and p38 kinase in pulmonary arteries. *Am. J. Respir. Cell Mol. Biol.* 23, 593–601. doi: 10.1165/ajrcmb.23.5.3921

Johansson, K., Metzendorf, C., and Soderhall, K. (2005). Microarray analysis of immune challenged hemocytes. *Exp. Cell Res.* 305, 145–155. doi: 10.1016/j.yexcr.2004.12.018

Jones, W., and Bianchi, K. (2015). Aerobic glycolysis: beyond proliferation. *Front. Immunol.* 6:227. doi: 10.3389/fimmu.2015.00227

Kacsoh, B. Z., and Schlenke, T. A. (2012). High hemocyte load is associated with increased resistance against parasitoids in *Drosophila suzukii*, a relative of *D. melanogaster*. *PLoS One* 7:e34721. doi: 10.1371/journal.pone.0034721

Kammerer, T., Faihs, V., Hulde, N., Stangl, M., Brettner, F., Rehm, M., et al. (2020). Hypoxic-inflammatory responses under acute hypoxia: in vitro experiments and prospective observational expedition trial. *Int. J. Mol. Sci.* 21:1034. doi: 10.3390/ijms21031034

Karnovsky, M. L. (1962). Metabolic basis of phagocytic activity. *Physiol. Rev.* 42, 143–168. doi: 10.1152/physrev.1962.42.1.143

Kazankov, K., Jørgensen, S. M. D., Thomsen, K. L., Møller, H. J., Vilstrup, H., George, J., et al. (2019). The role of macrophages in nonalcoholic fatty liver disease and nonalcoholic steatohepatitis. *Nat. Rev. Gastroenterol. Hepatol.* 16, 145–159. doi: 10.1038/s41575-018-0082-x

Kedia-Mehta, N., and Finlay, D. K. (2019). Competition for nutrients and its role in controlling immune responses. *Nat. Commun.* 10:2123. doi: 10.1038/s41467-019-10015-4

Khovidhunkit, W., Kim, M. S., Memon, R. A., Shigenaga, J. K., Moser, A. H., Feingold, K. R., et al. (2004). Effects of infection and inflammation on lipid and lipoprotein metabolism: mechanisms and consequences to the host. *J. Lipid Res.* 45, 1169–1196. doi: 10.1194/jlr.R300019-JLR200

Kierdorf, K., Hersperger, F., Sharrock, J., Vincent, C. M., Ustaoglu, P., Dou, J., et al. (2020). Muscle function and homeostasis require cytokine inhibition of AKT activity in *Drosophila*. *eLife* 9:e051595. doi: 10.7554/eLife.51595

Kim, J., Tchernyshyov, I., Semenza, G. L., and Dang, C. V. (2006). HIF-1-mediated expression of pyruvate dehydrogenase kinase: a metabolic switch required for cellular adaptation to hypoxia. *Cell Metab.* 3, 177–185. doi: 10.1016/j.cmet.2006.02.002

Koehler, F., Doehner, W., Hoernig, S., Witt, C., Anker, S. D., and John, M. (2007). Anorexia in chronic obstructive pulmonary disease — association to cachexia and hormonal derangement. *Int. J. Cardiol.* 119, 83–89. doi: 10.1016/j.ijcard.2006.07.088

Koelwyn, G. J., Corr, E. M., Erbay, E., and Moore, K. J. (2018). Regulation of macrophage immunometabolism in atherosclerosis. *Nat. Immunol.* 19, 526–537. doi: 10.1038/s41590-018-0113-3

Koivunen, P., Hirsilä, M., Remes, A. M., Hassinen, I. E., Kivirikko, K. I., and Myllyharju, J. (2007). Inhibition of Hypoxia-Inducible Factor (HIF) hydroxylases by citric acid cycle intermediates. *J. Biol. Chem.* 282, 4524–4532. doi: 10.1074/jbc.M610415200

Koltai, T. (2020). Cancer cachexia has many symptoms but only one cause: anoxia. *F1000Res.* 9:250. doi: 10.12688/f1000research.22624.1

Korbecki, J., and Bajdak-Rusinek, K. (2019). The effect of palmitic acid on inflammatory response in macrophages: an overview of molecular mechanisms. *Inflamm. Res.* 68, 915–932. doi: 10.1007/s00011-019-01273-5

Kraakman, M. J., Murphy, A. J., Jandeleit-Dahm, K., and Kammoun, H. L. (2014). Macrophage polarization in obesity and type 2 diabetes: weighing down our understanding of macrophage function? *Front. Immunol.* 5:470. doi: 10.3389/fimmu.2014.00470

Krejčová, G., Bajgar, A., Nedbalová, P., Kovářová, J., Kamps-Hughes, N., Zemanová, H., et al. (2020). Macrophage-derived insulin/IGF antagonist ImpL2 regulates systemic metabolism for mounting an effective acute immune response in *Drosophila*. *bioRxiv* [Preprint], doi: 10.1101/2020.09.24.311670

Krejčová, G., Danielová, A., Nedbalová, P., Kazek, M., Strych, L., Chawla, G., et al. (2019). *Drosophila* macrophages switch to aerobic glycolysis to mount effective antibacterial defense. *eLife* 8:e050414. doi: 10.7554/eLife.50414

Krishnan, J., Suter, M., Windak, R., Krebs, T., Felley, A., Montessuit, C., et al. (2009). Activation of a HIF1α-PPARγ axis underlies the integration of glycolytic and lipid anabolic pathways in pathologic cardiac hypertrophy. *Cell Metab.* 9, 512–524. doi: 10.1016/j.cmet.2009.05.005

Kühnlein, R. P. (2012). Lipid droplet-based storage fat metabolism in *Drosophila*. *J. Lipid Res.* 53, 1430–1436. doi: 10.1194/jlr.R024299

Kullmann, S., Valenta, V., Wagner, R., Tschritter, O., Machann, J., Häring, H.-U., et al. (2020). Brain insulin sensitivity is linked to adiposity and body fat distribution. *Nat. Commun.* 11:1841. doi: 10.1038/s41467-020-15686-y

Kwon, D., Cha, H.-J., Lee, H., Hong, S.-H., Park, C., Park, S.-H., et al. (2019). Protective effect of glutathione against oxidative stress-induced cytotoxicity in RAW 264.7 macrophages through activating the nuclear factor erythroid 2-Related Factor-2/Heme oxygenase-1 pathway. *Antioxidants* 8:82. doi: 10.3390/antiox8040082

Kwon, Y., Song, W., Droujinine, I. A., Hu, Y., Asara, J. M., and Perrimon, N. (2015). systemic organ wasting induced by localized expression of the secreted insulin/igf antagonist ImpL2. *Dev. Cell* 33, 36–46. doi: 10.1016/j.devcel.2015.02.012

Langin, D. (2013). Adipose tissue lipolysis and insulin sensitivity. *Endocr. Abstr.* 32:S32.3. doi: 10.1530/endoabs.32.S32.3

Lee, G. J., Han, G., Yun, H. M., Lim, J. J., Noh, S., Lee, J., et al. (2018). Steroid signaling mediates nutritional regulation of juvenile body growth via IGF-binding protein in *Drosophila*. *Proc. Natl. Acad. Sci. U.S.A.* 115, 5992–5997. doi: 10.1073/pnas.1718834115

Lee, S., and Dong, H. H. (2017). FoxO integration of insulin signaling with glucose and lipid metabolism. *J. Endocrinol.* 233, R67–R79. doi: 10.1530/JOE-17-0002

Leonard, E. J., Skeel, A., Chiang, P. K., and Cantoni, G. L. (1978). The action of the adenosylhomocysteine hydrolase inhibitor, 3-deazaadenosine, on phagocytic function of mouse macrophages and human monocytes. *Biochem. Biophys. Res. Commun.* 84, 102–109. doi: 10.1016/0006-291X(78)90269-3

Lewis, A., and Elks, P. M. (2019). Hypoxia induces macrophage tnfa expression via cyclooxygenase and prostaglandin E2 in vivo. *Front. Immunol.* 10:2321. doi: 10.3389/fimmu.2019.02321

Lewis, G. F., Carpentier, A., Adeli, K., and Giacca, A. (2002). Disordered fat storage and mobilization in the pathogenesis of insulin resistance and Type 2 diabetes. *Endocr. Rev.* 23, 201–229. doi: 10.1210/edrv.23.2.0461

Lim, Y.-M., Lim, H., Hur, K. Y., Quan, W., Lee, H.-Y., Cheon, H., et al. (2014). Systemic autophagy insufficiency compromises adaptation to metabolic stress

and facilitates progression from obesity to diabetes. *Nat. Commun.* 5:4934. doi: 10.1038/ncomms5934

Liou, G.-Y. (2017). Inflammatory cytokine signaling during development of pancreatic and prostate cancers. *J. Immunol. Res.* 2017, 1–10. doi: 10.1155/2017/7979637

Liu, Y., Wu, M., Ling, J., Cai, L., Zhang, D., Gu, H. F., et al. (2015). Serum IGFBP7 levels associate with insulin resistance and the risk of metabolic syndrome in a Chinese population. *Sci. Rep.* 5:10227. doi: 10.1038/srep10227

Loftus, R. M., and Finlay, D. K. (2016). Immunometabolism: cellular metabolism turns immune regulator. *J. Biol. Chem.* 291, 1–10. doi: 10.1074/jbc.R115.693903

Ma, J., Wei, K., Liu, J., Tang, K., Zhang, H., Zhu, L., et al. (2020). Glycogen metabolism regulates macrophage-mediated acute inflammatory responses. *Nat. Commun.* 11:1769. doi: 10.1038/s41467-020-15636-8

Maier, A., Wu, H., Cordasic, N., Oefner, P., Dietel, B., Thiele, C., et al. (2017). Hypoxia-inducible protein 2 Hig2/Hilpda mediates neutral lipid accumulation in macrophages and contributes to atherosclerosis in apolipoprotein E-deficient mice. *FASEB J.* 31, 4971–4984. doi: 10.1096/fj.201700235R

Mak, R. H., and Cheung, W. (2006). Energy homeostasis and cachexia in chronic kidney disease. *Pediatr. Nephrol.* 21, 1807–1814. doi: 10.1007/s00467-006-0194-3

Makki, K., Froguel, P., and Wolowczuk, I. (2013). Adipose tissue in obesity-related inflammation and insulin resistance: cells, cytokines, and chemokines. *ISRN Inflamm.* 2013, 1–12. doi: 10.1155/2013/139239

Marette, A. (2002). Mediators of cytokine-induced insulin resistance in obesity and other inflammatory settings. *Curr. Opin. Clin. Nutr. Metab. Care* 5, 377–383. doi: 10.1097/00075197-200207000-00005

Marik, P. E., and Bellomo, R. (2013). Stress hyperglycemia: an essential survival response!. *Crit. Care* 17:305. doi: 10.1186/cc12514

Martínez-Castillo, M., Rosique-Oramas, D., Medina-Avila, Z., Pérez-Hernández, J. L., Higuera-De la Tijera, F., Santana-Vargas, D., et al. (2020). Differential production of insulin-like growth factor-binding proteins in liver fibrosis progression. *Mol. Cell. Biochem.* 469, 65–75. doi: 10.1007/s11010-020-03728-4

Marxsen, J. H., Stengel, P., Doege, K., Heikkinen, P., Jokilehto, T., Wagner, T., et al. (2004). Hypoxia-inducible factor-1 (HIF-1) promotes its degradation by induction of HIF-α-prolyl-4-hydroxylases. *Biochem. J.* 381, 761–767. doi: 10.1042/BJ20040620

Matrone, C., Pignataro, G., Molinaro, P., Irace, C., Scorziello, A., Di Renzo, G. F., et al. (2004). HIF-1alpha reveals a binding activity to the promoter of iNOS gene after permanent middle cerebral artery occlusion. *J. Neurochem.* 90, 368–378. doi: 10.1111/j.1471-4159.2004.02483.x

Melcarne, C., Lemaitre, B., and Kurant, E. (2019). Phagocytosis in *Drosophila*: from molecules and cellular machinery to physiology. *Insect Biochem. Mol. Biol.* 109, 1–12. doi: 10.1016/j.ibmb.2019.04.002

Mihajlovic, Z., Tanasic, D., Bajgar, A., Perez-Gomez, R., Steffal, P., and Krejci, A. (2019). Lime is a new protein linking immunity and metabolism in *Drosophila*. *Dev. Biol.* 452, 83–94. doi: 10.1016/j.ydbio.2019.05.005

Mills, C. D., Lenz, L. L., and Ley, K. (2015). Macrophages at the fork in the road to health or disease. *Front. Immunol.* 6:59. doi: 10.3389/fimmu.2015.00059

Mills, E. L., and O'Neill, L. A. (2016). Reprogramming mitochondrial metabolism in macrophages as an anti-inflammatory signal. *Eur. J. Immunol.* 46, 13–21. doi: 10.1002/eji.201445427

Miska, J., Lee-Chang, C., Rashidi, A., Muroski, M. E., Chang, A. L., Lopez-Rosas, A., et al. (2019). HIF-1α is a metabolic switch between glycolytic-driven migration and oxidative phosphorylation-driven immunosuppression of tregs in glioblastoma. *Cell Rep.* 27, 226–237.e4. doi: 10.1016/j.celrep.2019.03.029

Molaei, M., Vandehoef, C., and Karpac, J. (2019). NF-κB shapes metabolic adaptation by attenuating foxo-mediated lipolysis in *Drosophila*. *Dev. Cell* 49, 802–810.e6. doi: 10.1016/j.devcel.2019.04.009

Morgantini, C., Jager, J., Li, X., Levi, L., Azzimato, V., Sulen, A., et al. (2019). Liver macrophages regulate systemic metabolism through non-inflammatory factors. *Nat. Metab.* 1, 445–459. doi: 10.1038/s42255-019-0044-9

Mosser, D. M., and Edwards, J. P. (2008). Exploring the full spectrum of macrophage activation. *Nat. Rev. Immunol.* 8, 958–969. doi: 10.1038/nri2448

Mylonis, I., Sembongi, H., Befani, C., Liakos, P., Siniossoglou, S., and Simos, G. (2012). Hypoxia causes triglyceride accumulation by HIF-1-mediated stimulation of lipin 1 expression. *J. Cell Sci.* 125, 3485–3493. doi: 10.1242/jcs.106682

Mylonis, I., Simos, G., and Paraskeva, E. (2019). Hypoxia-inducible factors and the regulation of lipid metabolism. *Cells* 8:214. doi: 10.3390/cells8030214

Nagao, A., Kobayashi, M., Koyasu, S., Chow, C. C. T., and Harada, H. (2019). HIF-1-dependent reprogramming of glucose metabolic pathway of cancer cells and its therapeutic significance. *Int. J. Mol. Sci.* 20:238. doi: 10.3390/ijms20020238

Nagy, C., and Haschemi, A. (2015). Time and demand are two critical dimensions of immunometabolism: the process of macrophage activation and the pentose phosphate pathway. *Front. Immunol.* 6:164. doi: 10.3389/fimmu.2015.00164

Narsale, A. A., and Carson, J. A. (2014). Role of interleukin-6 in cachexia. *Curr. Opin. Support. Palliat. Care* 8, 321–327. doi: 10.1097/SPC.0000000000000091

Nässel, D. R., and Broeck, J. V. (2016). Insulin/IGF signaling in *Drosophila* and other insects: factors that regulate production, release and post-release action of the insulin-like peptides. *Cell. Mol. Life Sci.* 73, 271–290. doi: 10.1007/s00018-015-2063-3

Nässel, D. R., Liu, Y., and Luo, J. (2015). Insulin/IGF signaling and its regulation in *Drosophila*. *Gen. Comp. Endocrinol.* 221, 255–266. doi: 10.1016/j.ygcen.2014.11.021

Newsholme, P., Curi, R., Gordon, S., and Newsholme, E. A. (1986). Metabolism of glucose, glutamine, long-chain fatty acids and ketone bodies by murine macrophages. *Biochem. J.* 239, 121–125. doi: 10.1042/bj2390121

Nonnenmacher, Y., and Hiller, K. (2018). Biochemistry of proinflammatory macrophage activation. *Cell. Mol. Life Sci.* 75, 2093–2109. doi: 10.1007/s00018-018-2784-1

Obach, M., Navarro-Sabaté, À, Caro, J., Kong, X., Duran, J., and Gómez, M. (2004). 6-Phosphofructo-2-kinase (pfkfb3) gene promoter contains hypoxia-inducible Factor-1 binding sites necessary for transactivation in response to hypoxia. *J. Biol. Chem.* 279, 53562–53570. doi: 10.1074/jbc.M406096200

Oldefest, M., Nowinski, J., Hung, C.-W., Neelsen, D., Trad, A., Tholey, A., et al. (2013). Upd3 - an ancestor of the four-helix bundle cytokines. *Biochem. Biophys. Res. Commun.* 436, 66–72. doi: 10.1016/j.bbrc.2013.04.107

Olefsky, J. M., and Glass, C. K. (2010). Macrophages, inflammation, and insulin resistance. *Annu. Rev. Physiol.* 72, 219–246. doi: 10.1146/annurev-physiol-021909-135846

Olson, J. M., Jinka, T. R., Larson, L. K., Danielson, J. J., Moore, J. T., Carpluck, J., et al. (2013). Circannual rhythm in body temperature, torpor, and sensitivity to A 1 adenosine receptor agonist in arctic ground squirrels. *J. Biol. Rhythms* 28, 201–207. doi: 10.1177/0748730413490667

O'Neill, L. A. J. (2015). A broken krebs cycle in macrophages. *Immunity* 42, 393–394. doi: 10.1016/j.immuni.2015.02.017

Owusu-Ansah, E., Song, W., and Perrimon, N. (2013). Muscle mitohormesis promotes longevity via systemic repression of insulin signaling. *Cell* 155, 699–712. doi: 10.1016/j.cell.2013.09.021

Palazon, A., Goldrath, A. W., Nizet, V., and Johnson, R. S. (2014). HIF transcription factors, inflammation, and immunity. *Immunity* 41, 518–528. doi: 10.1016/j.immuni.2014.09.008

Panday, A., Sahoo, M. K., Osorio, D., and Batra, S. (2015). NADPH oxidases: an overview from structure to innate immunity-associated pathologies. *Cell. Mol. Immunol.* 12, 5–23. doi: 10.1038/cmi.2014.89

Patel, H. J., and Patel, B. M. (2017). TNF-α and cancer cachexia: molecular insights and clinical implications. *Life Sci.* 170, 56–63. doi: 10.1016/j.lfs.2016.11.033

Pavlou, S., Wang, L., Xu, H., and Chen, M. (2017). Higher phagocytic activity of thioglycollate-elicited peritoneal macrophages is related to metabolic status of the cells. *J. Inflamm.* 14:4. doi: 10.1186/s12950-017-0151-x

Péan, C. B., Schiebler, M., Tan, S. W. S., Sharrock, J. A., Kierdorf, K., Brown, K. P., et al. (2017). Regulation of phagocyte triglyceride by a STAT-ATG2 pathway controls mycobacterial infection. *Nat. Commun.* 8:14642. doi: 10.1038/ncomms14642

Perry, R. J., Samuel, V. T., Petersen, K. F., and Shulman, G. I. (2014). The role of hepatic lipids in hepatic insulin resistance and type 2 diabetes. *Nature* 510, 84–91. doi: 10.1038/nature13478

Peyssonnaux, C., Cejudo-Martin, P., Doedens, A., Zinkernagel, A. S., Johnson, R. S., and Nizet, V. (2007). Cutting edge: essential role of hypoxia inducible Factor-1α in development of lipopolysaccharide-induced sepsis. *J. Immunol.* 178, 7516–7519. doi: 10.4049/jimmunol.178.12.7516

Pizarro, T. T., and Cominelli, F. (2007). Cloning IL-1 and the birth of a new era in cytokine biology. *J. Immunol.* 178, 5411–5412. doi: 10.4049/jimmunol.178.9.5411

Popa, C., Netea, M. G., van Riel, P. L. C. M., van der Meer, J. W. M., and Stalenhoef, A. F. H. (2007). The role of TNF-α in chronic inflammatory conditions, intermediary metabolism, and cardiovascular risk. *J. Lipid Res.* 48, 751–762. doi: 10.1194/jlr.R600021-JLR200

Porporato, P. E. (2016). Understanding cachexia as a cancer metabolism syndrome. *Oncogenesis* 5:e200. doi: 10.1038/oncsis.2016.3

Prabakaran, S. (2015). Mitochondria to nucleus: activate HIF1α. *Sci. Signal.* 8:ec330. doi: 10.1126/scisignal.aad8189

Puigserver, P., Rhee, J., Donovan, J., Walkey, C. J., Yoon, J. C., Oriente, F., et al. (2003). Insulin-regulated hepatic gluconeogenesis through FOXO1-PGC-1α interaction. *Nature* 423, 550–555. doi: 10.1038/nature01667

Rajan, A., and Perrimon, N. (2011). *Drosophila* as a model for interorgan communication: lessons from studies on energy homeostasis. *Dev. Cell* 21, 29–31. doi: 10.1016/j.devcel.2011.06.034

Ramond, E., Dudzic, J. P., and Lemaitre, B. (2020). Comparative RNA-Seq analyses of *Drosophila* plasmatocytes reveal gene specific signatures in response to clean injury and septic injury. *PLoS One* 15:e0235294. doi: 10.1371/journal.pone.0235294

Ramond, E., Jamet, A., Coureuil, M., and Charbit, A. (2019). Pivotal role of mitochondria in macrophage response to bacterial pathogens. *Front. Immunol.* 10:2461. doi: 10.3389/fimmu.2019.02461

Ratcliffe, N. A., and Rowley, A. F. (1975). Cellular defense reactions of insect hemocytes in vitro: phagocytosis in a new suspension culture system. *J. Invertebr. Pathol.* 26, 225–233. doi: 10.1016/0022-2011(75)90053-1

Park, Y. M. (2014). CD36, a scavenger receptor implicated in atherosclerosis. *Exp. Mol. Med.* 46:e99. doi: 10.1038/emm.2014.38

Remmerie, A., and Scott, C. L. (2018). Macrophages and lipid metabolism. *Cell. Immunol.* 330, 27–42. doi: 10.1016/j.cellimm.2018.01.020

Riddle, S. R., Ahmad, A., Ahmad, S., Deeb, S. S., Malkki, M., Schneider, B. K., et al. (2000). Hypoxia induces hexokinase II gene expression in human lung cell line A549. *Am. J. Physiol. Cell. Mol. Physiol.* 278, L407–L416. doi: 10.1152/ajplung.2000.278.2.L407

Riganti, C., Gazzano, E., Polimeni, M., Aldieri, E., and Ghigo, D. (2012). The pentose phosphate pathway: an antioxidant defense and a crossroad in tumor cell fate. *Free Radic. Biol. Med.* 53, 421–436. doi: 10.1016/j.freeradbiomed.2012.05.006

Ristow, M., and Schmeisser, K. (2014). Mitohormesis: promoting health and lifespan by increased levels of reactive oxygen species (ROS). *Dose Response* 12, 288–341. doi: 10.2203/dose-response.13-035.Ristow

Rossol, M., Heine, H., Meusch, U., Quandt, D., Klein, C., Sweet, M. J., et al. (2011). LPS-induced cytokine production in human monocytes and macrophages. *Crit. Rev. Immunol.* 31, 379–446. doi: 10.1615/CritRevImmunol.v31.i5.20

Roth, K. J., and Copple, B. L. (2015). Role of hypoxia-inducible factors in the development of liver fibrosis. *Cell. Mol. Gastroenterol. Hepatol.* 1, 589–597. doi: 10.1016/j.jcmgh.2015.09.005

Rouzer, C. A., Scott, W. A., Griffith, O. W., Hamill, A. L., and Cohn, Z. A. (1982). Glutathione metabolism in resting and phagocytizing peritoneal macrophages. *J. Biol. Chem.* 257, 2002–2008. doi: 10.1016/s0021-9258(19)68139-1

Ruan, W., Wu, M., Shi, L., Li, F., Dong, L., Qiu, Y., et al. (2017). Serum levels of IGFBP7 are elevated during acute exacerbation in COPD patients. *Int. J. Chron. Obstruct. Pulmon. Dis.* Volume 12, 1775–1780. doi: 10.2147/COPD.S132652

Ryter, S. W., Koo, J. K., and Choi, A. M. K. (2014). Molecular regulation of autophagy and its implications for metabolic diseases. *Curr. Opin. Clin. Nutr. Metab. Care* 17, 329–337. doi: 10.1097/MCO.0000000000000068

Sag, D., Carling, D., Stout, R. D., and Suttles, J. (2008). Adenosine 5′-monophosphate-activated protein Kinase promotes macrophage polarization to an anti-inflammatory functional phenotype. *J. Immunol.* 181, 8633–8641. doi: 10.4049/jimmunol.181.12.8633

Salazar, J., Bermúdez, V., Olivar, L. C., Torres, W., Palmar, J., Añez, R., et al. (2018). Insulin resistance indices and coronary risk in adults from Maracaibo city, Venezuela: a cross sectional study. *F1000Research* 7:44. doi: 10.12688/f1000research.13610.2

Sancho, D., Enamorado, M., and Garaude, J. (2017). Innate immune function of mitochondrial metabolism. *Front. Immunol.* 8:527. doi: 10.3389/fimmu.2017.00527

Santoleri, D., and Titchenell, P. M. (2019). Resolving the paradox of hepatic insulin resistance. *Cell. Mol. Gastroenterol. Hepatol.* 7, 447–456. doi: 10.1016/j.jcmgh.2018.10.016

Sarkar, P., Stefi, R. V., Pasupuleti, M., Paray, B. A., Al-Sadoon, M. K., and Arockiaraj, J. (2020). Antioxidant molecular mechanism of adenosyl homocysteinase from cyanobacteria and its wound healing process in fibroblast cells. *Mol. Biol. Rep.* 47, 1821–1834. doi: 10.1007/s11033-020-05276-y

Schrader, J., Haddy, F. J., and Gerlach, E. (1977). Release of adenosine, inosine and hypoxanthine from the isolated guinea pig heart during hypoxia, flow-autoregulation and reactive hyperemia. *Pflügers Arch. Eur. J. Physiol.* 369, 1–6. doi: 10.1007/BF00580802

Schwartsburd, P. M. (2017). Catabolic and anabolic faces of insulin resistance and their disorders: a new insight into circadian control of metabolic disorders leading to diabetes. *Futur. Sci. OA* 3:FSO201. doi: 10.4155/fsoa-2017-0015

Scialò, F., Fernández-Ayala, D. J., and Sanz, A. (2017). Role of mitochondrial reverse electron transport in ROS signaling: potential roles in health and disease. *Front. Physiol.* 8:428. doi: 10.3389/fphys.2017.00428

Scott, B. N. V., Sarkar, T., Kratofil, R. M., Kubes, P., and Thanabalasuriar, A. (2019). Unraveling the host's immune response to infection: seeing is believing. *J. Leukoc. Biol.* 106, 323–335. doi: 10.1002/JLB.4RI1218-503R

Shen, G., and Li, X. (2017). "The multifaceted role of hypoxia-inducible Factor 1 (HIF1) in lipid metabolism," in *Hypoxia and Human Diseases*, eds J. Zheng and C. Zhou (London: InTechopen), doi: 10.5772/65340

Shen, G.-M., Zhao, Y.-Z., Chen, M.-T., Zhang, F.-L., Liu, X.-L., Wang, Y., et al. (2012). Hypoxia-inducible factor-1 (HIF-1) promotes LDL and VLDL uptake through inducing VLDLR under hypoxia. *Biochem. J.* 441, 675–683. doi: 10.1042/BJ20111377

Shi, J., Fan, J., Su, Q., and Yang, Z. (2019). Cytokines and abnormal glucose and lipid metabolism. *Front. Endocrinol.* 10:703. doi: 10.3389/fendo.2019.00703

Shin, M., Cha, N., Koranteng, F., Cho, B., and Shim, J. (2020). Subpopulation of macrophage-like plasmatocytes attenuates systemic growth via JAK/STAT in the *Drosophila* fat body. *Front. Immunol.* 11:63. doi: 10.3389/fimmu.2020.00063

Shin, K. C., Hwang, I., Choe, S. S., Park, J., Ji, Y., Kim, J. I., et al. (2017). Macrophage VLDLR mediates obesity-induced insulin resistance with adipose tissue inflammation. *Nat. Commun.* 8:1087. doi: 10.1038/s41467-017-01232-w

Siegert, I., Schödel, J., Nairz, M., Schatz, V., Dettmer, K., Dick, C., et al. (2015). Ferritin-mediated iron sequestration stabilizes hypoxia-inducible Factor-1α upon LPS activation in the presence of ample oxygen. *Cell Rep.* 13, 2048–2055. doi: 10.1016/j.celrep.2015.11.005

Silva, D., Moreira, D., Cordeiro-da-Silva, A., Quintas, C., Gonçalves, J., and Fresco, P. (2020). Intracellular adenosine released from THP-1 differentiated human macrophages is involved in an autocrine control of Leishmania parasitic burden, mediated by adenosine A2A and A2B receptors. *Eur. J. Pharmacol.* 885:173504. doi: 10.1016/j.ejphar.2020.173504

Silva-Vilches, C., Ring, S., and Mahnke, K. (2018). ATP and its metabolite adenosine as regulators of dendritic cell activity. *Front. Immunol.* 9:2581. doi: 10.3389/fimmu.2018.02581

Soeters, M. R., and Soeters, P. B. (2012). The evolutionary benefit of insulin resistance. *Clin. Nutr.* 31, 1002–1007. doi: 10.1016/j.clnu.2012.05.011

Srikanthan, P., Hevener, A. L., and Karlamangla, A. S. (2010). Sarcopenia exacerbates obesity-associated insulin resistance and Dysglycemia: findings from the national health and nutrition examination survey III. *PLoS One* 5:e10805. doi: 10.1371/journal.pone.0010805

Stenholm, S., Harris, T. B., Rantanen, T., Visser, M., Kritchevsky, S. B., and Ferrucci, L. (2008). Sarcopenic obesity: definition, cause and consequences. *Curr. Opin. Clin. Nutr. Metab. Care* 11, 693–700. doi: 10.1097/MCO.0b013e328312c37d

Straub, R. H. (2014). Insulin resistance, selfish brain, and selfish immune system: an evolutionarily positively selected program used in chronic inflammatory diseases. *Arthritis Res. Ther.* 16:S4. doi: 10.1186/ar4688

Stuart, L. M., and Ezekowitz, R. A. (2008). Phagocytosis and comparative innate immunity: learning on the fly. *Nat. Rev. Immunol.* 8, 131–141. doi: 10.1038/nri2240

Stunault, M. I., Bories, G., Guinamard, R. R., and Ivanov, S. (2018). Metabolism plays a key role during macrophage activation. *Med. Inflamm.* 2018:2426138. doi: 10.1155/2018/2426138

Tadaishi, M., Toriba, Y., Shimizu, M., and Kobayashi-Hattori, K. (2018). Adenosine stimulates hepatic glycogenolysis via adrenal glands-liver crosstalk in mice. *PLoS One* 13:e0209647. doi: 10.1371/journal.pone.0209647

Tattikota, S. G., Cho, B., Liu, Y., Hu, Y., Barrera, V., Steinbaugh, M. J., et al. (2020). A single-cell survey of *Drosophila* blood. *eLife* 9:e54818. doi: 10.7554/eLife.54818

Tehlivets, O., Malanovic, N., Visram, M., Pavkov-Keller, T., and Keller, W. (2013). S-adenosyl-L-homocysteine hydrolase and methylation disorders: yeast as a model system. *Biochim. Biophys. Acta Mol. Basis Dis.* 1832, 204–215. doi: 10.1016/j.bbadis.2012.09.007

Teng, O., Ang, C. K. E., and Guan, X. L. (2017). Macrophage-bacteria interactions—a lipid-centric relationship. *Front. Immunol.* 8:1836. doi: 10.3389/fimmu.2017.01836

Texada, M. J., Jørgensen, A. F., Christensen, C. F., Koyama, T., Malita, A., Smith, D. K., et al. (2019). A fat-tissue sensor couples growth to oxygen availability by remotely controlling insulin secretion. *Nat. Commun.* 10:1955. doi: 10.1038/s41467-019-09943-y

Theret, M., Mounier, R., and Rossi, F. (2019). The origins and non-canonical functions of macrophages in development and regeneration. *Development* 146:dev156000. doi: 10.1242/dev.156000

Thomas, A. P., and Halestrap, A. P. (1981). The rôle of mitochondrial pyruvate transport in the stimulation by glucagon and phenylephrine of gluconeogenesis from l-lactate in isolated rat hepatocytes. *Biochem. J.* 198, 551–560. doi: 10.1042/bj1980551

Tilg, H., and Hotamisligil, G. S. (2006). Nonalcoholic fatty liver disease: cytokine-adipokine interplay and regulation of insulin resistance. *Gastroenterol.* 131, 934–945. doi: 10.1053/j.gastro.2006.05.054

Tonelli, C., Chio, I. I. C., and Tuveson, D. A. (2018). Transcriptional regulation by Nrf2. *Antioxid. Redox Signal.* 29, 1727–1745. doi: 10.1089/ars.2017.7342

Van den Berghe, G. (2002). Beyond diabetes: saving lives with insulin in the ICU. *Int. J. Obes.* 26, S3–S8. doi: 10.1038/sj.ijo.0802171

Van den Bossche, J., Baardman, J., and de Winther, M. P. J. (2015). Metabolic characterization of polarized M1 and M2 bone marrow-derived macrophages using real-time extracellular flux analysis. *J. Vis. Exp.* 2015:53424. doi: 10.3791/53424

van Niekerk, G., Davis, T., and Engelbrecht, A.-M. (2017). Hyperglycaemia in critically ill patients: the immune system's sweet tooth. *Crit. Care* 21:202. doi: 10.1186/s13054-017-1775-1

Vijayan, V., Pradhan, P., Braud, L., Fuchs, H. R., Gueler, F., Motterlini, R., et al. (2019). Human and murine macrophages exhibit differential metabolic responses to lipopolysaccharide - A divergent role for glycolysis. *Redox Biol.* 22:101147. doi: 10.1016/j.redox.2019.101147

Wang, A., Luan, H. H., and Medzhitov, R. (2019). An evolutionary perspective on immunometabolism. *Science* 363:eaar3932. doi: 10.1126/science.aar3932

Wang, C.-W., Purkayastha, A., Jones, K. T., Thaker, S. K., and Banerjee, U. (2016). In vivo genetic dissection of tumor growth and the Warburg effect. *eLife* 5:e018126. doi: 10.7554/eLife.18126

Wang, L., Sexton, T. R., Venard, C., Giedt, M., Guo, Q., Chen, Q., et al. (2014). Pleiotropy of the *Drosophila* JAK pathway cytokine Unpaired 3 in development and aging. *Dev. Biol.* 395, 218–231. doi: 10.1016/j.ydbio.2014.09.015

Wang, T., Liu, H., Lian, G., Zhang, S.-Y., Wang, X., and Jiang, C. (2017). HIF1 α -induced glycolysis metabolism is essential to the activation of inflammatory macrophages. *Med. Inflamm.* 2017, 1–10. doi: 10.1155/2017/9029327

Warburg, O. (1956). On the origin of cancer cells. *Science* 123, 309–314. doi: 10.1126/science.123.3191.309

Warburg, O., Wind, F., and Negelein, E. (1927). The metabolism of tumors in the body. *J. Gen. Physiol.* 8, 519–530. doi: 10.1085/jgp.8.6.519

Watts, E. R., and Walmsley, S. R. (2019). Inflammation and hypoxia: HIF and PHD isoform selectivity. *Trends Mol. Med.* 25, 33–46.

Werb, Z., and Cohn, Z. A. (1972). Plasma membrane synthesis in the macrophage following phagocytosis of polystyrene latex particles. *J. Biol. Chem.* 247, 2439–2446. doi: 10.1016/s0021-9258(19)45448-3

Wolowczuk, I., Verwaerde, C., Viltart, O., Delanoye, A., Delacre, M., Pot, B., et al. (2008). Feeding our immune system: impact on metabolism. *Clin. Dev. Immunol.* 2008:639803. doi: 10.1155/2008/639803

Woodcock, K. J., Kierdorf, K., Pouchelon, C. A., Vivancos, V., Dionne, M. S., and Geissmann, F. (2015). Macrophage-derived upd3 cytokine causes impaired glucose homeostasis and reduced lifespan in *Drosophila* fed a lipid-rich diet. *Immunity* 42, 133–144. doi: 10.1016/j.immuni.2014.12.023

Wynn, T. A., Chawla, A., and Pollard, J. W. (2013). Macrophage biology in development, homeostasis and disease. *Nature* 496, 445–455. doi: 10.1038/nature12034

Xing, J., and Lu, J. (2016). HIF-1α activation attenuates IL-6 and TNF-α pathways in hippocampus of rats following transient global ischemia. *Cell. Physiol. Biochem.* 39, 511–520. doi: 10.1159/000445643

Xu, Q., Choksi, S., Qu, J., Jang, J., Choe, M., Banfi, B., et al. (2016). NADPH oxidases are essential for macrophage differentiation. *J. Biol. Chem.* 291, 20030–20041. doi: 10.1074/jbc.M116.731216

Yamashita, A., Zhao, Y., Matsuura, Y., Yamasaki, K., Moriguchi-Goto, S., Sugita, C., et al. (2014). Increased metabolite levels of glycolysis and pentose phosphate pathway in rabbit atherosclerotic arteries and hypoxic macrophage. *PLoS One* 9:e86426. doi: 10.1371/journal.pone.0086426

Yang, H., and Hultmark, D. (2017). *Drosophila* muscles regulate the immune response against wasp infection via carbohydrate metabolism. *Sci. Rep.* 7:15713. doi: 10.1038/s41598-017-15940-2

Yang, H., Kronhamn, J., Ekström, J., Korkut, G. G., and Hultmark, D. (2015). JAK/STAT signaling in *Drosophila* muscles controls the cellular immune response against parasitoid infection. *EMBO Rep.* 16, 1664–1672. doi: 10.15252/embr.201540277

Yang, W., Huang, J., Wu, H., Wang, Y., Du, Z., Ling, Y., et al. (2020). Molecular mechanisms of cancer cachexia-induced muscle atrophy (Review). *Mol. Med. Rep.* 22, 4967–4980. doi: 10.3892/mmr.2020.11608

Zanin, R. F., Braganhol, E., Bergamin, L. S., Campesato, L. F. I., Filho, A. Z., Moreira, J. C. F., et al. (2012). differential macrophage activation alters the expression profile of NTPDase and Ecto-5′-nucleotidase. *PLoS One* 7:e31205. doi: 10.1371/journal.pone.0031205

Zeng, T., Zhang, C.-L., Xiao, M., Yang, R., and Xie, K.-Q. (2016). Critical roles of kupffer cells in the pathogenesis of alcoholic liver disease: from basic science to clinical trials. *Front. Immunol.* 7:538. doi: 10.3389/fimmu.2016.00538

Zhang, D., Zheng, H., Zhou, Y., Tang, X., Yu, B., and Li, J. (2007). Association of IL-1beta gene polymorphism with cachexia from locally advanced gastric cancer. *BMC Cancer* 7:45. doi: 10.1186/1471-2407-7-45

Conflict of Interest: The authors declare that the research was conducted in the absence of any commercial or financial relationships that could be construed as a potential conflict of interest.

frontiers in Cell and Developmental Biology

REVIEW
published: 18 February 2021
doi: 10.3389/fcell.2020.624213

From Species to Regional and Local Specialization of Intestinal Macrophages

Cynthia Arroyo Portilla[1,2], *Julie Tomas*[1], *Jean-Pierre Gorvel*[1] *and Hugues Lelouard*[1]*

[1] Aix Marseille Univ, CNRS, INSERM, CIML, Marseille, France, [2] Departamento de Análisis Clínicos, Facultad de Microbiología, Universidad de Costa Rica, San José, Costa Rica

Initially intended for nutrient uptake, phagocytosis represents a central mechanism of debris removal and host defense against invading pathogens through the entire animal kingdom. In vertebrates and also many invertebrates, macrophages (MFs) and MF-like cells (e.g., coelomocytes and hemocytes) are professional phagocytic cells that seed tissues to maintain homeostasis through pathogen killing, efferocytosis and tissue shaping, repair, and remodeling. Some MF functions are common to all species and tissues, whereas others are specific to their homing tissue. Indeed, shaped by their microenvironment, MFs become adapted to perform particular functions, highlighting their great plasticity and giving rise to high population diversity. Interestingly, the gut displays several anatomic and functional compartments with large pools of strikingly diversified MF populations. This review focuses on recent advances on intestinal MFs in several species, which have allowed to infer their specificity and functions.

Keywords: intestinal immunity, macrophages, microbiota, phagocytosis, stromal microenvironment, dietary antigens, metabolites, antigen sampling

OPEN ACCESS

Edited by:
Katrin Kierdorf,
University of Freiburg, Germany

Reviewed by:
Stephen J. Jenkins,
University of Edinburgh,
United Kingdom
Guy E. Boeckxstaens,
KU Leuven, Belgium

***Correspondence:**
Hugues Lelouard
lelouard@ciml.univ-mrs.fr

Specialty section:
This article was submitted to Cell Death and Survival, a section of the journal Frontiers in Cell and Developmental Biology

Received: *30 October 2020*
Accepted: *30 December 2020*
Published: *18 February 2021*

Citation:
Arroyo Portilla C, Tomas J, Gorvel J-P and Lelouard H (2021) From Species to Regional and Local Specialization of Intestinal Macrophages. Front. Cell Dev. Biol. 8:624213. doi: 10.3389/fcell.2020.624213

INTRODUCTION

The innate immune system encompasses different defense mechanisms selected over evolutionary time and encoded in the germline, hence passed to offspring with only minor refinements. Genome sequencing has established that much of these defense systems are conserved across animal phyla, reflecting their remarkable effectiveness and versatility (Litman and Cooper, 2007). These conserved defense mechanisms include the complement system, pattern recognition receptors (PRRs), and phagocytosis. The complement system is an ancient component of immunity that likely evolved from protection of the unicellular protists to essential defense functions in the blood of vertebrates (Elvington et al., 2016). Classical PRRs, such as Toll-like receptors (TLRs), C-type lectins, NOD-like receptors (NLRs), and perforin-2/MPEG-1, are already identified in non-bilaterian animals (Traylor-Knowles et al., 2019). Phagocytosis, from ancient Greek meaning "cell eating," is typically an eukaryote-specific process that consists in the ingestion of particulate matters larger than 0.4 μm by a cell through invagination of its membrane (Mills, 2020). Inside the Eukaryota domain, plant cells are not able to phagocyte due to their rigid cell wall. In addition, no phagocytosis has been reported in fungi, with the exception of the parasitic fungus *Rozella allomycis* (Yutin et al., 2009). By contrast, protists use phagocytosis for the intake of nutrients from the environment where these unicellular organisms reside. In parasitic infections, such as

trichomoniasis, the protozoan *Trichomonas vaginalis* uses phagocytosis to ingest *Saccharomyces cerevisiae* cells, vaginal epithelial cells, leucocytes, and erythrocytes (Pereira-Neves and Benchimol, 2007). Phagocytosis involves cell membrane receptors for target recognition. Thus, the scavenger receptor cysteine-rich (SRCR) domain family of receptors is encoded in the genomes from the most primitive sponges to mammals (Dzik, 2010). Receptors for phagocytosis bind the particles either directly or via opsonins (antibodies or complement components) that enhance phagocytosis (Richards and Endres, 2017). The specialized compartment resulting from membrane invagination around the targeted material is termed phagosome (Niedergang and Grinstein, 2018). Interestingly, the soil-living amoeba *Dictyostelium discoideum* uses molecular mechanisms of phagosome maturation very similar to higher eukaryotic cells, such as macrophages (MFs) (Gotthardt et al., 2002). This efficient "digestive" system of ingested material defines the primary function around which phagocytosis extends its functional ability throughout evolution (Desjardins et al., 2005). However, despite that phagocytosis is often proposed as an evolutionarily conserved mechanism, the diversity and variability of proteins associated with phagosomes across the different eukaryotic species suggest that phagocytosis may have evolved independently several times (Yutin et al., 2009; Mills, 2020).

The kingdom Animalia is composed of multicellular eukaryotic organisms. This cellular scaling has required the acquisition of cell–cell adhesion, communication, cooperation, and specialization (Niklas, 2014). Organism size has always been considered an important factor for the evolution of multicellularity. The advantages of increased size include predator evasion, increased motility, and an increased capacity to store nutrients. Interestingly, the organism size has an impact in cellular specialization, which may evolve more easily in larger organisms (Willensdorfer, 2008). In animals, phagocytosis has extended from the nutritional function to key roles in homeostasis, such as apoptotic cell removal, tissue remodeling, and immune defense (Desjardins et al., 2005). Hartenstein and Martinez have recently reviewed the role of phagocytosis in nutrition and have compared this function of invertebrate enteric phagocytes/enterocytes with MF ability to eliminate pathogens and damaged cells (Hartenstein and Martinez, 2019). Endodermal-derived enterocytes play indeed a prominent role in the invertebrate digestive system by taking up the extracellularly pre-digested material and completing the digestive process intracellularly. By contrast, MFs are mesodermally derived motile cells that engulf and digest foreign materials and cellular detritus that threaten the integrity of the organism. Thus, phagocytosis is an ancient process that likely evolved from the feeding of phagotrophic unicellular organisms to the defense against pathogens in complex organisms. Non-nutritional-related phagocytic cells observed in invertebrate species bear different names (e.g., amoebocytes, coelomocytes, or hemocytes) depending on the hosting species, but basically they have a MF-like appearance and have, to a certain extent, comparable functions as part of the innate immune system (**Table 1**) (Buchmann, 2014). The hypothesis of a common origin for immunity and digestion is mainly based on the existence of shared components such as enzymes, receptors, signaling pathways, and cellular processes (Broderick, 2015). Thus, many of the enzymes involved in immunity play also a role in digestion (e.g., lysozymes and proteases), with specific contexts for which these functions cannot be distinguished, e.g., for animals that capture and feed on bacteria. However, an extensive transcriptomic analysis done in different phagocytic cell types across widely divergent clades was inconclusive for homology assessments (Hartenstein and Martinez, 2019). Anyhow, in immunity, bacteria internalized via phagocytosis are typically sequestered within phagolysosomes where several antibacterial strategies are used to kill and degrade them, such as compartment acidification, enzyme production and activation, and generation of reactive oxygen species (ROS). Many types of eukaryotes produce ROS, which likely represent an ancient antimicrobial strategy for targeting intracellular bacteria (Richter and Levin, 2019).

Interestingly, phagocytosis shares molecular mechanisms with autophagy, a degradative cellular process in which eukaryotic cells digest their own components (Birgisdottir and Johansen, 2020). Like phagocytosis, autophagy is an ancient highly conserved process likely to date back to the common ancestor of all eukaryotes (Duszenko et al., 2011). Like phagocytosis, autophagy likely evolved from a cellular nutrition mechanism to become a key player in cellular homeostasis and defense against pathogens. Although autophagy and phagocytosis are activated by different mechanisms, they converge on similar pathways that are regulated by shared molecules. Thus, LC3-associated phagocytosis (LAP) involves engulfment of large extracellular particles through the engagement of components of the autophagy machinery among which Beclin 1, the phosphatidylinositol 3-kinase Vps34, ATG (autophagy) family proteins, and finally LC3 (Sanjuan et al., 2007; Martinez et al., 2011, 2015). LC3 recruitment to the phagosome favors phagosome fusion with lysosomes, acidification, and ingested material degradation. LAP is involved in several phagocyte functions, such as pathogen clearance, antigen presentation by major histocompatibility complex (MHC) class II molecules, regulation of proinflammatory cytokine production and efferocytosis (Martinez, 2018).

From its earliest beginnings, the study of innate immunity has greatly benefited from works carried out on simple organisms, starting from the discovery of phagocytosis significance in starfish larva by Elie Metchnikoff to the more recent discovery of PRRs in the fruit fly by Jules Hoffman (Lemaitre et al., 1996; Hoffmann and Reichhart, 2002; Buchmann, 2014; Gordon, 2016). Indeed, these organisms combine easy genetic manipulations and phenotypic analyses with fast generation renewal and simplified cell diversity and signaling pathways including key elements conserved across species. It is therefore important to appreciate the diversity of MFs across species to have a complete picture of them. With the tissue organization of complex organisms, MFs have acquired new functions within their residence niche where they maintain strong relationships with their neighboring cells, allowing their resident tissue to function properly. In this review, we describe the nature of MFs and MF-like cells across the animal kingdom with a special focus on the intestinal tissue of

TABLE 1 | Main features of MF-like cells across species.

	Diploblastic	Platyhelminths	Nematoda	Arthropoda	Echinodermata	Vertebrates		
						Zebrafish	Birds	Mouse	Human
Representative organism	Cnidaria, Porifera	Planarian	*Caenorhabditis elegans*	*Drosophila melanogaster*	Sea urchin				
Body cavity	No	Acoelomates	Pseudocoelomates	Coelomates					
Gut formation	No	Protostomia			Deuterostomia				
Adaptive immunity		No				Yes			
Phagocyte name	Amoebocytes	Reticular cells	Coelomocytes	Plasmatocytes (different subsets)	Hemocytes/Filopodial cells/Ovoid cells	Macrophages			
Gut-specific population	No			Proventriculus	No	Yes			
Main known functions	Digestive phagocytosis Nutrient transport	Digestive and immune phagocytosis Nutrient transport MORN2-mediated antimicrobial activity	Digestive phagocytosis Fat consumption Life span extension upon starvation Metal detoxification	**Exclusive immune phagocytosis** Efferocytosis Wound healing Antimicrobial signaling IESCs proliferation Glucose homeostasis	Digestive and immune phagocytosis Encapsulation Syncytia formation	**Exclusive immune phagocytosis** Protection against infection and inflammation Microbiota shaping Th17 cells/Tregs regulation Intestinal inflammatory lymphangiogenesis	**Exclusive immune phagocytosis** Antigen uptake Protection Against invading pathogens Antimicrobial activities	**Exclusive immune phagocytosis** Multiple functions depending on their location (see **Table 2**)	

IESCs: intestinal epithelial stem cells; Tregs, regulatory T cells.

each species when data are available. We consider more precisely the local and regional specialization of MFs in the mammalian intestine and discuss recent findings highlighting their great diversity of functions from one location to another.

MACROPHAGE-LIKE CELLS OF THE DIPLOBLASTS

Living cells depend on a constant supply of energy-rich organic molecules from the environment, making the emergence of a specialized system for food digestion and nutrient absorption a crucial innovation for multicellular organisms. The most ancient division within the animal kingdom is between diploblasts and triploblasts (**Figure 1**). Diploblasts are radially symmetrical animals with two distinct germ layers: an inner layer or endoderm/gut and an outer layer or ectoderm/skin. In between these two layers, triploblasts have an additional layer: the mesoderm (Telford et al., 2015). Because of the lack of this intermediate layer, mesodermal MFs *per se* are not found in diploblasts. Instead, the gelatinous matrix (mesoglea) between both layers contains large numbers of motile amoebocytes that carry out multiple functions, the most primitive being digestion (**Table 1**). Amoebocytes ingest and digest food caught by enterocytes and transport nutrients to the other cells. Amoebocytes have been reported in the different diploblastic phyla: Cnidaria (Menzel et al., 2015), Ctenophora (Traylor-Knowles et al., 2019), and Porifera (Adamska, 2016). However, in Placozoa, a sister phylum of Cnidaria, amoebocytes have not been described, probably because these animals are mostly composed of epithelial cells (Mayorova et al., 2019). The ability to phagocyte and move in the mesoglea makes the amoebocytes very similar to mesodermal MFs. Additionally, the presence in these animals of conserved innate defense mechanisms, such as PRRs and pore-forming proteins (e.g., the MF-expressed gene 1 protein, Mpeg1), supports the participation of these amoebocytes in innate immunity (Brennan and Gilmore, 2018; Walters et al., 2020).

MACROPHAGE-LIKE CELLS IN ACOELOMATE AND PSEUDOCOELOMATE PROTOSTOMES

The triploblasts have two major branches, the Protostomia and Deuterostomia (**Figure 1**). Their names reflect the fundamentally different fates of the blastopore, the primary embryonic gut opening (Nielsen et al., 2018). In protostomes, the blastopore forms the mouth with the anus forming secondarily (protostomy = mouth first); in the deuterostomes, it is the other way around (deuterostomy = mouth second). The presence of a mouth creates an asymmetry with an anterior–posterior axis making the triploblastic condition a synonym of Bilateria. The gastrointestinal tract (GIT) displays diversified levels of complexity according to species, with the endoderm-derived one-way gut of most bilaterians being the prevailing and more specialized form (Annunziata et al., 2019).

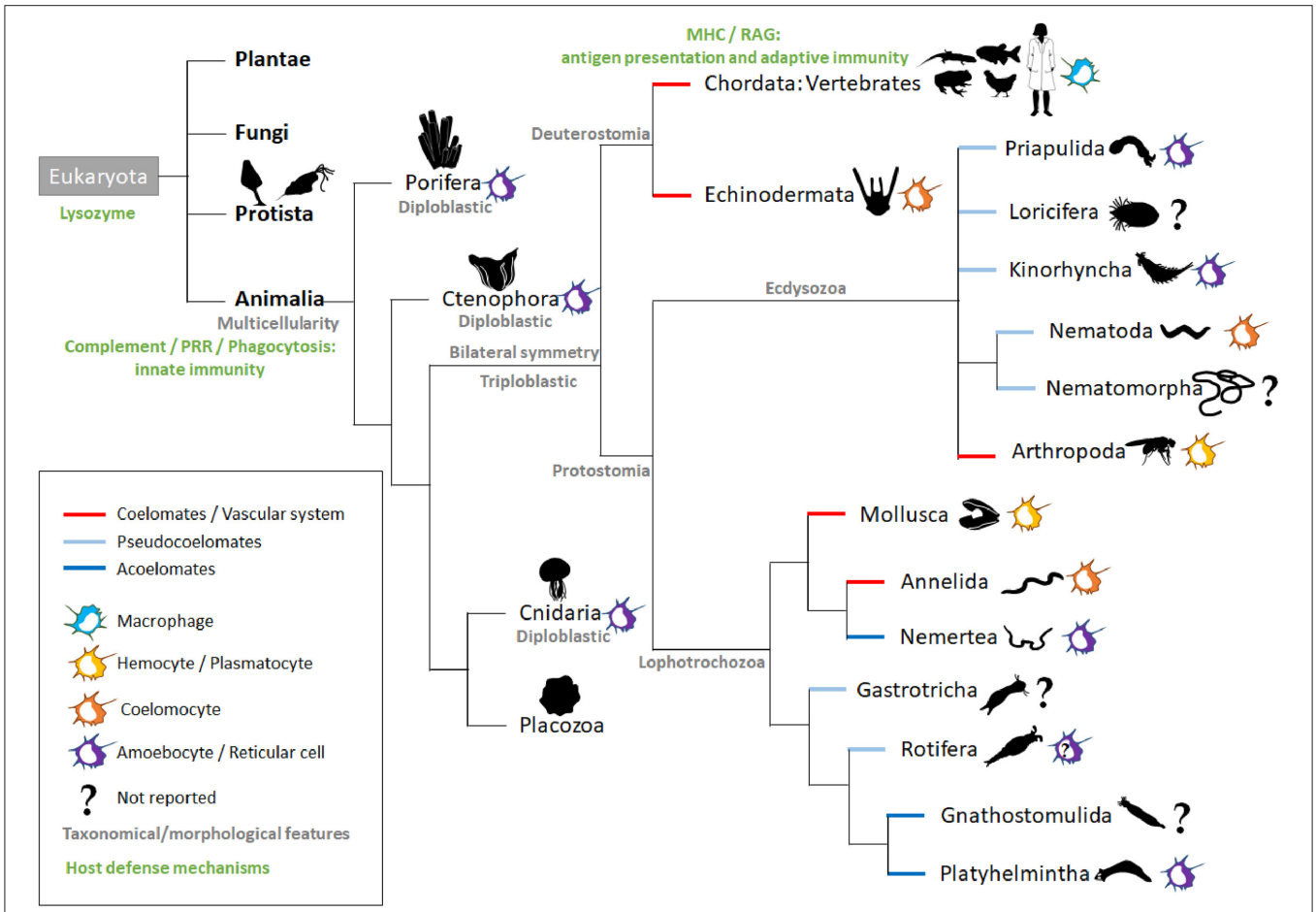

FIGURE 1 | Intestinal macrophage-like cell types across animal species. The main kingdoms (bold black) of the Eukaryota domain are listed. In animals, the representative phyla are named and ordered according to currently used phylogenetic trees (Peterson and Eernisse, 2016; Giribet and Edgecombe, 2017; Kocot et al., 2017). Additional information is added in gray (taxonomical or morphological) in green (host defense mechanisms; nutritional phagocytosis not taken into account) and by the colored lines (embryological development). For each phylum, colored icons on the right symbolize the macrophage-like cell type; the question marks indicate a lack of literature for the phylum. In Rotifera, amoebocytes have been described, but their function is more related to their motility, and there are no reports related to their immunological role (Baumann et al., 2000). MHC, Major Histocompatibility complex; PRR, pattern recognition receptors; RAG, recombination-activating gene.

The majority of invertebrates belong to Protostomia, whereas all vertebrates and few invertebrates belong to Deuterostomia (**Figure 1**). During embryonic development, if a split in the mesoderm forms a fluid-filled body cavity termed coelom, the animal is referred to as coelomate. When the space between the ectoderm and endoderm tissue layers is filled with a meshwork of mesodermal cells (or parenchyma), the animal is referred to as acoelomate. When the mesoderm has fluid-filled clefts in this meshwork, the animal is then termed pseudocoelomate (Monahan-Earley et al., 2013). Acoelomates and pseudocoelomates are found only in Protostomia (**Figure 1**). By contrast, coelomates are found in both lineages. In several invertebrate phyla, motile MF-like cells in the parenchyma or coelom take up cellular debris resulting from dying cells and actively distribute digested foodstuffs, receiving this material from enteric phagocytes lining the gut (Hartenstein and Martinez, 2019).

The acoelomate protostomes obtain their oxygen and food by simple diffusion across the skin and gut and throughout the intercellular medium. Freely moving reticular cells have been observed in the parenchyma of the platyhelminths (flatworms) (Morita, 1995). These reticular cells are mesenchymal cells that play an important role in nutrient transportation and phagocytosis of foreign material, acting as an immune surveillance system (**Table 1**). Planarian platyhelminth antimicrobial activities involve an orthologous protein for MORN2, which has been associated with LAP and resistance to bacterial infection in human MFs (Abnave et al., 2014). In Nemertea, amebocytes arising from the intestinal segment were reported to play a central role in graft rejection (Langlet and Bierne, 1984). To our knowledge, there are no reports on the presence of MF-like cells in gnathostomulids.

In pseudocoelomates, the pseudocoelomic fluid serves as the circulatory system for nutrients that are taken up, ingested,

degraded, and secreted into the pseudocoelom by the intestinal cells. We did not find any report of MF-like cells in the phyla Gastrotricha, Nematomorpha, and Loricifera. However, in Rotifera, the pseudocoelom of several taxa contains free motile amoeboid cells, but so far, no immune function has been reported for these cells (Baumann et al., 2000). By contrast, phagocytically active amoebocytes have been observed in Priapulida (Mattisson and Fänge, 1973) and Kinorhyncha (Neuhaus and Higgins, 2002). For Nematoda, the cells contained in the pseudocoelomic fluid are termed coelomocytes. *Caenorhabditis elegans* is a simple and genetically tractable nematode model that has enabled key advances in immunity (Willis et al., 2020). However, there is no evidence that their coelomocytes provide a potent defense against bacterial infection (**Table 1**). These six oblong MF-like scavenger cells located in the *C. elegans* body cavity are indeed dispensable to the viability and survival of the worm (Fares and Greenwald, 2001). Nevertheless, studies of *C. elegans* coelomocytes identified novel components of the endocytic machinery that are conserved in mammals (Fares and Greenwald, 2001; Sato et al., 2014). Moreover, *C. elegans* coelomocytes have been shown to regulate fat consumption and life span extension upon starvation (Buis et al., 2019). Finally, they participate in metal detoxification (Tang et al., 2020). Interestingly, old studies performed in another nematode, *Ascaris suum*, have documented the encapsulation of bacteria by coelomocytes (Bolla et al., 1972).

MACROPHAGE-LIKE CELLS IN COELOMATE PROTOSTOMES WITH AN OPEN CIRCULATORY SYSTEM

The advantage of a true coelom is the ability of the inner mesenteric layer to suspend the central gut in the middle of the animals, allowing them to increase their body size. In addition, a circulatory system helps size increase by reducing the functional diffusion distance of nutrients, gases, and metabolic waste products. In animals that have evolved coelom along with a vascular system, cells with the characteristics of MFs are prominent among the circulating cells, commonly referred to as coelomocytes or hemocytes (Hartenstein, 2006). During development, they represent the professional MFs that eliminate apoptotic cells. In addition, they cooperate with humoral factors to battle invading parasites and microbes, many of which enter through the digestive tract.

Blood vascular systems follow one of two principal designs: open or closed. In open circulatory system, the blood, referred to as hemolymph, empties from a contractile heart and major supply vessels into the body cavity termed hemocoel, where it directly bathes the organs. This occurs in arthropods and non-cephalopod molluscs.

In Arthropoda, the fruit fly *Drosophila melanogaster* has been widely used as a suitable model to study innate immunity and has provided invaluable contributions to the knowledge of innate immune system signaling pathways (Hoffmann and Reichhart, 2002). In *D. melanogaster*, hematopoiesis does not occur in adult but only during development through two waves (Wood and Martin, 2017; Banerjee et al., 2019; Sanchez Bosch et al., 2019). The first wave occurs in the embryo and gives rise to hemocytes that proliferate during the larval stages. The second wave of hematopoiesis occurs at the larval stage in an organ called the larval lymph gland. MF-like cells termed plasmatocytes represent about 95% of the total hemocyte population in adult. A single-cell transcriptome of hemocytes made it possible to characterize different subsets of plasmatocytes (ranging from 4 to 12 depending on the study), showing an interesting parallel with the great diversity of MFs in mammals (Cattenoz et al., 2020; Cho et al., 2020; Fu et al., 2020; Tattikota et al., 2020). Although the precise functions of each of these subsets remain to be established, plasmatocytes globally serve essential roles in immune response to infection and wound healing (**Table 1**). While lack of plasmatocytes does not impair fruit fly development, it indeed induces a strong susceptibility to infections by various microorganisms, due notably to an absence of phagocytosis in deficient fruit flies (Charroux and Royet, 2009). Plasmatocytes do not only patrol the body in the circulation but also associate with specific tissues, such as the intestinal epithelium. In the *D. melanogaster* model, the intestine is composed of three main parts: the foregut, the midgut, and the hindgut. The fore- and hindgut have an ectodermal origin, whereas the midgut, which is the functional equivalent of the mammalian small intestine (SI), has an endodermal origin. Plasmatocytes of embryonic origin specifically colonize a region at the foregut/midgut junction known as the proventriculus, where they form a discrete group of functional MFs able to phagocytose both apoptotic bodies and bacterial intruders (Charroux and Royet, 2009; Zaidman-Rémy et al., 2012). Plasmatocytes circulating in the hemolymph can also infiltrate the midgut when necessary (Ayyaz et al., 2015). In addition to their phagocytic activity, plasmatocytes relay intestinal infection-induced oxidative stress signal and nitric oxide production to the fat body, an organ equivalent to the vertebrate liver, which produces an antimicrobial peptide response (Wu et al., 2012). Like mammal MFs, plasmatocytes switch their metabolic program to aerobic glycolysis in order to mount an efficient antibacterial response (Krejčová et al., 2019). Upon injury, circulating plasmatocytes release the cytokines of the unpaired (Upd) family Upd2 and Upd3, which by retrospective alignments of type I cytokines and functional analogies are most closely related to the vertebrate leptins (Rajan and Perrimon, 2012; Beshel et al., 2017). These cytokines bind to the receptor Domeless that activates the JAK-STAT pathway in the fat body and in the gut, where it stimulates intestinal stem cell proliferation, thereby contributing to fly survival (Chakrabarti et al., 2016).

In bivalve molluscs, the distribution of blast-like cells suggests that hematopoiesis may be widespread in connective tissue, with further development of hemocytes in the hemolymph (Hine, 1999). Two main sub-populations of hemocytes have been identified: granulocytes containing many cytoplasmic granules and hyalinocytes containing few or no granules (Girón-Pérez, 2010). Granulocytes are the main cell type involved in the cellular immune defense of bivalves (Rolton et al., 2020). They are also involved in other physiological functions, such as wound healing and shell repair, digestion, and transport of nutrients. Indeed, in the gut lumen, hemocytes ingest and digest foreign materials and

transport the digested materials to the gut lining or other tissues. In addition to this digestive function, hemocytes can engulf and phagocytize foreign pathogens present on the mucosal surfaces of oysters as part of their innate immune functions. Hemocytes routinely traffic between the hemolymph and the outer surfaces of oysters (Provost et al., 2011).

MACROPHAGE-LIKE CELLS IN COELOMATE PROTOSTOMES WITH A CLOSED CIRCULATORY SYSTEM

Closed circulatory systems occur in a wide variety of invertebrates including annelids, cephalopods, and non-vertebrate chordates. Earthworms, which are the best known of all annelids, belong to the class Oligochaeta. Their gut surface is in permanent contact with ingested soil. Moreover, the nephridia and dorsal pores enable microorganisms to enter the coelomic cavity. Hence, both coelom and gut interact with naturally occurring soil microorganisms and have to face strong antigenic environment (Prochazkova et al., 2020). The free circulating immune cells of the coelomic cavity, termed coelomocytes, can be subdivided into two subpopulations, the eleocytes and the amoebocytes (Engelmann et al., 2016). Eleocytes are highly autofluorescent cells due to their large granules termed chloragosomes that contain riboflavin. Eleocytes originate from the chloragogen tissue surrounding the gut and are considered as the terminal differentiation stage of sessile chloragocytes released from this tissue. They have mainly accessory functions such as maintenance of pH and storage of glycogen and lipids. By contrast, amoebocytes are MF-like cells with a broad range of defense functions, including phagocytosis (Engelmann et al., 2016). Two types of amoebocytes have been described, hyaline and granular amoebocytes, without clear separate functions. PRRs [coelomic cytolytic factor (CCF) and lipopolysaccharide (LPS)-binding protein (LBP)] and the TLR signaling pathway molecule Myd88 genes are typically expressed by amoebocytes but not eleocytes, supporting the role of amoebocytes in pathogen detection and neutralization (Bodó et al., 2018). Moreover, amoebocytes express higher levels of the oxidative stress-related super oxide dismutase and antimicrobial lysozyme and lumbricin genes (Bodó et al., 2018). Dermal contact with immunostimulants decreases coelomocyte total number but increases the proportion of granular amoebocytes among them and induces ROS production (Homa et al., 2013, 2016). Experimental microbial challenge triggers the release of phagocytic coelomocytes from the mesenchymal lining of the coelom and thus increases the defense reaction in the coelomic cavity of earthworms (Dvorák et al., 2016).

MACROPHAGE-LIKE CELLS IN INVERTEBRATE DEUTEROSTOMES

Deuterostomes include two main phyla: Echinodermata and Chordata (**Figure 1**). In echinoderms, the circulating immune cells, i.e., the coelomocytes, are heterogeneous in morphology, size, relative abundance, and functions. This makes a single standard classification for all echinoderms a difficult task. The distribution of these cell types is also highly variable among species and even at the individual level (Smith et al., 2018). Nevertheless, phagocytes are present in all echinoderm classes and are the main effectors of the echinoderm immune system. These phagocytes respond to immune challenges through phagocytosis, encapsulation, syncytia formation, and expression of complement components (Golconda et al., 2019).

The sea urchin larva has five major types of immune cells that populate the body cavity (blastocoel), including two phagocytic cell types termed filopodial and ovoid cells (**Table 1**) (Ho et al., 2017). Filopodial cells extend long filopodia that form a reticular network in the blastocoel (Buckley and Rast, 2019). They are likely the MF-like cells observed by Elie Metchnikoff in his seminal works on phagocytosis. Ovoid cells are rarely present at steady state but rapidly appear upon immune challenge and could therefore represent an activation state of some of the filopodial cells. Upon sea urchin larva gut disturbance through the presence of pathogenic bacteria in the seawater, a coordinated immune response takes place (Ho et al., 2017). A subset of immune cells termed pigment cells rapidly migrates from the ectoderm to the gut epithelium where they secrete their antibacterial iron chelator pigment echinochrome A (Ho et al., 2017; Coates et al., 2018). Then, the number and duration of cell–cell interactions among immune cells and with the gut epithelium increase (Ho et al., 2017). Finally, filopodial cells quickly phagocytose bacteria that penetrate the blastocoel of larvae. This coordinated immune response is at least in part launched by secretion of IL-17 family members by gut epithelial cells (Buckley et al., 2017).

VERTEBRATE MACROPHAGES

The phylum Chordata consists of three subphyla: Urochordata, Cephalochordata, and Vertebrata. Vertebrates possess non-phagocytic enterocytes, and a clear dichotomy is made at this level between the digestive and immune function of phagocytosis (Hartenstein and Martinez, 2019). Moreover, vertebrates have evolved adaptive immunity that can recognize and respond to specific antigen determinants thanks to the somatic DNA rearrangement of segmental elements encoding the antigen binding regions of their T and B cell receptors (Cooper and Alder, 2006). Together with adaptive immunity appears a new type of mononuclear phagocytes termed dendritic cells (DCs). DCs make the link between innate and adaptive immunity by initiating and controlling antigen-specific immunity through presentation of antigenic epitopes on MHC class I and class II molecules (Banchereau and Steinman, 1998). Therefore, the vertebrate mononuclear phagocyte system comprises monocytes, MFs, and DCs, as well as their lineage-committed progenitors (Guilliams et al., 2014). The intestinal immune system of vertebrates comprises a unique array of innate and adaptive immune cells. Along the intestinal tract, immune cells are either disseminated throughout the mucosa forming a diffuse distribution or clustered in organized lymphoid tissues. The latter, termed organized gut-associated lymphoid tissues (GALT), initiate the intestinal immune response. Organized GALT have

been reported in their simplest forms in all classes of vertebrates but are especially well-developed in the endotherms, mainly mammals and birds.

The bone marrow is the hematopoietic organ in all vertebrates except some amphibians in which hematopoiesis can also occur in the liver and fishes in which hematopoiesis occurs only in the kidney. Fishes are the most primitive animals in which an adaptive immunity is present. In zebrafish, the first embryonic MFs originate from the mesoderm and migrate over the yolk ball before colonizing other tissues, whereas in adults, myeloid-lineage progenitors arise from the kidney (Stachura and Traver, 2011). MFs and DCs are especially abundant in the spleen and gut (Wittamer et al., 2011). In the adult zebrafish, the gut can be divided following the anterior–posterior axis into seven segments, from the proximal S1 to the most distal S7 (Wang et al., 2010). Each segment exhibits functional differences and also similarities to the mammalian GIT; e.g., the S7 represents the colon-like region (Wang et al., 2010; Lickwar et al., 2017). Distribution of MFs and DCs along these segments and the ability of these phagocytes to sample luminal antigens depending on their location have not been determined so far. Interestingly, Interferon Regulatory Factor 8 (IRF8) depletion leads to a lack of MFs during embryonic development with only partial recovery in adults (Li et al., 2011; Shiau et al., 2015; Ferrero et al., 2020). Thus, brain and gut resident MFs remain strongly impacted by IRF8 deficiency (Earley et al., 2018). Importantly, like in mammals, intestinal MFs are required for shaping the gut microbiota, and dysbiosis occurs in MF-deficient zebrafish (**Table 1**) (Earley et al., 2018). In addition, IRF8-dependent MFs are the main producers of the complement C1q genes in the intestine (Earley et al., 2018). Zebrafish intestinal MFs show other similarities with their mammal counterparts. Thus, like in mouse and human, $CD4^+$ MFs and regulatory T (Treg) cells reside in the zebrafish gut mucosa (Dee et al., 2016). Moreover, microbiota and inflammation promote G-protein-coupled receptor 35 expression in mouse and zebrafish intestinal MFs, which have a protective role during intestinal inflammation by inducing TNF synthesis upon lysophosphatidic acid binding (Kaya et al., 2020). Finally, like in mammals, intestinal inflammation entails infiltration into the gut mucosa of inflammatory MFs, which elicit a Th17 cell response together with a decrease of Treg cells (Coronado et al., 2019). Moreover, in a zebrafish colitis model, MFs promote intestinal inflammatory lymphangiogenesis via their vascular endothelial growth factor gene expression (*vegfa*, *vegfc*, and *vegfd*), highlighting the potential of the zebrafish model to investigate the mechanism of lymphangiogenesis in inflammatory bowel diseases (IBDs) (Okuda et al., 2015).

Amphibians rely heavily on MFs not only for immune defense but also for homeostasis and tissue remodeling/resorption. Most of the literature on amphibian MFs is related to programmed cell death and tissue remodeling during metamorphosis (Grayfer and Robert, 2016). Hematopoiesis of primitive and mainly aquatic amphibian species occurs in the liver, whereas hematopoiesis of more terrestrial amphibian species occurs in the bone marrow (Grayfer and Robert, 2016). In the frog *Xenopus laevis*, the principal site of hematopoiesis is still the liver subcapsular region, but myelopoiesis, i.e., the differentiation of the granulocyte MF precursor (GMP) into granulocytes and MFs, occurs in the bone marrow (Grayfer and Robert, 2013; Yaparla et al., 2016). Precursors with GMP potential migrate from the liver to the bone marrow under the influence of chemokines enriched in the bone marrow, such as CXCL12 (Yaparla et al., 2019). MF differentiation is controlled through binding of the main MF growth factor, colony-stimulating factor-1 (CSF1) to its CSF1 receptor (CSF1R), which is almost exclusively expressed on committed MF precursors (Grayfer and Robert, 2016). IL-34 is as an alternative CSF1R ligand, giving rise to morphologically and functionally distinct MFs (Yaparla et al., 2020). Unfortunately, to our knowledge, the literature on amphibian intestinal MFs consists mainly of old descriptive studies. Lymphoid aggregates resembling mammalian isolated lymphoid follicles (ILFs) have been observed in the urodele amphibians (Ardavín et al., 1982). In these structures, the number of goblet cells decreases, and lymphoid cells, including MFs, penetrate the intestinal epithelium. In the gut lamina propria of toads, MFs tend to cluster and interact with lymphocytes and plasma cells (Chin and Wong, 1977).

Most studies on reptile immune function have focused on systemic immune responses, leaving an important knowledge gap in the mucosal immune responses. Indeed, literature on reptile intestinal immunity consists mainly of descriptive studies (Borysenko and Cooper, 1972; Zapata and Solas, 1979; Solas and Zapata, 1980; Ashford et al., 2019). Reptiles possess primary lymphoid organs such as bone marrow and thymus but lack secondary lymphoid tissues such as Peyer's patches (PPs) or mesenteric lymph nodes (MLNs). Instead, numerous ILF-like lymphoid aggregates are located throughout the small and large intestines. These aggregates are enriched in small lymphocytes and MFs (Borysenko and Cooper, 1972; Zapata and Solas, 1979; Solas and Zapata, 1980; Ashford et al., 2019). MFs are dispersed in the lamina propria but can migrate to the intestinal epithelium in these lymphoid aggregates (Solas and Zapata, 1980). Interestingly, the number of lymphoid aggregates in the SI of poikilothermic snakes depends on the season, diminishing in spring and summer (Solomon et al., 1981). Moreover, temperature can affect functions of lizard MFs, which have an optimal phagocytic activity at 25°C (Mondal and Rai, 2001). In reptiles, the enteropathogenic bacteria *Salmonella enterica* colonize the intestinal tract without any signs of disease, but MFs seem not to be involved in this protection since *S. enterica* is able to kill turtle MFs (Pasmans et al., 2002).

Like mammals, birds have a well-developed mucosal immune system, with several organized GALT. They include the primary lymphoid organ termed bursa of Fabricius and several secondary lymphoid organs, namely, PPs, cecal tonsils, and Meckel's diverticulum (Casteleyn et al., 2010). The chicken gut lamina propria contains various innate immune cells such as heterophils (the avian polymorphonuclear cells), natural killer cells, DCs and MFs, although the differences between the latter two have not been carefully assessed (Broom and Kogut, 2018). Chicken MFs/DCs display a range of PRRs, expression of MHC class II, and phagocytic and antimicrobial activities. Like in mammals, early-life microbial colonization is critical for the immunological maturation of the avian gut, and short early-life antibiotic

treatment induces alteration of mucosal gene expression and a decrease of MF number in the gut lamina propria for at least 2 weeks (Schokker et al., 2017). In chicken duodenum, jejunum, and ileum, MFs/DCs are involved in antigen uptake and provide protection against invading pathogens (**Table 1**) (Taha-Abdelaziz et al., 2020). During coccidiosis, MFs are the principal cell type involved in the clearance of the sporozoites by phagocytosis (de Geus and Vervelde, 2013). During *Salmonella* infection, resistance depends on a genetic locus *SAL1* and has been linked to MFs with better oxidative killing activity and greater and faster expression of proinflammatory cytokines (Wigley, 2014). During dextran sulfate sodium (DSS)-induced intestinal inflammation, increased monocyte/MF infiltration occurs in all segments of laying hen intestine (Nii et al., 2020).

In mammals, embryonic MFs initially originate from yolk sac erythro-myeloid progenitors (Hoeffel and Ginhoux, 2018). Subsequently, early hematopoietic stem cells (HSCs) settle first in the fetal liver and later in bone marrow to form a permanent, self-renewing source of monocytes. Monocytes infiltrate tissues and can replace and differentiate into tissue-resident MFs to varying degrees depending on the organs and the encountered immune challenges, with most MFs keeping an embryonic origin and self-renewal (Hoeffel and Ginhoux, 2018; Liu et al., 2019). Importantly, MF renewal by monocytes is especially prevalent in the intestine, which is always subject to antigenic stimulation whether through food, drink, or microbiota (Bain et al., 2014). In rodents and in human, the GIT is complex and divided longitudinally from the duodenum to the rectum, with functional and morphological distinctions between the small (duodenum, jejunum, and ileum) and large (cecum and proximal and distal colon) intestines (Mowat and Agace, 2014). The SI is specialized in the absorption of nutrients, whereas the primary function of colon is the absorption of water and electrolytes. The SI has villi that increase its surface of exposure to the intestinal lumen content, a thinner and less well-organized mucus layer, and reduced microbial communities than the colon. Mammalian MFs can fulfill the auxiliary functions necessary for the homeostasis of each tissue of residence, such as peristaltic movements and tolerance induction toward dietary and microbiota-derived antigens in the intestine. In the recent years, single-cell RNA sequencing associated with high-resolution confocal microscopy, multiparameter flow cytometry, and functional assay analyses have allowed to reveal unsuspected aspects of the local and regional specialization of MFs in mouse and human intestine as discussed below and shown in **Table 2**.

TELL ME WHERE YOU LIVE AND I WILL TELL YOU WHAT KIND OF MACROPHAGE YOU ARE

We have seen that across species, specialized cells assume at least one of the main activities of what we call MF in vertebrates: phagocytosis. These cells show a remarkable plasticity according to their local microenvironment, i.e., the network of factors and cells with which they interact. With the increasing complexity of tissue functions occurring during the metazoan evolution, these cells have diversified even more and have acquired dedicated functions to offer protection and to sustain activity of their tissue of residence.

The specific stromal microenvironment that surrounds HSCs in the bone marrow has been identified decades ago as niches indispensable for the maintenance and differentiation of HSCs (Morrison and Scadden, 2014). However, it is only very recently that this concept of niche has been fully appreciated for peripheral tissues, especially for MF identity imprinting (Gosselin et al., 2014; Lavin et al., 2014; van de Laar et al., 2016). Two recent reviews have described how this local microenvironment is now crucial to be considered in order to better characterize and understand the functions of tissue-resident MFs (Blériot et al., 2020; Guilliams et al., 2020). Nowadays, studies dedicated to the conditioning of MFs by their local microenvironment are mainly developed in human and mouse in which a unique MF transcriptional program seems to correspond to each specific niche of the intestine (Bujko et al., 2018; De Schepper et al., 2018; Kang et al., 2020). Since phagocytic cells interact with and react to external factors and neighboring stromal and immune cells whatever the species considered, we however assume that this concept can be widely extended to other species.

In the following parts, we detail how intestinal MF identity and functions are impacted by their niche of residence. We particularly focus on the (re)categorization of the MFs according to their anatomical location within the intestinal mucosa (**Table 2**). We also consider the strong influence of two exogenous factors inseparable from the intestine, the intestinal microbiota and the dietary antigens.

A (Re)Categorization of Intestinal Macrophages by Their Radial Distribution and Local Compartmentalization: Protecting and Supporting Your Immediate Neighbors

Most intestinal MFs along the GIT share some common functions, such as the phagocytosis of microorganisms and dead cells. They also share some common specific markers, such as CX_3CR1 and F4/80 in mouse and CD14 and CD16 in human (Bain et al., 2013; Bujko et al., 2018). In addition, in both species, intestinal MFs express CD64, CD163, and MerTK. At the exception of immune inductive sites such as PPs as discussed later, gut MFs display anti-inflammatory properties at steady state. They indeed weakly respond to many different innate stimulations, constitutively express IL-10 and its receptor, participate in Treg cell expansion, and protect from colitis (Hadis et al., 2011; Bain et al., 2013; Shouval et al., 2014; Zigmond et al., 2014). According to their anatomical location, intestinal MFs interact with specific cells and detect and respond to specific factors that make them crucial support units of their microenvironment. In turn, the latter is decisive for MF recruitment and differentiation in relation to the different anatomic layers of the intestine. Therefore, from the serosa to the epithelium, MFs are territorialized to accomplish specific functions (**Table 2**).

TABLE 2 | Local and regional specialization of intestinal macrophages in human and mouse.

		Location	Name	Main neighbors	Main functions	Species	Key markers	References
Radial specialization	Effector sites: Villus and colonic MFs	Subepithelial SI and colon	LPM	IECs fibroblastic cells Immune cells	Antigen sampling Tissue protection and repair Treg and Th17 cell equilibrium	Mouse Human	CD64, CX_3CR1, F4/80, MerTK CD14, CD16, CD64, MerTK, CD163	Tamoutounour et al., 2012; Bain et al., 2013 Bujko et al., 2018
		Perivascular SI and colon	Perivascular MF	Endothelial cells	Regulation and strengthening of the vasculature Bacterial translocation blockade Systemic antigen uptake	Mouse	CX_3CR1, CD169, CD206	De Schepper et al., 2018; Honda et al., 2020; Kang et al., 2020
		Crypt base SI and colon	Crypt base-associated MF	$Lgr5^+$ epithelial stem cells Paneth cells	Maintain the renewal of the SI crypts Promote the crypt regenerative response Inflammatory monocyte recruitment	Mouse	CSF1R/CD115, CD169, CD206	Pull et al., 2005; Asano et al., 2015; Sehgal et al., 2018; Kang et al., 2020
		Submucosa/muscularis	Muscularis MF	Enteric neurons Smooth muscle cells	Smooth muscle contraction and Peristaltism Tissue-protective	Mouse Human	CX_3CR1, MHC-II, BPM2, β2 AR CD14, CD11b, CD209	Muller et al., 2014; Gabanyi et al., 2016; De Schepper et al., 2018 Bujko et al., 2018
	Inductive sites: Peyer's patch MFs	Subepithelial dome Upper follicle	$TIM\text{-}4^-$ LysoMac	FAE/M cells $RANKL^+$ stromal cells DCs, B and T cells	Uptake of particulate antigens Innate defense Apoptotic IEC removal	Mouse Human	MerTK, CX_3CR1, lysozyme, CD4 Lysozyme, CD11c, SIRPα	Bonnardel et al., 2015 Wagner et al., 2020
		Interfollicular regions Lower follicle	$TIM4^+$ LysoMac	T cells	Apoptotic T cell removal	Mouse Human	MerTK, CX_3CR1, CD4, TIM-4 Lysozyme, TIM-4	Bonnardel et al., 2015 Wagner et al., 2020
		Germinal center	Tingible body MF	B cells	Apoptotic B cell removal	Mouse Human	MerTK, CX_3CR1, CD4, TIM-4 Lysozyme, TIM-4	Bonnardel et al., 2015 Wagner et al., 2020
		Submucosa/muscularis externa	Serosal/muscularis MF	?	?	Mouse Human	MerTK, CX_3CR1, TIM-4 Lysozyme, TIM-4, CD163	Bonnardel et al., 2015 Wagner et al., 2020
Gut segment specialization	Antigen-inducible sampling mechanisms	SI lumen	Luminal MF	IECs	Immune exclusion by pathogen capture (*Salmonella* Typhimurium)	Mouse	CD11c, CX_3CR1, F4/80	Man et al., 2017
		Distal ileum	TED^+ LPM	IECs	Pathogenic bacteria uptake (*Salmonella* Typhimurium)	Mouse	CX_3CR1, CD11c, CD11b	Niess et al., 2005
		Peyer's patches	TMD^+ LysoDC	M cells	Pathogenic bacteria uptake (*Salmonella* Typhimurium)	Mouse	CX_3CR1, lysozyme, CD11c	Lelouard et al., 2012; Bonnardel et al., 2015; Wagner et al., 2020
		Distal colon	$BLPs^+$ LPM	IECs	Fluid sampling and fungus toxin detection IECs protection by regulating fluid absorption	Mouse	CD11c, CD11b, MHCII, F4/80, CX_3CR1, CD64	Chikina et al., 2020
	Adaptive immune responses	Distal ileum	LPM	?	Antigen-specific Th17 cells induction in response to SFB ileum colonization	Mouse	CD64, CSF1R	Panea et al., 2015
		Colon	LPM	?	Induction of Th17 cells and antibodies in response to fungus colon colonization Immune surveillance and maintenance of a balanced colonic fungal community	Mouse Human	CX_3CR1	Leonardi et al., 2018

SI, small intestine; MF, macrophages; LPM, lamina propria MF; DC, dendritic cells; IECs, intestinal epithelial cells; FAE, follicle-associated epithelium; TED, trans-epithelial dendrite; TMD, trans-M cell dendrite; BLP, balloon-like protrusion; SFB, segmented filamentous bacteria; CSF1R, colony-stimulating factor-1 receptor; β2 AR, β2 adrenergic receptor; ?, unknown.

Two main categories of MFs are present in the small and large intestines of mammals: *lamina propria* MFs (LPM) and muscularis MFs (MM) (Hume et al., 1984; Mikkelsen, 1995). LPM can be further subdivided into mucosal and submucosal LPM with different life span, transcriptional program, and functions (De Schepper et al., 2018). Mucosal LPM from the SI to the colon line the intestinal epithelium on the one hand and the vasculature on the other hand (Niess et al., 2005; Chieppa et al., 2006; Chikina et al., 2020; Honda et al., 2020). Mucosal subepithelial LPM are thus strategically positioned to sample luminal antigens and to protect the mucosa from enteropathogens that can penetrate the epithelial barrier. In the mouse SI, the pathogenic bacteria *Salmonella* Typhimurium induce the formation of paracellular transepithelial dendrites by subepithelial LPM, allowing them to capture bacteria directly from the lumen (Niess et al., 2005; Chieppa et al., 2006). In accordance with their bacteria-inducible nature, LPM transepithelial dendrites occur more frequently where bacteria are abundant, i.e., at the tip of villi of the terminal ileum rather than in other parts of the SI (Niess et al., 2005; Chieppa et al., 2006). Whether LPM transepithelial dendrites represent an important mechanism of antigen sampling that could occur in absence of pathogenic bacteria remains under debate (McDole et al., 2012). *Salmonella* Typhimurium induce also the migration of mouse subepithelial LPM into the gut lumen to participate in the immune exclusion of the bacteria from the gut (Arques et al., 2009; Man et al., 2017). Importantly, both transepithelial dendrites and luminal migration are dependent on CX_3CR1 expression by subepithelial LPM and on MyD88-dependent TLR signaling by intestinal epithelial cells (Chieppa et al., 2006; Arques et al., 2009; Man et al., 2017). Whether these partial (dendrites) or complete (luminal migration) transepithelial passages occur in human has yet to be established, especially since CX_3CR1 expression by human intestinal LPM is reduced as compared with that in mice (Bujko et al., 2018). Nevertheless, a missense mutation in the *CX3CR1* gene has been identified in Crohn's disease patients and was linked to an inefficient antifungal response (Leonardi et al., 2018). This suggests that CX_3CR1 is at least important in human for the control of the fungi gut community. Unlike conventional DC, mucosal LPM are unable to migrate into the gut-draining MLNs to present pathogen-derived antigens and prime naïve T cells (Schulz et al., 2009; Bravo-Blas et al., 2019). Nevertheless, they can transfer antigens via gap junctions to neighboring conventional DC that can in turn express CCR7, migrate to the MLNs, and prime naïve T cells (Mazzini et al., 2014). Mucosal conventional DC can also acquire soluble and particulate antigens directly from the lumen through several mechanisms (McDole et al., 2012; Farache et al., 2013), raising the question of the real contribution of MFs to the provision of antigens for antigenic presentation.

Another subpopulation of CX_3CR1^+ mucosal and also submucosal LPM is closely associated to the intestinal vasculature in mice (De Schepper et al., 2018; Honda et al., 2020). Perivascular LPM are either self-maintaining throughout adulthood, especially submucosal ones, or replaced by monocytes on a regular basis, especially mucosal ones (De Schepper et al., 2018). The full maturation of the latter from $Ly6^{hi}$ monocytes is ensured by the microbiota and by the transcription factor NR4A1, a master regulator of the conversion of $CCR2^{hi}CX_3CR1^{int}Ly6C^{hi}$ into $CCR2^{lo}CX_3CR1^{hi}Ly6C^{lo}$ monocytes (Honda et al., 2020). Mucosal perivascular LPM form tight interdigitating connections around all of the vasculature of both SI and colon by which they prevent bacteria translocation into the blood circulation (Honda et al., 2020). Therefore, both subepithelial and perivascular mucosal LPM are fully equipped to prevent penetration of pathogens through epithelial and vascular barriers, offering thus a double defensive line. By contrast, submucosal perivascular LPM are distant from the lumen, the microbiota, and potential pathogens. They acquire a transcriptional profile in relation to their niche, including angiogenesis-related genes, and are necessary for the repair and strengthening of the vasculature since lack of perivascular LPM disturbs the vasculature morphology and induces particle leakage from the blood (De Schepper et al., 2018).

At the base of SI and colonic crypts, a specific subset of submucosal LPM expressing CD169 is tightly associated with the epithelial stem cell niche (Pull et al., 2005; Hiemstra et al., 2014; Asano et al., 2015; Sehgal et al., 2018) (**Table 2**). In the SI, depletion of these stem cell niche-associated LPM following CSF1R blockade induces a defect in Paneth cell differentiation and a reduction in $LGR5^+$ intestinal stem cell numbers (Sehgal et al., 2018). This leads to reduced epithelial proliferation and imbalanced intestinal epithelial cell ratio, notably favoring goblet cells. Therefore, stem cell niche-associated LPM are crucial in the appropriate differentiation of SI epithelial cells. Surprisingly, in the colon, *Csf1*-deficient *op/op* mice with strong LPM depletion show normal colonic crypt morphology, suggesting that unlike SI, colon stem cell niche-associated LPM are not essential to maintain the colonic stem cell niche (Cecchini et al., 1994). Nevertheless, during injury, the colonic stem cell niche-associated LPM are essential to promote the regenerative response, i.e., the proliferation and the survival of colonic epithelial progenitors (Pull et al., 2005). Similarly, in fruit fly, plasmatocytes induce stem cell proliferation in the intestine in response to wounding via their secretion of Upd2 and Upd3 (Chakrabarti et al., 2016). Therefore, as for mouse stem cell niche-associated LPM, fruit fly plasmatocytes can be tightly associated with the intestinal epithelium and can play a major role in tissue repair, highlighting a highly conserved mechanism of cooperation between phagocytes and gut epithelial stem cells.

In mammals, MM display either bipolar (circular muscle and deep muscular plexus MM) or stellate (serosal and myenteric MM) shapes and are closely associated with smooth muscles and enteric neurons of the muscularis externa, distant from any luminal stimulation (Mikkelsen, 1995; Phillips and Powley, 2012). Accordingly, MM display a gene expression profile associated with tissue protection and neuronal development (Gabanyi et al., 2016; De Schepper et al., 2018). MM play a major role in regulating intestinal peristalsis by producing BMP2 and PGE2, which act on enteric neurons and smooth muscles, respectively (Muller et al., 2014; Luo et al., 2018). In addition, MM play a neuroprotective role by limiting infection-induced neuronal loss through an adrenergic/arginase 1/polyamines axis (Matheis et al., 2020). The development of MM is ensured

by CSF1 produced by their associated enteric neurons (Muller et al., 2014). However, other cells (e.g., endothelial cells or interstitial cells of Cajal) can replace enteric neurons since MM are not impacted in mice lacking enteric neurons, as well as in humans in whom the enteric nervous system is absent from the colon (Hirschsprung disease) (Avetisyan et al., 2018). Neuron-associated MFs are also present in the submucosal LP, where they could play a role in the regulation of the intestinal secretion induced by neurons (De Schepper et al., 2018).

From the SI to the colon, from rodents to humans, most mucosal LPM are continuously renewed by blood monocytes (Tamoutounour et al., 2012; Bain et al., 2013, 2014; Bujko et al., 2018). In mice, LPM differentiation from Ly6C^{hi} monocytes is phenotypically characterized by four developmental stages termed monocyte waterfall (Tamoutounour et al., 2012; Bain et al., 2013). Nonetheless, a large part of MM and of the submucosal LPM, especially those associated with neurons and vasculature, appears to be long-lived self-maintained cells and are barely replaced by circulating monocytes (De Schepper et al., 2018; Shaw et al., 2018). These MFs are indeed distant from the gut lumen and thus from microbiota and dietary antigens, the well-known drivers of intestinal MF replacement by circulating monocytes (Bain et al., 2014; Ochi et al., 2016). This may explain their self-maintaining property, which is very similar to that of MFs residing in other tissues (Hashimoto et al., 2013; Yona et al., 2013; Liu et al., 2019). In humans, a recent study went through the characterization of MFs within the upper part of the SI (Bujko et al., 2018). They encompass four well-defined subsets based on marker expression, transcriptional profiles, maturation stage, life span, and location. LPM and MM represent two of these subsets, whereas the other two are related to the monocyte to MF conversion.

(RE)CATEGORIZATION OF INTESTINAL MACROPHAGES BY THEIR GUT SEGMENT LOCATION: INFLUENCE OF DIETARY ANTIGENS AND OF MICROBIOTA

Local compartmentalization of intestinal MFs is broadly similar between the SI and the colon. However, MF numbers are generally higher in the colon than in the SI. Moreover, despite similar differentiation programs and markers, MFs of the SI and of the colon are clearly distinct. Thus, monocytes infiltrating the gut acquire intestinal segment-specific gene expression profiles (Gross-Vered et al., 2020). Their differences are mainly due to the specific functions of each segment of the GIT and to the different exogenous antigens they are exposed to. Thus, ileal MFs display higher expression of genes related to immune reaction and response to challenge than colonic MFs (Gross-Vered et al., 2020). In the following part, we will describe how phenotypically similar MFs can act differently according to their gut segment location.

As mentioned above, the main function of the SI is to absorb nutrients, and its large surface area is continually exposed to important amounts of dietary-derived products. Microbiota density increases drastically from the duodenum to the colon according to gut physico-chemical environment variations (e.g., oxygen and pH levels). Therefore, the colon faces a huge amount of diverse microorganisms (commensal bacteria, archaea, virus, and fungi) and their derived metabolites. The number of goblet cells also increases significantly from the SI to the colon. Consistent with this increased goblet cell frequency, the mammalian colon is protected by thicker and more organized mucus layers than the SI, keeping microorganisms at bay from the epithelium (Johansson et al., 2008; Bergstrom et al., 2020).

Whereas in the colon the microbiota promotes LPM renewal by circulating monocytes and contributes to their functional diversification (Bain et al., 2014; Kang et al., 2020), in the SI, intestinal microbiota is a major factor neither for the control of MF replenishment nor for their IL-10 production (Ochi et al., 2016). Consistently, there is no difference in the number of SI LPM populations between antibiotic-treated and untreated mice. However, dietary factors can directly regulate homeostasis of SI LPM, and a total deficiency in dietary amino acids or the inhibition of the mTOR-mediated amino acid sensing leads to a reduction of IL-10-producing MF number (Ochi et al., 2016). Actually, many other molecules resulting from the degradation of the food, such as vitamins and aryl hydrocarbon receptor (AHR) ligands, are susceptible either directly or indirectly to influence intestinal MF functions in the SI (Mowat and Agace, 2014).

Drosophila melanogaster is a good model to study the impact in the gut of imbalanced diets, such as the high-fat and Western diets, or of potential toxic products, such as fried food-derivatives. In the fruit fly, lipid peroxidation products of fried food induce an increase of ROS production and DNA damages in plasmatocytes (Demir and Marcos, 2017). A similar study was recently performed in mouse and confirmed that dietary peroxidized fats induce proinflammatory responses by peritoneal MFs and resident immune cells in PPs (Keewan et al., 2020). With regard to high-fat diet, Woodcock *et al.* showed that lipid-rich diets reduce the life span of *D. melanogaster* and impair its glucose metabolism (Woodcock et al., 2015). This is due to the activation of the JAK-STAT pathway in response to the Upd3 secreted by the plasmatocytes that become foamy, accumulating neutral triglycerides and other lipids in lipid vacuoles. In mouse, Kawano et al. highlighted that high-fat diet induces CCL2 expression by colonic IEC leading to CCR2-dependent proinflammatory MF infiltration in the colon, which results in inflammasome activation in these newly recruited MF, increased intestinal permeability, and glucose metabolism and insulin resistance impairment (Kawano et al., 2016). The western diet includes a high intake of proteins (mainly from animal-derived sources), saturated fatty acids (SFAs), sugar, processed food, and salt, together with a reduced consumption of vegetables, fruits, vitamins, minerals, and ω-3 polyunsaturated fatty acids (PUFAs). SFAs activate proinflammatory response in MFs through the TLR4-NF-κB pathway (Lee et al., 2003). By contrast, specialized proresolving mediators (SPMs) are a large class of signaling molecules that counteract the effect of proinflammatory dietary antigens on intestinal MFs. SPMs are derived from the metabolism of ω-3 PUFA supplied in the diet, giving rise to protectins, resolvins, and maresins. Alternatively, they are produced as eicosanoids (prostaglandin

D2 and E2 and lipoxin A4) by immune (including MFs) and non-immune cells (Na et al., 2019). SPMs influence MF differentiation toward a proresolving phenotype. Proresolving MFs dampen Th1 and Th17 responses, re-establish breached epithelial barrier, limit entry of neutrophils to the site of injury, and promote monocyte migration (Na et al., 2019). Thus, protectins and resolving D1 promote resolution of inflammation by increasing MF phagocytosis and suppressing inflammatory MFs in inflammatory diseases (Buckley et al., 2014). In summary, diet is a key element to take into account when studying variations in LPM functions. However, it is important to keep in mind that most of the research studying the interplay between the dietary antigens and the intestinal MFs have been performed *in vitro*. Therefore, more *in vivo* studies will be required to fully address the impact of diet on the different populations of intestinal MFs.

The main function of the colon is to absorb electrolytes and water and also to manage undigested foodstuffs. Through saccharolytic and proteolytic fermentations, the colon microbiota is involved in the catabolism of remaining indigestible food and produces a variety of metabolites in the colon including short-chain fatty acids (SCFAs), which are involved in colonic LPM conditioning. Thus, antibiotic treatments cause colonic LPM to express increased levels of proinflammatory cytokines following microbiota recolonization and to become responsive to LPS stimulation (Scott et al., 2018). Interestingly, supplementation of antibiotics with the SCFA butyrate, whose production is reduced under antibiotic treatment, restores the anti-inflammatory profile and hypo-responsiveness of colonic MFs (Scott et al., 2018). Administration of butyrate also promotes colonic LPM antimicrobial activities, such as lysozyme, calprotectin, and ROS production (Schulthess et al., 2019). Anti-inflammatory and anti-microbial effects of butyrate are mediated via inhibition of histone deacetylase 3, thus regulating MF transcriptional and metabolic program (Chang et al., 2014; Schulthess et al., 2019). More generally, microbiota contributes to the functional diversification of colon MFs (Kang et al., 2020). It supports in particular colonic LPM production of IL-10 and limits Th1 cell response while promoting Treg cell expansion (Kim et al., 2018).

Colonic LPM conditioning depends not only on microbiota but also on TGFβ and, above all, IL-10 signaling (Schridde et al., 2017; Biswas et al., 2018). Indeed, IL-10 signaling pathway promotes WASP and DOCK8 interaction leading to STAT3 phosphorylation and anti-inflammatory MF polarization (Biswas et al., 2018). By contrast, lack of IL-10 signaling induces a proinflammatory profile on colonic MFs highlighted by IL-23 and IL-1β production, leading to recruitment of Th17 cells and promoting colitis (Shouval et al., 2016; Bernshtein et al., 2019). Loss of IL-10 receptor signaling in mouse and human MFs indeed induces spontaneous colitis and severe infant-onset IBD, respectively (Shouval et al., 2014; Zigmond et al., 2014). Surprisingly, though more inflammatory, these MFs show defect in *Salmonella* Typhimurium killing due to prostaglandin E2 overproduction (Mukhopadhyay et al., 2020).

Depending on the location of encountered microorganisms, CX_3CR1^+ LPM induce regionalized antigen-specific Th17 responses (**Table 2**). Thus, CX_3CR1^+ LPM are involved in the induction in the SI of a specific and robust Th17 response against segmented filamentous bacteria (SFB) that colonize specifically the ileum (Panea et al., 2015). Unlike pathogen-elicited Th17 cells that are highly glycolytic inflammatory effector cells producing IFNγ, SFB-induced Th17 cells are non-inflammatory homeostatic tissue resident cells (Omenetti et al., 2019). By contrast, colonization with the fungus *Candida albicans* induces a strong Th17 response in the colon where it resides but not in the SI (Leonardi et al., 2018). Actually, colonic LPM are fully equipped to efficiently recognize and respond to the important fungal communities (mycobiota) found in the distal colon, notably via the C-type lectin receptors dectin-1, dectin-2, and mincle (Iliev et al., 2012; Leonardi et al., 2018). Dectin-1 promotes a proinflammatory program in colonic MFs, resulting in inflammasome-dependent IL-1β secretion and inflammatory monocyte recruitment to the inflamed colon (Rahabi et al., 2020). In contrast, Treg cells regulate the inflammatory properties of colonic MFs by inhibiting their IL-1β and IL-23 production (Bauché et al., 2018). This inhibition involves MHC class II engagement by latent activation gene-3 (LAG-3) expressed on Treg cells. Interestingly, the way by which LPM from the distal colon sense their microenvironment is completely different from that performed by SI and proximal colon LPM (**Table 2**). Indeed, distal colon LPM form balloon-like protrusions that insert between colonic epithelial cells but do not extend into the lumen like in the SI (Chikina et al., 2020). They remain instead confined in the intercellular space of the epithelium. These balloon-like protrusions, which are induced by the presence of fungi in the lumen, sample the fluids absorbed by epithelial cells to detect toxins among fungi metabolites. By instructing them to stop absorption, MFs with balloon-like protrusions protect colonic epithelial cells from dying of absorbing too much fungal toxins (Chikina et al., 2020).

SPECIFICITY OF INTESTINAL IMMUNE INDUCTIVE SITE MACROPHAGES

As mentioned above, the gastrointestinal mucosa of vertebrates has specialized sites dedicated to the detection of pathogens in contaminated food and water. Indeed, in reptiles, amphibians, and lungfishes, the gut contains lymphoid aggregates resembling the ILFs found in mammals (Borysenko and Cooper, 1972; Zapata and Solas, 1979; Solas and Zapata, 1980; Tacchi et al., 2015; Ashford et al., 2019). Like mammal ILFs, the number and size of these aggregates increase with microbial challenges (Tacchi et al., 2015; Ashford et al., 2019). Based on recent observations made on lungfish, it seems however that these lymphoid aggregates lack a well-structured organization, showing no segregation between B and T cells, no germinal center, no AID expression, and no somatic hypermutation (Tacchi et al., 2015). The cellular composition of these primitive aggregates is otherwise poorly described; and MFs, although observed by electron microscopy (Ardavín et al., 1982), have not been well-characterized.

In addition to ILFs, mammals and also birds have PPs that are distributed along the SI, especially in the last part of the

ileum (Jung et al., 2010). PPs consist of clustered B cell follicles forming domes on the surface of the mucosa. These domes are separated from each other by dome-associated villi (DAV) over interfollicular regions (IFRs) enriched in T cells. A specialized follicle-associated epithelium (FAE) separates the subepithelial dome (SED) above the follicle from the gut lumen. This FAE provides a permissive environment for pathogen entry. Indeed, it secretes no or few IgA and antimicrobial proteins and is covered by a reduced mucus layer. This is due to lack of polymeric Ig receptor expression, inhibition of IL-22 signaling, and diminished number of goblet cells (Bhalla and Owen, 1982; Pappo and Owen, 1988; Jinnohara et al., 2017). Moreover, the glycocalyx is attenuated over the FAE favoring interaction of luminal antigens with the mucosal surface (Frey et al., 1996; Mantis et al., 2000). Finally, the specialized FAE cell termed M cell efficiently binds and transports all kind of antigens from the lumen to the SED (Ohno, 2016; Kobayashi et al., 2019). Therefore, PP MFs are continually exposed to much more threatening elements than other intestinal MFs. They are accordingly equipped with a whole arsenal against pathogens and prone to promote an inflammatory response (Bonnardel et al., 2015; Wagner et al., 2018). Until now, these MFs have been mainly characterized in mice and to a much lesser extent in humans (**Table 2**). At the exception of DAV MFs that closely resemble LPM of standard villi, other PP MFs are profoundly different from all other MF populations (Wagner et al., 2018). This is exemplified by their lack of F4/80 and CD64 expression in mice and of CD163 in humans (Bonnardel et al., 2015; Wagner et al., 2018, 2020). Nevertheless, they share with most, if not all, mouse MFs the expression of the apoptotic receptor MerTK and high levels of the chemokine receptor CX_3CR1, both markers enabling their distinction from conventional DC (Bonnardel et al., 2015, 2017; Wagner et al., 2020). In relation to their important role in innate defense, PP MFs express very large amounts of the antibacterial protein lysozyme, which was the first reliable marker to identify monocyte-derived cells in PPs of mice, rats, and humans (Lelouard et al., 2010). This has given rise to their LysoMac nickname for lysozyme-expressing MFs (Bonnardel et al., 2015). Interestingly, monocytes give also rise in PPs to the unique lysozyme-expressing DC termed LysoDC. LysoDC have a transcriptional program close but not identical to that of PP MFs as they display additional functions, notably in terms of antigen presentation (Bonnardel et al., 2015; Martinez-Lopez et al., 2019; Wagner et al., 2020). Like conventional DC, mature LysoDC are indeed able to prime naïve T cells at least *in vitro* for IFNγ and IL-17 production (Bonnardel et al., 2015; Martinez-Lopez et al., 2019). This ability is strengthened by stimulation with a TLR7 ligand. In addition, TLR7 stimulation induces expression of CCR7 by subepithelial LysoDC and promotes their migration to the periphery of the IFR where they encounter naïve T cells and where they interact tightly with newly activated proliferative T cells (Wagner et al., 2020). At steady state, very few if any LysoDC are in the IFR, and only few of them are located in the follicle, with most of them being in the SED where they excel in antigen capture. Conversely, MFs have been observed in all regions of PPs (Bonnardel et al., 2015). In addition to LysoMac, mainly located in the SED, the follicle, and the IFR, there are indeed muscularis and serosal MFs, and germinal center tingible body MFs (TBM). Interestingly, these different anatomic locations are tightly linked to phenotypic distinctions between PP MFs (**Table 2**). Thus, muscularis and serosal MFs below the IFR express CD169, whereas other PP MFs do not. As well, TBM and interfollicular and lower follicular LysoMac express the phosphatidylserine receptor TIM-4, whereas subepithelial and upper follicular LysoMac do not. This suggests that an important regional specialization of MF functions exists inside the PPs itself (Wagner et al., 2018). Thus, TIM-4 mainly expressed by MFs in the regions of T cell priming and B cell selection belongs to the family of apoptotic cell receptors and is known to be involved in the regulation of the adaptive immune response and prevention of autoimmunity through removal of both B and T cells (Albacker et al., 2010, 2013; Rodriguez-Manzanet et al., 2010). Therefore, TIM-4^+ MFs could protect PPs from an exaggerated inflammatory reaction by regulating both T and B cell numbers.

As mentioned above, TIM-4^- LysoMac as well as LysoDC are close to the FAE, and they play key role in the uptake of particulate antigens and pathogenic bacteria (Lelouard et al., 2010, 2012; Disson et al., 2018). The mechanisms by which LysoDC and TIM-4^- LysoMac sample luminal antigens are different from either SI or colonic LPM. Indeed, phagocytosis of antigens by LysoDC and TIM-4^- LysoMac either follows M cell transcytosis or occurs through LysoDC dendrite extension into the lumen through M cell-specific transcellular pores (Lelouard et al., 2012; Bonnardel et al., 2015). Therefore, M cells tightly control both mechanisms. Accordingly, absence of M cells is associated with a strong downregulation of antigen uptake in PPs and of IgA production in villi (Rios et al., 2016). Unlike villus paracellular transepithelial dendrites, these LysoDC trans-M cell dendrites do not depend on CX_3CR1 expression (Bonnardel et al., 2015). LysoDC and TIM-4^- LysoMac also influence FAE properties to favor contact with exogenous antigens. Thus, they express *Il22ra2*, which encodes IL-22BP, an inhibitor of Il-22 (Da Silva et al., 2017). IL-22BP promotes microbial sampling by influencing the FAE transcriptional program, notably by inhibiting genes encoding antimicrobial proteins and also genes involved in surface glycosylation and mucus production (Jinnohara et al., 2017). PP MFs are also likely involved in M cell differentiation as long-term blockade of CSF1R, which is known to deplete MFs, impairs M cell differentiation (Sehgal et al., 2018). Finally, together with other immune cells, they could be involved in M cell maturation via the expression of the S100 family member S100a4 (Kunimura et al., 2019).

More globally, in relation to the fact that PPs are a permissive entry site for a large number of pathogens, PP MFs display a strong antiviral and antibacterial transcriptional program (Bonnardel et al., 2015). Moreover, PP MFs lack the typical anti-inflammatory properties of other intestinal MFs (Wagner et al., 2018). Thus, they do not produce IL-10 or express its receptor but instead secrete TNF and IL-6 upon stimulation (Bonnardel et al., 2015; Wagner et al., 2018). Therefore, unlike most intestinal MFs, they retain a strong ability to promote inflammation.

CONCLUSIONS AND PERSPECTIVES

There has been incredible progress in recent years in the appreciation of intestinal MF heterogeneity (**Table 2**). This obviously raises great hope for targeted therapies that would render possible to alter a defective population without disturbing the others or to promote one population over the others and thus restore homeostasis. However, much more work is needed to understand the signaling between MFs and their direct neighbors and how this can be used to remodel MF properties. As suggested by Guilliams et al. (2020), manipulation of the neighboring cells that imprint the MF with its functional properties instead of the MF itself could represent alternative and interesting strategies for deciphering the mechanisms that dictate the fate of intestinal MFs on the one hand and modifying key instructing factors according to pathologies on the other hand. Nutritional- and microbial-based intervention strategies to modulate intestinal MF properties have also become a promising therapeutic approach to treat and prevent intestinal diseases. A great challenge for all these approaches will be to deal with the complexity of the structure and diversity of potentially simultaneous signals (food, microbiota, pathogen, stromal, and immune cell-derived factors) that make the intestine such a special and diversified organ.

AUTHOR CONTRIBUTIONS

CAP, JT, and HL: writing—original draft. CAP, JT, HL, and J-PG: writing—revision. CAP: figure design. HL and J-PG: funding acquisition. All authors contributed to the article and approved the submitted version.

FUNDING

This work was supported by institutional funding from Center National de la Recherche Scientifique and Institut National de la Santé et de la Recherche Médicale, and by the Fondation pour la Recherche Médicale (FRM), Grant No. DEQ20170336745. CAP was supported by the University of Costa Rica.

ACKNOWLEDGMENTS

We thank Camille Wagner for her help in figure drawing.

REFERENCES

Abnave, P., Mottola, G., Gimenez, G., Boucherit, N., Trouplin, V., Torre, C., et al. (2014). Screening in planarians identifies MORN2 as a key component in LC3-associated phagocytosis and resistance to bacterial infection. *Cell Host Microbe* 16, 338–350. doi: 10.1016/j.chom.2014.08.002

Adamska, M. (2016). Sponges as models to study emergence of complex animals. *Curr. Opin. Genet. Dev* 39, 21–28. doi: 10.1016/j.gde.2016.05.026

Albacker, L. A., Karisola, P., Chang, Y. J., Umetsu, S. E., Zhou, M., Akbari, O., et al. (2010). TIM-4, a receptor for phosphatidylserine, controls adaptive immunity by regulating the removal of antigen-specific T cells. *J. Immunol.* 185, 6839–6849. doi: 10.4049/jimmunol.1001360

Albacker, L. A., Yu, S., Bedoret, D., Lee, W. L., Umetsu, S. E., Monahan, S., et al. (2013). TIM-4, expressed by medullary macrophages, regulates respiratory tolerance by mediating phagocytosis of antigen-specific T cells. *Mucosal Immunol.* 6, 580–590. doi: 10.1038/mi.2012.100

Annunziata, R., Andrikou, C., Perillo, M., Cuomo, C., and Arnone, M. I. (2019). Development and evolution of gut structures: from molecules to function. *Cell Tissue Res.* 377, 445–458. doi: 10.1007/s00441-019-03093-9

Ardavín, C. F., Zapata, A., Garrido, E., and Villena, A. (1982). Ultrastructure of gut-associated lymphoid tissue (GALT) in the amphibian urodele, Pleurodeles waltlii. *Cell Tissue Res.* 224, 663–671. doi: 10.1007/BF00213761

Arques, J. L., Hautefort, I., Ivory, K., Bertelli, E., Regoli, M., Clare, S., et al. (2009). Salmonella induces flagellin- and MyD88-dependent migration of bacteria-capturing dendritic cells into the gut lumen. *Gastroenterology* 137, 579–587, 87 e1–2. doi: 10.1053/j.gastro.2009.04.010

Asano, K., Takahashi, N., Ushiki, M., Monya, M., Aihara, F., Kuboki, E., et al. (2015). Intestinal CD169(+) macrophages initiate mucosal inflammation by secreting CCL8 that recruits inflammatory monocytes. *Nat. Commun.* 6:7802. doi: 10.1038/ncomms8802

Ashford, M. A., Palackdharry, S. M., Sadd, B. M., Bowden, R. M., and Vogel, L. A. (2019). Intestinal B cells in the red-eared slider turtle, *Trachemys scripta*: anatomical distribution and implications for ecological interactions with pathogenic microbes. *J. Exp. Zool.* 331, 407–415. doi: 10.1002/jez.2307

Avetisyan, M., Rood, J. E., Huerta Lopez, S., Sengupta, R., Wright-Jin, E., Dougherty, J. D., et al. (2018). Muscularis macrophage development in the absence of an enteric nervous system. *Proc. Natl. Acad. Sci. U.S.A.* 115, 4696–4701. doi: 10.1073/pnas.1802490115

Ayyaz, A., Li, H., and Jasper, H. (2015). Haemocytes control stem cell activity in the Drosophila intestine. *Nat. Cell Biol.* 17, 736–748. doi: 10.1038/ncb3174

Bain, C. C., Bravo-Blas, A., Scott, C. L., Gomez Perdiguero, E., Geissmann, F., Henri, S., et al. (2014). Constant replenishment from circulating monocytes maintains the macrophage pool in the intestine of adult mice. *Nat. Immunol.* 15, 929–937. doi: 10.1038/ni.2967

Bain, C. C., Scott, C. L., Uronen-Hansson, H., Gudjonsson, S., Jansson, O., Grip, O., et al. (2013). Resident and pro-inflammatory macrophages in the colon represent alternative context-dependent fates of the same Ly6Chi monocyte precursors. *Mucosal Immunol.* 6, 498–510. doi: 10.1038/mi.2012.89

Banchereau, J., and Steinman, R. M. (1998). Dendritic cells and the control of immunity. *Nature* 392, 245–252. doi: 10.1038/32588

Banerjee, U., Girard, J. R., Goins, L. M., and Spratford, C. M. (2019). Drosophila as a genetic model for hematopoiesis. *Genetics* 211, 367–417. doi: 10.1534/genetics.118.300223

Bauché, D., Joyce-Shaikh, B., Jain, R., Grein, J., Ku, K. S., Blumenschein, W. M., et al. (2018). LAG3(+) Regulatory T cells restrain interleukin-23-producing CX3CR1(+) gut-resident macrophages during group 3 innate lymphoid cell-driven colitis. *Immunity* 49, 342–352.e5. doi: 10.1016/j.immuni.2018.07.007

Baumann, O., Arlt, K., Römmling, K., Goller, H., and Walz, B. (2000). Characterization of an extremely motile cellular network in the rotifer Asplanchna spp. Structure, kinetics, and the cytoskeleton. *Cell Tissue Res.* 299, 159–172. doi: 10.1007/s004410050014

Bergstrom, K., Shan, X., Casero, D., Batushansky, A., Lagishetty, V., Jacobs, J. P., et al. (2020). Proximal colon-derived O-glycosylated mucus encapsulates and modulates the microbiota. *Science* 370, 467–472. doi: 10.1126/science.aay7367

Bernshtein, B., Curato, C., Ioannou, M., Thaiss, C. A., Gross-Vered, M., Kolesnikov, M., et al. (2019). IL-23-producing IL-10Rα-deficient gut macrophages elicit an IL-22-driven proinflammatory epithelial cell response. *Sci. Immunol* 4:eaau6571. doi: 10.1126/sciimmunol.aau6571

Beshel, J., Dubnau, J., and Zhong, Y. (2017). A leptin analog locally produced in the brain acts via a conserved neural circuit to modulate obesity-linked behaviors in drosophila. *Cell Metab.* 25, 208–217. doi: 10.1016/j.cmet.2016.12.013

Bhalla, D. K., and Owen, R. L. (1982). Cell renewal and migration in lymphoid follicles of Peyer's patches and cecum–an autoradiographic study in mice. *Gastroenterology* 82, 232–242. doi: 10.1016/0016-5085(82)90010-5

Birgisdottir, Å. B., and Johansen, T. (2020). Autophagy and endocytosis - interconnections and interdependencies. *J. Cell Sci.* 133:jcs228114. doi: 10.1242/jcs.228114

Biswas, A., Shouval, D. S., Griffith, A., Goettel, J. A., Field, M., Kang, Y. H., et al. (2018). WASP-mediated regulation of anti-inflammatory macrophages is IL-10 dependent and is critical for intestinal homeostasis. *Nat. Commun.* 9:1779. doi: 10.1038/s41467-018-03670-6

Blériot, C., Chakarov, S., and Ginhoux, F. (2020). Determinants of resident tissue macrophage identity and function. *Immunity* 52, 957–970. doi: 10.1016/j.immuni.2020.05.014

Bodó, K., Ernszt, D., Németh, P., and Engelmann, P. (2018). Distinct immune- and defense-related molecular fingerprints in sepatated coelomocyte subsets of *Eisenia andrei* earthworms. *Invertebrate Survival J.* 15, 338–345. doi: 10.25431/1824-307X/isj.v15i1.338-345

Bolla, R. I., Weinstein, P. P., and Cain, G. D. (1972). Fine structure of the coelomocyte of adult *Ascaris suum*. *J. Parasitol.* 58, 1025–1036. doi: 10.2307/3278127

Bonnardel, J., Da Silva, C., Henri, S., Tamoutounour, S., Chasson, L., Montanana-Sanchis, F., et al. (2015). Innate and adaptive immune functions of peyer's patch monocyte-derived cells. *Cell Rep.* 11, 770–784. doi: 10.1016/j.celrep.2015.03.067

Bonnardel, J., Da Silva, C., Wagner, C., Bonifay, R., Chasson, L., Masse, M., et al. (2017). Distribution, location, and transcriptional profile of Peyer's patch conventional DC subsets at steady state and under TLR7 ligand stimulation. *Mucosal Immunol.* 10, 1412–1430. doi: 10.1038/mi.2017.30

Borysenko, M., and Cooper, E. L. (1972). Lymphoid tissue in the snapping turtle, *Chelydra serpentina*. *J. Morphol.* 138, 487–497. doi: 10.1002/jmor.1051380408

Bravo-Blas, A., Utriainen, L., Clay, S. L., Kästele, V., Cerovic, V., Cunningham, A. F., et al. (2019). Salmonella enterica Serovar typhimurium travels to mesenteric lymph nodes both with host cells and autonomously. *J. Immunol.* 202, 260–267. doi: 10.4049/jimmunol.1701254

Brennan, J. J., and Gilmore, T. D. (2018). Evolutionary origins of toll-like receptor signaling. *Mol. Biol. Evol.* 35, 1576–1587. doi: 10.1093/molbev/msy050

Broderick, N. A. (2015). A common origin for immunity and digestion. *Front. Immunol.* 6:72. doi: 10.3389/fimmu.2015.00072

Broom, L. J., and Kogut, M. H. (2018). The role of the gut microbiome in shaping the immune system of chickens. *Vet. Immunol. Immunopathol.* 204, 44–51. doi: 10.1016/j.vetimm.2018.10.002

Buchmann, K. (2014). Evolution of innate immunity: clues from invertebrates via fish to mammals. *Front. Immunol.* 5:459. doi: 10.3389/fimmu.2014.00459

Buckley, C. D., Gilroy, D. W., and Serhan, C. N. (2014). Proresolving lipid mediators and mechanisms in the resolution of acute inflammation. *Immunity* 40, 315–327. doi: 10.1016/j.immuni.2014.02.009

Buckley, K. M., Ho, E. C. H., Hibino, T., Schrankel, C. S., Schuh, N. W., Wang, G., et al. (2017). IL17 factors are early regulators in the gut epithelium during inflammatory response to Vibrio in the sea urchin larva. *Elife* 6:e23481. doi: 10.7554/eLife.23481.025

Buckley, K. M., and Rast, J. P. (2019). Immune activity at the gut epithelium in the larval sea urchin. *Cell Tissue Res.* 377, 469–474. doi: 10.1007/s00441-019-03095-7

Buis, A., Bellemin, S., Goudeau, J., Monnier, L., Loiseau, N., Guillou, H., et al. (2019). Coelomocytes regulate starvation-induced fat catabolism and lifespan extension through the lipase LIPL-5 in *Caenorhabditis elegans*. *Cell Rep.* 28, 1041–1049.e4. doi: 10.1016/j.celrep.2019.06.064

Bujko, A., Atlasy, N., Landsverk, O. J. B., Richter, L., Yaqub, S., Horneland, R., et al. (2018). Transcriptional and functional profiling defines human small intestinal macrophage subsets. *J. Exp. Med.* 215, 441–458. doi: 10.1084/jem.20170057

Casteleyn, C., Doom, M., Lambrechts, E., Van den Broeck, W., Simoens, P., and Cornillie, P. (2010). Locations of gut-associated lymphoid tissue in the 3-month-old chicken: a review. *Avian Pathol.* 39, 143–150. doi: 10.1080/03079451003786105

Cattenoz, P. B., Sakr, R., Pavlidaki, A., Delaporte, C., Riba, A., Molina, N., et al. (2020). Temporal specificity and heterogeneity of Drosophila immune cells. *EMBO J.* 39:e104486. doi: 10.15252/embj.2020104486

Cecchini, M. G., Dominguez, M. G., Mocci, S., Wetterwald, A., Felix, R., Fleisch, H., et al. (1994). Role of colony stimulating factor-1 in the establishment and regulation of tissue macrophages during postnatal development of the mouse. *Development* 120, 1357–1372.

Chakrabarti, S., Dudzic, J. P., Li, X., Collas, E. J., Boquete, J. P., and Lemaitre, B. (2016). Remote control of intestinal stem cell activity by haemocytes in drosophila. *PLoS Genet.* 12:e1006089. doi: 10.1371/journal.pgen.1006089

Chang, P. V., Hao, L., Offermanns, S., and Medzhitov, R. (2014). The microbial metabolite butyrate regulates intestinal macrophage function via histone deacetylase inhibition. *Proc. Natl. Acad. Sci. U.S.A.* 111, 2247–2252. doi: 10.1073/pnas.1322269111

Charroux, B., and Royet, J. (2009). Elimination of plasmatocytes by targeted apoptosis reveals their role in multiple aspects of the Drosophila immune response. *Proc. Natl. Acad. Sci. U.S.A.* 106, 9797–9802. doi: 10.1073/pnas.0903971106

Chieppa, M., Rescigno, M., Huang, A. Y., and Germain, R. N. (2006). Dynamic imaging of dendritic cell extension into the small bowel lumen in response to epithelial cell TLR engagement. *J. Exp. Med.* 203, 2841–2852. doi: 10.1084/jem.20061884

Chikina, A. S., Nadalin, F., Maurin, M., San-Roman, M., Thomas-Bonafos, T., Li, X. V., et al. (2020). Macrophages maintain epithelium integrity by limiting fungal product absorption. *Cell* 183, 411–428.e16. doi: 10.1016/j.cell.2020.08.048

Chin, K. N., and Wong, W. C. (1977). Some ultrastructural observations on the intestinal mucosa of the toad (Bufo melanostictus). *J. Anatomy* 123, 331–339.

Cho, B., Yoon, S. H., Lee, D., Koranteng, F., Tattikota, S. G., Cha, N., et al. (2020). Single-cell transcriptome maps of myeloid blood cell lineages in Drosophila. *Nat. Commun.* 11:4483. doi: 10.1038/s41467-020-18135-y

Coates, C. J., McCulloch, C., Betts, J., and Whalley, T. (2018). Echinochrome a release by red spherule cells is an iron-withholding strategy of sea urchin innate immunity. *J. Innate Immun.* 10, 119–130. doi: 10.1159/000484722

Cooper, M. D., and Alder, M. N. (2006). The evolution of adaptive immune systems. *Cell* 124, 815–822. doi: 10.1016/j.cell.2006.02.001

Coronado, M., Solis, C. J., Hernandez, P. P., and Feijóo, C. G. (2019). Soybean meal-induced intestinal inflammation in zebrafish Is T cell-dependent and has a Th17 cytokine profile. *Front. Immunol.* 10:610. doi: 10.3389/fimmu.2019.00610

Da Silva, C., Wagner, C., Bonnardel, J., Gorvel, J. P., and Lelouard, H. (2017). The Peyer's patch mononuclear phagocyte system at steady state and during infection. *Front. Immunol.* 8:1254. doi: 10.3389/fimmu.2017.01254

de Geus, E. D., and Vervelde, L. (2013). Regulation of macrophage and dendritic cell function by pathogens and through immunomodulation in the avian mucosa. *Dev. Comp. Immunol.* 41, 341–351. doi: 10.1016/j.dci.2013.03.008

De Schepper, S., Verheijden, S., Aguilera-Lizarraga, J., Viola, M. F., Boesmans, W., Stakenborg, N., et al. (2018). Self-maintaining gut macrophages are essential for intestinal homeostasis. *Cell* 175, 400–415.e13. doi: 10.1016/j.cell.2018.07.048

Dee, C. T., Nagaraju, R. T., Athanasiadis, E. I., Gray, C., Fernandez Del Ama, L., Johnston, S. A., et al. (2016). CD4-transgenic zebrafish reveal tissue-resident Th2- and regulatory T cell-like populations and diverse mononuclear phagocytes. *J. Immunol.* 197, 3520–3530. doi: 10.4049/jimmunol.1600959

Demir, E., and Marcos, R. (2017). Assessing the genotoxic effects of two lipid peroxidation products (4-oxo-2-nonenal and 4-hydroxy-hexenal) in haemocytes and midgut cells of *Drosophila melanogaster* larvae. *Food Chem. Toxicol.* 105, 1–7. doi: 10.1016/j.fct.2017.03.036

Desjardins, M., Houde, M., and Gagnon, E. (2005). Phagocytosis: the convoluted way from nutrition to adaptive immunity. *Immunol. Rev.* 207, 158–165. doi: 10.1111/j.0105-2896.2005.00319.x

Disson, O., Bleriot, C., Jacob, J. M., Serafini, N., Dulauroy, S., Jouvion, G., et al. (2018). Peyer's patch myeloid cells infection by Listeria signals through gp38(+) stromal cells and locks intestinal villus invasion. *J. Exp. Med.* 215, 2936–2954. doi: 10.1084/jem.20181210

Duszenko, M., Ginger, M. L., Brennand, A., Gualdrón-López, M., Colombo, M. I., Coombs, G. H., et al. (2011). Autophagy in protists. *Autophagy* 7, 127–158. doi: 10.4161/auto.7.2.13310

Dvorák, J., Roubalov,á R., Procházková, P., Rossmann, P., Škanta, F., and Bilej, M. (2016). Sensing microorganisms in the gut triggers the immune response in *Eisenia andrei* earthworms. *Dev. Comp. Immunol.* 57, 67–74. doi: 10.1016/j.dci.2015.12.001

Dzik, J. M. (2010). The ancestry and cumulative evolution of immune reactions. *Acta Biochim. Pol.* 57, 443–466. doi: 10.18388/abp.2010_2431

Earley, A. M., Graves, C. L., and Shiau, C. E. (2018). Critical role for a subset of intestinal macrophages in shaping gut microbiota in adult zebrafish. *Cell Rep.* 25, 424–436. doi: 10.1016/j.celrep.2018.09.025

Elvington, M., Liszewski, M. K., and Atkinson, J. P. (2016). Evolution of the complement system: from defense of the single cell to guardian of the intravascular space. *Immunol. Rev*. 274, 9–15. doi: 10.1111/imr.12474

Engelmann, P., Hayashi, Y., Bodó, K., Ernszt, D., Somogyi, I., Steib, A., et al. (2016). Phenotypic and functional characterization of earthworm coelomocyte subsets: Linking light scatter-based cell typing and imaging of the sorted populations. *Dev. Comp. Immunol*. 65, 41–52. doi: 10.1016/j.dci.2016.06.017

Farache, J., Koren, I., Milo, I., Gurevich, I., Kim, K. W., Zigmond, E., et al. (2013). Luminal bacteria recruit CD103+ dendritic cells into the intestinal epithelium to sample bacterial antigens for presentation. *Immunity* 38, 581–595. doi: 10.1016/j.immuni.2013.01.009

Fares, H., and Greenwald, I. (2001). Genetic analysis of endocytosis in *Caenorhabditis elegans*: coelomocyte uptake defective mutants. *Genetics* 159, 133–145.

Ferrero, G., Gomez, E., Lyer, S., Rovira, M., Miserocchi, M., Langenau, D. M., et al. (2020). The macrophage-expressed gene (mpeg) 1 identifies a subpopulation of B cells in the adult zebrafish. *J. Leukoc. Biol*. 107, 431–443. doi: 10.1002/JLB.1A1119-223R

Frey, A., Giannasca, K. T., Weltzin, R., Giannasca, P. J., Reggio, H., Lencer, W. I., et al. (1996). Role of the glycocalyx in regulating access of microparticles to apical plasma membranes of intestinal epithelial cells: implications for microbial attachment and oral vaccine targeting. *J. Exp. Med.* 184, 1045–1059. doi: 10.1084/jem.184.3.1045

Fu, Y., Huang, X., Zhang, P., van de Leemput, J., and Han, Z. (2020). Single-cell RNA sequencing identifies novel cell types in Drosophila blood. *J. Genet. Genomics* 47, 175–186. doi: 10.1016/j.jgg.2020.02.004

Gabanyi, I., Muller, P. A., Feighery, L., Oliveira, T. Y., Costa-Pinto, F. A., and Mucida, D. (2016). Neuro-immune interactions drive tissue programming in intestinal macrophages. *Cell* 164, 378–391. doi: 10.1016/j.cell.2015.12.023

Giribet, G., and Edgecombe, G. D. (2017). Current understanding of ecdysozoa and its internal phylogenetic relationships. *Integr. Comp. Biol*. 57, 455–466. doi: 10.1093/icb/icx072

Girón-Pérez, M. I. (2010). Relationships between innate immunity in bivalve molluscs and environmental pollution. *Invertebrate Survival J.* 7:149–156.

Golconda, P., Buckley, K. M., Reynolds, C. R., Romanello, J. P., and Smith, L. C. (2019). The axial organ and the pharynx are sites of hematopoiesis in the Sea Urchin. *Front. Immunol*. 10:870. doi: 10.3389/fimmu.2019.00870

Gordon, S. (2016). Phagocytosis: the legacy of metchnikoff. *Cell* 166, 1065–1068. doi: 10.1016/j.cell.2016.08.017

Gosselin, D., Link, V. M., Romanoski, C. E., Fonseca, G. J., Eichenfield, D. Z., Spann, N. J., et al. (2014). Environment drives selection and function of enhancers controlling tissue-specific macrophage identities. *Cell* 159, 1327–1340. doi: 10.1016/j.cell.2014.11.023

Gotthardt, D., Warnatz, H. J., Henschel, O., Brückert, F., Schleicher, M., and Soldati, T. (2002). High-resolution dissection of phagosome maturation reveals distinct membrane trafficking phases. *Mol. Biol. Cell* 13, 3508–3520. doi: 10.1091/mbc.e02-04-0206

Grayfer, L., and Robert, J. (2013). Colony-stimulating factor-1-responsive macrophage precursors reside in the amphibian (Xenopus laevis) bone marrow rather than the hematopoietic subcapsular liver. *J. Innate Immun*. 5, 531–542. doi: 10.1159/000346928

Grayfer, L., and Robert, J. (2016). Amphibian macrophage development and antiviral defenses. *Dev. Comp. Immunol*. 58, 60–67. doi: 10.1016/j.dci.2015.12.008

Gross-Vered, M., Trzebanski, S., Shemer, A., Bernshtein, B., Curato, C., Stelzer, G., et al. (2020). Defining murine monocyte differentiation into colonic and ileal macrophages. *Elife* 9:e49998. doi: 10.7554/eLife.49998

Guilliams, M., Ginhoux, F., Jakubzick, C., Naik, S. H., Onai, N., Schraml, B. U., et al. (2014). Dendritic cells, monocytes and macrophages: a unified nomenclature based on ontogeny. *Nat. Rev. Immunol.*14, 571–578. doi: 10.1038/nri3712

Guilliams, M., Thierry, G. R., Bonnardel, J., and Bajenoff, M. (2020). Establishment and maintenance of the macrophage niche. *Immunity* 52, 434–451. doi: 10.1016/j.immuni.2020.02.015

Hadis, U., Wahl, B., Schulz, O., Hardtke-Wolenski, M., Schippers, A., Wagner, N., et al. (2011). Intestinal tolerance requires gut homing and expansion of FoxP3+ regulatory T cells in the lamina propria. *Immunity* 34, 237–246. doi: 10.1016/j.immuni.2011.01.016

Hartenstein, V. (2006). Blood cells and blood cell development in the animal kingdom. *Annu. Rev. Cell Dev. Biol.* 22, 677–712. doi: 10.1146/annurev.cellbio.22.010605.093317

Hartenstein, V., and Martinez, P. (2019). Phagocytosis in cellular defense and nutrition: a food-centered approach to the evolution of macrophages. *Cell Tissue Res*. 377, 527–547. doi: 10.1007/s00441-019-03096-6

Hashimoto, D., Chow, A., Noizat, C., Teo, P., Beasley, M. B., Leboeuf, M., et al. (2013). Tissue-resident macrophages self-maintain locally throughout adult life with minimal contribution from circulating monocytes. *Immunity* 38, 792–804. doi: 10.1016/j.immuni.2013.04.004

Hiemstra, I. H., Beijer, M. R., Veninga, H., Vrijland, K., Borg, E. G., Olivier, B. J., et al. (2014). The identification and developmental requirements of colonic CD169^{+} macrophages. *Immunology* 142, 269–278. doi: 10.1111/imm.12251

Hine, P. M. (1999). The inter-relationships of bivalve haemocytes. *Fish Shellfish Immunol*. 9, 367–385. doi: 10.1006/fsim.1998.0205

Ho, E. C., Buckley, K. M., Schrankel, C. S., Schuh, N. W., Hibino, T., Solek, C. M., et al. (2017). Perturbation of gut bacteria induces a coordinated cellular immune response in the purple sea urchin larva. *Immunol. Cell Biol.* 95:647. doi: 10.1038/icb.2017.40

Hoeffel, G., and Ginhoux, F. (2018). Fetal monocytes and the origins of tissue-resident macrophages. *Cell. Immunol*. 330, 5–15. doi: 10.1016/j.cellimm.2018.01.001

Hoffmann, J. A., and Reichhart, J. M. (2002). Drosophila innate immunity: an evolutionary perspective. *Nat. Immunol* 3, 121–126. doi: 10.1038/ni0202-121

Homa, J., Stalmach, M., Wilczek, G., and Kolaczkowska, E. (2016). Effective activation of antioxidant system by immune-relevant factors reversely correlates with apoptosis of *Eisenia andrei* coelomocytes. *J. Comp. Physiol. B* 186, 417–430. doi: 10.1007/s00360-016-0973-5

Homa, J., Zorska, A., Wesolowski, D., and Chadzinska, M. (2013). Dermal exposure to immunostimulants induces changes in activity and proliferation of coelomocytes of *Eisenia andrei*. *J. Comp. Physiol.* 183, 313–322. doi: 10.1007/s00360-012-0710-7

Honda, M., Surewaard, B. G. J., Watanabe, M., Hedrick, C. C., Lee, W. Y., Brown, K., et al. (2020). Perivascular localization of macrophages in the intestinal mucosa is regulated by Nr4a1 and the microbiome. *Nat. Commun*. 11:1329. doi: 10.1038/s41467-020-15068-4

Hume, D. A., Perry, V. H., and Gordon, S. (1984). The mononuclear phagocyte system of the mouse defined by immunohistochemical localisation of antigen F4/80: macrophages associated with epithelia. *Anat. Rec*. 210, 503–512. doi: 10.1002/ar.1092100311

Iliev, I. D., Funari, V. A., Taylor, K. D., Nguyen, Q., Reyes, C. N., Strom, S. P., et al. (2012). Interactions between commensal fungi and the C-type lectin receptor Dectin-1 influence colitis. *Science* 336, 1314–1317. doi: 10.1126/science.1221789

Jinnohara, T., Kanaya, T., Hase, K., Sakakibara, S., Kato, T., Tachibana, N., et al. (2017). IL-22BP dictates characteristics of Peyer's patch follicle-associated epithelium for antigen uptake. *J. Exp. Med*. 214, 1607–1618. doi: 10.1084/jem.20160770

Johansson, M. E. V., Phillipson, M., Petersson, J., Velcich, A., Holm, L., and Hansson, G. C. (2008). The inner of the two Muc2 mucin-dependent mucus layers in colon is devoid of bacteria. *Proc. Natl. Acad. Sci. U.S.A.* 105:15064. doi: 10.1073/pnas.0803124105

Jung, C., Hugot, J. P., and Barreau, F. (2010). Peyer's patches: the immune sensors of the intestine. *Int. J. Inflam*. 2010:823710. doi: 10.4061/2010/823710

Kang, B., Alvarado, L. J., Kim, T., Lehmann, M. L., Cho, H., He, J., et al. (2020). Commensal microbiota drive the functional diversification of colon macrophages. *Mucosal Immunol*. 13, 216–229. doi: 10.1038/s41385-019-0228-3

Kawano, Y., Nakae, J., Watanabe, N., Kikuchi, T., Tateya, S., Tamori, Y., et al. (2016). Colonic pro-inflammatory macrophages cause insulin resistance in an intestinal Ccl2/Ccr2-dependent manner. *Cell Metab*. 24, 295–310. doi: 10.1016/j.cmet.2016.07.009

Kaya, B., Doñas, C., Wuggenig, P., Diaz, O. E., Morales, R. A., Melhem, H., et al. (2020). Lysophosphatidic acid-mediated GPR35 signaling in CX3CR1(+) macrophages regulates intestinal homeostasis. *Cell Rep*. 32:107979. doi: 10.1016/j.celrep.2020.107979

Keewan, E., Narasimhulu, C. A., Rohr, M., Hamid, S., and Parthasarathy, S. (2020). Are fried foods unhealthy? the dietary peroxidized fatty acid, 13-HPODE, induces intestinal inflammation *in vitro* and *in vivo*. *Antioxidants* 9:926. doi: 10.3390/antiox9100926

Kim, M., Galan, C., Hill, A. A., Wu, W. J., Fehlner-Peach, H., Song, H. W., et al. (2018). Critical role for the microbiota in CX(3)CR1(+) intestinal mononuclear phagocyte regulation of intestinal T Cell responses. *Immunity* 49, 151–163.e5. doi: 10.1016/j.immuni.2018.05.009

Kobayashi, N., Takahashi, D., Takano, S., Kimura, S., and Hase, K. (2019). The roles of Peyer's patches and microfold cells in the gut immune system: relevance to autoimmune diseases. *Front. Immunol.* 10:2345. doi: 10.3389/fimmu.2019.02345

Kocot, K. M., Struck, T. H., Merkel, J., Waits, D. S., Todt, C., Brannock, P. M., et al. (2017). Phylogenomics of lophotrochozoa with consideration of systematic error. *Syst. Biol.* 66, 256–282. doi: 10.1093/sysbio/syw079

Krejčová, G., Danielová, A., Nedbalová, P., Kazek, M., Strych, L., Chawla, G., et al. (2019). Drosophila macrophages switch to aerobic glycolysis to mount effective antibacterial defense. *Elife* 8:e50414. doi: 10.7554/eLife.50414

Kunimura, K., Sakata, D., Tun, X., Uruno, T., Ushijima, M., Katakai, T., et al. (2019). S100A4 protein is essential for the development of mature microfold cells in Peyer's Patches. *Cell Rep.* 29, 2823-34.e7. doi: 10.1016/j.celrep.2019.10.091

Langlet, C., and Bierne, J. (1984). Immunocompetent cells requisite for graft rejection in Lineus (Invertebrata, Nemertea). *Dev. Comp. Immunol.* 8, 547–557. doi: 10.1016/0145-305X(84)90087-9

Lavin, Y., Winter, D., Blecher-Gonen, R., David, E., Keren-Shaul, H., Merad, M., et al. (2014). Tissue-resident macrophage enhancer landscapes are shaped by the local microenvironment. *Cell* 159, 1312–1326. doi: 10.1016/j.cell.2014.11.018

Lee, J. Y., Ye, J., Gao, Z., Youn, H. S., Lee, W. H., Zhao, L., et al. (2003). Reciprocal modulation of Toll-like receptor-4 signaling pathways involving MyD88 and phosphatidylinositol 3-kinase/AKT by saturated and polyunsaturated fatty acids. *J. Biol. Chem.* 278, 37041–37051. doi: 10.1074/jbc.M305213200

Lelouard, H., Fallet, M., de Bovis, B., Meresse, S., and Gorvel, J. P. (2012). Peyer's patch dendritic cells sample antigens by extending dendrites through M cell-specific transcellular pores. *Gastroenterology* 142, 592–601 e3. doi: 10.1053/j.gastro.2011.11.039

Lelouard, H., Henri, S., De Bovis, B., Mugnier, B., Chollat-Namy, A., Malissen, B., et al. (2010). Pathogenic bacteria and dead cells are internalized by a unique subset of Peyer's patch dendritic cells that express lysozyme. *Gastroenterology* 138, 173–184 e1–3. doi: 10.1053/j.gastro.2009.09.051

Lemaitre, B., Nicolas, E., Michaut, L., Reichhart, J. M., and Hoffmann, J. A. (1996). The dorsoventral regulatory gene cassette spätzle/Toll/cactus controls the potent antifungal response in Drosophila adults. *Cell* 86, 973–983. doi: 10.1016/S0092-8674(00)80172-5

Leonardi, I., Li, X., Semon, A., Li, D., Doron, I., Putzel, G., et al. (2018). CX3CR1(+) mononuclear phagocytes control immunity to intestinal fungi. *Science* 359, 232–236. doi: 10.1126/science.aao1503

Li, L., Jin, H., Xu, J., Shi, Y., and Wen, Z. (2011). Irf8 regulates macrophage versus neutrophil fate during zebrafish primitive myelopoiesis. *Blood* 117, 1359–1369. doi: 10.1182/blood-2010-06-290700

Lickwar, C. R., Camp, J. G., Weiser, M., Cocchiaro, J. L., Kingsley, D. M., Furey, T. S., et al. (2017). Genomic dissection of conserved transcriptional regulation in intestinal epithelial cells. *PLoS Biol.* 15:e2002054. doi: 10.1371/journal.pbio.2002054

Litman, G. W., and Cooper, M. D. (2007). Why study the evolution of immunity? *Nat. Immunol.* 8, 547–548. doi: 10.1038/ni0607-547

Liu, Z., Gu, Y., Chakarov, S., Bleriot, C., Kwok, I., Chen, X., et al. (2019). Fate mapping via Ms4a3-expression history traces monocyte-derived cells. *Cell* 178, 1509–1525.e19. doi: 10.1016/j.cell.2019.08.009

Luo, J., Qian, A., Oetjen, L. K., Yu, W., Yang, P., Feng, J., et al. (2018). TRPV4 Channel signaling in macrophages promotes gastrointestinal motility via direct effects on smooth muscle cells. *Immunity* 49, 107–119.e4. doi: 10.1016/j.immuni.2018.04.021

Man, A. L., Gicheva, N., Regoli, M., Rowley, G., De Cunto, G., Wellner, N., et al. (2017). CX3CR1+ cell-mediated salmonella exclusion protects the intestinal mucosa during the initial stage of infection. *J. Immunol.* 198, 335–343. doi: 10.4049/jimmunol.1502559

Mantis, N. J., Frey, A., and Neutra, M. R. (2000). Accessibility of glycolipid and oligosaccharide epitopes on rabbit villus and follicle-associated epithelium. *Am. J. Physiol. Gastrointest. Liver Physiol.* 278, G915–G923. doi: 10.1152/ajpgi.2000.278.6.G915

Martinez, J. (2018). LAP it up, fuzz ball: a short history of LC3-associated phagocytosis. *Curr. Opin. Immunol.* 55, 54–61. doi: 10.1016/j.coi.2018.09.011

Martinez, J., Almendinger, J., Oberst, A., Ness, R., Dillon, C. P., Fitzgerald, P., et al. (2011). Microtubule-associated protein 1 light chain 3 alpha (LC3)-associated phagocytosis is required for the efficient clearance of dead cells. *Proc. Natl. Acad. Sci. U.S.A.* 108, 17396–17401. doi: 10.1073/pnas.1113421108

Martinez, J., Malireddi, R. K., Lu, Q., Cunha, L. D., Pelletier, S., Gingras, S., et al. (2015). Molecular characterization of LC3-associated phagocytosis reveals distinct roles for Rubicon, NOX2 and autophagy proteins. *Nat. Cell Biol.* 17, 893–906. doi: 10.1038/ncb3192

Martinez-Lopez, M., Iborra, S., Conde-Garrosa, R., Mastrangelo, A., Danne, C., Mann, E. R., et al. (2019). Microbiota sensing by mincle-syk axis in dendritic cells regulates interleukin-17 and−22 production and promotes intestinal barrier integrity. *Immunity* 50, 446–461 e9. doi: 10.1016/j.immuni.2018.12.020

Matheis, F., Muller, P. A., Graves, C. L., Gabanyi, I., Kerner, Z. J., Costa-Borges, D., et al. (2020). Adrenergic signaling in muscularis macrophages limits infection-induced neuronal loss. *Cell* 180, 64–78.e16. doi: 10.1016/j.cell.2019.12.002

Mattisson, A., and Fänge, R. (1973). Ultrastructure of erythrocytes and leucocytes of *Priapulus caudatus* (de Lamarck) (Priapulida). *J. Morphol.* 140, 367–379. doi: 10.1002/jmor.1051400309

Mayorova, T. D., Hammar, K., Winters, C. A., Reese, T. S., and Smith, C. L. (2019). The ventral epithelium of *Trichoplax adhaerens* deploys in distinct patterns cells that secrete digestive enzymes, mucus or diverse neuropeptides. *Biol. Open* 8:bio045674. doi: 10.1242/bio.045674

Mazzini, E., Massimiliano, L., Penna, G., and Rescigno, M. (2014). Oral tolerance can be established via gap junction transfer of fed antigens from $CX3CR1^{+}$ macrophages to $CD103^{+}$ dendritic cells. *Immunity* 40, 248–261. doi: 10.1016/j.immuni.2013.12.012

McDole, J. R., Wheeler, L. W., McDonald, K. G., Wang, B., Konjufca, V., Knoop, K. A., et al. (2012). Goblet cells deliver luminal antigen to CD103+ dendritic cells in the small intestine. *Nature* 483, 345–349. doi: 10.1038/nature10863

Menzel, L. P., Tondo, C., Stein, B., and Bigger, C. H. (2015). Histology and ultrastructure of the coenenchyme of the octocoral Swiftia exserta, a model organism for innate immunity/graft rejection. *Zoology* 118, 115–124. doi: 10.1016/j.zool.2014.09.002

Mikkelsen, H. B. (1995). Macrophages in the external muscle layers of mammalian intestines. *Histol. Histopathol* 10, 719–736.

Mills, D. B. (2020). The origin of phagocytosis in Earth history. *Interface Focus* 10:20200019. doi: 10.1098/rsfs.2020.0019

Monahan-Earley, R., Dvorak, A. M., and Aird, W. C. (2013). Evolutionary origins of the blood vascular system and endothelium. *J. Thrombosis Haemostasis* 11(Suppl 1):46–66. doi: 10.1111/jth.12253

Mondal, S., and Rai, U. (2001). *In vitro* effect of temperature on phagocytic and cytotoxic activities of splenic phagocytes of the wall lizard, *Hemidactylus flaviviridis*. *Comparative Biochem. Physiol. A* 129, 391–398. doi: 10.1016/S1095-6433(00)00356-1

Morita, M. (1995). Structure and function of the reticular cell in the planarian Dugesia dorotocephala. *Hydrobiologia* 305, 189–196. doi: 10.1007/978-94-011-0045-8_32

Morrison, S. J., and Scadden, D. T. (2014). The bone marrow niche for haematopoietic stem cells. *Nature* 505, 327–334. doi: 10.1038/nature12984

Mowat, A. M., and Agace, W. W. (2014). Regional specialization within the intestinal immune system. *Nat. Rev. Immunol.* 14, 667–685. doi: 10.1038/nri3738

Mukhopadhyay, S., Heinz, E., Porreca, I., Alasoo, K., Yeung, A., Yang, H. T., et al. (2020). Loss of IL-10 signaling in macrophages limits bacterial killing driven by prostaglandin E2. *J. Exp. Med.* 217:e20180649. doi: 10.1084/jem.20180649

Muller, P. A., Koscs,ó B., Rajani, G. M., Stevanovic, K., Berres, M. L., Hashimoto, D., et al. (2014). Crosstalk between muscularis macrophages and enteric neurons regulates gastrointestinal motility. *Cell* 158, 300–313. doi: 10.1016/j.cell.2014.04.050

Na, Y. R., Stakenborg, M., Seok, S. H., and Matteoli, G. (2019). Macrophages in intestinal inflammation and resolution: a potential therapeutic target in IBD. *Nat. Rev. Gastroenterol. Hepatol.* 16, 531–543. doi: 10.1038/s41575-019-0172-4

Neuhaus, B., and Higgins, R. P. (2002). Ultrastructure, biology, and phylogenetic relationships of kinorhyncha. *Integr. Comp. Biol.* 42, 619–632. doi: 10.1093/icb/42.3.619

Niedergang, F., and Grinstein, S. (2018). How to build a phagosome: new concepts for an old process. *Curr. Opin. Cell Biol.* 50, 57–63. doi: 10.1016/j.ceb.2018.01.009

Nielsen, C., Brunet, T., and Arendt, D. (2018). Evolution of the bilaterian mouth and anus. *Nat. Ecol. Evolution* 2, 1358–1376. doi: 10.1038/s41559-018-0641-0

Niess, J. H., Brand, S., Gu, X., Landsman, L., Jung, S., McCormick, B. A., et al. (2005). CX3CR1-mediated dendritic cell access to the intestinal lumen and bacterial clearance. *Science* 307, 254–258. doi: 10.1126/science.1102901

Nii, T., Bungo, T., Isobe, N., and Yoshimura, Y. (2020). Intestinal inflammation induced by dextran sodium sulphate causes liver inflammation and lipid metabolism disfunction in laying hens. *Poult. Sci.* 99, 1663–1677. doi: 10.1016/j.psj.2019.11.028

Niklas, K. J. (2014). The evolutionary-developmental origins of multicellularity. *Am. J. Bot.* 101, 6–25. doi: 10.3732/ajb.1300314

Ochi, T., Feng, Y., Kitamoto, S., Nagao-Kitamoto, H., Kuffa, P., Atarashi, K., et al. (2016). Diet-dependent, microbiota-independent regulation of IL-10-producing lamina propria macrophages in the small intestine. *Sci. Rep.* 6:27634. doi: 10.1038/srep27634

Ohno, H. (2016). Intestinal M cells. *J. Biochem.* 159, 151–160. doi: 10.1093/jb/mvv121

Okuda, K. S., Misa, J. P., Oehlers, S. H., Hall, C. J., Ellett, F., Alasmari, S., et al. (2015). A zebrafish model of inflammatory lymphangiogenesis. *Biol. Open* 4, 1270–1280. doi: 10.1242/bio.013540

Omenetti, S., Bussi, C., Metidji, A., Iseppon, A., Lee, S., Tolaini, M., et al. (2019). The intestine harbors functionally distinct homeostatic tissue-resident and inflammatory Th17 cells. *Immunity* 51, 77–89.e6. doi: 10.1016/j.immuni.2019.05.004

Panea, C., Farkas, A. M., Goto, Y., Abdollahi-Roodsaz, S., Lee, C., Koscso, B., et al. (2015). Intestinal monocyte-derived macrophages control commensal-specific Th17 responses. *Cell Rep.* 12, 1314–1324. doi: 10.1016/j.celrep.2015.07.040

Pappo, J., and Owen, R. L. (1988). Absence of secretory component expression by epithelial cells overlying rabbit gut-associated lymphoid tissue. *Gastroenterology* 95, 1173–1177. doi: 10.1016/0016-5085(88)90347-2

Pasmans, F., De Herdt, P., and Haesebrouck, F. (2002). Interactions of Salmonella enterica serovar Muenchen with macrophages of the turtle *Trachemys scripta* scripta. *Dev. Comp. Immunol.* 26, 295–304. doi: 10.1016/S0145-305X(01)00075-1

Pereira-Neves, A., and Benchimol, M. (2007). Phagocytosis by Trichomonas vaginalis: new insights. *Biol. Cell* 99, 87–101. doi: 10.1042/BC20060084

Peterson, K. J., and Eernisse, D. J. (2016). The phylogeny, evolutionary developmental biology, and paleobiology of the Deuterostomia: 25 years of new techniques, new discoveries, and new ideas. *Organisms Diversity Evol.* 16, 401–418. doi: 10.1007/s13127-016-0270-x

Phillips, R. J., and Powley, T. L. (2012). Macrophages associated with the intrinsic and extrinsic autonomic innervation of the rat gastrointestinal tract. *Autonomic Neurosci.* 169, 12–27. doi: 10.1016/j.autneu.2012.02.004

Prochazkova, P., Roubalova, R., Dvorak, J., Navarro Pacheco, N. I., and Bilej, M. (2020). Pattern recognition receptors in annelids. *Dev. Comp. Immunol.* 102:103493. doi: 10.1016/j.dci.2019.103493

Provost, K., Dancho, B. A., Ozbay, G., Anderson, R. S., Richards, G. P., and Kingsley, D. H. (2011). Hemocytes are sites of enteric virus persistence within oysters. *Appl. Environ. Microbiol.* 77, 8360–8369. doi: 10.1128/AEM.06887-11

Pull, S. L., Doherty, J. M., Mills, J. C., Gordon, J. I., and Stappenbeck, T. S. (2005). Activated macrophages are an adaptive element of the colonic epithelial progenitor niche necessary for regenerative responses to injury. *Proc. Natl. Acad. Sci. U.S.A.* 102, 99–104. doi: 10.1073/pnas.0405979102

Rahabi, M., Jacquemin, G., Prat, M., Meunier, E., AlaEddine, M., Bertrand, B., et al. (2020). Divergent roles for macrophage C-type lectin receptors, dectin-1 and mannose receptors, in the intestinal inflammatory response. *Cell Rep.* 30, 4386–4398.e5. doi: 10.1016/j.celrep.2020.03.018

Rajan, A., and Perrimon, N. (2012). Drosophila cytokine unpaired 2 regulates physiological homeostasis by remotely controlling insulin secretion. *Cell* 151, 123–137. doi: 10.1016/j.cell.2012.08.019

Richards, D. M., and Endres, R. G. (2017). How cells engulf: a review of theoretical approaches to phagocytosis. *Rep. Prog. Phys.* 80:126601. doi: 10.1088/1361-6633/aa8730

Richter, D. J., and Levin, T. C. (2019). The origin and evolution of cell-intrinsic antibacterial defenses in eukaryotes. *Curr. Opin. Genet. Dev.* 58-59, 111–122. doi: 10.1016/j.gde.2019.09.002

Rios, D., Wood, M. B., Li, J., Chassaing, B., Gewirtz, A. T., and Williams, I. R. (2016). Antigen sampling by intestinal M cells is the principal pathway initiating mucosal IgA production to commensal enteric bacteria. *Mucosal Immunol.* 9, 907–916. doi: 10.1038/mi.2015.121

Rodriguez-Manzanet, R., Sanjuan, M. A., Wu, H. Y., Quintana, F. J., Xiao, S., Anderson, A. C., et al. (2010). T and B cell hyperactivity and autoimmunity associated with niche-specific defects in apoptotic body clearance in TIM-4-deficient mice. *Proc. Natl. Acad. Sci. U.S.A.* 107, 8706–8711. doi: 10.1073/pnas.0910359107

Rolton, A., Delisle, L., Berry, J., Venter, L., Webb, S. C., Adams, S., et al. (2020). Flow cytometric characterization of hemocytes of the flat oyster, *Ostrea chilensis*. *Fish Shellfish Immunol.* 97, 411–420. doi: 10.1016/j.fsi.2019.12.071

Sanchez Bosch, P., Makhijani, K., Herboso, L., Gold, K. S., Baginsky, R., Woodcock, K. J., et al. (2019). Adult drosophila lack hematopoiesis but rely on a blood cell reservoir at the respiratory epithelia to relay infection signals to surrounding tissues. *Dev. Cell* 51, 787–803.e5. doi: 10.1016/j.devcel.2019.10.017

Sanjuan, M. A., Dillon, C. P., Tait, S. W., Moshiach, S., Dorsey, F., Connell, S., et al. (2007). Toll-like receptor signalling in macrophages links the autophagy pathway to phagocytosis. *Nature* 450, 1253–1257. doi: 10.1038/nature06421

Sato, K., Norris, A., Sato, M., and Grant, B. D. (2014). "*C. elegans* as a model for membrane traffic". in *WormBook*, ed. The *C. elegans* Research Community. doi: 10.1895/wormbook.1.77.2

Schokker, D., Jansman, A. J., Veninga, G., de Bruin, N., Vastenhouw, S. A., de Bree, F. M., et al. (2017). Perturbation of microbiota in one-day old broiler chickens with antibiotic for 24 hours negatively affects intestinal immune development. *BMC Genomics* 18:241. doi: 10.1186/s12864-017-3625-6

Schridde, A., Bain, C. C., Mayer, J. U., Montgomery, J., Pollet, E., Denecke, B., et al. (2017). Tissue-specific differentiation of colonic macrophages requires TGFbeta receptor-mediated signaling. *Mucosal Immunol.* 10, 1387–1399. doi: 10.1038/mi.2016.142

Schulthess, J., Pandey, S., Capitani, M., Rue-Albrecht, K. C., Arnold, I., Franchini, F., et al. (2019). The short chain fatty acid butyrate imprints an antimicrobial program in macrophages. *Immunity* 50, 432–445.e7. doi: 10.1016/j.immuni.2018.12.018

Schulz, O., Jaensson, E., Persson, E. K., Liu, X., Worbs, T., Agace, W. W., et al. (2009). Intestinal CD103+, but not CX3CR1+, antigen sampling cells migrate in lymph and serve classical dendritic cell functions. *J. Exp. Med.* 206, 3101–3114. doi: 10.1084/jem.20091925

Scott, N. A., Andrusaite, A., Andersen, P., Lawson, M., Alcon-Giner, C., Leclaire, C., et al. (2018). Antibiotics induce sustained dysregulation of intestinal T cell immunity by perturbing macrophage homeostasis. *Sci. Transl. Med.* 10:eaao4755. doi: 10.1126/scitranslmed.aao4755

Sehgal, A., Donaldson, D. S., Pridans, C., Sauter, K. A., Hume, D. A., and Mabbott, N. A. (2018). The role of CSF1R-dependent macrophages in control of the intestinal stem-cell niche. *Nat. Commun.* 9:1272. doi: 10.1038/s41467-018-03638-6

Shaw, T. N., Houston, S. A., Wemyss, K., Bridgeman, H. M., Barbera, T. A., Zangerle-Murray, T., et al. (2018). Tissue-resident macrophages in the intestine are long lived and defined by Tim-4 and CD4 expression. *J. Exp. Med.* 215, 1507–1518. doi: 10.1084/jem.20180019

Shiau, C. E., Kaufman, Z., Meireles, A. M., and Talbot, W. S. (2015). Differential requirement for irf8 in formation of embryonic and adult macrophages in zebrafish. *PLoS ONE* 10:e0117513. doi: 10.1371/journal.pone.0117513

Shouval, D. S., Biswas, A., Goettel, J. A., McCann, K., Conaway, E., Redhu, N. S., et al. (2014). Interleukin-10 receptor signaling in innate immune cells regulates mucosal immune tolerance and anti-inflammatory macrophage function. *Immunity* 40, 706–719. doi: 10.1016/j.immuni.2014.03.011

Shouval, D. S., Biswas, A., Kang, Y. H., Griffith, A. E., Konnikova, L., Mascanfroni, I. D., et al. (2016). Interleukin 1β mediates intestinal inflammation in mice and patients with interleukin 10 receptor deficiency. *Gastroenterology* 151, 1100–1104. doi: 10.1053/j.gastro.2016.08.055

Smith, L. C., Arizza, V., Barela Hudgell, M. A., Barone, G., Bodnar, A. G., Buckley, K. M., et al. (2018). "Echinodermata: the complex immune system in echinoderms," In *Advances in Comparative Immunology* ed. E. L. Cooper. (Cham: Springer International Publishing). p. 409–501. doi: 10.1007/978-3-319-76768-0_13

Solas, M. T., and Zapata, A. (1980). Gut-associated lymphoid tissue (GALT) in reptiles: intraepithelial cells. *Dev. Comp. Immunol.* 4, 87–97. doi: 10.1016/S0145-305X(80)80011-5

Solomon, J. B., Developmental ISo., and Immunology C. (1981). *Aspects of Developmental and Comparative Immunology: Proceedings of the 1st Congress of Developmental and Comparative Immunology, 27 July-1 August 1980*, Aberdeen: Pergamon Press.

Stachura, D. L., and Traver, D. (2011). "Chapter 4 - cellular dissection of zebrafish hematopoiesis," in *Methods in Cell Biology*. eds H. W. Detrich, M. Westerfield, L. I. Zon. (Academic Press). 101, *p*. 75–110. doi: 10.1016/B978-0-12-387036-0.00004-9

Tacchi, L., Larragoite, E. T., Muñoz, P., Amemiya, C. T., and Salinas, I. (2015). African lungfish reveal the evolutionary origins of organized mucosal lymphoid tissue in vertebrates. *Curr. Biol.* 25, 2417–2424. doi: 10.1016/j.cub.2015.07.066

Taha-Abdelaziz, K., Astill, J., Shojadoost, B., Borrelli, S., M. A. M., and Sharif, S. (2020). Campylobacter-derived ligands induce cytokine and chemokine expression in chicken macrophages and cecal tonsil mononuclear cells. *Vet. Microbiol.* 246:108732. doi: 10.1016/j.vetmic.2020.108732

Tamoutounour, S., Henri, S., Lelouard, H., de Bovis, B., de Haar, C., van der Woude, C. J., et al. (2012). CD64 distinguishes macrophages from dendritic cells in the gut and reveals the Th1-inducing role of mesenteric lymph node macrophages during colitis. *Eur. J. Immunol.* 42, 3150–3166. doi: 10.1002/eji.201242847

Tang, B., Williams, P. L., Xue, K. S., Wang, J. S., and Tang, L. (2020). Detoxification mechanisms of nickel sulfate in nematode *Caenorhabditis elegans*. *Chemosphere* 260:127627. doi: 10.1016/j.chemosphere.2020.127627

Tattikota, S. G., Cho, B., Liu, Y., Hu, Y., Barrera, V., Steinbaugh, M. J., et al. (2020). A single-cell survey of Drosophila blood. *Elife* 9:e54818. doi: 10.7554/eLife.54818.sa2

Telford, M. J., Budd, G. E., and Philippe, H. (2015). Phylogenomic insights into animal evolution. *Curr. Biol.* 25, R876–R887. doi: 10.1016/j.cub.2015.07.060

Traylor-Knowles, N., Vandepas, L. E., and Browne, W. E. (2019). Still enigmatic: innate immunity in the ctenophore *Mnemiopsis leidyi*. *Integr. Comp. Biol.* 59, 811–818. doi: 10.1093/icb/icz116

van de Laar, L., Saelens, W., De Prijck, S., Martens, L., Scott, C. L., Van Isterdael, G., et al. (2016). Yolk sac macrophages, fetal liver, and adult monocytes can colonize an empty niche and develop into functional tissue-resident macrophages. *Immunity* 44, 755–768. doi: 10.1016/j.immuni.2016.02.017

Wagner, C., Bonnardel, J., Da Silva, C., Martens, L., Gorvel, J. P., and Lelouard, H. (2018). Some news from the unknown soldier, the Peyer's patch macrophage. *Cell. Immunol.* 330, 159–167. doi: 10.1016/j.cellimm.2018.01.012

Wagner, C., Bonnardel, J., Da Silva, C., Spinelli, L., Portilla, C. A., Tomas, J., et al. (2020). Differentiation paths of Peyer's patch LysoDCs are linked to sampling site positioning, migration, and T cell priming. *Cell Rep* 31:107479. doi: 10.1016/j.celrep.2020.03.043

Walters, B. M., Connelly, M. T., Young, B., and Traylor-Knowles, N. (2020). The complicated evolutionary diversification of the Mpeg-1/Perforin-2 family in cnidarians. *Front. Immunol.* 11:1690. doi: 10.3389/fimmu.2020.01690

Wang, Z., Du, J., Lam, S. H., Mathavan, S., Matsudaira, P., and Gong, Z. (2010). Morphological and molecular evidence for functional organization along the rostrocaudal axis of the adult zebrafish intestine. *BMC Genomics* 11:392. doi: 10.1186/1471-2164-11-392

Wigley, P. (2014). *Salmonella enterica* in the chicken: how it has helped our understanding of immunology in a non-biomedical model species. *Front. Immunol.* 5:482. doi: 10.3389/fimmu.2014.00482

Willensdorfer, M. (2008). Organism size promotes the evolution of specialized cells in multicellular digital organisms. *J. Evol. Biol.* 21, 104–110. doi: 10.1111/j.1420-9101.2007.01466.x

Willis, A. R., Sukhdeo, R., and Reinke, A. W. (2020). Remembering your enemies: mechanisms of within-generation and multigenerational immune priming in *Caenorhabditis elegans*. *FEBS J.* doi: 10.1111/febs.15509

Wittamer, V., Bertrand, J. Y., Gutschow, P. W., and Traver, D. (2011). Characterization of the mononuclear phagocyte system in zebrafish. *Blood* 117, 7126–7135. doi: 10.1182/blood-2010-11-321448

Wood, W., and Martin, P. (2017). Macrophage functions in tissue patterning and disease: new insights from the fly. *Dev. Cell* 40, 221–233. doi: 10.1016/j.devcel.2017.01.001

Woodcock, K. J., Kierdorf, K., Pouchelon, C. A., Vivancos, V., Dionne, M. S., and Geissmann, F. (2015). Macrophage-derived upd3 cytokine causes impaired glucose homeostasis and reduced lifespan in Drosophila fed a lipid-rich diet. *Immunity* 42, 133–144. doi: 10.1016/j.immuni.2014.12.023

Wu, S. C., Liao, C. W., Pan, R. L., and Juang, J. L. (2012). Infection-induced intestinal oxidative stress triggers organ-to-organ immunological communication in Drosophila. *Cell Host Microbe* 11, 410–417. doi: 10.1016/j.chom.2012.03.004

Yaparla, A., Koubourli, D. V., Popovic, M., and Grayfer, L. (2020). Exploring the relationships between amphibian (*Xenopus laevis*) myeloid cell subsets. *Dev. Comp. Immunol.* 113:103798. doi: 10.1016/j.dci.2020.103798

Yaparla, A., Reeves, P., and Grayfer, L. (2019). Myelopoiesis of the Amphibian *Xenopus laevis* is segregated to the bone marrow, away from their hematopoietic peripheral liver. *Front. Immunol.* 10:3015. doi: 10.3389/fimmu.2019.03015

Yaparla, A., Wendel, E. S., and Grayfer, L. (2016). The unique myelopoiesis strategy of the amphibian *Xenopus laevis*. *Dev. Comp. Immunol.* 63, 136–143. doi: 10.1016/j.dci.2016.05.014

Yona, S., Kim, K. W., Wolf, Y., Mildner, A., Varol, D., Breker, M., et al. (2013). Fate mapping reveals origins and dynamics of monocytes and tissue macrophages under homeostasis. *Immunity* 38, 79–91. doi: 10.1016/j.immuni.2012.12.001

Yutin, N., Wolf, M. Y., Wolf, Y. I., and Koonin, E. V. (2009). The origins of phagocytosis and eukaryogenesis. *Biol. Direct* 4:9. doi: 10.1186/1745-6150-4-9

Zaidman-Rémy, A., Regan, J. C., Brandão, A. S., and Jacinto, A. (2012). The Drosophila larva as a tool to study gut-associated macrophages: PI3K regulates a discrete hemocyte population at the proventriculus. *Dev. Comp. Immunol.* 36, 638–647. doi: 10.1016/j.dci.2011.10.013

Zapata, A., and Solas, M. T. (1979). Gut-associated lymphoid tissue (GALT) in reptilla: structure of mucosal accumulations. *Dev. Comp. Immunol.* 3, 477–487. doi: 10.1016/S0145-305X(79)80043-9

Zigmond, E., Bernshtein, B., Friedlander, G., Walker, C. R., Yona, S., Kim, K. W., et al. (2014). Macrophage-restricted interleukin-10 receptor deficiency, but not IL-10 deficiency, causes severe spontaneous colitis. *Immunity* 40, 720–733. doi: 10.1016/j.immuni.2014.03.012

Conflict of Interest: The authors declare that the research was conducted in the absence of any commercial or financial relationships that could be construed as a potential conflict of interest.

frontiers in Cell and Developmental Biology

BRIEF RESEARCH REPORT
published: 04 March 2021
doi: 10.3389/fcell.2021.643712

Toward a Consensus in the Repertoire of Hemocytes Identified in *Drosophila*

Pierre B. Cattenoz[1,2,3,4]*, *Sara Monticelli*[1,2,3,4], *Alexia Pavlidaki*[1,2,3,4] and *Angela Giangrande*[1,2,3,4]*

[1] Institut de Génétique et de Biologie Moléculaire et Cellulaire, Illkirch, France, [2] Centre National de la Recherche Scientifique, UMR 7104, Illkirch, France, [3] Institut National de la Santé et de la Recherche Médicale, U1258, Illkirch, France, [4] Université de Strasbourg, Illkirch, France

OPEN ACCESS

Edited by:
Marc S. Dionne,
Imperial College London,
United Kingdom

Reviewed by:
Iwan Robert Evans,
The University of Sheffield,
United Kingdom
Ioannis Eleftherianos,
George Washington University,
United States

***Correspondence:**
Pierre B. Cattenoz
cattenoz@igbmc.fr
orcid.org/0000-0001-5301-1975
Angela Giangrande
angela@igbmc.fr
orcid.org/0000-0001-6278-5120

Specialty section:
This article was submitted to Cell Death and Survival, a section of the journal Frontiers in Cell and Developmental Biology

Received: 18 December 2020
Accepted: 12 February 2021
Published: 04 March 2021

Citation:
Cattenoz PB, Monticelli S, Pavlidaki A and Giangrande A (2021) Toward a Consensus in the Repertoire of Hemocytes Identified in Drosophila. Front. Cell Dev. Biol. 9:643712. doi: 10.3389/fcell.2021.643712

The catalog of the *Drosophila* immune cells was until recently limited to three major cell types, based on morphology, function and few molecular markers. Three recent single cell studies highlight the presence of several subgroups, revealing a large diversity in the molecular signature of the larval immune cells. Since these studies rely on somewhat different experimental and analytical approaches, we here compare the datasets and identify eight common, robust subgroups associated to distinct functions such as proliferation, immune response, phagocytosis or secretion. Similar comparative analyses with datasets from different stages and tissues disclose the presence of larval immune cells resembling embryonic hemocyte progenitors and the expression of specific properties in larval immune cells associated with peripheral tissues.

Keywords: macrophage, single cell RNA seq, drosophila, lamellocyte, innate immunity

INTRODUCTION

Immune cells are able to move and connect distant tissues and organs. This feature likely accounts for their pleiotropic role as sensors and regulators of the internal state in homeostatic, challenged and pathological conditions. While pleiotropy seems to arise from immune cell heterogeneity, the cause and nature of cell diversity is still poorly understood. How much does it depend on intrinsic differences dictated by cell autonomous cues vs. environmental conditions met by these cells during their life? To address the longstanding question on the impact of nature vs. nurture, of cell identity vs. cell state, we first need to characterize the different subtypes in depth.

Beside a lower complexity of the immune cell lineages, *Drosophila* shares with vertebrates several factors controlling the differentiation of the myeloid lineage [e.g., GATA and Runx proteins (Wood and Jacinto, 2007)], immune cell migration [e.g., integrins and Rho GTPases (Paladi and Tepass, 2004; Siekhaus et al., 2010; Comber et al., 2013)], phagocytosis [e.g., the CED-1 family member Draper and the CD36-related receptor Croquemort (Franc et al., 1996; Manaka et al., 2004)] and immune response [i.e., JAK/STAT, IMD, and Toll pathways (Buchon et al., 2014)]. Hence, it represents a simple yet evolutionary conserved model to address the origin of the immune cell diversity.

The immune cells of *Drosophila*, the hemocytes, have been classically subdivided in three types: the plasmatocytes, the crystal cells and the lamellocytes, which are thought to derive from the same lineage, similar to the myeloid cells in mammals (Banerjee et al., 2019). The plasmatocytes are macrophage-like cells that phagocytose pathogens as well as cell debris and constitute ∼95% of the hemocytes. The remaining hemocytes are the crystal cells, platelet-like cells in charge of melanization, a process that is necessary for wound closure and immune response to pathogens. The third type of immune cells, the lamellocytes, appears only after immune/inflammatory challenge from progenitors or by plasmatocyte transdifferentiation (Banerjee et al., 2019).

Until recently, the hemocytes were identified using distinctive morphological features and a handful of molecular markers. The plasmatocytes are small cells of ∼10 μm of diameter. They can be round or present cytoplasmic projections [i.e., podocytes (Rizki and Rizki, 1980)]. They express several markers such as the transmembrane receptors Nimrod C1 (NimC1), Eater, Hemese (He) and Croquemort (Crq), the fascin Singed (Sn) and the secreted proteins Hemolectin (Hml), Peroxidasin (Pxn), and Collagen type IV alpha 1 (Col4a1) (Nelson et al., 1994; Franc et al., 1996; Goto et al., 2001; Kurucz et al., 2003; Kocks et al., 2005; Zanet et al., 2009). The crystal cells have the same size than the plasmatocytes and are characterized by the presence of crystals. They express the transcription factors Lozenge (Lz) and Pebbled (Peb) as well as Prophenoloxidases 1 and 2 (PPO1 and PPO2) (Rizki and Rizki, 1959; Binggeli et al., 2014). PPO2 is a major constituent of the crystals, which are released upon wounding to initiate the melanization reaction (Binggeli et al., 2014). The lamellocytes are large melanized cells (>60 μm of diameter) with heterogeneous shapes. They are strongly labeled with the actin filament probe called phalloidin and express the Prophenoloxidase 3 (PPO3), the kinase Misshapen (Msn), the integrins Myospheroid (Mys, Integrin beta or L4), and Integrin alphaPS4 subunit (ItgaPS4 or L5), the actin binding protein Cheerio (Cher, L5), and the glycosylphosphatidylinositol (GPI)-anchored protein Atilla (L1) (Braun et al., 1997; Irving et al., 2005; Rus et al., 2006; Honti et al., 2009).

The development of single cell RNA sequencing (scRNAseq) techniques has made it possible to significantly enlarge the panel of the *Drosophila* immune cells based on their transcriptional profile. ScRNAseq consists of sequencing the transcriptome of single cells in a high throughput fashion. The cells are then grouped according to their expression profiles (reviewed in Potter, 2018; See et al., 2018). Three scRNAseq studies recently revealed the diversity of the hemocytes present in the *Drosophila* larva (Cattenoz et al., 2020; Fu et al., 2020; Tattikota et al., 2020). We perform here a comparative study to refine immune cell diversity, origin and localization within the organism. Our comparison defines subgroups robustly found in the three datasets from steady state larval hemocytes, despite the different experimental and analytical approaches. The common subgroups reflect the differentiation state, intermediary vs. mature hemocytes, as well as their main functions (phagocytosis, immune response/antimicrobial peptide (AMP) production, secretion and proliferation). Finally, we analyze the hemocytes present in available single cell datasets from larval eye discs and brains as well as from stage 6 embryos in order to link specific subgroups to distinct environments/developmental trajectories.

MATERIALS AND METHODS

Comparison of scRNAseq Data on Wandering 3rd Instar Larval Hemocytes

The list of markers for each subgroup were retrieved from the publications [Dataset_EV2 in Cattenoz et al. (2020) and **Supplementary File 2** in Tattikota et al. (2020)]. The two lists were generated with the same tool [function "FindMarkers" in Seurat R toolkit (Butler et al., 2018; Stuart et al., 2019)] and provide comparable parameters including the enrichment levels for all the subgroup markers. The two tables were compiled in R and plotted using the package ggplot2 (Villanueva and Chen, 2019). The markers described in Fu et al. (2020) dataset were retrieved from the figure of the manuscript. Of note, the PM12 cells in Tattikota et al. (2020) appear exclusively in wounding condition, an experimental set up that was not assessed by the two other studies. To keep the comparison as homogenous as possible, the markers of the subgroup PM12 were excluded from our analysis.

The dot plots were generated using the function "DotPlot" in the Seurat R toolkit (Butler et al., 2018; Stuart et al., 2019) with the non-infested data from Cattenoz et al. deposited in the ArrayExpress database at EMBL-EBI[1] under the accession number E-MTAB-8698. The list of markers for the CAH7 PM, the Lsp PM, the Ppn PM, the thanacytes, and the primocytes were retrieved from the figures in Fu et al. (2020). The top PSC markers were retrieved from the lymph gland scRNAseq data from Cho et al. (2020; **Supplementary Table S2**): the markers presenting the highest enrichment in the PSC were selected.

Comparison of the WL Hemocyte scRNAseq Data With Stage 6 Embryo, Larval Eye Disc and Larval Brain scRNAseq Data

The normalized expression matrix of the stage 6 embryos (Karaiskos et al., 2017) was downloaded from https://shiny.mdc-berlin.de/DVEX/ and analyzed with the standard workflow from Seurat toolkit[2] (Butler et al., 2018; Stuart et al., 2019). Briefly, first the data were normalized (function NormalizeData), the variable genes were identified (function FindVariableFeatures, selection method "vst," number of feature = 2,000), the data were scaled (function ScaleData, features = all.genes), linear dimensional reduction was carried out on the variable genes (function RunPCA), the dimensionality of the dataset was determined and set

[1] www.ebi.ac.uk/arrayexpress

[2] https://satijalab.org/seurat/v3.2/pbmc3k_tutorial.html

to 15 (function ElbowPlot), the cells were then clustered (functions FindNeighbors, dims = 1:15 and FindClusters, resolution = 1.2), at last non-linear dimensional reductions were carried out (functions RunUMAP and RunTSNE). This pipeline generated a single subgroup enriched for all the markers of the hemocyte subgroup described in Karaiskos et al. (2017): i.e., Gcm, Ham, Ttk, CrebA, Shep, RhoL, Fok, Knrl, Kni, Zfh1, CG33099, Srp, Btd, and NetB. This subgroup was used for the downstream analyses.

The normalized expression matrix of the wild type larval eye disc (Ariss et al., 2018) was downloaded from https://www.ebi.ac.uk/gxa/sc/experiments/E-MTAB-7195/downloads and analyzed following the same pipeline than stage 6 embryos described above with modification: the dimensionality was set to 17 and the cells were clustered with a resolution of 0.5. The hemocyte subgroup was unambiguously identified using the hemocyte markers Srp, Hml, Pxn, NimC1, Crq, and Sn and used for the downstream analyses.

The expression matrices of the normal 1st instar larval brains (Brunet Avalos et al., 2019) were downloaded from https://www.ncbi.nlm.nih.gov/geo/query/acc.cgi?acc=GSE134722. The expression matrices GSM3964166, GSM3964167, GSM3964168, and GSM4132287 were merged and integrated following Seurat standard pipeline (Butler et al., 2018; Stuart et al., 2019): each matrix was normalized (function NormalizeData), the variable features and the common anchors were identified (function FindVariableFeatures, method "vst," function FindIntegrationAnchors, dimension 1:50) and the matrices were integrated (function IntegrateData, dimension: 1:50). The integrated matrix was analyzed following the same pipeline as described above for the stage 6 embryos with the following parameters: the dimensionality was set to 50 and the cells were clustered with a resolution of 0.4. The hemocyte subgroup was unambiguously identified using the hemocyte markers Srp, Hml, Pxn, NimC1, and He and used for the downstream analyses.

The expression matrices of the brains from 2nd instar larvae [24 h after larval hatching (h ALH)], feeding 3rd instar larvae (48 h ALH) and wandering 3rd instar larvae (96 h ALH) (Cocanougher et al., 2019) were downloaded from https://www.ncbi.nlm.nih.gov/geo/query/acc.cgi?acc=GSE135810. The following matrices were used: GSM4030602, GSM4030604, and GSM4030607 for the 2nd instar larvae, GSM4030600 and GSM4030606 for the feeding 3rd instar larvae and GSM4030623, GSM4030624, GSM4030625, and GSM4030626 for the wandering 3rd instar larvae. The matrices were integrated for each stage and analyzed as described for the 1st instar larval brain described above with the following parameters: the dimensionality was set to 30 and the cells were clustered with a resolution of 0.4 for the 2nd instar larvae and 2.4 for the feeding and wandering 3rd instar larvae. The hemocyte subgroups were unambiguously identified using the hemocyte markers Srp, Hml, Pxn, NimC1, He, and Nplp2 (described by the authors) and used for the downstream analyses.

Pearson correlation were computed as follow. Pseudo-transcriptomes were generated for the hemocyte subgroups from the stage 6 embryos data (Karaiskos et al., 2017), from the eye disc data (Ariss et al., 2018), for the brain data (Brunet Avalos et al., 2019) as well as for each subgroup of the non-infested dataset from Cattenoz et al. (2020) using the function "AverageExpression" from the Seurat R toolkit (Butler et al., 2018; Stuart et al., 2019). The correlation between the pseudo-transcriptomes were then measured using the Pearson correlation coefficient. The pseudo-transcriptomes of the hemocyte subgroups from Cattenoz et al. were compared to the pseudo-transcriptome of stage 6 embryos' hemocytes in **Supplementary Figure S3G**, to the pseudo-transcriptome of the eye disc associated hemocytes in **Supplementary Figure S3C** and to the pseudo-transcriptome of the brain associated hemocytes in **Supplementary Figure S3E**.

The dot plot (**Figure 4D**) was generated using the function "DotPlot" from the Seurat R toolkit with the non-infested data from Cattenoz et al. (2020) and the expression matrices from stage 6 embryos and larval eye discs (Karaiskos et al., 2017; Ariss et al., 2018). The dot plot was compiled in Adobe Illustrator CS6.

Regulon Analysis

To identify the regulons enriched in the lamellocytes, we ran Single-Cell regulatory Network Inference and Clustering (SCENIC) (Aibar et al., 2017) through its Python implementation pySCENIC, version 0.9.19[3]. The source code was downloaded from the GitHub repository https://github.com/aertslab/pySCENIC.git. The **Supplementary Files** necessary to run SCENIC were obtained from https://resources-mirror.aertslab.org/cistarget/. The analysis was carried out on the wasp infested expression matrix from Cattenoz et al. deposited in the ArrayExpress database at EMBL-EBI[4] under the accession number E-MTAB-8698.

The motifs version 8,[5] the regulatory elements within 5 kb upstream the TSS and the transcript introns[6] were used for the analysis. The most significant regulons showing differential activity among clusters were determined with Mann-Whitney *U*-test (Mann and Whitney, 1947), between the AUC scores given by SCENIC in a specific cluster versus all the rest of the clusters. The regulons displaying a z-score above 2 or below -2 for the lamellocytes subgroups were selected to build the heatmap shown in **Figure 3A**. The heatmap was generated with the R package "pheatmap" (Kolde, 2019).

The scatter plot (**Figure 3B**) was generated with the pseudo-transcriptomes of LM1 and LM2 subgroups from the wasp infested dataset in Cattenoz et al. (2020). The pseudo-transcriptomes were estimated with the function "AverageExpression" from the Seurat R toolkit (Butler et al., 2018; Stuart et al., 2019).

Fly Strains and Genetics

All flies were raised on standard media at 25°C. The following strains were used: *Oregon-R, srp(hemo)-3xmcherry*

[3]https://pyscenic.readthedocs.io/en/latest/

[4]www.ebi.ac.uk/arrayexpress

[5]cistarget/motif2tf/motifs-v8-nr.flybase-m0.001-o0.0.tbl

[6]cistarget/databases/drosophila_melanogaster/dm6/flybase_r6.02/mc8nr/gene_based/dm6-5kb-upstream-full-tx-11species.mc8nr.feather

[*srp(hemo) > RFP*, gift from D. Siekhaus (Gyoergy et al., 2018)], *BAC-gcm-Flag* (Laneve et al., 2013).

Immunolabelling and Image Acquisition

For hemocyte labeling, 10 wandering 3rd instar larvae were bled in Schneider medium complemented with 10% Fetal Calf Serum (FCS), 0.5% penicillin, 0.5% streptomycin (PS), and few crystals of N-phenylthiourea ≥98% (PTU). The cells were cytospinned on a glass slide at 700 rpm for 3 min at room temperature (RT), then the samples were fixed for 10 min in 4% paraformaldehyde/PBS at RT and rinsed with PTX (PBS 1x, 0.5% triton X-100).

For the embryos, overnight collections were washed on a 100 μm mesh and dechorionated in bleach for 5 min. The fixation was carried out for 25 min at RT under agitation in a solution of 4% paraformaldehyde in PBS 1x/heptane (1/1 vol.). The vitelline membrane of the embryos was then removed by replacing the PFA solution by methanol and strong agitation for 30 s. The methanol/heptane solution was removed and the embryos were washed with PTX for 15 min at RT.

For the lymph gland and filet preparation, wandering 3rd instar larvae were dissected in cold PBS 1x, then transferred in 4% paraformaldehyde in PBS 1x for at least 30 min at RT and rinsed in PTX for 15 min.

Following the PFA fixation and PTX wash, the samples were incubated with blocking reagent (Roche) for 1 h at RT, incubated overnight at 4°C with primary antibodies diluted in blocking reagent, washed three times for 10 min with PTX, incubated for 1 h with secondary antibodies, washed twice for 10 min with PTX, incubated for 30 min with DAPI and phalloidin TRITC (1:1,000, Sigma #P1951), and then mounted in Aqua-Poly/Mount (Polysciences, Inc.). The following primary antibodies were used: rabbit anti-Srp [1:500, (Bazzi et al., 2018)], rabbit anti-Flag (1:100, Sigma S3165), chicken anti-GFP (1:500, abcam ab13970), rat anti-RFP (1:500, Chromotek 5F8-100), rabbit anti-Pxn [1:5,000; gift from J. Shim, (Yoon et al., 2017)], mouse anti-Hemese [1:50 gifts from I. Ando, (Kurucz et al., 2003)].

The following secondary antibodies were used at 1:500: FITC donkey anti-chicken IgG (Jackson ImmunoResearch Labs Cat# 703-095-155), FITC goat anti-mouse IgG (Jackson ImmunoResearch Labs Cat# 115-095-166), Cy3 donkey anti-mouse IgG (Jackson ImmunoResearch Labs Cat# 715-165-151), Cy3 goat anti-rat IgG (Jackson ImmunoResearch Labs Cat# 112-165-167), Cy3 donkey anti-rabbit IgG (Jackson ImmunoResearch Labs Cat# 711-165-152), Cy5 goat anti-mouse IgG (Jackson ImmunoResearch Labs Cat# 115-175-003) and Cy5 goat anti-rat IgG (Jackson ImmunoResearch Labs Cat# 112-175-167), Cy5 goat anti-rabbit IgG (Jackson ImmunoResearch Labs Cat# 111-175-144), Alexa Fluor 647 goat anti-mouse IgG (Jackson ImmunoResearch Labs Cat# 115-605-166).

The slides were analyzed by confocal microscopy (Leica Spinning Disk and Leica SP8) with 20x, 40x, and 63x objectives, using hybrid detectors in photon counting mode. DAPI was excited at 350 nm, the emission filters 410–510 were used to collect the signal; FITC was excited at 488 nm, the emission filters 498–551 were used to collect the signal; Cy3 was excited at 568 nm, emission filters 648–701 were used to collect the signal, and Cy5 was excited at 633 nm; emission signal was collected at 729–800 nm. The images were analyzed with Fiji (Schindelin et al., 2012).

RESULTS

Characterization of the *Drosophila* Larval Hemocytes by scRNAseq

The first hematopoietic wave occurs at early embryonic stages 6–9, in the procephalic mesoderm (PM). The progenitors undergo several rounds of division, differentiate into plasmatocytes and crystal cells and migrate along stereotyped routes to spread throughout the organism (PM hemocytes) (Tepass et al., 1994; Gold and Bruckner, 2014). The second hematopoietic wave occurs in the lymph gland (LG) of the larva to generate cells that are only released in the hemolymph after puparium formation, upon lymph gland histolysis (LG hemocytes) (Jung et al., 2005; reviewed by Banerjee et al., 2019). The larval infestation from parasitoid wasps such as *Leptopilina boulardi* as well as wounding triggers precocious lymph gland histolysis. These challenges also lead to the differentiation of lamellocytes that encapsulate the wasp eggs or participate to the wound closure (**Figure 1A**) and the same cell type is found upon the activation of pro-inflammatory pathways (Lemaitre et al., 1995; Luo et al., 1995; Markus et al., 2005; Fleury et al., 2009; Kim-Jo et al., 2019).

The larval PM hemocytes were recently analyzed in three scRNAseq studies (Cattenoz et al., 2020; Fu et al., 2020; Tattikota et al., 2020), following different experimental parameters (**Figure 1B**). Tattikota et al. analyzed hemocytes from feeding 3rd instar larvae and wandering 3rd instar larvae (WL) in steady state conditions or after inducing an immune reaction (clean wounding, or wasp infestation). Three sequencing technologies were used and the animals were of two genotypes. The merge of these datasets identified twelve subgroups of plasmatocytes, two of crystal cells and two of lamellocytes (Tattikota et al., 2020). Fu et al. analyzed hemocytes from WL of one genotype in steady state conditions using 10x Genomics technology. They identified four subgroups of plasmatocytes, one of crystal cells, one of lamellocytes and two minor cell populations called primocytes and thanacytes (Fu et al., 2020). Cattenoz et al. analyzed hemocytes from female WL of one genotype, in steady state conditions and after wasp infestations, using 10x Genomics technology. They identified thirteen subgroups of plasmatocytes, one of crystal cells and two of lamellocytes, the latter ones being specifically found in the dataset from the challenged condition (Cattenoz et al., 2020). In the three datasets, the definition of the subgroups was followed by lineage prediction analyses to identify distinct developmental trajectories amongst the hemocyte subgroups. The trajectories are defined by organizing the cells along a pseudo-time axis based on the progression of the expression of the variable genes (Kester and van Oudenaarden, 2018).

The systematic comparison of the lists of markers from the three studies allows the identification of common subgroups (**Figure 2A**). The markers are defined by their levels of enrichment in a specific subgroup compared to the whole hemocyte population [Log2(enrichment) >0.25, adjusted

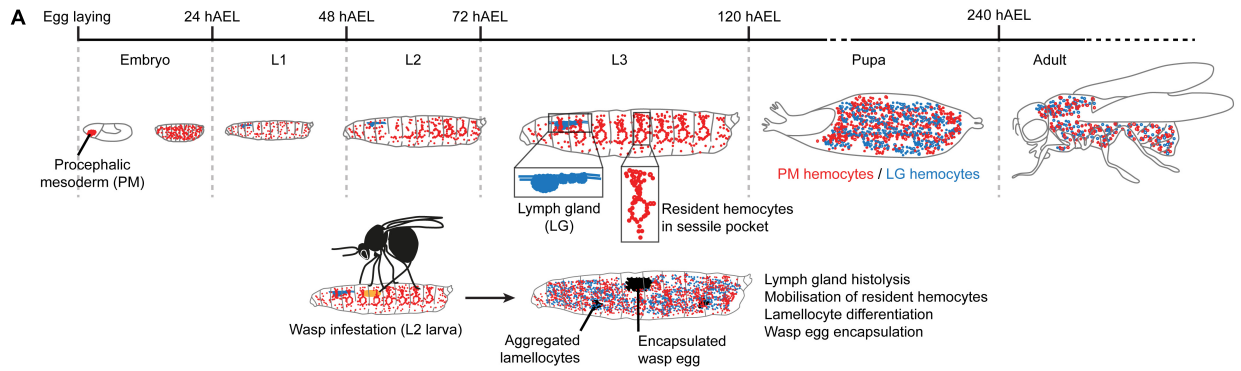

B

Ref	(Cattenoz *et al.*, 2020)	(Tattikota *et al.*, 2020)	(Fu *et al.*, 2020)
Stage	Wandering L3 (120 hAEL)	Feeding L3 (96 hAEL) and wandering L3	Wandering L3
Challenge	Steady state/ Wasp infestation	Steady stage/ Wasp infestation/ Sterile wound	Steady state
Genotype	*Oregon-R* (females only)	Wasp: *Oregon-R* Wound and steady state: *hml>EGFP*	w^{1118}
Sequencing technology	10x Genomics	10x Genomics, Drop-seq, inDrop	10x Genomics
Total cell number	15664 (7606 steady state + 8058 after wasp infestation)	19458 (4110 steady state, 6170 after wasp infestation, 9178 after clean wound)	3424
Subgroup/marker identification	Seurat v3.0 R package	Seurat v3.0 R package	Seurat v2.3 R package
Lineage prediction	Monocle 2 and Velocyto v0.17.17	Monocle 3	Monocle 2
Regulon analysis	SCENIC (pySCENIC v0.9.19)	Not available	Not available
Dataset ID	E-MTAB-8698	GSE146596	Not available
Number of hemocyte subgroups	13 plasmatocytes 1 crystal cell 2 lamellocytes	12 plasmatocytes 2 crystal cells 2 lamellocytes	4 plasmatocytes 1 crystal cell 1 lamellocyte 2 others

FIGURE 1 | Experimental procedures used to generate the scRNAseq datasets on larval hemocytes. **(A)** Overview of the two hematopoietic waves during *Drosophila* development. The first wave starts in the procephalic mesoderm (PM) of the early embryo. By the end of embryogenesis, the PM hemocytes spread across the whole embryo and constitute the whole population of hemocytes present in the hemolymph of the larva. By the 2nd larval instar, the majority of the PM hemocytes become resident between the muscle and the cuticle to form the sessile pockets. After pupariation, the hemocytes are mobilized in the hemolymph. The second wave occurs in the lymph gland (LG) during the larval stages, the LG hemocytes being released in circulation after pupariation. When the wasp infests the larva (2nd instar), it induces a strong immune response, which includes precocious lymph gland histolysis and the release of the LG hemocytes in 3rd instar larvae. The response also includes the mobilization of the resident hemocytes and the differentiation of lamellocytes to encapsulate the wasp egg. The lamellocytes spontaneously aggregate and form melanized masses called melanotic tumors. The developmental stages and their duration at 25°C are indicated in gray in hours After Egg Laying (hAEL). **(B)** Experimental parameters of the three single cell sequencing analyses of PM hemocytes.

$p < 0.01$ in Cattenoz et al. (2020) and Tattikota et al. (2020)]. The correlation between the subgroups of each dataset is inferred from the cross-comparison of all plasmatocyte markers found in the three studies (**Figure 2A**). The number of markers as well as their level of enrichments are taken into consideration (**Supplementary Figures S1A,B, S2A,C–E**). An additional level of comparison among the datasets is the developmental trajectory. If our comparison based on markers is accurate, the developmental trajectories between the distinct subgroups should be preserved across the three studies, and we find that this is the case. Thus, the subgroups presenting the highest number of common markers, the highest levels of markers' enrichment and similar developmental trajectories likely define equivalent subgroup (**Figures 2B,C**).

For example, PM9 in Tattikota et al. dataset shares a significant number of markers with PL-0, PL-3, PL-vir1, PL-prolif, PL-Inos, and PL-robo2 in Cattenoz et al. dataset (**Figure 2A**). The subgroup presenting the highest number of markers with the highest enrichments is PL-prolif (**Supplementary Figure S1A**). The second closest subgroup is PL-robo2, which also displays markers with relatively high enrichments. However, PL-robo2/PM9 markers are expressed in most hemocyte subgroups while PL-prolif/PM9 markers are highly specific (**Supplementary Figure S1B**). At last, lineage predictions carried out in both studies suggest that PM9 and PL-prolif are sitting at the beginning of the developmental trajectories of the hemocytes (Cattenoz et al., 2020; Tattikota et al., 2020). Altogether, these data suggest that PM9 and PL-prolif represent the same subgroup.

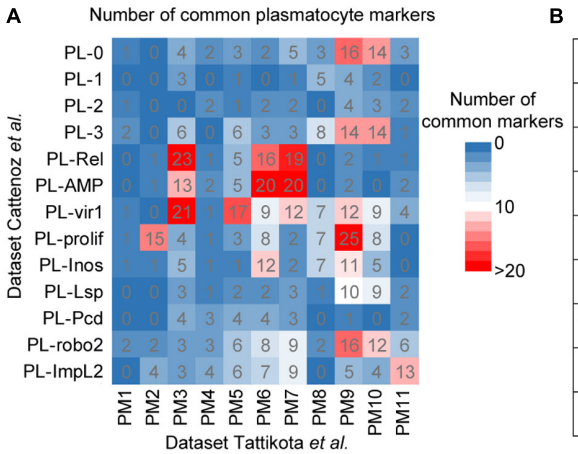

B

	Subgroup ID (Cattenoz et al., 2020)	Subgroup ID (Tattikota et al., 2020)	Subgroup ID (Fu et al., 2020)
Crystal cells	CC	CC1, CC2	Crystal cell (cluster 2)
Lamellocytes	Intermediate (LM-2), mature (LM-1)	Intermediate (LM1), mature (LM2)	Lamellocyte (cluster 3)
Unspecified plasmatocytes	PL-0, PL-1, PL-2, PL-3	PM1	Reservoir PM
Proliferative plasmatocytes	PL-prolif/PL-Inos	PM2, PM9	Ppn+ PM (?)
PSC-like hemocytes	PL-ImpL2	PM11	Primocyte
Antimicrobial plasmatocytes	PL-Rel, PL-vir1, PL-AMP	PM3, PM5, PM6, PM7	NA
Phagocytic plasmatocytes	PL-robo2	NA	CAH7+ PM
Secretory plasmatocytes	PL-Lsp PL-Pcd	NA	Lsp+ PM Thanacyte

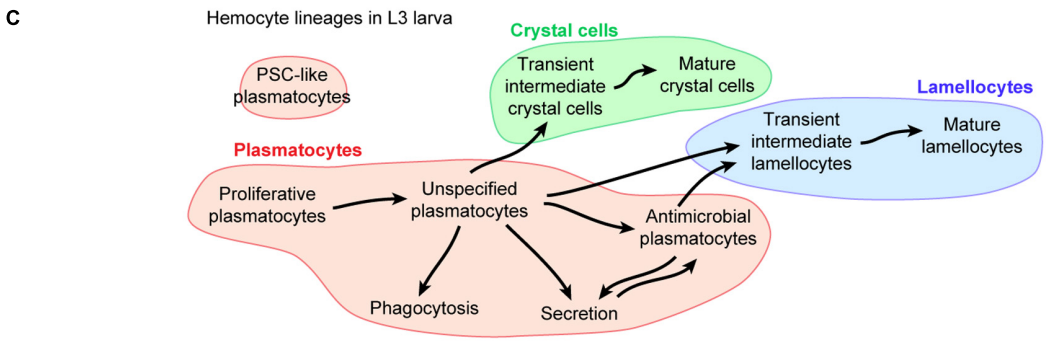

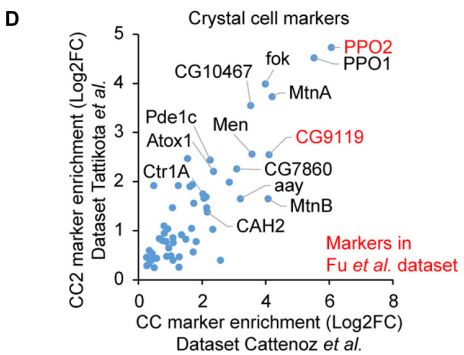

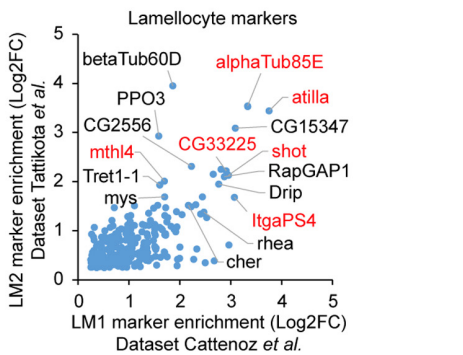

FIGURE 2 | Defining a consensual repertoire of the hemocyte subgroups. **(A)** Number of common markers between the plasmatocyte subgroups identified in Cattenoz et al. (2020) (rows) and in Tattikota et al. (2020) (column). The number of markers is highlighted by the color gradient (from 0 in blue to >20 in red). **(B)** Concordance amongst the hemocyte subgroups across the three datasets. **(C)** Outline of the lineage predictions among the hemocyte subgroups, based on the prediction analyses in Cattenoz et al. (2020) and Tattikota et al. (2020) and on the present comparative analysis. The proliferative plasmatocytes are at the origin of most hemocytes, they give rise to a large pool of unspecified plasmatocytes that further differentiate to acquire specific properties such as phagocytosis, secretion or antimicrobial peptide production. Subsets of unspecified plasmatocytes and antimicrobial plasmatocytes transdifferentiate to produce crystal cells or lamellocytes. **(D)** Scatter plot representing the enrichment levels of the crystal cell markers common to the subgroups CC2 (y-axis) from Tattikota et al. (2020) and CC (x-axis) from Cattenoz et al. (2020). The Log2 fold change (Log2FC) of the enrichment is represented. The markers with the strongest enrichment are indicated on the graph, those also identified in Fu et al. (2020) are highlighted in red. **(E)** Scatter plot representing the enrichment of the lamellocyte markers in the indicated subgroups. The representation is as in panel **(D)**.

The marker comparison shows a large correlation across studies for crystal cells and lamellocytes: 53 crystal cell markers and 265 lamellocyte markers are commonly found by Tattikota et al. and Cattenoz et al. (**Figures 2D,E**). All the markers previously used to label the crystal cells and the lamellocytes are present in the two datasets. Such tight correlation is expected

for subgroups that present strong physiological differences compared to the plasmatocytes. Fu et al. disclosed a limited list of markers for crystal cells and lamellocytes; all of them are nevertheless present in the crystal cell and lamellocyte subgroups identified in two other datasets, further confirming the identity of these subgroups. The three studies consistently found a large subgroup of "unspecified plasmatocytes" presenting no distinctive marker and encompassing more than 50% of plasmatocytes (PM1 in Tattikota et al.; PL-0, 1, 2, and 3 in Cattenoz et al.; reservoir PM in Fu et al.), as well as several smaller subgroups enriched for specific markers: the proliferative, the antimicrobial, the posterior signaling center-like, the phagocytic and the secretory plasmatocytes (**Figure 2B**).

Proliferative Plasmatocytes

The markers involved in mitosis, including Cyclin B (CycB) (Gavet and Pines, 2010), the phosphatase String (Stg) (Edgar and O'Farrell, 1990), the importin Pendulin (Pen) (Kussel and Frasch, 1995) and the kinase Polo (Sunkel and Glover, 1988) are enriched in clusters PM2 as well as PM9 in Tattikota et al., and in the PL-prolif cluster in Cattenoz et al. (**Supplementary Figures S2A,B**). These proliferative subgroups are positioned at the beginning of the developmental trajectories and give rise to the pool of unspecified plasmatocytes. The PL-prolif subgroup represents a hemocyte subset of the PL-Inos subgroup, which lacks the proliferative genes but expresses all the other markers of PL-prolif (Cattenoz et al., 2020), suggesting that PL-prolif and PL-Inos represent two states (dividing/quiescent) of the same subgroup.

Antimicrobial Plasmatocytes

Two datasets contain subgroups of plasmatocytes enriched in transcripts involved in immune pathways: PL-AMP, PL-Rel and PL-vir1 in Cattenoz et al.; PM3, PM5, PM6, and PM7 in Tattikota et al. The comparison of the markers indicates a correlation between PL-Rel/PL-AMP and PM3/PM6/PM7 as well as between PL-vir1 and PM3/PM5 (**Supplementary Figures S2C,D**).

PM6/7 and PL-AMP are highly enriched for AMP expression [i.e., Cecropins A1, A2, and C (CecA1, CecA2, CecC), Diptericin B (DptB), Drosomycin (Drs), Metchnikowin (Mtk), Mtk-like (Mtkl)]. Of note, the AMPs Mtk, DptB, and Drs are enriched at higher levels in the dataset from Tattikota et al. than in the one from Cattenoz et al. This is likely due to the induction of these AMPs by clean wounding, a condition specific to the dataset from Tattikota et al. All these subgroups also express high levels of Matrix metalloproteinase 1 (Mmp1), involved in wound healing (Stevens and Page-McCaw, 2012). PM3 and PL-Rel express elements of the IMD and JNK pathways and lower levels of AMP, which suggests weaker or different mode of activation of the immune response. This may reflect different microenvironments and/or different intrinsic properties compared to PM6/7 and PL-AMP.

PM5 and PL-vir1 present common expression profiles, distinctive from the other subgroups. They are not enriched in AMPs (**Supplementary Figure S2D**) and seem specialized in xenobiotic detoxification, as suggested by the expression of the Ferritin 1 heavy chain homolog, the Ferritin 2 light chain homolog and the Multidrug resistance protein (Chahine and O'Donnell, 2009; Tang and Zhou, 2013).

Posterior Signaling Center-Like Plasmatocytes

The comparison of the markers consistently identifies a subgroup of cells representing less than 1% of the hemocyte population across the three studies: PL-ImpL2 (Cattenoz et al., 2020), PM11 (Tattikota et al., 2020), and the primocytes (Fu et al., 2020) (**Supplementary Figures S2E,F**). This subgroup expresses typical markers of the posterior signaling center (PSC) present in the lymph gland, such as the transcription factors Knot (Kn) (Makki et al., 2010) and Antennapedia (Antp) (Mandal et al., 2007). The comparison of the markers of this subgroup with the PSC markers identified by the scRNAseq assay on the lymph gland (Cho et al., 2020) also identifies this subgroup as PSC-like plasmatocytes (**Supplementary Figure S2G**).

Phagocytic Plasmatocytes and Secretory Plasmatocytes

The datasets from Fu et al. and from Cattenoz et al. identified phagocytic plasmatocytes, plasmatocytes secreting storage proteins and plasmatocytes secreting opsonins.

Phagocytic plasmatocytes: CAH7 + PM (Fu et al.) and PL-robo2 (Cattenoz *et* al.*)* are enriched for the phagocytic receptor NimC2 (Kurucz et al., 2007), the cytoskeleton proteins Myoblast city (Erickson et al., 1997), the Tenascin accessory (Mosca et al., 2012), the transmembrane receptor Lipophorin receptor 2 (LpR2) and Mmp2 (**Supplementary Figure S2H**). Lineage predictions call for PL-robo2/CAH7 + PM being directly issued from the unspecified plasmatocytes and since the strongest markers for PL-robo2 are also enriched to a lower extent in a subset of unspecified plasmatocytes (PL-0/PL-2), PL-robo2 may specifically represent the phagocytic, active state, of this subset.

Secretory plasmatocytes: Lsp + PM (Fu et al.) and PL-Lsp (Cattenoz et al.) display a highly distinctive expression pattern of proteins secreted in the hemolymph such as Larval serum protein 1 alpha (Lsp1alpha), Larval serum protein 2 (Lsp2), Apolipophorin (Apolpp), and Odorant binding protein 99b (Obp99b) (**Supplementary Figure S2I**). All these proteins are mostly expressed by the fat body (Chintapalli et al., 2007) and serve as storage proteins (Telfer and Kunkel, 1991; Handke et al., 2013), suggesting common functions between the fat body and these secretory plasmatocytes.

At last, the thanacytes (Fu et al.) and PL-Pcd (Cattenoz et al.) express low levels of NimC1 and secrete the opsonins Thioester-containing protein 2 and 4 (Tep2 and Tep4) that promote the phagocytosis of bacteria and the activation of the Toll pathway (Dostalova et al., 2017; **Supplementary Figure S2J**). The thanacyte markers are consistently enriched in both PL-AMP and PL-Pcd, yet differ from PL-AMP by the lack of AMP production (**Supplementary Figure S2J**). Thus, PL-AMP may represent an activated state of PL-Pcd/thanacyte, in which the inflammatory pathways are triggered and antimicrobial peptides are secreted.

These three subgroups were not identified in Tattikota et al. dataset. Their markers are detected in some cells but these

cells are not clustered together and are associated with the pool of unspecified plasmatocytes, with whom they share the majority of the markers.

Lamellocytes

The datasets from Tattikota et al. and Cattenoz et al. include conditions promoting the differentiation of the lamellocytes and identify two subgroups. One of them expresses both plasmatocyte and lamellocyte markers and likely corresponds to plasmatocytes that are transdifferentiating into lamellocytes (LM1 in Tattikota et al., LM-2 in Cattenoz et al.). The second subgroup lacks most of the plasmatocyte markers and expresses the lamellocyte markers strongly (LM2 in Tattikota et al., LM-1 in Cattenoz et al.). For the sake of simplicity, we will call the first and the second subgroups intermediary and mature lamellocytes, respectively.

To identify the molecular pathways activated during lamellocyte differentiation, we carried out a regulon analysis using SCENIC (Aibar et al., 2017) on the dataset from wasp infested larvae generated by Cattenoz et al. (2020). This analysis relies on two steps. First, the genes presenting covariation are identified across the whole single cell dataset. Then, the promoters of the covariating genes are scanned for canonical transcription factor binding sites. The genes presenting similar expression profiles and carrying the same transcription factor binding site(s) are grouped in one regulon named after the transcription factor. This analysis highlights two regulons, Kayak (Kay) and Jun-related antigen (Jra), which regroup the targets of the two main transcription factors of the JNK pathway (reviewed in La Marca and Richardson, 2020; **Figure 3A**), known to promote the differentiation of lamellocytes (Tokusumi et al., 2009). We have pulled together the transcriptomes of all cells from the intermediary and mature lamellocytes from Cattenoz et al. dataset to generate pseudo-transcriptomes. The comparison of the pseudo-transcriptomes shows that the genes regulated by the JNK pathways are expressed at higher levels in the mature lamellocytes than in the intermediary ones (**Figure 3B**). Strikingly, this analysis also reveals for the first time seven novel regulons associated with lamellocyte differentiation: Cyclic-AMP response element binding protein B (CrebB), Forkhead box sub-group O (Foxo), REPTOR-binding partner (REPTOR-BP), Pannier (Pnr), Maf-S, Zinc-finger protein (Zif), and Checkpoint suppressor 1-like (CHES-1-like). These regulons are highly enriched in lamellocytes and display an enhanced activation from the intermediary lamellocytes to the mature lamellocytes (**Figure 3A**).

The regulons CrebB, Foxo and REPTOR-BP are involved in the maintenance of energy metabolism upon food restriction or molecular stress (Dionne et al., 2006; Iijima et al., 2009; Tiebe et al., 2015). They may be responsible for the induction of specific glucose transporters and the metabolic shift from lipolytic to glycolytic observed during the transdifferentiation of plasmatocytes into lamellocyte (Cattenoz et al., 2020; Tattikota et al., 2020). These pathways may also maintain the high metabolic activity of lamellocytes, while the metabolism of other organs is inhibited to privilege the immune response over the developmental processes (Bajgar et al., 2015; Dolezal, 2015). Maf-S along with Foxo regulate oxidative stress resistance (Rahman et al., 2013; Gumeni et al., 2019) and CHES-1-like is involved in the DNA-damage response (Busygina et al., 2006). Both oxidative stress and DNA damage can be associated with the high metabolism of lamellocytes, a phenomenon usually observed in cancerous cells in mammals (Moretton and Loizou, 2020).

Hemocyte Populations in Other Single Cell Datasets

In mammals, macrophages are conditioned by their microenvironment, which leads to molecular signatures specific to the tissues in which they reside (van de Laar et al., 2016; Guilliams et al., 2020). To assess if specific hemocyte subgroups are associated to different tissues in *Drosophila*, we have screened tissue specific or embryonic scRNAseq datasets containing hemocytes (i.e., larval eye discs, larval brains, and stage 6 embryos) and compared their molecular signatures to the dataset of Cattenoz et al.

Hemocytes Associated With the Larval Eye Disc Resemble Unspecified Plasmatocytes

The scRNAseq analyses on larval eye discs (Ariss et al., 2018) reveal a small subgroup of cells in line with the hemocytes observed in close contact with this disc (Holz et al., 2003; **Figure 4A** and **Supplementary Figures S3A,B**). Since the eye disc associated hemocytes express a large panel of hemocyte markers, their pseudo-transcriptome was compared to the pseudo-transcriptome of each of the subgroups identified in Cattenoz et al. dataset using Pearson correlation coefficient. This analysis highlights a strong correlation between the eye disc associated hemocytes and unspecified plasmatocytes (PL-1/PL-3, **Supplementary Figure S3C**), which do not express strong markers. Moreover, the eye disc associated hemocytes do not express subgroup-exclusive markers, like Lsp1alpha in PL-Lsp or Kn and Tau in PL-ImpL2 (**Figure 4D**). Altogether, these evidence suggest that the eye disc associated hemocytes are unspecified plasmatocytes.

Next, to determine if the eye disc associated hemocytes represent a subgroup that was not defined in Cattenoz et al. dataset, we compared their pseudo-transcriptome to the combined pseudo-transcriptome of all subgroups from Cattenoz et al. (**Supplementary Figure S4A**). This comparison did not return a strong signature for the eye disc associated hemocytes (less than 10 genes specifically expressed in the eye disc hemocytes), which is concordant with the high correlations measured between almost all subgroups and the eye-associated hemocytes (**Supplementary Figure S3C**). Thus, at this level of resolution, the hemocytes in the eye disc cannot be distinguished from unspecified plasmatocytes.

One of the main characteristics of the unspecified plasmatocytes is the expression of Extra Cellular Matrix (ECM) components such as Pxn, which is necessary for the assembly of the basement membrane (Bhave et al., 2012). Pxn is indeed strongly expressed in the hemocytes associated to the eye disc and is detected at the basement membrane of the disc (**Figure 4A**). Similar analyses will reveal whether this feature

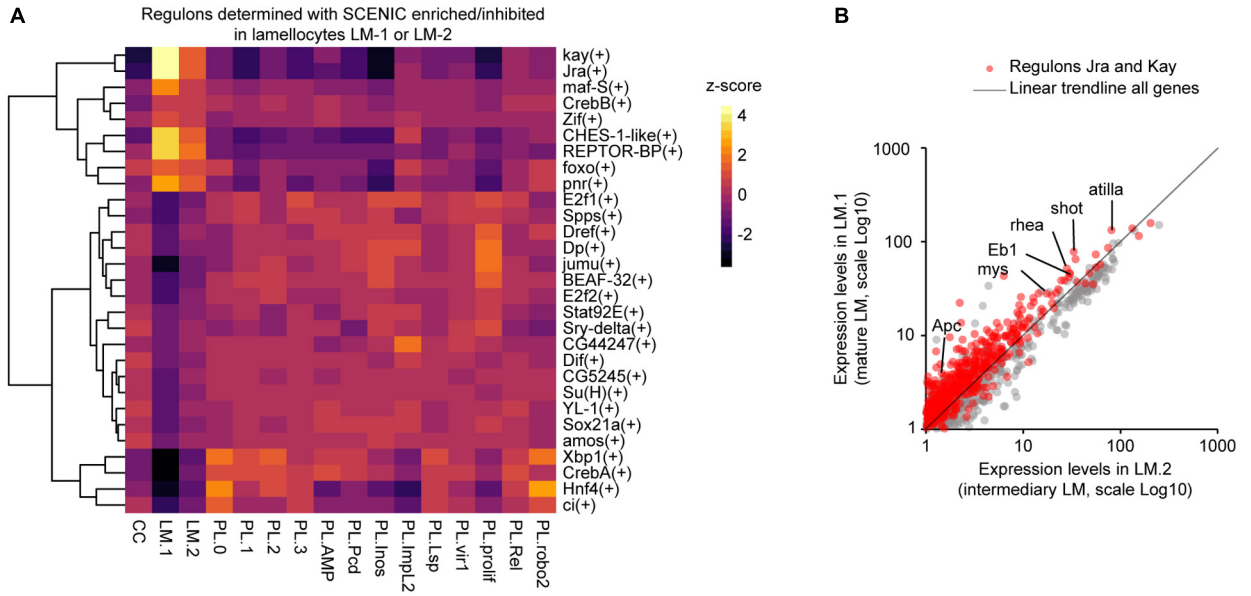

FIGURE 3 | Characterization of the regulatory network controlling lamellocyte differentiation. **(A)** Heatmap representing the z-score for the regulons enriched or underrepresented in the lamellocyte subgroups (*z*-score >2 or < -2) determined with SCENIC. The dendrogram on the left side of the panel indicates the correlation between the regulons across the dataset. The *z*-score is indicated with a gradient from black (*z*-score < 0, underrepresented regulons) to red and then yellow (*z*-score > 0, overrepresented regulons). **(B)** Scatter plot comparing the pseudo-transcriptomes of mature lamellocytes (y-axis) and transient intermediary lamellocytes (x-axis). The pseudo-transcriptomes were generated from the dataset obtained upon wasp infestation (Cattenoz et al., 2020). The genes belonging to the regulons Jra and Kay are indicated in red, the trendline of all genes expressions is in black, the axes are in Log10 scale.

is common to the hemocytes associated to the other imaginal tissues. Interestingly, larval hemocytes secrete ECM compounds to build the basement membrane of the ovaries and the fat body (Shahab et al., 2015; Van De Bor et al., 2015).

Hemocytes Associated With the Brain Resemble the Proliferative Plasmatocytes (PL-Inos, PL-Prolif)

Two scRNAseq datasets on the larval brain from 1st instar to 3rd instar larvae (Brunet Avalos et al., 2019; Cocanougher et al., 2019) report the presence of hemocytes (**Supplementary Figure S3D**), in line with the hemocytes observed in close contact with this tissue (**Figure 4B**). The comparison of the pseudo-transcriptomes of hemocytes from the 1st instar brain and of Cattenoz et al. subgroups highlights the highest correlation with the PL-prolif and PL-Inos subgroups (**Supplementary Figure S3E**). The correlation coefficients are much weaker than in the comparison with the eye disc associated hemocytes. In addition, the comparison of the pseudo-transcriptomes of brain associated hemocytes with the pseudo-transcriptome of all subgroups from Cattenoz et al. suggests a specific molecular signature for these hemocytes (**Supplementary Figure S4B**). PL-prolif markers are represented in the brain associated hemocytes, together with dozens of genes that are consistently expressed from 1st instar to 3rd instar larval brains (**Figure 4D**, **Supplementary Table S1** and **Supplementary Figure S4C**). Altogether, these data suggest that the brain hemocytes represent a discrete subgroup with a specific molecular signature. The strong markers of PL-Inos/PL-prolif are preserved during development as they are observed from the 1st to the 3rd instar datasets (**Figure 4D**).

PSC-Like Plasmatocytes and Proliferative Plasmatocytes Resemble Prohemocytes From Stage 6 Embryos

The single cell analyses suggest that the larval hemocytes originate from the proliferative subgroup. We therefore predicted that the prohemocytes present at the early embryonic stages may resemble this subgroup and compared the larval dataset from Cattenoz et al. with the one obtained from scRNAseq on embryos at stage 6 (**Supplementary Figure S3F**; Karaiskos et al., 2017). At this stage, the cells of the procephalic mesoderm express the earliest hemocyte-specific transcription factors Glial Cell Missing/Glial Cell Deficient (Gcm) and Serpent (Srp) (**Figure 4C**; Sam et al., 1996; Bernardoni et al., 1997; Waltzer et al., 2003). The comparison of the pseudo-transcriptomes indeed shows that the prohemocytes from stage 6 embryos present the highest correlation with the subgroups PL-prolif/PL-Inos (i.e., proliferative plasmatocytes) and PL-ImpL2 (i.e., PSC-like plasmatocytes), and express the strongest markers of these subgroups (**Figure 4D** and **Supplementary Figure S3G**).

DISCUSSION

The comparative analysis of the scRNAseq datasets confirms the diversity of the immune cells present in the *Drosophila* larva. Molecular features consistently found across the studies allow the identification of robust plasmatocyte subgroups in addition to crystal cells and lamellocytes. The proliferative subgroup resembles the prohemocytes present in the early embryonic

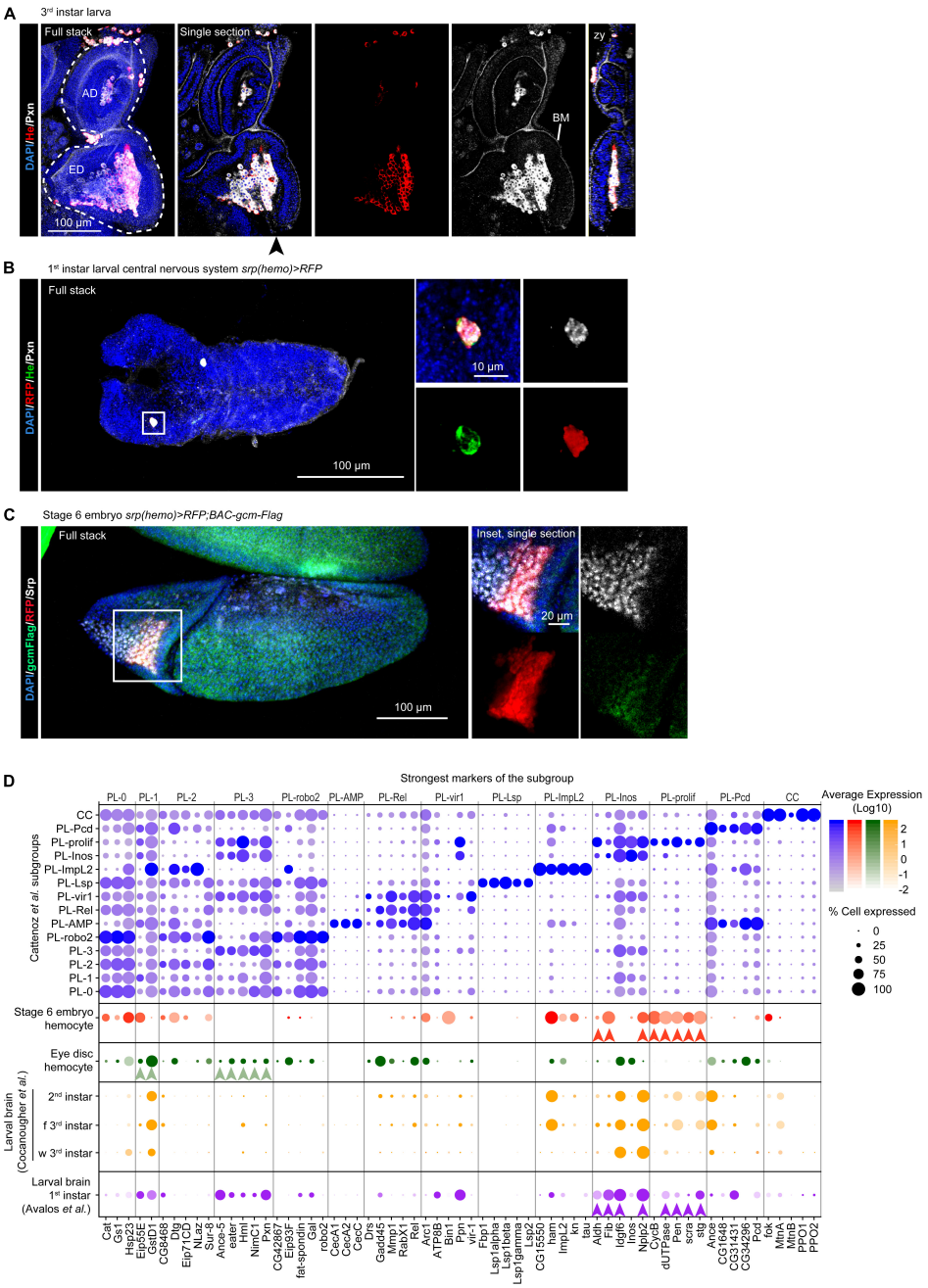

FIGURE 4 | The molecular signatures of the hemocytes from larval eye discs, larval brains and stage 6 embryos. **(A)** Eye disc from 3rd instar larva. The immunolabelling assay used anti-He (in red), anti-Pxn (in white) and the nuclei were labeled with DAPI (blue). The left panel shows the full stack, the eye disc (ED) and the antenna disc (AD) are indicated with a white dashed line, the next panels show a single section with all the channels, He labeling only and Pxn labeling only, respectively. Pxn labeling is present at the basement membrane (BM). The rightmost panel shows an orthogonal projection along the z-y axes from the position indicated by the black arrowhead. The scale bar represents 100 µm. **(B)** Central Nervous System from 1st instar larva carrying the *srp(hemo) > RFP* transgene, which allows for hemocyte detection (Gyoergy et al., 2018). The immunolabelling assay used three hemocyte markers [anti-RFP (in red), anti-He (in green), anti-Pxn (in gray)], and the nuclei were labeled with DAPI (blue). The left panel shows the full stack, the right panels (partial stacks) show the inset at high magnification (merged and individual channels). The scale bars represent 100 µm in the full stack and 10 µm in the inset. The hemocyte lays on the surface of the nervous system. **(C)** Stage 6 embryo *srp(hemo) > RFP; BAC-gcm-Flag*. The BAC was used to reveal the Gcm protein (Laneve et al., 2013). The immunolabelling assay used anti-RFP (in red), anti-Flag (in green), anti-Srp (in gray), and the nuclei were labeled with DAPI (blue). The left panel shows the full stack, the right panels show a single section of the inset at high magnification (merged and individual channels). The scale bars represent 100 µm in the stack and 20 µm in the inset. **(D)** Dot plot representing the expression levels and percentage of cells expressing the top markers of each subgroup identified by Cattenoz et al. (2020). The violet dots represent the expression in Cattenoz et al. (2020) subgroups, the red dots, expression in the hemocytes from stage 6 embryos (E6 embryos), the green dots in the hemocytes from larval eye discs, the purple and orange dots in the hemocytes from larval brains at the indicated stages (f 3rd instar: feeding 3rd instar larvae; w 3rd instar: wandering 3rd instar larvae). The arrowheads (red, green, purple) indicate the strongest markers linking the tissue-specific hemocytes with the subgroups from Cattenoz et al. (2020).

stages and the plasmatocytes associated with different larval tissues seem to present specific features.

Identification of Robust Subgroups

The present analysis identifies common subgroups with specific potentials (proliferation, AMP production, PSC-like, phagocytosis, secretion, crystal cells and lamellocytes) or lacking specific properties (unspecified plasmatocytes) (summarized in **Figures 2B,C**).

The proliferative plasmatocytes seem the sole source of larval hemocytes, including the crystal cells (Cattenoz et al., 2020; Tattikota et al., 2020). This subgroup may represent cells retaining a progenitor state, in line with their resemblance with the molecular signature of the hemocyte progenitors present in the early embryo. Lineage predictions suggest that the proliferative subgroup generates the unspecified plasmatocytes, which constitute more than 50% of the hemocytes and represent intermediary states between proliferative and differentiated cells (Cattenoz et al., 2020; Tattikota et al., 2020). The unspecified plasmatocytes seem to constitute the majority of the hemocytes associated with the eye discs, where they produce ECM proteins. The antimicrobial subgroup is the largest specified subgroup. It encompasses plasmatocytes enriched in transcripts coding for proteins associated to the immune response, including elements of the IMD and the Toll pathways and AMPs. The PSC-like subgroup displays a signature highly similar to that of the PSC in the lymph gland. Future studies will determine whether this subgroup plays a similar signaling role in the hemolymph and/or in specific niches. The phagocytic plasmatocytes are enriched for markers involved in engulfment, phagocytosis and actin remodeling. The secretory plasmatocytes are subdivided into two subgroups, one secreting storage proteins and the other secreting opsonins. The phagocytic and the storage protein secreting subgroups resemble strongly the unspecified plasmatocytes, as the number of specific markers is quite limited. The lack of a strong distinctive signature suggests that these cells may be associated with specific microenvironments/challenges, which would induce the expression of proteins on-demand, without drastically affecting hemocyte properties and identity. In other terms, we hypothesize that these two clusters are of common nature and that their differences rely on different "nurture."

In addition to the plasmatocyte subgroups, the three studies identified lamellocyte and crystal cell subgroups. Both subgroups are characterized by a specific list of markers, suggesting a well-defined nature of these cells. Some markers are already known (Rizki and Rizki, 1959; Braun et al., 1997; Irving et al., 2005; Rus et al., 2006; Honti et al., 2009; Binggeli et al., 2014), some are new. The datasets from Tattikota et al. and Cattenoz et al. include similar experimental immune challenges (i.e., wasp infestation) to activate the production of lamellocytes and display two subgroups of lamellocytes, one intermediary and one mature. The regulons analysis identifies the transcription factors involved in lamellocyte transdifferentiation/functions. These include the transcription factors of the JNK pathway known to promote lamellocyte differentiation and seven novel transcription factors potentially required for lamellocytes maturation. Further investigations will determine the roles of these transcription factors in the differentiation of the lamellocytes.

Advantages and Biases of the Computational Approach

The comparison of the different hemocyte scRNAseq datasets allows the identification of common molecular signatures, despite the heterogeneity of the experimental procedures. This straightforward approach is based on the marker lists provided by each study and is not computationally demanding. The downside is that it highlights only the subgroups presenting the strongest markers and biologically relevant minor variations can be hidden by the differences between the parameters chosen for the computational analysis. This is the case of the secretory and phagocytic subgroups, which were not identified in Tattikota et al. (2020). In addition to the different analytic parameters, the absence of these subgroups may also be explained by the different experimental conditions. Tattikota et al. dataset includes three experimental conditions with a majority of the cells coming from wounded larvae. Such set up may favor the identification of subgroups specific to wounded conditions at the expense of subgroups present in steady state conditions.

The molecular signature of the subgroups defined in Cattenoz et al. have been used to determine the identity of hemocytes present in the scRNAseq from larval eye discs and brains as well as from stage 6 embryos. The strong molecular signature of the hemocytes permits a clear distinction of these cells within each dataset and then the comparison with the hemocyte subgroups' signatures allows the identification of the closest subgroups. Typically, the hemocytes associated with the brain display the distinctive profile of the small, proliferative, subgroup. The main caveat of this analysis is related to the limited number of hemocytes recovered in assay (<100 cells in each dataset). We cannot exclude that discrete subgroups were not found because of their low frequencies in the specific tissue. This may notably be the case of the hemocytes associated with the eye discs, which display markers of the large subgroup of unspecified plasmatocytes. In addition, the dissection procedure may remove the less tightly associated cells, rendering our interpretation incomplete. The development of *ad hoc* protocols to analyze the hemocytes in the whole animal will help significantly.

The comparison of scRNAseq datasets brings robustness to the precise information on the cellular diversity gained with a single dataset. However, this approach is highly dependent on the analysis pipelines followed within each study. Since the number of studies using scRNAseq are currently booming and in parallel, new analytical tools are constantly generated, the comparability between datasets is not always straightforward (Vieth et al., 2019; Gao et al., 2020). Generating a universal pipeline of scRNAseq analysis will be highly valuable as it will facilitate the comparison between datasets.

In sum, the comparison of the three scRNAseq datasets allows the definition of common features and robust subgroups, an important asset to understand the biology of hemocyte heterogeneity. Some subgroups show a distinctive transcriptomic signature, while others present many shared

markers, suggesting an origin according to nature and nurture, respectively. Increasing evidence highlight the influence of the microenvironment in governing the gene expression profile in mammalian tissue-specific macrophages, despite their common embryonic origin (Gautier et al., 2012; Lavin et al., 2014). We expect that similar mechanisms in *Drosophila* lead to the differentiation of specific subgroups. Future lineage tracing assays will help assessing the relative impact of intrinsic and environmental cues on the presence of the different subgroups as well as their stability. The generation of subgroup specific drivers will make it possible to assess the role of the different subgroups in physiological and pathological conditions. Finally, bulk RNAseq of distinct subgroups (sorted according to the markers from the scRNAseq) will generate deeper molecular signatures. The combination of more refined experimental and analytical approaches will determine with higher precision the similarities and differences between subgroups and reveal the function of the subgroups. This will contribute to unravel the heterogeneity and the biology of the macrophage populations.

DATA AVAILABILITY STATEMENT

The data was deposited in the ArrayExpress database at EMBLEBI (www.ebi.ac.uk/arrayexpress) under the accession number E-MTAB-8698.

AUTHOR CONTRIBUTIONS

PC and AG: conceptualization, investigation, writing—original draft, funding acquisition, and supervision. PC, AG, AP, and SM: methodology and writing—review and editing. AG: resources. All authors contributed to the article and approved the submitted version.

FUNDING

This work was supported by INSERM, CNRS, UDS, Ligue Régionale contre le Cancer, Hôpital de Strasbourg, ARC, CEFIPRA, ANR grants and by the CNRS/University LIA Calim. AP was an IGBMC International Ph.D. Program fellow supported by LabEx INRT funds. SM benefits from a CEFIPRA fellowship. The IGBMC was also supported by a French state fund through the ANR labex.

ACKNOWLEDGMENTS

We thank the Imaging Center of the IGBMC for technical assistance. This study was supported by the grant ANR-10-LABX-0030-INRT, a French State fund managed by the Agence Nationale de la Recherche under the frame program Investissements d'Avenir ANR-10-IDEX-0002-02. We thank I. Ando, J. Shim, D. Siekhaus for providing fly stocks and antibodies. In addition, stocks obtained from the Bloomington Drosophila Stock Center (NIH P40OD018537) as well as antibodies obtained from the Developmental Studies Hybridoma Bank created by the NICHD of the NIH and maintained at The University of Iowa (Department of Biology, Iowa City, IA 52242) were used in this study. We thank Dr. A. Riba for his assistance in the regulon analysis, C. Delaporte for technical assistance, R. Sakr, T. Boutet, and C. Riet for critical reading of the manuscript.

SUPPLEMENTARY MATERIAL

The Supplementary Material for this article can be found online at: https://www.frontiersin.org/articles/10.3389/fcell.2021.643712/full#supplementary-material

REFERENCES

Aibar, S., Gonzalez-Blas, C. B., Moerman, T., Huynh-Thu, V. A., Imrichova, H., Hulselmans, G., et al. (2017). SCENIC: single-cell regulatory network inference and clustering. *Nat. Methods* 14, 1083–1086. doi: 10.1038/nmeth.4463

Ariss, M. M., Islam, A., Critcher, M., Zappia, M. P., and Frolov, M. V. (2018). Single cell RNA-sequencing identifies a metabolic aspect of apoptosis in Rbf mutant. *Nat. Commun.* 9:5024.

Bajgar, A., Kucerova, K., Jonatova, L., Tomcala, A., Schneedorferova, I., Okrouhlik, J., et al. (2015). Extracellular adenosine mediates a systemic metabolic switch during immune response. *PLoS Biol.* 13:e1002135. doi: 10.1371/journal.pbio.1002135

Banerjee, U., Girard, J. R., Goins, L. M., and Spratford, C. M. (2019). Drosophila as a genetic model for hematopoiesis. *Genetics* 211, 367–417.

Bazzi, W., Cattenoz, P. B., Delaporte, C., Dasari, V., Sakr, R., Yuasa, Y., et al. (2018). Embryonic hematopoiesis modulates the inflammatory response and larval hematopoiesis in Drosophila. *Elife* 7:e34890.

Bernardoni, R., Vivancos, V., and Giangrande, A. (1997). glide/gcm is expressed and required in the scavenger cell lineage. *Dev. Biol.* 191, 118–130. doi: 10.1006/dbio.1997.8702

Bhave, G., Cummings, C. F., Vanacore, R. M., Kumagai-Cresse, C., Ero-Tolliver, I. A., Rafi, M., et al. (2012). Peroxidasin forms sulfilimine chemical bonds using hypohalous acids in tissue genesis. *Nat. Chem. Biol.* 8, 784–790. doi: 10.1038/nchembio.1038

Binggeli, O., Neyen, C., Poidevin, M., and Lemaitre, B. (2014). Prophenoloxidase activation is required for survival to microbial infections in Drosophila. *PLoS Pathogens* 10:e1004067. doi: 10.1371/journal.ppat.1004067

Braun, A., Lemaitre, B., Lanot, R., Zachary, D., and Meister, M. (1997). Drosophila immunity: analysis of larval hemocytes by P-element-mediated enhancer trap. *Genetics* 147, 623–634. doi: 10.1093/genetics/147.2.623

Brunet Avalos, C., Maier, G. L., Bruggmann, R., and Sprecher, S. G. (2019). Single cell transcriptome atlas of the *Drosophila larval* brain. *Elife* 8:e50354.

Buchon, N., Silverman, N., and Cherry, S. (2014). Immunity in *Drosophila melanogaster*–from microbial recognition to whole-organism physiology. *Nat. Rev. Immunol.* 14, 796–810. doi: 10.1038/nri3763

Busygina, V., Kottemann, M. C., Scott, K. L., Plon, S. E., and Bale, A. E. (2006). Multiple endocrine neoplasia type 1 interacts with forkhead transcription factor CHES1 in DNA damage response. *Cancer Res.* 66, 8397–8403. doi: 10.1158/0008-5472.can-06-0061

Butler, A., Hoffman, P., Smibert, P., Papalexi, E., and Satija, R. (2018). Integrating single-cell transcriptomic data across different conditions, technologies, and species. *Nat. Biotechnol.* 36, 411–420. doi: 10.1038/nbt.4096

Cattenoz, P. B., Sakr, R., Pavlidaki, A., Delaporte, C., Riba, A., Molina, N., et al. (2020). Temporal specificity and heterogeneity of Drosophila immune cells. *EMBO J.* 39:e104486.

Chahine, S., and O'Donnell, M. J. (2009). Physiological and molecular characterization of methotrexate transport by Malpighian tubules of adult

Drosophila melanogaster. *J. Insect Physiol.* 55, 927–935. doi: 10.1016/j.jinsphys.2009.06.005

Chintapalli, V. R., Wang, J., and Dow, J. A. (2007). Using FlyAtlas to identify better *Drosophila melanogaster* models of human disease. *Nat. Genet.* 39, 715–720. doi: 10.1038/ng2049

Cho, B., Yoon, S. H., Lee, D., Koranteng, F., Tattikota, S. G., Cha, N., et al. (2020). Single-cell transcriptome maps of myeloid blood cell lineages in Drosophila. *Nat. Commun.* 11:4483.

Cocanougher, B., Wittenbach, J., Long, X. S., Kohn, A., Norekian, T., Yan, J., et al. (2019). Comparative single-cell transcriptomics of complete insect nervous systems. *bioRxiv [Preprint]* doi: 10.1101/785931

Comber, K., Huelsmann, S., Evans, I., Sanchez-Sanchez, B. J., Chalmers, A., Reuter, R., et al. (2013). A dual role for the betaPS integrin myospheroid in mediating *Drosophila embryonic* macrophage migration. *J. Cell Sci.* 126(Pt 15), 3475–3484. doi: 10.1242/jcs.129700

Dionne, M. S., Pham, L. N., Shirasu-Hiza, M., and Schneider, D. S. (2006). Akt and FOXO dysregulation contribute to infection-induced wasting in Drosophila. *Curr. Biol.* 16, 1977–1985. doi: 10.1016/j.cub.2006.08.052

Dolezal, T. (2015). Adenosine: a selfish-immunity signal? *Oncotarget* 6, 32307–32308. doi: 10.18632/oncotarget.4685

Dostalova, A., Rommelaere, S., Poidevin, M., and Lemaitre, B. (2017). Thioester-containing proteins regulate the Toll pathway and play a role in Drosophila defence against microbial pathogens and parasitoid wasps. *BMC Biol.* 15:79.

Edgar, B. A., and O'Farrell, P. H. (1990). The three postblastoderm cell cycles of Drosophila embryogenesis are regulated in G2 by string. *Cell* 62, 469–480. doi: 10.1016/0092-8674(90)90012-4

Erickson, M. R. S., Galletta, B. J., and Abmayr, S. M. (1997). Drosophila myoblast city encodes a conserved protein that is essential for myoblast fusion, dorsal closure, and cytoskeletal organization. *J. Cell Biol.* 138, 589–603. doi: 10.1083/jcb.138.3.589

Fleury, F., Gibert, P., Ris, N., and Allemand, R. (2009). Ecology and life history evolution of frugivorous drosophila parasitoids. *Adv. Parasitol.* 70, 3–44. doi: 10.1016/s0065-308x(09)70001-6

Franc, N. C., Dimarcq, J. L., Lagueux, M., Hoffmann, J., and Ezekowitz, R. A. (1996). Croquemort, a novel Drosophila hemocyte/macrophage receptor that recognizes apoptotic cells. *Immunity* 4, 431–443. doi: 10.1016/s1074-7613(00)80410-0

Fu, Y., Huang, X., Zhang, P., van de Leemput, J., and Han, Z. (2020). Single-cell RNA sequencing identifies novel cell types in Drosophila blood. *J. Genet. Genomics* 47, 175–186. doi: 10.1016/j.jgg.2020.02.004

Gao, M., Ling, M., Tang, X., Wang, S., Xiao, X., Qiao, Y., et al. (2020). Comparison of high-throughput single-cell RNA sequencing data processing pipelines. *bioRxiv [Preprint]* doi: 10.1101/2020.02.09.940221

Gautier, E. L., Shay, T., Miller, J., Greter, M., Jakubzick, C., Ivanov, S., et al. (2012). Gene-expression profiles and transcriptional regulatory pathways that underlie the identity and diversity of mouse tissue macrophages. *Nat. Immunol.* 13, 1118–1128. doi: 10.1038/ni.2419

Gavet, O., and Pines, J. (2010). Activation of cyclin B1-Cdk1 synchronizes events in the nucleus and the cytoplasm at mitosis. *J. Cell Biol.* 189, 247–259. doi: 10.1083/jcb.200909144

Gold, K. S., and Bruckner, K. (2014). Drosophila as a model for the two myeloid blood cell systems in vertebrates. *Exp. Hematol.* 42, 717–727. doi: 10.1016/j.exphem.2014.06.002

Goto, A., Kumagai, T., Kumagai, C., Hirose, J., Narita, H., Mori, H., et al. (2001). A Drosophila haemocyte-specific protein, hemolectin, similar to human von willebrand factor. *Biochem. J.* 359(Pt 1), 99–108. doi: 10.1042/0264-6021:3590099

Guilliams, M., Thierry, G. R., Bonnardel, J., and Bajenoff, M. (2020). Establishment and maintenance of the macrophage niche. *Immunity* 52, 434–451. doi: 10.1016/j.immuni.2020.02.015

Gumeni, S., Evangelakou, Z., Tsakiri, E. N., Scorrano, L., and Trougakos, I. P. (2019). Functional wiring of proteostatic and mitostatic modules ensures transient organismal survival during imbalanced mitochondrial dynamics. *Redox Biol.* 24:101219. doi: 10.1016/j.redox.2019.101219

Gyoergy, A., Roblek, M., Ratheesh, A., Valoskova, K., Belyaeva, V., Wachner, S., et al. (2018). Tools allowing independent visualization and genetic manipulation of *Drosophila melanogaster* macrophages and surrounding tissues. *G3* 8, 845–857. doi: 10.1534/g3.117.300452

Handke, B., Poernbacher, I., Goetze, S., Ahrens, C. H., Omasits, U., Marty, F., et al. (2013). The hemolymph proteome of fed and starved *Drosophila larvae*. *PLoS One* 8:e67208. doi: 10.1371/journal.pone.0067208

Holz, A., Bossinger, B., Strasser, T., Janning, W., and Klapper, R. (2003). The two origins of hemocytes in Drosophila. *Development* 130, 4955–4962. doi: 10.1242/dev.00702

Honti, V., Kurucz, E., Csordas, G., Laurinyecz, B., Markus, R., and Ando, I. (2009). In vivo detection of lamellocytes in *Drosophila melanogaster*. *Immunol. Lett.* 126, 83–84. doi: 10.1016/j.imlet.2009.08.004

Iijima, K., Zhao, L., Shenton, C., and Iijima-Ando, K. (2009). Regulation of energy stores and feeding by neuronal and peripheral CREB activity in Drosophila. *PLoS One* 4:e8498. doi: 10.1371/journal.pone.0008498

Irving, P., Ubeda, J. M., Doucet, D., Troxler, L., Lagueux, M., Zachary, D., et al. (2005). New insights into *Drosophila larval* haemocyte functions through genome-wide analysis. *Cell Microbiol.* 7, 335–350. doi: 10.1111/j.1462-5822.2004.00462.x

Jung, S. H., Evans, C. J., Uemura, C., and Banerjee, U. (2005). The Drosophila lymph gland as a developmental model of hematopoiesis. *Development* 132, 2521–2533. doi: 10.1242/dev.01837

Karaiskos, N., Wahle, P., Alles, J., Boltengagen, A., Ayoub, S., Kipar, C., et al. (2017). The Drosophila embryo at single-cell transcriptome resolution. *Science* 358, 194–199.

Kester, L., and van Oudenaarden, A. (2018). Single-cell transcriptomics meets lineage tracing. *Cell Stem Cell* 23, 166–179. doi: 10.1016/j.stem.2018.04.014

Kim-Jo, C., Gatti, J. L., and Poirie, M. (2019). Drosophila cellular immunity against parasitoid wasps: a complex and time-dependent process. *Front. Physiol.* 10:603.

Kocks, C., Cho, J. H., Nehme, N., Ulvila, J., Pearson, A. M., Meister, M., et al. (2005). Eater, a transmembrane protein mediating phagocytosis of bacterial pathogens in Drosophila. *Cell* 123, 335–346. doi: 10.1016/j.cell.2005.08.034

Kolde, R. (2019). *pheatmap: Pretty Heatmaps*. Available online at: https://CRAN.R-project.org/package=pheatmap

Kurucz, E., Markus, R., Zsamboki, J., Folkl-Medzihradszky, K., Darula, Z., Vilmos, P., et al. (2007). Nimrod, a putative phagocytosis receptor with EGF repeats in Drosophila plasmatocytes. *Curr. Biol.* 17, 649–654. doi: 10.1016/j.cub.2007.02.041

Kurucz, E., Zettervall, C. J., Sinka, R., Vilmos, P., Pivarcsi, A., Ekengren, S., et al. (2003). Hemese, a hemocyte-specific transmembrane protein, affects the cellular immune response in Drosophila. *Proc. Natl. Acad. Sci. U.S.A.* 100, 2622–2627.

Kussel, P., and Frasch, M. (1995). Pendulin, a drosophila protein with cell cycle-dependent nuclear-localization, is required for normal-cell proliferation. *J. Cell Biol.* 129, 1491–1507.

La Marca, J. E., and Richardson, H. E. (2020). Two-faced: roles of JNK signalling during tumourigenesis in the drosophila model. *Front. Cell Dev. Biol.* 8:42.

Laneve, P., Delaporte, C., Trebuchet, G., Komonyi, O., Flici, H., Popkova, A., et al. (2013). The Gcm/Glide molecular and cellular pathway: new actors and new lineages. *Dev. Biol.* 375, 65–78.

Lavin, Y., Winter, D., Blecher-Gonen, R., David, E., Keren-Shaul, H., Merad, M., et al. (2014). Tissue-resident macrophage enhancer landscapes are shaped by the local microenvironment. *Cell* 159, 1312–1326.

Lemaitre, B., Meister, M., Govind, S., Georgel, P., Steward, R., Reichhart, J. M., et al. (1995). Functional-analysis and regulation of nuclear import of dorsal during the immune-response in Drosophila. *Embo J.* 14, 536–545.

Luo, H., Hanratty, W. P., and Dearolf, C. R. (1995). An amino-acid substitution in the drosophila hop(Tum-L) jak kinase causes leukemia-like hematopoietic defects. *Embo J.* 14, 1412–1420.

Makki, R., Meister, M., Pennetier, D., Ubeda, J. M., Braun, A., Daburon, V., et al. (2010). A short receptor downregulates JAK/STAT signalling to control the Drosophila cellular immune response. *PLoS Biol.* 8:e1000441.

Manaka, J., Kuraishi, T., Shiratsuchi, A., Nakai, Y., Higashida, H., Henson, P., et al. (2004). Draper-mediated and phosphatidylserine-independent phagocytosis of apoptotic cells by Drosophila hemocytes/macrophages. *J. Biol. Chem.* 279, 48466–48476.

Mandal, L., Martinez-Agosto, J. A., Evans, C. J., Hartenstein, V., and Banerjee, U. (2007). A Hedgehog- and Antennapedia-dependent niche maintains Drosophila haematopoietic precursors. *Nature* 446, 320–324.

Mann, H. B., and Whitney, D. R. (1947). On a test of whether one of two random variables is stochastically larger than the other. *Ann. Math. Stat.* 18, 50–60.

Markus, R., Kurucz, T., Rus, F., and Ando, I. (2005). Sterile wounding is a minimal and sufficient trigger for a cellular immune response in *Drosophila melanogaster*. *Immunol. Lett.* 101, 108–111.

Moretton, A., and Loizou, J. I. (2020). Interplay between cellular metabolism and the DNA damage response in cancer. *Cancers* 12:2051.

Mosca, T. J., Hong, W., Dani, V. S., Favaloro, V., and Luo, L. (2012). Trans-synaptic Teneurin signalling in neuromuscular synapse organization and target choice. *Nature* 484, 237–241.

Nelson, R. E., Fessler, L. I., Takagi, Y., Blumberg, B., Keene, D. R., Olson, P. F., et al. (1994). Peroxidasin: a novel enzyme-matrix protein of Drosophila development. *EMBO J.* 13, 3438–3447.

Paladi, M., and Tepass, U. (2004). Function of Rho GTPases in embryonic blood cell migration in Drosophila. *J. Cell Sci.* 117(Pt 26), 6313–6326.

Potter, S. S. (2018). Single-cell RNA sequencing for the study of development, physiology and disease. *Nat. Rev. Nephrol.* 14, 479–492.

Rahman, M. M., Sykiotis, G. P., Nishimura, M., Bodmer, R., and Bohmann, D. (2013). Declining signal dependence of Nrf2-MafS-regulated gene expression correlates with aging phenotypes. *Aging Cell* 12, 554–562.

Rizki, M. T., and Rizki, R. M. (1959). Functional significance of the crystal cells in the larva of *Drosophila melanogaster*. *J. Biophys. Biochem. Cytol.* 5, 235–240.

Rizki, T. M., and Rizki, R. M. (1980). Properties of the larval hemocytes of *Drosophila melanogaster*. *Experientia* 36, 1223–1226.

Rus, F., Kurucz, E., Markus, R., Sinenko, S. A., Laurinyecz, B., Pataki, C., et al. (2006). Expression pattern of Filamin-240 in Drosophila blood cells. *Gene Expr. Patterns* 6, 928–934.

Sam, S., Leise, W., and Hoshizaki, D. K. (1996). The serpent gene is necessary for progression through the early stages of fat-body development. *Mech. Dev.* 60, 197–205. doi: 10.1016/S0925-4773(96)00615-6

Schindelin, J., Arganda-Carreras, I., Frise, E., Kaynig, V., Longair, M., Pietzsch, T., et al. (2012). Fiji: an open-source platform for biological-image analysis. *Nat. Methods* 9, 676–682. doi: 10.1038/nmeth.2019

See, P., Lum, J., Chen, J. M., and Ginhoux, F. (2018). A single-cell sequencing guide for immunologists. *Front. Immunol.* 9:2425. doi: 10.3389/fimmu.2018.02425

Shahab, J., Baratta, C., Scuric, B., Godt, D., Venken, K. J., and Ringuette, M. J. (2015). Loss of SPARC dysregulates basal lamina assembly to disrupt larval fat body homeostasis in *Drosophila melanogaster*. *Dev. Dyn.* 244, 540–552. doi: 10.1002/dvdy.24243

Siekhaus, D., Haesemeyer, M., Moffitt, O., and Lehmann, R. (2010). RhoL controls invasion and Rap1 localization during immune cell transmigration in Drosophila. *Nat. Cell Biol.* 12, 605–610. doi: 10.1038/ncb2063

Stevens, L. J., and Page-McCaw, A. (2012). A secreted MMP is required for reepithelialization during wound healing. *Mol. Biol. Cell* 23, 1068–1079. doi: 10.1091/mbc.e11-09-0745

Stuart, T., Butler, A., Hoffman, P., Hafemeister, C., Papalexi, E., Mauck, W. M., et al. (2019). Comprehensive integration of single-cell data. *Cell* 188:e1821. doi: 10.1016/j.cell.2019.05.031

Sunkel, C. E., and Glover, D. M. (1988). polo, a mitotic mutant of Drosophila displaying abnormal spindle poles. *J. Cell Sci.* 89(Pt 1), 25–38.

Tang, X., and Zhou, B. (2013). Ferritin is the key to dietary iron absorption and tissue iron detoxification in *Drosophila melanogaster*. *FASEB J.* 27, 288–298. doi: 10.1096/fj.12-213595

Tattikota, S. G., Cho, B., Liu, Y., Hu, Y., Barrera, V., Steinbaugh, M. J., et al. (2020). A single-cell survey of Drosophila blood. *Elife* 9:e54818. doi: 10.7554/eLife.54818.sa2

Telfer, W. H., and Kunkel, J. G. (1991). The function and evolution of insect storage hexamers. *Annu. Rev. Entomol.* 36, 205–228. doi: 10.1146/annurev.en.36.010191.001225

Tepass, U., Fessler, L. I., Aziz, A., and Hartenstein, V. (1994). Embryonic origin of hemocytes and their relationship to cell-death in drosophila. *Development* 120, 1829–1837.

Tiebe, M., Lutz, M., De La Garza, A., Buechling, T., Boutros, M., and Teleman, A. A. (2015). REPTOR and REPTOR-BP regulate organismal metabolism and transcription downstream of TORC1. *Dev. Cell* 33, 272–284. doi: 10.1016/j.devcel.2015.03.013

Tokusumi, T., Sorrentino, R. P., Russell, M., Ferrarese, R., Govind, S., and Schulz, R. A. (2009). Characterization of a lamellocyte transcriptional enhancer located within the misshapen gene of *Drosophila melanogaster*. *PLoS One* 4:e6429. doi: 10.1371/journal.pone.0006429

Van De Bor, V., Zimniak, G., Papone, L., Cerezo, D., Malbouyres, M., Juan, T., et al. (2015). Companion blood cells control ovarian stem cell niche microenvironment and homeostasis. *Cell Rep.* 13, 546–560. doi: 10.1016/j.celrep.2015.09.008

van de Laar, L., Saelens, W., De Prijck, S., Martens, L., Scott, C. L., Van Isterdael, G., et al. (2016). Yolk sac macrophages, fetal liver, and adult monocytes can colonize an empty niche and develop into functional tissue-resident macrophages. *Immunity* 44, 755–768. doi: 10.1016/j.immuni.2016.02.017

Vieth, B., Parekh, S., Ziegenhain, C., Enard, W., and Hellmann, I. (2019). A systematic evaluation of single cell RNA-seq analysis pipelines. *Nat. Commun.* 10:4667. doi: 10.1038/s41467-019-12266-7

Villanueva, R. A. M., and Chen, Z. J. (2019). ggplot2: elegant graphics for data analysis, 2nd edition. *Meas. Interdisciplinary Res. Perspect.* 17, 160–167. doi: 10.1080/15366367.2019.1565254

Waltzer, L., Ferjoux, G., Bataille, L., and Haenlin, M. (2003). Cooperation between the GATA and RUNX factors serpent and lozenge during Drosophila hematopoiesis. *EMBO J.* 22, 6516–6525. doi: 10.1093/emboj/cdg622

Wood, W., and Jacinto, A. (2007). *Drosophila melanogaster* embryonic haemocytes: masters of multitasking. *Nat. Rev. Mol. Cell Biol.* 8, 542–551. doi: 10.1038/nrm2202

Yoon, S., Cho, B., Shin, M., Koranteng, F., Cha, N., and Shim, J. (2017). Iron homeostasis controls myeloid blood cell differentiation in drosophila. *Mol. Cells* 40, 976–985.

Zanet, J., Stramer, B., Millard, T., Martin, P., Payre, F., and Plaza, S. (2009). Fascin is required for blood cell migration during Drosophila embryogenesis. *Development* 136, 2557–2565. doi: 10.1242/dev.036517

Conflict of Interest: The authors declare that the research was conducted in the absence of any commercial or financial relationships that could be construed as a potential conflict of interest.

frontiers in Cell and Developmental Biology

MINI REVIEW
published: 11 March 2021
doi: 10.3389/fcell.2021.630272

Macrophages and Their Organ Locations Shape Each Other in Development and Homeostasis – A *Drosophila* Perspective

Anjeli Mase[1†], Jordan Augsburger[1†] and Katja Brückner[1,2,3]*

[1] Department of Cell and Tissue Biology, University of California, San Francisco, San Francisco, CA, United States, [2] Eli and Edythe Broad Center of Regeneration Medicine and Stem Cell Research, University of California, San Francisco, San Francisco, CA, United States, [3] Cardiovascular Research Institute, University of California, San Francisco, San Francisco, CA, United States

OPEN ACCESS

Edited by:
Katrin Kierdorf,
University of Freiburg, Germany

Reviewed by:
Angela Giangrande,
Conseil National Pour La Recherche Scientifique, France
Jonathon Coates,
Queen Mary University of London, United Kingdom

***Correspondence:**
Katja Brückner
katja.brueckner@ucsf.edu

[†] These authors have contributed equally to this work

Specialty section:
This article was submitted to Cell Death and Survival, a section of the journal Frontiers in Cell and Developmental Biology

Received: 17 November 2020
Accepted: 25 January 2021
Published: 11 March 2021

Citation:
Mase A, Augsburger J and Brückner K (2021) Macrophages and Their Organ Locations Shape Each Other in Development and Homeostasis – A Drosophila Perspective. Front. Cell Dev. Biol. 9:630272. doi: 10.3389/fcell.2021.630272

Across the animal kingdom, macrophages are known for their functions in innate immunity, but they also play key roles in development and homeostasis. Recent insights from single cell profiling and other approaches in the invertebrate model organism *Drosophila melanogaster* reveal substantial diversity among *Drosophila* macrophages (plasmatocytes). Together with vertebrate studies that show genuine expression signatures of macrophages based on their organ microenvironments, it is expected that *Drosophila* macrophage functional diversity is shaped by their anatomical locations and systemic conditions. *In vivo* evidence for diverse macrophage functions has already been well established by *Drosophila* genetics: *Drosophila* macrophages play key roles in various aspects of development and organogenesis, including embryogenesis and development of the nervous, digestive, and reproductive systems. Macrophages further maintain homeostasis in various organ systems and promote regeneration following organ damage and injury. The interdependence and interplay of tissues and their local macrophage populations in *Drosophila* have implications for understanding principles of organ development and homeostasis in a wide range of species.

Keywords: *Drosophila melanogaster*, macrophage, plasmatocyte, hemocyte, organ microenvironment, regeneration, development, homeostasis

INTRODUCTION

Macrophages have a wide range of functions across species. While best known for their roles in innate immunity, macrophages also perform vital tissue-specific roles in development and homeostasis (Gold and Brückner, 2015; Okabe and Medzhitov, 2016). At the same time, macrophages are defined by their local microenvironments (Lavin et al., 2015). In this review, we discuss these underappreciated dual ways that macrophages and their microenvironment shape one another, focusing on insights from the invertebrate model organism *Drosophila melanogaster*.

The *Drosophila* blood cell system closely parallels the hematopoietic system of vertebrates both developmentally and functionally, making it an especially apt model for studying macrophage development, heterogeneity, and function (Hartenstein, 2006; Gold and Brückner, 2014, 2015; Banerjee et al., 2019). Since the 1970s, the concept of the mononuclear macrophage system

dominated the vertebrate field, proposing that hematopoietic progenitors of the bone marrow give rise to monocytes, which are the source of all macrophages as they enter the tissues (van Furth et al., 1972; Dzierzak and Speck, 2008; Morrison and Scadden, 2014). However, over the last decade or more, this view has been dismissed in favor of a new model of two independent lineages of macrophages (Frame et al., 2013; Lavin et al., 2015; Ginhoux et al., 2016; Perdiguero and Geissmann, 2016). Based on modern genetic lineage tracing, an independent lineage of blood cells gives rise to the majority of tissue-resident macrophages in vertebrates. This independent lineage derives from erythro-myeloid progenitors that originate in the embryonic yolk sac and mature in the fetal liver, and subsequently colonize organs throughout the body, giving rise to local macrophage populations such as the microglia of the brain, Langerhans cells of the skin, Kupffer cells of the liver, and resident macrophages of the lung (Herbomel et al., 2001; Merad et al., 2002; Ajami et al., 2007; Geissmann et al., 2010; Hoeffel et al., 2012; Schulz et al., 2012; Davies et al., 2013; Hashimoto et al., 2013; Sieweke and Allen, 2013; Gomez Perdiguero et al., 2015). In some, but not all, organs this independent lineage of tissue macrophages is complemented by macrophages of the monocyte lineage (Davies et al., 2013; Frame et al., 2013; Sieweke and Allen, 2013; Lavin et al., 2015; Ginhoux et al., 2016; Perdiguero and Geissmann, 2016).

Interestingly, much like vertebrates, *Drosophila* also has two independent lineages of blood cells, or hemocytes:

(1) The embryonic/resident lineage, which parallels the vertebrate erythro-myeloid progenitor lineage of tissue macrophages, is based on self-renewing differentiated macrophages (Makhijani et al., 2011; Davies et al., 2013; Gold and Brückner, 2014, 2015; Ratheesh et al., 2015; Banerjee et al., 2019). Hemocytes of this lineage arise in the embryonic head mesoderm, quickly differentiate into macrophage-like plasmatocytes, migrate throughout the embryo in stereotyped routes (Tepass et al., 1994; Siekhaus et al., 2010), and then colonize organ and tissue microenvironments in the larva where they proliferate over time (Gold and Brückner, 2014, 2015). Examples include the prominent tissue-resident clusters of hemocytes in segmentally repeated epidermal-muscular pockets (hematopoietic pockets), and resident hemocytes at the proventriculus of the gastrointestinal system (Zaidman-Rémy et al., 2012). Homing and adhesion of hemocytes to these sites depends on active sensory neurons of the hematopoietic pockets and their expression of the Transforming Growth Factor-β (TGF-β) family ligand Activin-β (Actβ) and other predicted factors (Makhijani et al., 2011, 2017). Neuron signals may also play a role in the localization of hemocytes at the proventriculus (Cognigni et al., 2011). In hemocytes, actin cytoskeleton regulators such as Rho1 and Rac appear to be required for their tissue localization and adhesion (Williams, 2006; Makhijani et al., 2011). Likewise, Nimrod family transmembrane receptors such as Nimrod C1 (NimC1) and Eater, expressed on plasmatocytes, play roles in adhesion (Bretscher et al., 2015; Melcarne et al., 2019), the latter through interaction with the collagen XV/XVIII ortholog Multiplexin in the basement membrane of tissues (Csordás et al., 2020). Hemocyte adhesion is negatively regulated by factors from other tissues such as NimB5, secreted from the fat body upon nutrient starvation, driving hemocyte release into circulation (Ramond et al., 2020b). Resident hemocytes also lose adhesion and enter circulation upon various immune challenges, or changes in cell signaling (Williams, 2006; Stofanko et al., 2008; Markus et al., 2009), while wounds induce local adhesion of circulating hemocytes (Babcock et al., 2008). However, under unchallenged conditions, in the first and second instar larva, the vast majority of hemocytes are resident (Makhijani et al., 2011; Petraki et al., 2015). Starting in the late second to early third instar, an increasing number of hemocytes enter circulation (Markus et al., 2009; Makhijani et al., 2011; Petraki et al., 2015), establishing a steady state exchange with various resident locations (Welman et al., 2010; Makhijani et al., 2011; Makhijani and Brückner, 2012).

(2) The lymph gland lineage, which is based on progenitors, parallels the vertebrate lineage of hematopoietic stem and progenitor cells (Jung, 2005; Krzemien et al., 2010a,b; Gold and Brückner, 2014; Banerjee et al., 2019). Developmentally, the lymph gland originates from the cardiogenic mesoderm of the embryo, echoing the emergence of hematopoietic stem cells from the endothelium of the aorta in vertebrates (Hartenstein, 2006; Gold and Brückner, 2014, 2015; Banerjee et al., 2019). Blood progenitors of the lymph gland proliferate in the embryo and the larval stages, and only start in the mid-second instar to differentiate into plasmatocytes and other immune cell types (Jung, 2005; Krzemien et al., 2010a; Gold and Brückner, 2015; Banerjee et al., 2019). In addition, differentiated plasmatocytes proliferate to a certain extent, in particular in third instar larvae (Jung, 2005; Banerjee et al., 2019). Immune assaults and environmental challenges accelerate the differentiation of lymph gland progenitors and the release of differentiated plasmatocytes and other immune cells into circulation (Sorrentino et al., 2002; Crozatier et al., 2004; Márkus et al., 2005; Owusu-Ansah and Banerjee, 2009; Shim et al., 2013; Letourneau et al., 2016; Banerjee et al., 2019). Likewise, dysregulation of various major signaling pathways that usually tightly control normal lymph gland development can result in premature, or precocious, differentiation, including signaling by Notch (N), Hedgehog (Hh), Wingless (Wg), the Bone Morphogenetic Protein (BMP) Decapentaplegic (Dpp), receptor tyrosine kinases such as the PDGFR/VEGFR-related Receptor (PVR) and Fibroblast Growth Factor Receptor (FGFR), Hippo, JAK/STAT, NFκB- related Toll signaling and transcriptional regulators such as the zinc finger transcription factor Zfrp8 and the GATA factor Pannier (Qiu et al., 1998; Myrick and Dearolf, 2000; Lebestky et al., 2003; Crozatier et al., 2004; Mandal et al., 2007; Minakhina et al., 2007, 2011; Sinenko et al., 2009; Pennetier et al., 2012; Dragojlovic-Munther and Martinez-Agosto, 2013; Ferguson and Martinez-Agosto, 2014; Milton et al., 2014; Destalminil-Letourneau et al., 2021). In contrast, under unchallenged conditions, the lymph gland disintegrates and releases all of its hemocytes at the beginning of metamorphosis (Grigorian et al., 2011).

The two hemocyte lineages persist into the adult animal, with the embryonic lineage contributing the major part of immune cells, at least under unchallenged conditions (Holz et al., 2003; Sanchez Bosch et al., 2019). No significant new blood cell production has been detected in the adult, even under conditions of immune challenge (Sanchez Bosch et al., 2019), and a decline in both hemocyte number and phagocytic activity has been documented as adult flies age (Mackenzie et al., 2011; Horn et al., 2014). Both hemocyte lineages give rise to common cell types: plasmatocytes (>90% of immune cells at most developmental stages), which are analogous to vertebrate macrophages and function as the primary phagocytic cells in *Drosophila*; crystal cells (∼5% of immune cells), which function in clotting and wound healing through prophenoloxidase (PPO)-mediated melanization; and lamellocytes, stress- or immune challenge-induced cells involved in encapsulation, analogous to granuloma formation in vertebrates (Gold and Brückner, 2014, 2015; Banerjee et al., 2019).

Across species, macrophages have many important functions during development and homeostasis (**Figure 1**). Macrophages play vital roles in phagocytosis of pathogens and apoptotic cells, through scavenger receptors such as Croqumort (Crq), and Nimrod-domain (NIM) containing receptors including Eater, Nimrod C1 (NimC1), Draper (Drpr), and Six-microns-under (Simu) (Franc, 1999; Manaka et al., 2004; Kocks et al., 2005; MacDonald et al., 2006; Kurucz et al., 2007; Kurant et al., 2008; Krzemien et al., 2010b; Melcarne et al., 2019; Roddie et al., 2019). Related to this, macrophages participate in wound healing (Stramer et al., 2005; Babcock et al., 2008; Pastor-Pareja et al., 2008; Koh and DiPietro, 2011; Wang et al., 2014). They play a central role in innate immunity, producing antimicrobial and pro-inflammatory mediators (Lemaitre and Hoffmann, 2007; Lazzaro, 2008; Buchon et al., 2014). In addition, macrophages have homeostatic functions such as regulation of dietary stress (Woodcock et al., 2015) and detection and regulation of the metabolic state (Parupalli et al., 2020). *Drosophila* macrophages also produce and deposit extracellular matrix (ECM) components (Fessler and Fessler, 1989; Wood and Jacinto, 2007) such as Collagen IV, Laminin, Perlecan, and Peroxidasin, an ECM-associated peroxidase, as they migrate along surfaces and reside in specific anatomical locations (Nelson et al., 1994; Bunt et al., 2010; Martinek et al., 2011; Van De Bor et al., 2015; Matsubayashi et al., 2017; Sánchez-Sánchez et al., 2017). Moreover, *Drosophila* macrophages regulate stem cells and other tissue-specific cell populations, often through localized secretion of signals such as cytokines of the Unpaired (Upd) family, which signal through the receptor Domeless (Dome) and the JAK/STAT pathway (Hopscotch and Stat2E in *Drosophila*), promoting proliferation and differentiation of target tissues (Chakrabarti et al., 2016; Guillou et al., 2016). In *Drosophila*, at least some macrophage-like plasmatocytes have the plasticity to give rise to crystal cells (Bretscher et al., 2015; Leitão and Sucena, 2015; Corcoran et al., 2020) and, upon immune challenge, lamellocytes (Markus et al., 2009; Anderl et al., 2016).

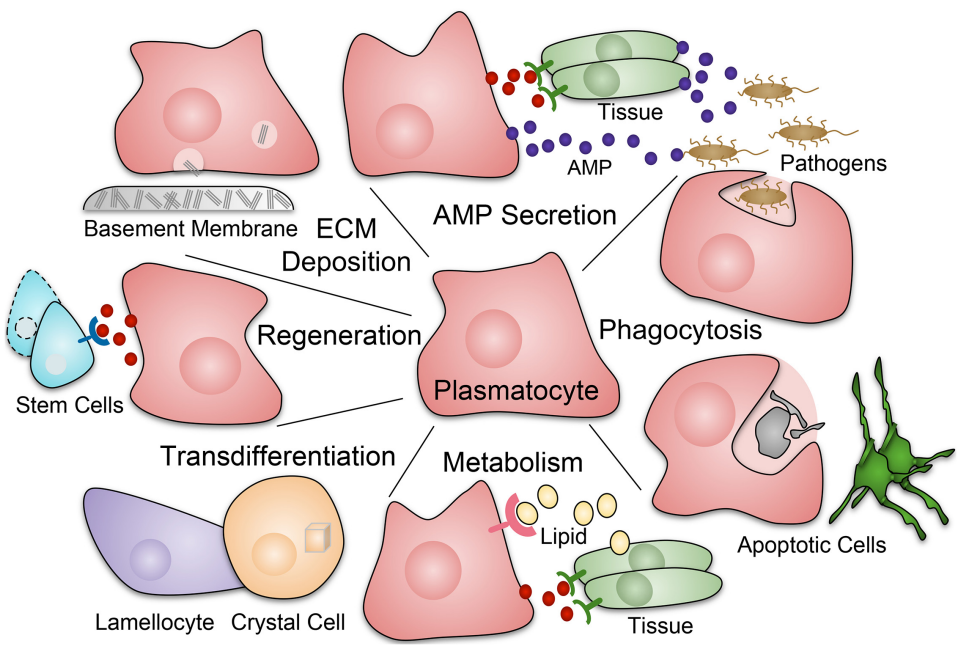

FIGURE 1 | Roles of macrophage-like plasmatocytes in *Drosophila*. Plasmatocytes (red) perform a diverse array of functions during development, homeostasis, injury, and infection. Responses include phagocytosis of pathogens and apoptotic cells; production of AMPs (antimicrobial peptides) and inflammatory mediators; production and deposition of ECM (extracellular matrix) components such as collagen that are often part of the basement membrane; tissue repair and regeneration, including stimulation of stem cell function; roles in metabolic homeostasis including uptake of lipids and secretion of metabolic mediators. In addition, at least some *Drosophila* plasmatocytes have plasticity to transdifferentiate into other hemocyte types, specifically crystal cells and, upon immune challenge, lamellocytes.

NEW INSIGHTS INTO MACROPHAGE DIVERSITY

A recent body of research suggests that not all macrophages are equal, rather they can be categorized into phenotypically and functionally unique subpopulations. Single cell RNA sequencing and functional studies in *Drosophila* identify transcriptionally and functionally distinct clusters of plasmatocytes, which are modulated by developmental time, lineage, injury, and infection status (Cattenoz et al., 2020; Cho et al., 2020; Coates et al., 2020; Ramond et al., 2020a; Tattikota et al., 2020). Vertebrate single cell studies identify similar heterogeneity among macrophages, modulated by developmental stage and lineage (Gordon and Taylor, 2005; Martinez et al., 2006; Paul et al., 2015; Lin et al., 2019; Lantz et al., 2020). Under pathologic conditions, macrophages may take on a spectrum of activation states, mirrored by their transcriptional profiles, dependent on disease severity (Lin et al., 2019; Mould et al., 2019; Weinstock et al., 2019; Lantz et al., 2020). Additionally, through analyses of enhancer landscapes and tissue-specific single cell RNA sequencing, it has become clear that macrophage subpopulations of organs including the liver, spleen, lung, peritoneal cavity, colon, small intestine, brain, and kidney, are shaped by their tissue of residence in vertebrate models (Gosselin et al., 2014; Lavin et al., 2014; MacParland et al., 2018; Mould et al., 2019; Van Hove et al., 2019; Zimmerman et al., 2019). In *Drosophila*, it is expected that heterogeneity of macrophages stems from the complex interactions between these cells and their microenvironment. A recent sequencing study identified cross-species markers between *Drosophila* and vertebrate macrophages, although their functional significance remains to be determined (Fu et al., 2020).

In addition to parallels in the local regulation of macrophages, *Drosophila* and vertebrates rely on conserved systemic signaling that regulates macrophages. Vertebrate macrophages express colony stimulating factor 1 receptor (CSF-1R), a receptor tyrosine kinase (RTK) of the family of Platelet-Derived Growth Factor Receptors and Vascular Endothelial Growth Factor Receptors (PDGFRs and VEGFRs) (Lemmon and Schlessinger, 2010). Vertebrate CSF-1R is activated by colony-stimulating factor-1 (CSF-1) and interleukin-34 (IL-34), promoting proliferation, differentiation, survival, chemotactic migration and differentiation of macrophages during development, homeostasis, and innate immunity (Stanley and Chitu, 2014). Similarly in *Drosophila,* the molecularly conserved ortholog PDGFR/VEGFR-related Receptor (PVR) is expressed in hemocytes. PVR recognizes PDGF/VEGF related factors Pvf1, Pvf2, and Pvf3, and is essential for trophic survival, proliferation, plasmatocyte activation, and some aspects of chemotactic migration (Munier et al., 2002; Brückner et al., 2004; Wood et al., 2006; Wood and Jacinto, 2007; Kelsey et al., 2012; Parsons and Foley, 2013; Sopko et al., 2015).

Despite the apparent necessity of macrophages in development and homeostasis, ablation studies suggest that hemocytes are not essential for survival in *Drosophila* (Braun et al., 1998; Charroux and Royet, 2009; Defaye et al., 2009; Arefin et al., 2015). However, plasmatocytes and PVR expression are fundamental to embryonic development, as they promote the essential process of central nervous system (CNS) condensation (Zhou et al., 1995; Sears, 2003; Olofsson and Page, 2005; Defaye et al., 2009; Evans et al., 2010). Lack of macrophages is seemingly compatible with larval and pupal development, although it causes a shift in immune effector pathways – specifically, induction of the Toll pathway and repression of the Imd pathway – which leads to a proinflammatory state and aberrant leg development, in turn resulting in reduced likelihood of eclosion (Arefin et al., 2015). In adult *Drosophila*, lack of macrophages increases susceptibility to bacterial infection (Braun et al., 1998; Charroux and Royet, 2009; Defaye et al., 2009; Arefin et al., 2015), demonstrating their immune functions and role as sentinels of infection that induce antimicrobial peptide (AMP) gene expression in other tissues (Sanchez Bosch et al., 2019).

It is clear that plasmatocytes are a diverse population of cells that modulate a wide variety of processes during development. Genetic studies in *Drosophila* have provided broad evidence of tissue-specific macrophage function. How do macrophages and their microenvironment shape one another in different organ systems? We address this question in the following paragraphs and **Figure 2**.

NERVOUS SYSTEM

The *Drosophila* central nervous system consists of the brain and ventral nerve cord, and the peripheral nervous system includes sensory and motor neurons (Landgraf and Thor, 2006; Sánchez-Soriano et al., 2007; Hartenstein et al., 2008; Singhania and Grueber, 2014; Schirmeier et al., 2016; Doe, 2017; Li et al., 2018; Sugie et al., 2018; Akin and Zipursky, 2020). Major roles of macrophages in the nervous system, together with glia, are the phagocytic removal of apoptotic cells and the production of ECM (Zheng et al., 2017; Bittern et al., 2020; Hilu-Dadia and Kurant, 2020). Hemocytes invade the posterior end of the embryo during the germband extended stage and subsequently disperse throughout the embryo by migration, also entering the ventral nerve cord (VNC) (Tepass et al., 1994; Brückner et al., 2004). Some aspects of this migration, in particular invasion of the posterior end and migration along the VNC are mediated by PVR (Brückner et al., 2004; Wood et al., 2006), although PVR is primarily required for anti-apoptotic survival of hemocytes (Brückner et al., 2004). In the VNC, a significant amount of programmed cell death takes place in various cell types from the early stages of CNS formation to the end of embryogenesis (Abrams et al., 1993; White et al., 1994; Sonnenfeld and Jacobs, 1995; Zhou et al., 1995; Hidalgo et al., 2001; Peterson et al., 2002; Lundell, 2003; Miguel-Aliaga, 2004; Karcavich and Doe, 2005; Rogulja-Ortmann et al., 2007). Hemocytes phagocytose apoptotic bodies, opening up spaces and allowing for condensation of the nervous system (Olofsson and Page, 2005; Evans et al., 2010). Inhibition of hemocyte development or function causes mispositioning of glia, which, in turn, results in CNS axon scaffold and patterning defects (Sears, 2003); this phenotype is also observed when either *PVR* or *Crq* are RNAi silenced in hemocytes (Sears, 2003). CNS axon scaffold malformation forms a physical barrier to hemocyte migration along the VNC

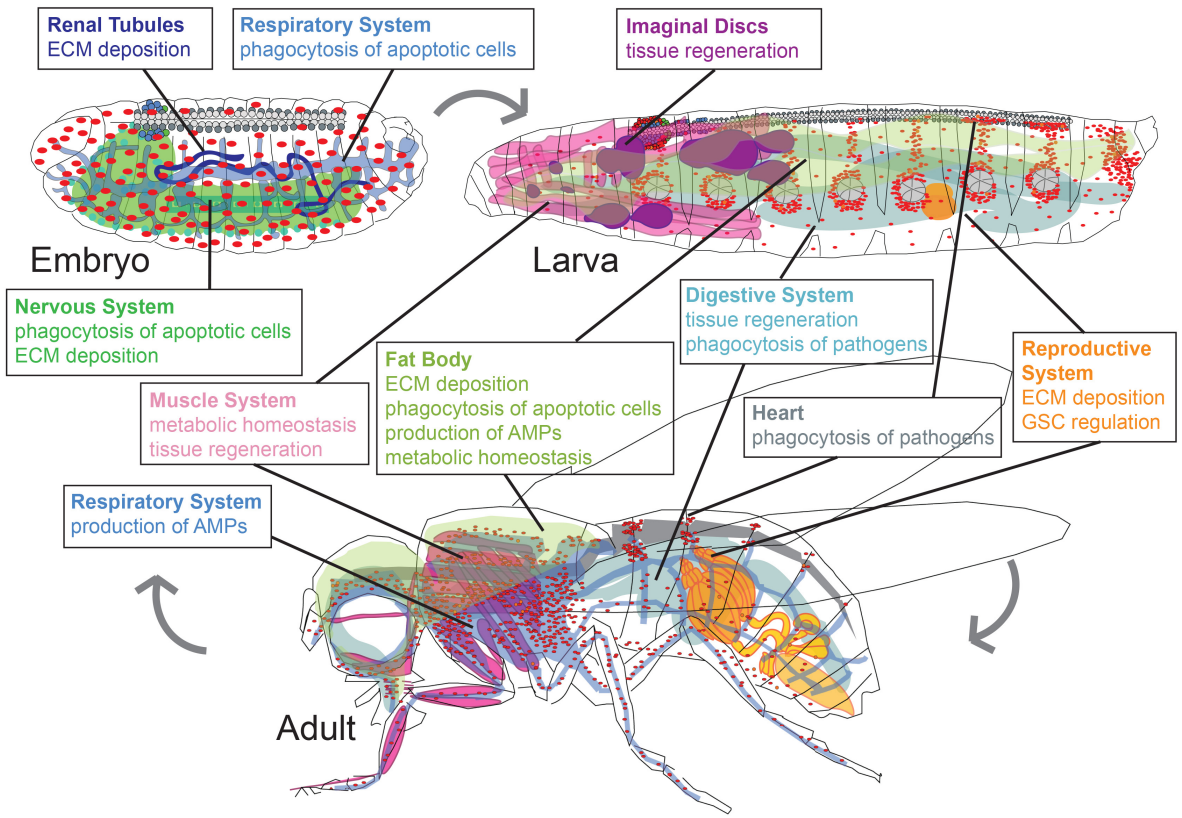

FIGURE 2 | *Drosophila* macrophages play life stage and tissue-specific roles in development, homeostasis, and infection. Major roles of plasmatocytes (macrophages, red) during developmental stages of embryo, larva, and adult (pupal stage is omitted). Organ systems regulated by macrophages are renal tubules (dark blue), respiratory system (light blue), nervous system (green), fat body (olive green), muscle system (pink), imaginal discs (purple), digestive system (teal), reproductive system (orange), heart (gray). Organ shapes adapted from Hartenstein (1995).

(Evans et al., 2010). When hemocytes cannot migrate, VNC condensation was proposed to also be disrupted due to a lack of ECM deposition by the migrating hemocytes (Olofsson and Page, 2005; Evans et al., 2010). Consistent with this, hemocytes deficient in *laminin B1 (LanB1)* exhibit slower migration along the ventral nerve cord (VNC) and defects in VNC condensation (Sánchez-Sánchez et al., 2017).

As development proceeds, in the larva, and especially during metamorphosis and in the adult, functions of hemocytes are more predominantly adopted by glia. In particular, glia mediate phagocytosis of dead cells and neuron fragments during axonal and dendrite pruning, and following injury (Sonnenfeld and Jacobs, 1995; Watts et al., 2004; Kurant, 2011; Bittern et al., 2020; Furusawa and Emoto, 2020; Hilu-Dadia and Kurant, 2020). Hemocytes and glia show molecular parallels regarding their phagocytic receptors such as Simu and Drpr (MacDonald et al., 2006; Kurant et al., 2008; Shklyar et al., 2014; Evans et al., 2015; Weavers et al., 2016; Shlyakhover et al., 2018; Davidson and Wood, 2020), and their mutual dependence on the transcription factors glial cells missing (gcm) and glial cells missing 2 (gcm2), during embryonic development (Bernardoni et al., 1997; Alfonso and Jones, 2002; Trébuchet et al., 2019).

Plasmatocytes also play roles in the development and homeostasis of the peripheral nervous system (PNS). During larval development, macrophages were proposed to function in neuronal pruning by severing destabilized dendritic branches and engulfing neuronal debris (Williams, 2005). More recently, however, it has been shown that non-traditional phagocytes, including glia and epidermal cells, play more central roles in neuronal pruning during development (Han et al., 2014). Macrophages may also have other roles in PNS development: a study suggested that hemocytes may promote aspects of glial cell biology necessary for peripheral nerve elongation (Pandey et al., 2011).

Conversely, the peripheral nervous system (PNS) can shape its resident macrophages and other hemocytes. Hemocytes associate with sensory neurons of the PNS in segmentally repeated hematopoietic pockets of the larval body wall (Makhijani et al., 2011; Makhijani and Brückner, 2012). These sensory neurons detect a variety of environmental and internal cues such as mechanical inputs, chemical stimuli, temperature, and light (Tracey et al., 2003; Hughes and Thomas, 2007; Song et al., 2007; Xiang et al., 2010; Han et al., 2014) and serve as a microenvironment for macrophages and other hemocytes (Makhijani et al., 2011, 2017; Makhijani and Brückner, 2012;

Corcoran et al., 2020). Within the microenvironments, neurons promote macrophage survival (Makhijani et al., 2011) through Dscam1 expression (Ouyang et al., 2020), and proliferation and localization by the expression of Actβ (Makhijani et al., 2017). Moreover, a specific set of caudal sensory neurons promotes transdifferentiation of plasmatocytes into crystal cells in the presence of oxygen, providing evidence that environmental inputs to the sensory nervous system can impact hematopoietic processes (Corcoran et al., 2020).

DIGESTIVE SYSTEM

The digestive system of *Drosophila* is maintained throughout all developmental stages based on intestinal stem cell (ISC) proliferation and differentiation (Murakami et al., 1999; Micchelli and Perrimon, 2006; Ohlstein and Spradling, 2006; Lemaitre and Miguel-Aliaga, 2013). Macrophages and other hemocytes form aggregates in folds of the intestine: at all developmental stages, they are enriched at the proventriculus, a structure where the esophagus, crop, and midgut converge (Tepass et al., 1994; Lebestky et al., 2000; Brückner et al., 2004; Charroux and Royet, 2009; Zaidman-Rémy et al., 2012). Hemocytes at the proventriculus are regulated by phosphoinositide 3-kinase (PI3K): PI3K signaling decreases hemocyte adhesion at the proventriculus, although it does not interfere with initial recruitment (Zaidman-Rémy et al., 2012). Hemocyte localization and responses may be further regulated by the innervation of the proventriculus (Cognigni et al., 2011), similar to hemocyte dependence on active sensory neurons in the hematopoietic pockets (Makhijani et al., 2011, 2017; Gold and Brückner, 2014, 2015). Macrophages are also enriched in clusters at the midgut, especially upon damage or infection (Ayyaz et al., 2015), and it has been debated whether some hemocytes are inserted in the midgut epithelium (Charroux and Royet, 2009; Zaidman-Rémy et al., 2012).

The macrophages of the intestine play important roles in innate immunity, maintaining homeostasis of gut microbiota both under basal conditions and after pathogen ingestion via the secretion of AMPs and phagocytosis (Nehme et al., 2007; Charroux and Royet, 2009; Ayyaz et al., 2015; Bonfini et al., 2016; Guillou et al., 2016). In addition, under conditions of tissue damage, inflammation, and infection, local and systemic macrophages function to promote and control tissue regeneration of the intestine (Takeishi et al., 2013; Ayyaz et al., 2015; Chakrabarti et al., 2016). Septic injury triggers upregulation of Upd ligands in hemocytes (Pastor-Pareja et al., 2008; Chakrabarti et al., 2016), inducing systemic changes including intestinal stem cell activation via JAK/STAT signaling (Chakrabarti et al., 2016; Guillou et al., 2016); this mechanism plays a role in many situations of gut regeneration and homeostasis (Jiang et al., 2009). Upon gut damage by oxidative stress or oral infection, local hemocytes produce the BMP Dpp, inducing proliferation of ISCs through activation of the signal transducer dSmad2, followed by signaling through the signal transducer Mothers against Dpp (Mad) that restores ISC quiescence (Ayyaz et al., 2015). This pathway also maintains normal gut homeostasis and limits ISC proliferation (Guo et al., 2013; Zhou et al., 2015). As the fly ages, repeated Dpp secretion by hemocytes can lead to dysregulated dSmad2 activity, resulting in dysplasia as ISCs over-proliferate, an intriguing model for colon cancer (Ayyaz et al., 2015). Similarly, in mouse models, macrophages in the colon directly promote the proliferation of epithelial progenitors as a wound response (Pull et al., 2005).

REPRODUCTIVE SYSTEM

The *Drosophila* reproductive organs, the female ovary and the male testis, carry germline stem cells and produce the gametes (Fuller and Spradling, 2007). In the *Drosophila* ovary, the basement membrane, a specialized ECM underlying the basal side of epithelial cells (LeBleu et al., 2007; Yurchenco, 2011), is important for the stability and function of the gonad and the developing egg chambers (follicles) (Denef et al., 2008; Van De Bor et al., 2015). While follicular epithelial cells contribute to the basement membrane in the adult ovary (Denef et al., 2008), a population of ovarian macrophages deposits collagen IV in the larval gonad, forming a stable basement membrane that persists from the larval to the adult stage (Van De Bor et al., 2015). This basement membrane regulates the stem cell niche of the gonad by limiting diffusion of the BMP Dpp, which prevents excessive Dpp in the ovaries from triggering over-proliferation of the germline stem cells (Van De Bor et al., 2015). The gradient of Dpp is also known to be limited by heparan sulfate proteoglycans (HSPGs) (Guo et al., 2013; Zhou et al., 2015). In the absence of hemocyte-produced collagen, larvae develop malformed basement membranes, which, in turn, lead to dysregulated stem cell proliferation, ultimately resulting in decreased reproductive fitness (Wang et al., 2008; Van De Bor et al., 2015). In the male testis, macrophages were suggested to be required for the regeneration of germline stem cells from dedifferentiating spermatogonial cells, a process that may depend on JAK/STAT signaling (Varga et al., 2020). In the mammalian ovary, macrophages play various roles, although mechanistic parallels with *Drosophila* remain to be determined (Wu et al., 2004). For example, macrophages are located along the basement membrane and support follicular development during the estrous cycle (Cohen et al., 1997). Their exact role in tissue remodeling during ovulation is unclear, although mice lacking ovarian macrophages have decreased reproductive success (Cohen et al., 1997).

RESPIRATORY SYSTEM

The *Drosophila* respiratory system consists of a tubular system of trachea that develop over the embryonic and larval stages; it is then remodeled during metamorphosis, forming the extensive air sacs of the head and thorax, as well as tubular tracheal structures in the abdomen of the adult animal (Whitten, 1957; Manning and Krasnow, 1993; Hayashi and Kondo, 2018). In the tracheal system, hemocytes exist alongside respiratory tubes and epithelia

to assist with development (Hartenstein et al., 1994; Baer et al., 2010) and prevention of infection (Sanchez Bosch et al., 2019). Specifically, during embryonic development, tracheal cells at the base of the dorsal branch undergo apoptosis in response to microenvironmental cues, detach from the epithelium, and are engulfed by macrophages (Baer et al., 2010). Tracheal cells also undergo apoptosis as part of tracheal remodeling during metamorphosis, suggesting a possible role for phagocytosing macrophages at this stage of development (Chen and Krasnow, 2014). Following pupariation, macrophages of the embryonic lineage and dispersed lymph gland hemocytes (Holz et al., 2003; Grigorian et al., 2011) associate with the respiratory epithelia (air sacs) in the head and thorax of the adult animal, forming the major blood cell reservoir (Sanchez Bosch et al., 2019). Here, macrophages act as sentinels of infection, engulfing pathogens and instructing the respiratory epithelia and neighboring cells of the fat body via secretion of Upd3 to produce e.g., the AMP Drosocin (Tzou et al., 2000; Sanchez Bosch et al., 2019), which defends against bacterial infection (Lemaitre et al., 1995; Sanchez Bosch et al., 2019).

FAT BODY

The *Drosophila* fat body is a site of energy storage, detoxification and immune response that functionally parallels the vertebrate liver (Miller et al., 2002; Dionne, 2014). It forms an extensive tissue in the embryo and larva, and lines the majority of the adult cuticle and epidermis (Zhang and Xi, 2015). During larval development, macrophages contribute critically to basement membrane formation of the fat body via the deposition of SPARC, a glycoprotein involved in the assembly of collagen IV (Shahab et al., 2015). Later, during metamorphosis, larval fat body cells undergo remodeling, resulting in fat body dissociation and apoptosis (Nelliot et al., 2006; Sanchez Bosch et al., 2019). Macrophages associate with these decaying cells and are involved in the phagocytosis of the cellular debris, a process that lasts well into adulthood (Nelliot et al., 2006; Sanchez Bosch et al., 2019).

Macrophages affect many aspects of metabolic regulation, homeostasis and immunity in the fat body (Dionne, 2014). For example, when larvae are raised on a high fat diet, or exposed to parasitic wasp infestation, plasmatocytes produce excess Upd3, inducing Jak/Stat signaling in the fat body, which downregulates insulin production, decreases larval growth, and reduces lifespan (Woodcock et al., 2015; Shin et al., 2020). This mechanism is mirrored in animals on a high sucrose diet (Parupalli et al., 2020). In response to bacterial infection, hemocytes communicate to the fat body through signals including Upd3 and the Toll ligand Spätzle to induce AMP expression, in both the larva and adult (Agaisse et al., 2003; Brennan et al., 2007; Charroux and Royet, 2009; Shia et al., 2009; Honti et al., 2014; Sanchez Bosch et al., 2019). Bacterial infection also stimulates hemocytes to release ImpL2, an insulin/IGF antagonist, which induces the release of lipoproteins and carbohydrates from the fat body to fuel the immune response (Gabriela et al., 2020); in turn, hemocytes switch to aerobic glycolysis, which supports the antibacterial defense (Krejèová et al., 2019).

Conversely, fat body cells regulate hemocyte populations during instances of nutrient deprivation and immune challenge. During starvation, macrophages move from the hematopoietic pockets and other locations to infiltrate the larval fat body (Shim et al., 2012). Specifically, the fat body releases NimB5, which acts on hemocytes to downregulate adhesion and proliferation (Ramond et al., 2020b). This mechanism redirects resources to essential functions only, promoting animal survival (Ramond et al., 2020b). Under immune challenge such as parasitic wasp infestation, signals from the fat body promote hemocyte responses: Toll signaling in the fat body promotes the Toll-dependent activation of macrophages (Schmid et al., 2014). Moreover, fat body cells upregulate expression of Edin (elevated during infection), a secreted peptide that promotes an increase in macrophage number and also triggers their release from the hematopoietic pockets and other resident locations, thereby facilitating the encapsulation response (Vanha-aho et al., 2015).

MUSCLE SYSTEM

Drosophila has a complex muscle system at all stages of development (Bothe and Baylies, 2016). Macrophages and the muscular system form another axis of communication in *Drosophila.* In the adult animal, under non-inflammatory physiology, hemocytes constitutively produce Upd3, which promotes basal JAK/STAT activity in muscle cells (Kierdorf et al., 2020). When disrupting this signaling by loss of the *dome* receptor in muscles, a systemic metabolic pathology develops, characterized by hyperactivation of the kinase AKT, an insulin signaling mediator, and reduced lifespan (Kierdorf et al., 2020). While this study raises new interesting questions, the interactions between muscle, insulin signaling, metabolism, and growth have been an intense focus of investigation (Demontis and Perrimon, 2009, 2010; Kwon et al., 2015).

Molecular communication in both directions, including signaling from the muscles to macrophages, is central in establishing immune responses (Yang et al., 2015; Yang and Hultmark, 2017). In the *Drosophila* larva, muscles regulate plasmatocytes in the immune response to parasitic wasp infestation. This effect is initially triggered by the release of Upd2 and Upd3 from plasmatocytes during wasp infestation, activating the JAK/STAT pathway in muscle tissue beyond basal levels (Yang et al., 2015; Shin et al., 2020). In turn, muscle cells control the plasmatocyte response, promoting the number of plasmatocyte-derived lamellocytes and enhancing the encapsulation response (Yang et al., 2015). This effect appears to depend on altered feeding behavior and is mediated by insulin signaling via TOR (target of rapamycin) in the muscles, which indirectly enhances JAK/STAT signaling in hemocytes, driving lamellocyte formation (Yang et al., 2015; Anderl et al., 2016; Yang and Hultmark, 2017). Interestingly, larval muscles are an anatomical part of the hematopoietic pockets where plasmatocytes reside in clusters, suggesting that muscle cells are an active player of this instructive microenvironment (Makhijani et al., 2011; Makhijani and Brückner, 2012; Yang et al., 2015).

HEART

In *Drosophila* and in insects in general, macrophages accumulate in clusters at the ostia (intake valves) of the heart (Gupta, 1979), a tubular structure running along the dorsal side of the animal (Ocorr et al., 2007). Macrophages in these clusters monitor the streaming hemolymph of the open circulatory system and fulfill immune functions, phagocytosing bacteria and foreign particles (Gupta, 1979; Elrod-Erickson et al., 2000; Dionne et al., 2003; King and Hillyer, 2012; Cevik et al., 2019). Relatively little is known about interactions between macrophages and heart tissue. In *Drosophila* third instar larvae, hemocytes from resident sites increasingly enter circulation and subsequently accumulate in clusters at the ostia and pericardial nephrocytes of the larval heart (dorsal vessel) (Frasch, 1999), forming dorsal vessel-associated clusters (Markus et al., 2009; Makhijani et al., 2011; Petraki et al., 2015; Cevik et al., 2019). Hemocytes accumulate in the ECM of the dorsal vessel, which is facilitated by the heart-specific collagen Pericardin (Cevik et al., 2019). In addition, some aspects of this accumulation may be mechanical (Petraki et al., 2015; Cevik et al., 2019). In adult *Drosophila*, hemocytes accumulate at the ostia of the heart in a mesh of ECM that likewise contains Pericardin and Laminin A (Ghosh et al., 2015; Sessions et al., 2017). One study suggested that the heart serves as a 'hematopoietic hub' for new hemocyte production (Ghosh et al., 2015), however, this model was disproven based on evidence of a developmental mechanism of macrophage accumulation at the heart, and the absence of any significant hematopoietic activity using multiple orthogonal approaches (Sanchez Bosch et al., 2019).

RENAL TUBULES

Drosophila Malpighian tubules (renal tubules) are excretory organs with similarity to the vertebrate kidney; they secrete waste and maintain ionic and osmotic homeostasis (Maddrell, 1972; Denholm and Skaer, 2009). During the embryonic development of the Malpighian tubules, macrophages are attracted to these growing structures through tubule expression of PVF ligands (Bunt et al., 2010). Macrophages, in turn, secrete components of the basement membrane (Bunt et al., 2010). Collagen IV is part of this, sensitizing tubule cells to the BMP ligand Dpp, which is required to promote the outgrowth of the tubules (Bunt et al., 2010). While it is known that Dpp is secreted locally, the source remains unknown; however, in the gut, Dpp is sourced from hemocytes (Guo et al., 2013; Ayyaz et al., 2015) and hemocytes could have a similar function for the Malpighian tubules. The process of macrophage-mediated tubule elongation is conserved in mice where tissue-resident macrophages contribute to renal organogenesis (Munro and Hughes, 2017).

IMAGINAL DISCS

Imaginal discs are the larval precursors to the adult fly eyes, wings, legs, and other appendages (Worley et al., 2012). They develop as epithelial sacs, which serve as intriguing models to study patterning, morphogenesis, and regeneration (Hariharan and Serras, 2017). Imaginal disc damage stimulates increase in macrophages that adhere to the wound (Bryant and Fraser, 1988; McClure et al., 2008; Pastor-Pareja et al., 2008; Katsuyama and Paro, 2013). In response to UV damage to the eye imaginal disc, macrophages actively promote tissue regeneration (Kelsey et al., 2012). Specifically, damaged disc cells upregulate Shnurri (Shn), a transcriptional regulator that induces *Pvf1*, which then signals to disc-associated hemocytes to activate their macrophage-like behavior (Kelsey et al., 2012). Activated hemocytes engulf apoptotic cells in the eye disc and clear debris to limit tissue damage (Kelsey et al., 2012). The activation of macrophages in this model relies at least in part on the induction of mesencephalic astrocyte-derived neurotrophic factor (MANF) (Neves et al., 2016). MANF shifts the expression of hemocyte markers and induces expression of the *Drosophila* homolog of the mammalian M2 marker *arginase1*, suggesting a process similar to the alternative activation of macrophages in vertebrates (Neves et al., 2016). Importantly, PDGF/MANF signaling of macrophages in response to retinal damage is conserved in mammals (Neves et al., 2016). Hemocytes also trigger tissue regeneration via epithelial cell proliferation in response to reactive oxygen species (ROSs) released from damaged epithelial disc cells (Fogarty et al., 2016). In a model of apoptosis-induced proliferation (AiP), in which eye disc cells were induced to die by the pro-apoptotic gene head involution defect (hid), while apoptosis was concomitantly blocked by p35 (Ryoo et al., 2004), activity of the caspase Dronc in epithelial disc cells promotes activation of the NADPH oxidase Duox that generates extracellular ROSs (Fogarty et al., 2016). ROS release activates disc-associated macrophages and induces them to secrete the TNF (tumor necrosis factor) family ligand Eiger, which activates JNK signaling in disc cells leading to proliferation (Fogarty et al., 2016). Similar mechanisms of ROS-induced JNK signaling may apply to the regeneration of damaged wing discs, although the role of hemocytes in this context remains to be investigated (Santabárbara-Ruiz et al., 2015). One study reported hemocytes to be dispensable for the regenerative growth of aseptic wounds of wing discs or transplanted leg disc fragments under conditions of combined ablation of hemocytes and fat body (Katsuyama and Paro, 2013). However, these experiments were performed in developmentally arrested larvae fed with *erg2*Δ mutant yeast (Katsuyama and Paro, 2013) that does not provide sterols necessary for the formation of the fly hormone ecdysone (Parkin and Burnet, 1986). Ecdysone controls molting, but also stimulates hemocyte phagocytic activity and mobility, and the encapsulation response (Sorrentino et al., 2002; Regan et al., 2013; Sampson et al., 2013), which could have affected experimental outcomes (Katsuyama and Paro, 2013).

DISCUSSION

Drosophila and vertebrates share many parallels in their macrophage systems, which in both cases are based on two lineages. While the anatomical origins of tissue macrophages in *Drosophila* and vertebrates differ, there are many evolutionary

parallels at the molecular, cellular, and functional level. Considering that this lineage is the predominant source of macrophages in *Drosophila* (Sanchez Bosch et al., 2019), we propose that tissue macrophages may represent the ancient mechanism of macrophage production and regulation, allowing immediate adaptation to organismal and environmental conditions. This may be particularly important in species that heavily rely on innate immunity.

The diverse functional roles of *Drosophila* macrophages predict defined subpopulations, influenced by local signals from their tissue of residence, and possibly lineage and other conditions. This resembles vertebrates, in which macrophage populations have been characterized based on their polarization, i.e., their distinct functional phenotypes, regulated by microenvironmental and systemic stimuli (Gordon and Taylor, 2005; Martinez, 2008; Lavin et al., 2015; Zhu et al., 2015; Shapouri-Moghaddam et al., 2018). Vertebrate macrophages exhibit functional plasticity to differentiate into classically activated macrophages (M1) with roles in infection, and alternatively activated macrophages (M2) active in tissue repair and anti-inflammatory responses; further subdivisions are based on their prototypical activating stimuli and functionality (Martinez, 2008; Tarique et al., 2015; Zhu et al., 2015; Shapouri-Moghaddam et al., 2018). Recent analyses suggest an even greater spectrum of activation states exceeding these classifications (Mosser and Edwards, 2008; Xue et al., 2014), and lineage also plays a role in determining the properties and activation states of macrophages (Gundra et al., 2014). Macrophages may adopt potentially distinct activation states when mediating previously unknown functions, such as the transfer of mitochondria to and from target tissues including neurons and heart cells, which promotes repair after tissue damage, and stimulates the macrophage innate immune response, respectively (Jackson et al., 2016; Brestoff et al., 2020; Nicolás-Ávila et al., 2020; Raoof et al., 2020).

Research in *Drosophila* suggests that the characteristics of macrophages are changed following priming by an immune encounter, such as phagocytosis of apoptotic cells (Weavers et al., 2016; Nonaka et al., 2017; Roddie et al., 2019; Chakrabarti and Visweswariah, 2020). This interaction leads to "immune training", consisting of changes in intracellular signaling and the repertoire of phagocytic receptors, which can determine behavior in future encounters (Weavers et al., 2016; Nonaka et al., 2017; Roddie et al., 2019; Chakrabarti and Visweswariah, 2020). Consistent with this, a study provided molecular evidence of *Drosophila* macrophages taking on an alternatively activated (M2) status in response to local cues in tissue regeneration (Neves et al., 2016). Single cell RNA sequencing and functional studies further support the hypothesis of distinct activation states in *Drosophila* macrophages, identifying subpopulations that have differential involvement in phagocytosis, metabolic homeostasis, and the humoral AMP response (Cattenoz et al., 2020; Cho et al., 2020; Coates et al., 2020; Fu et al., 2020; Ramond et al., 2020a; Shin et al., 2020; Tattikota et al., 2020). Functional distinctions are driven by developmental stage (Cattenoz et al., 2020; Cho et al., 2020), injury, and immune challenge (Coates et al., 2020; Fu et al., 2020; Ramond et al., 2020a; Tattikota et al., 2020).

Additional research will link many of the observed cellular differences between macrophage populations with their roles in specific organ systems, as exemplified in this review. A particular gap in knowledge is how microenvironmental cues shape the molecular and phenotypic status of macrophages to adapt to their distinct tasks, and how interactions between immune cell types and lineages may affect their response. In vertebrates, organ microenvironments regulate tissue macrophages through local production of CSF1, IL-34, and paracrine and autocrine TGF-β (Lavin et al., 2015). However, findings from *Drosophila* (Makhijani et al., 2011, 2017; Gold and Brückner, 2014, 2015; Corcoran et al., 2020) suggest the existence of more elaborate regulatory systems also in vertebrates, comprising, e.g., peripheral innervation or cell based environmental sensors that regulate local tissue macrophage populations through molecular signals. Understanding cellular and molecular principles of organ-macrophage communication in *Drosophila* will further broaden our insights into vertebrate macrophage systems, and contribute to approaches that harness the power of macrophages in regenerative medicine and immunology.

AUTHOR CONTRIBUTIONS

AM and JA wrote the text and designed the figures. KB revised the text and figures, designed figure elements, and coordinated the content of the review. All authors contributed to the article and approved the submitted version.

FUNDING

This work was supported by grants from the National Institutes of Health 1R01GM112083 and 1R01GM131094 (to KB).

ACKNOWLEDGMENTS

We apologize to authors whose work was not cited due to space constraints or accidental oversight.

REFERENCES

Abrams, J. M., White, K., Fessler, L. I., and Steller, H. (1993). Programmed cell death during *Drosophila embryogenesis*. *Development* 117, 29–43.

Agaisse, H., Petersen, U. M., Boutros, M., Mathey-Prevot, B., and Perrimon, N. (2003). Signaling role of hemocytes in *Drosophila* JAK/STAT-dependent response to septic injury. *Dev. Cell* 5, 441–450. doi: 10.1016/s1534-5807(03)00244-2

Ajami, B., Bennett, J. L., Krieger, C., Tetzlaff, W., and Rossi, F. M. V. (2007). Local self-renewal can sustain CNS microglia maintenance and function throughout adult life. *Nat. Neurosci.* 10, 1538–1543. doi: 10.1038/nn2014

Akin, O., and Zipursky, S. L. (2020). Activity regulates brain development in the fly. *Curr. Opin. Genet. Dev.* 65, 8–13. doi: 10.1016/j.gde.2020.04.005

Alfonso, T. B., and Jones, B. W. (2002). gcm2 promotes glial cell differentiation and is required with glial cells missing for macrophage development in *Drosophila*. *Dev. Biol.* 248, 369–383. doi: 10.1006/dbio.2002.0740

Anderl, I., Vesala, L., Ihalainen, T. O., Vanha-aho, L.-M., Andó, I., Rämet, M., et al. (2016). Transdifferentiation and proliferation in two distinct hemocyte lineages in *Drosophila melanogaster* Larvae after Wasp infection. *PLoS Pathog.* 12:e1005746. doi: 10.1371/journal.ppat.1005746

Arefin, B., Kucerova, L., Krautz, R., Kranenburg, H., Parvin, F., and Theopold, U. (2015). Apoptosis in hemocytes induces a shift in effector mechanisms in the *Drosophila* immune system and leads to a pro-inflammatory state. *PLoS One* 10:e0136593. doi: 10.1371/journal.pone.0136593

Ayyaz, A., Li, H., and Jasper, H. (2015). Haemocytes control stem cell activity in the *Drosophila* intestine. *Nat. Cell Biol.* 17, 736–748. doi: 10.1038/ncb3174

Babcock, D. T., Brock, A. R., Fish, G. S., Wang, Y., Perrin, L., Krasnow, M. A., et al. (2008). Circulating blood cells function as a surveillance system for damaged tissue in *Drosophila larvae*. *Proc. Natl. Acad. Sci. U.S.A.* 105, 10017–10022. doi: 10.1073/pnas.0709951105

Baer, M. M., Bilstein, A., Caussinus, E., Csiszar, A., Affolter, M., and Leptin, M. (2010). The role of apoptosis in shaping the tracheal system in the *Drosophila embryo*. *Mech. Dev.* 127, 28–35. doi: 10.1016/j.mod.2009.11.003

Banerjee, U., Girard, J. R., Goins, L. M., and Spratford, C. M. (2019). *Drosophila* as a genetic model for hematopoiesis. *Genetics* 211, 367–417. doi: 10.1534/genetics.118.300223

Bernardoni, R., Vivancos, V., and Giangrande, A. (1997). glide/gcm is expressed and required in the scavenger cell lineage. *Dev. Biol.* 191, 118–130. doi: 10.1006/dbio.1997.8702

Bittern, J., Pogodalla, N., Ohm, H., Brüser, L., Kottmeier, R., Schirmeier, S., et al. (2020). Neuron-glia interaction in the *Drosophila* nervous system. *Dev. Neurobiol.* doi: 10.1002/dneu.22737 [Epub ahead of print].

Bonfini, A., Liu, X., and Buchon, N. (2016). From pathogens to microbiota: how *Drosophila* intestinal stem cells react to gut microbes. *Dev. Comp. Immunol.* 64, 22–38. doi: 10.1016/j.dci.2016.02.008

Bothe, I., and Baylies, M. K. (2016). *Drosophila* myogenesis. *Curr. Biol.* 26, R786–R791. doi: 10.1016/j.cub.2016.07.062

Braun, A., Hoffmann, J. A., and Meister, M. (1998). Analysis of the *Drosophila* host defense in domino mutant larvae, which are devoid of hemocytes. *Proc. Natl. Acad. Sci. U.S.A.* 95, 14337–14342. doi: 10.1073/pnas.95.24.14337

Brennan, C. A., Delaney, J. R., Schneider, D. S., and Anderson, K. V. (2007). Psidin is required in *Drosophila* blood cells for both phagocytic degradation and immune activation of the fat body. *Curr. Biol.* 17, 67–72. doi: 10.1016/j.cub.2006.11.026

Brestoff, J. R., Wilen, C. B., Moley, J. R., Li, Y., Zou, W., Malvin, N. P., et al. (2020). Intercellular mitochondria transfer to macrophages regulates white adipose tissue homeostasis and is impaired in obesity. *Cell Metab.* doi: 10.1016/j.cmet.2020.11.008 [Epub ahead of print].

Bretscher, A. J., Honti, V., Binggeli, O., Burri, O., Poidevin, M., Kurucz, E., et al. (2015). The Nimrod transmembrane receptor Eater is required for hemocyte attachment to the sessile compartment in *Drosophila melanogaster*. *Biol. Open* 4, 355–363. doi: 10.1242/bio.201410595

Brückner, K., Kockel, L., Duchek, P., Luque, C. M., Rørth, P., and Perrimon, N. (2004). The PDGF/VEGF receptor controls blood cell survival in *Drosophila*. *Dev. Cell* 7, 73–84. doi: 10.1016/j.devcel.2004.06.007

Bryant, P. J., and Fraser, S. E. (1988). Wound healing, cell communication, and DNA synthesis during imaginal disc regeneration in *Drosophila*. *Dev. Biol.* 127, 197–208. doi: 10.1016/0012-1606(88)90201-1

Buchon, N., Silverman, N., and Cherry, S. (2014). Immunity in *Drosophila melanogaster* — from microbial recognition to whole-organism physiology. *Nat. Rev. Immunol.* 14, 796–810. doi: 10.1038/nri3763

Bunt, S., Hooley, C., Hu, N., Scahill, C., Weavers, H., and Skaer, H. (2010). Hemocyte-secreted Type IV collagen enhances BMP signaling to guide renal tubule morphogenesis in *Drosophila*. *Dev. Cell* 19, 296–306. doi: 10.1016/j.devcel.2010.07.019

Cattenoz, P. B., Sakr, R., Pavlidaki, A., Delaporte, C., Riba, A., Molina, N., et al. (2020). Temporal specificity and heterogeneity of *Drosophila* immune cells. *EMBO J.* 39:e104486. doi: 10.15252/embj.2020104486

Cevik, D., Acker, M., Michalski, C., and Jacobs, J. R. (2019). Pericardin, a *Drosophila collagen*, facilitates accumulation of hemocytes at the heart. *Dev. Biol.* 454, 52–65. doi: 10.1016/j.ydbio.2019.06.006

Chakrabarti, S., Dudzic, J. P., Li, X., Collas, E. J., Boquete, J.-P., and Lemaitre, B. (2016). Remote control of intestinal stem cell activity by haemocytes in *Drosophila*. *PLoS Genet.* 12:e1006089. doi: 10.1371/journal.pgen.1006089

Chakrabarti, S., and Visweswariah, S. S. (2020). Intramacrophage ROS primes the innate immune system via JAK/STAT and toll activation. *Cell Rep.* 33:108368. doi: 10.1016/j.celrep.2020.108368

Charroux, B., and Royet, J. (2009). Elimination of plasmatocytes by targeted apoptosis reveals their role in multiple aspects of the *Drosophila* immune response. *Proc. Natl. Acad. Sci. U.S.A.* 106, 9797–9802. doi: 10.1073/pnas.0903971106

Chen, F., and Krasnow, M. A. (2014). Progenitor outgrowth from the niche in *Drosophila trachea* is guided by FGF from decaying branches. *Science* 343, 186–189. doi: 10.1126/science.1241442

Cho, B., Yoon, S.-H., Lee, D., Koranteng, F., Tattikota, S. G., Cha, N., et al. (2020). Single-cell transcriptome maps of myeloid blood cell lineages in *Drosophila*. *Nat. Commun.* 11:4483. doi: 10.1038/s41467-020-18135-y

Coates, J. A., Brittle, A., Armitage, E. L., Zeidler, M. P., and Evans, I. R. (2020). Identification of functionally-distinct macrophage subpopulations regulated by efferocytosis in *Drosophila*. *Dev. Biol.* doi: 10.1101/2020.04.17.047472 [Epub ahead of print].

Cognigni, P., Bailey, A. P., and Miguel-Aliaga, I. (2011). Enteric neurons and systemic signals couple nutritional and reproductive status with intestinal homeostasis. *Cell Metab.* 13, 92–104. doi: 10.1016/j.cmet.2010.12.010

Cohen, P. E., Zhu, L., and Pollard, J. W. (1997). Absence of colony stimulating factor-1 in osteopetrotic (csfmop/csfmop) mice disrupts estrous cycles and ovulation. *Biol. Reprod.* 56, 110–118. doi: 10.1095/biolreprod56.1.110

Corcoran, S., Mase, A., Hashimi, Y., Ouyang, D., Augsburger, J., Jacobs, T., et al. (2020). Regulation of blood cell transdifferentiation by oxygen sensing neurons in *Drosophila*. *bioRxiv* [Preprint] doi: 10.1101/2020.04.22.056622

Crozatier, M., Ubeda, J.-M., Vincent, A., and Meister, M. (2004). Cellular immune response to parasitization in *Drosophila* requires the EBF orthologue collier. *PLoS Biol.* 2:e196. doi: 10.1371/journal.pbio.0020196

Csordás, G., Grawe, F., and Uhlirova, M. (2020). Eater cooperates with Multiplexin to drive the formation of hematopoietic compartments. *eLife* 9:e57297. doi: 10.7554/eLife.57297

Davidson, A. J., and Wood, W. (2020). Phagocyte responses to cell death in flies. *Cold Spring Harb. Perspect. Biol.* 12:a036350. doi: 10.1101/cshperspect.a036350

Davies, L. C., Jenkins, S. J., Allen, J. E., and Taylor, P. R. (2013). Tissue-resident macrophages. *Nat. Immunol.* 14, 986–995. doi: 10.1038/ni.2705

Defaye, A., Evans, I., Crozatier, M., Wood, W., Lemaitre, B., and Leulier, F. (2009). Genetic ablation of *Drosophila* phagocytes reveals their contribution to both development and resistance to bacterial infection. *J. Innate Immun.* 1, 322–334. doi: 10.1159/000210264

Demontis, F., and Perrimon, N. (2009). Integration of Insulin receptor/Foxo signaling and dMyc activity during muscle growth regulates body size in *Drosophila*. *Development* 136, 983–993. doi: 10.1242/dev.027466

Demontis, F., and Perrimon, N. (2010). FOXO/4E-BP signaling in *Drosophila* muscles regulates organism-wide proteostasis during aging. *Cell* 143, 813–825. doi: 10.1016/j.cell.2010.10.007

Denef, N., Chen, Y., Weeks, S. D., Barcelo, G., and Schüpbach, T. (2008). Crag regulates epithelial architecture and polarized deposition of basement membrane proteins in *Drosophila*. *Dev. Cell* 14, 354–364. doi: 10.1016/j.devcel.2007.12.012

Denholm, B., and Skaer, H. (2009). Bringing together components of the fly renal system. *Curr. Opin. Genet. Dev.* 19, 526–532. doi: 10.1016/j.gde.2009.08.006

Destalminil-Letourneau, M., Morin-Poulard, I., Tian, Y., Vanzo, N., and Crozatier, M. (2021). The vascular niche controls *Drosophila* hematopoiesis via fibroblast growth factor signaling. *eLife* 10:64672. doi: 10.7554/eLife.64672

Dionne, M. (2014). Immune-metabolic interaction in *Drosophila*. *Fly (Austin)* 8, 75–79. doi: 10.4161/fly.28113

Dionne, M. S., Ghori, N., and Schneider, D. S. (2003). *Drosophila melanogaster* is a genetically tractable model host for *Mycobacterium marinum*. *Infect. Immun.* 71, 3540–3550. doi: 10.1128/iai.71.6.3540-3550.2003

Doe, C. Q. (2017). Temporal patterning in the *Drosophila* CNS. *Annu. Rev. Cell Dev. Biol.* 33, 219–240. doi: 10.1146/annurev-cellbio-111315-125210

Dragojlovic-Munther, M., and Martinez-Agosto, J. A. (2013). Extracellular matrix-modulated Heartless signaling in Drosophila blood progenitors regulates their differentiation via a Ras/ETS/FOG pathway and target of rapamycin function. *Dev. Biol.* 384, 313–330. doi: 10.1016/j.ydbio.2013.04.004

Dzierzak, E., and Speck, N. A. (2008). Of lineage and legacy: the development of mammalian hematopoietic stem cells. *Nat. Immunol.* 9, 129–136. doi: 10.1038/ni1560

Elrod-Erickson, M., Mishra, S., and Schneider, D. (2000). Interactions between the cellular and humoral immune responses in *Drosophila*. *Curr. Biol.* 10, 781–784. doi: 10.1016/s0960-9822(00)00569-8

Evans, I. R., Hu, N., Skaer, H., and Wood, W. (2010). Interdependence of macrophage migration and ventral nerve cord development in *Drosophila embryos*. *Development* 137, 1625–1633. doi: 10.1242/dev.046797

Evans, I. R., Rodrigues, F. S. L. M., Armitage, E. L., and Wood, W. (2015). Draper/CED-1 mediates an ancient damage response to control inflammatory blood cell migration in vivo. *Curr. Biol.* 25, 1606–1612. doi: 10.1016/j.cub.2015.04.037

Ferguson, G. B., and Martinez-Agosto, J. A. (2014). Yorkie and scalloped signaling regulates notch-dependent lineage specification during *Drosophila* hematopoiesis. *Curr. Biol.* 24, 2665–2672. doi: 10.1016/j.cub.2014.09.081

Fessler, J. H., and Fessler, L. I. (1989). *Drosophila* extracellular matrix. *Annu. Rev. Cell. Biol.* 5, 309–339. doi: 10.1146/annurev.cb.05.110189.001521

Fogarty, C. E., Diwanji, N., Lindblad, J. L., Tare, M., Amcheslavsky, A., Makhijani, K., et al. (2016). Extracellular reactive oxygen species drive apoptosis-induced proliferation via *Drosophila* macrophages. *Curr. Biol.* 26, 575–584. doi: 10.1016/j.cub.2015.12.064

Frame, J. M., McGrath, K. E., and Palis, J. (2013). Erythro-myeloid progenitors: "Definitive" hematopoiesis in the conceptus prior to the emergence of hematopoietic stem cells. *Blood Cells Mol. Dis.* 51, 220–225. doi: 10.1016/j.bcmd.2013.09.006

Franc, N. C. (1999). Requirement for croquemort in phagocytosis of apoptotic cells in *Drosophila*. *Science* 284, 1991–1994. doi: 10.1126/science.284.5422.1991

Frasch, M. (1999). Intersecting signalling and transcriptional pathways in *Drosophila* heart specification. *Semin. Cell Dev. Biol.* 10, 61–71. doi: 10.1006/scdb.1998.0279

Fu, Y., Huang, X., Zhang, P., van de Leemput, J., and Han, Z. (2020). Single-cell RNA sequencing identifies novel cell types in *Drosophila* blood. *J. Genet. Genomics* 47, 175–186. doi: 10.1016/j.jgg.2020.02.004

Fuller, M. T., and Spradling, A. C. (2007). Male and female *Drosophila germline* stem cells: two versions of immortality. *Science* 316, 402–404. doi: 10.1126/science.1140861

Furusawa, K., and Emoto, K. (2020). Spatiotemporal regulation of developmental neurite pruning: molecular and cellular insights from *Drosophila* models. *Neurosci. Res.* doi: 10.1016/j.neures.2020.11.010 [Epub ahead of print].

Gabriela, K., Adam, B., Pavla, N., Julie, K., Nick, K.-H., Helena, Z., et al. (2020). Macrophage-derived insulin/IGF antagonist ImpL2 regulates systemic metabolism for mounting an effective acute immune response in *Drosophila*. *bioRxiv* [Preprint] doi: 10.1101/2020.09.24.311670

Geissmann, F., Manz, M. G., Jung, S., Sieweke, M. H., Merad, M., and Ley, K. (2010). Development of monocytes, macrophages, and dendritic cells. *Science* 327, 656–661. doi: 10.1126/science.1178331

Ghosh, S., Singh, A., Mandal, S., and Mandal, L. (2015). Active hematopoietic hubs in *Drosophila* adults generate hemocytes and contribute to immune response. *Dev. Cell* 33, 478–488. doi: 10.1016/j.devcel.2015.03.014

Ginhoux, F., Schultze, J. L., Murray, P. J., Ochando, J., and Biswas, S. K. (2016). New insights into the multidimensional concept of macrophage ontogeny, activation and function. *Nat. Immunol.* 17, 34–40. doi: 10.1038/ni.3324

Gold, K. S., and Brückner, K. (2014). Drosophila as a model for the two myeloid blood cell systems in vertebrates. *Exp. Hematol.* 42, 717–727. doi: 10.1016/j.exphem.2014.06.002

Gold, K. S., and Brückner, K. (2015). Macrophages and cellular immunity in *Drosophila melanogaster*. *Semin. Immunol.* 27, 357–368. doi: 10.1016/j.smim.2016.03.010

Gomez Perdiguero, E., Klapproth, K., Schulz, C., Busch, K., Azzoni, E., Crozet, L., et al. (2015). Tissue-resident macrophages originate from yolk-sac-derived erythro-myeloid progenitors. *Nature* 518, 547–551. doi: 10.1038/nature13989

Gordon, S., and Taylor, P. R. (2005). Monocyte and macrophage heterogeneity. *Nat. Rev. Immunol.* 5, 953–964. doi: 10.1038/nri1733

Gosselin, D., Link, V. M., Romanoski, C. E., Fonseca, G. J., Eichenfield, D. Z., Spann, N. J., et al. (2014). Environment drives selection and function of enhancers controlling tissue-specific macrophage identities. *Cell* 159, 1327–1340. doi: 10.1016/j.cell.2014.11.023

Grigorian, M., Mandal, L., and Hartenstein, V. (2011). Hematopoiesis at the onset of metamorphosis: terminal differentiation and dissociation of the *Drosophila* lymph gland. *Dev. Genes Evol.* 221, 121–131. doi: 10.1007/s00427-011-0364-6

Guillou, A., Troha, K., Wang, H., Franc, N. C., and Buchon, N. (2016). The *Drosophila* CD36 homologue croquemort is required to maintain immune and gut homeostasis during development and aging. *PLoS Pathog.* 12:e1005961. doi: 10.1371/journal.ppat.1005961

Gundra, U. M., Girgis, N. M., Ruckerl, D., Jenkins, S., Ward, L. N., Kurtz, Z. D., et al. (2014). Alternatively activated macrophages derived from monocytes and tissue macrophages are phenotypically and functionally distinct. *Blood* 123, e110–e122. doi: 10.1182/blood-2013-08-520619

Guo, Z., Driver, I., and Ohlstein, B. (2013). Injury-induced BMP signaling negatively regulates *Drosophila* midgut homeostasis. *J. Cell Biol.* 201, 945–961. doi: 10.1083/jcb.201302049

Gupta, A. P. (1979). *Insect Hemocytes: Development, Forms, Functions, and Techniques*. New York, NY: Cambridge University Press.

Han, C., Song, Y., Xiao, H., Wang, D., Franc, N. C., Jan, L. Y., et al. (2014). Epidermal cells are the primary phagocytes in the fragmentation and clearance of degenerating dendrites in *Drosophila*. *Neuron* 81, 544–560. doi: 10.1016/j.neuron.2013.11.021

Hariharan, I. K., and Serras, F. (2017). Imaginal disc regeneration takes flight. *Curr. Opin. Cell Biol.* 48, 10–16. doi: 10.1016/j.ceb.2017.03.005

Hartenstein, V. (1995). *Atlas of Drosophila Development*, 1 Edn. Cold Spring Harbor, NY: Cold Spring Harbor Laboratory Press.

Hartenstein, V. (2006). Blood cells and blood cell development in the animal kingdom. *Annu. Rev. Cell Dev. Biol.* 22, 677–712. doi: 10.1146/annurev.cellbio.22.010605.093317

Hartenstein, V., Spindler, S., Pereanu, W., and Fung, S. (2008). "The development of the *Drosophila* larval brain," in *Brain Development in Drosophila melanogaster Advances in Experimental Medicine and Biology*, ed. G. M. Technau (New York, NY: Springer New York), 1–31. doi: 10.1007/978-0-387-78261-4_1

Hartenstein, V., Tepass, U., and Gruszynski-Defeo, E. (1994). Embryonic development of the stomatogastric nervous system in *Drosophila*. *J. Comp. Neurol.* 350, 367–381. doi: 10.1002/cne.903500304

Hashimoto, D., Chow, A., Noizat, C., Teo, P., Beasley, M. B., Leboeuf, M., et al. (2013). Tissue-resident macrophages self-maintain locally throughout adult life with minimal contribution from circulating monocytes. *Immunity* 38, 792–804. doi: 10.1016/j.immuni.2013.04.004

Hayashi, S., and Kondo, T. (2018). Development and function of the *Drosophila* tracheal system. *Genetics* 209, 367–380. doi: 10.1534/genetics.117.300167

Herbomel, P., Thisse, B., and Thisse, C. (2001). Zebrafish early macrophages colonize cephalic mesenchyme and developing brain, retina, and epidermis through a M-CSF receptor-dependent invasive process. *Dev. Biol.* 238, 274–288. doi: 10.1006/dbio.2001.0393

Hidalgo, A., Kinrade, E. F. V., and Georgiou, M. (2001). The *Drosophila* neuregulin vein maintains glial survival during axon guidance in the CNS. *Dev. Cell* 1, 679–690. doi: 10.1016/S1534-5807(01)00074-0

Hilu-Dadia, R., and Kurant, E. (2020). Glial phagocytosis in developing and mature *Drosophila* CNS: tight regulation for a healthy brain. *Curr. Opin. Immunol.* 62, 62–68. doi: 10.1016/j.coi.2019.11.010

Hoeffel, G., Wang, Y., Greter, M., See, P., Teo, P., Malleret, B., et al. (2012). Adult Langerhans cells derive predominantly from embryonic fetal liver monocytes with a minor contribution of yolk sac-derived macrophages. *J. Exp. Med.* 209, 1167–1181. doi: 10.1084/jem.20120340

Holz, A., Bossinger, B., Strasser, T., Janning, W., and Klapper, R. (2003). The two origins of hemocytes in *Drosophila*. *Development* 130, 4955–4962. doi: 10.1242/dev.00702

Honti, V., Csordás, G., Kurucz, É, Márkus, R., and Andó, I. (2014). The cell-mediated immunity of *Drosophila melanogaster*: hemocyte lineages, immune compartments, microanatomy and regulation. *Dev. Comp. Immunol.* 42, 47–56. doi: 10.1016/j.dci.2013.06.005

Horn, L., Leips, J., and Starz-Gaiano, M. (2014). Phagocytic ability declines with age in adult *Drosophila* hemocytes. *Aging Cell* 13, 719–728. doi: 10.1111/acel.12227

Hughes, C. L., and Thomas, J. B. (2007). A sensory feedback circuit coordinates muscle activity in *Drosophila*. *Mol. Cell Neurosci.* 35, 383–396. doi: 10.1016/j.mcn.2007.04.001

Jackson, M. V., Morrison, T. J., Doherty, D. F., McAuley, D. F., Matthay, M. A., Kissenpfennig, A., et al. (2016). Mitochondrial transfer via tunneling nanotubes is an important mechanism by which mesenchymal stem cells enhance macrophage phagocytosis in the in vitro and in vivo models of ARDS:

mitochondrial transfer from MSC to macrophages. *Stem Cells* 34, 2210–2223. doi: 10.1002/stem.2372

Jiang, H., Patel, P. H., Kohlmaier, A., Grenley, M. O., McEwen, D. G., and Edgar, B. A. (2009). Cytokine/Jak/Stat signaling mediates regeneration and homeostasis in the *Drosophila* midgut. *Cell* 137, 1343–1355. doi: 10.1016/j.cell.2009.05.014

Jung, S.-H. (2005). The *Drosophila* lymph gland as a developmental model of hematopoiesis. *Development* 132, 2521–2533. doi: 10.1242/dev.01837

Karcavich, R., and Doe, C. Q. (2005). Drosophila neuroblast 7-3 cell lineage: a model system for studying programmed cell death, Notch/Numb signaling, and sequential specification of ganglion mother cell identity. *J. Comp. Neurol.* 481, 240–251. doi: 10.1002/cne.20371

Katsuyama, T., and Paro, R. (2013). Innate immune cells are dispensable for regenerative growth of imaginal discs. *Mech. Dev.* 130, 112–121. doi: 10.1016/j.mod.2012.11.005

Kelsey, E. M., Luo, X., Bruckner, K., and Jasper, H. (2012). Schnurri regulates hemocyte function to promote tissue recovery after DNA damage. *J. Cell Sci.* 125, 1393–1400. doi: 10.1242/jcs.095323

Kierdorf, K., Hersperger, F., Sharrock, J., Vincent, C. M., Ustaoglu, P., Dou, J., et al. (2020). Muscle function and homeostasis require cytokine inhibition of AKT activity in *Drosophila*. *eLife* 9:e51595. doi: 10.7554/eLife.51595

King, J. G., and Hillyer, J. F. (2012). Infection-induced interaction between the mosquito circulatory and immune systems. *PLoS Pathog.* 8:e1003058. doi: 10.1371/journal.ppat.1003058

Kocks, C., Cho, J. H., Nehme, N., Ulvila, J., Pearson, A. M., Meister, M., et al. (2005). Eater, a transmembrane protein mediating phagocytosis of bacterial pathogens in *Drosophila*. *Cell* 123, 335–346. doi: 10.1016/j.cell.2005.08.034

Koh, T. J., and DiPietro, L. A. (2011). Inflammation and wound healing: the role of the macrophage. *Expert Rev. Mol. Med.* 13, e23. doi: 10.1017/S1462399411001943

Krejèová, G., Danielová, A., Nedbalová, P., Kazek, M., Strych, L., Chawla, G., et al. (2019). Drosophila macrophages switch to aerobic glycolysis to mount effective antibacterial defense. *eLife* 8:e50414. doi: 10.7554/eLife.50414

Krzemien, J., Crozatier, M., and Vincent, A. (2010a). Ontogeny of the *Drosophila* larval hematopoietic organ, hemocyte homeostasis and the dedicated cellular immune response to parasitism. *Int. J. Dev. Biol.* 54, 1117–1125. doi: 10.1387/ijdb.093053jk

Krzemien, J., Oyallon, J., Crozatier, M., and Vincent, A. (2010b). Hematopoietic progenitors and hemocyte lineages in the Drosophila lymph gland. *Dev. Biol.* 346, 310–319. doi: 10.1016/j.ydbio.2010.08.003

Kurant, E. (2011). Keeping the CNS clear: glial phagocytic functions in *Drosophila*. *Glia* 59, 1304–1311. doi: 10.1002/glia.21098

Kurant, E., Axelrod, S., Leaman, D., and Gaul, U. (2008). Six-microns-under acts upstream of Draper in the glial phagocytosis of apoptotic neurons. *Cell* 133, 498–509. doi: 10.1016/j.cell.2008.02.052

Kurucz, É, Márkus, R., Zsámboki, J., Folkl-Medzihradszky, K., Darula, Z., Vilmos, P., et al. (2007). Nimrod, a putative phagocytosis receptor with EGF repeats in *Drosophila* plasmatocytes. *Curr. Biol.* 17, 649–654. doi: 10.1016/j.cub.2007.02.041

Kwon, Y., Song, W., Droujinine, I. A., Hu, Y., Asara, J. M., and Perrimon, N. (2015). Systemic organ wasting induced by localized expression of the secreted insulin/IGF antagonist ImpL2. *Dev. Cell* 33, 36–46. doi: 10.1016/j.devcel.2015.02.012

Landgraf, M., and Thor, S. (2006). Development of *Drosophila* motoneurons: specification and morphology. *Semin. Cell Dev. Biol.* 17, 3–11. doi: 10.1016/j.semcdb.2005.11.007

Lantz, C., Radmanesh, B., Liu, E., Thorp, E. B., and Lin, J. (2020). Single-cell RNA sequencing uncovers heterogenous transcriptional signatures in macrophages during efferocytosis. *Sci. Rep.* 10, 14333. doi: 10.1038/s41598-020-70353-y

Lavin, Y., Mortha, A., Rahman, A., and Merad, M. (2015). Regulation of macrophage development and function in peripheral tissues. *Nat. Rev. Immunol.* 15, 731–744. doi: 10.1038/nri3920

Lavin, Y., Winter, D., Blecher-Gonen, R., David, E., Keren-Shaul, H., Merad, M., et al. (2014). Tissue-resident macrophage enhancer landscapes are shaped by the local microenvironment. *Cell* 159, 1312–1326. doi: 10.1016/j.cell.2014.11.018

Lazzaro, B. P. (2008). Natural selection on the *Drosophila* antimicrobial immune system. *Curr. Opin. Microbiol.* 11, 284–289. doi: 10.1016/j.mib.2008.05.001

Lebestky, T., Chang, T., Hartenstein, V., and Banerjee, U. (2000). Specification of *Drosophila* hematopoietic lineage by conserved transcription factors. *Science* 288, 146–149. doi: 10.1126/science.288.5463.146

Lebestky, T., Jung, S.-H., and Banerjee, U. (2003). A Serrate-expressing signaling center controls *Drosophila* hematopoiesis. *Genes Dev.* 17, 348–353. doi: 10.1101/gad.1052803

LeBleu, V. S., Macdonald, B., and Kalluri, R. (2007). Structure and function of basement membranes. *Exp. Biol. Med. (Maywood)* 232, 1121–1129. doi: 10.3181/0703-MR-72

Leitão, A. B., and Sucena, É (2015). *Drosophila* sessile hemocyte clusters are true hematopoietic tissues that regulate larval blood cell differentiation. *eLife* 4:e06166. doi: 10.7554/eLife.06166

Lemaitre, B., and Hoffmann, J. (2007). The host defense of *Drosophila melanogaster*. *Annu. Rev. Immunol.* 25, 697–743. doi: 10.1146/annurev.immunol.25.022106.141615

Lemaitre, B., Kromer-Metzger, E., Michaut, L., Nicolas, E., Meister, M., Georgel, P., et al. (1995). A recessive mutation, immune deficiency (imd), defines two distinct control pathways in the *Drosophila* host defense. *Proc. Natl. Acad. Sci. U.S.A.* 92, 9465–9469. doi: 10.1073/pnas.92.21.9465

Lemaitre, B., and Miguel-Aliaga, I. (2013). The digestive tract of *Drosophila melanogaster*. *Annu. Rev. Genet.* 47, 377–404. doi: 10.1146/annurev-genet-111212-133343

Lemmon, M. A., and Schlessinger, J. (2010). Cell signaling by receptor tyrosine kinases. *Cell* 141, 1117–1134. doi: 10.1016/j.cell.2010.06.011

Letourneau, M., Lapraz, F., Sharma, A., Vanzo, N., Waltzer, L., and Crozatier, M. (2016). *Drosophila* hematopoiesis under normal conditions and in response to immune stress. *FEBS Lett.* 590, 4034–4051. doi: 10.1002/1873-3468.12327

Li, H., Shuster, S. A., Li, J., and Luo, L. (2018). Linking neuronal lineage and wiring specificity. *Neural Dev.* 13:5. doi: 10.1186/s13064-018-0102-0

Lin, J.-D., Nishi, H., Poles, J., Niu, X., Mccauley, C., Rahman, K., et al. (2019). Single-cell analysis of fate-mapped macrophages reveals heterogeneity, including stem-like properties, during atherosclerosis progression and regression. *JCI Insight* 4:e124574. doi: 10.1172/jci.insight.124574

Lundell, M. J. (2003). The regulation of apoptosis by Numb/Notch signaling in the serotonin lineage of *Drosophila*. *Development* 130, 4109–4121. doi: 10.1242/dev.00593

MacDonald, J. M., Beach, M. G., Porpiglia, E., Sheehan, A. E., Watts, R. J., and Freeman, M. R. (2006). The *Drosophila* cell corpse engulfment receptor Draper mediates glial clearance of severed axons. *Neuron* 50, 869–881. doi: 10.1016/j.neuron.2006.04.028

Mackenzie, D. K., Bussière, L. F., and Tinsley, M. C. (2011). Senescence of the cellular immune response in *Drosophila melanogaster*. *Exp. Gerontol.* 46, 853–859. doi: 10.1016/j.exger.2011.07.004

MacParland, S. A., Liu, J. C., Ma, X.-Z., Innes, B. T., Bartczak, A. M., Gage, B. K., et al. (2018). Single cell RNA sequencing of human liver reveals distinct intrahepatic macrophage populations. *Nat. Commun.* 9:4383. doi: 10.1038/s41467-018-06318-7

Maddrell, S. H. P. (1972). The mechanisms of insect excretory systems. *Adv. Insect Physiol.* 8, 199–331. doi: 10.1016/S0065-2806(08)60198-8

Makhijani, K., Alexander, B., Rao, D., Petraki, S., Herboso, L., Kukar, K., et al. (2017). Regulation of *Drosophila* hematopoietic sites by Activin-β from active sensory neurons. *Nat. Commun.* 8, 15990. doi: 10.1038/ncomms15990

Makhijani, K., Alexander, B., Tanaka, T., Rulifson, E., and Brückner, K. (2011). The peripheral nervous system supports blood cell homing and survival in the *Drosophila* larva. *Development* 138, 5379–5391. doi: 10.1242/dev.067322

Makhijani, K., and Brückner, K. (2012). Of blood cells and the nervous system: hematopoiesis in the *Drosophila* larva. *Fly (Austin)* 6, 254–260. doi: 10.4161/fly.22267

Manaka, J., Kuraishi, T., Shiratsuchi, A., Nakai, Y., Higashida, H., Henson, P., et al. (2004). Draper-mediated and Phosphatidylserine-independent phagocytosis of apoptotic cells by *Drosophila* hemocytes/macrophages. *J. Biol. Chem.* 279, 48466–48476. doi: 10.1074/jbc.M408597200

Mandal, L., Martinez-Agosto, J. A., Evans, C. J., Hartenstein, V., and Banerjee, U. (2007). A Hedgehog- and Antennapedia-dependent niche maintains *Drosophila* haematopoietic precursors. *Nature* 446, 320–324. doi: 10.1038/nature05585

Manning, G., and Krasnow, M. A. (1993). "Development of the *Drosophila* tracheal system," in *The Development of Drosophila melanogaster*, eds M. Bate and A. M. Arias (Cold Spring Harbor, NY: Cold Spring Harbor Laboratory Press).

Márkus, R., Kurucz, E., Rus, F., and Andó, I. (2005). Sterile wounding is a minimal and sufficient trigger for a cellular immune response in *Drosophila melanogaster*. *Immunol. Lett.* 101, 108–111. doi: 10.1016/j.imlet.2005.03.021

Markus, R., Laurinyecz, B., Kurucz, E., Honti, V., Bajusz, I., Sipos, B., et al. (2009). Sessile hemocytes as a hematopoietic compartment in *Drosophila melanogaster*. *Proc. Natl. Acad. Sci. U.S.A.* 106, 4805–4809. doi: 10.1073/pnas.0801766106

Martinek, N., Shahab, J., Saathoff, M., and Ringuette, M. (2011). Haemocyte-derived SPARC is required for collagen-IV-dependent stability of basal laminae in *Drosophila* embryos. *J. Cell Sci.* 124:670. doi: 10.1242/jcs.086819

Martinez, F. O. (2008). Macrophage activation and polarization. *Front. Biosci.* 13:453. doi: 10.2741/2692

Martinez, F. O., Gordon, S., Locati, M., and Mantovani, A. (2006). Transcriptional profiling of the human monocyte-to-macrophage differentiation and polarization: new molecules and patterns of gene expression. *J. Immunol.* 177, 7303–7311. doi: 10.4049/jimmunol.177.10.7303

Matsubayashi, Y., Louani, A., Dragu, A., Sánchez-Sánchez, B. J., Serna-Morales, E., Yolland, L., et al. (2017). A moving source of matrix components is essential for de novo basement membrane formation. *Curr. Biol.* 27, 3526–3534.e4. doi: 10.1016/j.cub.2017.10.001

McClure, K. D., Sustar, A., and Schubiger, G. (2008). Three genes control the timing, the site and the size of blastema formation in *Drosophila*. *Dev. Biol.* 319, 68–77. doi: 10.1016/j.ydbio.2008.04.004

Melcarne, C., Ramond, E., Dudzic, J., Bretscher, A. J., Kurucz, É, Andó, I., et al. (2019). Two Nimrod receptors, NimC1 and Eater, synergistically contribute to bacterial phagocytosis in *Drosophila melanogaster*. *FEBS J.* 286, 2670–2691. doi: 10.1111/febs.14857

Merad, M., Manz, M. G., Karsunky, H., Wagers, A., Peters, W., Charo, I., et al. (2002). Langerhans cells renew in the skin throughout life under steady-state conditions. *Nat. Immunol.* 3, 1135–1141. doi: 10.1038/ni852

Micchelli, C. A., and Perrimon, N. (2006). Evidence that stem cells reside in the adult *Drosophila* midgut epithelium. *Nature* 439, 475–479. doi: 10.1038/nature04371

Miguel-Aliaga, I. (2004). Segment-specific prevention of pioneer neuron apoptosis by cell-autonomous, postmitotic Hox gene activity. *Development* 131, 6093–6105. doi: 10.1242/dev.01521

Miller, J. M., Oligino, T., Pazdera, M., López, A. J., and Hoshizaki, D. K. (2002). Identification of fat-cell enhancer regions in *Drosophila melanogaster*. *Insect Mol. Biol.* 11, 67–77. doi: 10.1046/j.0962-1075.2001.00310.x

Milton, C. C., Grusche, F. A., Degoutin, J. L., Yu, E., Dai, Q., Lai, E. C., et al. (2014). The Hippo pathway regulates hematopoiesis in *Drosophila melanogaster*. *Curr. Biol.* 24, 2673–2680. doi: 10.1016/j.cub.2014.10.031

Minakhina, S., Druzhinina, M., and Steward, R. (2007). Zfrp8, the *Drosophila* ortholog of PDCD2, functions in lymph gland development and controls cell proliferation. *Development* 134, 2387–2396. doi: 10.1242/dev.003616

Minakhina, S., Tan, W., and Steward, R. (2011). JAK/STAT and the GATA factor Pannier control hemocyte maturation and differentiation in *Drosophila*. *Dev. Biol.* 352, 308–316. doi: 10.1016/j.ydbio.2011.01.035

Morrison, S. J., and Scadden, D. T. (2014). The bone marrow niche for haematopoietic stem cells. *Nature* 505, 327–334. doi: 10.1038/nature12984

Mosser, D. M., and Edwards, J. P. (2008). Exploring the full spectrum of macrophage activation. *Nat. Rev. Immunol.* 8, 958–969. doi: 10.1038/nri2448

Mould, K. J., Jackson, N. D., Henson, P. M., Seibold, M., and Janssen, W. J. (2019). Single cell RNA sequencing identifies unique inflammatory airspace macrophage subsets. *JCI Insight* 4:e126556. doi: 10.1172/jci.insight.126556

Munier, A., Doucet, D., Perrodou, E., Zachary, D., Meister, M., Hoffmann, J. A., et al. (2002). PVF2, a PDGF/VEGF-like growth factor, induces hemocyte proliferation in *Drosophila* larvae. *EMBO Rep.* 3, 1195–1200. doi: 10.1093/embo-reports/kvf242

Munro, D. A. D., and Hughes, J. (2017). The origins and functions of tissue-resident macrophages in kidney development. *Front. Physiol.* 8:837. doi: 10.3389/fphys.2017.00837

Murakami, R., Takashima, S., and Hamaguchi, T. (1999). Developmental genetics of the *Drosophila* gut: specification of primordia, subdivision and overt-differentiation. *Cell Mol. Biol.* 45, 661–676.

Myrick, K. V., and Dearolf, C. R. (2000). Hyperactivation of the *Drosophila* Hop Jak kinase causes the preferential overexpression of eIF1A transcripts in larval blood cells. *Gene* 244, 119–125. doi: 10.1016/S0378-1119(99)00568-5

Nehme, N. T., Liégeois, S., Kele, B., Giammarinaro, P., Pradel, E., Hoffmann, J. A., et al. (2007). A model of bacterial intestinal infections in *Drosophila melanogaster*. *PLoS Pathog.* 3:e173. doi: 10.1371/journal.ppat.0030173

Nelliot, A., Bond, N., and Hoshizaki, D. K. (2006). Fat-body remodeling in *Drosophila melanogaster*. *Genesis* 44, 396–400. doi: 10.1002/dvg.20229

Nelson, R. E., Fessler, L. I., Takagi, Y., Blumberg, B., Keene, D. R., Olson, P. F., et al. (1994). Peroxidasin: a novel enzyme-matrix protein of *Drosophila* development. *EMBO J.* 13, 3438–3447.

Neves, J., Zhu, J., Sousa-Victor, P., Konjikusic, M., Riley, R., Chew, S., et al. (2016). Immune modulation by MANF promotes tissue repair and regenerative success in the retina. *Science* 353:aaf3646. doi: 10.1126/science.aaf3646

Nicolás-Ávila, J. A., Lechuga-Vieco, A. V., Esteban-Martínez, L., Sánchez-Díaz, M., Díaz-García, E., Santiago, D. J., et al. (2020). A network of macrophages supports mitochondrial homeostasis in the heart. *Cell* 183, 94–109.e23. doi: 10.1016/j.cell.2020.08.031

Nonaka, S., Ando, Y., Kanetani, T., Hoshi, C., Nakai, Y., Nainu, F., et al. (2017). Signaling pathway for phagocyte priming upon encounter with apoptotic cells. *J. Biol. Chem.* 292, 8059–8072. doi: 10.1074/jbc.M116.769745

Ocorr, K., Perrin, L., Lim, H.-Y., Qian, L., Wu, X., and Bodmer, R. (2007). Genetic control of heart function and aging in *Drosophila*. *Trends Cardiovasc. Med.* 17, 177–182. doi: 10.1016/j.tcm.2007.04.001

Ohlstein, B., and Spradling, A. (2006). The adult *Drosophila* posterior midgut is maintained by pluripotent stem cells. *Nature* 439, 470–474. doi: 10.1038/nature04333

Okabe, Y., and Medzhitov, R. (2016). Tissue biology perspective on macrophages. *Nat. Immunol.* 17, 9–17. doi: 10.1038/ni.3320

Olofsson, B., and Page, D. T. (2005). Condensation of the central nervous system in embryonic *Drosophila* is inhibited by blocking hemocyte migration or neural activity. *Dev. Biol.* 279, 233–243. doi: 10.1016/j.ydbio.2004.12.020

Ouyang, D., Xiao, X., Mase, A., Li, G., Corcoran, S., Wang, F., et al. (2020). Dscam1 promotes blood cell survival in Drosophila melanogaster through a dual role in blood cells and neurons. *bioRxiv* [Preprint] doi: 10.1101/2020.09.26.314997

Owusu-Ansah, E., and Banerjee, U. (2009). Reactive oxygen species prime *Drosophila* haematopoietic progenitors for differentiation. *Nature* 461, 537–541. doi: 10.1038/nature08313

Pandey, R., Blanco, J., and Udolph, G. (2011). The glucuronyltransferase GlcAT-P is required for stretch growth of peripheral nerves in *Drosophila*. *PLoS One* 6:e28106. doi: 10.1371/journal.pone.0028106

Parkin, C. A., and Burnet, B. (1986). Growth arrest of *Drosophila melanogaster* on erg-2 and erg-6 sterol mutant strains of *Saccharomyces cerevisiae*. *J. Insect Physiol.* 32, 463–471. doi: 10.1016/0022-1910(86)90007-7

Parsons, B., and Foley, E. (2013). The *Drosophila* platelet-derived growth factor and vascular endothelial growth factor-receptor related (Pvr) protein ligands Pvf2 and Pvf3 control hemocyte viability and invasive migration. *J. Biol. Chem.* 288, 20173–20183. doi: 10.1074/jbc.M113.483818

Parupalli, P., Tomar, A., Madhwal, S., and Mukherjee, T. (2020). Immune control of animal growth in homeostasis and nutritional stress in *Drosophila*. *Front. Immunol.* 11:1528. doi: 10.3389/fimmu.2020.01528

Pastor-Pareja, J. C., Wu, M., and Xu, T. (2008). An innate immune response of blood cells to tumors and tissue damage in *Drosophila*. *Dis. Models Mech.* 1, 144–154. doi: 10.1242/dmm.000950

Paul, F., Arkin, Y., Giladi, A., Jaitin, D. A., Kenigsberg, E., Keren-Shaul, H., et al. (2015). Transcriptional heterogeneity and lineage commitment in myeloid progenitors. *Cell* 163, 1663–1677. doi: 10.1016/j.cell.2015.11.013

Pennetier, D., Oyallon, J., Morin-Poulard, I., Dejean, S., Vincent, A., and Crozatier, M. (2012). Size control of the *Drosophila* hematopoietic niche by bone morphogenetic protein signaling reveals parallels with mammals. *Proc. Natl. Acad. Sci. U.S.A.* 109, 3389–3394. doi: 10.1073/pnas.1109407109

Perdiguero, E. G., and Geissmann, F. (2016). The development and maintenance of resident macrophages. *Nat. Immunol.* 17, 2–8. doi: 10.1038/ni.3341

Peterson, C., Carney, G. E., Taylor, B. J., and White, K. (2002). reaper is required for neuroblast apoptosis during *Drosophila* development. *Development* 129, 1467–1476.

Petraki, S., Alexander, B., and Brückner, K. (2015). Assaying blood cell populations of the *Drosophila melanogaster* larva. *J. Vis. Exp.* 105, 52733. doi: 10.3791/52733

Pull, S. L., Doherty, J. M., Mills, J. C., Gordon, J. I., and Stappenbeck, T. S. (2005). Activated macrophages are an adaptive element of the colonic epithelial

progenitor niche necessary for regenerative responses to injury. *Proc. Natl. Acad. Sci. U.S.A.* 102, 99–104. doi: 10.1073/pnas.0405979102

Qiu, P., Pan, P. C., and Govind, S. (1998). A role for the *Drosophila* Toll/Cactus pathway in larval hematopoiesis. *Development* 125, 1909–1920.

Ramond, E., Dudzic, J. P., and Lemaitre, B. (2020a). Comparative RNA-Seq analyses of *Drosophila* plasmatocytes reveal gene specific signatures in response to clean injury and septic injury. *PLoS One* 15:e0235294. doi: 10.1371/journal.pone.0235294

Ramond, E., Petrignani, B., Dudzic, J. P., Boquete, J., Poidevin, M., Kondo, S., et al. (2020b). The adipokine NimrodB5 regulates peripheral hematopoiesis in *Drosophila*. *FEBS J.* 287, 3399–3426. doi: 10.1111/febs.15237

Raoof, R., van der Vlist, M., Willemen, H. L. D. M., Prado, J., Versteeg, S., Vos, M., et al. (2020). Macrophages transfer mitochondria to sensory neurons to resolve inflammatory pain. *bioRxiv* [Preprint] doi: 10.1101/2020.02.12.940445

Ratheesh, A., Belyaeva, V., and Siekhaus, D. E. (2015). *Drosophila* immune cell migration and adhesion during embryonic development and larval immune responses. *Curr. Opin. Cell Biol.* 36, 71–79. doi: 10.1016/j.ceb.2015.07.003

Regan, J. C., Brandão, A. S., Leitão, A. B., Mantas Dias, A. R., Sucena, E., Jacinto, A., et al. (2013). Steroid hormone signaling is essential to regulate innate immune cells and fight bacterial infection in *Drosophila*. *PLoS Pathog.* 9:e1003720. doi: 10.1371/journal.ppat.1003720

Roddie, H. G., Armitage, E. L., Coates, J. A., Johnston, S. A., and Evans, I. R. (2019). Simu-dependent clearance of dying cells regulates macrophage function and inflammation resolution. *PLoS Biol.* 17:e2006741. doi: 10.1371/journal.pbio.2006741

Rogulja-Ortmann, A., Luer, K., Seibert, J., Rickert, C., and Technau, G. M. (2007). Programmed cell death in the embryonic central nervous system of *Drosophila melanogaster*. *Development* 134, 105–116. doi: 10.1242/dev.02707

Ryoo, H. D., Gorenc, T., and Steller, H. (2004). Apoptotic cells can induce compensatory cell proliferation through the JNK and the Wingless signaling pathways. *Dev. Cell* 7, 491–501. doi: 10.1016/j.devcel.2004.08.019

Sampson, C. J., Amin, U., and Couso, J.-P. (2013). Activation of *Drosophila* hemocyte motility by the ecdysone hormone. *Biol. Open* 2, 1412–1420. doi: 10.1242/bio.20136619

Sanchez Bosch, P., Makhijani, K., Herboso, L., Gold, K. S., Baginsky, R., Woodcock, K. J., et al. (2019). Adult *Drosophila* lack hematopoiesis but rely on a blood cell reservoir at the respiratory epithelia to relay infection signals to surrounding tissues. *Dev. Cell* 51, 787–803.e5. doi: 10.1016/j.devcel.2019.10.017

Sánchez-Sánchez, B. J., Urbano, J. M., Comber, K., Dragu, A., Wood, W., Stramer, B., et al. (2017). *Drosophila* embryonic hemocytes produce laminins to strengthen migratory response. *Cell Rep.* 21, 1461–1470. doi: 10.1016/j.celrep.2017.10.047

Sánchez-Soriano, N., Tear, G., Whitington, P., and Prokop, A. (2007). *Drosophila* as a genetic and cellular model for studies on axonal growth. *Neural Dev.* 2, 9. doi: 10.1186/1749-8104-2-9

Santabárbara-Ruiz, P., López-Santillán, M., Martínez-Rodríguez, I., Binagui-Casas, A., Pérez, L., Milán, M., et al. (2015). ROS-induced JNK and p38 signaling is required for unpaired cytokine activation during *Drosophila* regeneration. *PLoS Genet.* 11:e1005595. doi: 10.1371/journal.pgen.1005595

Schirmeier, S., Matzat, T., and Klämbt, C. (2016). Axon ensheathment and metabolic supply by glial cells in *Drosophila*. *Brain Res.* 1641, 122–129. doi: 10.1016/j.brainres.2015.09.003

Schmid, M. R., Anderl, I., Vesala, L., Vanha-aho, L.-M., Deng, X.-J., Rämet, M., et al. (2014). Control of *Drosophila* blood cell activation via Toll signaling in the fat body. *PLoS One* 9:e102568. doi: 10.1371/journal.pone.0102568

Schulz, C., Gomez Perdiguero, E., Chorro, L., Szabo-Rogers, H., Cagnard, N., Kierdorf, K., et al. (2012). A lineage of myeloid cells independent of Myb and hematopoietic stem cells. *Science* 336, 86–90. doi: 10.1126/science.1219179

Sears, H. C. (2003). Macrophage-mediated corpse engulfment is required for normal *Drosophila* CNS morphogenesis. *Development* 130, 3557–3565. doi: 10.1242/dev.00586

Sessions, A. O., Kaushik, G., Parker, S., Raedschelders, K., Bodmer, R., Van Eyk, J. E., et al. (2017). Extracellular matrix downregulation in the *Drosophila* heart preserves contractile function and improves lifespan. *Matrix Biol.* 62, 15–27. doi: 10.1016/j.matbio.2016.10.008

Shahab, J., Baratta, C., Scuric, B., Godt, D., Venken, K. J. T., and Ringuette, M. J. (2015). Loss of SPARC dysregulates basal lamina assembly to disrupt larval fat body homeostasis in *Drosophila melanogaster*. *Dev. Dyn.* 244, 540–552. doi: 10.1002/dvdy.24243

Shapouri-Moghaddam, A., Mohammadian, S., Vazini, H., Taghadosi, M., Esmaeili, S.-A., Mardani, F., et al. (2018). Macrophage plasticity, polarization, and function in health and disease. *J. Cell Physiol.* 233, 6425–6440. doi: 10.1002/jcp.26429

Shia, A. K. H., Glittenberg, M., Thompson, G., Weber, A. N., Reichhart, J.-M., and Ligoxygakis, P. (2009). Toll-dependent antimicrobial responses in *Drosophila* larval fat body require Spätzle secreted by haemocytes. *J. Cell Sci.* 122, 4505–4515. doi: 10.1242/jcs.049155

Shim, J., Mukherjee, T., and Banerjee, U. (2012). Direct sensing of systemic and nutritional signals by haematopoietic progenitors in *Drosophila*. *Nat. Cell Biol.* 14, 394–400. doi: 10.1038/ncb2453

Shim, J., Mukherjee, T., Mondal, B. C., Liu, T., Young, G. C., Wijewarnasuriya, D. P., et al. (2013). Olfactory control of blood progenitor maintenance. *Cell* 155, 1141–1153. doi: 10.1016/j.cell.2013.10.032

Shin, M., Cha, N., Koranteng, F., Cho, B., and Shim, J. (2020). Subpopulation of macrophage-like plasmatocytes attenuates systemic growth via JAK/STAT in the *Drosophila* fat body. *Front. Immunol.* 11:63. doi: 10.3389/fimmu.2020.00063

Shklyar, B., Sellman, Y., Shklover, J., Mishnaevski, K., Levy-Adam, F., and Kurant, E. (2014). Developmental regulation of glial cell phagocytic function during *Drosophila* embryogenesis. *Dev. Biol.* 393, 255–269. doi: 10.1016/j.ydbio.2014.07.005

Shlyakhover, E., Shklyar, B., Hakim-Mishnaevski, K., Levy-Adam, F., and Kurant, E. (2018). Drosophila GATA factor serpent establishes phagocytic ability of embryonic macrophages. *Front. Immunol.* 9:266. doi: 10.3389/fimmu.2018.00266

Siekhaus, D., Haesemeyer, M., Moffitt, O., and Lehmann, R. (2010). RhoL controls invasion and Rap1 localization during immune cell transmigration in *Drosophila*. *Nat. Cell Biol.* 12, 605–610. doi: 10.1038/ncb2063

Sieweke, M. H., and Allen, J. E. (2013). Beyond stem cells: self-renewal of differentiated macrophages. *Science* 342:1242974. doi: 10.1126/science.1242974

Sinenko, S. A., Mandal, L., Martinez-Agosto, J. A., and Banerjee, U. (2009). Dual role of wingless signaling in stem-like hematopoietic precursor maintenance in *Drosophila*. *Dev. Cell* 16, 756–763. doi: 10.1016/j.devcel.2009.03.003

Singhania, A., and Grueber, W. B. (2014). Development of the embryonic and larval peripheral nervous system of *Drosophila*. *Wiley Interdiscip. Rev. Dev. Biol.* 3, 193–210. doi: 10.1002/wdev.135

Song, W., Onishi, M., Jan, L. Y., and Jan, Y. N. (2007). Peripheral multidendritic sensory neurons are necessary for rhythmic locomotion behavior in *Drosophila* larvae. *Proc. Natl. Acad. Sci. U.S.A.* 104, 5199–5204. doi: 10.1073/pnas.0700895104

Sonnenfeld, M. J., and Jacobs, J. R. (1995). Macrophages and glia participate in the removal of apoptotic neurons from theDrosophila embryonic nervous system. *J. Comp. Neurol.* 359, 644–652. doi: 10.1002/cne.903590410

Sopko, R., Lin, Y. B., Makhijani, K., Alexander, B., Perrimon, N., and Brückner, K. (2015). A systems-level interrogation identifies regulators of *Drosophila* blood cell number and survival. *PLoS Genet.* 11:e1005056. doi: 10.1371/journal.pgen.1005056

Sorrentino, R. P., Carton, Y., and Govind, S. (2002). Cellular immune response to parasite infection in the Drosophila lymph gland is developmentally regulated. *Dev. Biol.* 243, 65–80. doi: 10.1006/dbio.2001.0542

Stanley, E. R., and Chitu, V. (2014). CSF-1 receptor signaling in myeloid cells. *Cold Spring Harb. Perspect. Biol.* 6:a021857. doi: 10.1101/cshperspect.a021857

Stofanko, M., Kwon, S. Y., and Badenhorst, P. (2008). A misexpression screen to identify regulators of drosophila larval hemocyte development. *Genetics* 180, 253–267. doi: 10.1534/genetics.108.089094

Stramer, B., Wood, W., Galko, M. J., Redd, M. J., Jacinto, A., Parkhurst, S. M., et al. (2005). Live imaging of wound inflammation in *Drosophila* embryos reveals key roles for small GTPases during in vivo cell migration. *J. Cell Biol.* 168, 567–573. doi: 10.1083/jcb.200405120

Sugie, A., Marchetti, G., and Tavosanis, G. (2018). Structural aspects of plasticity in the nervous system of *Drosophila*. *Neural Dev.* 13:14. doi: 10.1186/s13064-018-0111-z

Takeishi, A., Kuranaga, E., Tonoki, A., Misaki, K., Yonemura, S., Kanuka, H., et al. (2013). Homeostatic epithelial renewal in the gut is required for dampening a

fatal systemic wound response in *Drosophila*. *Cell Rep.* 3, 919–930. doi: 10.1016/j.celrep.2013.02.022

Tarique, A. A., Logan, J., Thomas, E., Holt, P. G., Sly, P. D., and Fantino, E. (2015). Phenotypic, functional, and plasticity features of classical and alternatively activated human macrophages. *Am. J. Respir. Cell Mol. Biol.* 53, 676–688. doi: 10.1165/rcmb.2015-0012OC

Tattikota, S. G., Cho, B., Liu, Y., Hu, Y., Barrera, V., Steinbaugh, M. J., et al. (2020). A single-cell survey of *Drosophila* blood. *eLife* 9:e54818. doi: 10.7554/eLife.54818

Tepass, U., Fessler, L. I., Aziz, A., and Hartenstein, V. (1994). Embryonic origin of hemocytes and their relationship to cell death in *Drosophila*. *Development* 120, 1829–1837.

Tracey, W. D., Wilson, R. I., Laurent, G., and Benzer, S. (2003). painless, a *Drosophila* gene essential for nociception. *Cell* 113, 261–273. doi: 10.1016/S0092-8674(03)00272-1

Trébuchet, G., Cattenoz, P. B., Zsámboki, J., Mazaud, D., Siekhaus, D. E., Fanto, M., et al. (2019). The repo homeodomain transcription factor suppresses hematopoiesis in *Drosophila* and preserves the glial fate. *J. Neurosci.* 39, 238–255. doi: 10.1523/JNEUROSCI.1059-18.2018

Tzou, P., Ohresser, S., Ferrandon, D., Capovilla, M., Reichhart, J. M., Lemaitre, B., et al. (2000). Tissue-specific inducible expression of antimicrobial peptide genes in *Drosophila* surface epithelia. *Immunity* 13, 737–748. doi: 10.1016/s1074-7613(00)00072-8

Van De Bor, V., Zimniak, G., Papone, L., Cerezo, D., Malbouyres, M., Juan, T., et al. (2015). Companion blood cells control ovarian stem cell niche microenvironment and homeostasis. *Cell Rep.* 13, 546–560. doi: 10.1016/j.celrep.2015.09.008

van Furth, R., Cohn, Z. A., Hirsch, J. G., Humphrey, J. H., Spector, W. G., and Langevoort, H. L. (1972). The mononuclear phagocyte system: a new classification of macrophages, monocytes, and their precursor cells. *Bull. World Health Organ.* 46, 845–852.

Van Hove, H., Martens, L., Scheyltjens, I., De Vlaminck, K., Pombo Antunes, A. R., De Prijck, S., et al. (2019). A single-cell atlas of mouse brain macrophages reveals unique transcriptional identities shaped by ontogeny and tissue environment. *Nat. Neurosci.* 22, 1021–1035. doi: 10.1038/s41593-019-0393-4

Vanha-aho, L.-M., Anderl, I., Vesala, L., Hultmark, D., Valanne, S., and Rämet, M. (2015). Edin expression in the fat body is required in the defense against parasitic wasps in *Drosophila melanogaster*. *PLoS Pathog.* 11:e1004895. doi: 10.1371/journal.ppat.1004895

Varga, V. B., Szikszai, F., Szinyákovics, J., Manzéger, A., Puska, G., Kovács, T., et al. (2020). Role of hemocytes in the regeneration of germline stem cells in *Drosophila*. *bioRxiv* [Preprint] doi: 10.1101/2020.08.31.275255

Wang, L., Kounatidis, I., and Ligoxygakis, P. (2014). Drosophila as a model to study the role of blood cells in inflammation, innate immunity and cancer. *Front. Cell. Infect. Microbiol.* 3:113. doi: 10.3389/fcimb.2013.00113

Wang, X., Harris, R. E., Bayston, L. J., and Ashe, H. L. (2008). Type IV collagens regulate BMP signalling in *Drosophila*. *Nature* 455, 72–77.

Watts, R. J., Schuldiner, O., Perrino, J., Larsen, C., and Luo, L. (2004). Glia engulf degenerating axons during developmental axon pruning. *Curr. Biol.* 14, 678–684. doi: 10.1016/j.cub.2004.03.035

Weavers, H., Evans, I. R., Martin, P., and Wood, W. (2016). Corpse engulfment generates a molecular memory that primes the macrophage inflammatory response. *Cell* 165, 1658–1671. doi: 10.1016/j.cell.2016.04.049

Weinstock, A., Brown, E. J., Garabedian, M. L., Pena, S., Sharma, M., Lafaille, J., et al. (2019). Single-cell RNA sequencing of visceral adipose tissue leukocytes reveals that caloric restriction following obesity promotes the accumulation of a distinct macrophage population with features of phagocytic cells. *Immunometabolism* 1:e190008. doi: 10.20900/immunometab20190008

Welman, A., Serrels, A., Brunton, V. G., Ditzel, M., and Frame, M. C. (2010). Two-color photoactivatable probe for selective tracking of proteins and cells. *J. Biol. Chem.* 285, 11607–11616. doi: 10.1074/jbc.M110.102392

White, K., Grether, M. E., Abrams, J. M., Young, L., Farrell, K., and Steller, H. (1994). Genetic control of programmed cell death in *Drosophila*. *Science* 264, 677–683. doi: 10.1126/science.8171319

Whitten, J. M. (1957). The post-embryonic development of the tracheal system in *Drosophila melanogaster*. *J. Cell Sci.* 98, 123.

Williams, D. W. (2005). Cellular mechanisms of dendrite pruning in *Drosophila*: insights from in vivo time-lapse of remodeling dendritic arborizing sensory neurons. *Development* 132, 3631–3642. doi: 10.1242/dev.01928

Williams, M. J. (2006). Rac1 signalling in the *Drosophila* larval cellular immune response. *J. Cell Sci.* 119, 2015–2024. doi: 10.1242/jcs.02920

Wood, W., Faria, C., and Jacinto, A. (2006). Distinct mechanisms regulate hemocyte chemotaxis during development and wound healing in *Drosophila melanogaster*. *J. Cell Biol.* 173, 405–416. doi: 10.1083/jcb.200508161

Wood, W., and Jacinto, A. (2007). *Drosophila melanogaster* embryonic haemocytes: masters of multitasking. *Nat. Rev. Mol. Cell Biol.* 8, 542–551. doi: 10.1038/nrm2202

Woodcock, K. J., Kierdorf, K., Pouchelon, C. A., Vivancos, V., Dionne, M. S., and Geissmann, F. (2015). Macrophage-derived upd3 cytokine causes impaired glucose homeostasis and reduced lifespan in *Drosophila* fed a lipid-rich diet. *Immunity* 42, 133–144. doi: 10.1016/j.immuni.2014.12.023

Worley, M. I., Setiawan, L., and Hariharan, I. K. (2012). Regeneration and transdetermination in *Drosophila* imaginal discs. *Annu. Rev. Genet.* 46, 289–310. doi: 10.1146/annurev-genet-110711-155637

Wu, R., Van der Hoek, K. H., Ryan, N. K., Norman, R. J., and Robker, R. L. (2004). Macrophage contributions to ovarian function. *Hum. Reprod. Update* 10, 119–133. doi: 10.1093/humupd/dmh011

Xiang, Y., Yuan, Q., Vogt, N., Looger, L. L., Jan, L. Y., and Jan, Y. N. (2010). Light-avoidance-mediating photoreceptors tile the *Drosophila* larval body wall. *Nature* 468, 921–926. doi: 10.1038/nature09576

Xue, J., Schmidt, S. V., Sander, J., Draffehn, A., Krebs, W., Quester, I., et al. (2014). Transcriptome-based network analysis reveals a spectrum model of human macrophage activation. *Immunity* 40, 274–288. doi: 10.1016/j.immuni.2014.01.006

Yang, H., and Hultmark, D. (2017). Drosophila muscles regulate the immune response against wasp infection via carbohydrate metabolism. *Sci. Rep.* 7:15713. doi: 10.1038/s41598-017-15940-2

Yang, H., Kronhamn, J., Ekström, J.-O., Korkut, G. G., and Hultmark, D. (2015). JAK/STAT signaling in *Drosophila* muscles controls the cellular immune response against parasitoid infection. *EMBO Rep.* 16, 1664–1672. doi: 10.15252/embr.201540277

Yurchenco, P. D. (2011). Basement membranes: cell scaffoldings and signaling platforms. *Cold Spring Harb. Perspect. Biol.* 3:a004911. doi: 10.1101/cshperspect.a004911

Zaidman-Rémy, A., Regan, J. C., Brandão, A. S., and Jacinto, A. (2012). The *Drosophila* larva as a tool to study gut-associated macrophages: PI3K regulates a discrete hemocyte population at the proventriculus. *Dev. Comp. Immunol.* 36, 638–647. doi: 10.1016/j.dci.2011.10.013

Zhang, Y., and Xi, Y. (2015). Fat body development and its function in energy storage and nutrient sensing in *Drosophila melanogaster*. *J. Tissue Sci. Eng.* 6:1. doi: 10.4172/2157-7552.1000141

Zheng, Q., Ma, A., Yuan, L., Gao, N., Feng, Q., Franc, N. C., et al. (2017). Apoptotic cell clearance in *Drosophila melanogaster*. *Front. Immunol.* 8:1881. doi: 10.3389/fimmu.2017.01881

Zhou, J., Florescu, S., Boettcher, A.-L., Luo, L., Dutta, D., Kerr, G., et al. (2015). Dpp/Gbb signaling is required for normal intestinal regeneration during infection. *Dev. Biol.* 399, 189–203. doi: 10.1016/j.ydbio.2014.12.017

Zhou, L., Hashimi, H., Schwartz, L. M., and Nambu, J. R. (1995). Programmed cell death in the *Drosophila* central nervous system midline. *Curr. Biol.* 5, 784–790. doi: 10.1016/S0960-9822(95)00155-2

Zhu, L., Zhao, Q., Yang, T., Ding, W., and Zhao, Y. (2015). Cellular metabolism and macrophage functional polarization. *Int. Rev. Immunol.* 34, 82–100. doi: 10.3109/08830185.2014.969421

Zimmerman, K. A., Bentley, M. R., Lever, J. M., Li, Z., Crossman, D. K., Song, C. J., et al. (2019). Single-cell RNA sequencing identifies candidate renal resident macrophage gene expression signatures across species. *J. Am. Soc. Nephrol.* 30, 767–781. doi: 10.1681/ASN.2018090931

Conflict of Interest: The authors declare that the research was conducted in the absence of any commercial or financial relationships that could be construed as a potential conflict of interest.

frontiers in Cell and Developmental Biology

REVIEW
published: 26 March 2021
doi: 10.3389/fcell.2021.628991

From Flies to Men: ROS and the NADPH Oxidase in Phagocytes

Zohreh Mansoori Moghadam[1,2], *Philipp Henneke*[1,3] *and Julia Kolter*[1]*

[1] *Institute for Immunodeficiency, Center for Chronic Immunodeficiency (CCI), Medical Center – University of Freiburg, Faculty of Medicine, University of Freiburg, Freiburg, Germany,* [2] *Faculty of Biology, University of Freiburg, Freiburg, Germany,* [3] *Center for Pediatrics and Adolescent Medicine, Medical Center – University of Freiburg, Freiburg, Germany*

The cellular formation of reactive oxygen species (ROS) represents an evolutionary ancient antimicrobial defense system against microorganisms. The NADPH oxidases (NOX), which are predominantly localized to endosomes, and the electron transport chain in mitochondria are the major sources of ROS. Like any powerful immunological process, ROS formation has costs, in particular collateral tissue damage of the host. Moreover, microorganisms have developed defense mechanisms against ROS, an example for an arms race between species. Thus, although NOX orthologs have been identified in organisms as diverse as plants, fruit flies, rodents, and humans, ROS functions have developed and diversified to affect a multitude of cellular properties, i.e., far beyond direct antimicrobial activity. Here, we focus on the development of NOX in phagocytic cells, where the so-called respiratory burst in phagolysosomes contributes to the elimination of ingested microorganisms. Yet, NOX participates in cellular signaling in a cell-intrinsic and -extrinsic manner, e.g., via the release of ROS into the extracellular space. Accordingly, in humans, the inherited deficiency of NOX components is characterized by infections with bacteria and fungi and a seemingly independently dysregulated inflammatory response. Since ROS have both antimicrobial and immunomodulatory properties, their tight regulation in space and time is required for an efficient and well-balanced immune response, which allows for the reestablishment of tissue homeostasis. In addition, distinct NOX homologs expressed by non-phagocytic cells and mitochondrial ROS are interlinked with phagocytic NOX functions and thus affect the overall redox state of the tissue and the cellular activity in a complex fashion. Overall, the systematic and comparative analysis of cellular ROS functions in organisms of lower complexity provides clues for understanding the contribution of ROS and ROS deficiency to human health and disease.

Keywords: NADPH, reactive oxygen species, myeloid cells, inflammation, CGD, mitochondrial ROS, neutrophils, macrophages

OPEN ACCESS

Edited by:
Efstathios G. Stamatiades, Charité – Universitätsmedizin Berlin, Germany

Reviewed by:
Zengli Guo, The University of North Carolina at Chapel Hill, United States
David Thomas, Imperial College London, United Kingdom

***Correspondence:**
Julia Kolter
Julia.kolter@uniklinik-freiburg.de

Specialty section:
This article was submitted to Cell Death and Survival, a section of the journal Frontiers in Cell and Developmental Biology

Received: *13 November 2020*
Accepted: *26 February 2021*
Published: *26 March 2021*

Citation:
Moghadam ZM, Henneke P and Kolter J (2021) From Flies to Men: ROS and the NADPH Oxidase in Phagocytes. Front. Cell Dev. Biol. 9:628991. doi: 10.3389/fcell.2021.628991

INTRODUCTION

The biological system involving the formation and scavenging of reactive oxygen species (ROS) emerged more than 3 billion years ago, together with the appearance of photosynthetic organisms (Inupakutika et al., 2016). Upon discovery of ROS, their radical function was primarily considered to damage exposed cells and tissue structures. Later, it became clear that ROS are versatile in

function and integral to cellular signaling in most organisms. NADPH oxidases (NOX), as major sources of ROS, play an important role in this context. Within this group, the phagocyte NADPH oxidase (NOX2) is the best-studied member. It generates large amounts of ROS in phagosomes, which function to kill ingested microbes in a direct or indirect fashion. However, homologs exist in nearly all cells of plant or animal origin (Nauseef, 2019), suggesting functions of NOX beyond the mammalian immune system.

In this review, we focus on the role of NOX and ROS signaling in professional phagocytes, where ROS have mainly been studied for their role in pathogen elimination. Yet, NOX2 can also be recruited to the plasma membrane of phagocytes leading to the generation of extracellular H_2O_2 (Aviello and Knaus, 2018), and NOX2-derived ROS participate in major signaling pathways, both within the individual phagocyte and surrounding cells. Additionally, mitochondria contribute substantial amounts of ROS during oxidative phosphorylation (Hamanaka and Chandel, 2010). These pathways require tight regulation, as excessive ROS produced by phagocytes may cause oxidative stress and damage in the tissues and contribute to e.g., neurodegeneration (Wu et al., 2006). A dysfunction of phagocyte NOX, on the other hand, results in chronic granulomatous disease (CGD) in humans, characterized by recurrent bacterial and fungal infections as well as granuloma formation and hyperinflammation.

Due to the different sources and potential paracrine effects, studying the effect of ROS on certain cell types and tissues is rather complex. Thus, the analysis of organisms of lower complexity can provide valuable insights. While mammals possess different types of phagocytes, i.e., granulocytes, dendritic cells, macrophages, and monocytes, the cellular immune system of insects consists only of one phagocytic cell type called hemocyte. Hemocytes can either circulate in the hemolymph or adhere to certain tissues and recognize and phagocytose foreign material, resulting in assembly of NOX and superoxide production (Browne et al., 2013). In zebrafish, on the other hand, macrophages and neutrophils can be distinguished, which share multiple characteristics with the mammalian counterparts (Linnerz and Hall, 2020). Here, we will compare ROS formation and function in phagocytes of different species and discuss the impact of phagocyte-derived ROS on cellular and tissular signaling.

ROS FORMATION IN DIFFERENT SPECIES

The Evolution of NADPH Oxidase Enzymes

NOX enzymes emerged at the transition from unicellular to multicellular life (Bedard et al., 2007) and thus exist in fungi, plants, and animals. The mammalian NOX family currently contains seven members, i.e., NOX1–5 and the dual oxidases DUOX1 and 2. The enzyme evolved early in eukaryotic development. It was postulated that the ancestral type was similar to NOX1–4 (Kawahara et al., 2007). NOX1–3 and NOX4, on the other hand, emerged from a common branch, as both of these subgroups depend on the presence of $p22^{phox}$ to be activated or stable (Kawahara et al., 2007) (**Figure 1**).

The first mammalian NADPH oxidase to be discovered was NOX2, the phagocyte NADPH oxidase. The active form comprises six subunits: the integral membrane units $gp91^{phox}$ and $p22^{phox}$ and the regulatory subunits $p40^{phox}$, $p47^{phox}$, and $p67^{phox}$ as well as the GTPase Rac, which are localized in the cytoplasm. The other NOX isoforms were discovered later and vary at the molecular level (Panday et al., 2015). In NOX1, 3, and 4, $gp91^{phox}$ homologs form together with $p22^{phox}$ the flavocytochrome b_{558}, which facilitates the transfer of electrons from NADPH to reduce O_2 to O_2^-. NOX1 additionally recruits Nox organizing protein 1 (NOXO1) and NOX activator 1 (NOXA1), which are homologs of $p47^{phox}$ and $p67^{phox}$, respectively (Panday et al., 2015). In contrast, the activation of NOX5 and DUOX1 and 2 is mediated via Ca^{2+} and does not rely on regulatory subunits.

NOX1 is widely expressed in different cell types, with particularly high expression in colonic epithelial cells (Szanto et al., 2005) and endothelial cells of the colon, and vascular smooth muscles (Hanna et al., 2004). NOX2 is predominantly expressed in phagocytes, with lower expression in vascular smooth muscle cells (Briones et al., 2011) and human endothelial cells (Buul et al., 2005). It is generally accepted to be the major ROS source in humans (Lam et al., 2010) and it is expressed in all metazoan organisms, except for nematodes and arthropodes (Sumimoto, 2008). NOX2 is the most stringently conserved NOX enzyme among vertebrates (Kawahara et al., 2007). NOX3 was detected in the inner ear of mice (Bánfi et al., 2004) and is primarily expressed in fetal tissues (Cheng et al., 2001). It is not present in frog, zebrafish, and teleost fish, which led to the conclusion that NOX3 evolved after the emergence of fish and amphibians (Kawahara et al., 2007). NOX4 is expressed in fetal tissues and the kidney (Cheng et al., 2001). It is a main NOX isoform in non-phagocytic cells, where it is located in the endoplasmic reticulum (Chen et al., 2008). Finally, NOX5 evolved from NOX1-4 through the acquisition of a Ca^{2+}-binding EF hand motif, which enables activation by cytosolic calcium (Bedard et al., 2007; Kawahara et al., 2007; Touyz et al., 2019) (**Figure 1**). These Ca^{2+}-binding motifs evolved early during evolution, as NOX5-like isoforms are also found in protists and plants, whereas insects, nematodes, and rodents do not express NOX5 (Bedard et al., 2007; Kawahara et al., 2007). In humans, NOX5 is expressed in lymphoid organs, testis, and spleen (Touyz et al., 2019).

DUOX1 and DUOX2 enzymes emerged from NOX5 by the addition of a peroxidase homology domain (Kawahara et al., 2007; Touyz et al., 2019). DUOX enzymes were first described to be involved in thyroid hormone biosynthesis as a source of hydrogen peroxide (Dupuy et al., 1999). This is in contrast to the other NOX family members that produce only superoxide. In addition to mammals, peroxidase activity of DUOX has been shown in the nematode *Caenorhabditis elegans* (Meitzler and Ortiz de Montellano, 2009; Morand et al., 2009). In humans, DUOX1 is expressed in the lung, salivary glands, pancreas, placenta, and testis (Edens et al., 2001), whereas DUOX2 is

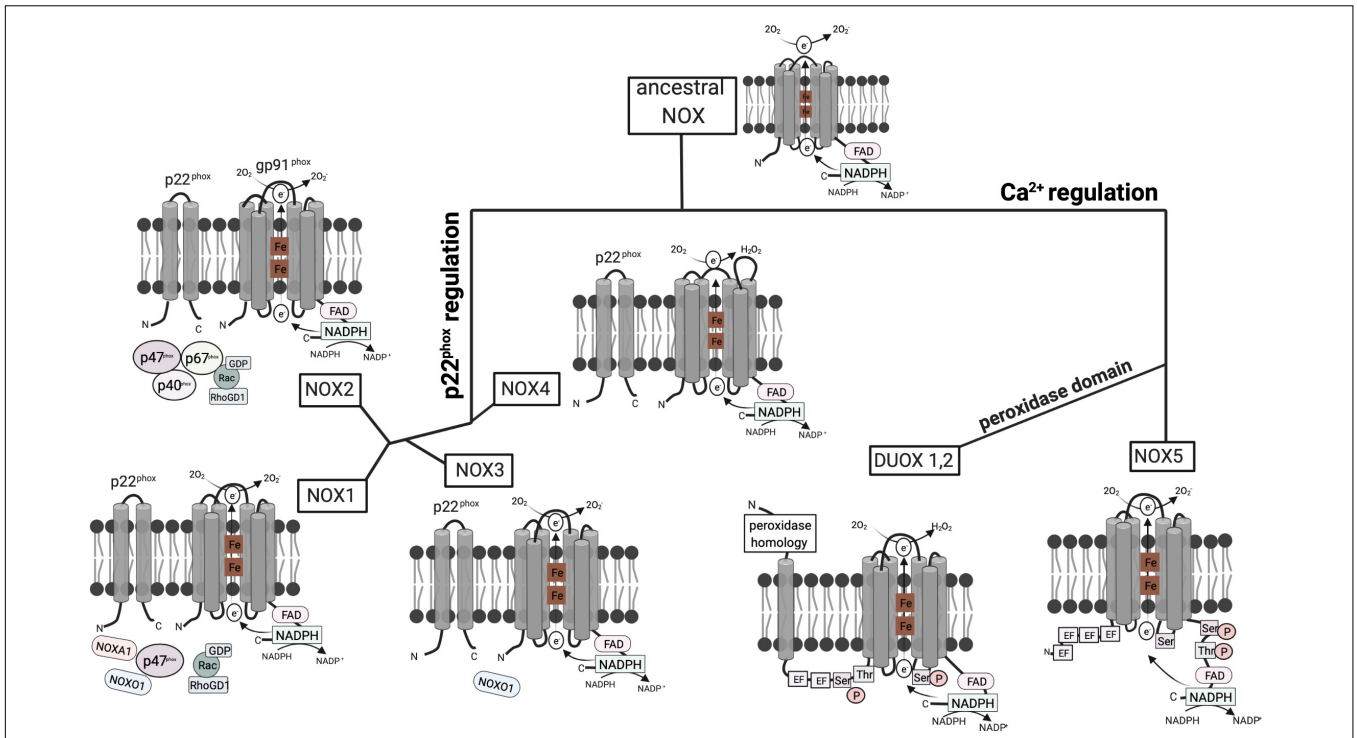

FIGURE 1 | Structure and hypothetical evolution of NOX isoforms. The ancestral NOX enzyme consists of a conserved C-terminal core region including six transmembrane a-helices, two heme (Fe) groups, and a NADPH-binding cytoplasmic C-terminal domain. The conserved gp91^{phox} subunit transfers electrons from NADPH to reduce oxygen (O_2) to superoxide anion (O_2^-). Later NOX isoforms acquired dependence on the activating subunit p22^{phox} or calcium. NOX1–3 and NOX4 emerged from a common branch, as both of these subgroups depend on the presence of the p22^{phox} subunit with two transmembrane a-helices. However, NOX4 solely relies on p22^{phox}, while NOX1–3 require additional cytoplasmic subunits. Mammalian NOX2 additionally relies on the cytoplasmic regulators p47^{phox}, p67^{phox}, p40^{phox}, and Rac. In contrast, NOX1 is regulated by NOXO1 and NOXA1. NOXO1 also contributes to NOX3 activation. NOX5 evolved from ancestral NOX through the acquisition of four EF hand motifs containing a Ca^{2+}-binding domain, which enables activation by cytosolic calcium rather than other subunits. DUOX1/2 enzymes then emerged from NOX5 isoforms by the addition of a peroxidase domain in the N-terminal region enabling H_2O_2 production (Bedard et al., 2007; Kawahara et al., 2007).

expressed in the trachea, stomach, colon, and rectum (Edens et al., 2001; Geiszt et al., 2003). In polarized cells, DUOX localizes to the apical plasma membrane (El Hassani et al., 2005; Forteza et al., 2005) and is involved in antimicrobial defense via hydrogen peroxide production in secretory glands and on mucosal surfaces (Geiszt et al., 2003).

NOX in Phagocytes Across Different Species

NADPH oxidases family members fulfill distinct roles in various species. In the following, we will discuss the expression patterns of NOX orthologs across common model organisms to resolve the diverse function of these enzymes in phagocytes.

Nematodes

The nematode *C. elegans* is a powerful model organism to study the conserved host innate immune mechanisms, given that its genome was the first one to be entirely sequenced, its easy culturability under laboratory conditions, and the existence of conserved host–microbe interactions (Kumar et al., 2020). The NADPH oxidases in *C. elegans*, termed Ce-DUOX, consists of a gp91^{phox} homology region, and a peroxidase homology domain (Edens et al., 2001). The peroxidase domain forms two bonds with heme that have a catalytic function (Meitzler and Ortiz de Montellano, 2009). Ce-DUOX1 plays imperative roles in the protection against pathogens, e.g., *Enterococcus faecalis* (Chávez et al., 2007, 2009) and *Candida albicans* (van der Hoeven et al., 2015). Less Ce-DUOX expression leads to decreased ROS production and increases susceptibility to *E. faecalis* (Chávez et al., 2009). ROS production activates SKN-1, an ortholog of the mammalian NRF transcription factor family, via p38 MAPK signaling (Van Der Hoeven et al., 2011).

Zebrafish

The study of zebrafish has provided new insights due to the availability of transgenic models of innate immunity disorders, combined with superior opportunities of *in vivo* imaging, given the transparency of the larvae (Harvie and Huttenlocher, 2015; Masud et al., 2019). Zebrafish express NOX1, NOX2, NOX4, NOX5, and a single isoform of DUOX (Kawahara et al., 2007). They possess all innate immune cell types and exhibit a similar functional diversity in phagocytes as mammals (Linnerz and Hall, 2020). NOX2 is expressed and functioning in both neutrophils and

macrophages and transgenic lines are available to fluorescently label and genetically manipulate the specific subsets. As discussed below, $p22^{phox}$-deficient larvae show increased susceptibility to fungal infection with excessive inflammation (Schoen et al., 2020).

Insects

Insects possess phagocytic cells, which engulf and kill pathogens under superoxide production (Browne et al., 2013). Plasmatocytes, the most common hemocytes, are macrophage-like cells similar to mammalian tissue macrophages (Buchon et al., 2014). In *Lepidoptera*, the cellular defense is mediated by plasmatocytes and granular cells, while in *Drosophila*, plasmatocytes and lamellocytes are key players (Browne et al., 2013). However, single-cell sequencing recently indicated that multiple populations and states of hemocytes exist (Tattikota et al., 2020), suggesting further functional diversity.

Drosophila has proven to be highly useful for studying the evolutionarily conserved innate immune system. This particularly concerns the gastrointestinal tract given the similarity to mammalian intestinal physiology and the less complex microbiota profile (Broderick and Lemaitre, 2012; Wang et al., 2014; Liu et al., 2017; Trinder et al., 2017). Gut infection in *Drosophila* induces rapid ROS production (Ha et al., 2005b). The two NADPH oxidase enzymes in *Drosophila*, which control intestinal microbes, are DUOX and NOX (Ha et al., 2005a). Microbiota-derived lactate leads to the activation of intestinal NOX (Iatsenko et al., 2018), while DUOX is activated through pathogen-derived uracil (Lee et al., 2013). It was shown that the two isoforms are present in different gut regions of *Drosophila* (Dutta et al., 2015; Iatsenko et al., 2018). Presumably, the two oxidase enzymes have distinct functions due to the different roles of lactate and uracil in host metabolism. In the intestine, DUOX-derived ROS are mainly involved in host defense, and regeneration, while NOX-derived ROS mediate epithelial renewal (Iatsenko et al., 2018).

Macrophage-like plasmatocytes are involved in the phagocytosis and encapsulation of pathogens (Fauvarque and Williams, 2011). Upon infection, a biphasic ROS response occurs (Myers et al., 2018). Initially, upon stimulation, all hemocytes, including non-phagocytic prohemocytes and crystal cells, mount a transient ROS response, which, in turn, influences plasmatocyte activation. Subsequently, after bacterial uptake, a strong ROS signal can be detected in phagocytes. The ROS responses in *Drosophila* are thus distinct in different cell types, with respect to timing, activation mechanisms, and functions. Potentially, the rapid ROS pulse is produced by mitochondria, and the later ROS response by the NADPH oxidase (Myers et al., 2018). However, further investigations are required to fully comprehend the mechanisms of these two ROS responses and their cell-type-specific effects. While regulatory NOX subunits were not found in *Drosophila* (Kawahara and Lambeth, 2007; Sumimoto, 2008), hemocytes of the Lepidopteran species *Galleria mellonella* contain proteins homologous to $p67^{phox}$ and $p47^{phox}$, which translocate upon PMA stimulation (Bergin et al., 2005; Renwick et al., 2007).

Mammals

Most mammalian species express seven NOX isoforms: NOX1–5 and DUOX1–2. Rodents are an exception, as they do not possess NOX5 (Sumimoto, 2008). NOX2 is expressed in mononuclear phagocytes as well as all three types of granulocytes, i.e., neutrophils, eosinophils, and basophils (Buvelot et al., 2016). Phagocytes can release ROS both into the phagosome and the extracellular space due to expression of NOX2 on both the phagosomal and the plasma membrane, while eosinophils express it only on the plasma membrane (Holmdahl et al., 2016). B lymphocytes also express NOX2, albeit at lower levels (Holmdahl et al., 2016).

Similar gene loci and protein sizes for the different subunits of NOX2 have been identified in humans and mice. The *Cybb* gene that encodes $gp91^{phox}$ is localized on chromosome Xp21.1. The molecular size of the $gp91^{phox}$ protein in humans and rodents is similar, approximately 65.3 kDa (Lambeth et al., 2000). In humans, the chromosomal position of the *Ncf1* gene, which encodes $p47^{phox}$, is 7q11, whereas in mice, it resides in the distal region of chromosome 5, in a region of high homology to human 7q11. While the mouse gene shows a reduced size, the number of exons and introns are conserved and exons exhibit a high degree of sequence homology (DeSilva et al., 2000).

Activation of Phagocyte NOX

The activation of the mammalian phagocyte NOX is tightly regulated and predominantly depends on the engagement of surface receptors by dedicated ligands. Subsequent to their activation, enzymatic subunits assemble at the membrane (**Figure 2**). The $gp91^{phox}$ subunit provides a conserved electron transportation region and NADPH and FAD binding sites. It forms, together with $p22^{phox}$, the catalytic core, a non-covalent heterodimer that resides at phagosomal, granule, and the plasma membrane. The regulatory subunits $p67^{phox}$, $p47^{phox}$, and $p40^{phox}$ reside in the cytoplasm as complex. Upon stimulation, $p47^{phox}$ undergoes phosphorylation, and the complex translocates to the membrane along with the small GTPase Rac2 in order to activate flavocytochrome b_{558} (Lambeth, 2004; Nauseef, 2004; Sumimoto et al., 2005). The underlying molecular events have recently been reviewed in detail (Brandes et al., 2014; Nguyen et al., 2017; Belambri et al., 2018).

Some cell surface receptors, including Toll-like receptors (TLRs), G-protein-coupled receptors (GPCRs), and TNF receptors (TNFRs), can prime the phagocytes for NOX2 activation (Nguyen et al., 2017). Priming may include conformational changes or partial phosphorylation of the regulatory subunits, which renders the cells more susceptible to a secondary stimulus but does not lead to superoxide production. Stimulation of other receptors, including Fc and integrin receptors, and the GPCR recognizing *N*-Formylmethionine-leucyl-phenylalanine (fMLP) result in direct activation of NOX2 (Nguyen et al., 2017). Their interaction with enzymes such as phospholipase C leads to the activation of protein kinase C (PKC) family members, which phosphorylate the cytosolic subunits of NOX2. PMA, on the other hand, penetrates the plasma membrane and directly induces PKCα and β activation

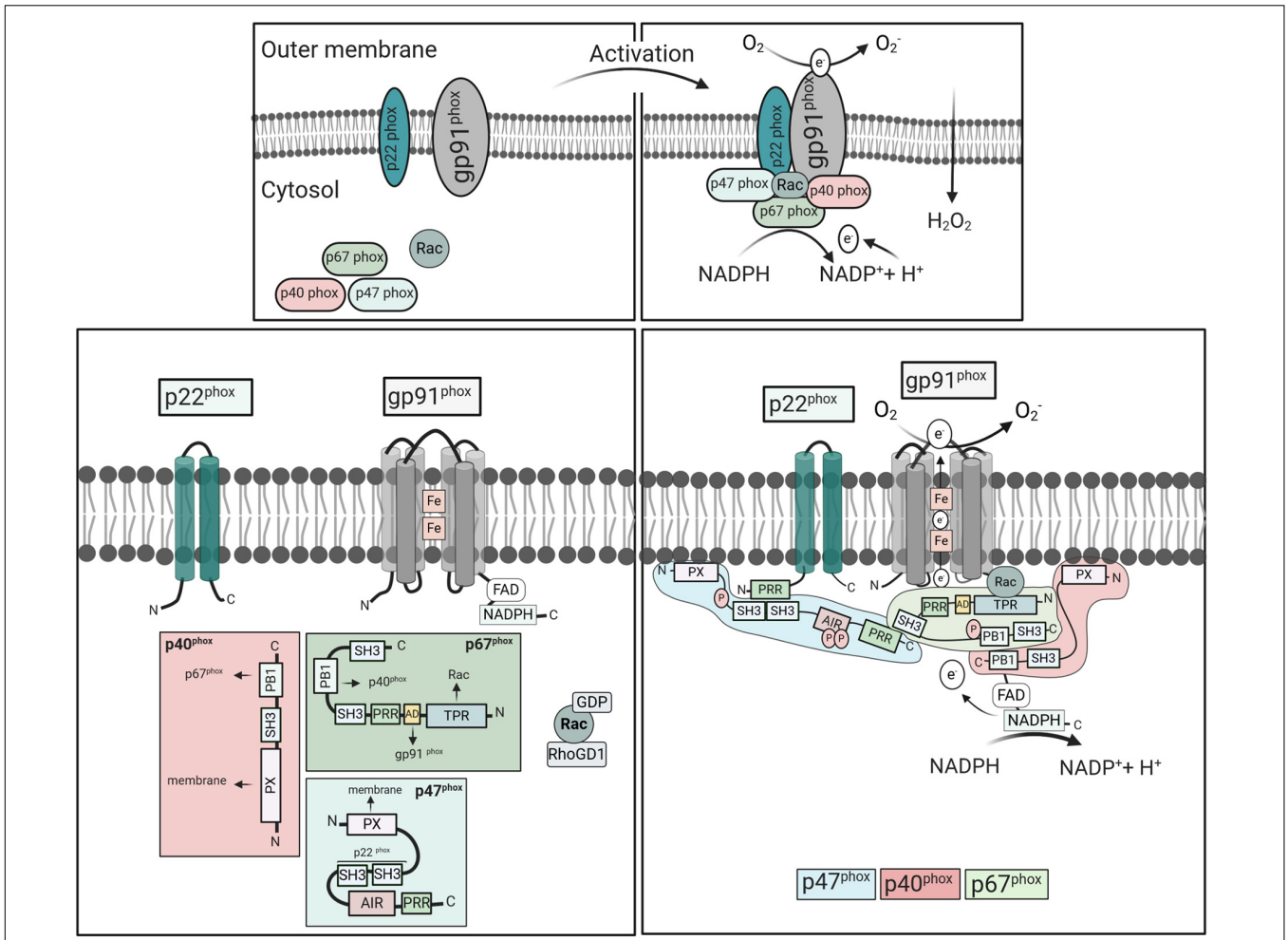

FIGURE 2 | Activation and assembly of mammalian NOX2. NOX2 consists of the cytosolic components p67^{phox}, p47^{phox}, p40^{phox}, Rac2, and the integral membrane subunits gp91^{phox} and p22^{phox}. Upon cell stimulation, the cytosolic subunits translocate to the membranes to form an active complex with gp91^{phox} and p22^{phox}. Meanwhile, Rac exchanges GDP to GTP, and dissociates from Rho-GDI. In the resting state, the p47^{phox}-SH3 tandem domain interacts with AIR keeping p47^{phox} in an inactive conformation (Belambri et al., 2018). Cell stimulation induces phosphorylation of AIR, releasing the interactive domains, i.e., SH3, PX, and PRR, which mediate oxidase assembly. The PRR of p47^{phox} binds to the SH3 region of p67^{phox}, while p67^{phox} links with p40^{phox} through their PB1 domains. The p47^{phox}-SH3 regions then bind to the p22^{phox}-PRR domains promoting p67^{phox} interaction with gp91^{phox} and moving p40^{phox}-PX domains in close proximity to the membrane. Activated NOX2 uses cytosolic NADPH to induce oxygen reduction and superoxide anion (O_2·-) generation. Abbreviations: SH3, Src homology 3 (SH3),; PX, phox homology (PX),; AIR, auto-inhibitory region (AIR),; PRR, proline-rich region (PRR),; TPR, tetratricopeptide-rich regions; PB1, phox and Bem1 domain; and AD, activation domain.

and phosphorylation of p47^{phox} (Fontayne et al., 2002). The p47^{phox} subunit harbors a tandem Src homology 3 (SH3), an auto-inhibitory region (AIR), and a proline-rich region (PRR) at the C-terminus (**Figure 2**). A phosphoinositide-interacting PX domain in the N-terminus mediates binding to phosphoinositides [PI(3,4)P2] of the plasma membrane (Hiroaki et al., 2001). In the cytoplasm of resting phagocytes, the SH3 domains are blocked due to the intramolecular interaction with AIR. Upon stimulation, phosphorylation leads to the release of the PRR/AIR domain and the open structure can bind to the other subunits (Yuzawa et al., 2004; Minakami and Sumimoto, 2006). The SH3 domain then binds to p22^{phox} of flavocytochrome b_{558} and the PX domain to the plasma membrane, bringing p67^{phox} in close proximity to Nox2. The p67^{phox} subunit contains an activation domain in the center, which subsequently activates NOX2.

The third component of the cytosolic complex, p40^{phox}, contains a PX domain that mediates binding to phosphatidylinositol-3-phosphate [PI(3)P] in phagosomal membranes (Suh et al., 2006). This binding domain was shown to be essential for oxidase activation in response to fungal particles in human, but not mouse neutrophils (Bagaitkar et al., 2012). Consequently, mouse neutrophils do not depend on p40^{phox} for NOX activation. In addition, p40^{phox}-deficient patients show a selective loss of NOX activity in response to ingested particles in neutrophils, but not mononuclear phagocytes (van de Geer et al., 2018). Accordingly, mouse macrophages and monocytes may also be capable of signaling independently of p40^{phox}. Finally,

Rac, a member of the Rho family of small GTPases, critically regulates the oxidase activity (Miyano and Sumimoto, 2012). The isoform Rac1 is ubiquitously expressed, while Rac2 is only expressed in hematopoietic cells where it is mainly responsible for NOX2 activation (Panday et al., 2015). The inactive form is bound to GDP and Rho-GDI, the GDP dissociation inhibitor. In response to stimulation, GDP is converted to GTP, mediating dissociation of Rho-GDI and Rac translocation.

ROS as Signaling Molecules

Reactive oxygen species are involved in a range of cellular and tissue responses. Additionally, ROS derived from different NOX influence distinct downstream signaling pathways, which may be the reason for co-expression of more than one isoform of NOX in specific cell types (Dworakowski et al., 2006). Upon NOX assembly, electrons are shuttled from cytosolic NADPH to FAD to membrane-embedded heme groups, which then reduce molecular oxygen to superoxide (O_2^-). The superoxide anion is a highly reactive "non-diffusible" state that is spontaneously or enzymatically converted to hydrogen peroxide (H_2O_2). In granulocytes, H_2O_2 is rapidly transformed to bactericidal hypochlorous acid (HOCl) via the action of the granule-contained myeloperoxidase (Chen et al., 2011; Nguyen et al., 2017). H_2O_2, on the other hand, is a stable "diffusible" oxidant, which may induce cytoplasmic signaling molecules (Gough and Cotter, 2011).

Reactive oxygen species play a role in various signaling pathways as second messenger. They can influence MAPK cascades and calcium signaling via oxidation of signaling intermediates (Zhang et al., 2016), and may affect cellular proliferation as well as cell death (Lambeth, 2004; Morgan and Liu, 2010; Schenk and Fulda, 2015). ROS can regulate actin and microtubule dynamics due to the oxidation of certain amino acid residues in microtubules and actin microfilaments (Wilson and González-Billault, 2015). H_2O_2 can promote cell migration through the regulation of actin dynamics and cytoskeleton organization (Kim et al., 2009). The release of DUOX-derived H_2O_2 by the zebrafish epithelium attracts leukocytes to the wound (Niethammer et al., 2009). In human, ROS are critical for wound healing via induction of thrombus formation; recruitment of peripheral blood cells, endothelial cells, keratinocytes, and fibroblasts; and promotion of cell division (Lambeth, 2004; Dunnill et al., 2017). Generally, the effects of ROS strongly depend on the amount, source, reactivity, and half-life of the produced ROS and the cellular compartment of its production. In the following, we will thus focus on effects of ROS generated by phagocytes and emphasize on the source of ROS wherever possible, e.g., through the use of genetically deficient animals or patients with CGD, where monogenetic aberrations abrogate ROS formation (see below).

Expression of NOX Homologs in Phagocytes

Apart from NOX2 expression in phagocytes, it has been reported that NOX1 (Maitra et al., 2009), NOX4 (Lee et al., 2010), and NOX5 (Marzaioli et al., 2017) are also expressed in phagocytes. In murine macrophages, stimulation with LPS leads to activation of NOX1. IRAK-1, downstream intracellular signaling components of TLR4, induces the transcription of NOX1 via NF-κB and other related transcription factors (Maitra et al., 2009). In addition, NOX1 was shown to play a role together with NOX2 in M2 polarization and macrophage differentiation by induction of the JNK and ERK signaling pathways (Xu et al., 2016). NOX4, on the other hand, localizes to the endoplasmic reticulum and mediates intracellular ROS generation in human monocytes and mature macrophages (Lee et al., 2010). Furthermore, NOX4 contributes to the polarization of macrophages. It appears to have an anti-inflammatory role in macrophages, as NOX4 deficiency favors the polarization of proinflammatory human macrophages and promotes NF-κB activity (Helfinger et al., 2019). Furthermore, expression of NOX1 (Chéret et al., 2008) and NOX4 (Li et al., 2009) was shown in microglia.

Finally, NOX5 expression was detected in the THP-1 cell line and primary $CD14^+$ human monocytes (Manea et al., 2015). Immunohistochemical staining data confirmed the presence of the NOX5 in $CD68^+$ macrophages. A recent publication demonstrated that NOX5 expression is strongly increased during the differentiation of monocytes into dendritic cells (DCs), but not macrophages (Marzaioli et al., 2017). Additionally, NOX5 expression was detected in circulating myeloid DC. Mechanistically, the NOX5–$p22^{phox}$ complex mediates DC differentiation from monocytes through regulation of the JAK/STAT/MAPK and NF-κB pathways (Marzaioli et al., 2017). Collectively, these studies demonstrate that phagocytes may express other NOX isoforms except for NOX2 at certain developmental stages and after polarization. The relative contribution of these alternative ROS sources remains unclear at this stage. However, they should be considered in situations when regulatory subunits are lost, such as $p22^{phox}$ with functions in several isoforms, or general ROS inhibitors are used for investigations in phagocytes.

NOX-Independent ROS Formation by Phagocytes

Next to NOX, cell organelles may contribute to ROS formation in phagocytes. Mitochondria are the main ROS source besides NOX in mammals, while the endoplasmic reticulum and peroxisomes are less important. In mitochondria, superoxide anions are produced during oxidative phosphorylation by reduction of molecular oxygen, which are further converted to H_2O_2 by superoxide dismutases (Hamanaka and Chandel, 2010). Mitochondria can produce ROS (mtROS) in a TLR-dependent fashion and are recruited to macrophage phagosomes (West et al., 2011). MtROS-derived H_2O_2 may then be directly delivered to bacteria-containing phagosomes via mitochondria-derived vesicles (Abuaita et al., 2018). These mechanisms can directly contribute to bactericidal activity in macrophages. In zebrafish, it was shown that macrophages use fatty acid β-oxidation in infection to produce mtROS, which is regulated via Irg1 (immunoresponsive gene 1) (Hall et al., 2013). For *Drosophila*, the impact of mtROS on the innate immune response is less clear. Biphasic ROS production after bacterial infection may suggest

that hemocytes produce mitochondrial and enzyme-derived ROS upon infection as well (Myers et al., 2018). While macrophages can produce high amounts of mtROS, especially after stimulation, neutrophils contain only low numbers of active mitochondria (Dupre-Crochet et al., 2013).

A cross-talk between NOXs-derived ROS and mitochondria, which was termed "ROS-induced ROS release," may amplify ROS generation at different subcellular compartments (Fukai and Ushio-Fukai, 2020). NOX4-derived H_2O_2 may augment mtROS, which could be limited by NOX2 siRNA (Kim et al., 2017). It was thus suggested that NOX2 can sense H_2O_2 and regulate mtROS generation (Kim et al., 2017). In addition, NOX-derived H_2O_2 of phagocytes can stimulate NOX in non-phagocytic cell types in a positive feedback loop to generate more oxidant species, which may be involved in vascular cell injury (Li et al., 2001). In addition to cell organelles, ROS may be produced in small amounts as a by-product in other enzymatic reactions, e.g., in the cytoplasm. The different sources of ROS were reviewed in more detail elsewhere (Dupre-Crochet et al., 2013).

FUNCTIONAL ROLES OF NOX-DERIVED OXIDANTS IN PHAGOCYTES

Myeloid Lineage-Specific Aspects

Phagocyte lineages differ in NOX2 expression and activity. After activation, neutrophils produce more ROS compared to monocytes and macrophages (Nauseef, 2019). DCs express little NOX2 and accordingly less ROS after activation (Mantegazza et al., 2008). In neutrophils, generation of H_2O_2 in the phagosomes activates myeloperoxidase in primary granules, which catalyzes the production of the highly antimicrobial and oxidative hypochlorous acid (Nguyen et al., 2017; Nauseef, 2019). Moreover, neutrophils are recruited to wounds via tissue-derived H_2O_2 and the myeloperoxidase was shown to clear H_2O_2 at the wound site in zebrafish (Yoo et al., 2011; Pase et al., 2012; Linnerz and Hall, 2020). Additionally, NOX2 activates granular proteases and triggers the generation of neutrophil extracellular traps (NETs) (Singel and Segal, 2016; Nguyen et al., 2017). These filamentous protein and chromatin structures are released extracellularly and aid in killing extracellular bacteria. Neutrophils of CGD patients are incapable of NETosis, which was restored by gene therapy in a CGD patient (Bianchi et al., 2009). NET formation was also absent in lungs of $p47^{phox}$-deficient mice after *Aspergillus* infection (Röhm et al., 2014). As excessive neutrophil activity after infection may cause tissue damage, cell death of activated neutrophils is physiologically important and tightly regulated. In the context of infection, this process, termed pathogen-induced cell death, depends on NOX activity (Lawrence et al., 2020). Impaired NETosis and reduced efferocytosis may thus contribute to the overall hyperinflammatory phenotype in CGD patients. As neutrophils contain only few mitochondria, the impact of mtROS is considered to be low (Dupre-Crochet et al., 2013).

Mononuclear phagocytes, on the other hand, do not express myeloperoxidase and thus contain more H_2O_2 in their phagosomes (Nauseef, 2019). In addition, mitochondrial H_2O_2 is delivered to phagosomes (Abuaita et al., 2018). As ROS production is a hallmark of classically activated M1 macrophages, ROS are essential for induction and function of the M1 phenotype (Mills and O'Neill, 2016; Rendra et al., 2019). However, it was found that superoxide is also produced during alternative macrophage activation and that the inhibition of ROS blocks the polarization to M2 macrophages (Zhang et al., 2013). Yet, since the inhibitors, which were employed in this study, also interrupted mitochondrial ROS, the source of ROS remained unclear. Another study found that M2 polarization is impaired in macrophages with a combined deficiency in NOX1 and 2, which was connected to wound healing deficits (Xu et al., 2016). Overall, it is not yet clear how polarization of macrophages is influenced by ROS, as it likely depends on several parameters including phagocyte differentiation stage and source of ROS. Similarly, it is not understood how ROS affect the differentiation of tissue macrophages. At least in the murine brain, NOX2 is activated during the development of microglia, the resident macrophages, and promotes their infiltration into the subventricular zone of the cerebral cortex (Lelli et al., 2013).

P47-deficient mice, which were complemented with a functional allele of p47 only in CD68+ cells (i.e., monocytes and macrophages), were shown to be more resistant to staphylococcal and *Aspergillus* infection, indicating that NOX2 in mononuclear phagocytes is crucial in the systemic defense against bacteria and fungi (Pizzolla et al., 2012; Grimm et al., 2013). Moreover, patients with a macrophage-specific mutation in *Cybb* ($gp91^{phox}$) are particularly prone to mycobacterial disease (Bustamante et al., 2011). In these patients, a germline mutation in the *Cybb* allele impairs NOX assembly and respiratory burst in macrophages, but not in monocytes and neutrophils. Accordingly, the assembly of NOX depends on cell-specific thresholds.

NOX2 is also expressed in DCs, albeit at lower levels. In these cells, the enzyme is recruited to early phagosomes where it utilizes protons for ROS production, thereby limiting acidification of the phagosomes. In the absence of NOX2, phagosomes of mouse DCs show decreased proteolysis and consequently degradation of antigen, resulting in impaired antigen cross-presentation skills (Savina et al., 2006; Rybicka et al., 2012). Cross-presentation of tumor antigens is also impaired in DCs from human CGD patients (Mantegazza et al., 2008). In contrast, the acidification of phagosomes of macrophages, which exhibit much higher NOX2 activity, is positively affected by ROS production (Bagaitkar et al., 2018). In efferocytosis, phagosomes of peritoneal macrophages of CGD mice showed delayed maturation and acidification, resulting in decelerated disposal of apoptotic cells (Bagaitkar et al., 2018). In addition, cross-presentation of antigens was increased in these cells. The opposed function of NOX2 in macrophages and DCs might relate to the higher expression of the V-ATPase and lysosomal proteases in macrophages.

Cell-Intrinsic Effects

The functions of NOX2 and of NOX2-derived oxidants can generally be subclassified in effects on the individual cell level and the population/tissue level. Effects due to autocrine signaling occur in the individual phagocyte after NOX2 activation.

Neutrophils of CGD patients show globally increased expression of proinflammatory mediators in steady state (Kobayashi et al., 2004). In response to toll-like receptor ligands, human and mouse leukocytes exhibit increased production of proinflammatory cytokines such as IL-6 and TNF along with elevated NF-κB activation (Bylund et al., 2007; Brown et al., 2008). Notably, increased expression of inflammatory cytokines has also been described in $p22^{phox}$-deficient larvae of zebrafish in steady state as well as in response to fungal infection (Schoen et al., 2020). In the past, the activation of NOX2 was linked to the activation of the inflammasome, multimeric cytosolic pathogen sensors. According to some earlier studies, NOX2-derived ROS were described as essential second stimuli for the activation of the NLRP3 inflammasome (Dostert et al., 2008). However, it was later shown that the NLRP3 inflammasome does not depend on NOX1–4-derived ROS for its activation (van Bruggen et al., 2010), but instead on mitochondrial ROS (Zhou et al., 2011; Netea et al., 2015). On the contrary, monocytes from CGD patients exhibited increased caspase activation and IL-1β secretion in comparison to controls (Meissner et al., 2010; van de Veerdonk et al., 2010). de Luca et al. (2014) showed that macrophages from CGD mice and monocytes from CGD patients were deficient in autophagy, leading to increased IL-1β release after stimulation. Blockage of the IL-1β receptor limited inflammasome activation and restored autophagy, resulting in decreased neutrophil recruitment and amelioration of colitis in some CGD patients. Thus, NOX2 appears to be important for the negative regulation of IL-1β-dependent signaling. Moreover, NOX2-derived ROS are involved in the induction of a non-canonical autophagy pathway, called LC3-associated phagocytosis (LAP) (Huang et al., 2009; de Luca et al., 2014; Martinez et al., 2015). In LAP, components of the autophagy pathway, i.e., LC3, are targeted to phagosomal membranes, leading to efficient fusion with lysosomes and destruction of contained pathogens. Notably, this pathway is particularly important for the clearance of *Aspergillus fumigatus*, which often causes invasive infections in CGD patients.

Additionally, the hyperinflammatory phenotype in CGD has been linked to defective tryptophane metabolism, as the kynurenine pathway, the major pathway for tryptophane degradation, was supposedly dependent on superoxide (Romani et al., 2008). However, several later studies found tryptophan catabolism to be normal in NOX2-deficient patients and mice (De Ravin et al., 2010; Jürgens et al., 2010; Maghzal et al., 2014). The increased cytokine expression in response to stimuli in CGD was instead traced back to impaired activation of the nuclear factor erythroid 2-related factor 2 (Nrf2), a key redox-sensitive transcription factor (Segal et al., 2010). Nrf2 regulates oxidative stress pathways and acts anti-inflammatory by suppressing the transcription of proinflammatory cytokines (Kobayashi et al., 2016). Consequently, mononuclear cells from peripheral blood from CGD patients show reduced Nrf2 activity and increased NF-κB activation (Han et al., 2013; Singel and Segal, 2016). Furthermore, it was suggested that NOX2 deficiency promotes nuclear accumulation of thioredoxin-1, an antioxidant protein with a disulfide reductase activity (Trevelin et al., 2016). Thioredoxin-1 in turn contributes to the DNA binding of NF-κB subunits by posttranslational modification (Matthews et al., 1992; Trevelin et al., 2016; Muri et al., 2020). Thus, the activity of NOX2 may influence the NF-κB pathway via interaction with multiple nuclear proteins, ensuring the regulation of proinflammatory cytokines. These processes are largely conserved from zebrafish to mammals.

In general, ROS derived from mitochondria contribute to cellular signaling as well. MtROS contribute to proinflammatory cytokine secretion by disulfide linkage of the essential modulator of NF-κB NEMO (Herb et al., 2019) and stimulate the activation of the NLRP3 inflammasome (Zhou et al., 2011). Thus, the effect of ROS on cytokine secretion depends additionally on the cellular source and localization of ROS. In line with that, a recent study suggested that mtROS are elevated in CGD phagocytes, which paradoxically leads to oxidative stress and increased MAPK activation and may thus further contribute to production of proinflammatory cytokines (Sundqvist et al., 2017).

Cell-Extrinsic Effects

The assembly of NOX2 at the plasma membrane allows for the production of extracellular ROS intermediates (Nauseef, 2019). Production of extracellular H_2O_2 may thus affect cells of the surrounding tissue. In general, NOX2 is recognized to play an important role in the calibration of the immune response, i.e., to limit inflammatory responses after injury or infection (Singel and Segal, 2016). This effect may be achieved by dampening of the IL-1β response in macrophages, thereby leading to the recruitment of less neutrophils (de Luca et al., 2014). The effect of ROS also depends on the production site. Warnatsch et al. (2017) showed that neutrophils produced intracellular ROS in mice infected with small microbes, while ROS were secreted into the extracellular space in infection with large microbes such as filamentous fungi. Intracellular ROS suppressed IL-1β expression in these neutrophils, thus limiting recruitment of additional neutrophils, while extracellular ROS amplified IL-1β secretion and neutrophil clustering. Hence, the assembly of NOX2 on the phagosomal or the plasma membrane impacts on the outcome of the entire tissue reaction.

Secondly, the production of large quantities of superoxide during the respiratory burst may lead to the depletion of oxygen in the surrounding tissue, e.g., in the context of acute colitis. Transmigrating neutrophils rapidly deplete microenvironmental oxygen in the lamina propria, leading to stabilization of the hypoxia-inducible factor HIF and HIF-dependent responses in intestinal epithelial cells (Campbell et al., 2014). Furthermore, $gp91^{phox}$-deficient mice showed increased infiltration of granulocytes, but diminished hypoxia and worsened colitis. Thus, the NOX2-dependent modulation of extracellular oxygen may be protective in colitis, due to activation of hypoxic responses in neighboring cells, highlighting the complexity of ROS signaling on the tissular level.

Recently, a paracrine effect of NOX2 was shown to facilitate interaction between neutrophils and macrophages after liver injury (Yang et al., 2019). Genetic deficiency in $gp91^{phox}$ delayed liver recovery, due to a failure of pro-inflammatory $Ly6C^{hi}CX_3CR1^{low}$ macrophages to convert into pro-resolving $Ly6C^{low}CX_3CR1^{high}$ macrophages. Adoptive transfer of

WT, but not gp91^{phox}-deficient neutrophils, rescued the conversion in neutropenic mice. Thus, NOX2-derived ROS from neutrophils appear to shape the phenotype of tissue macrophages and thereby orchestrate tissue repair. A ROS-dependent bidirectional communication was also observed between hemocytes, the macrophages of *Drosophila*, and epithelial cells (Fogarty et al., 2016). Extracellular DUOX-derived ROS formed by epithelial cells led to macrophage activation, which in turn triggered apoptosis-induced proliferation in epithelial cells via TNF. Accordingly, the diffusion of ROS and in particular H_2O_2 within the tissue or even across membranes (Nauseef, 2019; Yang et al., 2019) may influence signaling and cellular processes of other cell types within the same tissue or even across membranes in distant tissues. In *Drosophila*, increased levels of ROS sensitize hematopoietic progenitors to differentiate into mature innate blood cells (Owusu-Ansah and Banerjee, 2009), and after parasite infection, induction of ROS in hematopoietic cells leads to secretion of epidermal growth-factor like cytokine resulting in differentiation of specialized innate immune cells (Sinenko et al., 2012). Consistent with this model, hematopoietic stem cells were found to be diminished in bone marrow and peripheral blood of CGD patients (Weisser et al., 2016).

NOX2 might also affect adaptive immunity. A type 1 interferon signature was found in CGD mice and patients, accompanied by the presence of autoantibodies, pointing toward autoimmune features of NOX2 deficiency (Kelkka et al., 2014). Notably, CGD patients exhibit an increased frequency of autoimmune diseases (Schäppi M. G. et al., 2008). Female carriers of X-linked CGD with varying degrees of inactivation in the mutated X chromosome also show autoimmune manifestations, which, in some cases, included lupus-like symptoms (Cale et al., 2007; Marciano et al., 2018). In mice, gp91^{phox} deficiency led to a heightened susceptibility for autoimmune arthritis (George-Chandy et al., 2008). Generally, the increased expression of proinflammatory cytokines may enhance T cell activation by antigen-presenting cells (George-Chandy et al., 2008). In addition, NOX2-deficient rat and human macrophages are less capable to induce regulatory T cells (Kraaij et al., 2010). For more details on the impact of ROS on lymphocyte signaling, we refer the reader to recent reviews (Cachat et al., 2015; Holmdahl et al., 2016). Altogether, NOX2-derived ROS may shape the regulation of the adaptive immune response and play a role in the resolution of the inflammatory response. The mechanisms discussed in the previous paragraph, such as enhanced secretion of proinflammatory mediators and decelerated disposal of apoptotic cells may contribute to this effect.

PHAGOCYTE-DERIVED ROS IN HEALTH AND DISEASE

In general, ROS are recognized to play a role in physiological as well as pathological states and the literature covering this subject has increased extensively. While NOX-derived ROS are important for basic physiological functions such as the regulation of blood pressure and gut motility, excess ROS may promote cellular stress and contribute to the development of autoimmunity or cancer (Sorescu et al., 2002; Block and Gorin, 2012; Gray Stephen et al., 2013; Nayernia et al., 2013; Panday et al., 2015; Konaté et al., 2020). As an example, it was found that in acute myeloid leukemia, NOX-derived ROS promote proliferation of leukemic cells (Hole et al., 2013). For the present review, we will finally focus on two aspects directly related to the expression of NOX in phagocytes, i.e., the interplay with the microbiota and the clinical perspective of CGD.

The Specific Role of NOX in the Cross-Talk With the Microbiota

In steady state, NOX-derived ROS are involved in the interspecies cross-talk with the individual microbiota. This has been exemplified in *Drosophila*, which exhibits a low degree of bacterial diversity in the microbiota (Wong et al., 2011). Both in fruit flies and mice, commensal bacteria induce NOX1-dependent ROS and thereby stimulate the proliferation of intestinal stem cells (Jones et al., 2013). In contrast, an overgrowth of commensals with increased formation of lactic acid induces excessive intestinal NOX activity and ROS production, and, as a result, intestinal damage in *Drosophila* (Iatsenko et al., 2018). The underlying mechanism is the oxidation of lactate by the host lactate dehydrogenase, which produces NADH for NOX, uncovering a metabolic cross-talk between microbiota and host with contribution by ROS. Analogous mechanisms in mammals involve symbionts inducing ROS generation by intestinal epithelial cells, thereby impacting on host physiology (Jones and Neish, 2017). In contrast, few studies have investigated the direct impact of phagocytic NOX on the host–microbiome interaction. In p47^{phox}-deficient mice, susceptibility for DSS colitis was reversed by standardizing the microflora from birth on (Falcone et al., 2016), indicating that impaired NOX2 activity might have a lasting impact on the microbiome composition. In case the microbiome is disturbed by antibiotics, NOX2 is required for host survival in a *Citrobacter rodentium* infection model (Pircalabioru et al., 2016; Knaus et al., 2017). Thus, the commensal microbiota may act in concert with NOX2 to protect the intestine from the invasion of virulent microorganisms.

In patients suffering from CGD, the spectrum of microbes causing infections is surprisingly narrow, indicating which pathogens are targeted in particular by NOX2. Patients frequently present with severe fungal infections, especially by *Aspergillus* spp., which also account for most infection-related deaths in CGD (Henriet et al., 2012; Marciano et al., 2015). Next to the prevalent *A. fumigatus*, *Aspergillus nidans* imposes a specific risk pathogen in CGD patients, which is uncommon in other immunodeficiencies (Henriet et al., 2012). Interestingly, zebrafish larvae with p22^{phox}-deficiency are also more susceptible to *Aspergillus nidulans* infection with enhanced inflammation, which was attributed to both excessive neutrophil recruitment as well as fungal growth (Schoen et al., 2020). Potentially, increased inflammation caused by this normally avirulent fungus results in its fast clearance but, in case of CGD deficiency, leads to detrimental inflammatory damage to the host instead.

With regard to bacteria, *Staphylococcus*, *Burkholderia*, and *Serratia* are leading causes of infection in CGD (Marciano et al., 2015). Similarly, NOX2-deficient rodents show increased

susceptibility to *Staphylococcus aureus* and *Aspergillus* (Pollock et al., 1995; Pizzolla et al., 2012; Grimm et al., 2013). In a cohort of 268 patients, about one third suffered from severe infections with *S. aureus*, which was isolated from lymph nodes and liver abscesses (Marciano et al., 2015). Notably, neutrophils of CGD patients show a decreased capacity to kill *S. aureus* but not *Escherichia coli* (Rosen and Michel, 1997). It is not entirely clear why NOX2 is particularly important in the defense against *S. aureus*, as the bacterium possesses multiple resistance mechanisms such as catalase and superoxide dismutase (Buvelot et al., 2016). Next to the direct killing capacity, ROS may directly modify staphylococcal gene regulation (Rothfork et al., 2004; Buvelot et al., 2016). On the other hand, the regulation of the immune response by NOX2, in particular the inflammatory response as discussed above, may be essential to eliminate *S. aureus*. Also in *Aspergillus*, antioxidant pathways may overcome direct damage by ROS (Lambou et al., 2010; Wiemann et al., 2017; Schoen et al., 2020). This demonstrates a large degree of adaptation by the pathogens, which are particularly affected by this host defense mechanism. Thus, next to direct damage of bacterial DNA or proteins, the control and regulation of the inflammatory response may be equally important in the containment of these pathogens.

Finally, CGD patients show an increased susceptibility for mycobacteria, i.e., *Mycobacterium tuberculosis* in endemic countries and *Mycobacterium bovis* (BCG) after vaccination (Deffert et al., 2014; Conti et al., 2016). As mentioned above, patients with a macrophage-specific mutation in *Cybb* are particularly prone to mycobacterial disease (Bustamante et al., 2011). P47^{phox}-deficient mice also show increased growth of *Mycobacterium tuberculosis* in the lungs at early stages of pulmonary infection (Cooper et al., 2000). Moreover, NOX-dependent mechanisms are essential for neutrophil-mediated killing of *Mycobacterium marinum* in zebrafish larvae after granuloma formation (Yang et al., 2012). Thus, oxidative killing of mycobacteria is a conserved mechanism by which phagocytes protect their respective hosts.

In addition to monogenetic and deleterious aberrations, single-nucleotide polymorphisms and hypomorphic mutations in *Nox* subunit genes have been associated with increased risks for IBD (Dhillon et al., 2014; Aviello and Knaus, 2018). IBD, on the other hand, is often associated with dysbiosis. Yet, it is unclear if this is causal for or a result of increased inflammation. As almost every second CGD patient suffers from intestinal inflammation (Marks et al., 2009; Falcone et al., 2016), further research is needed on the role of NOX2 in intestinal integrity, in particular in terms of local immune homeostasis and the microbiota.

CGD: Clinics and Animal Models

Chronic granulomatous disease is an immunodeficiency disease caused by defects in any of the five structural components of the NOX enzyme, i.e., X-linked recessive mutations in *Cybb* (gp91^{phox}), or autosomal recessive mutations in *Cyba* (p22^{phox}), *Ncf1* (p47^{phox}), *Ncf2* (p67^{phox}), or *Ncf4* (p40^{phox}) (Kuhns et al., 2010; Arnold and Heimall, 2017; van de Geer et al., 2018). Gp91^{phox}-deficient CGD is the most common and severe form of this disease in human (Kuhns et al., 2010). Gp91^{phox}-deficient patients produce very low amounts of ROS, while neutrophils in patients with mutations in *Ncf1* form higher amounts, leading to an overall increased survival rate. Recently, a novel cause for CGD was discovered in patients with a deficiency in the *Cybc1* gene (Arnadottir et al., 2018; Thomas et al., 2019). Cybc1 encodes the ER-resident protein EROS (Essential for Reactive Oxygen Species), which is required for stable expression of the gp91^{phox} and p22^{phox} proteins and putatively acts as chaperone for the heterodimer in humans and mice (Thomas et al., 2017; Arnadottir et al., 2018).

The CGD incidence is between 1 in 200,000–250,000 newborns in Europe and the United States (Winkelstein et al., 2000; Arnold and Heimall, 2017). As described in the previous paragraph, invasive bacterial and fungal infections are pivotal contributors to morbidity and mortality in CGD patients. Bacterial infections typically affect the lungs, skin, liver, and lymph nodes (Arnold and Heimall, 2017). Dysregulated inflammation on the other hand most commonly affects the gastrointestinal tract, followed by lungs, urogenital tract, and eyes. In addition, liver abnormalities including nodular regenerative hyperplasia and non-cirrhotic portal hypertension have been observed in NOX2-deficient patients (Hussain et al., 2007). In gp91^{phox}-deficient individuals, inflammatory complications occur twice as often as in patients with autosomal recessive NOX gene mutations (Arnold and Heimall, 2017). Moreover, X-linked CGD patients exhibit a strong and early disease phenotype, and an earlier age of death (van den Berg et al., 2009).

Granuloma formation is a typical CGD manifestation (Schäppi M. G. et al., 2008). Granulomas can occur in various organs such as colon, lung, and skin and may functionally impair the respective organs. While granulomas can form as a reaction to chronic infection, they may also form in the absence of overt infection, i.e., the absence of cultivable microbes. In CGD patients, their response to immunosuppressants rather than antibiotics clearly indicates immunodysregulation (Schäppi M. G. et al., 2008). In NOX2-deficient mice, persistent inflammatory lesions develop in response to sterile preparations of fungal cell walls in the lung and skin (Morgenstern et al., 1997; Schäppi M. et al., 2008). Furthermore, mice deficient in *Ncf1* or *Cyba* were reported to develop spontaneous granulomas in the lung, even if housed under SPF conditions (van der Weyden et al., 2018). Thus, granulomatous lesions in CGD patients may not just deflect impaired microbial killing, but rather the dysregulation of the inflammatory response and the failure to efficiently clear debris.

The CGD models in zebrafish comprise deficiencies in gp91^{phox} and p22^{phox}. CGD zebrafish models are susceptible to *Pseudomonas aeruginosa* and to *A. nidulans* (Henriet et al., 2012; Yang et al., 2012). Additionally, excessive neutrophil recruitment is observed (Schoen et al., 2020). Both the fungal growth and the neutrophilic inflammation could be limited by expression of NOX in neutrophils alone, indicating that the aberrant signaling in neutrophils contributes to both higher microbial susceptibility and the hyperinflammatory phenotype in zebrafish (Schoen et al., 2020).

Around 50% of patients with CGD suffer from severe intestinal inflammation, which shares features with inflammatory bowel disease (IBD), according to a report of the National Institutes of Health (Falcone et al., 2016). The gastrointestinal manifestations show striking similarities with Crohn's disease (Marks et al., 2009) and mostly affect the colon, which shows microgranulomas, pigmented macrophages, and tissue eosinophilia (Alimchandani et al., 2013).

To understand the mechanisms of colitis in NOX2 deficiency, animal models have been extensively used. In NOX2-deficient mice, however, colitis does not develop spontaneously and requires induction, most commonly achieved by chemicals. In the trinitrobenzenesulfonic acid (TNBS) model, colitis is stimulated via T lymphocyte responses due to haptenization of host or microbiota-derived proteins (Antoniou et al., 2016). Dextran sulfate sodium (DSS) treatment, on the other hand, exhibits toxicity against of intestinal epithelial cells, which stimulates disintegration of the mucosal membrane (Perše and Cerar, 2012; Wirtz et al., 2017). Thus, while the DSS model represents a wound model, the TNBS model is considered an acute-to-chronic inflammation model (Campbell and Colgan, 2019). For CGD, it was demonstrated that gp91^{phox}-deficient mice are susceptible to the TNBS colitis model (Campbell et al., 2014). In contrast, DSS did not efficiently induce colitis in gp91-deficient mice; weight loss and colitis severity were less pronounced than in wild-type mice (Bao et al., 2011; Aviello et al., 2019). In addition, it was suggested that mice with gp91^{phox} deficiency also do not develop severe colitis after *C. rodentium* infection (Fattouh et al., 2013). Conversely, p47^{phox}-deficient mice developed strong disease after DSS administration (Rodrigues-Sousa et al., 2014; Falcone et al., 2016) and p40^{phox}-deficient mice were more susceptible to DSS colitis than wild-type mice (Conway et al., 2012). One explanation for these differences may be individual roles of each subunit in NOX-independent signaling pathways. On the other hand, external environmental influences such as the prevalence of commensal/pathogenic microorganisms may contribute to the variability, particularly as the microbiota has a large impact on IBD (Nell et al., 2010; Perše and Cerar, 2012). Finally, the mechanism of colitis induction is probably critical. Recently, a study demonstrated that mice with a hypomorphic mutation in *Cyba* (p22^{phox}) showed loss of the mucus layer, dysbiosis, and increased inflammation while *Cyba*-deficient mice did not display any predisposition to DSS colitis (Aviello et al., 2019). Notably, ROS generation in neutrophils was also absent in the mice with the hypomorphic mutation, but, opposed to the complete p22^{phox} deficiency, NOX4 remained functional. Hence, compensation by other ROS sources in the intestine, e.g., NOX4 in epithelial cells, may affect the disease phenotype, at least in rodents.

CONCLUSION

Intensive studies in human and mouse systems have led to a comprehensive understanding of the contribution of phagocyte-derived ROS to health and disease. Yet, gaps of knowledge remain especially with regard to the specific targeting of individual ROS sources or the transferability of results originating in rodent models. As one example, NOX2-deficient mice do not spontaneously develop intestinal bowel disease, which is a prevalent symptom of CGD patients. On the other hand, the conservation of the signaling components in ROS pathways presents also an opportunity for performing studies in animals of lower complexity. *Drosophila* might be an excellent model to study the effects of mitochondrial ROS (Salminen and Vale, 2020), considering the availability of suitable genetic tools. The zebrafish, on the other hand, exhibits a CGD-like phenotype upon NOX2 deficiency (Schoen et al., 2020) and offers the possibility to investigate the individual role of ROS in both granulocytes and mononuclear phagocytes.

A more profound knowledge of the involved pathways and downstream effects is crucial, as both an excessive and a diminished production of ROS have proven to be harmful. Additionally, the development of specific inhibitors, e.g., small molecules or plant-based substances, is still in its infancy (Panday et al., 2015). Further research in this area will thus serve the purpose of not only developing more specific therapeutics for CGD, for which the current standard therapy is bone marrow transplantation, but also understanding the regulation of a balanced immune response in general.

AUTHOR CONTRIBUTIONS

ZM, PH, and JK wrote and edited the manuscript. All authors contributed to the article and approved the submitted version.

FUNDING

JK was funded by EQUIP—Funding for medical scientists, Faculty of Medicine, University of Freiburg. Further funding was provided by the German Ministry of Education and Research (grants 01EO0803, 01GL1746A, and 01EK1602A to PH) and the German Research Council (grants HE3127/9-1, HE3127/12-1, and SFB/TRR167 to PH). The article processing charge was funded by the Baden-Wuerttemberg Ministry of Science, Research and Art and the University of Freiburg in the funding programme Open Access Publishing.

REFERENCES

Abuaita, B. H., Schultz, T. L., and O'Riordan, M. X. (2018). Mitochondria-Derived vesicles deliver antimicrobial reactive oxygen species to control phagosome-localized *Staphylococcus aureus*. *Cell Host Microbe* 24, 625-636.e5. doi: 10.1016/j.chom.2018.10.005

Alimchandani, M., Lai, J.-P., Aung, P. P., Khangura, S., Kamal, N., Gallin, J. I., et al. (2013). Gastrointestinal histopathology in chronic granulomatous disease: a study of 87 patients. *Am. J. Surg. Pathol.* 37, 1365–1372. doi: 10.1097/PAS.0b013e318297427d

Antoniou, E., Margonis, G. A., Angelou, A., Pikouli, A., Argiri, P., Karavokyros, I., et al. (2016). The TNBS-induced colitis animal model: an overview. *Ann. Med. Surg.* 11, 9–15. doi: 10.1016/j.amsu.2016.07.019

Arnadottir, G. A., Norddahl, G. L., Gudmundsdottir, S., Agustsdottir, A. B., Sigurdsson, S., Jensson, B. O., et al. (2018). A homozygous loss-of-function

mutation leading to CYBC1 deficiency causes chronic granulomatous disease. *Nat. Commun.* 9:4447. doi: 10.1038/s41467-018-06964-x

Arnold, D. E., and Heimall, J. R. (2017). A review of chronic granulomatous disease. *Adv. Ther.* 34, 2543–2557. doi: 10.1007/s12325-017-0636-2

Aviello, G., and Knaus, U. G. (2018). NADPH oxidases and ROS signaling in the gastrointestinal tract. *Mucosal. Immunol.* 11, 1011–1023. doi: 10.1038/s41385-018-0021-8

Aviello, G., Singh, A. K., O'Neill, S., Conroy, E., Gallagher, W., D'Agostino, G., et al. (2019). Colitis susceptibility in mice with reactive oxygen species deficiency is mediated by mucus barrier and immune defense defects. *Mucosal. Immunol.* 12, 1316–1326. doi: 10.1038/s41385-019-0205-x

Bagaitkar, J., Huang, J., Zeng, M. Y., Pech, N. K., Monlish, D. A., Perez-Zapata, L. J., et al. (2018). NADPH oxidase activation regulates apoptotic neutrophil clearance by murine macrophages. *Blood* 131, 2367–2378. doi: 10.1182/blood-2017-09-809004

Bagaitkar, J., Matute, J. D., Austin, A., Arias, A. A., and Dinauer, M. C. (2012). Activation of neutrophil respiratory burst by fungal particles requires phosphatidylinositol 3-phosphate binding to p40phox in humans but not in mice. *Blood* 120, 3385–3387. doi: 10.1182/blood-2012-07-445619

Bánfi, B., Malgrange, B., Knisz, J., Steger, K., Dubois-Dauphin, M., and Krause, K.-H. (2004). NOX3, a superoxide-generating NADPH oxidase of the inner ear. *J. Biol. Chem.* 279, 46065–46072. doi: 10.1074/jbc.M403046200

Bao, S., Carr, E. D., Xu, Y. H., and Hunt, N. H. (2011). Gp91phox contributes to the development of experimental inflammatory bowel disease. *Immunol. Cell Biol.* 89, 853–860. doi: 10.1038/icb.2011.4

Bedard, K., Lardy, B., and Krause, K.-H. (2007). NOX family NADPH oxidases: not just in mammals. *Biochimie* 89, 1107–1112. doi: 10.1016/j.biochi.2007.01.012

Belambri, S. A., Rolas, L., Raad, H., Hurtado-Nedelec, M., Dang, P. M.-C., and El-Benna, J. (2018). NADPH oxidase activation in neutrophils: role of the phosphorylation of its subunits. *Eur. J. Clin. Invest.* 48:e12951. doi: 10.1111/eci.12951

Bergin, D., Reeves, E. P., Renwick, J., Wientjes, F. B., and Kavanagh, K. (2005). Superoxide production in *Galleria mellonella* hemocytes: identification of proteins homologous to the NADPH oxidase complex of human neutrophils. *Infect. Immun.* 73, 4161–4170. doi: 10.1128/iai.73.7.4161-4170.2005

Bianchi, M., Hakkim, A., Brinkmann, V., Siler, U., Seger, R. A., Zychlinsky, A., et al. (2009). Restoration of NET formation by gene therapy in CGD controls aspergillosis. *Blood* 114, 2619–2622. doi: 10.1182/blood-2009-05-221606

Block, K., and Gorin, Y. (2012). Aiding and abetting roles of NOX oxidases in cellular transformation. *Nat. Rev. Cancer* 12, 627–637. doi: 10.1038/nrc3339

Brandes, R. P., Weissmann, N., and Schröder, K. (2014). Nox family NADPH oxidases: molecular mechanisms of activation. *Free Radic. Biol. Med.* 76, 208–226. doi: 10.1016/j.freeradbiomed.2014.07.046

Briones, A. M., Tabet, F., Callera, G. E., Montezano, A. C., Yogi, A., He, Y., et al. (2011). Differential regulation of Nox1, Nox2 and Nox4 in vascular smooth muscle cells from WKY and SHR. *J. Am. Soc. Hypertens.* 5, 137–153. doi: 10.1016/j.jash.2011.02.001

Broderick, N. A., and Lemaitre, B. (2012). Gut-associated microbes of *Drosophila melanogaster*. *Gut microbes* 3, 307–321. doi: 10.4161/gmic.19896

Brown, K. L., Bylund, J., MacDonald, K. L., Song-Zhao, G. X., Elliott, M. R., Falsafi, R., et al. (2008). ROS-deficient monocytes have aberrant gene expression that correlates with inflammatory disorders of chronic granulomatous disease. *Clin. Immunol.* 129, 90–102. doi: 10.1016/j.clim.2008.06.005

Browne, N., Heelan, M., and Kavanagh, K. (2013). An analysis of the structural and functional similarities of insect hemocytes and mammalian phagocytes. *Virulence* 4, 597–603. doi: 10.4161/viru.25906

Buchon, N., Silverman, N., and Cherry, S. (2014). Immunity in *Drosophila melanogaster*–from microbial recognition to whole-organism physiology. *Nat. Rev. Immunol.* 14, 796–810. doi: 10.1038/nri3763

Bustamante, J., Arias, A. A., Vogt, G., Picard, C., Galicia, L. B., Prando, C., et al. (2011). Germline CYBB mutations that selectively affect macrophages in kindreds with X-linked predisposition to tuberculous mycobacterial disease. *Nat. Immunol.* 12, 213–221. doi: 10.1038/ni.1992

Buul, J. V., Fernandez-Borja, M., Anthony, E., and Hordijk, P. (2005). Expression and localization of NOX2 and NOX4 in primary human endothelial cells. *Antioxid. Redox Signal.* 7, 308–317. doi: 10.1089/ars.2005.7.308

Buvelot, H., Posfay-Barbe, K. M., Linder, P., Schrenzel, J., and Krause, K.-H. (2016). *Staphylococcus aureus*, phagocyte NADPH oxidase and chronic granulomatous disease. *FEMS Microbiol. Rev.* 41, 139–157. doi: 10.1093/femsre/fuw042

Bylund, J., MacDonald, K. L., Brown, K. L., Mydel, P., Collins, L. V., Hancock, R. E. W., et al. (2007). Enhanced inflammatory responses of chronic granulomatous disease leukocytes involve ROS-independent activation of NF-κB. *Eur. J. Immunol.* 37, 1087–1096. doi: 10.1002/eji.200636651

Cachat, J., Deffert, C., Hugues, S., and Krause, K.-H. (2015). Phagocyte NADPH oxidase and specific immunity. *Clin. Sci.* 128, 635–648. doi: 10.1042/CS20140635

Cale, C. M., Morton, L., and Goldblatt, D. (2007). Cutaneous and other lupus-like symptoms in carriers of X-linked chronic granulomatous disease: incidence and autoimmune serology. *Clin. Exp. Immunol.* 148, 79–84. doi: 10.1111/j.1365-2249.2007.03321.x

Campbell, E. L., Bruyninckx, W. J., Kelly, C. J., Glover, L. E., McNamee, E. N., Bowers, B. E., et al. (2014). Transmigrating neutrophils shape the mucosal microenvironment through localized oxygen depletion to influence resolution of inflammation. *Immunity* 40, 66–77. doi: 10.1016/j.immuni.2013.11.020

Campbell, E. L., and Colgan, S. P. (2019). Control and dysregulation of redox signalling in the gastrointestinal tract. *Nat. Rev. Gastroenterol. Hepatol.* 16, 106–120. doi: 10.1038/s41575-018-0079-5

Chávez, V., Mohri-Shiomi, A., and Garsin, D. A. (2009). Ce-Duox1/BLI-3 generates reactive oxygen species as a protective innate immune mechanism in *Caenorhabditis elegans*. *Infect. Immun.* 77, 4983–4989. doi: 10.1128/IAI.00627-09

Chávez, V., Mohri-Shiomi, A., Maadani, A., Vega, L. A., and Garsin, D. A. (2007). Oxidative stress enzymes are required for DAF-16-mediated immunity due to generation of reactive oxygen species by *Caenorhabditis elegans*. *Genetics* 176, 1567–1577. doi: 10.1534/genetics.107.072587

Chen, K., Kirber, M. T., Xiao, H., Yang, Y., and Keaney, J. F. Jr. (2008). Regulation of ROS signal transduction by NADPH oxidase 4 localization. *J. Cell Biol.* 181, 1129–1139. doi: 10.1083/jcb.200709049

Chen, X., Lee, K.-A., Ha, E.-M., Lee, K. M., Seo, Y. Y., Choi, H. K., et al. (2011). A specific and sensitive method for detection of hypochlorous acid for the imaging of microbe-induced HOCl production. *Chem. Commun.* 47, 4373–4375. doi: 10.1039/C1CC10589B

Cheng, G., Cao, Z., Xu, X., Van Meir, E. G., and Lambeth, J. D. (2001). Homologs of gp91phox: cloning and tissue expression of Nox3. Nox4, and Nox5. *Gene* 269, 131–140. doi: 10.1016/S0378-1119(01)00449-8

Chéret, C., Gervais, A., Lelli, A., Colin, C., Amar, L., Ravassard, P., et al. (2008). Neurotoxic activation of microglia is promoted by a Nox1-dependent NADPH Oxidase. *J. Neurosci.* 28:12039. doi: 10.1523/JNEUROSCI.3568-08.2008

Conti, F., Lugo-Reyes, S. O., Blancas Galicia, L., He, J., Aksu, G., Borges de Oliveira, E. Jr., et al. (2016). Mycobacterial disease in patients with chronic granulomatous disease: a retrospective analysis of 71 cases. *J. Allergy Clin. Immunol.* 138, 241–248.e3. doi: 10.1016/j.jaci.2015.11.041

Conway, K. L., Goel, G., Sokol, H., Manocha, M., Mizoguchi, E., Terhorst, C., et al. (2012). p40phox expression regulates neutrophil recruitment and function during the resolution phase of intestinal inflammation. *J. Immunol.* 189, 3631–3640. doi: 10.4049/jimmunol.1103746

Cooper, A. M., Segal, B. H., Frank, A. A., Holland, S. M., and Orme, I. M. (2000). Transient loss of resistance to pulmonary tuberculosis in p47phox-/- Mice. *Infect. Immun.* 68, 1231–1234. doi: 10.1128/iai.68.3.1231-1234.2000

de Luca, A., Smeekens, S. P., Casagrande, A., Iannitti, R., Conway, K. L., Gresnigt, M. S., et al. (2014). IL-1 receptor blockade restores autophagy and reduces inflammation in chronic granulomatous disease in mice and in humans. *Proc. Natl. Acad. Sci. U.S.A.* 111:3526. doi: 10.1073/pnas.1322831111

De Ravin, S. S., Zarember, K. A., Long-Priel, D., Chan, K. C., Fox, S. D., Gallin, J. I., et al. (2010). Tryptophan/kynurenine metabolism in human leukocytes is independent of superoxide and is fully maintained in chronic granulomatous disease. *Blood* 116, 1755–1760. doi: 10.1182/blood-2009-07-233734

Deffert, C., Schappi, M. G., Pache, J. C., Cachat, J., Vesin, D., Bisig, R., et al. (2014). *Bacillus* calmette-guerin infection in NADPH oxidase deficiency: defective mycobacterial sequestration and granuloma formation. *PLoS Pathog.* 10:e1004325. doi: 10.1371/journal.ppat.1004325

DeSilva, U., Miller, E., Görlach, A., Foster, C. B., Green, E. D., and Chanock, S. J. (2000). Molecular characterization of the mouse p47-phox (Ncf1) gene and comparative analysis of the mouse p47-phox (Ncf1) gene to the human NCF1 gene. *Mol. Cell Biol. Res. Commun.* 3, 224–230. doi: 10.1006/mcbr.2000.0214

Dhillon, S. S., Fattouh, R., Elkadri, A., Xu, W., Murchie, R., Walters, T., et al. (2014). Variants in nicotinamide adenine dinucleotide phosphate oxidase complex

components determine susceptibility to very early onset inflammatory bowel disease. *Gastroenterology* 147, 680–689.e2. doi: 10.1053/j.gastro.2014.06.005

Dostert, C., Pétrilli, V., Van Bruggen, R., Steele, C., Mossman, B. T., and Tschopp, J. (2008). Innate immune activation through Nalp3 inflammasome sensing of asbestos and silica. *Science* 320, 674–677. doi: 10.1126/science.1156995

Dunnill, C., Patton, T., Brennan, J., Barrett, J., Dryden, M., Cooke, J., et al. (2017). Reactive oxygen species (ROS) and wound healing: the functional role of ROS and emerging ROS-modulating technologies for augmentation of the healing process. *Int. Wound J.* 14, 89–96. doi: 10.1111/iwj.12557

Dupre-Crochet, S., Erard, M., and Nubetae, O. (2013). ROS production in phagocytes: why, when, and where? *J. Leukoc. Biol.* 94, 657–670. doi: 10.1189/jlb.1012544

Dupuy, C., Ohayon, R., Valent, A., Noël-Hudson, M.-S., Dème, D., and Virion, A. (1999). Purification of a novel flavoprotein involved in the thyroid NADPH oxidase cloning of the porcine and human cdnas. *J. Biol. Chem.* 274, 37265–37269. doi: 10.1074/jbc.274.52.37265

Dutta, D., Dobson, A. J., Houtz, P. L., Gläßer, C., Revah, J., Korzelius, J., et al. (2015). Regional cell-specific transcriptome mapping reveals regulatory complexity in the adult *Drosophila* midgut. *Cell Rep.* 12, 346–358. doi: 10.1016/j.celrep.2015.06.009

Dworakowski, R., Anilkumar, N., Zhang, M., and Shah, A. M. (2006). Redox signalling involving NADPH oxidase-derived reactive oxygen species. *Biochem. Soc. Trans.* 34, 960–964. doi: 10.1042/bst0340960

Edens, W. A., Sharling, L., Cheng, G., Shapira, R., Kinkade, J. M., Lee, T., et al. (2001). Tyrosine cross-linking of extracellular matrix is catalyzed by Duox, a multidomain oxidase/peroxidase with homology to the phagocyte oxidase subunit gp91 phox. *J. Cell Biol.* 154, 879–892. doi: 10.1083/jcb.200103132

El Hassani, R. A., Benfares, N., Caillou, B., Talbot, M., Sabourin, J.-C., Belotte, V., et al. (2005). Dual oxidase2 is expressed all along the digestive tract. *Am. J. Physiol. Gastrointest. Liver Physiol.* 288, G933–G942. doi: 10.1152/ajpgi.00198.2004

Falcone, E. L., Abusleme, L., Swamydas, M., Lionakis, M. S., Ding, L., Hsu, A. P., et al. (2016). Colitis susceptibility in p47(phox-/-) mice is mediated by the microbiome. *Microbiome* 4:13. doi: 10.1186/s40168-016-0159-0

Fattouh, R., Guo, C.-H., Lam, G. Y., Gareau, M. G., Ngan, B.-Y., Glogauer, M., et al. (2013). Rac2-deficiency leads to exacerbated and protracted colitis in response to *Citrobacter rodentium* infection. *PLoS One* 8:e61629. doi: 10.1371/journal.pone.0061629

Fauvarque, M. O., and Williams, M. J. (2011). Drosophila cellular immunity: a story of migration and adhesion. *J. Cell Sci.* 124, 1373–1382. doi: 10.1242/jcs.064592

Fogarty, C. E., Diwanji, N., Lindblad, J. L., Tare, M., Amcheslavsky, A., Makhijani, K., et al. (2016). Extracellular reactive oxygen species drive apoptosis-induced proliferation via *Drosophila Macrophages*. *Curr. Biol.* 26, 575–584. doi: 10.1016/j.cub.2015.12.064

Fontayne, A., Dang, P. M.-C., Gougerot-Pocidalo, M.-A., and El Benna, J. (2002). Phosphorylation of p47phox Sites by PKC α, βII, δ, and ζ:? effect on binding to p22phox and on NADPH oxidase activation. *Biochemistry* 41, 7743–7750. doi: 10.1021/bi011953s

Forteza, R., Salathe, M., Miot, F., Forteza, R., and Conner, G. E. (2005). Regulated hydrogen peroxide production by Duox in human airway epithelial cells. *Am. J. Respir. Cell Mol. Biol.* 32, 462–469. doi: 10.1165/rcmb.2004-0302OC

Fukai, T., and Ushio-Fukai, M. (2020). Cross-Talk between NADPH oxidase and mitochondria: role in ROS signaling and angiogenesis. *Cells* 9:1849. doi: 10.3390/cells9081849

Geiszt, M., Witta, J., Baff, J., Lekstrom, K., and Leto, T. L. (2003). Dual oxidases represent novel hydrogen peroxide sources supporting mucosal surface host defense. *FASEB J.* 17, 1502–1504. doi: 10.1096/fj.02-1104fje

George-Chandy, A., Nordström, I., Nygren, E., Jonsson, I. M., Postigo, J., Collins, L. V., et al. (2008). Th17 development and autoimmune arthritis in the absence of reactive oxygen species. *Eur. J. Immunol.* 38, 1118–1126. doi: 10.1002/eji.200737348

Gough, D. R., and Cotter, T. G. (2011). Hydrogen peroxide: a Jekyll and Hyde signalling molecule. *Cell Death Dis.* 2:e213. doi: 10.1038/cddis.2011.96

Gray Stephen, P., Di Marco, E., Okabe, J., Szyndralewiez, C., Heitz, F., Montezano Augusto, C., et al. (2013). NADPH Oxidase 1 plays a key role in diabetes mellitus–accelerated atherosclerosis. *Circulation* 127, 1888–1902. doi: 10.1161/CIRCULATIONAHA.112.132159

Grimm, M. J., Vethanayagam, R. R., Almyroudis, N. G., Dennis, C. G., Khan, A. N. H., D'Auria, A. C., et al. (2013). Monocyte- and macrophage-targeted NADPH oxidase mediates antifungal host defense and regulation of acute inflammation in mice. *J. Immunol.* 190:4175. doi: 10.4049/jimmunol.1202800

Ha, E.-M., Oh, C.-T., Bae, Y. S., and Lee, W.-J. (2005a). A direct role for dual oxidase in *Drosophila* gut immunity. *Science* 310, 847–850. doi: 10.1126/science.1117311

Ha, E.-M., Oh, C.-T., Ryu, J.-H., Bae, Y.-S., Kang, S.-W., Jang, I.-H., et al. (2005b). An antioxidant system required for host protection against gut infection in *Drosophila*. *Dev. Cell* 8, 125–132. doi: 10.1016/j.devcel.2004.11.007

Hall, C. J., Boyle, R. H., Astin, J. W., Flores, M. V., Oehlers, S. H., Sanderson, L. E., et al. (2013). Immunoresponsive gene 1 augments bactericidal activity of macrophage-lineage cells by regulating β-oxidation-dependent mitochondrial ROS production. *Cell Metab.* 18, 265–278. doi: 10.1016/j.cmet.2013.06.018

Hamanaka, R. B., and Chandel, N. S. (2010). Mitochondrial reactive oxygen species regulate cellular signaling and dictate biological outcomes. *Trends Biochem. Sci.* 35, 505–513. doi: 10.1016/j.tibs.2010.04.002

Han, W., Li, H., Cai, J., Gleaves, L. A., Polosukhin, V. V., Segal, B. H., et al. (2013). NADPH oxidase limits lipopolysaccharide-induced lung inflammation and injury in mice through reduction-oxidation regulation of NF-κB activity. *J. Immunol.* 190, 4786–4794. doi: 10.4049/jimmunol.1201809

Hanna, I. R., Hilenski, L. L., Dikalova, A., Taniyama, Y., Dikalov, S., Lyle, A., et al. (2004). Functional association of nox1 with p22phox in vascular smooth muscle cells. *Free Radic. Biol. Med.* 37, 1542–1549. doi: 10.1016/j.freeradbiomed.2004.08.011

Harvie, E. A., and Huttenlocher, A. (2015). Neutrophils in host defense: new insights from zebrafish. *J. Leukoc. Biol.* 98, 523–537. doi: 10.1189/jlb.4MR1114-524R

Helfinger, V., Palfi, K., Weigert, A., and Schröder, K. (2019). The NADPH oxidase Nox4 controls macrophage polarization in an NFκB-dependent manner. *Oxid. Med. Cell. Longev.* 2019:3264858. doi: 10.1155/2019/3264858

Henriet, S. S. V., Verweij, P. E., and Warris, A. (2012). *Aspergillus nidulans* and chronic granulomatous disease: a unique host–pathogen interaction. *J. Infect. Dis.* 206, 1128–1137. doi: 10.1093/infdis/jis473

Herb, M., Gluschko, A., Wiegmann, K., Farid, A., Wolf, A., Utermöhlen, O., et al. (2019). Mitochondrial reactive oxygen species enable proinflammatory signaling through disulfide linkage of NEMO. *Sci. Signal.* 12:eaar5926. doi: 10.1126/scisignal.aar5926

Hiroaki, H., Ago, T., Ito, T., Sumimoto, H., and Kohda, D. (2001). Solution structure of the PX domain, a target of the SH3 domain. *Nat. Struct. Biol.* 8, 526–530. doi: 10.1038/88591

Hole, P. S., Zabkiewicz, J., Munje, C., Newton, Z., Pearn, L., White, P., et al. (2013). Overproduction of NOX-derived ROS in AML promotes proliferation and is associated with defective oxidative stress signaling. *Blood* 122, 3322–3330. doi: 10.1182/blood-2013-04-491944

Holmdahl, R., Sareila, O., Olsson, L. M., Bäckdahl, L., and Wing, K. (2016). Ncf1 polymorphism reveals oxidative regulation of autoimmune chronic inflammation. *Immunol. Rev.* 269, 228–247. doi: 10.1111/imr.12378

Huang, J., Canadien, V., Lam, G. Y., Steinberg, B. E., Dinauer, M. C., Magalhaes, M. A. O., et al. (2009). Activation of antibacterial autophagy by NADPH oxidases. *Proc. Natl. Acad. Sci. U.S.A.* 106:6226. doi: 10.1073/pnas.0811045106

Hussain, N., Feld, J. J., Kleiner, D. E., Hoofnagle, J. H., Garcia-Eulate, R., Ahlawat, S., et al. (2007). Hepatic abnormalities in patients with chronic granulomatous disease. *Hepatology* 45, 675–683. doi: 10.1002/hep.21524

Iatsenko, I., Boquete, J. P., and Lemaitre, B. (2018). Microbiota-Derived lactate activates production of reactive oxygen species by the intestinal NADPH oxidase nox and shortens *Drosophila* lifespan. *Immunity* 49, 929–942e5. doi: 10.1016/j.immuni.2018.09.017

Inupakutika, M. A., Sengupta, S., Devireddy, A. R., Azad, R. K., and Mittler, R. (2016). The evolution of reactive oxygen species metabolism. *J. Exp. Bot.* 67, 5933–5943. doi: 10.1093/jxb/erw382

Jones, R. M., Luo, L., Ardita, C. S., Richardson, A. N., Kwon, Y. M., Mercante, J. W., et al. (2013). Symbiotic *Lactobacilli* stimulate gut epithelial proliferation via Nox-mediated generation of reactive oxygen species. *EMBO J.* 32, 3017–3028. doi: 10.1038/emboj.2013.224

Jones, R. M., and Neish, A. S. (2017). Redox signaling mediated by the gut microbiota. *Free Radic. Biol. Med.* 105, 41–47. doi: 10.1016/j.freeradbiomed.2016.10.495

Jürgens, B., Fuchs, D., Reichenbach, J., and Heitger, A. (2010). Intact indoleamine 2,3-dioxygenase activity in human chronic granulomatous disease. *Clin. Immunol.* 116, 1–4. doi: 10.1016/j.clim.2010.05.007

Kawahara, T., and Lambeth, J. D. (2007). Molecular evolution of Phox-related regulatory subunits for NADPH oxidase enzymes. *BMC Evol. Biol.* 7:178. doi: 10.1186/1471-2148-7-178

Kawahara, T., Quinn, M. T., and Lambeth, J. D. (2007). Molecular evolution of the reactive oxygen-generating NADPH oxidase (Nox/Duox) family of enzymes. *BMC Evol. Biol.* 7:109. doi: 10.1186/1471-2148-7-109

Kelkka, T., Kienhöfer, D., Hoffmann, M., Linja, M., Wing, K., Sareila, O., et al. (2014). Reactive oxygen species deficiency induces autoimmunity with type 1 interferon signature. *Antioxid. Redox Signal.* 21, 2231–2245. doi: 10.1089/ars.2013.5828

Kim, J.-S., Huang, T. Y., and Bokoch, G. M. (2009). Reactive oxygen species regulate a slingshot-cofilin activation pathway. *Mol. Biol. Cell* 20, 2650–2660. doi: 10.1091/mbc.e09-02-0131

Kim, Y.-M., Kim, S.-J., Tatsunami, R., Yamamura, H., Fukai, T., and Ushio-Fukai, M. (2017). ROS-induced ROS release orchestrated by Nox4, Nox2, and mitochondria in VEGF signaling and angiogenesis. *Am. J. Physiol. Cell Physiol.* 312, C749–C764. doi: 10.1152/ajpcell.00346.2016

Knaus, U. G., Hertzberger, R., Pircalabioru, G. G., Yousefi, S. P. M., and Branco dos Santos, F. (2017). Pathogen control at the intestinal mucosa – H2O2 to the rescue. *Gut Microbes* 8, 67–74. doi: 10.1080/19490976.2017.1279378

Kobayashi, E. H., Suzuki, T., Funayama, R., Nagashima, T., Hayashi, M., Sekine, H., et al. (2016). Nrf2 suppresses macrophage inflammatory response by blocking proinflammatory cytokine transcription. *Nat. Commun.* 7:11624. doi: 10.1038/ncomms11624

Kobayashi, S. D., Voyich, J. M., Braughton, K. R., Whitney, A. R., Nauseef, W. M., Malech, H. L., et al. (2004). Gene expression profiling provides insight into the pathophysiology of chronic granulomatous disease. *J. Immunol.* 172:636. doi: 10.4049/jimmunol.172.1.636

Konaté, M. M., Antony, S., and Doroshow, J. H. (2020). Inhibiting the activity of NADPH oxidase in cancer. *Antioxid. Redox Signal.* 33, 435–454. doi: 10.1089/ars.2020.8046

Kraaij, M. D., Savage, N. D. L., van der Kooij, S. W., Koekkoek, K., Wang, J., van den Berg, J. M., et al. (2010). Induction of regulatory T cells by macrophages is dependent on production of reactive oxygen species. *Proc. Natl. Acad. Sci. U.S.A.* 107, 17686–17691. doi: 10.1073/pnas.1012016107

Kuhns, D. B., Alvord, W. G., Heller, T., Feld, J. J., Pike, K. M., Marciano, B. E., et al. (2010). Residual NADPH oxidase and survival in chronic granulomatous disease. *N. Engl. J. Med.* 363, 2600–2610. doi: 10.1056/NEJMoa1007097

Kumar, A., Baruah, A., Tomioka, M., Iino, Y., Kalita, M. C., and Khan, M. (2020). Caenorhabditis elegans: a model to understand host–microbe interactions. *Cell. Mol. Life Sci.* 77, 1229–1249. doi: 10.1007/s00018-019-03319-7

Lam, G. Y., Huang, J., and Brumell, J. H. (2010). The many roles of NOX2 NADPH oxidase-derived ROS in immunity. *Semin. Immunopathol.* 32, 415–430. doi: 10.1007/s00281-010-0221-0

Lambeth, J. D. (2004). NOX enzymes and the biology of reactive oxygen. *Nat. Rev. Immunol.* 4, 181–189. doi: 10.1038/nri1312

Lambeth, J. D., Cheng, G., Arnold, R. S., and Edens, W. A. (2000). Novel homologs of gp91phox. *Trends Biochem. Sci.* 25, 459–461. doi: 10.1016/s0968-0004(00)01658-3

Lambou, K., Lamarre, C., Beau, R., Dufour, N., and Latge, J.-P. (2010). Functional analysis of the superoxide dismutase family in *Aspergillus fumigatus*. *Mol. Microbiol.* 75, 910–923. doi: 10.1111/j.1365-2958.2009.07024.x

Lawrence, S. M., Corriden, R., and Nizet, V. (2020). How neutrophils meet their end. *Trends Immunol.* 41, 531–544. doi: 10.1016/j.it.2020.03.008

Lee, C. F., Qiao, M., Schröder, K., Zhao, Q., and Asmis, R. (2010). Nox4 is a novel inducible source of reactive oxygen species in monocytes and macrophages and mediates OxLDL-induced macrophage death. *Circ. Res.* 106:1489. doi: 10.1161/CIRCRESAHA.109.215392

Lee, K.-A., Kim, S.-H., Kim, E.-K., Ha, E.-M., You, H., Kim, B., et al. (2013). Bacterial-derived uracil as a modulator of mucosal immunity and gut-microbe homeostasis in *Drosophila*. *Cell* 153, 797–811. doi: 10.1016/j.cell.2013.04.009

Lelli, A., Gervais, A., Colin, C., Chéret, C., de Almodovar, C. R., Carmeliet, P., et al. (2013). The NADPH oxidase Nox2 regulates VEGFR1/CSF-1R-mediated microglial chemotaxis and promotes early postnatal infiltration of phagocytes in the subventricular zone of the mouse cerebral cortex. *Glia* 61, 1542–1555. doi: 10.1002/glia.22540

Li, B., Bedard, K., Sorce, S., Hinz, B., Dubois-Dauphin, M., and Krause, K. H. (2009). NOX4 expression in human microglia leads to constitutive generation of reactive oxygen species and to constitutive IL-6 expression. *J. Innate Immun.* 1, 570–581. doi: 10.1159/000235563

Li, W.-G., Miller, F. J., Zhang, H. J., Spitz, D. R., Oberley, L. W., and Weintraub, N. L. (2001). H2O2-induced O? 2production by a non-phagocytic NAD (P) H oxidase causes oxidant injury. *J. Biol. Chem.* 276, 29251–29256. doi: 10.1074/jbc.M102124200

Linnerz, T., and Hall, C. J. (2020). The diverse roles of phagocytes during bacterial and fungal infections and sterile inflammation: lessons from zebrafish. *Front. Immunol.* 11:1094. doi: 10.3389/fimmu.2020.01094

Liu, X., Hodgson, J. J., and Buchon, N. (2017). Drosophila as a model for homeostatic, antibacterial, and antiviral mechanisms in the gut. *PLoS Pathogens* 13:e1006277. doi: 10.1371/journal.ppat.1006277

Maghzal, G. J., Winter, S., Wurzer, B., Chong, B. H., Holmdahl, R., and Stocker, R. (2014). Tryptophan catabolism is unaffected in chronic granulomatous disease. *Nature* 514, E16–E17. doi: 10.1038/nature13844

Maitra, U., Singh, N., Gan, L., Ringwood, L., and Li, L. (2009). IRAK-1 contributes to lipopolysaccharide-induced reactive oxygen species generation in macrophages by inducing NOX-1 transcription and Rac1 activation and suppressing the expression of antioxidative enzymes. *J. Biol. Chem.* 284, 35403–35411. doi: 10.1074/jbc.M109.059501

Manea, A., Manea, S.-A., Gan, A. M., Constantin, A., Fenyo, I. M., Raicu, M., et al. (2015). Human monocytes and macrophages express NADPH oxidase 5; a potential source of reactive oxygen species in atherosclerosis. *Biochem. Biophys. Res. Commun.* 461, 172–179. doi: 10.1016/j.bbrc.2015.04.021

Mantegazza, A. R., Savina, A., Vermeulen, M., Pérez, L., Geffner, J., Hermine, O., et al. (2008). NADPH oxidase controls phagosomal pH and antigen cross-presentation in human dendritic cells. *Blood* 112, 4712–4722. doi: 10.1182/blood-2008-01-134791

Marciano, B. E., Spalding, C., Fitzgerald, A., Mann, D., Brown, T., Osgood, S., et al. (2015). Common severe infections in chronic granulomatous disease. *Clin. Infect. Dis.* 60, 1176–1183. doi: 10.1093/cid/ciu1154

Marciano, B. E., Zerbe, C. S., Falcone, E. L., Ding, L., DeRavin, S. S., Daub, J., et al. (2018). X-linked carriers of chronic granulomatous disease: illness, lyonization, and stability. *J. Allergy Clin. Immunol.* 141, 365–371. doi: 10.1016/j.jaci.2017.04.035

Marks, D. J., Miyagi, K., Rahman, F. Z., Novelli, M., Bloom, S. L., and Segal, A. W. (2009). Inflammatory bowel disease in CGD reproduces the clinicopathological features of Crohn's disease. *Am. J. Gastroenterol.* 104, 117–124. doi: 10.1038/ajg.2008.72

Martinez, J., Malireddi, R. K. S., Lu, Q., Cunha, L. D., Pelletier, S., Gingras, S., et al. (2015). Molecular characterization of LC3-associated phagocytosis reveals distinct roles for Rubicon. NOX2 and autophagy proteins. *Nat. Cell Biol.* 17, 893–906. doi: 10.1038/ncb3192

Marzaioli, V., Hurtado-Nedelec, M., Pintard, C., Tlili, A., Marie, J. C., Monteiro, R. C., et al. (2017). NOX5 and p22phox are 2 novel regulators of human monocytic differentiation into dendritic cells. *Blood* 130, 1734–1745. doi: 10.1182/blood-2016-10-746347

Masud, S., Prajsnar, T. K., Torraca, V., Lamers, G. E. M., Benning, M., Van Der Vaart, M., et al. (2019). Macrophages target *Salmonella* by Lc3-associated phagocytosis in a systemic infection model. *Autophagy* 15, 796–812. doi: 10.1080/15548627.2019.1569297

Matthews, J. R., Wakasugi, N., Virelizier, J. L., Yodoi, J., and Hay, R. T. (1992). Thioredoxin regulates the DNA binding activity of NF-kappa B by reduction of a disulphide bond involving cysteine 62. *Nucleic Acids Res.* 20, 3821–3830. doi: 10.1093/nar/20.15.3821

Meissner, F., Seger, R. A., Moshous, D., Fischer, A., Reichenbach, J., and Zychlinsky, A. (2010). Inflammasome activation in NADPH oxidase defective mononuclear phagocytes from patients with chronic granulomatous disease. *Blood* 116, 1570–1573. doi: 10.1182/blood-2010-01-264218

Meitzler, J. L., and Ortiz de Montellano, P. R. (2009). *Caenorhabditis elegans* and human dual oxidase 1 (DUOX1) "peroxidase" domains: insights into heme

binding and catalytic activity. *J. Biol. Chem.* 284, 18634–18643. doi: 10.1074/jbc.M109.013581

Mills, E. L., and O'Neill, L. A. (2016). Reprogramming mitochondrial metabolism in macrophages as an anti-inflammatory signal. *Eur. J. Immunol.* 46, 13–21. doi: 10.1002/eji.201445427

Minakami, R., and Sumimoto, H. (2006). Phagocytosis-coupled activation of the superoxide-producing phagocyte oxidase, a member of the NADPH oxidase (nox) family. *Int. J. Hematol.* 84, 193–198. doi: 10.1532/IJH97.06133

Miyano, K., and Sumimoto, H. (2012). "Assessment of the role for Rho family GTPases in NADPH oxidase Activation," in *Rho GTPases: Methods and Protocols*, ed. F. Rivero (New York, NY: Springer).

Morand, S., Ueyama, T., Tsujibe, S., Saito, N., Korzeniowska, A., and Leto, T. L. (2009). Duox maturation factors form cell surface complexes with Duox affecting the specificity of reactive oxygen species generation. *FASEB J.* 23, 1205–1218. doi: 10.1096/fj.08-120006

Morgan, M. J., and Liu, Z.-G. (2010). Reactive oxygen species in TNFα-induced signaling and cell death. *Mol. Cells* 30, 1–12.

Morgenstern, D. E., Gifford, M. A., Li, L. L., Doerschuk, C. M., and Dinauer, M. C. (1997). Absence of respiratory burst in X-linked chronic granulomatous disease mice leads to abnormalities in both host defense and inflammatory response to *Aspergillus fumigatus*. *J. Exp. Med.* 185, 207–218. doi: 10.1084/jem.185.2.207

Muri, J., Thut, H., Feng, Q., and Kopf, M. (2020). Thioredoxin-1 distinctly promotes NF-κB target DNA binding and NLRP3 inflammasome activation independently of Txnip. *eLife* 9:e53627. doi: 10.7554/eLife.53627

Myers, A. L., Harris, C. M., Choe, K.-M., and Brennan, C. A. (2018). Inflammatory production of reactive oxygen species by *Drosophila* hemocytes activates cellular immune defenses. *Biochem. Biophys. Res. Commun.* 505, 726–732. doi: 10.1016/j.bbrc.2018.09.126

Nauseef, W. M. (2004). Assembly of the phagocyte NADPH oxidase. *Histochem. Cell Biol.* 122, 277–291. doi: 10.1007/s00418-004-0679-8

Nauseef, W. M. (2019). The phagocyte NOX2 NADPH oxidase in microbial killing and cell signaling. *Curr. Opin. Immunol.* 60, 130–140. doi: 10.1016/j.coi.2019.05.006

Nayernia, Z., Jaquet, V., and Krause, K.-H. (2013). New insights on NOX enzymes in the central nervous system. *Antioxid. Redox Signal.* 20, 2815–2837. doi: 10.1089/ars.2013.5703

Nell, S., Suerbaum, S., and Josenhans, C. (2010). The impact of the microbiota on the pathogenesis of IBD: lessons from mouse infection models. *Nat. Rev. Microbiol.* 8, 564–577. doi: 10.1038/nrmicro2403

Netea, M. G., van de Veerdonk, F. L., van der Meer, J. W. M., Dinarello, C. A., and Joosten, L. A. B. (2015). Inflammasome-independent regulation of IL-1-Family Cytokines. *Annu. Rev. Immunol.* 33, 49–77. doi: 10.1146/annurev-immunol-032414-112306

Nguyen, G. T., Green, E. R., and Mecsas, J. (2017). Neutrophils to the ROScue: mechanisms of NADPH oxidase activation and bacterial resistance. *Front. Cell Infect. Microbiol.* 7:373. doi: 10.3389/fcimb.2017.00373

Niethammer, P., Grabher, C., Look, A. T., and Mitchison, T. J. (2009). A tissue-scale gradient of hydrogen peroxide mediates rapid wound detection in zebrafish. *Nature* 459, 996–999. doi: 10.1038/nature08119

Owusu-Ansah, E., and Banerjee, U. (2009). Reactive oxygen species prime *Drosophila* haematopoietic progenitors for differentiation. *Nature* 461, 537–541. doi: 10.1038/nature08313

Panday, A., Sahoo, M. K., Osorio, D., and Batra, S. (2015). NADPH oxidases: an overview from structure to innate immunity-associated pathologies. *Cell. Mol. Immunol.* 12, 5–23. doi: 10.1038/cmi.2014.89

Pase, L., Layton, J. E., Wittmann, C., Ellett, F., Nowell, C. J., Reyes-Aldasoro, C. C., et al. (2012). Neutrophil-delivered myeloperoxidase dampens the hydrogen peroxide burst after tissue wounding in zebrafish. *Curr. Biol.* 22, 1818–1824. doi: 10.1016/j.cub.2012.07.060

Perše, M., and Cerar, A. (2012). Dextran sodium sulphate colitis mouse model: traps and tricks. *J. Biomed. Biotechnol.* 2012, 718617. doi: 10.1155/2012/718617

Pircalabioru, G., Aviello, G., Kubica, M., Zhdanov, A., Paclet, M.-H., Brennan, L., et al. (2016). Defensive mutualism rescues NADPH oxidase inactivation in gut infection. *Cell Host Microbe* 19, 651–663. doi: 10.1016/j.chom.2016.04.007

Pizzolla, A., Hultqvist, M., Nilson, B., Grimm, M. J., Eneljung, T., Jonsson, I. M., et al. (2012). Reactive oxygen species produced by the NADPH oxidase 2 complex in monocytes protect mice from bacterial infections. *J. Immunol.* 188, 5003–5011. doi: 10.4049/jimmunol.1103430

Pollock, J. D., Williams, D. A., Gifford, M. A. C., Li, L. L., Du, X., Fisherman, J., et al. (1995). Mouse model of X–linked chronic granulomatous disease, an inherited defect in phagocyte superoxide production. *Nat. Genet.* 9, 202–209. doi: 10.1038/ng0295-202

Rendra, E., Riabov, V., Mossel, D. M., Sevastyanova, T., Harmsen, M. C., and Kzhyshkowska, J. (2019). Reactive oxygen species (ROS) in macrophage activation and function in diabetes. *Immunobiology* 224, 242–253. doi: 10.1016/j.imbio.2018.11.010

Renwick, J., Reeves, E. P., Wientjes, F. B., and Kavanagh, K. (2007). Translocation of proteins homologous to human neutrophil p47phox and p67phox to the cell membrane in activated hemocytes of *Galleria mellonella*. *Dev. Comp. Immunol.* 31, 347–359. doi: 10.1016/j.dci.2006.06.007

Rodrigues-Sousa, T., Ladeirinha, A. F., Santiago, A. R., Carvalheiro, H., Raposo, B., Alarcão, A., et al. (2014). Deficient production of reactive oxygen species leads to severe chronic DSS-induced colitis in Ncf1/p47 phox-mutant mice. *PLoS One* 9:e97532. doi: 10.1371/journal.pone.0097532

Röhm, M., Grimm, M. J., D'Auria, A. C., Almyroudis, N. G., Segal, B. H., and Urban, C. F. (2014). NADPH oxidase promotes neutrophil extracellular trap formation in pulmonary aspergillosis. *Infect. Immun.* 82, 1766–1777. doi: 10.1128/iai.00096-14

Romani, L., Fallarino, F., De Luca, A., Montagnoli, C., D'Angelo, C., Zelante, T., et al. (2008). Defective tryptophan catabolism underlies inflammation in mouse chronic granulomatous disease. *Nature* 451, 211–215. doi: 10.1038/nature06471

Rosen, H., and Michel, B. R. (1997). Redundant contribution of myeloperoxidase-dependent systems to neutrophil-mediated killing of *Escherichia coli*. *Infect. Immun.* 65, 4173–4178. doi: 10.1128/IAI.65.10.4173-4178.1997

Rothfork, J. M., Timmins, G. S., Harris, M. N., Chen, X., Lusis, A. J., Otto, M., et al. (2004). Inactivation of a bacterial virulence pheromone by phagocyte-derived oxidants: new role for the NADPH oxidase in host defense. *Proc. Natl. Acad. Sci. U.S.A.* 101:13867. doi: 10.1073/pnas.0402996101

Rybicka, J. M., Balce, D. R., Chaudhuri, S., Allan, E. R. O., and Yates, R. M. (2012). Phagosomal proteolysis in dendritic cells is modulated by NADPH oxidase in a pH-independent manner. *EMBO J.* 31, 932–944. doi: 10.1038/emboj.2011.440

Salminen, T. S., and Vale, P. F. (2020). *Drosophila* as a Model system to investigate the effects of mitochondrial variation on innate immunity. *Front. Immunol.* 11:521. doi: 10.3389/fimmu.2020.00521

Savina, A., Jancic, C., Hugues, S., Guermonprez, P., Vargas, P., Moura, I. C., et al. (2006). NOX2 controls phagosomal pH to regulate antigen processing during crosspresentation by dendritic cells. *Cell* 126, 205–218. doi: 10.1016/j.cell.2006.05.035

Schäppi, M., Deffert, C., Fiette, L., Gavazzi, G., Herrmann, F., Belli, D., et al. (2008). Branched fungal beta-glucan causes hyperinflammation and necrosis in phagocyte NADPH oxidase-deficient mice. *J. Pathol.* 214, 434–444. doi: 10.1002/path.2298

Schäppi, M. G., Jaquet, V., Belli, D. C., and Krause, K. H. (2008). Hyperinflammation in chronic granulomatous disease and anti-inflammatory role of the phagocyte NADPH oxidase. *Semin. Immunopathol.* 30, 255–271. doi: 10.1007/s00281-008-0119-2

Schenk, B., and Fulda, S. (2015). Reactive oxygen species regulate Smac mimetic/TNFα-induced necroptotic signaling and cell death. *Oncogene* 34, 5796–5806. doi: 10.1038/onc.2015.35

Schoen, T. J., Rosowski, E. E., Knox, B. P., Bennin, D., Keller, N. P., and Huttenlocher, A. (2020). Neutrophil phagocyte oxidase activity controls invasive fungal growth and inflammation in zebrafish. *J. Cell Sci.* 133, jcs236539. doi: 10.1242/jcs.236539

Segal, B. H., Han, W., Bushey, J. J., Joo, M., Bhatti, Z., Feminella, J., et al. (2010). NADPH oxidase limits innate immune responses in the lungs in mice. *PLoS One* 5:e9631. doi: 10.1371/journal.pone.0009631

Sinenko, S. A., Shim, J., and Banerjee, U. (2012). Oxidative stress in the haematopoietic niche regulates the cellular immune response in *Drosophila*. *EMBO Rep.* 13, 83–89. doi: 10.1038/embor.2011.223

Singel, K. L., and Segal, B. H. (2016). NOX2-dependent regulation of inflammation. *Clin. Sci.* 130, 479–490. doi: 10.1042/CS20150660

Sorescu, D., Weiss, D., Lassègue, B., Clempus Roza, E., Szöcs, K., Sorescu George, P., et al. (2002). Superoxide production and expression of nox family proteins in human atherosclerosis. *Circulation* 105, 1429–1435. doi: 10.1161/01.CIR.0000012917.74432.66

Suh, C. I., Stull, N. D., Li, X. J., Tian, W., Price, M. O., Grinstein, S., et al. (2006). The phosphoinositide-binding protein p40phox activates the NADPH oxidase during FcgammaIIA receptor-induced phagocytosis. *J. Exp. Med.* 203, 1915–1925. doi: 10.1084/jem.20052085

Sumimoto, H. (2008). Structure, regulation and evolution of Nox-family NADPH oxidases that produce reactive oxygen species. *FEBS J.* 275, 3249–3277. doi: 10.1111/j.1742-4658.2008.06488.x

Sumimoto, H., Miyano, K., and Takeya, R. (2005). Molecular composition and regulation of the Nox family NAD (P) H oxidases. *Biochem. Biophys. Res. Commun.* 338, 677–686.

Sundqvist, M., Christenson, K., Björnsdottir, H., Osla, V., Karlsson, A., Dahlgren, C., et al. (2017). Elevated mitochondrial reactive oxygen species and cellular redox imbalance in human NADPH-oxidase-deficient phagocytes. *Front. Immunol.* 8:1828. doi: 10.3389/fimmu.2017.01828

Szanto, I., Rubbia-Brandt, L., Kiss, P., Steger, K., Banfi, B., Kovari, E., et al. (2005). Expression of NOX1, a superoxide-generating NADPH oxidase, in colon cancer and inflammatory bowel disease. *J. Pathol.* 207, 164–176. doi: 10.1002/path.1824

Tattikota, S. G., Cho, B., Liu, Y., Hu, Y., Barrera, V., Steinbaugh, M. J., et al. (2020). A single-cell survey of *Drosophila* blood. *eLife* 9:e54818. doi: 10.7554/eLife.54818

Thomas, D. C., Charbonnier, L.-M., Schejtman, A., Aldhekri, H., Coomber, E. L., Dufficy, E. R., et al. (2019). EROS/CYBC1 mutations: decreased NADPH oxidase function and chronic granulomatous disease. *J. Allergy Clin. Immunol.* 143, 782–785.e1. doi: 10.1016/j.jaci.2018.09.019

Thomas, D. C., Clare, S., Sowerby, J. M., Pardo, M., Juss, J. K., Goulding, D. A., et al. (2017). Eros is a novel transmembrane protein that controls the phagocyte respiratory burst and is essential for innate immunity. *J. Exp. Med.* 214, 1111–1128. doi: 10.1084/jem.20161382

Touyz, R. M., Anagnostopoulou, A., Rios, F., Montezano, A. C., and Camargo, L. L. (2019). NOX5: molecular biology and pathophysiology. *Exp. Physiol.* 104, 605–616. doi: 10.1113/EP086204

Trevelin, S. C., dos Santos, C. X., Ferreira, R. G., de Sá Lima, L., Silva, R. L., Scavone, C., et al. (2016). Apocynin and Nox2 regulate NF-κB by modifying thioredoxin-1 redox-state. *Sci. Rep.* 6:34581. doi: 10.1038/srep34581

Trinder, M., Daisley, B. A., Dube, J. S., and Reid, G. (2017). *Drosophila melanogaster* as a high-throughput model for host-microbiota interactions. *Front. Microbiol.* 8:751. doi: 10.3389/fmicb.2017.00751

van Bruggen, R., Köker, M. Y., Jansen, M., van Houdt, M., Roos, D., Kuijpers, T. W., et al. (2010). Human NLRP3 inflammasome activation is Nox1-4 independent. *Blood* 115, 5398–5400. doi: 10.1182/blood-2009-10-250803

van de Geer, A., Nieto-Patlán, A., Kuhns, D. B., Tool, A. T. J., Arias, A. A., Bouaziz, M., et al. (2018). Inherited p40phox deficiency differs from classic chronic granulomatous disease. *J. Clin. Invest.* 128, 3957–3975. doi: 10.1172/JCI97116

van de Veerdonk, F. L., Smeekens, S. P., Joosten, L. A. B., Kullberg, B. J., Dinarello, C. A., van der Meer, J. W. M., et al. (2010). Reactive oxygen species–independent activation of the IL-1β inflammasome in cells from patients with chronic granulomatous disease. *PNAS* 107, 3030–3033. doi: 10.1073/pnas.0914795107

van den Berg, J. M., van Koppen, E., Ahlin, A., Belohradsky, B. H., Bernatowska, E., Corbeel, L., et al. (2009). Chronic granulomatous disease: the European experience. *PLoS One* 4:e5234. doi: 10.1371/journal.pone.0005234

van der Hoeven, R., Cruz, M. R., Chávez, V., and Garsin, D. A. (2015). Localization of the dual oxidase BLI-3 and characterization of its NADPH oxidase domain during infection of *Caenorhabditis elegans*. *PloS One* 10:e0124091. doi: 10.1371/journal.pone.0124091

Van Der Hoeven, R., McCallum, K. C., Cruz, M. R., and Garsin, D. A. (2011). Ce-Duox1/BLI-3 generated reactive oxygen species trigger protective SKN-1 activity via p38 MAPK signaling during infection in C. elegans. *PLoS Pathog* 7:e1002453. doi: 10.1371/journal.ppat.1002453

van der Weyden, L., Speak, A. O., Swiatkowska, A., Clare, S., Schejtman, A., Santilli, G., et al. (2018). Pulmonary metastatic colonisation and granulomas in NOX2-deficient mice. *J,. Pathol.* 246, 300–310. doi: 10.1002/path.5140

Wang, L., Kounatidis, I., and Ligoxygakis, P. (2014). Drosophila as a model to study the role of blood cells in inflammation, innate immunity and cancer. *Front. Cell. Infect. Microbiol.* 3:113. doi: 10.3389/fcimb.2013.00113

Warnatsch, A., Tsourouktsoglou, T.-D., Branzk, N., Wang, Q., Reincke, S., Herbst, S., et al. (2017). Reactive oxygen species localization programs inflammation to clear microbes of different size. *Immunity* 46, 421–432. doi: 10.1016/j.immuni.2017.02.013

Weisser, M., Demel, U. M., Stein, S., Chen-Wichmann, L., Touzot, F., Santilli, G., et al. (2016). Hyperinflammation in patients with chronic granulomatous disease leads to impairment of hematopoietic stem cell functions. *J. Allergy Clin. Immunol.* 138, 219–228.e9. doi: 10.1016/j.jaci.2015.11.028

West, A. P., Brodsky, I. E., Rahner, C., Woo, D. K., Erdjument-Bromage, H., Tempst, P., et al. (2011). TLR signalling augments macrophage bactericidal activity through mitochondrial ROS. *Nature* 472, 476–480. doi: 10.1038/nature09973

Wiemann, P., Perevitsky, A., Lim, F. Y., Shadkchan, Y., Knox, B. P., Landero Figueora, J. A., et al. (2017). *Aspergillus fumigatus* copper export machinery and reactive oxygen intermediate defense counter host copper-mediated oxidative antimicrobial offense. *Cell Rep.* 19, 1008–1021. doi: 10.1016/j.celrep.2017.04.019

Wilson, C., and González-Billault, C. (2015). Regulation of cytoskeletal dynamics by redox signaling and oxidative stress: implications for neuronal development and trafficking. *Front. Cell. Neurosci.* 9:381. doi: 10.3389/fncel.2015.00381

Winkelstein, J. A., Marino, M. C., Johnston, R. B. Jr., Boyle, J., Curnutte, J., Gallin, J. I., et al. (2000). Chronic granulomatous disease: report on a national registry of 368 patients. *Medicine* 79, 155–169. doi: 10.1097/00005792-200005000-00003

Wirtz, S., Popp, V., Kindermann, M., Gerlach, K., Weigmann, B., Fichtner-Feigl, S., et al. (2017). Chemically induced mouse models of acute and chronic intestinal inflammation. *Nat. Protoc.* 12, 1295–1309. doi: 10.1038/nprot.2017.044

Wong, C. N., Ng, P., and Douglas, A. E. (2011). Low-diversity bacterial community in the gut of the fruitfly *Drosophila melanogaster*. *Environ. Microbiol.* 13, 1889–1900. doi: 10.1111/j.1462-2920.2011.02511.x

Wu, D.-C., Ré, D. B., Nagai, M., Ischiropoulos, H., and Przedborski, S. (2006). The inflammatory NADPH oxidase enzyme modulates motor neuron degeneration in amyotrophic lateral sclerosis mice. *Proc. Natl. Acad. Sci.* 103:12132. doi: 10.1073/pnas.0603670103

Xu, Q., Choksi, S., Qu, J., Jang, J., Choe, M., Banfi, B., et al. (2016). NADPH oxidases are essential for macrophage differentiation. *J. Biol. Chem.* 291, 20030–20041. doi: 10.1074/jbc.M116.731216

Yang, C.-T., Cambier, C. J., Davis, J. M., Hall, Christopher, J., Crosier, P. S., et al. (2012). Neutrophils exert protection in the early tuberculous granuloma by oxidative killing of mycobacteria phagocytosed from infected macrophages. *Cell Host Microbe* 12, 301–312. doi: 10.1016/j.chom.2012.07.009

Yang, W., Tao, Y., Wu, Y., Zhao, X., Ye, W., Zhao, D., et al. (2019). Neutrophils promote the development of reparative macrophages mediated by ROS to orchestrate liver repair. *Nat. Commun.* 10:1076. doi: 10.1038/s41467-019-09046-8

Yoo, S. K., Starnes, T. W., Deng, Q., and Huttenlocher, A. (2011). Lyn is a redox sensor that mediates leukocyte wound attraction in vivo. *Nature* 480, 109–112. doi: 10.1038/nature10632

Yuzawa, S., Ogura, K., Horiuchi, M., Suzuki, N. N., Fujioka, Y., Kataoka, M., et al. (2004). Solution structure of the tandem Src homology 3 domains of p47phox in an autoinhibited form. *J. Biol. Chem.* 279, 29752–29760. doi: 10.1074/jbc.M401457200

Zhang, J., Wang, X., Vikash, V., Ye, Q., Wu, D., Liu, Y., et al. (2016). ROS and ROS-mediated cellular signaling. *Oxid. Med. Cell. Longev.* 2016:4350965. doi: 10.1155/2016/4350965

Zhang, Y., Choksi, S., Chen, K., Pobezinskaya, Y., Linnoila, I., and Liu, Z.-G. (2013). ROS play a critical role in the differentiation of alternatively activated macrophages and the occurrence of tumor-associated macrophages. *Cell Res.* 23, 898–914. doi: 10.1038/cr.2013.75

Zhou, R., Yazdi, A. S., Menu, P., and Tschopp, J. (2011). A role for mitochondria in NLRP3 inflammasome activation. *Nature* 469, 221–225. doi: 10.1038/nature09663

Conflict of Interest: The authors declare that the research was conducted in the absence of any commercial or financial relationships that could be construed as a potential conflict of interest.

frontiers in Cell and Developmental Biology

REVIEW
published: 08 April 2021
doi: 10.3389/fcell.2021.649937

Prenatal Development and Function of Human Mononuclear Phagocytes

Mohi Miah[1†], *Issac Goh*[1†] *and Muzlifah Haniffa*[1,2,3*]

[1] Biosciences Institute, Newcastle University, Newcastle upon Tyne, United Kingdom, [2] Department of Dermatology and NIHR Newcastle Biomedical Research Centre, Newcastle Hospitals NHS Foundation Trust, Newcastle upon Tyne, United Kingdom, [3] Wellcome Sanger Institute, Hinxton, United Kingdom

OPEN ACCESS

Edited by:
Efstathios G. Stamatiades, Charité – Universitätsmedizin Berlin, Germany

Reviewed by:
Christian Schulz, Ludwig Maximilian University of Munich, Germany
Slava Epelman, University Health Network (UHN), Canada
Marc Dalod, Centre National de la Recherche Scientifique (CNRS), France

***Correspondence:**
Muzlifah Haniffa
m.a.haniffa@ncl.ac.uk

[†] These authors have contributed equally to this work

Specialty section:
This article was submitted to Cell Death and Survival, a section of the journal Frontiers in Cell and Developmental Biology

Received: 05 January 2021
Accepted: 01 March 2021
Published: 08 April 2021

Citation:
Miah M, Goh I and Haniffa M (2021) Prenatal Development and Function of Human Mononuclear Phagocytes. Front. Cell Dev. Biol. 9:649937. doi: 10.3389/fcell.2021.649937

The human mononuclear phagocyte (MP) system, which includes dendritic cells, monocytes, and macrophages, is a critical regulator of innate and adaptive immune responses. During embryonic development, MPs derive sequentially in yolk sac progenitors, fetal liver, and bone marrow haematopoietic stem cells. MPs maintain tissue homeostasis and confer protective immunity in post-natal life. Recent evidence – primarily in animal models – highlight their critical role in coordinating the remodeling, maturation, and repair of target organs during embryonic and fetal development. However, the molecular regulation governing chemotaxis, homeostasis, and functional diversification of resident MP cells in their respective organ systems during development remains elusive. In this review, we summarize the current understanding of the development and functional contribution of tissue MPs during human organ development and morphogenesis and its relevance to regenerative medicine. We outline how single-cell multi-omic approaches and next-generation *ex-vivo* organ-on-chip models provide new experimental platforms to study the role of human MPs during development and disease.

Keywords: human mononuclear phagocytes, developmental immunology, monopoiesis, prenatal human mononuclear phagocytes, organoids, single cell transcriptomics, immunobiology, sc-RNA seq

INTRODUCTION

The mononuclear phagocyte (MP) system includes macrophages, monocytes, and their precursors, classified based on their morphology, function, and origin, with macrophages initially assumed to be differentiated monocytes (van Furth and Cohn, 1968). Dendritic cells (DCs) were discovered later. Defined by their probing morphology and ability to activate naïve T-cells, they were incorporated into the MP system (Steinman and Cohn, 1973; Collin and Bigley, 2018).

In 1882, Elie Metchnikoff suggested that macrophages participate in the maintenance of tissue integrity and homeostasis. This required macrophages to be able to discriminate between the self and non-self, recognize tissue damage, and sense invading pathogens (Tauber, 2003). Since then, multitudes of studies have continuously refined and redefined our understanding of MP function. The roles MPs play in post-natal life have been studied in depth; however, the functional

heterogeneity of the MP system during human gestation is still poorly understood (Ginhoux and Jung, 2014; Hoeffel and Ginhoux, 2015; Hoeffel et al., 2015). Recent studies have shown MPs are present from 6 post-conception weeks (PCW) in a human pathogen-free *in utero* environment (Popescu et al., 2019; Park et al., 2020), thus suggesting that MPs may play a non-canonical role – a role unrelated to protective immunity – in organogenesis and tissue morphogenesis during development.

In this review, we summarize the consensus view on human MP development, outline the diverse functions of MPs in prenatal life and compare them to their roles in post-natal life. We also explore the use of organoids and organ-on-chip (OoC) models to interrogate MP function *ex vivo*. We further provide a web portal of manually curated MP markers and associated protein interaction networks stratified by species, organ, and developmental time[1].

DEVELOPMENT OF THE HUMAN MP SYSTEM

Human embryonic haematopoiesis occurs in several transient waves. Generation and differentiation of haematopoietic progenitors begin in the human yolk sac (YS), giving rise to the first myeloid cells appearing in the human YS at 2–3 PCW and to macrophage populations (Ginhoux and Jung, 2014; Hoeffel and Ginhoux, 2015; Bian et al., 2020).

Definitive haematopoiesis then follows in the human aorta-gonad-mesonephros (AGM) from 3 to 4 PCW (CS12), characterized by haematopoietic stem cells (HSCs) formed from the haemogenic endothelium (Migliaccio et al., 1986; Ginhoux and Jung, 2014; Hoeffel and Ginhoux, 2015). These HSCs rapidly enter the circulation and seed the fetal liver (FL), which produces the first population of granulocyte-monocyte progenitors (GMPs) and blood monocytes at 4–5 PCW/CS15 (Hoeffel and Ginhoux, 2015; Hoeffel et al., 2015; **Figure 1A**). In humans, MPs arise from YS progenitors and the AGM-derived HSCs that seed the haematopoietic organs, including the FL; the FL then serves as the main haematopoietic organ during embryonic and early fetal development (<20 PCW) (Ginhoux and Jung, 2014; Haniffa et al., 2015; Hume et al., 2019; Popescu et al., 2019). After birth, adult bone marrow (BM)-derived monocytes can also give rise to macrophages (Hume et al., 1985).

Monocytes

Monocytes comprise a remarkably plastic population circulating through the blood to surrounding tissues where they differentiate into macrophages or monocyte-derived dendritic cells (mo-DCs).

Three types of monocytes have been observed in adult humans: $CD14^{++}CD16^{-}$ classical monocytes, $CD14^{+}CD16^{++}$ non-classical monocytes, and $CD14^{+}CD16^{+}$ human intermediate monocytes (Ziegler-Heitbrock et al., 2010). The closest equivalent of human $CD14^{++}CD16^{-}$ and $CD14^{+}CD16^{++}$ monocytes in mice are $Ly6C^{+}$ classical monocytes and $Ly6C^{-}$ non-classical monocytes, respectively. Murine $Ly6C^{-}$ non-classical monocytes have been shown to differentiate from circulating $Ly6C^{+}$ monocytes and patrol the vascular system (Ginhoux and Jung, 2014).

Comparison of human fetal and post-natal monocytes has shown that both fetal and adult populations show a high expression of myeloid and monocyte surface markers CD11b, CD11c, CCR2, and CX3CR1 (Krow-Lucal et al., 2014). Upon interferon γ (IFN- γ) stimulation, post-natal monocytes upregulate antigen presentation genes. Conversely, fetal monocytes upregulate genes involved in innate antimicrobial responses to evade activating adaptive immunity, which could cause anti-self/anti-maternal rejection (Krow-Lucal et al., 2014).

Macrophages

Macrophages have been observed both morphologically and transcriptionally from the earliest wave of mouse YS haematopoiesis and as early as 6 PCW/CS19 in human YS and decidua (Banaei-Bouchareb et al., 2006; Menassa and Gomez-Nicola, 2018; Vento-Tormo et al., 2018; Popescu et al., 2019). Hofbauer cells, observed from 2.5 PCW, are used to describe any fetal-derived placental macrophage that resides within the placental villous core, amnion, and chorionic larvae (Vento-Tormo et al., 2018; Thomas et al., 2020). Hofbauer cells isolated from the human placenta express CD14, CD163, and secrete anti-inflammatory TGFβ and IL-10, which is suggestive of immune-suppressive and pro-vasculo/angiogenic functions (Johnson and Chakraborty, 2012).

Tissue-resident macrophages (TRM) are perfectly adapted to their resident tissues and have been named based on anatomical location, protein, and transcriptional signatures (Guilliams et al., 2014). The surface markers of macrophages include those shared with monocytes (CD14, CD16, CD68, and CCR5), general macrophage program markers (C1QC and VEGF), and tissue-specific markers, such as VCAM1 for fetal Kupffer cells and PPARγ for alveolar macrophages (Asada et al., 2004; Ginhoux and Jung, 2014; Spivia et al., 2014; Hoeffel and Ginhoux, 2015). TRMs can be long-lived and self-renewing following prenatal seeding but can also be replaced by circulating monocytes (McGovern et al., 2014; Scott et al., 2016; Bajpai et al., 2018; MacParland et al., 2018).

DCs

Major human dendritic cell (DC) subsets include plasmacytoid DCs (pDC), conventional DC1 (cDC1) and DC2 (cDC2), monocyte-derived DCs (moDC), and Langerhans cells (LCs) (Dzionek et al., 2000; Collin and Bigley, 2018). Although human DC origin has been attributed to BM-derived HSCs, fetal DCs have been observed as early as 6 PCW, suggesting that FL HSCs may also generate DCs (Popescu et al., 2019). Compared to adult DCs, fetal DCs possess an immature phenotype but can induce allogeneic T-cell proliferation upon culture (McGovern et al., 2015). Their presence during early development is attributed to ensuring tolerogenic responses to self and maternal antigens (McGovern et al., 2015).

[1]https://developmentcellatlas.ncl.ac.uk/MPS_development_review

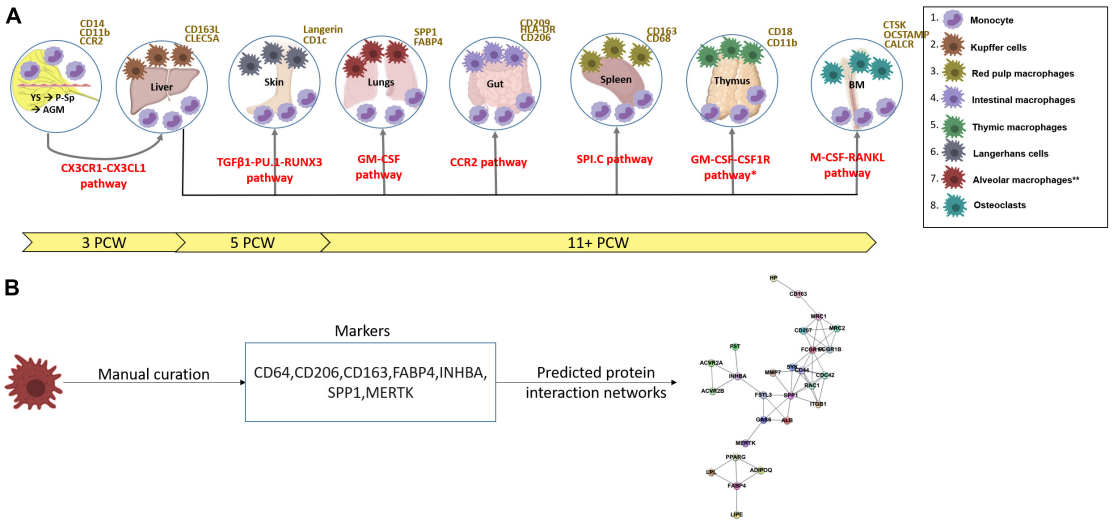

FIGURE 1 | (A) A scheme showing the functional timeline and earliest characterization of mononuclear phagocytes and the pathways involved (red) from the yolk sac into the fetal liver (Migliaccio et al., 1986; Ginhoux and Jung, 2014; Hoeffel and Ginhoux, 2015; Bian et al., 2020), thymus, spleen, gut, skin, lungs (alveolar macrophages denoted with ** as they arise post-natally) detected from 11 post-conception weeks (Audiger et al., 2017), and bone marrow. Arrows show the journey of circulating monocytes before tissue infiltration. Surface markers of monocytes and tissue residing mononuclear phagocytes are in yellow. *Data from mouse studies – may not have been verified in human studies. YS, yolk sac; P-Sp, para-aortic-splanchnopleura; AGM, aorta-gonad-mesonephros; BM, bone marrow; CS, Carnegie stage; PCW, post-conception weeks. Figures were produced with assistance from Biorender.com. **(B)** A schematic showing how markers for cell states were manually curated and used to compute predicted protein interaction networks. All markers and predicted networks curated are available on an interactive online portal: (https://developmentcellatlas.ncl.ac.uk/MPS_development_review).

Post-natally, DCs function to sense pathogens and activate the adaptive immune system (Collin and Bigley, 2018). DCs can arise from both myeloid and lymphoid progenitors (Notta et al., 2016), with studies showing monocyte participation in the DC pool following inflammation (Segura et al., 2013; Tamoutounour et al., 2013).

FUNCTIONAL DIVERSIFICATION OF MPs IN PRENATAL LIFE

The distribution of MPs in prenatal organs is carefully coordinated with key timelines of specific organ development, allowing for the continuous survival and development of the fetus (Krow-Lucal et al., 2014; McGrath et al., 2015). Discoveries, including MP origin from progenitors to their post-natal immunological and repair functions, have overshadowed the important roles they play during development and in organogenesis (Hoeffel and Ginhoux, 2015; Hoeffel et al., 2015).

The functional absence of the MP system is embryonically lethal, which shows the importance of MPs for survival during development (De Groote et al., 2014; Rojo et al., 2019). We and others have shown that macrophages, monocytes, and DCs are present from 6 PCW of human life in a relatively pathogen-free *in utero* environment (Popescu et al., 2019; Park et al., 2020). This raises the hypothesis that MPs may play an important role in tissue modeling and homeostasis in addition to immunity during early prenatal life. Below, we synthesize the literature on MP function in the BM, lymphoid, and non-lymphoid barrier organs during human development.

All MP markers and predicted protein interaction are available via an interactive web portal: (see text footnote 1). Markers were stratified by species, organ, cell type, and developmental time. Each set of markers per cell type were submitted as a string protein query using the RCY3 (v3.12) and the STRINGDB module in cytoscape (v3.8). The top 10 interactions per marker with a Stringdb confidence score of >0.9 were embedded in a network plot with nodes representing proteins and edges representing interactions (**Figure 1B**).

Bone Marrow

Osteoclasts, the TRMs of the BM, are identified by protein-based surface markers: CTSK, CALCR, SIGLEC15, ACP5, DCSTAMP, OCSTAMP, and TNFRSF11A (Weivoda et al., 2020). Osteoclasts differentiate from common myeloid progenitors via cytokine-dependent signaling involving M-CSF (macrophage-CSF/CSF-1) and receptor-activated NF-κB ligand (RANKL) (Atkins et al., 2003; Tokunaga et al., 2020). They function to assist with the clearance/resorption of bone tissue and are critical in the maintenance, repair, and remodeling of the skeleton (Park et al., 2017).

Osteopetrotic (CSF-1 deficient) mice have excessive bone deposition, deformed bone marrow cavities, and massively altered haematopoiesis. This is due to impaired cell fusion in the absence of CSF-1 required to form osteoclasts (Rojo et al., 2019). *Tnfrsf11a*^{cre};*Csf1r*$^{fl/fl}$ mice are phenotypically similar to CSF1R-deficient mice, presenting with decreased TRMs, impaired tooth eruption, misshapen skulls, and shorter long bones. However, in contrast to CSF1R-deficient mice, HSCs colonize the bone

marrow post-natally in *Tnfrsf11a*^{cre};*Csf1r*$^{fl/fl}$ mice, leading to the development of osteoclasts, but the prenatally determined deformities persist throughout life (Jacome-Galarza et al., 2019). This suggests that prenatal precursors provide functions required for tooth eruption, skull shape, and long bone development prenatally, whilst post-natal HSC-derived osteoclasts function to maintain bone mass.

Human osteoclasts promote the formation of HSC niches whilst BM macrophages determine haematopoietic egress through the phagocytosis of cells not expressing the "don't eat me" signaling CD47 ligand (Sacchetti et al., 2007; Witt et al., 2018). Erythroblastic island macrophages in the human BM are in contact with BM erythroblasts to support erythropoiesis. They contribute to heme synthesis and iron recycling (Leimberg et al., 2008), erythropoietin (EPO) feedback sensing (Sawada et al., 1989; Lifshitz et al., 2010), and expression of cytokines, including insulin-like growth factor (IGF) and bone morphogenetic protein (Sawada et al., 1989; Liu et al., 2015), which promote erythropoiesis. Decreased MPs in the BM affects the HSC niche and induces HSC mobilization into the blood due to niche collapse, resulting in a decline in erythro-/haematopoiesis due to bone endosteal niche disruptions (Kaur et al., 2017).

A study on adult human BM DCs showed reduced activity of canonical DC-functionalities when compared to matched DCs in the peripheral blood (van Leeuwen-Kerkhoff et al., 2018). For example, BM-derived cDC2s were less able to upregulate T-cell stimulatory molecules like CD80 upon TLR-triggering when compared to peripheral blood cDC2s (van Leeuwen-Kerkhoff et al., 2018). The BM niche was concluded to be primarily a DC developmental location. Murine BM studies have shown the contribution of DCs in the regulation of haematopoiesis: ablation of murine BM cDCs resulted in HSC mobilization into peripheral blood to transiently lodge into other haematopoietic organs such as the spleen. BM cDC ablation in the mice also led to a loss of BM macrophages, increased BM vascular permeability, and the expansion of BM endothelial cells, which are required for haematopoietic regulation (Zhang et al., 2019). These studies demonstrate the need for MPs in the BM niches during development and how they coincide with post-natal functions to maintain skeletal and BM haematopoietic niches.

Lymphoid Organs

Liver

Kupffer cells, identified by CD163, VCAM1, and CLEC5A in humans (Gonzalez-Dominguez et al., 2015), are the TRMs of the liver, lining the sinusoids. Kupffer cells assist in the proliferation and enucleation of erythroblasts as well as in iron recycling to facilitate erythropoiesis in the FL (Pourcher et al., 2011; Palis, 2016). Definitive erythropoiesis occurs in the human FL and requires HIF2A and EPO expression for progenitor survival. This process is MYB dependent and relies on transcriptional regulators, such as Sox6 and Bcl11A, that down-regulate embryonic (Gower 1 – $\zeta_2\varepsilon_2$, Gower 2 – $\alpha_2\varepsilon_2$) and fetal globin expression ($\alpha_2\gamma_2$) (Cantu et al., 2011; Bjurström et al., 2016). At the stage of active FL haematopoiesis, macrophages can migrate from the sinusoids to the parenchyma to form erythroblastic islands consisting of a central macrophages surrounded by erythroblasts (Li et al., 2019). The central macrophages express VCAM1, CD163, and EPOR to mediate interactions with early erythroid cells and EPO, stimulating erythroblast enucleation, proliferation, and differentiation (Li et al., 2019; Popescu et al., 2019).

A non-canonical function of human Kupffer cells is to prevent the pathogenic accumulation of lipids in the liver. Peroxisome proliferator-activated receptor gamma (PPARγ) was identified as an important regulator of macrophage activator programs linked to the fatty acid oxidation function of Kupffer cells (Scott et al., 2016; Luo et al., 2017). PPARγ also regulates pro-proliferative interleukin (IL)-4 driven programs (basophil recruitment) during damage to assist during liver generation/regeneration (Daniel et al., 2018). These studies demonstrate a common non-canonical function between human fetal and post-natal Kupffer cells in coordinating erythropoiesis and restoring damaged tissue during fetal development and post-natal liver regeneration.

Like adult DCs, human FL DCs can migrate to lymph nodes and initiate T-cell proliferation in response to toll-like receptor (TLR) ligation. Additionally, it was observed that after TLR ligation, FL cDC2s show markedly reduced TNFα cytokine production when compared to adult DCs to mediate immunosuppressive responses during gestation (McGovern et al., 2017).

Thymus

During early human gestation, CD45$^+$ early lymphoid progenitors (ELP) have been reported to colonize the fetal thymus from the FL and BM and give rise to plasmacytoid and conventional DC subsets and T-cells (Patel et al., 2009; Park et al., 2020). T-cells undergo positive and negative selection during development. Double positive CD4$^+$/CD8$^+$ cells that do not recognize MHCs on thymic stromal cells and single positive cells that respond to self-antigens are eliminated by apoptosis. Human DCs have been reported to mediate recognition and clearance of negatively selected cells, whilst thymic epithelial cells (TECs) have been shown to play an essential role in positive selection (Hu et al., 2015). Deactivated DCs characterized in the fetal thymus revealed gene expression programs adapted for this role, with AIRE supporting the negative selection of T-cells, and chemokines (CCL17, CCL19, and CCL22), enabling recruitment of CD4 T-cells and Tregs to the thymic medulla (Park et al., 2020). Thus, DC depletion in the thymus could lead to an increased propensity for autoimmunity reactions due to a lack of negative selection (Audiger et al., 2017; Park et al., 2020).

The early thymic MP system is composed of Mac1$^+$ (CD11b/CD18) thymic macrophages (TMs) observable from 8 PCW (Park et al., 2020), but little is known of their prenatal function. During murine development, TMs phagocytose apoptotic thymocytes, assisting with the clearance of negatively selected cells, carrying out DNA fragmentation via DNase-II-dependent degradation in lysosomes (Kawane et al., 2003). DNase-II knockout mice with impaired macrophage function during development displayed reduced brain, kidney, and thymic size due to the accumulation of undigested apoptotic cell debris within phagocytes (Kawane et al., 2003). A study on E14.5 mice

thymi demonstrated $CD4^+/CD11b^+$ macrophages exhibiting phagocytosis of apoptotic thymocytes (Esashi et al., 2003). RUNX1 knockout mice have impaired macrophage development and display impaired thymic development, including the accumulation of double-negative thymocytes (Putz et al., 2006).

Spleen

Splenic TRMs originate from the FL and fetal BM. The spleen functions to clear blood-borne pathogens and acts as an early haematopoietic organ during development, bridging erythro-/haematopoiesis between the FL and BM. It is divided into red pulp and white pulp fractions separated by the marginal zone. The macrophages in each zone have specific functions and interactions (Hoeffel and Ginhoux, 2015).

Human red pulp macrophages (RPM) form a vast network required for the uptake of senescent red blood cells and iron homeostasis. They express CD163 and CD68 and are SPI-C dependent. RPMs selectively upregulate SPI-C expression, driving HMOX1 expression, which encodes the essential heme recycling enzyme, Heme Oxygenase 1 (HO-1) (Haldar et al., 2014; Nagelkerke et al., 2018). Splenic monocytes may also express SPI-C when induced by free heme from red-blood-cell degradation, generating new RPMs (Haldar et al., 2014). Prenatally, RPMs localize in splenic cords and assess the condition of erythrocytes. CD47 expression on erythrocytes inhibits phagocytosis via interaction with the signal regulatory protein α (SIRPα) found on RPMs. Conformational changes to CD47 indicates erythrocyte senescence leading to phagocytosis by fetal RPMs (Murata et al., 2014; Hayes et al., 2020).

Formation of white pulp and the germinal center occurs in the presence of CD209 in humans and $SIGN\text{-}R1^+$ in murine marginal zone macrophages (MZM) (Steiniger et al., 2007; Endo et al., 2015; Pirgova et al., 2020). After birth, MZM and marginal metallophilic macrophage generation are dependent upon the nuclear liver X receptor (LXR) and function to filter the blood as it is released into the marginal zone (A-Gonzalez et al., 2013). The macrophages act like scavenger cells via scavenger receptors, such as MARCO, which recognize non-opsonised molecules and blood-borne antigens. MARCO also directly binds and mediates the phagocytosis of bacteria such as *Escherichia coli* and *Staphylococcus aureus* and works in conjunction with TLRs to mediate pathogen control (Kellermayer et al., 2014).

Splenic pre-follicular DCs secreting CXCL13 and driving B-cell chemotaxis also contribute to white pulp and marginal zone development after birth (Pirgova et al., 2020). Human fetal spleen cDC1s and cDC2s, observed by 13 PCW, have been observed to induce differentiation of T-regulatory (Treg) cells *in vitro* from adult T-cells. Fetal spleen cDCs also show significantly less pro-inflammatory cytokine production when compared to adult spleen DCs, including increased expression of arginase-2, consistent with the notion of fetal tolerance establishment (McGovern et al., 2017).

Barrier Organs

Lung

Human alveolar macrophages (AMs) express CD64, CD206 and CD163, FABP4, INHBA, SPP1, and MERTK (Mitsi et al., 2018; Morse et al., 2019). AMs reside on the luminal surfaces of the alveoli and are in direct contact with commensal bacteria, inhaled particles, and host-epithelial-derived factors such as surfactants.

In the post-natal steady state, AMs phagocytose excessive surfactant proteins. Mice and humans lacking AMs due to a dysfunction in GM-CSF signaling develop pulmonary alveolar proteinosis as a result of defective surfactant clearance, suggesting a vital function for AMs (Stanley et al., 1994; Robb et al., 1995; Ferretti et al., 2016). Surfactant production in the human fetus has been observed to start between 22 and 24 PCW and needs careful regulation to prevent build up (Hashimoto et al., 2013; Izquierdo et al., 2018).

Interstitial macrophages, present between the airways in the lung tissue interstitium, are involved in tissue remodeling, maintenance, and antigen presentation (van Furth and Cohn, 1968). They interact with DCs to influence airway allergic responses (Bedoret et al., 2009).

Gut

The human intestinal tract develops distinct morphological crypt-villus features by 12 PCW (Moxey and Trier, 1978). MPs such as $CD103^+$ and $CCR7^+$ DCs and macrophages are observed from as early as 14 PCW (Stras et al., 2019). Human intestinal macrophages have been shown to express HLA-DR, CD206, and CD209 (Bujko et al., 2018). Intestinal macrophages assist with epithelial homeostasis during development as they do in post-natal life (D'Angelo et al., 2013; Hoeffel and Ginhoux, 2015). The intestinal epithelium rapidly divides and requires constant and continuous ECM remodeling, which the macrophage provides via Wnt1 signaling and secretion of hepatocyte growth factor (HGF) (D'Angelo et al., 2013; Ortiz-Masia et al., 2014).

Post-natally, intestinal macrophages and DCs can penetrate the epithelium through *trans*-epithelial dendrites (TEDs). TED formation was found to be dependent upon the expression of CX_3CR1 and the membrane ligand fractalkine (CX_3CL1). This process allows them to sample and capture luminal bacteria for antigen presentation (Chieppa et al., 2006; Vallon-Eberhard et al., 2006). Intestinal goblet cells assist the transfer of antigens from the intestinal lumen to $CD103^+$ DCs (Mazzini et al., 2014; Knoop et al., 2015). These DCs then migrate from the lamina propria (LP) to the mesenteric lymph nodes (MLN) in a CCR7-dependent manner, or within the Peyer's Patches, into T-cell zones (Jang et al., 2006; Scott et al., 2015).

The human intestinal cDC populations are characterized by their expression of CD103 and SIRPα (Watchmaker et al., 2014). LP DCs are considered tolerogenic and assist with gut homeostasis. $CD103^+$ DCs have been observed to metabolize retinoic acid secreted by the liver to induce homing of protective $CCR9^+\alpha_4{}^+\beta_7{}^+$ T and B-cells to the gut (Bakdash et al., 2015; Roe et al., 2017). Other transcription factors, such as transforming growth factor β receptor II (TGFβII) (Ramalingam et al., 2012) and tumor necrosis factor receptor-associated factor 6 (TRAF6) (Han et al., 2013), maintain cDC tolerance of gut microbiota. cDC antigen presentation promotes the generation of forkhead box $P3^+$ ($FoxP3^+$)-inducible Tregs in the MLN and is key to the development of the symbiotic relationship with microbiota (Esterhazy et al., 2016). Human fetuses start swallowing amniotic

fluid from 8 to 12 PCW with data indicating the possible existence of an *in-utero* microbiome in the amniotic fluid and fetal gastrointestinal tract. This evidence thus suggests a potential role for cDC education and tolerance in fetal gut development (Collado et al., 2016; Martinez et al., 2018).

Skin

Various populations of MPs reside in the skin, including Langerhans cells (LCs) and dermal DCs. LCs are found in human fetal skin at 4–5 PCW, detected as HLA-DR$^+$ and CD1a$^+$, harboring a mixed DC/macrophage signature (Foster et al., 1986; Carpentier et al., 2016). LC precursors were observed to acquire CD1c and langerin expression at 9 PCW and grow in number throughout development (Schuster et al., 2009, 2012).

Dermal MPs (macrophages and DCs) are seeded prenatally but are replaced over time by circulating CD14^{++}CD16$^+$ human monocytes (Chorro et al., 2009; Malissen et al., 2014). CD14^{++}CD16$^+$ human monocytes can also be recruited to replace LCs when they are unable to self-renew (Chorro et al., 2009; Malissen et al., 2014). In humans, LCs express CD1A, CD11B, CD11C, CD207, and MHC class II. Dermal DCs express lower amounts of CD1A, CD1C, CD11B, CD206, CD209, and MHC class II. Dermal macrophages express CD163 and factor XIIIa (Valladeau et al., 2000; Nestle et al., 2009).

Dermal macrophages also promote the proliferation of fibroblasts in damaged tissue to assist with repair in a TGFα, fibroblast growth factor (FGF), and platelet-derived growth-factor-dependent mechanism (Shook et al., 2018; Etich et al., 2019).

Although human LCs are prenatally derived and share a similar origin with prenatal macrophages, they have additional "DC properties" in their ability to migrate to draining lymph nodes and initiate an immune response (Furio et al., 2010). LCs coordinate a state of immune tolerance in the postnatal skin but can instruct the adaptive immune system when skin integrity is compromised (Seneschal et al., 2012). During the early stages of wound healing, LCs are present as an immune barrier and coordinate with dermal macrophages to promote repair in a fibroblast-dependent manner (Shook et al., 2018; Etich et al., 2019). Little is known about the function of LCs during development, but data suggests they could be involved in ECM remodeling alongside dermal macrophages (Furio et al., 2010). More work is required to fully clarify their role during organogenesis.

Post-natally, dermal DCs function as migratory antigen-presenting cells whilst maintaining tolerance to self-antigens (Haniffa et al., 2012). The equivalent of murine dermal cDC1 in humans is defined as CD141$^+$ DCs and co-expresses: XCR1, CADM1, CLEC9A, and TLR3. Skin-draining lymph nodes contain migratory and resident CD141$^+$ (Haniffa et al., 2012; Collin and Bigley, 2018).

Developmental macrophage cell programs were recently shown to be co-opted in two common inflammatory skin conditions, psoriasis, and atopic dermatitis (Chorro et al., 2009; Reynolds et al., 2020). These new observations highlight the importance of developmental pathways in inflammatory disease pathogenesis that could be therapeutically targeted.

ORGANOID AND ORGAN-ON-CHIP PLATFORMS TO STUDY PRENATAL MPs

Studies on human MPs have focused on *in vitro* culture systems from BM-HSC, peripheral blood monocytes, induced pluripotent stem cells (iPSC) (Caux et al., 1992; Sallusto and Lanzavecchia, 1994; Merad et al., 2002; Poulin et al., 2010; Balan et al., 2018; Kirkling et al., 2018), and *ex vivo* primary MPs isolated from peripheral blood tissues (Haniffa et al., 2013; McGovern et al., 2014; Takata et al., 2017). Such culture systems allow the study of MP interactions with specific cells in the tissues through co-culture. Murine iPSC-derived macrophages (iMacs) can differentiate into microglia in co-culture with iPSC-derived neurons. Murine iMacs can be differentiated into functional TRMs of the lung and brain when transplanted *in vivo* showcasing the remarkable plasticity of MPs (Takata et al., 2017). These studies have provided new insights into the classification and roles of primary MPs but suffer from a failure to allow dissection into how MP ontogeny and functions are shaped by their physiological tissue of residence. Recent developments in human tissue organoid culture systems provide new opportunities to interrogate human MPs. Organoids are 3D culture systems that attempt to model *in vivo* settings by leveraging the intrinsic ability of cells for self-assembly and organization. The most common form of organoid culture, spheroids, organize aggregated cells with or without hydrogen scaffold substrates and aim to replicate three key features of a specific tissue: the spatial distribution of cells, the biochemical environment, and its mechanical environment (Iakobachvili and Peters, 2017; Shanti et al., 2018; Kim et al., 2020). Organoids can facilitate studies on organogenesis, disease pathophysiology, and drug discovery in an *ex vivo* setting (Broutier et al., 2017). A study by Neal et al. (2018) used an air-liquid interface to generate patient-derived tumoral organoids with preserved immune cell types including CD68$^+$ CD14$^+$ macrophages (Neal et al., 2018). Bourgine et al. (2018) used a perfusion bioreactor system to create a BM organoid with a human osteoblastic environment that supports HSC function (Bourgine et al., 2018).

Organ-on-Chip Systems

Organoids can replicate organ-level function but may lack key chemical, spatial, or other tissue physico-biomechanical properties distinct from those *in vivo,* e.g., fluid flow, and are labor intensive (Shanti et al., 2018; Jang et al., 2019; Kim et al., 2020). Microfluidic organ-on-chips (OoCs) enable organoids to be cultured in perfused, multiplexed chips that recapitulate tissue-specific mechanical and biochemical parameters at higher throughput (Shanti et al., 2018).

Mononuclear phagocyte migration and its role in development and disease have been studied using OoC models (Biselli et al., 2017; Sasserath et al., 2020). Monocytes and macrophages embedded in OoCs respond to hypoxia and injury-associated signals, such as MCP-1 and IL-6, by migrating down chemokine gradients (Liu et al., 2018; Shanti et al., 2018). These MPs express gene-expression programs similar to those observed to be crucial in development, such as programs

involved in angiogenesis (VEGF, COX2, Wnt5a, FGF2), tissue remodeling (MMP9), glucose transport (e.g., solute carrier family 2 member 1), and glycolytic metabolism (enolase 2) (Chou et al., 2018; Shanti et al., 2018; Jang et al., 2019; Sriram et al., 2019). Other OoC models incorporating MPs have been developed for the spleen (Rigat-Brugarolas et al., 2014), skin (Sriram et al., 2019), bone marrow (Chou et al., 2018), liver (Jang et al., 2019), the feto-maternal interface (Richardson et al., 2020), and an inter-connected multi-organ platform (Sasserath et al., 2020).

Sieber et al. (2018) developed a BM-on-a-chip model consisting of two media perfused micro-channels filled with BM progenitor, stromal, and endothelial cells. Cells were embedded in a hydroxyapatite scaffold to mimic the 3D physiology of BM (Sieber et al., 2018). The BM OoC successfully demonstrated key expression programs known to be essential for sustaining the BM HSC niche *in vivo,* with qPCR assays showing upregulation of *nestin, osteopontin, VEGF, angiopoietin 1,* and *fibronectin* expression (Chou et al., 2018; Sieber et al., 2018). $CD34^+$ cells isolated from the OoCs could form colony-forming units of erythrocytes, macrophages, granulocyte/macrophage, and granulocyte-erythrocyte-macrophage-megakaryocytes, demonstrating the ability of OoC derived BM HSCs to differentiate into various progenies and maintain functional HSC niches *in vitro* for up to 4 weeks (Sieber et al., 2018). In a separate study by Chou et al. (2018), BM OoCs supported differentiation into myeloid and erythroid-primed lineages, whilst improving maintenance of $CD34^+$ progenitors (Chou et al., 2018). Interestingly, post differentiation, myeloid mobilization, and remodeling were also observed across 4 weeks of OoC culture. Selective drug toxicity and recovery from 5-fluoracil and radiation exposures using BM OoCs demonstrated increased biologically mimetic toxicity responses and recoveries compared to their static gel-spheroid counterparts.

Liver OoCs recapitulate the hepatic lobule by patterning hepatocytes and other associated cells via micropillar arrays, which introduce perfusion to maintain functionality over time (Rennert et al., 2015). Liver-on-a-chip platforms have been designed to model and investigate various functions of the liver including metabolism, detoxification, and response to pharmaceutical interventions (Rennert et al., 2015; Groger et al., 2016). Groger et al. (2016) assessed the interaction of circulating monocytes and their ability to trigger tissue repair and the repolarization of Kupffer cells within a polystyrol scaffold embedded in a liver on-a-chip. Inflammation stimulated by TLR1 and 2 agonists and lipopolysaccharide (LPS) in the liver OoC caused the release of pro-inflammatory IL-1β, IL-6, and TNFα within 72 h and anti-inflammatory cytokine IL-10 post 72 h. The OoC exhibited similar responses to livers undergoing sepsis, *in vivo*, which caused hepatocellular dysfunction and cell death. There was also a shift from LPS-induced inflammatory macrophages to regenerative polarization with the introduction of THP-1 monocytes to the system (Groger et al., 2016). These results demonstrate crosstalk of the liver microenvironment and immune system with higher-throughput phenotypic readouts when compared to spheroid cultures (Hotchkiss and Opal, 2010).

A single tissue OoC cannot fully recapitulate physiologically relevant pharmacokinetic properties and toxicity responses across multiple tissues. To achieve crosstalk of organs, long-term multi-OoC cultures have been developed to better mimic these multi-tissue interactions (Zhao et al., 2019). A multi-OoC model comprising cardiomyocytes, skeletal muscle, and the liver was successfully used to study the THP-1 macrophage response to drug and inflammatory stimuli (Sasserath et al., 2020). The multi-OoC model incorporated biological microelectromechanical systems (BioMEMS) to non-invasively measure cardiomyocyte electrical (microelectrode array) and muscle mechanical function (cantilever). Liver function was monitored using biomarker quantification of CYP1A1, 3A4, 2C9, urea, and albumin. The system facilitated a multi-organ response to the drug amiodarone and revealed the selective THP-1 monocyte activation and infiltration in the cardiac OoC due to cytokines released by cardiomyocytes. LPS and IFNγ treatment of the chip system elicited a sepsis-like response characterized by TNFα, IL-6, and CCL5 and decreased cardiac, skeletal muscle, and liver function.

Taken together, these studies demonstrate the effectiveness of OoC systems to study MPs within tissues, as well as their responses to chemical stimuli (Rennert et al., 2015; Groger et al., 2016; Hulsmans et al., 2016; Prabhu and Frangogiannis, 2016; Sieber et al., 2018). However, despite the promising applications of organoids and OoCs, challenges in recapitulating organs to scale with accurate tissue architecture (size, cell number, and distribution) remain (Rennert et al., 2015; Groger et al., 2016).

The Future of Studying the MP System

To fully establish an atlas of fetal MP populations, studies must go beyond murine models to incorporate biomimetic OoC models with human fetal/embryonic samples (Behjati et al., 2018). Increasingly, international consortia initiatives, such as the Human Development Cell Atlas (HDCA), have leveraged high-throughput, unbiased technologies, such as single-cell RNA sequencing (scRNA-seq), and spatial techniques to create tissue-specific cellular atlases of the developing human (Behjati et al., 2018). In a recent HDCA publication, Popescu et al. (2019) applied scRNA-seq alongside the spatially resolved Hyperion to define the cellular and spatial composition of the human FL and YS, highlighting potential pathways for Kupffer cells to instruct B lineage survival in FL. This data demonstrates the potential for high-throughput omics technologies to inform on the *in vivo* cellular interactions between MPs and their microenvironment.

Organoid culture models have also benefited from the recent surge of accessibility and data generated by omics technologies (Kanton et al., 2019; Lee et al., 2020). Information gleaned from these data repositories can be used to increase the biomimetic capability and complexity of organoid models (Chorro et al., 2009; Haniffa et al., 2012; Popescu et al., 2019). Conversely, the application of high-throughput omics technologies on OoC and organoid models may also inform *in vivo* developmental trajectories and populations (Chorro et al., 2009; Haniffa et al., 2012). In a 2020 study, Lee et al. (2020) developed hair-bearing human skin organoids. These organoids were characterized by scRNA-seq at 1 week and 1-month timepoints and morphologically compared to human 18 PCW fetal skin (Lee et al., 2020). FGF and a BMP-inhibitor were used to induce differentiation of human pluripotent stem cell (hPSC)

spheroids into cranial neural crest cell populations, which is key in later assembly of the epidermis. Crucially, differential expression analysis of organoid scRNA-seq data revealed key signaling modulators for self-organization; expression of WNT modulators in the epidermal (*WNT6 and LEF1*) and dermal (*SFRP2*, *TCF4*, *WIF1*, and *APCDD1*) layers may govern the self-assembly and interactions between the respective layers *in vivo*. Furthermore, dermal expression of *FGF7* (Keratinocyte Growth Factor) was also identified as a key driver of epidermal stratification in the organoids (Lee et al., 2020). Similarly, Kanton et al. (2019) recapitulated HDCA scRNA-seq data to reveal the potential and limits of cerebral organoids. Comparison of fetal brain and cerebral organoid scRNA-seq data showed consistent gene-expression patterns of the earliest stage of developmental differentiation trajectories. This could provide an atlas of the budding human brain and offer a baseline for future inclusion of MP cells into cerebral organoid studies (Kanton et al., 2019).

High-throughput scRNA-seq technologies have transformed our understanding of complex cell populations. High-throughput multi-omic approaches can now enable combined scRNAs and cell-surface proteins (CITE-seq) analysis and single nucleus RNA and chromatin accessibility (snATAC-seq) to be performed (Stoeckius et al., 2017). Stephenson et al. (2021) recently used CITE-seq to characterize the cellular immune response to COVID-19 in peripheral blood.

The identification of key modulators driving self-organization and stratification of dermal and epidermal layers provides insight into how factors such as FGF7 and WNT signaling modulators (Lee et al., 2020) may be incorporated into skin OoC models to better regulate organoid cell fates, cell-cell interactions and improve organoid maturation. Data accrued from the HDCA and other international consortia can be leveraged to instruct more complex developmental organoids with the intention of incorporating their associative immune cell and MP populations.

CONCLUSION

A thorough understanding of MP contribution to tissue repair and regeneration will have important repercussions for regenerative medicine and therapy. The key roles of MPs in human organogenesis and organ morphogenesis are beginning to be explored and have thus far been reliant on pre-clinical animal models. Several logistical challenges remain to facilitate studies of MPs in human prenatal tissues. Organoids and OoC technologies, in tandem with data generated by emerging omics technologies and international collaborative consortia, provide a new experimental avenue to recapitulate human development and physiology. They have shown early success, but important hurdles remain including successful incorporation of the full complement of immune cells and physiologically relevant vascularization and perfusion of these culture systems.

AUTHOR CONTRIBUTIONS

IG and MM contributed equally to literature review, selection, synthesis, and writing. MH contributed to reviewing and editing the manuscript. All authors contributed to the article and approved the submitted version.

FUNDING

We acknowledge funding from the Wellcome Human Cell Atlas Strategic Science Support (WT211276/Z/18/Z); MH was funded by Wellcome (WT107931/Z/15/Z), The Lister Institute of Preventive Medicine, and Newcastle NIHR Biomedical Research Centre (BRC).

ACKNOWLEDGMENTS

We would like to thank Bayanne Olabi, Simone Webb, and Elizabeth Poyner for their comments and efforts in proof-reading the manuscript.

SUPPLEMENTARY MATERIAL

The Supplementary Material for this article can be found online at: https://www.frontiersin.org/articles/10.3389/fcell.2021.649937/full#supplementary-material

REFERENCES

A-Gonzalez, N., Guillen, J. A., Gallardo, G., Diaz, M., de la Rosa, J. V., Hernandez, I. H., et al. (2013). The nuclear receptor LXRalpha controls the functional specialization of splenic macrophages. *Nat. Immunol.* 14, 831–839. doi: 10.1038/ni.2622

Asada, K., Sasaki, S., Suda, T., Chida, K., and Nakamura, H. (2004). Antiinflammatory roles of peroxisome proliferator-activated receptor gamma in human alveolar macrophages. *Am. J. Respir Crit. Care Med.* 169, 195–200. doi: 10.1164/rccm.200207-740oc

Atkins, G. J., Kostakis, P., Pan, B., Farrugia, A., Gronthos, S., Evdokiou, A., et al. (2003). RANKL expression is related to the differentiation state of human osteoblasts. *J. Bone Miner. Res.* 18, 1088–1098. doi: 10.1359/jbmr.2003.18.6.1088

Audiger, C., Rahman, M. J., Yun, T. J., Tarbell, K. V., and Lesage, S. (2017). The importance of dendritic cells in maintaining immune tolerance. *J. Immunol.* 198, 2223–2231. doi: 10.4049/jimmunol.1601629

Bajpai, G., Schneider, C., Wong, N., Bredemeyer, A., Hulsmans, M., Nahrendorf, M., et al. (2018). The human heart contains distinct macrophage subsets with divergent origins and functions. *Nat. Med.* 24, 1234–1245. doi: 10.1038/s41591-018-0059-x

Bakdash, G., Vogelpoel, L. T., van Capel, T. M., Kapsenberg, M. L., and de Jong, E. C. (2015). Retinoic acid primes human dendritic cells to induce gut-homing, IL-10-producing regulatory T cells. *Mucosal Immunol.* 8, 265–278. doi: 10.1038/mi.2014.64

Balan, S., Arnold-Schrauf, C., Abbas, A., Couespel, N., Savoret, J., Imperatore, F., et al. (2018). Large-Scale human dendritic cell differentiation revealing notch-dependent lineage bifurcation and heterogeneity. *Cell Rep.* 24, 1902–1915 e6.

Banaei-Bouchareb, L., Peuchmaur, M., Czernichow, P., and Polak, M. (2006). A transient microenvironment loaded mainly with macrophages in the early developing human pancreas. *Endocrinol.* 188, 467–480.

Bedoret, D., Wallemacq, H., Marichal, T., Desmet, C., Quesada Calvo, F., Henry, E., et al. (2009). Lung interstitial macrophages alter dendritic cell functions to

prevent airway allergy in mice. *J. Clin. Invest.* 119, 3723–3738. doi: 10.1172/jci39717

Behjati, S., Lindsay, S., Teichmann, S. A., and Haniffa, M. (2018). Mapping human development at single-cell resolution. *Development* 145, dev152561. doi: 10.1242/dev.152561

Bian, Z., Gong, Y., Huang, T., Lee, C. Z. W., Bian, L., Bai, Z., et al. (2020). Deciphering human macrophage development at single-cell resolution. *Nature* 582, 571–576. doi: 10.1038/s41586-020-2316-7

Biselli, E., Agliari, E., Barra, A., Bertani, F. R., Gerardino, A., De Ninno, A., et al. (2017). Organs on chip approach: a tool to evaluate cancer -immune cells interactions. *Sci. Rep.* 7:12737.

Bjurström, C. F., Mojadidi, M., Phillips, J., Kuo, C., Lai, S., Lill, G. R., et al. (2016). Reactivating fetal hemoglobin expression in human adult erythroblasts through bcl11a knockdown using targeted endonucleases. *Mol. Ther. Nucleic Acids* 5:e351. doi: 10.1038/mtna.2016.52

Bourgine, P. E., Klein, T., Paczulla, A. M., Shimizu, T., Kunz, L., Kokkaliaris, K. D., et al. (2018). In vitro biomimetic engineering of a human hematopoietic niche with functional properties. *Proc Natl Acad Sci U.S.A.* 115, E5688–E5695.

Broutier, L., Mastrogiovanni, G., Verstegen, M. M., Francies, H. E., Gavarró, L. M., Bradshaw, C. R., et al. (2017). Human primary liver cancer-derived organoid cultures for disease modeling and drug screening. *Nat. Med.* 23, 1424–1435. doi: 10.1038/nm.4438

Bujko, A., Atlasy, N., Landsverk, O. J. B., Richter, L., Yaqub, S., Horneland, R., et al. (2018). Transcriptional and functional profiling defines human small intestinal macrophage subsets. *J. Exp. Med.* 215, 441–458. doi: 10.1084/jem.20170057

Cantu, C., Ierardi, R., Alborelli, I., Fugazza, C., Cassinelli, L., Piconese, S., et al. (2011). Sox6 enhances erythroid differentiation in human erythroid progenitors. *Blood* 117, 3669–3679. doi: 10.1182/blood-2010-04-282350

Carpentier, S., Vu Manh, T.-P., Chelbi, R., Henri, S., Malissen, B., Haniffa, M., et al. (2016). Comparative genomics analysis of mononuclear phagocyte subsets confirms homology between lymphoid tissue-resident and dermal XCR1(+) DCs in mouse and human and distinguishes them from Langerhans cells. *J. Immunol. Methods* 432, 35–49. doi: 10.1016/j.jim.2016.02.023

Caux, C., Dezutter-Dambuyant, C., Schmitt, D., and Banchereau, J. (1992). GM-CSF and TNF-alpha cooperate in the generation of cells. *Nature* 360, 258–261. doi: 10.1038/360258a0

Chieppa, M., Rescigno, M., Huang, A. Y. C., and Germain, R. N. (2006). Dynamic imaging of dendritic cell extension into the small bowel lumen in response to epithelial cell TLR engagement. *J.Exp. Med.* 203, 2841–2852. doi: 10.1084/jem.20061884

Chorro, L., Sarde, A., Li, M., Woollard, K. J., Chambon, P., Malissen, B., et al. (2009). Langerhans cell (LC) proliferation mediates neonatal development, homeostasis, and inflammation-associated expansion of the epidermal LC network. *J. Exp. Med.* 206, 3089–3100. doi: 10.1084/jem.20091586

Chou, D. B., Frismantas, V., Milton, Y., David, R., Pop-Damkov, P., Ferguson, D., et al. (2018). Human bone marrow disorders recapitulated in vitro using organ chip technology. *bioRxiv*[preprint] bioRxiv 458935,

Collado, M. C., Rautava, S., Aakko, J., Isolauri, E., and Salminen, S. (2016). Human gut colonisation may be initiated in utero by distinct microbial communities in the placenta and amniotic fluid. *Sci. Rep.* 6:23129.

Collin, M., and Bigley, V. (2018). Human dendritic cell subsets: an update. *Immunology.* 154, 3–20. doi: 10.1111/imm.12888

D'Angelo, F., Bernasconi, E., Schafer, M., Moyat, M., Michetti, P., Maillard, M. H., et al. (2013). Macrophages promote epithelial repair through hepatocyte growth factor secretion. *Clin. Exp. Immunol.* 174, 60–72. doi: 10.1111/cei.12157

Daniel, B., Nagy, G., Horvath, A., Czimmerer, Z., Cuaranta-Monroy, I., Poliska, S., et al. (2018). The IL-4/STAT6/PPARγ signaling axis is driving the expansion of the RXR heterodimer cistrome, providing complex ligand responsiveness in macrophages. *Nucleic Acids Res.* 46, 4425–4439. doi: 10.1093/nar/gky157

De Groote, M. A., Johnson, L., Podell, B., Brooks, E., Basaraba, R., and Gonzalez-Juarrero, M. (2014). GM-CSF knockout mice for preclinical testing of agents with antimicrobial activity against Mycobacterium abscessus. *J. Antimicrob. Chemother.* 69, 1057–1064. doi: 10.1093/jac/dkt451

Dzionek, A., Fuchs, A., Schmidt, P., Cremer, S., Zysk, M., Miltenyi, S., et al. (2000). BDCA-2, BDCA-3, and BDCA-4: three markers for distinct subsets of dendritic cells in human peripheral blood. *J. Immun.* 165, 6037–6046. doi: 10.4049/jimmunol.165.11.6037

Endo, A., Ueno, S., Yamada, S., Uwabe, C., and Takakuwa, T. (2015). Morphogenesis of the spleen during the human embryonic period. *Anat Rec (Hoboken).* 298, 820–826. doi: 10.1002/ar.23099

Esashi, E., Sekiguchi, T., Ito, H., Koyasu, S., and Miyajima, A. (2003). Cutting Edge: a possible role for CD4+ thymic macrophages as professional scavengers of apoptotic thymocytes. *J. Immunol.* 171, 2773–2777. doi: 10.4049/jimmunol.171.6.2773

Esterhazy, D., Loschko, J., London, M., Jove, V., Oliveira, T. Y., and Mucida, D. (2016). Classical dendritic cells are required for dietary antigen-mediated induction of peripheral T(reg) cells and tolerance. *Nat. Immunol.* 17, 545–555. doi: 10.1038/ni.3408

Etich, J., Koch, M., Wagener, R., Zaucke, F., Fabri, M., and Brachvogel, B. (2019). Gene expression profiling of the extracellular matrix signature in macrophages of different activation status: relevance for skin wound healing. *Int. J. Mol. Sci.* 20:5086. doi: 10.3390/ijms20205086

Ferretti, A., Fortwendel, J. R., Gebb, S. A., and Barrington, R. A. (2016). Autoantibody-mediated pulmonary alveolar proteinosis in rasgrp1-deficient mice. *J. Immunol.* 197, 470–479. doi: 10.4049/jimmunol.1502248

Foster, C. A., Holbrook, K. A., and Farr, A. G. (1986). Ontogeny of Langerhans cells in human embryonic and fetal skin: expression of HLA-DR and OKT-6 determinants. *J. Invest. Dermatol.* 86, 240–243. doi: 10.1111/1523-1747.ep12285201

Furio, L., Briotet, I., Journeaux, A., Billard, H., and Peguet-Navarro, J. (2010). Human langerhans cells are more efficient than CD14(-)CD1c(+) dermal dendritic cells at priming naive CD4(+) T cells. *J. Invest. Dermatol.* 130, 1345–1354. doi: 10.1038/jid.2009.424

Ginhoux, F., and Jung, S. (2014). Monocytes and macrophages: developmental pathways and tissue homeostasis. *Nat Rev Immunol.* 14, 392–404. doi: 10.1038/nri3671

Gonzalez-Dominguez, E., Samaniego, R., Flores-Sevilla, J. L., Campos-Campos, S. F., Gomez-Campos, G., Salas, A., et al. (2015). CD163L1 and CLEC5A discriminate subsets of human resident and inflammatory macrophages in vivo. *J. Leukoc Biol.* 98, 453–466. doi: 10.1189/jlb.3hi1114-531r

Groger, M., Rennert, K., Giszas, B., Weiss, E., Dinger, J., Funke, H., et al. (2016). Monocyte-induced recovery of inflammation-associated hepatocellular dysfunction in a biochip-based human liver model. *Sci. Rep.* 6:21868.

Guilliams, M., Ginhoux, F., Jakubzick, C., Naik, S. H., Onai, N., Schraml, B. U., et al. (2014). Dendritic cells, monocytes and macrophages: a unified nomenclature based on ontogeny. *Nat. Rev. Immunol.* 14, 571–578. doi: 10.1038/nri3712

Haldar, M., Kohyama, M., So, A. Y., Kc, W., Wu, X., Briseno, C. G., et al. (2014). Heme-mediated SPI-C induction promotes monocyte differentiation into iron-recycling macrophages. *Cell* 156, 1223–1234. doi: 10.1016/j.cell.2014.01.069

Han, D., Walsh, M. C., Cejas, P. J., Dang, N. N., Kim, Y. F., Kim, J., et al. (2013). Dendritic cell expression of the signaling molecule TRAF6 is critical for gut microbiota-dependent immune tolerance. *Immunity* 38, 1211–1222. doi: 10.1016/j.immuni.2013.05.012

Haniffa, M., Bigley, V., and Collin, M. (2015). Human mononuclear phagocyte system reunited. *Semin. Cell Dev. Biol.* 41, 59–69. doi: 10.1016/j.semcdb.2015.05.004

Haniffa, M., Collin, M., and Ginhoux, F. (2013). Identification of human tissue cross-presenting dendritic cells: a new target for cancer vaccines. *Oncoimmunology* 2:e23140. doi: 10.4161/onci.23140

Haniffa, M., Shin, A., Bigley, V., McGovern, N., Teo, P., See, P., et al. (2012). Human tissues contain CD141hi cross-presenting dendritic cells with functional homology to mouse CD103+ nonlymphoid dendritic cells. *Immunity.*37, 60–73. doi: 10.1016/j.immuni.2012.04.012

Hashimoto, D., Chow, A., Noizat, C., Teo, P., Beasley, M. B., Leboeuf, M., et al. (2013). Tissue-resident macrophages self-maintain locally throughout adult life with minimal contribution from circulating monocytes. *Immunity* 38, 792–804. doi: 10.1016/j.immuni.2013.04.004

Hayes, B. H., Tsai, R. K., Dooling, L. J., Kadu, S., Lee, J. Y., Pantano, D., et al. (2020). Macrophages show higher levels of engulfment after disruption of cis interactions between CD47 and the checkpoint receptor SIRPα. *J. Cell Sci.* 133:jcs237800. doi: 10.1242/jcs.237800

Hoeffel, G., Chen, J., Lavin, Y., Low, D., Almeida, F. F., See, P., et al. (2015). C-Myb(+) erythro-myeloid progenitor-derived fetal monocytes give rise to adult tissue-resident macrophages. *Immunity* 42, 665–678. doi: 10.1016/j.immuni.2015.03.011

Hoeffel, G., and Ginhoux, F. (2015). Ontogeny of tissue-resident macrophages. *Front. Immunol.* 6:486.

Hotchkiss, R. S., and Opal, S. (2010). Immunotherapy for sepsis–a new approach against an ancient foe. *N. Engl. J. Med.* 363, 87–89. doi: 10.1056/nejmcibr1004371

Hu, Z., Lancaster, J. N., Sasiponganan, C., and Ehrlich, L. I. R. (2015). CCR4 promotes medullary entry and thymocyte-dendritic cell interactions required for central tolerance. *J. Exp. Med.* 212, 1947–1965. doi: 10.1084/jem.20150178

Hulsmans, M., Sam, F., and Nahrendorf, M. (2016). Monocyte and macrophage contributions to cardiac remodeling. *J. Mol. Cell Cardiol.* 93, 149–155. doi: 10.1016/j.yjmcc.2015.11.015

Hume, D. A., Allan, W., Golder, J., Stephens, R. W., Doe, W. F., and Warren, H. S. (1985). Preparation and characterization of human bone marrow-derived macrophages. *J. Leukoc. Biol.* 38, 541–552. doi: 10.1002/jlb.38.4.541

Hume, D. A., Irvine, K. M., and Pridans, C. (2019). The Mononuclear Phagocyte System: The Relationship between Monocytes and Macrophages. *Trends Immunol.* 40, 98–112. doi: 10.1016/j.it.2018.11.007

Iakobachvili, N., and Peters, P. J. (2017). Humans in a dish: the potential of organoids in modeling immunity and infectious diseases. *Front. Microbiol.* 8:2402.

Izquierdo, H. M., Brandi, P., Gómez, M.-J., Conde-Garrosa, R., Priego, E., Enamorado, M., et al. (2018). Von hippel-lindau protein is required for optimal alveolar macrophage terminal differentiation, self-renewal, and function. *Cell Rep.* 24, 1738–1746. doi: 10.1016/j.celrep.2018.07.034

Jacome-Galarza, C. E., Percin, G. I., Muller, J. T., Mass, E., Lazarov, T., Eitler, J., et al. (2019). Developmental origin, functional maintenance and genetic rescue of osteoclasts. *Nature* 568, 541–545. doi: 10.1038/s41586-019-1105-7

Jang, K. J., Otieno, M. A., Ronxhi, J., Lim, H. K., Ewart, L., Kodella, K. R., et al. (2019). Reproducing human and cross-species drug toxicities using a Liver-Chip. *Sci. Transl. Med.* 11:eaax5516. doi: 10.1126/scitranslmed.aax5516

Jang, M. H., Sougawa, N., Tanaka, T., Hirata, T., Hiroi, T., Tohya, K., et al. (2006). CCR7 is critically important for migration of dendritic cells in intestinal lamina propria to mesenteric lymph nodes. *J. Immunol.* 176, 803–810. doi: 10.4049/jimmunol.176.2.803

Johnson, E. L., and Chakraborty, R. (2012). Placental Hofbauer cells limit HIV-1 replication and potentially offset mother to child transmission (MTCT) by induction of immunoregulatory cytokines. *Retrovirology* 9:101.

Kanton, S., Boyle, M. J., He, Z., Santel, M., Weigert, A., Sanchis-Calleja, F., et al. (2019). Organoid single-cell genomic atlas uncovers human-specific features of brain development. *Nature* 574, 418–422. doi: 10.1038/s41586-019-1654-9

Kaur, S., Raggatt, L. J., Batoon, L., Hume, D. A., Levesque, J. P., and Pettit, A. R. (2017). Role of bone marrow macrophages in controlling homeostasis and repair in bone and bone marrow niches. *Semin. Cell Dev. Biol.* 61, 12–21. doi: 10.1016/j.semcdb.2016.08.009

Kawane, K., Fukuyama, H., Yoshida, H., Nagase, H., Ohsawa, Y., Uchiyama, Y., et al. (2003). Impaired thymic development in mouse embryos deficient in apoptotic DNA degradation. *Nat. Immunol.* 4, 138–144. doi: 10.1038/ni881

Kellermayer, Z., Fisi, V., Mihalj, M., Berta, G., Kobor, J., and Balogh, P. (2014). Marginal zone macrophage receptor mARCO is trapped in conduits formed by follicular dendritic cells in the spleen. *J. Histochem. Cytochem.* 62, 436–449. doi: 10.1369/0022155414529595

Kim, J., Koo, B. K., and Knoblich, J. A. (2020). Human organoids: model systems for human biology and medicine. *Nat. Rev. Mol. Cell Biol.* 21, 571–584. doi: 10.1038/s41580-020-0259-3

Kirkling, M. E., Cytlak, U., Lau, C. M., Lewis, K. L., Resteu, A., Khodadadi-Jamayran, A., et al. (2018). Notch signaling facilitates in vitro generation of cross-presenting classical dendritic cells. *Cell Rep.* 23, 3658–72e6.

Knoop, K. A., McDonald, K. G., McCrate, S., McDole, J. R., and Newberry, R. D. (2015). Microbial sensing by goblet cells controls immune surveillance of luminal antigens in the colon. *Mucosal. Immunol.* 8, 198–210. doi: 10.1038/mi.2014.58

Krow-Lucal, E. R., Kim, C. C., Burt, T. D., and McCune, J. M. (2014). Distinct functional programming of human fetal and adult monocytes. *Blood* 123, 1897–1904. doi: 10.1182/blood-2013-11-536094

Lee, J., Rabbani, C. C., Gao, H., Steinhart, M. R., Woodruff, B. M., Pflum, Z. E., et al. (2020). Hair-bearing human skin generated entirely from pluripotent stem cells. *Nature* 582, 399–404. doi: 10.1038/s41586-020-2352-3

Leimberg, M. J., Prus, E., Konijn, A. M., and Fibach, E. (2008). Macrophages function as a ferritin iron source for cultured human erythroid precursors. *J. Cell Biochem.* 103, 1211–1218. doi: 10.1002/jcb.21499

Li, W., Wang, Y., Zhao, H., Zhang, H., Xu, Y., Wang, S., et al. (2019). Identification and transcriptome analysis of erythroblastic island macrophages. *Blood* 134, 480–491. doi: 10.1182/blood.2019000430

Lifshitz, L., Tabak, G., Gassmann, M., Mittelman, M., and Neumann, D. (2010). Macrophages as novel target cells for erythropoietin. *Haematologic.* 95, 1823–1831. doi: 10.3324/haematol.2010.025015

Liu, M., Jin, X., He, X., Pan, L., Zhang, X., and Zhao, Y. (2015). Macrophages support splenic erythropoiesis in 4T1 tumor-bearing mice. *PLoS One.* 10:e0121921. doi: 10.1371/journal.pone.0121921

Liu, Y., Gao, X., Miao, Y., Wang, Y., Wang, H., Cheng, Z., et al. (2018). NLRP3 regulates macrophage M2 polarization through up-regulation of IL-4 in asthma. *Biochem. J.* 475, 1995–2008. doi: 10.1042/bcj20180086

Luo, W., Xu, Q., Wang, Q., Wu, H., and Hua, J. (2017). Effect of modulation of PPAR-gamma activity on kupffer cells M1/M2 polarization in the development of non-alcoholic fatty liver disease. *Sci Rep.* 7:44612.

MacParland, S. A., Liu, J. C., Ma, X.-Z., Innes, B. T., Bartczak, A. M., Gage, B. K., et al. (2018). Single cell RNA sequencing of human liver reveals distinct intrahepatic macrophage populations. *Nat. Commun.* 9:4383.

Malissen, B., Tamoutounour, S., and Henri, S. (2014). The origins and functions of dendritic cells and macrophages in the skin. *Nat. Rev. Immunol.* 14, 417–428. doi: 10.1038/nri3683

Martinez, K. A. II, Romano-Keeler, J., Zackular, J. P., Moore, D. J., Brucker, R. M., Hooper, C., et al. (2018). Bacterial DNA is present in the fetal intestine and overlaps with that in the placenta in mice. *PLoS One.* 13:e0197439. doi: 10.1371/journal.pone.0197439

Mazzini, E., Massimiliano, L., Penna, G., and Rescigno, M. (2014). Oral tolerance can be established via gap junction transfer of fed antigens from CX3CR1(+) macrophages to CD103(+) dendritic cells. *Immunity* 40, 248–261. doi: 10.1016/j.immuni.2013.12.012

McGovern, N., Chan, J. K., and Ginhoux, F. (2015). Dendritic cells in humans–from fetus to adult. *Int. Immunol.* 27, 65–72. doi: 10.1093/intimm/dxu091

McGovern, N., Schlitzer, A., Gunawan, M., Jardine, L., Shin, A., Poyner, E., et al. (2014). Human dermal $CD14^{+}$ cells are a transient population of monocyte-derived macrophages. *Immunity* 41, 465–477. doi: 10.1016/j.immuni.2014.08.006

McGovern, N., Shin, A., Low, G., Low, D., Duan, K., Yao, L. J., et al. (2017). Human fetal dendritic cells promote prenatal T-cell immune suppression through arginase-2. *Nature* 546, 662–666.

McGrath, K. E., Frame, J. M., Fegan, K. H., Bowen, J. R., Conway, S. J., Catherman, S. C., et al. (2015). Distinct sources of hematopoietic progenitors emerge before hscs and provide functional blood cells in the mammalian embryo. *Cell Rep.* 11, 1892–1904. doi: 10.1016/j.celrep.2015.05.036

Menassa, D. A., and Gomez-Nicola, D. (2018). Microglial dynamics during human brain development. *Front. Immunol.* 9:1014.

Merad, M., Manz, M. G., Karsunky, H., Wagers, A., Peters, W., Charo, I., et al. (2002). Langerhans cells renew in the skin throughout life under steady-state conditions. *Nat. Immun.* 3, 1135–1141. doi: 10.1038/ni852

Migliaccio, G., Migliaccio, A. R., Petti, S., Mavilio, F., Russo, G., Lazzaro, D., et al. (1986). Human embryonic hemopoiesis. kinetics of progenitors and precursors underlying the yolk sac—-liver transition. *J. Clin. Invest.* 78, 51–60. doi: 10.1172/jci112572

Mitsi, E., Kamng'ona, R., Rylance, J., Solorzano, C., Jesus Reine, J., Mwandumba, H. C., et al. (2018). Human alveolar macrophages predominately express combined classical M1 and M2 surface markers in steady state. *Respir Res.* 19:66.

Morse, C., Tabib, T., Sembrat, J., Buschur, K. L., Bittar, H. T., Valenzi, E., et al. (2019). Proliferating SPP1/MERTK-expressing macrophages in idiopathic pulmonary fibrosis. *Eur. Respir J.* 54:1802441. doi: 10.1183/13993003.02441-2018

Moxey, P. C., and Trier, J. S. (1978). Specialized cell types in the human fetal small intestine. *Anat. Rec.* 191, 269–285. doi: 10.1002/ar.1091910302

Murata, Y., Kotani, T., Ohnishi, H., and Matozaki, T. (2014). The CD47-SIRPalpha signalling system: its physiological roles and therapeutic application. *J. Biochem.* 155, 335–344. doi: 10.1093/jb/mvu017

Nagelkerke, S. Q., Bruggeman, C. W., den Haan, J. M. M., Mul, E. P. J., van den Berg, T. K., van Bruggen, R., et al. (2018). Red pulp macrophages in the human spleen are a distinct cell population with a unique expression of Fc-gamma receptors. *Blood Adv.* 2, 941–953. doi: 10.1182/bloodadvances.2017015008

Neal, J. T., Li, X., Zhu, J., Giangarra, V., Grzeskowiak, C. L., Ju, J., et al. (2018). Organoid modeling of the tumor immune microenvironment. *Cell* 175, 1972–1988 e16.

Nestle, F. O., Di Meglio, P., Qin, J. Z., and Nickoloff, B. J. (2009). Skin immune sentinels in health and disease. *Nat. Rev. Immunol.* 9, 679–691. doi: 10.1038/nri2622

Notta, F., Zandi, S., Takayama, N., Dobson, S., Gan, O. I., Wilson, G., et al. (2016). Distinct routes of lineage development reshape the human blood hierarchy across ontogeny. *Science* 351:aab2116. doi: 10.1126/science.aab2116

Ortiz-Masia, D., Cosin-Roger, J., Calatayud, S., Hernandez, C., Alos, R., Hinojosa, J., et al. (2014). Hypoxic macrophages impair autophagy in epithelial cells through Wnt1: relevance in IBD. *Mucosal. Immunol.* 7, 929–938. doi: 10.1038/mi.2013.108

Palis, J. (2016). Interaction of the macrophage and primitive erythroid lineages in the mammalian embryo. *Front. Immunol.* 7:669.

Park, J. E., Botting, R. A., Dominguez Conde, C., Popescu, D. M., Lavaert, M., Kunz, D. J., et al. (2020). A cell atlas of human thymic development defines T cell repertoire formation. *Science* 367:eaay3224.

Park, J. H., Lee, N. K., and Lee, S. Y. (2017). Current understanding of RANK signaling in osteoclast differentiation and maturation. *Mol. Cells.* 40, 706–713.

Patel, E., Wang, B., Lien, L., Wang, Y., Yang, L. J., Moreb, J. S., et al. (2009). Diverse T-cell differentiation potentials of human fetal thymus, fetal liver, cord blood and adult bone marrow CD34 cells on lentiviral Delta-like-1-modified mouse stromal cells. *Immunology* 128(1 Suppl), e497–e505.

Pirgova, G., Chauveau, A., MacLean, A. J., Cyster, J. G., and Arnon, T. I. (2020). Marginal zone SIGN-R1(+) macrophages are essential for the maturation of germinal center B cells in the spleen. *Proc. Natl. Acad. Sci. U.S.A.* 117, 12295–12305. doi: 10.1073/pnas.1921673117

Popescu, D. M., Botting, R. A., Stephenson, E., Green, K., Webb, S., Jardine, L., et al. (2019). Decoding human fetal liver haematopoiesis. *Nature* 574, 365–371.

Poulin, L. F., Salio, M., Griessinger, E., Anjos-Afonso, F., Craciun, L., Chen, J. L., et al. (2010). Characterization of human DNGR-1+ BDCA3+ leukocytes as putative equivalents of mouse CD8alpha+ dendritic cells. *J. Exp. Med.* 207, 1261–1271. doi: 10.1084/jem.20092618

Pourcher, G., Mazurier, C., King, Y. Y., Giarratana, M.-C., Kobari, L., Boehm, D., et al. (2011). Human fetal liver: an in vitro model of erythropoiesis. *Stem. Cells Int.* 2011:405429.

Prabhu, S. D., and Frangogiannis, N. G. (2016). The biological basis for cardiac repair after myocardial infarction: from inflammation to fibrosis. *Circ. Res.* 119, 91–112. doi: 10.1161/circresaha.116.303577

Putz, G., Rosner, A., Nuesslein, I., Schmitz, N., and Buchholz, F. (2006). AML1 deletion in adult mice causes splenomegaly and lymphomas. *Oncogene* 25, 929–939. doi: 10.1038/sj.onc.1209136

Ramalingam, R., Larmonier, C. B., Thurston, R. D., Midura-Kiela, M. T., Zheng, S. G., Ghishan, F. K., et al. (2012). Dendritic cell-specific disruption of TGF-beta receptor II leads to altered regulatory T cell phenotype and spontaneous multiorgan autoimmunity. *J. Immunol.* 189, 3878–3893. doi: 10.4049/jimmunol.1201029

Rennert, K., Steinborn, S., Groger, M., Ungerbock, B., Jank, A. M., Ehgartner, J., et al. (2015). A microfluidically perfused three dimensional human liver model. *Biomaterials.*71, 119–131. doi: 10.1016/j.biomaterials.2015.08.043

Reynolds, G., Vegh, P., Fletcher, J., Poyner, E. F. M., Stephenson, E., Goh, I., et al. (2020). Poised cell circuits in human skin are activated in disease. *bioRxiv*[preprint] bioRxiv 2020.11.05.369363,

Richardson, L., Gnecco, J., Ding, T., Osteen, K., Rogers, L. M., Aronoff, D. M., et al. (2020). Fetal membrane organ-on-chip: an innovative approach to study cellular interactions. *Reprod Sci.* 27, 1562–1569. doi: 10.1007/s43032-020-00184-9

Rigat-Brugarolas, L. G., Elizalde-Torrent, A., Bernabeu, M., De Niz, M., Martin-Jaular, L., Fernandez-Becerra, C., et al. (2014). A functional microengineered model of the human splenon-on-a-chip. *Lab Chip* 14, 1715–1724. doi: 10.1039/c3lc51449h

Robb, L., Drinkwater, C. C., Metcalf, D., Li, R., Köntgen, F., Nicola, N. A., et al. (1995). Hematopoietic and lung abnormalities in mice with a null mutation of the common beta subunit of the receptors for granulocyte-macrophage colony-stimulating factor and interleukins 3 and 5. *Proc. Natl. Acad. Sci. U.S.A.* 92, 9565–9569. doi: 10.1073/pnas.92.21.9565

Roe, M. M., Swain, S., Sebrell, T. A., Sewell, M. A., Collins, M. M., Perrino, B. A., et al. (2017). Differential regulation of CD103 (alphaE integrin) expression in human dendritic cells by retinoic acid and Toll-like receptor ligands. *J. Leukoc Biol.* 101, 1169–1180. doi: 10.1189/jlb.1ma0316-131r

Rojo, R., Raper, A., Ozdemir, D. D., Lefevre, L., Grabert, K., Wollscheid-Lengeling, E., et al. (2019). Deletion of a Csf1r enhancer selectively impacts CSF1R expression and development of tissue macrophage populations. *Nat. Commun.* 10:3215.

Sacchetti, B., Funari, A., Michienzi, S., Di Cesare, S., Piersanti, S., Saggio, I., et al. (2007). Self-renewing osteoprogenitors in bone marrow sinusoids can organize a hematopoietic microenvironment. *Cell* 131, 324–336. doi: 10.1016/j.cell.2007.08.025

Sallusto, F., and Lanzavecchia, A. (1994). Efficient presentation of soluble antigen by cultured human dendritic cells is maintained by granulocyte/macrophage colony-stimulating factor plus interleukin 4 and downregulated by tumor necrosis factor alpha. *J. Exp. Med.* 179, 1109–1118. doi: 10.1084/jem.179.4.1109

Sasserath, T., Rumsey, J. W., McAleer, C. W., Bridges, L. R., Long, C. J., Elbrecht, D., et al. (2020). Differential monocyte actuation in a three-organ functional innate immune system-on-a-chip. *Adv. Sci. (Weinh).* 7:2000323. doi: 10.1002/advs.202000323

Sawada, K., Krantz, S. B., Dessypris, E. N., Koury, S. T., and Sawyer, S. T. (1989). Human colony-forming units-erythroid do not require accessory cells, but do require direct interaction with insulin-like growth factor I and/or insulin for erythroid development. *J. Clin. Invest.* 83, 1701–1709. doi: 10.1172/jci114070

Schuster, C., Vaculik, C., Fiala, C., Meindl, S., Brandt, O., Imhof, M., et al. (2009). HLA-DR+ leukocytes acquire CD1 antigens in embryonic and fetal human skin and contain functional antigen-presenting cells. *J. Exp. Med.* 206, 169–181. doi: 10.1084/jem.20081747

Schuster, C., Vaculik, C., Prior, M., Fiala, C., Mildner, M., Eppel, W., et al. (2012). Phenotypic characterization of leukocytes in prenatal human dermis. *J. Invest. Dermatol.* 132, 2581–2592. doi: 10.1038/jid.2012.187

Scott, C. L., Bain, C. C., Wright, P. B., Sichien, D., Kotarsky, K., Persson, E. K., et al. (2015). CCR2+CD103- intestinal dendritic cells develop from DC-committed precursors and induce interleukin-17 production by T cells. *Mucosal. Immun.* 8, 327–339. doi: 10.1038/mi.2014.70

Scott, C. L., Zheng, F., De Baetselier, P., Martens, L., Saeys, Y., De Prijck, S., et al. (2016). Bone marrow-derived monocytes give rise to self-renewing and fully differentiated Kupffer cells. *Nat. Commun.* 7:10321.

Segura, E., Touzot, M., Bohineust, A., Cappuccio, A., Chiocchia, G., Hosmalin, A., et al. (2013). Human inflammatory dendritic cells induce Th17 cell differentiation. *Immunity* 38, 336–348. doi: 10.1016/j.immuni.2012.10.018

Seneschal, J., Clark, R. A., Gehad, A., Baecher-Allan, C. M., and Kupper, T. S. (2012). Human epidermal Langerhans cells maintain immune homeostasis in skin by activating skin resident regulatory T cells. *Immunity* 36, 873–884. doi: 10.1016/j.immuni.2012.03.018

Shanti, A., Teo, J., and Stefanini, C. (2018). In vitro immune organs-on-chip for drug development: a review. *Pharmaceutics* 10:278. doi: 10.3390/pharmaceutics10040278

Shook, B. A., Wasko, R. R., Rivera-Gonzalez, G. C., Salazar-Gatzimas, E., Lopez-Giraldez, F., Dash, B. C., et al. (2018). Myofibroblast proliferation and heterogeneity are supported by macrophages during skin repair. *Science* 362:eaar2971. doi: 10.1126/science.aar2971

Sieber, S., Wirth, L., Cavak, N., Koenigsmark, M., Marx, U., Lauster, R., et al. (2018). Bone marrow-on-a-chip: long-term culture of human haematopoietic stem cells in a three-dimensional microfluidic environment. *J. Tissue Eng. Regen Med.* 12, 479–489.

Spivia, W., Magno, P. S., Le, P., and Fraser, D. A. (2014). Complement protein C1q promotes macrophage anti-inflammatory M2-like polarization during the clearance of atherogenic lipoproteins. *Inflamm. Res.* 63, 885–893. doi: 10.1007/s00011-014-0762-0

Sriram, G., Bigliardi, P. L., and Bigliardi-Qi, M. (2019). Full-thickness human skin equivalent models of atopic dermatitis. *Methods Mol. Biol.* 1879, 367–383. doi: 10.1007/7651_2018_163

Stanley, E., Lieschke, G. J., Grail, D., Metcalf, D., Hodgson, G., Gall, J. A., et al. (1994). Granulocyte/macrophage colony-stimulating factor-deficient mice

show no major perturbation of hematopoiesis but develop a characteristic pulmonary pathology. *Proc. Natl. Acad. Sci. U.S.A.* 91, 5592–5596. doi: 10.1073/pnas.91.12.5592

Steiniger, B., Ulfig, N., Risse, M., and Barth, P. J. (2007). Fetal and early post-natal development of the human spleen: from primordial arterial B cell lobules to a non-segmented organ. *Histochem. Cell Biol.* 128, 205–215. doi: 10.1007/s00418-007-0296-4

Steinman, R. M., and Cohn, Z. A. (1973). Identification of a novel cell type in peripheral lymphoid organs of mice. I. morphology, quantitation, tissue distribution. *J. Exp. Med.* 137, 1142–1162. doi: 10.1084/jem.137.5.1142

Stephenson, E., Reynolds, G., Botting, R. A., Calero-Nieto, F. J., Morgan, M., Tuong, Z. K., et al. (2021). The cellular immune response to COVID-19 deciphered by single cell multi-omics across three UK centres. *medRxiv*[preprint] medRxiv 2021.01.13.21249725,

Stoeckius, M., Hafemeister, C., Stephenson, W., Houck-Loomis, B., Chattopadhyay, P. K., Swerdlow, H., et al. (2017). Simultaneous epitope and transcriptome measurement in single cells. *Nat. Methods.* 14, 865–868. doi: 10.1038/nmeth.4380

Stras, S. F., Werner, L., Toothaker, J. M., Olaloye, O. O., Oldham, A. L., McCourt, C. C., et al. (2019). Maturation of the human intestinal immune system occurs early in fetal development. *Dev. Cell* 51, 357–373 e5.

Takata, K., Kozaki, T., Lee, C. Z. W., Thion, M. S., Otsuka, M., Lim, S., et al. (2017). Induced-pluripotent-stem-cell-derived primitive macrophages provide a platform for modeling tissue-resident macrophage differentiation and function. *Immunity* 47, 183–198 e6.

Tamoutounour, S., Guilliams, M., Montanana Sanchis, F., Liu, H., Terhorst, D., Malosse, C., et al. (2013). Origins and functional specialization of macrophages and of conventional and monocyte-derived dendritic cells in mouse skin. *Immunity* 39, 925–938. doi: 10.1016/j.immuni.2013.10.004

Tauber, A. I. (2003). Metchnikoff and the phagocytosis theory. *Nat. Rev. Mol. Cell Biol.* 4, 897–901. doi: 10.1038/nrm1244

Thomas, J. R., Appios, A., Zhao, X., Dutkiewicz, R., Donde, M., Lee, C. Y. C., et al. (2020). Phenotypic and functional characterization of first-trimester human placental macrophages, hofbauer cells. *J. Exp. Med.* 218: e20200891.

Tokunaga, T., Mokuda, S., Kohno, H., Yukawa, K., Kuranobu, T., Oi, K., et al. (2020). TGFβ1 Regulates human rankl-induced osteoclastogenesis via suppression of nfatc1 expression. *Int. J. Mol. Sci.* 21:800. doi: 10.3390/ijms21030800

Valladeau, J., Ravel, O., Dezutter-Dambuyant, C., Moore, K., Kleijmeer, M., Liu, Y., et al. (2000). Langerin, a novel C-type lectin specific to Langerhans cells, is an endocytic receptor that induces the formation of Birbeck granules. *Immunity* 12, 71–81. doi: 10.1016/s1074-7613(00)80160-0

Vallon-Eberhard, A., Landsman, L., Yogev, N., Verrier, B., and Jung, S. (2006). Transepithelial pathogen uptake into the small intestinal lamina propria. *J. Immunol.* 176, 2465–2469. doi: 10.4049/jimmunol.176.4.2465

van Furth, R., and Cohn, Z. A. (1968). The origin and kinetics of mononuclear phagocytes. *J. Exp. Med.* 128, 415–435. doi: 10.1084/jem.128.3.415

van Leeuwen-Kerkhoff, N., Lundberg, K., Westers, T. M., Kordasti, S., Bontkes, H. J., Lindstedt, M., et al. (2018). human bone marrow-derived myeloid dendritic cells show an immature transcriptional and functional profile compared to their peripheral blood counterparts and separate from slan+ non-classical monocytes. *Front. Immun.* 9:1619.

Vento-Tormo, R., Efremova, M., Botting, R. A., Turco, M. Y., Vento-Tormo, M., Meyer, K. B., et al. (2018). Single-cell reconstruction of the early maternal-fetal interface in humans. *Nature* 563, 347–353.

Watchmaker, P. B., Lahl, K., Lee, M., Baumjohann, D., Morton, J., Kim, S. J., et al. (2014). Comparative transcriptional and functional profiling defines conserved programs of intestinal DC differentiation in humans and mice. *Nat. Immunol.* 15, 98–108. doi: 10.1038/ni.2768

Weivoda, M. M., Chew, C. K., Monroe, D. G., Farr, J. N., Atkinson, E. J., Geske, J. R., et al. (2020). Identification of osteoclast-osteoblast coupling factors in humans reveals links between bone and energy metabolism. *Nat. Commun.* 11:87.

Witt, R. G., Wang, B., Nguyen, Q. H., Eikani, C., Mattis, A. N., and MacKenzie, T. C. (2018). Depletion of murine fetal hematopoietic stem cells with c-Kit receptor and CD47 blockade improves neonatal engraftment. *Blood Adv.* 2, 3602–3607. doi: 10.1182/bloodadvances.2018022020

Zhang, J., Supakorndej, T., Krambs, J. R., Rao, M., Abou-Ezzi, G., Ye, R. Y., et al. (2019). Bone marrow dendritic cells regulate hematopoietic stem/progenitor cell trafficking. *J Clin Invest.* 129, 2920–2931. doi: 10.1172/jci124829

Zhao, Y., Kankala, R. K., Wang, S.-B., and Chen, A.-Z. (2019). Multi-organs-on-chips: towards long-term biomedical investigations. *Molecules* 24:675. doi: 10.3390/molecules24040675

Ziegler-Heitbrock, L., Ancuta, P., Crowe, S., Dalod, M., Grau, V., Hart, D. N., et al. (2010). Nomenclature of monocytes and dendritic cells in blood. *Blood* 116, e74–e80.

Conflict of Interest: The authors declare that the research was conducted in the absence of any commercial or financial relationships that could be construed as a potential conflict of interest.

Advantages of publishing in Frontiers

OPEN ACCESS
Articles are free to read for greatest visibility and readership

FAST PUBLICATION
Around 90 days from submission to decision

HIGH QUALITY PEER-REVIEW
Rigorous, collaborative, and constructive peer-review

TRANSPARENT PEER-REVIEW
Editors and reviewers acknowledged by name on published articles

Frontiers
Avenue du Tribunal-Fédéral 34
1005 Lausanne | Switzerland

Visit us: www.frontiersin.org
Contact us: frontiersin.org/about/contact

REPRODUCIBILITY OF RESEARCH
Support open data and methods to enhance research reproducibility

DIGITAL PUBLISHING
Articles designed for optimal readership across devices

FOLLOW US
@frontiersin

IMPACT METRICS
Advanced article metrics track visibility across digital media

EXTENSIVE PROMOTION
Marketing and promotion of impactful research

LOOP RESEARCH NETWORK
Our network increases your article's readership